GEOLOGICAL SURVEY OF CANADA
COMMISSION GÉOLOGIQUE DU CANADA

PAPER 80-1C
ÉTUDE

This document was produced
by scanning the original publication.

Ce document est le produit d'une
numérisation par balayage
de la publication originale.

CURRENT RESEARCH
PART C

RECHERCHES EN COURS
PARTIE C

Energy, Mines and Resources Canada
Énergie, Mines et Ressources Canada

1980

Notice to Librarians and Indexers

The Geological Survey's thrice-yearly *Current Research* series contains many reports comparable in scope and subject matter to those appearing in scientific journals and other serials. All contributions to the Scientific and Technical Report section of *Current Research* include an abstract and bibliographic citation. It is hoped that these will assist you in cataloguing and indexing these reports and that this will result in a still wider dissemination of the results of the Geological Survey's research activities.

Avis aux bibliothécaires et préparateurs d'index

La série Recherches en cours *de la Commission géologique paraît trois fois par année; elle contient plusieurs rapports dont la portée et la nature sont comparable à ceux qui paraissent dans les revues scientifiques et autres périodiques. Tous les articles publiés dans la section des rapports scientifiques et techniques de la publication* Recherches en cours *sont accompagnés d'un résumé et d'une bibliographie, ce qui vous permettra, nous l'espérons, de cataloguer et d'indexer ces rapports, d'où une meilleure diffusion des résultats de recherche de la Commission géologique.*

Technical editing and compilation
Rédaction et compilation techniques
R.G. Blackadar
P.J. Griffin
H. Dumych
E.R.W. Neale

Production editing and layout
Préparation et mise en page
Leona R. Mahoney

Typed and checked by
Dactylographie et vérification
Madeleine Aiken
Debby Busby
Janet Gilliland
Sharon Parnham

GEOLOGICAL SURVEY
PAPER 80-1C

COMMISSION GÉOLOGIQUE
ÉTUDE 80-1C

CURRENT RESEARCH
PART C

Including

Rubidium-Strontium and Uranium-Lead Isotopic Age Studies, Report 3

1980

©Minister of Supply and Services Canada 1980

Available in Canada through

authorized bookstore agents
and other bookstores

or by mail from

Canadian Government Publishing Centre
Supply and Services Canada
Hull, Québec, Canada K1A 0S9

and from

Geological Survey of Canada
601 Booth Street
Ottawa, Canada K1A 0E8

A deposit copy of this publication is also available
for reference in public libraries across Canada

Cat. No. M44-80-ICE Canada: $6.00
ISBN 0-660-10721-X Other countries: $7.20

Price subject to change without notice

Geological Survey of Canada – *Commission géologique du Canada*

D.J. McLAREN
Director General
Directeur général

J.G. FYLES
Chief Geologist
Géologue en chef

E. HALL
Scientific Executive Officer
Agent exécutif scientifique

M.J. KEEN
Director, Atlantic Geoscience Centre, Dartmouth, Nova Scotia
Directeur du Centre géoscientifique de l'Atlantique, Dartmouth (Nouvelle-Ecosse)

J.A. MAXWELL
Director, Central Laboratories and Technical Services Division
Directeur de la Division des laboratoires centraux et des services techniques

R.G. BLACKADAR
Director, Geological Information Division
Directeur de la Division de l'information géologique

W.W. NASSICHUK
Director, Institute of Sedimentary and Petroleum Geology, Calgary, Alberta
Directeur de l'Institut de géologie sédimentaire et pétrolière, Calgary (Alberta)

J.E. REESOR
Director, Precambrian Geology Division
Directeur de la Division de la géologie du Précambrien

A.G. DARNLEY
Director, Resource Geophysics and Geochemistry Division
Directeur de la Division de la géophysique et de la géochimie appliquées

J.S. SCOTT
Director, Terrain Sciences Division
Directeur de la Division de la science des terrains

G.B. LEECH
Director, Economic Geology Division
Directeur de la Division de la géologie économique

R.B. CAMPBELL
Director, Cordilleran Geology Division, Vancouver, British Columbia
Directeur de la Division de la géologie de la Cordillère, Vancouver (Colombie-Britannique)

Separates

A limited number of separates of the papers that appear in this volume are available by direct request to the individual authors. The addresses of the Geological Survey of Canada offices follow:

601Booth Street,
OTTAWA, Ontario
K1A 0E8

Institute of Sedimentary and Petroleum Geology,
3303-33rd Street N.W.,
CALGARY, Alberta
T2L 2A7

Cordilleran Geology Division
100 West Pender Street,
VANCOUVER, B.C.
V6B 1R8

Atlantic Geoscience Centre,
Bedford Institute of Oceanography,
P.O. Box 1006,
DARTMOUTH, N.S.
B2Y 4A2

When no location accompanies an author's name in the title of a paper, the Ottawa address should be used.

Tirés à part

On peut obtenir un nombre limité de "tirés à part" des articles qui paraissent dans cette publication en s'adressant directement à chaque auteur. Les adresses des différents bureaux de la Commission géologique du Canada sont les suivantes:

601, rue Booth
OTTAWA, Ontario
K1A 0E8

Institut de géologie sédimentaire et pétrolière
3303-33rd, St. N.W.,
CALGARY, Alberta
T2L 2A7

Division de la géologie de la Cordillère
100 West Pender Street
VANCOUVER, Colombie-Britannique
V6B 1R8

Centre géoscientifique de l'Atlantique
Institut océanographique de Bedford
B.P. 1006
DARTMOUTH, Nouvelle-Ecosse
B2Y 4A2

Lorsque l'adresse de l'auteur ne figure pas sous le titre d'un document, on doit alors utiliser l'adresse d'Ottawa.

SCIENTIFIC AND TECHNICAL REPORTS

RAPPORTS SCIENTIFIQUES ET TECHNIQUES

SCIENTIFIC AND TECHNICAL NOTES

NOTES SCIENTIFIQUES ET TECHNIQUES

RUBIDIUM-STRONTIUM AND URANIUM-LEAD ISOTOPIC AGE STUDIES

ÉTUDES DES DATATIONS ISOTOPIQUES PAR LES MÉTHODES RUBIDIUM-STRONTIUM ET URANIUM-PLOMB

SCIENTIFIC AND TECHNICAL REPORTS
RAPPORTS SCIENTIFIQUES ET TECHNIQUES

1. **OVERBURDEN CHARACTERISTICS IN THE ALFRED-HAWKESBURY AREA, ONTARIO, OBTAINED BY D.C. ELECTRICAL SOUNDINGS**

Project 730004

Ajit K. Sinha
Resource Geophysics and Geochemistry Division

Sinha, Ajit K., Overburden characteristics in the Alfred-Hawkesbury area, Ontario, obtained by d.c. electrical soundings; in Current Research, Part C, Geological Survey of Canada, Paper 80-1C, p. 1-12, 1980.

Abstract

A direct current Schlumberger resistivity survey was carried out in an area around Alfred, Ontario. A total of 62 electrical soundings were made in the area with maximum current electrode separation of 1200 m. The station spacings were variable but averaged about 1.5 km from each other.

The geology of the area is not complex, the surface layers being composed of a number of quasi-parallel beds of varying resistivity and thickness. Because of the presence of an extremely conductive clay layer (Champlain clay beds) in much of the area, the analysis of the data yielded information on the presence and extent of this layer along with information like its conductance values and the drift thickness in the area. The field data have been interpreted using two different approaches to the layered earth model: the graphical auxiliary point method, and a computer-assisted interactive inversion program. Analysis of the data clearly delineated the areas where the clays are absent, thin, shallow or thick. The interpreted results of the survey have been presented in terms of the depth and thickness values of the highly conducting clay layers and also in terms of its conductance values, which provide a more accurate indication of the total effect of the clay beds at any station. A drift thickness map of the area has also been prepared which agrees well with a similar map prepared by the Ontario Ministry of Natural Resources based on information from water wells.

Introduction

The Alfred-Hawkesbury area of Eastern Ontario forms a part of the Ottawa-St. Lawrence Lowland. Geological studies in this region were initiated by Sir William Logan and recorded in various Geological Survey of Canada reports of progress from 1843 to 1864. Although considerable contributions were made by a number of other workers during and after Logan's work (Murray, 1852; Ells, 1898; Giroux, 1896; Johnston, 1917), the most exhaustive studies in this area were made by A.E. Wilson (1946), who described the stratigraphy and structure of the area as well as the economic geology aspects of the region.

In addition to surface bedrock mapping, some subsurface stratigraphical and structural data are available from a number of wells drilled for water and a few drilled for oil and natural gas. In recent years, Gadd (1963) has made extensive studies on the Quaternary deposits in the Ottawa area. The drift characteristics and Quaternary geology of the Alfred-Hawkesbury area have also been studied by Gwyn and Thibault (1973, 1975) who published maps indicating drift and bedrock characteristics based on examinations of natural and man-made exposures, aerial photographs and information from wells.

Surface geophysical exploration techniques (which depend on the contrasts in the physical properties of the different strata in the ground to generate observable anomalies) may also be used for mapping the subsurface layers. The first geophysical technique to be used in the area was a modified Barringer INPUT system which has been described by Dyck et al. (1974). To provide ground truths, a number of d.c. (direct current) Schlumberger resistivity[1] soundings were undertaken in the same area (Andrieux, 1968).

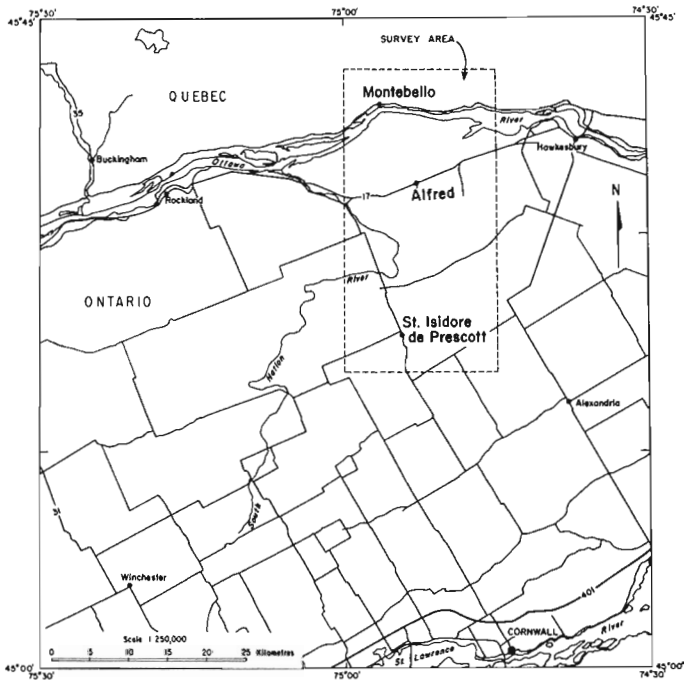

Figure 1.1. *Location map for the Schlumberger resistivity survey in the Alfred-Hawkesbury area.*

[1] Resistivity is a term indicating the property of a material that resists the flow of electrical current. The reciprocal of resistivity is conductivity. The product of conductivity and thickness of a conductor is termed its conductance. This parameter describes the total influence of the conductive bed better than either its conductivity or thickness considered separately.

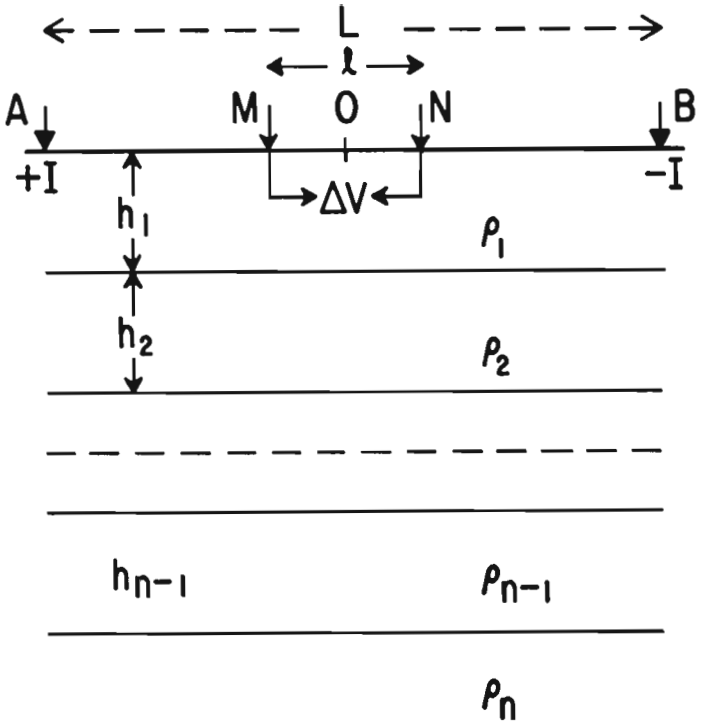

Figure 1.2. Arrangement of electrodes for the Schlumberger resistivity system.

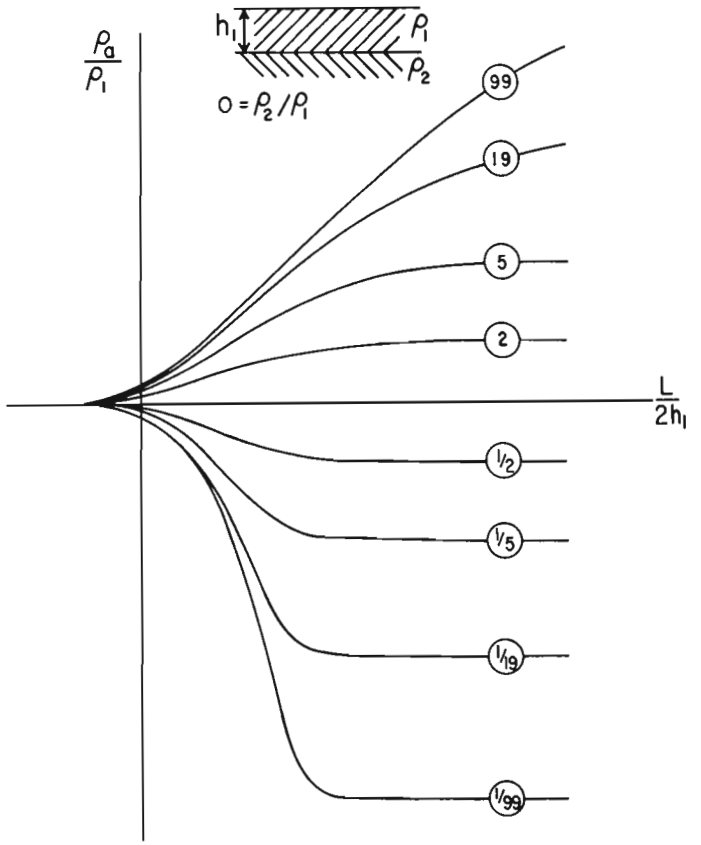

Figure 1.3. Master curves for the Schlumberger array over two-layer ground.

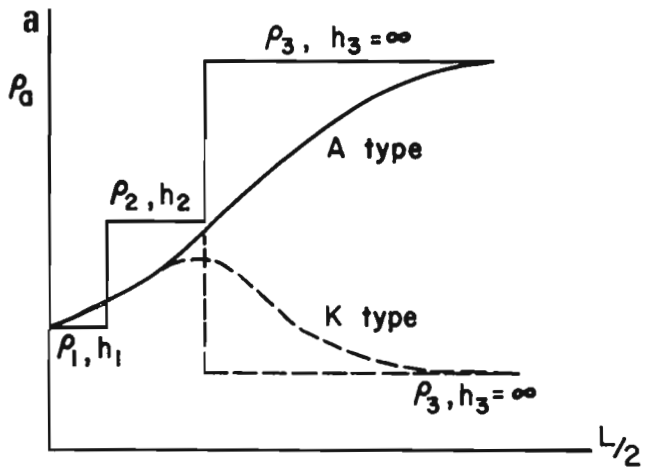

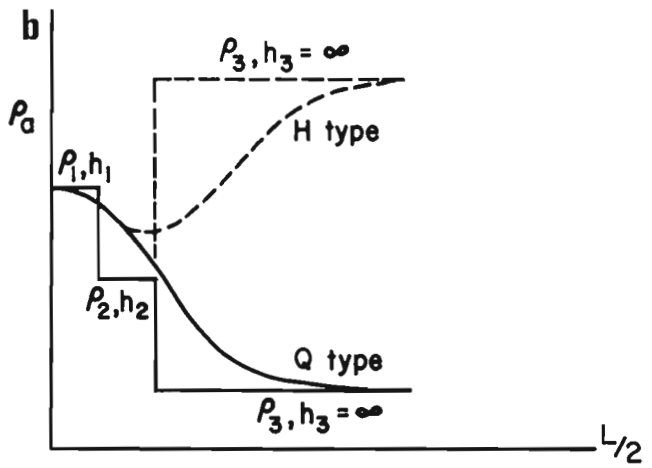

Figure 1.4a. Three layer master curves for the Schlumberger array (A and K types).

1.4b. Three layer master curves for the Schlumberger array (H and Q types).

As mentioned later in the paper, the geological setting for the area is relatively simple with a number of quasi-parallel beds lying over a highly resistive bedrock. The Schlumberger resistivity soundings are relatively easy to perform and the field data may be interpreted in terms of a number of layers with discrete thickness and resistivity values using widely available master curves. The area was later surveyed with the Tridem three frequency airborne electromagnetic system (Becker and Roy, 1977) and by a ground multifrequency e.m. system called the Maxiprobe, which has been described previously by Sinha (1979). The area was also mapped with the help of the newly developed Geonics EM-34 ground electromagnetic mapping system (Sinha, 1980). Geophysical techniques provide an extra dimension to surface geological mapping and may be used for determining overburden and bedrock characteristics in an area. In this area, the d.c. resistivity sounding data may be used to supplement existing geological information by providing information about layers and structures at depth.

The purpose of the present study is to analyze the resistivity sounding data in order to determine the topography of the bedrock surface and determine the thickness and distribution of the various Pleistocene and recent sediments (clays and sands). Such subsurface information is of considerable value in delineating future water-bearing reservoirs and deposits of sand, gravel, and other

construction materials. The resistivity data were analyzed using two different methods, the graphical auxiliary point method (Zohdy, 1965) and a computer-assisted semi-automatic interactive inversion program. The interpreted results are used to delineate areas where thick clay layers may be present and also regions of high resistivity which are normally due to the presence of dry sand layers or, to resistive bedrock exposed at the surface. Since the drift thickness may be obtained at each sounding station, a plot of these drift thicknesses in the area provided a crude map of the bedrock topography. In addition, several equiresistivity maps for different current electrode spacings have been plotted, which permits a reader to get some idea about the nature of the variation of the overburden materials with depth. Based on the resistivity data, a cross-sectional profile of the area along a line running north-south has been plotted. The diagram shows the nature of the variations in the thicknesses of the overburden and clay layers above the irregular bedrock surface along that line. Finally, the drift thicknesses obtained from resistivity soundings are compared to those obtained from geological mapping. It should be mentioned, however, that the station positions used in the two sets of drift measurements were different and the map obtained from water wells information (geological) had some uncertainty since some of the wells did not reach the bedrock. Therefore, total correlation between the two data sets should not be expected. Despite that, the general agreement between the two drift thickness maps is remarkably good.

Acknowledgments

The data presented in this paper were collected by P. Andrieux in 1968, with the help of D.C. Butterfield. The author is grateful to several colleagues in the Geological Survey of Canada who critically reviewed the manuscript. The author also thanks S. Wardlaw for some help in the computer-assisted interpretation of some of the sounding data.

Location and Access to the Area

The survey area is located around the town of Alfred, Ontario, about 65 km east of Ottawa. It straddles NTS map areas 31 G/7 and 10. The survey area shown in Figure 1.1 is rectangular with dimensions of 39.5 and 20 km along north-south and east-west directions, respectively. The area lies just south of the Canadian Shield, most of it south of the Ottawa River. Accessibility to the area is very good, being served by two highways, 17 and 417 (linking Ottawa to Montreal). There is an excellent network of side roads in the area, paved as well as unpaved which makes it possible to use a 2-wheel drive truck for most of the field operations. The road network is shown in greater detail in Figure 1.5.

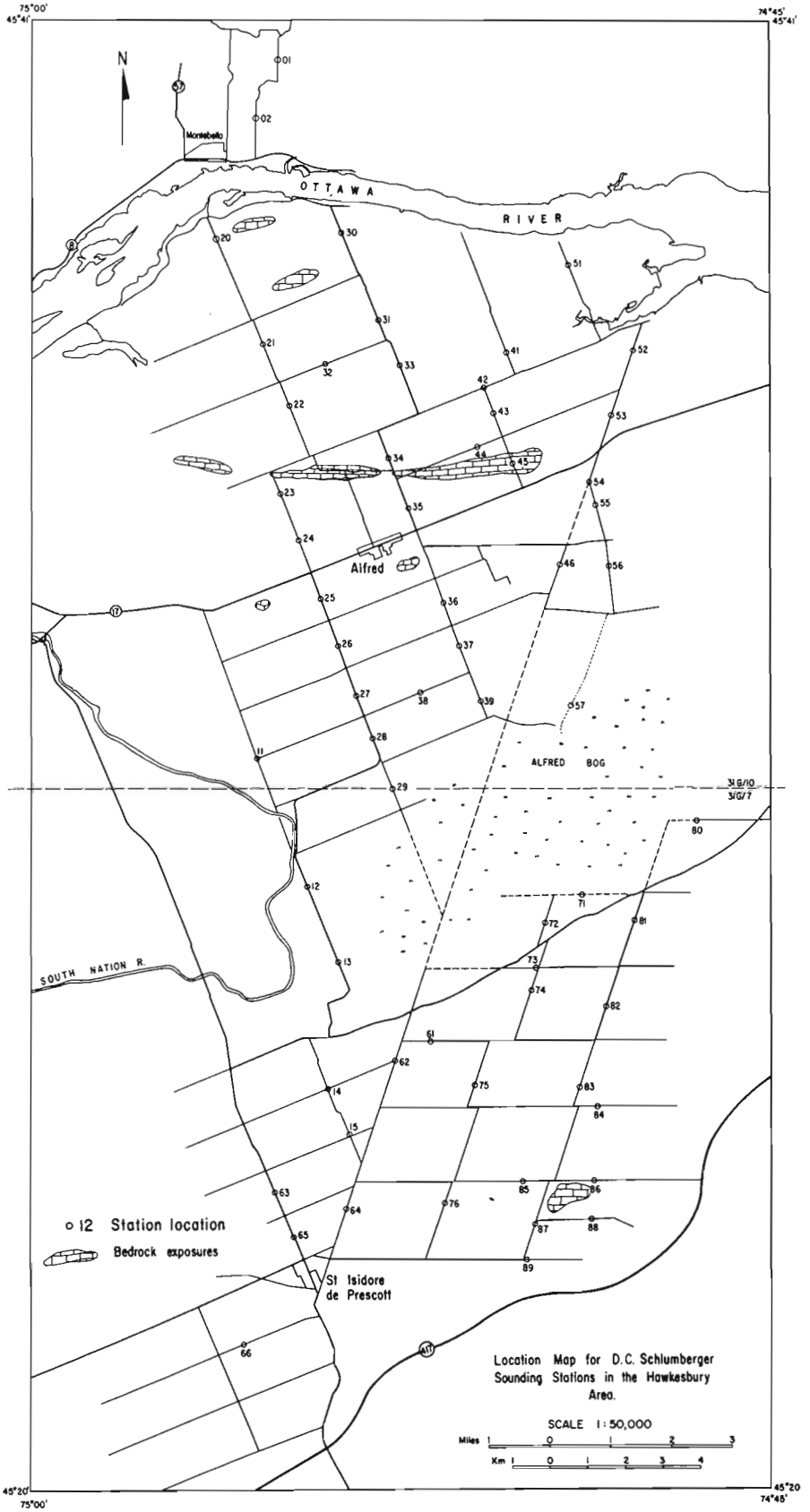

Figure 1.5. Location of the resistivity sounding stations in the Alfred area.

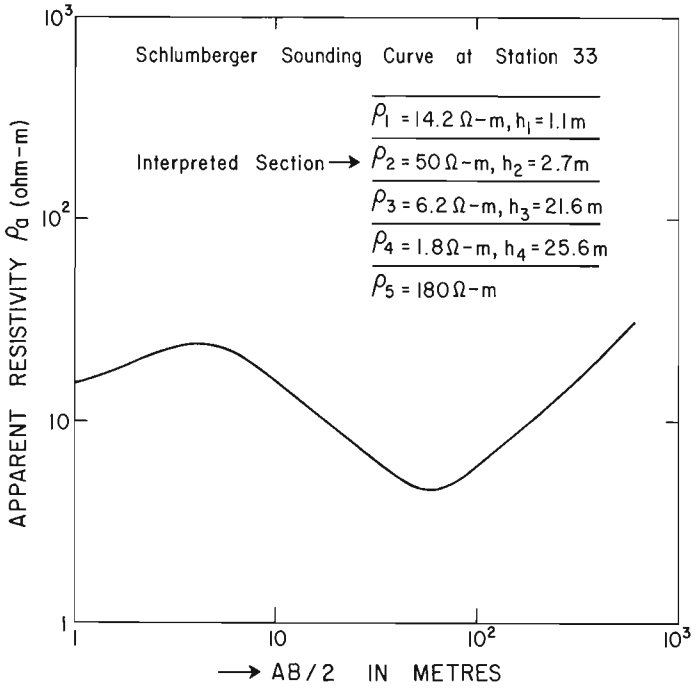

Figure 1.6. Schlumberger resistivity sounding curve at station 33.

Geology of the Area

The geological setting for the area has been described in detail by Wilson (1946). The bedrock in the area is similar to that described for the Ottawa area which consists of Precambrian granitic rocks and Grenville type metasedimentary gneisses and crystalline limestones. These rocks, in general, are overlain by sandstone, dolomitic sandstone, shale and limestone horizons of Ordovician age with a maximum thickness of 670 m in the area (Wilson, 1946). The Ordovician sediments are well indurated and have high resistivity values comparable to the Precambrian rocks. It is, therefore, difficult to differentiate the Ordovician sediments from the Precambrian rocks on the basis of resistivity data only.

An immense interval elapsed between the deposition of the Ordovician sediments and the beginning of the glacial period. The area was then invaded by the Champlain Sea which deposited sand and marine clay which are very conductive. The thickness of the Champlain clay deposits ranges from zero to about 100 m. After the withdrawal of the Champlain Sea, fresh water river currents deposited alluvium in several areas. The erosion of the older rocks also led to the deposition of fresh water clay and lacustrine marls which do not have very high conductivity values, in contrast to the highly conductive Champlain clay beds.

The bedrock strata have irregular dip and strike and are broken by normal faults. The Quaternary clay and sand beds lying over them are generally subhorizontal. The bedrock is quite shallow in several places and is even exposed north of Alfred and in southern part of the survey area.

It should be pointed out that the interpretation of resistivity sounding data over an area does not provide unique answers as to the type of geological material at depth. This is because the inversion of sounding data solves the electric problem but not necessarily the geologic problem, because given rock types and geological formations are not associated with definite resistivities except in a broad and general manner. In this area, it is generally acknowledged that much of the very low resistivity material (1-4 ohm·m) is conductive sea clays. The soil and alluvium layers lying near the surface have resistivity values varying from 20 to 50 ohm·m. High resistivity materials (resistivities greater than 500 ohm·m) usually indicate the presence of resistive bedrock. Therefore, interpretation of resistivity sounding data over this area which will yield the thickness and resistivity values of discrete subsurface layers should indicate the presence and extent of conductive clay layers and resistive sandstone or dolomitic sandstone beds along with drift thickness values at each sounding station.

Direct Current Resistivity Sounding

One of the main purposes of this study was to see whether geophysical, especially electrical methods may be used to map the bedrock and overlying Quaternary sediments in the area. Direct current resistivity sounding technique using the Schlumberger array was chosen for the simplicity of field operations and easy availability of required instrumentation and relatively great depth of investigation that may be achieved with this system. The rest of this section will be devoted to a discussion of the various facets of the direct current Schlumberger resistivity method of sounding.

Theory

The theory of direct current (henceforth abbreviated to d.c.) resistivity sounding methods are well known (Bhattacharya and Patra, 1968) and so, only an outline of the theory of the method will be presented. Figure 1.2 shows the arrangement of the electrodes for the symmetrical Schlumberger array. A and B are two current electrodes which put in currents of strength +I and -I into a layered ground, the resistivities and the thicknesses of the layers being $\rho_1, \rho_2, \rho_3 \ldots . \rho_n$ and $h_1, h_2, h_3, \ldots . h_{n-1}$ respectively. The centre point of the array is indicated by 0. The location of the two potential electrodes are shown by M and N and these are placed symmetrically with respect to the centre of the array. If L and ℓ are the current and the potential electrode separations, respectively, the potential difference Δv measured between M and N in the case of a homogeneous ground may be shown to be equal to

$$\Delta v = \frac{I\rho}{2\pi}\left[\frac{4}{L-\ell} - \frac{4}{L+\ell}\right] \qquad \ldots.(1)$$

where ρ is the resistivity of the homogeneous ground.

or

$$\rho = \frac{\pi}{4} \cdot \frac{\Delta v}{I} \cdot \frac{(L^2-\ell^2)}{\ell} \qquad \ldots.(2)$$

When the ground is layered as shown in Figure 1.2, the measured resistivity ρ shown in equation (2) will be a function of the layer parameters $\rho_1, \rho_2, \rho_3 \ldots . \rho_n$, $h_1, h_2, \ldots . h_{n-1}$ and the electrode separations L and ℓ. Hence, when the ground is heterogeneous, the resistivity measured in the field with the help of equation (2) is called the apparent resistivity and indicated by ρ_a. For the Schlumberger array, L is at least five times greater than ℓ. Under such conditions

$$\rho_a \simeq \frac{\pi}{4} \cdot L^2 \cdot \frac{E}{I} \qquad \ldots.(3)$$

where E is the electric intensity at the point 0 given by $E = \Delta v/\ell$. Hence, this array is also known as the gradient arrangement.

The Schlumberger array was used in the area for operational convenience (since the potential electrodes do not have to be moved every time the current electrodes change position) as well as for the fact that interpretation techniques and theoretical master curves are simpler and more readily available than for other electrode arrays.

Resistivity Sounding Curves

The field data obtained with the Schlumberger array are normally plotted on double-log graph sheets with a modulus of 62.5 mm with apparent resistivity values in ohm·meters along the ordinate and the parameter AB/2 or L/2 along the abscissa. When the electrode separation L is small, the current lines are confined to shallow depths. Hence, apparent resistivity values measured with very small L values reflect the resistivity of the top layer. As the electrode separation L increases, the current lines penetrate deeper layers. Hence, the apparent resistivity values are influenced more and more by the resistivities of the deeper layers as the current electrode separation L is increased. When the separation is very large, the influence of the top layers is much less since the current lines are mostly confined to the deeper strata and so the apparent resistivity value is mostly affected by these layers.

Figure 1.3 shows the theoretical master chart for a two-layer ground on a double-log paper. The dimensionless parameter ρ_a/ρ_1 is plotted along the ordinate and the parameter $L/2h_1$ along the abscissa, where ρ_1 and h_1 are the resistivity and the thickness of the top layer. The top set is for the case when ρ_2/ρ_1 is greater than 1 and the bottom set is for the case when ρ_2/ρ_1 is less than 1. At low values of L, ρ_a values approach ρ_1 and at large values of L, the ρ_a values approach the resistivity of the bottom layer ρ_2.

There are four basic types of three layer sounding curves for different combinations of the resistivity values ρ_1, ρ_2 and ρ_3 as shown in Figure 1.4. When $\rho_1 < \rho_2 < \rho_3$ the

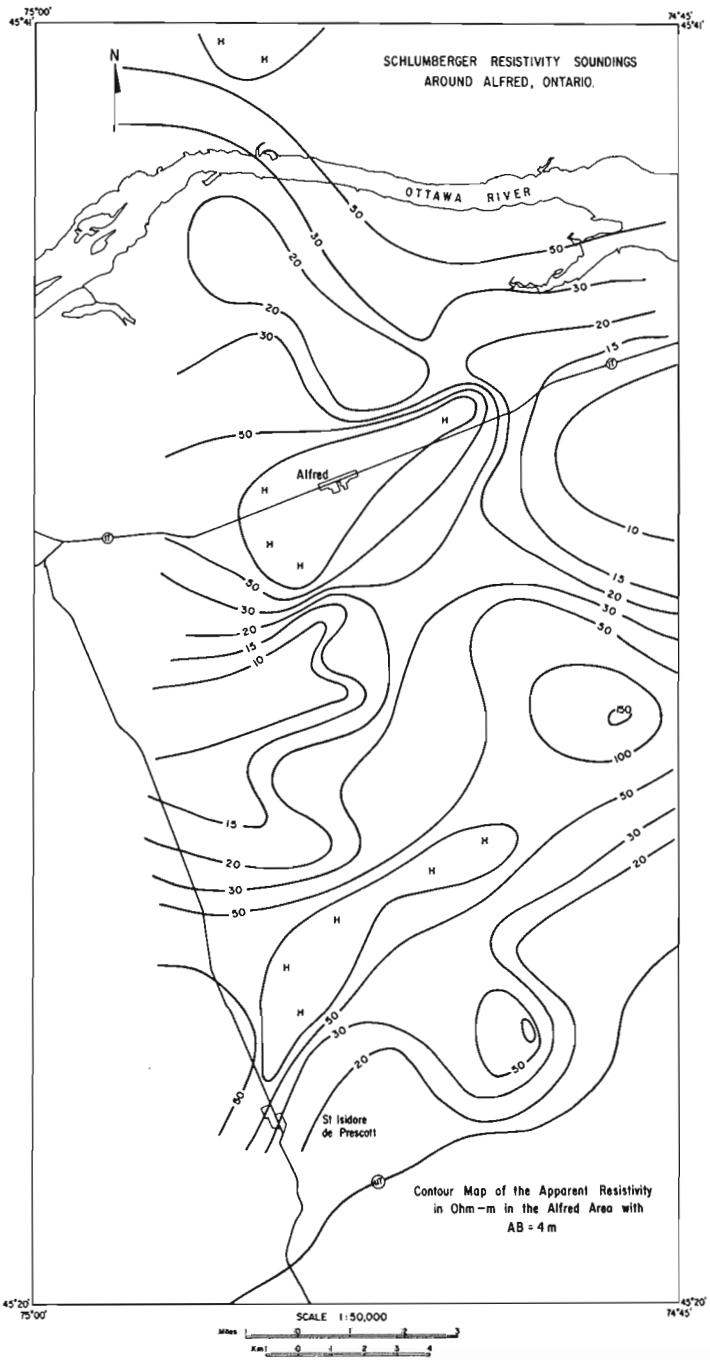

Figure 1.7. Equiresistivity map of the area with current electrode separation of 4 m.

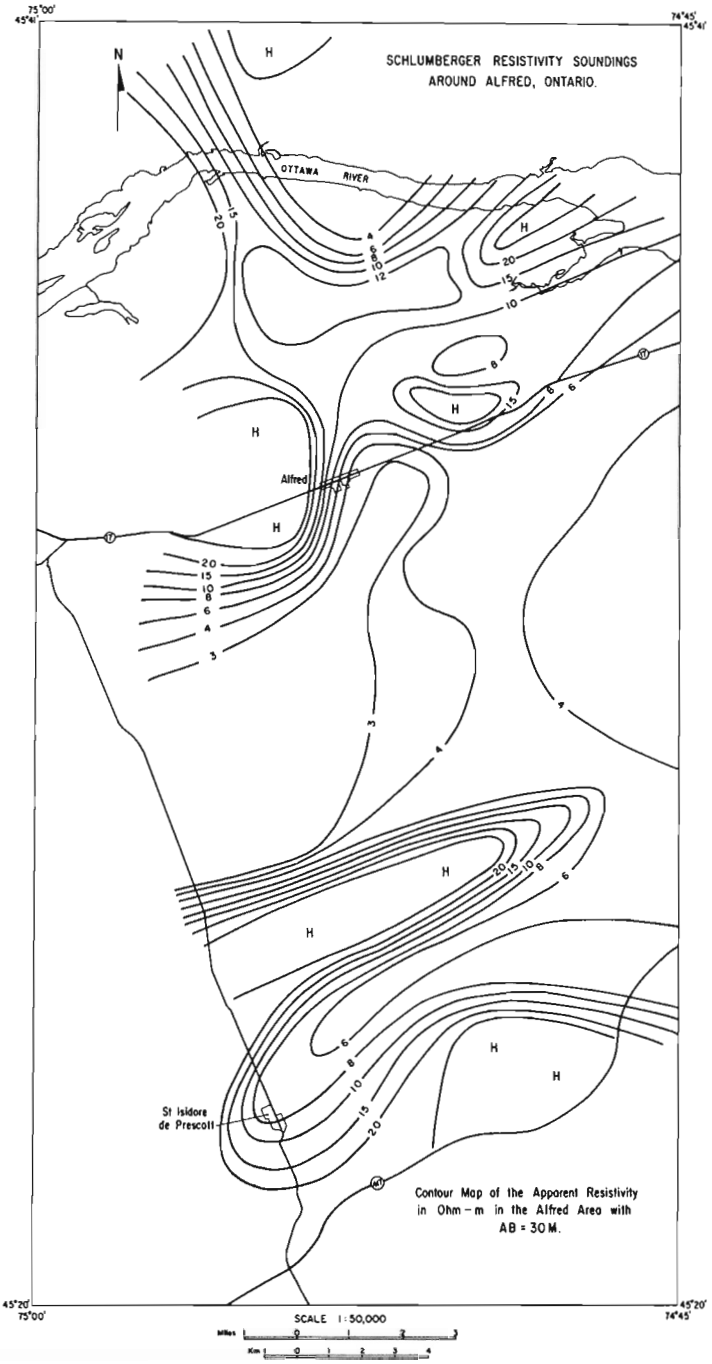

Figure 1.8. Equiresistivity map of the area with current electrode separation of 30 m.

curve is called double ascending or A type curve as shown in Figure 1.4a. When the third layer is less resistive than the second, ie., $\rho_1 < \rho_2 > \rho_3$ the curve is called K type as shown in Figure 1.4a. For the case when $\rho_1 > \rho_2 < \rho_3$, the curve is called H type and when $\rho_1 > \rho_2 > \rho_3$, the curve is called the Q type as shown in Figure 1.4b. When the number of layers is greater than 3, the curve shapes are combinations of the four basic types shown in Figure 1.4. For example, for the case of $\rho_1 > \rho_2 < \rho_3 > \rho_4$, the curve will be called HK type since its first and last parts will resemble H and K types, respectively.

For the Alfred-Hawkesbury area, most of the sounding curves resemble the H type curve, ie., there is a conductive layer in the middle sandwiched between two resistive media. However, K type curves are also common specially when the conducting Champlain clay beds are absent or very thin and the bottom layer is, for example, a water-saturated sandstone bed. However, the sounding curves are rarely as simple as three layer cases. At most sounding stations, the ground has at least four and in several places as many as seven distinct layers.

Field Equipment Used

A McPhar Resistivity System (Model R201) was used for conducting the resistivity soundings. The power supply consisted of ten 45 volt dry cell batteries (Eveready # 482) that could be connected in various ways of series and parallel combinations. The cells thus provided maximum voltage of 450 volts and 70 mA current or 90 volts with a maximum current of 220 mA. The d.c. voltage was transformed into square waves with a frequency of 0.3125 Hz by the use of Mercury relays. A salford (Salford Selectest Model K) meter is used to measure the current. The whole power supply including the cells is mounted on a portable backpack and weighs about 69 lbs.

The potential differences were measured with a specially designed voltmeter. It consisted of amplifiers, filters, rectifiers and a d.c. meter. Its maximum sensitivity was 100 microvolts full scale. Its accuracy was in the order of 1 per cent for full scale deflection, but less in the lower part of the scale. The receiver is battery operated and weighs about 20 lbs.

The cables used for connecting the current and potential electrodes to the instruments were lightweight, well insulated and could be wound on reels mechanically. The current and potential electrodes used during the field work were plain steel stakes. The voltage from the power supply was adjusted till a reasonable voltage could be recorded between the potential electrodes. The current flowing into the ground was read off the ammeter attached to the power supply unit.

Field Procedure

Most of the soundings were performed along roads in order to avoid carrying the instruments over long distances. During the survey, the maximum separation of the current electrodes was 1200 m. The vehicle carrying the instruments was driven to the central spot of the sounding array for unloading the instruments. The vehicle was used to unwind the current cables on both sides of the truck and two men were put in charge of the two current electrodes while a third man at the sounding point took care of the instruments and recorded the data. Measurements were first made with the largest separation and subsequent readings were taken for closer electrode separations using distance markers in the cable itself. Two and half to three hours were normally needed to complete one set of soundings.

The main source of error in the field data was the parasitic power line signals at 60 Hz. Although the bandpass of the receiver was quite narrow, a signal as high as 50 microvolt could be picked up between the potential electrodes 40 m apart due to the power line noise. Such noises were removed by using a parallel T filter (Collett and Ahrens, 1964). For parasitic signals of 10 microvolts or less, the filter was not used and the subtraction of the initial recording from the final reading after the injection of the 0.3125 Hz current removed the noise. It should be noted that such a filter should be designed to meet the specific characteristics of the receiver unit.

Interpretation Procedure

A total of 62 soundings were carried out in the area. The location of the sounding stations is indicated in Figure 1.5. The field data were interpreted by using two different approaches to the layered earth model interpretation. Initially, the data were interpreted using the graphical auxiliary point method of curve matching (Zohdy, 1965; Bhattacharya and Patra, 1968). To use this method, the field data were plotted on semi-transparent, double log graph sheets with modulus of 62.5 mm. Using published two-, three-, and four-layer master curves and the auxiliary point charts (Orellana and Mooney, 1966; Bhattacharya and Patra, 1968), the curves are interpreted in terms of the resistivity and thickness of a finite number of horizontal layers. It may be noted here that some smoothing of the field curve may be necessary before the interpretation is made. The steps involved in the graphical technique of interpreting sounding curves has been described in detail by Bhattacharya and Patra (1968). Because the geology of the area is rather simple, the subsurface being composed of a number of quasi-parallel horizontal layers, the method works quite well in this area.

The data were also interpreted using a computer-assisted interactive inversion program modelled after the inversion program of Zohdy (1975). Basically, this consists of getting an automatic inversion of data on a computer in terms of a number of layers with an acceptable root mean square error. An attempt is then made to fit the observed data to several plausible layered models with the help of an interactive terminal until a satisfactory model is obtained that is geologically acceptable and has a very low root mean square error compared with the observed data. Normally, this means considering four to eight models before an acceptable model is found. In general, the agreements between the models obtained by graphical and interactive means are good although the number of layers obtained from computer inversion are generally higher. In case of any divergence between the two interpretations, the results obtained by computer assisted interactive method is considered to be more accurate, since there is far greater flexibility in modeling by this method. It may be mentioned again that before attempting the computer inversion some smoothing of the data may be necessary in order to avoid wastage of computer time.

Results

As mentioned earlier, most of the sounding curves in the area look like H type curves (see Fig. 4b) although, at most locations, more than three layers are present (there being three distinct groups of layers). The top layers are composed of soil and till and hence not very conductive. Thus, for small current electrode separations, the apparent resistivity values are generally about 20-30 ohm·m reflecting the resistivity of this top cover. Beneath this soil cover lie the conductive Champlain Sea clay layers which produce sharply lower values of apparent resistivity as the current

electrode separation is increased. When the electrode separation is increased even further, the highly resistive bedrock begins to affect the apparent resistivity values resulting in sharply increased apparent resistivity values. It may be shown theoretically that even when the resistivity contrasts between two layers is infinitely large, the slope of the apparent resistivity curve cannot exceed 45 degrees. In this area, since the bedrock is extremely resistive and the clay layers very conductive, the resistivity contrast is extremely large, and hence, the last part of the apparent resistivity plot frequently rises with a 45 degree slope. In fact, at some locations, the slope even exceeds 45 degrees which, although theoretically impossible for layered ground, may be caused by the presence of lateral inhomogeneities.

Figure 1.6 illustrates a typical Schlumberger resistivity sounding curve obtained in the area. The curve was obtained over sounding station no. 33 (see Fig. 1.5) north of Alfred. From a quick glance at the curve, it is clear that there are at least four distinct layers beneath the station with resistivities of ρ_1, ρ_2, ρ_3 and ρ_4 such that $\rho_1 < \rho_2 > \rho_3 < \rho_4$. Thus the curve may be called a KH type since the first and last segments of the curve resemble K and H types respectively. However, when one begins to interpret the curve, it becomes clear that the descending section of the curve cannot be interpreted as being caused by one layer. Rather, it becomes necessary to put two layers with resistivities of 6.2 and 1.8 ohm·m in order to interpret the descending part of the curve satisfactorily. The interpretation for the sounding curve in terms of the thicknesses and resistivities of the various layers is also indicated in the diagram.

Figure 1.7 shows a plot of the equiresistivity contours of the area in ohm·metres for a small current electrode separation of 4 m. Since the energizing currents are confined

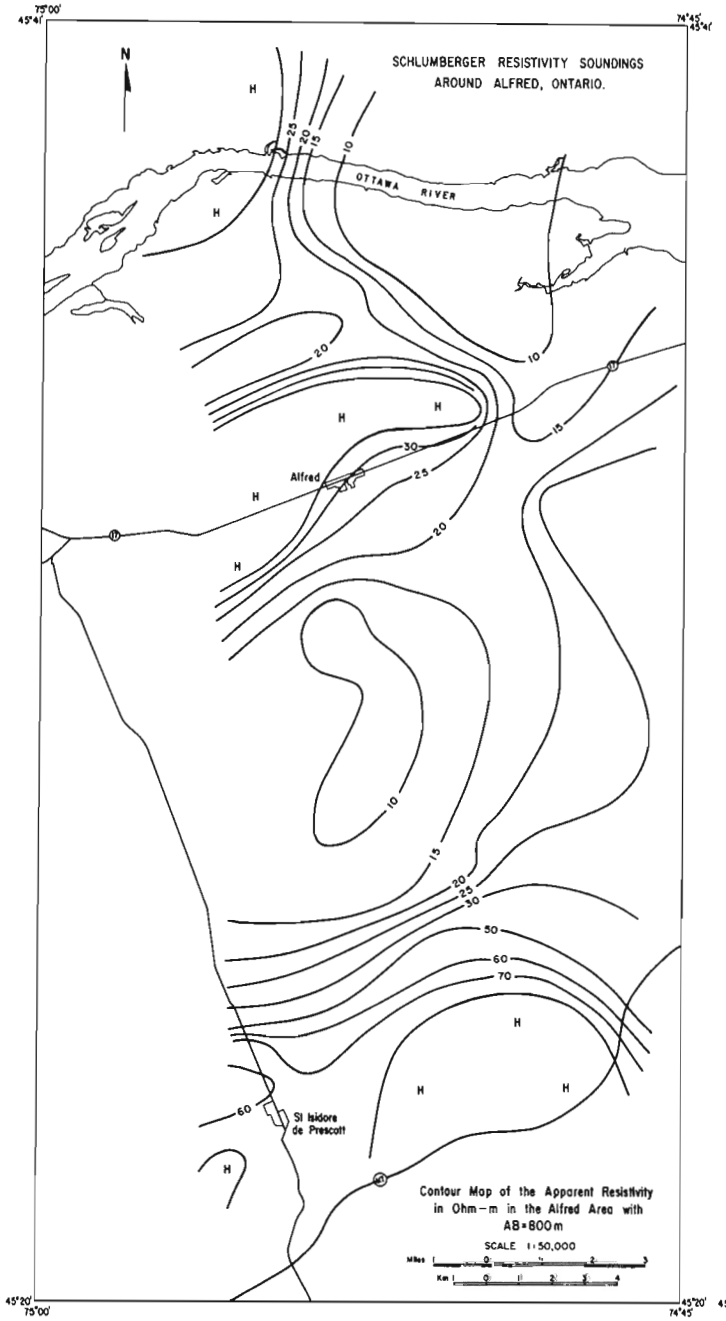

Figure 1.9. *Equiresistivity map of the area with current electrode separation of 800 m.*

Figure 1.10. *Contour map of the depths to the conductive clay layer in metres.*

close to the surface at such a small electrode separation, the plot reflects the variation of the resistivity of the upper layers of the ground. In this diagram, two areas, one around Alfred, and the other in the southern part (just north of St. Isidore de Prescott) are characterized by high apparent resistivity values and are indicated by the symbol H. In those areas, the apparent resistivities are in excess of 150 ohm·m which might be either due to the presence of dry sand or to exposure of bedrocks in those areas. There are also a few regions in the northern, southern, and southeastern parts of the map area where the apparent resistivity values reach 50 to 100 ohm·m, indicating areas where the surface materials are quite resistive and where conducting clay layers are deep or nonexistent. Low resistivity ground (10-20 ohm·m) occurs in several places which would indicate possible regions where clay layers are near the surface or where the resistive sand or bedrock may be missing.

The shapes of the equiresistivity contours are quite different when a similar plot is made for a current electrode separation of 30 m as shown in Figure 1.8. With the increase in current electrode separation, the currents are penetrating more deeply into the ground. Therefore, the effect of the conducting clay beds below the soil cover is having a greater influence. The high resistivity around Alfred shown in Figure 1.7 is split into two separate highs east and west of Alfred. Additional resistivity highs appear in the extreme south and northeast of the Alfred area which possibly indicate areas where the bedrock is quite shallow and covered with thin layers of soil. In several regions of the map area, the apparent resistivity values of the ground are 3 ohm·m or less indicating the presence of conducting clay in these regions. The high resistivity areas indicated by 'H' generally agree with the location of the bedrock exposures as shown in Figure 1.5. The area south of Alfred seems to have extensive clay deposits with the apparent resistivity values in the 3-4 ohm·m range. The resistivity values north of Alfred near Ottawa River are quite low indicating the presence of clay beds. Interestingly, Figure 1.7 shows the same area as having high apparent resistivity values. The clay beds here are generally covered by dry sand beds which are quite resistive. These sand beds would tend to give the large resistivity response for the short electrode spread as is the case for Figure 1.7.

Figure 1.9 displays the equiresistivity plot for a current electrode separation of 800 m. With such a large current electrode separation, most current lines are penetrating deep into the ground and are thus being affected most by the high resistivity of the bedrock. The region south of Alfred, which exhibited extremely low resistivity values in Figure 1.8, still indicates low values but the absolute values of apparent resistivity are higher because of the influence of the bedrock. The high in apparent resistivity north of St. Isidore de Prescott has become only moderately high possibly because of the presence of some low resistivity material at depth. The same is true in the northeastern corner of the map area where a high has been replaced by a moderate resistivity of 10 ohm·m. The two highs east and west of Alfred have merged again as in Figure 1.7 The area east of St. Isidore de Prescott has remained a high resistivity area in all three diagrams possibly indicating that the bedrock extends all the way up to the surface. Surface examination of the rock types confirms this. The area near Ottawa River exhibits moderate resistivity values, the low values of Figure 1.8 being increased due to the influence of the resistive bedrock.

Figures 1.7, 1.8 and 1.9 were plotted using raw field data without any interpretation and hence are somewhat qualitative. The next few diagrams present the results of the interpretations carried out on the field data. Figure 1.10 shows a contour map of the depths to the conductive clay layer in metres in the area. The area north of Alfred exhibits a basin-like structure with the top of the clay layers being at a maximum depth of 25 m from the surface in the central area but the depths decrease sharply both north and south of it. The apparent resistivity contours with a current electrode separation of 30 m shows a similar trend (Fig. 1.8) in that region. It is clear that if the clay is at a greater depth as in the centre of the basin, the apparent resistivity values would be higher at the centre with lows on both sides ot it. This is precisely what is seen in Figure 1.8. North of Alfred, near the Ottawa River, the clay layers are shallow. Hence, this area should show as a low resistivity ground as is seen in the apparent resistivity contours in Figure 1.8. The hatched areas in Figure 1.10 indicate places where clay layers are not present and these regions match, in general, with areas of high resistivity shown in Figure 1.8. A cross-sectional profile for the area has been plotted along the line AB shown in Figure 1.10 and will be discussed later in the paper.

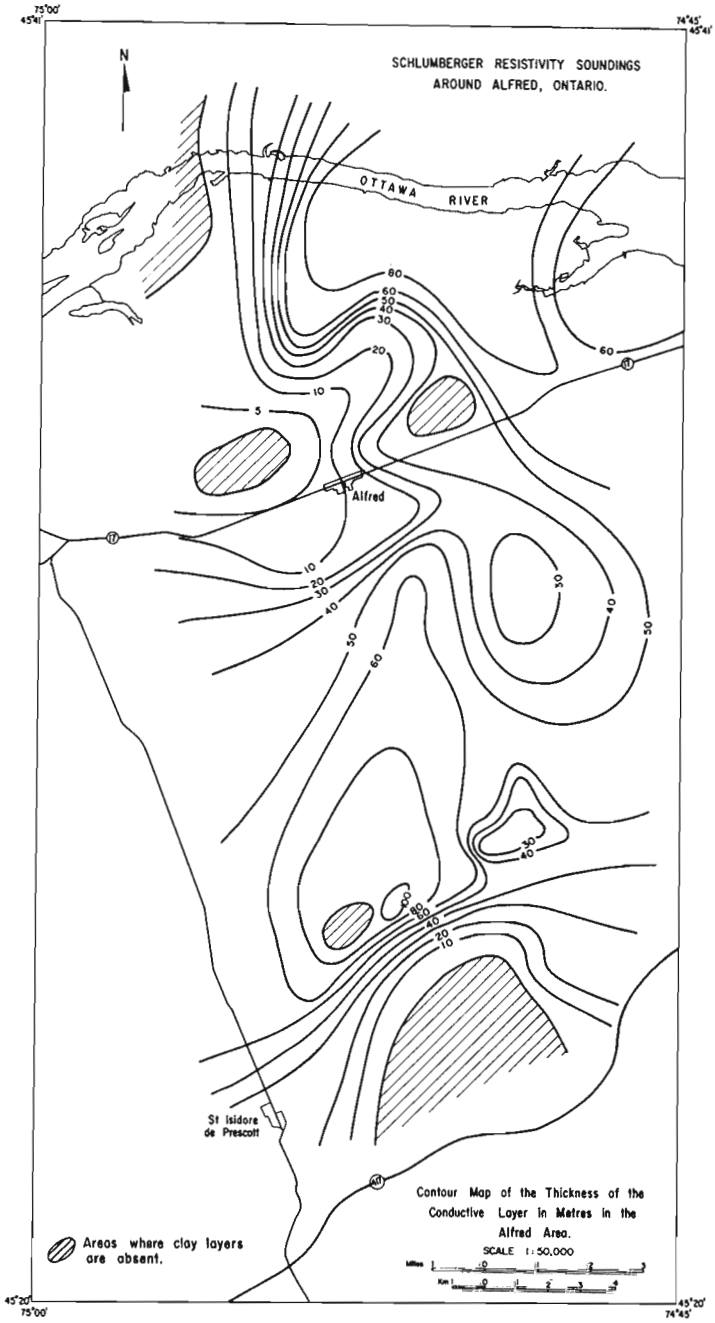

Figure 1.11. *Contour map of the thickness of the conductive clay layer in metres.*

Figure 1.11 illustrates a contour map with the thickness of the clay layer in metres. The conductive clay layers are thickest about 8 km northeast of St. Isidore de Prescott (100 m) and north of Alfred near Ottawa River (over 80 m). The clay layers are fairly thick south of Alfred and continue the gradual increase in thickness toward south until about 100 m. Beyond that, the clay layers decrease in thickness. The clay thickness around Alfred is low (10 m). The hatched regions in the map again indicate areas where clay layers are absent. In general, such areas are surrounded by regions with thin clay layers except in the region northeast of St. Isidore de Prescott where the maximum clay thickness zone is right next to a clayless area. This could have been caused by uneven bedrock topography when the clay deposition took place.

When conductors of high conductivity and limited thickness are encountered in the course of geophysical exploration, their effects are generally described in terms of their thickness-conductivity products or the conductance values. It was noted that the resistivity of the clay layers varied from 1 to 4 ohm·m at different locations in the area and their thickness values varied from zero to 100 m. Since both thickness and conductivity parameters varied so widely in the area, it was felt that the thickness-conductivity product of the clay layers would provide a useful parameter for understanding the contribution of the clay layers to the resistivity data. Figure 1.12 shows the contoured plot of the conductance parameter (thickness conductivity product) in Siemens over the area. This diagram is qualitatively somewhat similar to Figure 1.11 which shows the thickness of the clay layers. The highest conductance values are near the

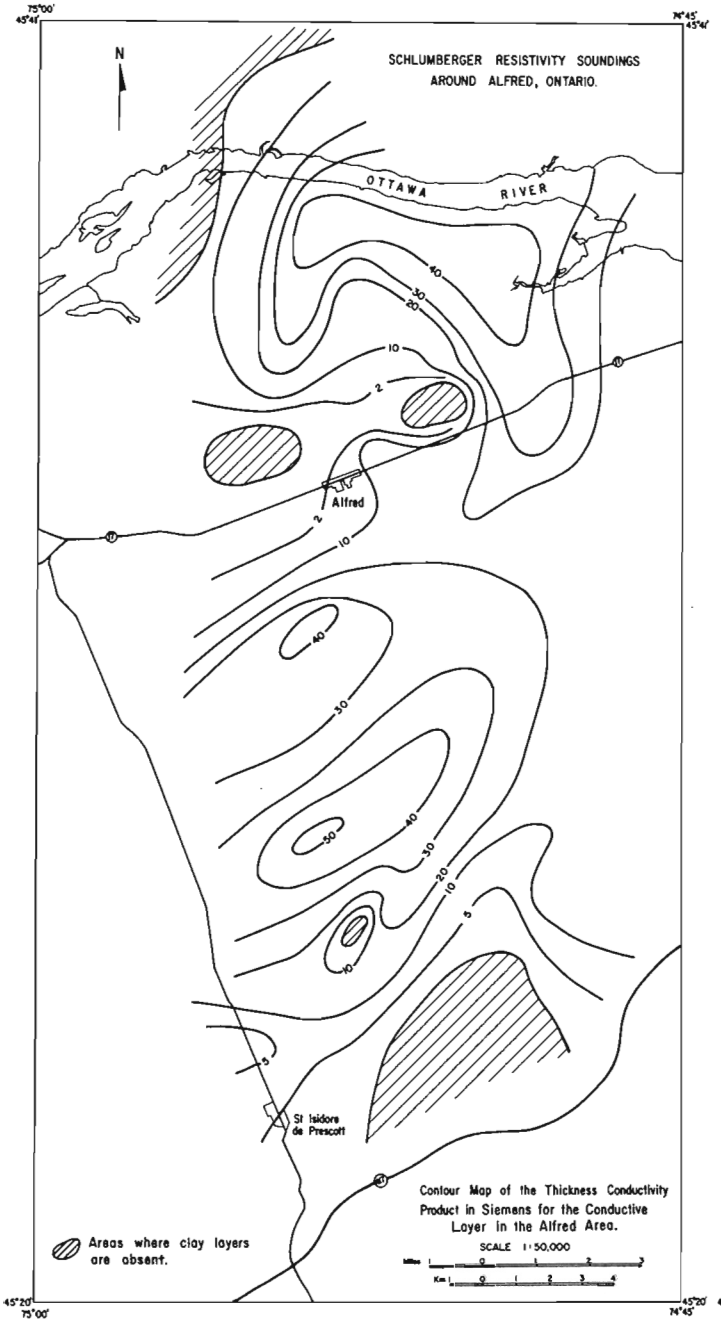

Figure 1.12. *Plot of the conductance of the clay layers in Siemens in the Alfred area.*

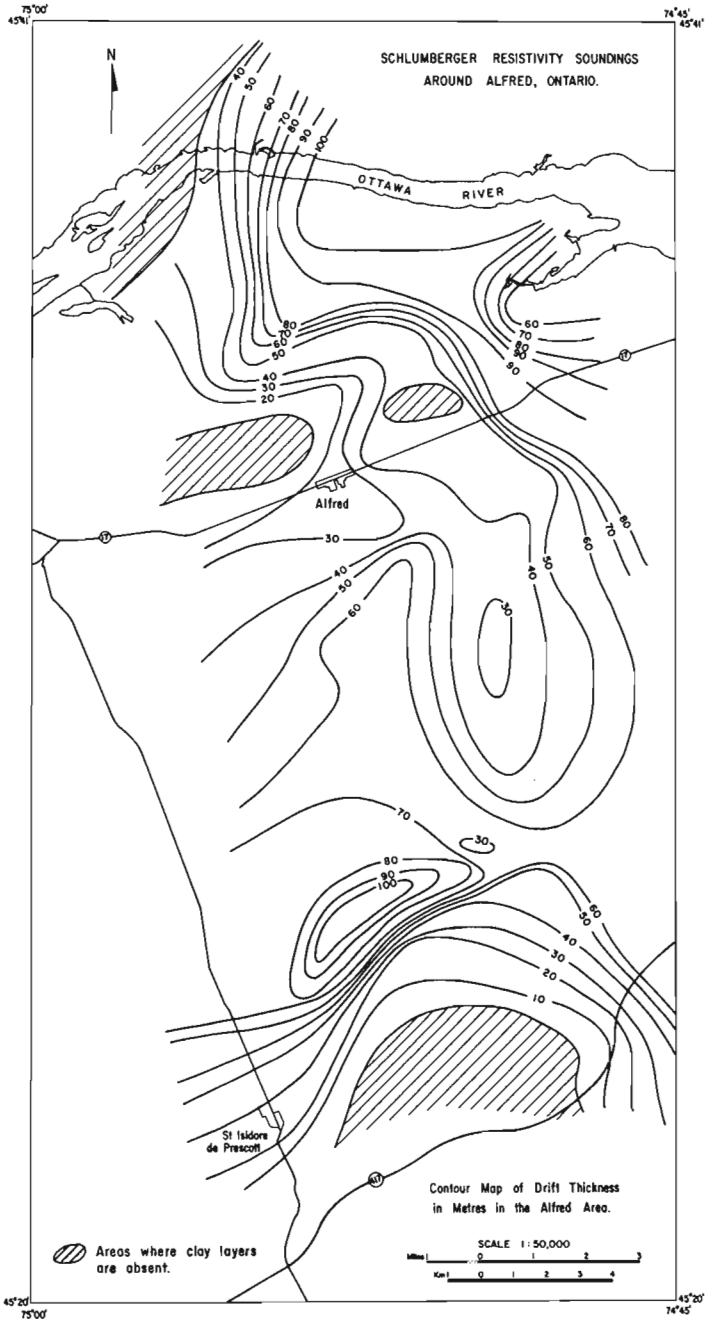

Figure 1.13. *Drift thickness map of the area obtained from resistivity soundings.*

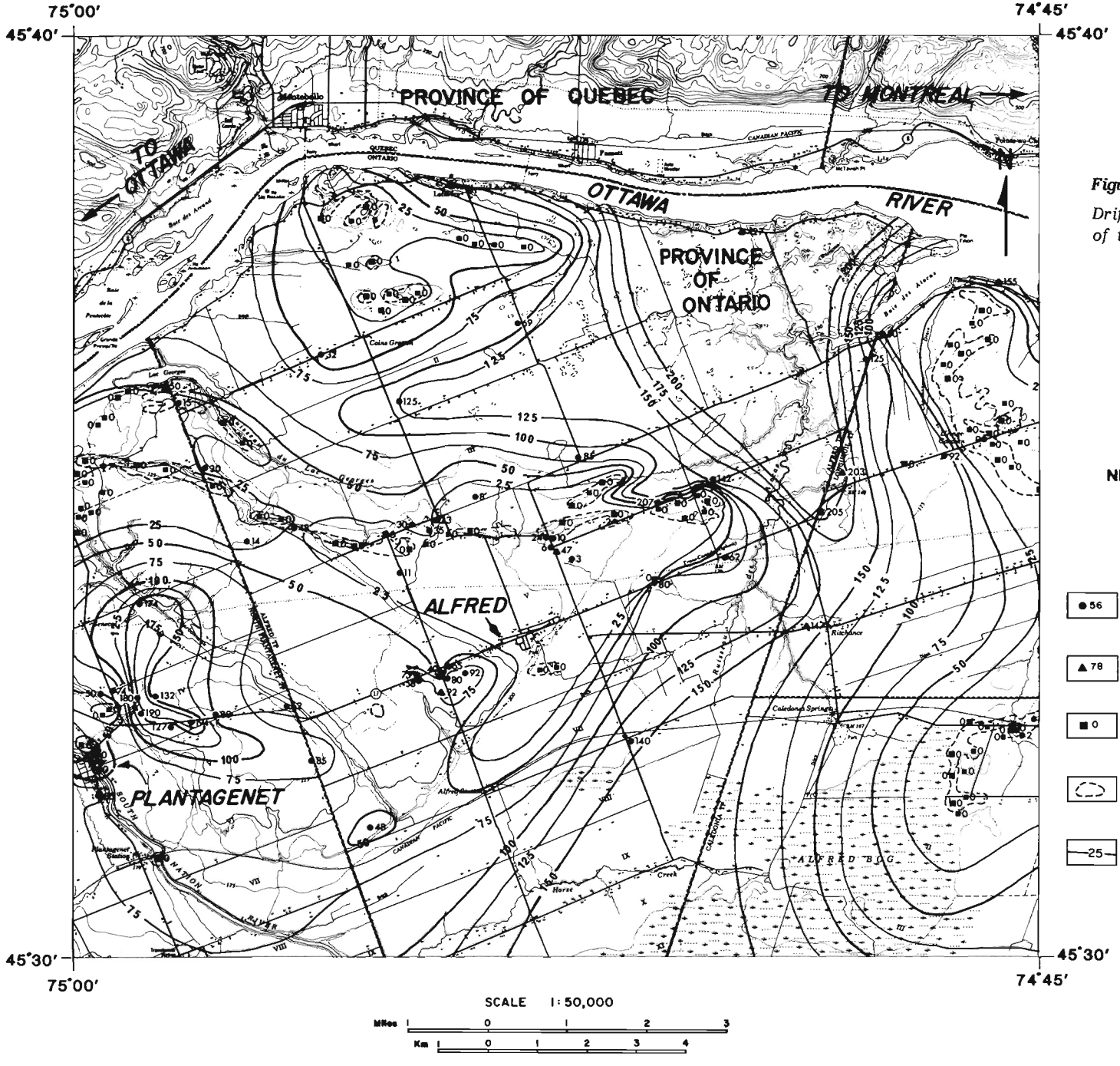

Figure 1.14

Drift thickness map of the northern half of the area (from Gwyn and Thibault, 1973).

NB. DRIFT THICKNESS ARE IN FEET

SYMBOLS

- ●56 — Water well which reached bedrock with drift thickness
- ▲78 — Water well which does not reach bedrock with minimum drift thickness
- ■0 — Small bedrock outcrop
- Area of bedrock outcrop
- —25— Drift thickness contour

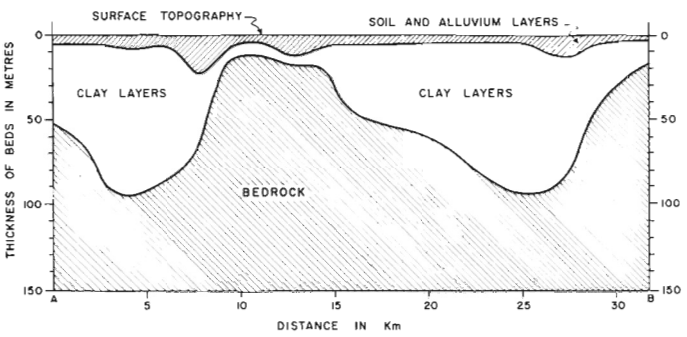

Figure 1.15. Cross-sectional profile along the line AB based on Schlumberger sounding in the area.

centre of the map somewhat midway between Alfred and St. Isidore de Prescott, where the conductance reaches 50 Siemens. North of Alfred, near the Ottawa River, the conductance values rise to 40 Siemens. The conductance values around Alfred and St. Isidore de Prescott vary from 2 to 10 Siemens. Since the effect of a clay layer on the resistivity values recorded at any place at the surface depends on its conductance value and the depth of the layer, it is clear that the clay layers south of Alfred will have a greater influence on the resistivity values than those north of it, where the depths are greater. An examination of Figure 1.8 confirms this. As before, the hatched areas indicate the regions where clay layers are not present.

Figure 1.13 shows a plot of the drift thickness in the area in metres obtained from resistivity sounding. The drift thickness values are largest about 8 km northeast of St. Isidore de Prescott and about 7 km north of Alfred where they are 100 m or more. The drift thickness over Alfred and St. Isidore de Prescott have values between 20 and 30 m. The thickness increases north and south of Alfred with the gradient being larger on the northern side. The drift map shows a few local low values which indicate the possible existence of local breaks in bedrock topography. The elliptical structure northeast of St. Isidore de Prescott indicates a deep basin-like structure with steep slopes. The hatched areas in the map indicate areas where the soundings could not be interpreted in terms of layered structure and possibly indicate bedrock covered with soil. This drift thickness map may be compared with a drift thickness map published by the Ontario Division of Mines (Gwyn and Thibault, 1973) for the northern half of our map area. Figure 1.14 shows the drift thickness map (Gwyn and Thibault, 1973) based on data from water wells, some of which do not reach the bedrock. It should be noted that the contour values in the map are given in feet and not metres. The general agreement between the two maps for the north side is quite good. However, the thickness values from the resistivity sounding data are generally somewhat greater. This may be explained by (a) the fact that thickness data in Figure 1.14 are based on information provided from wells some of which did not reach the bedrock and hence they are minimum values, and (b) the distribution of the wells is very irregular, there being no wells in several regions thus forcing the authors (Gwyn and Thibault) to be somewhat subjective in the plotting of thickness contours.

A cross-sectional profile of the area along the line AB running north-south (see Fig. 1.10) has been plotted in Figure 1.15. The line running just west of Alfred passes through areas with varying thicknesses of soil and the clay layers. As interpreted earlier from Figures 1.10, 1.11, and 1.13, the area has two basin-like depressions in the bedrock north and south of Alfred, the gradients of the basin walls being sharper on the north side. The soil and alluvium layers do not exhibit great variation in their thickness values in the area, their average thickness being of the order of 5-10 m. Only at three locations, does the thickness of the soil cover exceed 10 m. Generally speaking, the drift thicknesses along the northern end of line AB from Figure 1.15 agree well with the drift thickness values that would be obtained if a similar section were drawn in Figure 1.14 (Gwyn and Thibault, 1973).

Concluding Remarks

Sixty-two Schlumberger resistivity soundings were performed over the Alfred-Hawkesbury area for the purpose of determining the overburden characteristics of the area. The area presents an attractive site for the testing and use of electrical mapping systems. The geology of the area is relatively simple with semi-horizontal layers of sand, clay and limestones. As a result, several d.c. and electromagnetic methods have been tested to determine the overburden and bedrock characteristics in the area. From a geophysical point of view, there are mainly three dominant layers present: 1) The top layer consisting of soil, sand and unconsolidated sediments has thickness values ranging from zero to 25 m, the thickest occurring north of Alfred. The resistivity of this layer varies from 20 to 50 ohm·m. 2) Beneath them lie extremely conductive saline Champlain clay deposits whose thickness and resistivity values vary from zero to 100 m and 1 to 4 ohm·m, respectively. 3) Beneath the clay deposits lie resistive Paleozoic rocks comprising limestone, shale and sandstone beds. The resistivity contrasts between these Paleozoic formations and the underlying Precambrian rocks is not great enough to be detectable by resistivity measurements. The top of the bedrock surface is, in general, not smooth and a study of the drift thickness contours yield evidence of the roughness of the bedrock topography. Information about the depth and extent of clay deposits as well as the depth and extent of water bearing horizons have use in agriculture and in groundwater exploration. Information which can lead to the detection of highly resistive sand and gravel deposits is useful to the construction industry.

The main purpose for this study was to see if d.c. resistivity soundings could be used successfully for geological mapping of the different horizons in the area. This was achieved, since the strata in the area have distinct resistivity contrasts and interpretations could be performed in terms of a number of distinct layers of finite resistivity and thickness. The drift thickness map provides a concept of the bedrock topography and the conductance map provides a concept of the extent of the clay layers. A comparison of the d.c. sounding interpretations with known geological information indicates the validity of the interpretations made in the paper.

References

Andrieux, P.
1968: Electrical resistivity survey of the surficial geology in the Alfred area, Ontario; Unpublished report.

Becker, A. and Roy, J.
1977: Interpretation of frequency domain airborne electromagnetic data; Unpublished report prepared for Geological Survey of Canada by IREM-MERI, Montreal, available as Geological Survey of Canada Open File 605-Part II.

Bhattacharya, P.K. and Patra, H.P.
1968: Direct current geoelectric sounding; Elsevier Publishing Company, 135 p.

Collett, L.S. and Ahrens, R.H.
1964: Frequency rejection filter for use in d.c. resistivity surveys; Geological Survey of Canada, Paper 64-41, 10 p.

Dyck, A.V., Becker, A., and Collett, L.S.
1974: Surficial conductivity mapping with the airborne INPUT system; Canadian Institute of Mining and Metallurgy Bulletin, v. 77, no. 4, p. 1-6.

Ells, R.W.
1898: Sands and clays of the Ottawa basin; Geological Society of America Bulletin, v. 9, p. 211-222.

Gadd, N.R.
1963: Surficial geology of the Ottawa map-area, Ontario and Quebec, 31 G/5; Geological Survey of Canada, Paper 62-16, 4 p.

Giroux, N.J.
1896: Report of field work in the St. Lawrence Valley, Ontario and Quebec; Geological Survey of Canada, Annual Report 8, Pt. A, p. 68-74.

Gwyn, Q.H.J. and Thibault, J.J.L.
1973: Drift thickness of the Hawkesbury-Lachute area, Southern Ontario; Ontario Division of Mines, Preliminary Map P. 909, Drift thickness Series, Scale 1:50,000. Geology 1973.

1975: Quaternary geology of the Hawkesbury-Lachute area, Southern Ontario; Ontario Division of Mines, Preliminary Map P. 1010, Geology Series, Scale 1:50,000. Geology 1974.

Johnston, W.A.
1917: Pleistocene and recent deposits in the vicinity of Ottawa, with a description of the soils; Geological Survey of Canada, Memoir 101.

Murray, A.
1852: Report on the geology of the region between the Ottawa, St. Lawrence and Rideau rivers; Geological Survey of Canada, Report of Progress 1851-52, p. 57-91.

Orellana, E. and Mooney, H.M.
1966: Master tables and curves for vertical electric sounding over layered structures; Interscienia, Madrid, 150 p.

Sinha, A.K.
1976: Interpretation of Tridem airborne EM data; in Report of Activities, Part C, Geological Survey of Canada, Paper 76-1C, p. 221-224.

1979: Maxiprobe EMR-16: A new wide-band multi-frequency ground EM system; in Current Research, Part B, Geological Survey of Canada, Paper 79-1B, p. 23-26.

1980: Electromagnetic resistivity mapping of the area around Alfred, Ontario, with Geonics EM 34 system; in Current Research, Part A, Geological Survey of Canada, Paper 80-1A, p. 293-300.

Wilson, A.E.
1946: Geology of the Ottawa-St. Lawrnece lowland, Ontario and Quebec; Geological Survey of Canada, Memoir 241, 66 p.

Zohdy, A.A.R.
1965: The auxiliary point method of electrical sounding interpretation and its relationship to the Dar Zarrouk parameters; Geophysics, v. 30, no. 4, p. 644-660.

1975: Automatic interpretation of Schlumberger sounding curves, using modified Dar Zarrouk functions; United States Geological Survey, Bulletin 1313-E, 39 p.

2.

COLONIAL CORAL ASSEMBLAGES AND ASSOCIATED FOSSILS FROM THE LATE ORDOVICIAN HONORAT GROUP AND WHITE HEAD FORMATION, GASPÉ PENINSULA, QUÉBEC

Project 740084

Thomas E. Bolton
Director General's Office, Special Projects

Bolton, Thomas E., Colonial coral assemblages and associated fossils from the Late Ordovician Honorat Group and White Head Formation, Gaspé Peninsula, Québec; in Current Research, Part C, Geological Survey of Canada, Paper 80-1C, p. 13-28, 1980.

Abstract

Four distinct coral assemblages are recognizable in the Late Ordovician rocks of Gaspé Peninsula, two in the Honorat Group and two in the White Head Formation. The Honorat Group faunules consist of an association of: 1) ***Favistina honoratensis*** *Bolton,* ***Calapoecia anticostiensis*** *Billings and* ***Saffordophyllum*** *sp. A, overlain by 2)* ***Plasmoporella rarivesiculosa*** *n. sp.,* ***Propora*** *sp., and* ***Paleofavosites*** *sp. A, along with the stromatoporoid* ***Beatricea*** *[****Aulacera****] sp. The White Head Formation assemblages consist of: 1)* ***Propora conferta*** *Milne-Edwards and Haime,* ***P. speciosa*** *(Billings),* ***Calapoecia anticostiensis*** *Billings,* ***Catenipora*** *sp. aff.* ***C. aequabilis*** *(Teichert),* ***Paleofavosites*** *sp. B,* ***Lobocorallium vaurealensis*** *(Twenhofel), and* ***Bodophyllum****(?) sp. in the lower assemblage, and 2)* ***Paleofavosites capax*** *(Billings),* ***Propora*** *sp. aff.* ***P. speciosa*** *(Billings),* ***Catenipora*** *sp. and* ***Lobocorallium vaurealensis*** *(Twenhofel) in the upper assemblage. Several of the White Head species are common to Late Ordovician rocks of Anticosti Island, Québec.*

Introduction

The Ordovician corals of Eastern Canada are poorly known. The most comprehensive examinations were by Billings (1858, 1859, 1865, 1866), Lambe (1900, 1901), Twenhofel (1928, 1938), Foerste (1924), and Cox (1936). Most of these studies involved coral collections from southwestern Ontario, and Mingan and Anticosti islands, Québec. In recent years, the coralline faunas from the Ottawa-St. Lawrence region have been described by Wilson (1948) and Steele and Sinclair (1971), and the Late Ordovician proporid corals of Anticosti Island by Dixon (1974).

The greatest concentrations of corals throughout Eastern Canada are in the biostromes of Manitoulin Island (Copper, 1978; Copper and Grawbarger, 1978) and the bioherms of Anticosti Island, Québec (Bolton, 1972, 1979). Each area is characterized by distinctive coral assemblages (Copper, 1980), but some genera and species are common to both. The Gaspé Ordovician faunas described herein also are distinct, but again sufficient forms are present for correlation, particularly with Anticosti Island.

For the Gaspé region, only a list of corals found within the White Head Formation of the Percé area has been published (Schuchert and Cooper, 1930, p. 169). Recently, however, an assemblage from the Honorat Group of the Mount Saint Joseph area was detailed (Bolton, 1979). The present report records additional taxa from the same 3 m thick conglomerate to coarse sandstone beds that produced the first described fauna and a second, different coral assemblage from the top of the same section. Two younger, distinct coral assemblages and associated fossils also are defined from the White Head Formation of the Percé region.

1. **Calapoecia, Propora, Plasmoporella,** and **Paleofavosites** from the Honorat Group, Gaspé Peninsula, Québec

The colonial coral assemblage originally described from the Honorat Group exposed near the bottom of the section on the north side of the road leading to Mount Saint Joseph shrine north of Carleton, Québec (Béland and Vennat, 1979, fig. 2.2) consisted of **Favistina honoratensis** Bolton (Pl. 2.1, fig. 1, 2, 5) and **Saffordophyllum** sp. A (Bolton, 1979, p. 1-4). Additional collections (1979) by G.S. Nowlan, Geological Survey of Canada, from this same unit (GSC locality 96395) confirmed the presence of **Calapoecia anticostiensis** Billings within this faunule, a genus reported by St-Julien et al. (1972, p. 87) but not recognized in the first study. Other fossils identified from this unit include minute crinoid columnals, two small indeterminable trepostome bryozoan colonies, fragments of a coarse ribbed and a strophomenid-like brachiopod, and part of a cheirurid(?) trilobite glabella. J.E. Béland, Université de Montréal, and W.H. Poole, Geological Survey of Canada, in 1979 also collected several well preserved tabulate coral colonies from a second unit located farther uphill along the Mount Saint Joseph shrine road (GSC locality 97220). The fossils were collected from a 0.9 m thick exposure of medium grey siltstone to highly weathered bioclastic siltstone located at least 450 to 540 m stratigraphically above the first coral-bearing conglomerates.

The coral taxa **Plasmoporella rarivesiculosa** n. sp., **Propora** sp. A and **Paleofavosites** sp. A are described herein from these collections. The presence of the stromatoporoid **Beatricea** sp. aff. **Aulacera plummeri** Galloway and St. Jean (hypotypes, GSC 53506-53508; Pl. 2.1, fig. 8; Pl. 2.3, fig. 2, 6) strengthens the Late Ordovician assignment for these rocks. Poorly preserved fragments of the chain coral **Catenipora** sp. indet. (small round corallites in ranks of one or two forming lacunae like **C. aequabilis** (Teichert), a suggestion of numerous short septal spines), solitary streptelasmids, minute crinoid columnals, a small glyptorthid brachiopod, a small hormotomid gastropod, and a small orthoconic cephalopod with central siphuncle were also recognized in this upper unit.

Anthozoa, Tabulata

Genus **Calapoecia** Billings, 1865

Type species. **Calapoecia anticostiensis** Billings, 1865

Calapoecia anticostiensis Billings, 1865

Plate 2.1, figures 3, 4, 6, 7

Honorat coralla are bowl-shaped (100 mm wide and 40 mm high – hypotype, GSC 53510) to massive (180 mm wide and 90 mm high – hypotype, GSC 53511). In transverse sections, mature corallites are circular, 2.4 to 3.0 mm in diameter, but 1.5 to 2.0 mm near the base of one small

colony, with centres 3.0 to 3.5 mm apart up to a maximum of 5.0 mm, rarely in contact; septal spines within corallites are very short, at least 20 per corallite, and extend into the coenenchyme as short, blunt to long thin, continuous radiating 'costae' (Cox, 1936, p. 13). In longitudinal section, corallite tabulae are complete, flat to slightly sagging (Pl. 2.1, fig. 4) to anastomosing (Pl. 2.1, fig. 7), 7 to 12 in 5 mm corallite length; coenenchyme thick.

Discussion. The Honorat specimens differ from the type species (Bolton and Nowlan, 1979, p. 10, Pl. 5, fig. 5, 8) by the slightly narrower coenenchyme and shorter 'costae'. They differ from the White Head forms (Pl. 2.3, fig. 4, 7-9) in possessing flatter and closer spaced tabulae. Both types of colonies of **C. ungava** Cox (Bolton and Nowlan, 1979, p. 10, Pl. 5, fig. 1-3, 6) from Maysvillian rocks of Akpatok Island have larger corallites whereas in the lectotype from the Richmondian of southern Ontario (Jull, 1976, p. 464) the corallites are smaller and closer than in the Honorat forms.

Types. Hypotypes, GSC 53509-53511. GSC locality 96395; Honorat Group, Upper Ordovician.

Genus **Propora** Milne-Edwards and Haime, 1849

Type species. **Porites tubulatus** Lonsdale, 1839

Propora sp. A

Plate 2.2, figures 1, 2

A single hemispherical corallum, at least 40 mm high. In transverse section, corallites are round, 1.4 to 1.5 mm in diameter, thin walled with 12 very short septal spines, separated by highly vesicular coenenchyme of varying thickness. In longitudinal section, tabulae are incomplete, mainly horizontal, 6 in 5 mm corallite length.

Discussion. This Honorat proporid lies within the range of corallite diameters assigned to **P. conferta** Milne-Edwards and Haime by Dixon (1974), common to the Upper Ordovician Ellis Bay Formation of Anticosti Island, Québec, but the tabulae spacing is greater. The corallites are smaller than those of **P. speciosa** (Billings) from the same formation.

Type. Figured specimen, GSC 53514. GSC locality 97220; Honorat Group, Upper Ordovician.

Genus **Plasmoporella** Kiaer, 1899

Type species. **Plasmoporella convexotubulata** Kiaer, 1899

Plasmoporella rarivesiculosa n. sp.

Plate 2.2, figures 3-8; Plate 2.3, figure 1

Coralla are spherical, ranging in diameter from 35 mm (holotype, GSC 53515; paratype, GSC 53517) to 145 mm (paratype, GSC 53518), to turbinate, 110 mm high and 70 mm wide at apex (paratype, GSC 53516). In transverse section, walls are thick, most of the corallites are round to subcircular, 1.7 to 2.0 mm in diameter but ranging from 1.5 to 2.3 mm, with centres 2.0 to 3.0 mm apart and only rarely in contact; in the turbinate colony, the corallites usually are closely packed, frequently touching or separated by narrow coenenchyme (Pl. 2.2, fig. 3), 1.2 to 1.5 mm in diameter with centres 1.5 to 2.0 mm apart; 12 to 13 horizontal to upwardly curving septal spines are preserved up to 0.7 mm in apparent length although shorter in the turbinate colony, occasionally extending into the coenenchyme (Pl. 2.2, fig. 7). In longitudinal section, tabulae are abundant, complete (Pl. 2.2, fig. 6, 8), mainly horizontal to slightly concave or convex-vesiculate, 10 to 16 in 5 mm corallite length with no pronounced zoning; the coenenchyme is never very pronounced and varies from strongly vesicular at various levels of a colony but best developed in the peripheral regions

Plate 2.1

Figures 1, 2, 5. **Favistina honoratensis** Bolton. Honorat Group, Upper Ordovician, road-cut on road from Carleton to shrine on Mount Saint Joseph, Québec (GSC locality 96395).

1, 2. Transverse section showing major septa extending nearly to centres of most corallites and short minor septa, and longitudinal section showing uniformly spaced flat to slightly downturned tabulae, X10. Hypotype, GSC 53512.

5. Transverse section with major septa extending just to the centres of corallite with no twisting, X10. Hypotype, GSC 53513.

3, 4, 6, 7. **Calapoecia anticostiensis** Billings. Same horizon and locality as figures 1, 2, 5.

3, 4. Transverse and longitudinal (attached to a **F. honoratensis** colony) sections, showing coenenchymal thickness and variation in length of 'costae', X5. Hypotype, GSC 53509.

6, 7. Transverse and longitudinal sections showing long 'costae' and open relationship between corallite and coenenchyme, X10. Hypotype, GSC 53510.

8. **Beatricea** sp. aff. **Aulacera plummeri** Galloway and St. Jean. Transverse section of coenosteum, X2. Honorat Group, Upper Ordovician, exposure near top of hill on road from Carleton to shrine on Mount Saint Joseph, Québec (GSC locality 97220). Hypotype, GSC 53506 (also Pl. 2.3, figs. 2, 6).

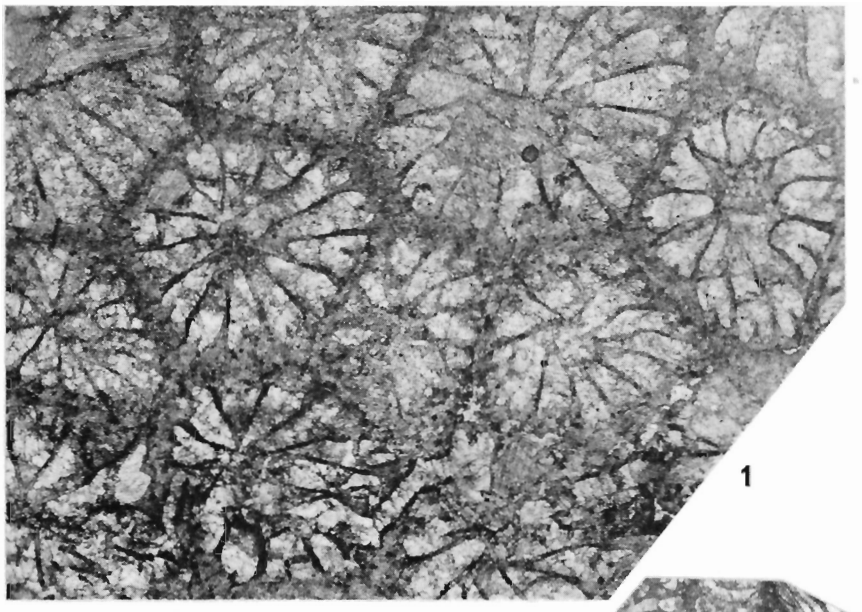
1

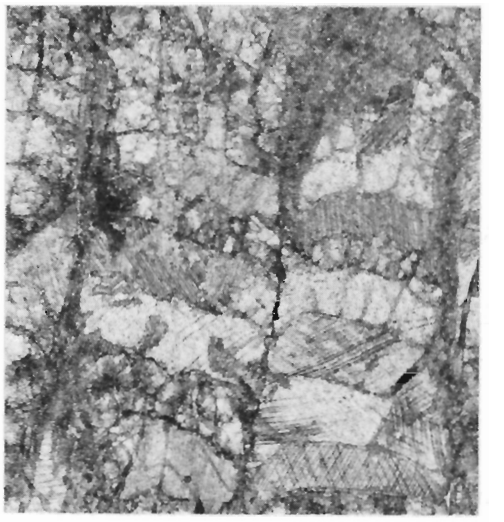
2

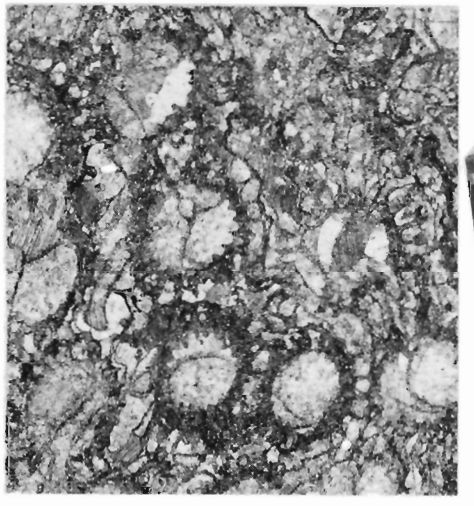
3

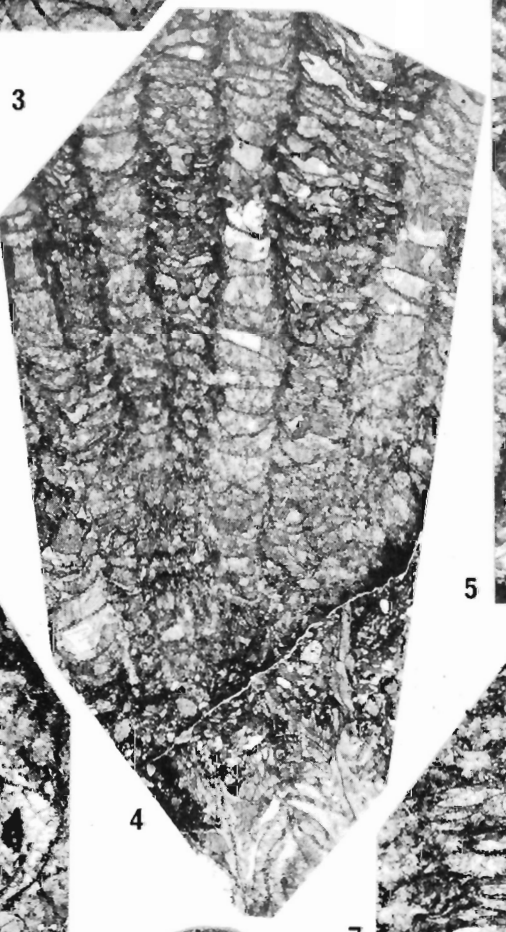
4

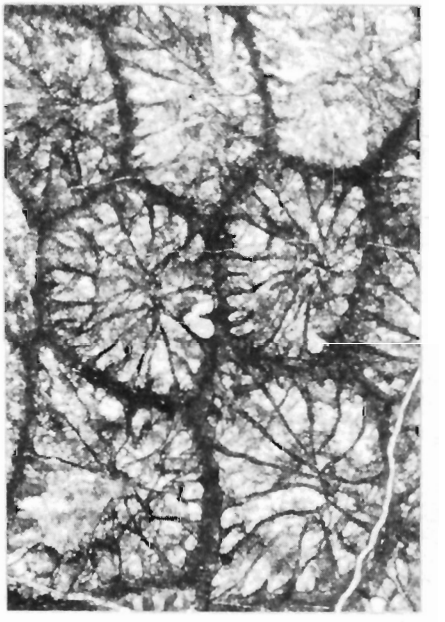
5


6

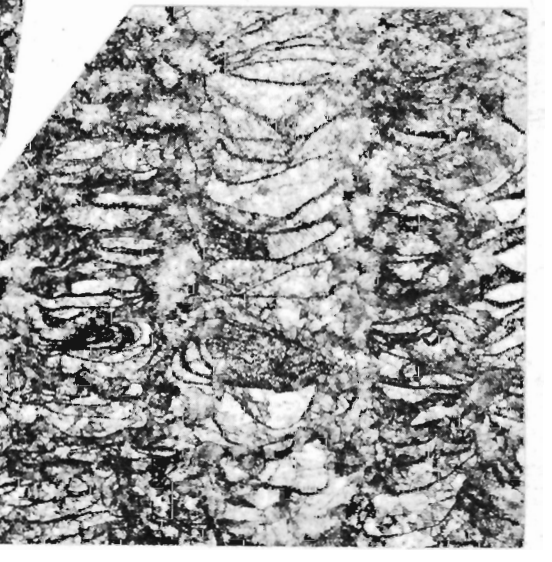
7


8

and with trabecular rods, to narrow 'tubes' with a single row of flat to vesicular dissepiments; the walls are thick and discontinuous with some localized trabecular thickening in both the axial and peripheral regions.

Discussion. This new species differs from all other **Plasmoporella** species in the closer crowding of corallites and consequent predominance of flat tabulae over vesicular coenenchyme. Its closest relationship is with **P. subchekiangensis** Bondarenko, 1963 and **P. spinosa** Bondarenko, 1963. In these species, however, the vesicular coenenchyme is more strongly developed and accordingly the corallites are farther apart. Their corallite diameters are 1.1 to 1.6 mm and 2.2 to 2.5 mm respectively. **P. contigua** Hall from the Upper Ordovician beds of New South Wales, Australia (Hall, 1975), has coenenchyme only irregularly developed, but it is distinguished by strongly arched tabulae and smaller diameter corallites.

Features of a number of different genera can be recognized in this new taxon. The turbinate form in longitudinal section (Pl. 2.3, fig. 1) resembles **Sibiriolites sibiricus** Sokolov, 1955 in the dominance of corallites over coenenchyme and tabular spacing, as well as in corallite diameters as recognized by Sokolov and Tesakov (1963), but the trabecular thickening is more pronounced in that genus (Bondarenko, 1977). The Honorat form resembles **Mcleodea** Flower and Duncan, 1975 in the coenenchymal variation of anastomosing domeshaped plates to horizontal dissepiments and well-defined walls (compare Pl. 2.2, fig. 6 with Flower and Duncan, 1975, Pl. 2, fig. 3). In some zones where the coenenchyme is undeveloped, there is a similarity to **Taeniolites** Bondarenko, 1961 (compare Pl. 2.2, fig. 8 with Bondarenko, 1963, Pl. 1, fig. 4, 6).

Types. Holotype, GSC 53515; paratypes, GSC 53516-53520. GSC locality 97220; Honorat Group, Upper Ordovician.

Genus **Paleofavosites** Twenhofel, 1914

Type species. **Favosites asper** d'Orbigny, 1850

Paleofavosites sp. A

Plate 2.3, figure 3

Larger corallum is 90 mm wide and 110 mm high. In transverse section, corallites are subpolygonal, 1.5 to 2.0 mm to a maximum of 2.5 mm in diameter; walls are thin and curved; mural pores are never abundant, located at the corners, and in the smaller, very short walled corallites 'solenia-like' corner pores develop (Powell and Scrutton, 1978). In longitudinal section, tabulae are complete, horizontal, from 4 to 6 in 5 mm corallite length; very short septal spines/squamulae are abundant locally; mural pores are located rarely in corallite corners.

Discussion. This form resembles several **Paleofavosites** colonies found within the Upper Ordovician Vauréal Formation of Anticosti Island, Québec.

Types. Figured specimen, GSC 53521; hypotype, GSC 53522. GSC locality 97220; Honorat Group, Upper Ordovician.

2. Late Ordovician tabulate corals and associated fossils of the White Head Formation, Percé, Québec

The Ordovician part of the White Head Formation is exposed in a series of fault blocks from Percé south to Cap Blanc and northwest along the coast to the Grande Coupe-Priest Road region (Poole and Rodgers, 1972). It consists of thinly interbedded greenish calcareous shale to argillaceous limestone, light brownish grey limestone, and minor amounts of dolomite, siltstone and sandstone. Major descriptions of the fauna of these rocks have been by Schuchert and Cooper (1930), Cooper and Kindle (1936), Foerste (1936), Lespérance (1968, 1968a, 1974), Lespérance and Sheehan (1976), Sheehan and Lespérance (1979), and Martin (1980). The regional distribution and paleogeographic implications of the Ordovician shelly faunas within the Northern Appalachian Magog belt were examined by Neuman (1968).

The brachiopod (Sheehan and Lespérance, 1979, p. 952) and trilobite (Lespérance, 1974, p. 21) faunas recognized in the White Head Formation both show close faunal relationship with the Ashgillian of northern Europe (North European zoogeographic province) and less with the Late Ordovician of Anticosti Island, Québec and central North America (North American zoogeographic province). Within the White Head, Lespérance has established, in ascending order, the Ashgillian **Stenoporeia** and **Remipyga [Ceraurinus]** faunas, and the Hirnantian **Mucronaspis-Hirnantia** fauna. According to Foerste (1936, p. 373) the cephalopod fauna from Grande Coupe has little in common specifically with the faunas of Anticosti Island, the closest affinities being with the Richmondian of interior North America. Martin (1980) recognized both Caradocian and Ashgillian microfaunal assemblages including species from central United States, Anticosti Island, and northwestern Europe.

From the Grande Coupe section, 2.4 km northwest of Percé, Schuchert and Cooper (1930, table, p. 169) identified **Paleofavosites prolificus, P. capax, Halysites catenularia, H. gracilis, Lyellia affinis, Calapoecia anticostiensis** and **Calapoecia** with small corallites, and Cooper and Kindle (1936, p. 350) added **Streptelasma** and **Nyctopora.** The fossils described herein were collected by G.W. Sinclair in 1956, W.B. Skidmore and P.J. Lespérance in 1961-64, and G.S. Nowlan in 1979. Most were found at Grande Coupe (GSC locality 27910) and Flynn road (GSC locality 96607). The opportunity to study these collections is greatly appreciated. B.L. Mamet, Université de Montréal, R.J. Elias, University of Manitoba, and O.A. Dixon, University of Ottawa, offered many useful suggestions.

The corals now recognized from Grande Coupe-Petite Coupe sections include: **Calapoecia anticostiensis** Billings, **Propora conferta** Milne-Edwards and Haime, **P. speciosa** (Billings), **Paleofavosites** sp. B, **Catenipora** sp. aff. **C. aequabilis** (Teichert), **Bodophyllum**(?) sp. (Pl. 2.5, fig. 9, 10)

Plate 2.2

Figures 1, 2. **Propora** sp. A. Longitudinal sections, one cutting centre of corallum, showing thick coenenchyme, X4. Honorat Group, Upper Ordovician, exposure near top of hill on road from Carleton to shrine on Mount Saint Joseph, Québec (GSC locality 97220). Figured specimen, GSC 53514.

3-8. **Plasmoporella rarivesiculosa** n. sp. Same horizon and locality as figures 1, 2.

3, 6. Transverse and longitudinal sections showing the short septa, well-defined corallite walls, and complete tabulae, X10 and X40. Paratype, GSC 53516 (also Pl. 2.3, fig. 1).

4, 5, 7. Longitudinal sections showing variation within colony of vesicular coenenchyme and trabecular rods, X2, and transverse section showing abundant septa, X15. Holotype, GSC 53515.

8. Longitudinal section showing abundant horizontal tabulae, with wide zones of vesicular coenenchyme at periphery, X4. Paratype, GSC 53517.

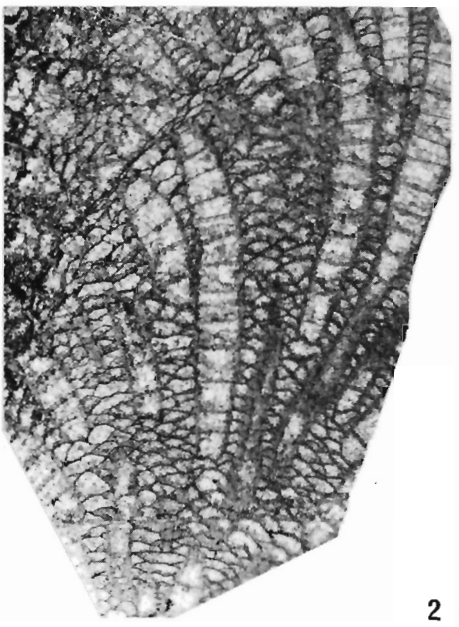

1

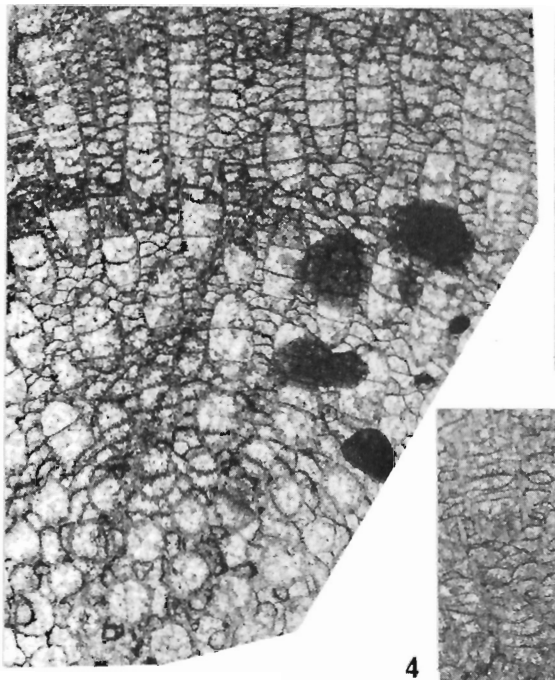

2

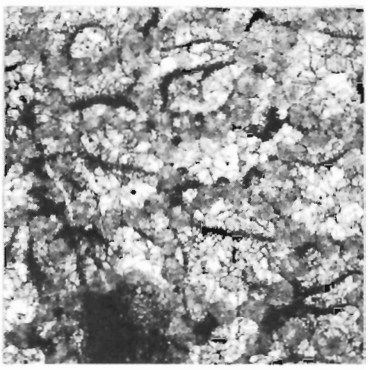

3

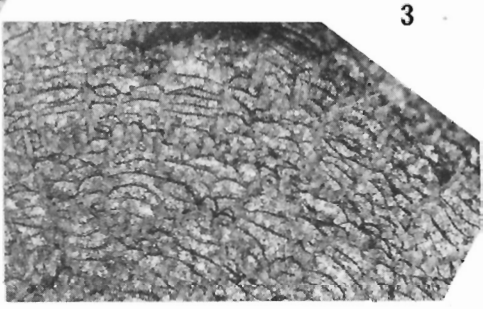

4

6

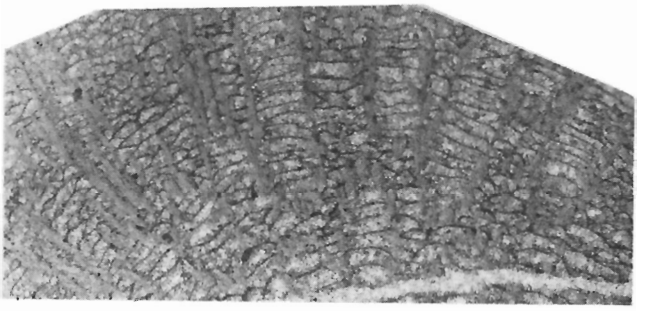

5

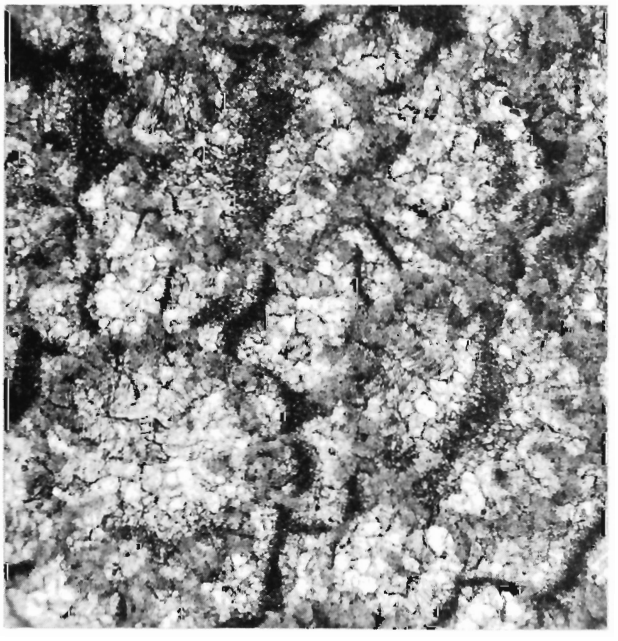

7

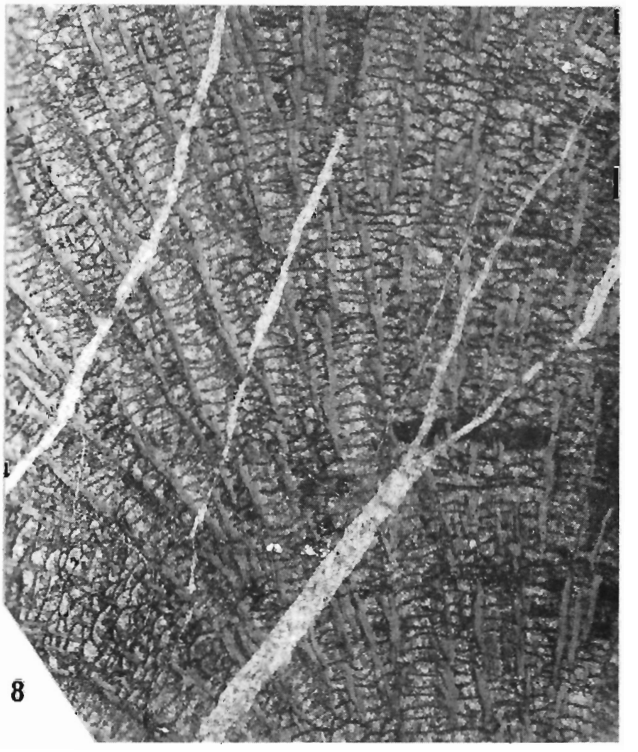

8

and **Lobocorallium vaurealensis** (Twenhofel) (Pl. 2.4, fig. 4). They are part of the total **Stenopareia** fauna; associated trilobites include: **Heterocyclopyge insolens** (Cooper), **Lonchodomas longirostris** Cooper, **Sphaerexochus bridgei** Cooper and Kindle, **Symphysops spinifera** Cooper and Kindle, **Tretaspis cerioides** (Angelin), **Novaspis elevata** (Cooper and Kindle), and **Cyclopyge vigilens** (Cooper and Kindle). The trepostome bryozoan **Hallopora** sp. and a bifoliate form are present in these beds. The alga **Rauserina notata** (Antropov) (Pl. 2.4, fig. 5-7; Pl. 2.5, fig. 2), **Kazakhstaniella**(?) sp. (Pl. 2.5, fig. 4), etc., Chitinozoa(?) (Pl. 2.5, fig. 5, 8) and minute ostracodes are abundant between **Catenipora** chains. **Paleofavosites** sp. B, **Catenipora** sp., and **Rauserina notata** (Antropov) are present in the **Remipyga** [**Ceraurinus**] fauna of Priest Road. The youngest coral fauna is composed of **Paleofavosites capax** (Billings), **Propora** sp. aff. **P. speciosa** (Billings), **Catenipora** sp., and **Lobocorallium vaurealensis** (Twenhofel) (Pl. 2.7, fig. 2, 3). It occurs on the Flynn road 32 m below the base of the Hirnantian mudstone. Trepostome Bryozoa also have been collected from these beds.

The closest relationship of both coral assemblages described herein is with the Richmondian fauna of Anticosti Island. Common to each area are **Propora conferta, P. speciosa, Calapoecia anticostiensis, Lobocorallium vaurealensis** and **Paleofavosites capax.** These same taxa are present throughout the Late Ordovician shallow carbonate platform deposits of North America, and the genera are recognized throughout the Late Ordovician Canadian-Arctic-Siberian paleozoogeographical province (equatorial faunal realm). Heliolitid corals, however, are never the dominant element in the tabulate coral megafauna in that province as they are in the White Head fauna. In addition, most of the colonial coralla are massive in the platform deposits whereas in the White Head the coralla are all consistently small.

Genus **Calapoecia** Billings, 1865

Type species. **Calapoecia anticostiensis** Billings, 1865

Calapoecia anticostiensis Billings

Plate 2.3, figures 4, 5, 7-9

White Head coralla (Pl. 2.3, fig. 4, 7-9) range in shape from oval (70 mm in diameter) to turbinate (90 mm wide and 120 mm high). In transverse section, corallites are circular, ranging in diameter from 2.2 to 2.5 mm, with centres 3 to 4 mm apart in smaller coralla to 2.5 to 3.0 mm with centres 4 to 5 mm apart in the largest coralla; 20 very short septal spines within corallites extend into the coenenchyme as short pointed to tear-shaped 'costae'. In longitudinal section, corallite tabulae range from slightly convex to sagging to anastomosing, 8 to 10 in 5 mm corallite length.

Discussion. The White Head specimens fall well within the range of specimens from the Upper Ordovician Ellis Bay Formation of Anticosti Island, Québec (Pl. 2.3, fig. 5) that have been included in this taxon. The only difference is that in the larger corallites the tabulae are wider apart and hence fewer in number.

Types. Hypotypes, GSC 53523-53526. GSC locality 27910; White Head Formation, Upper Ordovician. Hypotype, GSC 53527. GSC locality 76172, La Loutre road, Anticosti Island, Québec; Ellis Bay Formation, Upper Ordovician.

Plate 2.3

Figure 1. **Plasmoporella rarivesiculosa** n. sp. Longitudinal section, X4. Honorat Group, Upper Ordovician, exposure near top of hill on road from Carleton to shrine on Mount Saint Joseph, Québec (GSC locality 97220). Paratype, GSC 53516 (also Pl. 2.2, figs. 3, 6).

2, 6. **Beatricea** sp. aff. **Aulacera plummeri** Galloway and St. Jean. Transverse and longitudinal views of coenostea, X4 and X2 (also Pl. 2.1, fig. 8). Same horizon and locality as figure 1. Hypotypes, GSC 53506, 53507.

3. **Paleofavosites** sp. A. Longitudinal section showing septal spines/squamulae, complete tabulae, and thin corallite walls, X15. Same horizon and locality as figure 1. Figured specimen, GSC 53521.

4, 7-9. **Calapoecia anticostiensis** Billings. White Head Formation, Upper Ordovician, Grande Coupe, Percé, Québec (GSC locality 27910).

4, 7. Longitudinal section showing relatively narrow coenenchyme (compare with figure 5) and transverse section showing septal spines and 'costae', X5. Hypotype, GSC 53523.

8, 9. Transverse section showing 'costae' and longitudinal section through corallum with wide coenenchyme and open relationship between it and corallites, X5. Hypotype, GSC 53524.

5. **Calapoecia anticostiensis** Billings. Longitudinal section showing relatively narrow coenenchyme, X4. Ellis Bay Formation, Upper Ordovician, La Loutre road, Anticosti Island, Québec (GSC locality 76172). Hypotype, GSC 53527.

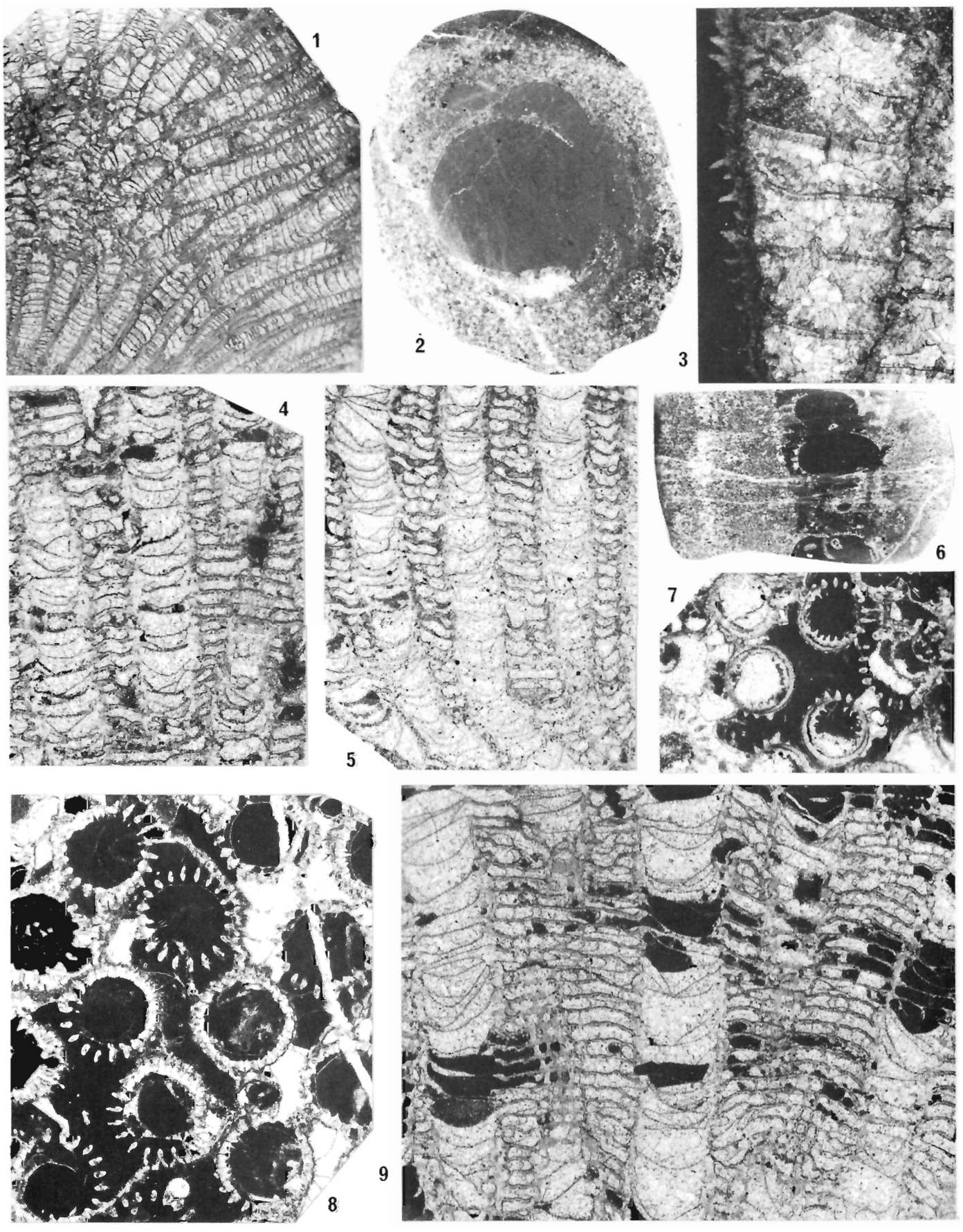
1
2
3
4
5
6
7
8
9

Genus **Propora** Milne-Edwards and Haime, 1849

Type species. **Porites tubulatus** Lonsdale, 1839

Propora conferta Milne-Edwards and Haime emend. Dixon, 1974

Plate 2.4, figures 1-3, 9, 10; Plate 2.5, figure 7

White Head coralla are small, spheroidal forms, 60 to 80 mm wide and 40 to 65 mm high. In transverse section, corallites are circular to subcircular, with thin and distinct walls, that range in diameter from 1.2 mm (hypotype, GSC 53528) to 1.6 mm (hypotype, GSC 53530) to 1.8 mm (hypotype, GSC 53529) with centres varying from 1.5 to 2.5 mm apart, most being 2.0 mm; coenenchyme is never very thick, corallites frequently in contact; minute spines are rarely preserved although in one colony (Pl. 2.5, fig. 7) 12 exothecal septal spines are exceedingly well developed (compare Dixon, 1974, Pl. 1, fig. 7-9). In longitudinal section, walls are thin, continuous and distinct (as in **Mcleodea** Flower and Duncan, 1975), tabulae are thin, horizontal to slightly sagging, normally 4 to 7 in 5 mm corallite length although in the smaller diameter corallite colonies, 10 to 11 can occur in 5 mm length; intercorallite spaces are occupied by single cells or vesicular coenenchyme, also abruptly ending at corallite walls although rarely a cystose element appears to curve downward into a wall resulting, in single coenenchymal tubes, in the development of beaded 'mesopore-like' structures (as in the Bryozoa genera **Diplotrypa** and **Trematopora**).

Discussion. The various modes of formation of corallites from cystoliths (Bondarenko, 1978) are well displayed in these colonies. Rejuvenation surfaces are present locally in some colonies. All the White Head forms are well within the range of morphological variations recognized by Dixon (1974) within continuous-walled corallite **P. conferta** specimens from the Ellis Bay Formation of Anticosti Island.

Types. Hypotypes, GSC 53528-53530. GSC locality 27910; White Head Formation, Upper Ordovician.

Propora speciosa (Billings)

Plate 2.5, figures 1, 3, 6

The White Head coralla range in form from oval (60 mm in diameter) to cylindrical (60 mm long and 30 mm wide). In transverse section, corallites are thick walled, subcircular, 1.9 to 2.5 mm in diameter with centres 2.5 to 4.0 mm apart; 12 septal spines or ridges are well developed producing crenulated margins; spacing between corallites is never very wide but corallites are rarely in contact. In longitudinal section, walls are thick varying from continuous to discontinuous with abundant septal spines pointing upwards; tabulae are thin, complete, horizontal, rarely gently arched or incomplete, 6 to 7 in 5 mm corallite length in hypotype, GSC 53531 and 9 to 11 in length in hypotype, GSC 53532; coenenchyme is strongly arched, cysts of variable size with abundant vertical trabeculae ranging from short spines to long rods.

Discussion. The corallite diameters of the White Head forms lie within the minimum to maximum diameter range of the Ellis Bay Formation specimens described from Anticosti Island. The difference in tabular spacing between vertical and lateral growing corallites as noted by Dixon (1974, p. 582) also is well displayed by the two Gaspé growth forms.

Types. Hypotypes, GSC 53531, 53532. GSC locality 27910, and Lespérance locality 62-L45, Petite Coupe, 2 km northwest of Grande Coupe, Gaspé Peninsula, Québec; White Head Formation, Upper Ordovician.

Plate 2.4

Figures 1-3, 9, 10. **Propora conferta** Milne-Edwards and Haime. White Head Formation, Upper Ordovician, Grande Coupe, Percé, Québec (GSC locality 27910).

1. Longitudinal section, slightly oblique, showing corallites in contact, X10. Hypotype, GSC 53528 (also Pl. 2.5, fig. 7).

2, 3. Longitudinal section through central region of colony, and transverse section showing smaller corallites in central zone (bottom of photo) and larger in peripheral region, X5. Hypotype, GSC 53529.

9, 10. Longitudinal section showing corallites in contact in central lower region of colony and development of beaded 'mesopore-like' coenenchyme (central tube), and transverse section showing variation in coenenchymal thickness, X10. Hypotype, GSC 53530.

4. **Lobocorallium vaurealensis** (Twenhofel). Transverse section, X2. Same horizon and locality as figure 1. Hypotype, GSC 53545.

5-7. **Rauserina rotata** (Antropov). X130. White Head Formation, Upper Ordovician, Priest Road (fig. 5) and Grande Coupe, Percé, Québec. Hypotypes, GSC 53549-53551.

8. **Lobocorallium vaurealensis** (Twenhofel). Transverse section, X2. Vauréal Formation, first creek before shore, Bay Martin road, Anticosti Island, Québec (GSC locality 36163). Hypotype, GSC 53556.

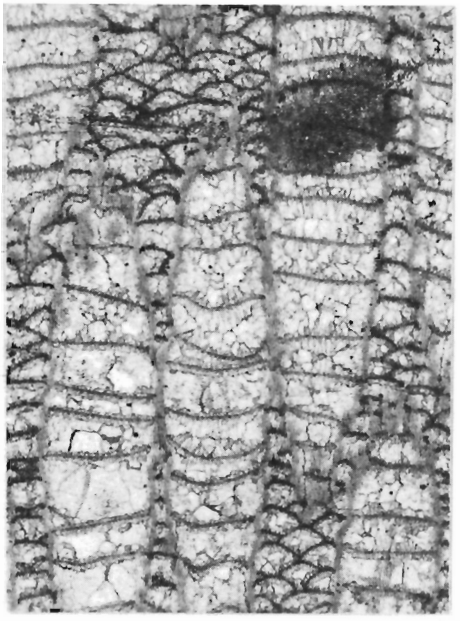

1

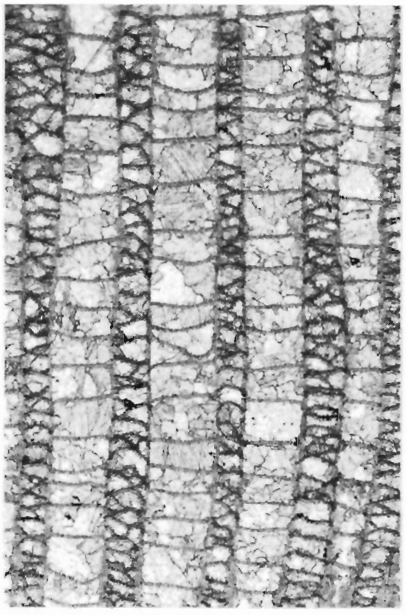

2

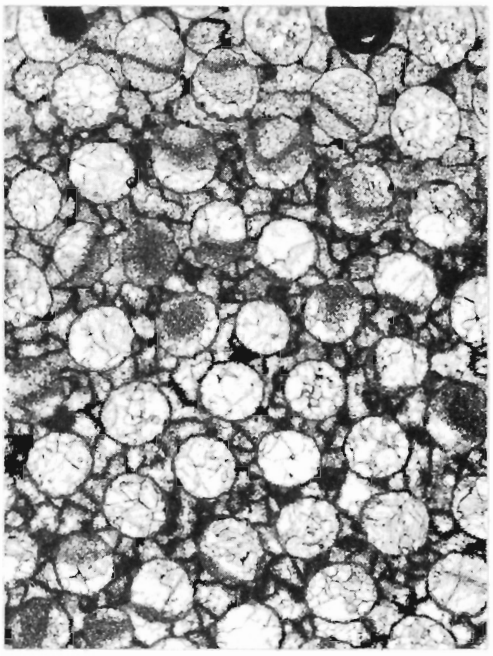

3

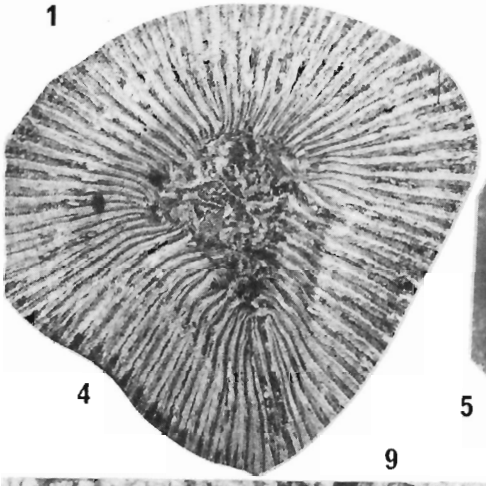

4

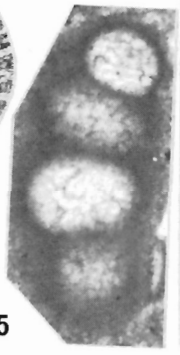

5

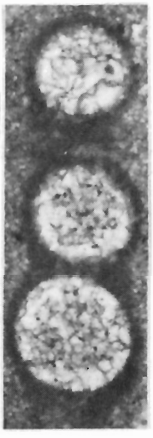

6

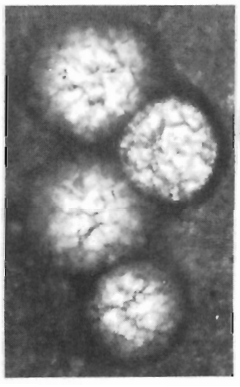

7

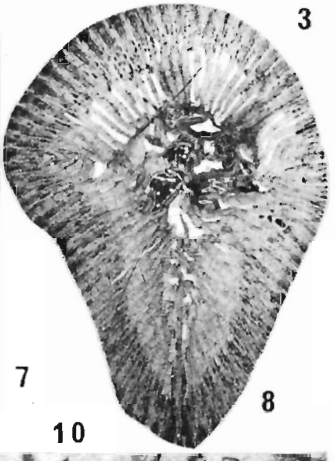

8

9

10

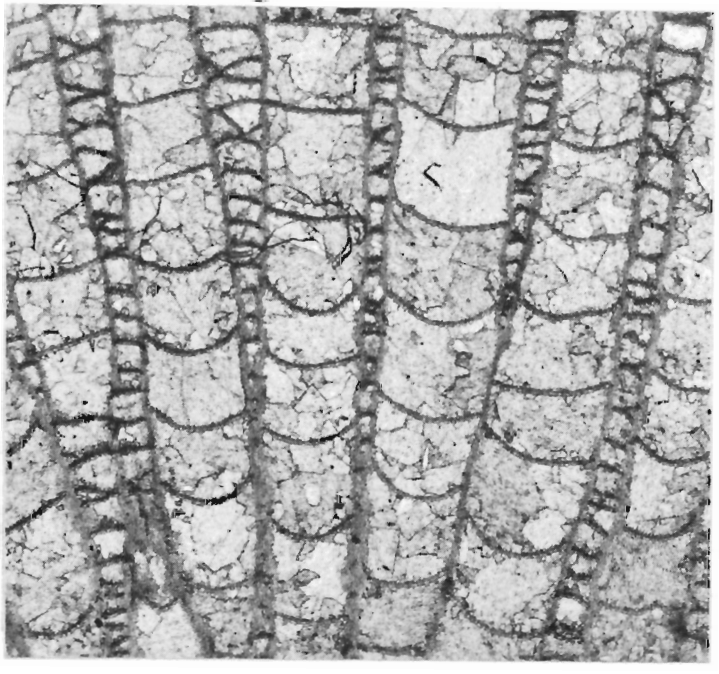

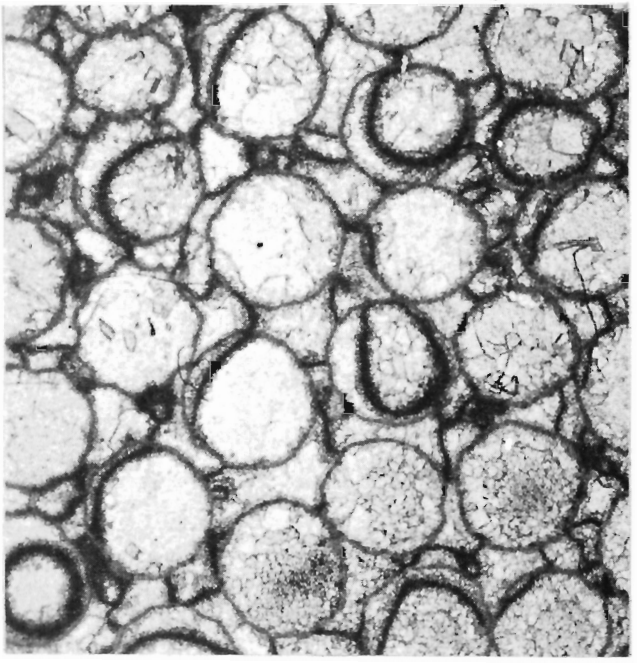

Table 2.1

Data for six **Paleofavosites** sp. B colonies.

Specimen	Corallite diameter (mm)	Tabulae per 5 mm	Spine length (mm)	Angle pore diameter (mm)
GSC 53533	1.1 to 1.2, 1.9 to 2.0	4 to 5	0.2, 0.5 max.	0.2 to 0.4
GSC 53535	rare 1.7, 2.0 to 2.4	3 to 7	0.3 to 0.5 (abundant)	0.5 to 0.8
GSC 53537	rare 1.1, 1.6 to 1.8, rare 2.2	4 to 6 (inner zone) 8 to 10 (outer zone)	0.3 to 0.8 (abundant)	0.3 to 0.4
GSC 53536	2.5 to 3.6	4 to 6	0.3	0.2
GSC 53534	rare 1.9, 2.4 to 2.7, rare 3.1	3 to 5	0.3, rare 0.5	0.2
GSC 53538	1.5 to 1.7, rare 2.2	5 to 9	-	0.4 to 0.6

Genus **Paleofavosites** Twenhofel, 1914

Paleofavosites sp. B

Plate 2.6, figures 1-9

Coralla are turbinate (40 mm wide and 50 mm high) to laminar (120 mm long and 40 mm high). In transverse section, the corallites are polygonal, 4- to 6-sided with thin, straight to gently curving walls, diameters vary considerably both intercolony and intracolony (Table 2.1); mural pores are located in corners with some 'solenia-like' structures, but no wall pores were observed; spines are mainly short spikes, rarely 0.5 mm in length, varying from few to very abundant. In longitudinal section, the tabulae are complete, essentially horizontal to slightly sagging, especially in larger diameter corallites, farther apart in the centre of some colonies (Table 2.1); spines/squamulae are normally directed upwards, straight to hooked (Pl. 2.6, fig. 3, 4); mural pores are circular.

Discussion. **Paleofavosites asper** (d'Orbigny) is characterized by adult corallite diameters in the range of 0.87 to 1.13 mm (Powell and Scrutton, 1978, p. 314), with a diameter of 1.1 predominating (Stel, 1978, 1979; Oekentorp, 1976). All the White Head species have greater diameters. As recognized by Twenhofel (1928), **P. prolificus** (Billings) from the Upper Ordovician rocks of Anticosti Island, Québec, has consistently smaller corallites ranging from 1.0 to 1.5 mm in diameter, and **P. capax** (Billings) from the same rocks has corallites of two sizes, 0.6 to 2.0 mm and 3.2 to 4.2 mm in diameter.

Types. Hypotypes, GSC 53533-53538. GSC locality 27910, and Lespérance locality 62-L47A, Priest Road, northwest of Percé, Québec; White Head Formation, Upper Ordovician.

Paleofavosites capax (Billings)

Plate 2.7, figures 1, 4-6

White Head incomplete coralla are 60 mm wide and 40 mm high. In transverse section, coralla are composed of a mixture of large 6-sided or more corallites 3.3 to 4.0 mm in diameter surrounded by smaller 4-sided corallites 0.6 to 1.3 mm in diameter; corallite walls are thin, straight to gently curved; small angle pores are abundant and a rare wall mural pore is present with walls thickening around the pores (Pl. 2.7, fig. 1, 4); no septal spines were observed. In longitudinal section, tabulae are complete, flat to slightly sagging, 1 to 1.5 per 5 mm corallite length; pores are 0.3-0.8 mm in diameter.

Plate 2.5

Figures 1, 3, 6. **Propora speciosa** (Billings). White Head Formation, Upper Ordovician.

1, 6. Longitudinal section showing wide coenenchyme, and transverse section showing septal spines in close corallites, X5. Grande Coupe, Percé, Québec (GSC locality 27910). Hypotype, GSC 53531.

3. Longitudinal section through centre of colony, X5. Petite Coupe, Percé, Québec (Lespérance locality 62-L45). Hypotype, GSC 53532.

2. **Rauserina notata** (Antropov). X130. Same horizon and locality as figures 1, 6. Hypotype, GSC 53552.

4. **Kazakhstaniella**(?) sp. X40. Same horizon and locality as figures 1, 6. Figured specimen, GSC 53553.

5, 8. Chitinozoa(?). X130. Same horizon and locality as figures 1, 6. Figured specimens, GSC 53554, 53555, a-c.

7. **Propora conferta** Milne-Edwards and Haime. Transverse section showing close corallites with septa spines, X10. Same horizon and locality as figures 1, 6. Hypotype, GSC 53528 (also Pl. 2.4, fig. 1).

9, 10. **Bodophyllum**(?) sp. Transverse and longitudinal sections, X2. White Head Formation, Upper Ordovician, Priest Road northwest of Percé, Québec (Lespérance locality 62-L47). Hypotype, GSC 53548.

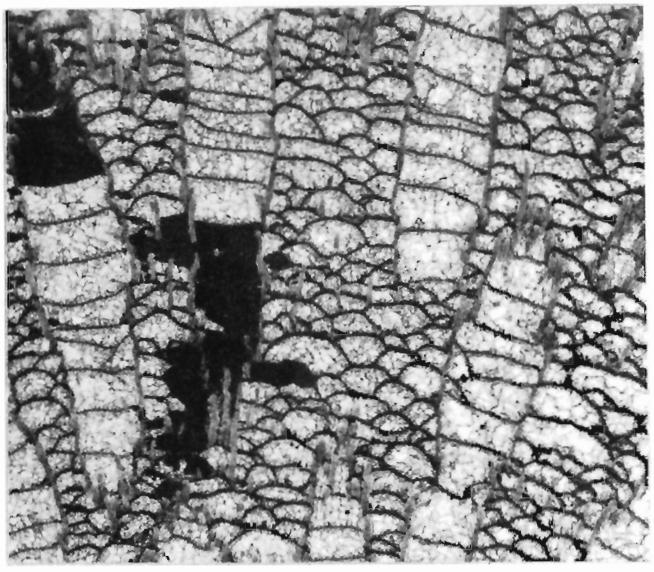

1

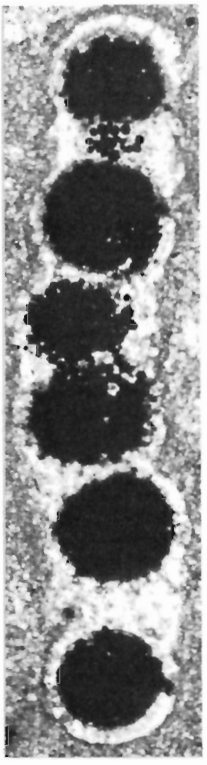

2

3

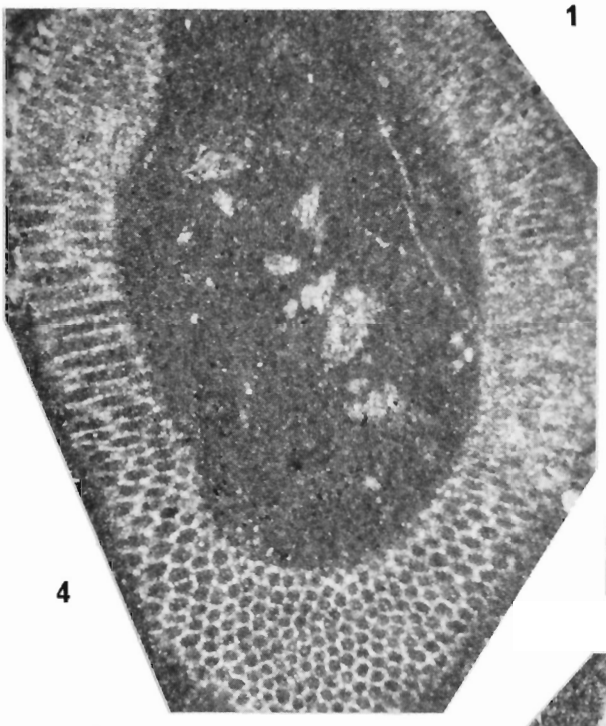

4

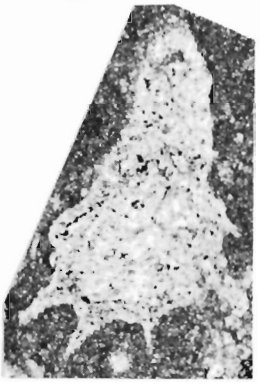

5

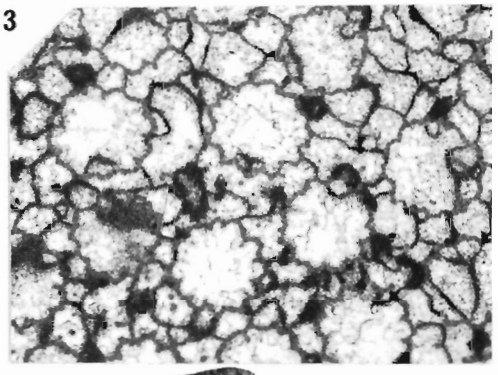

6

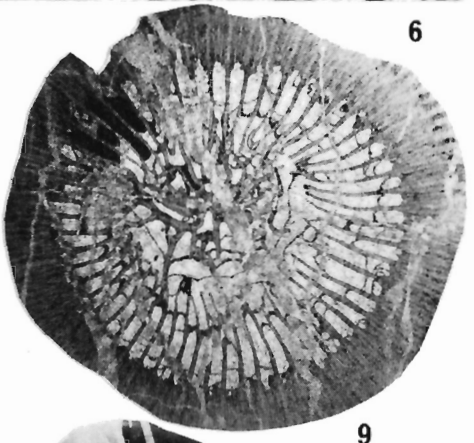

9

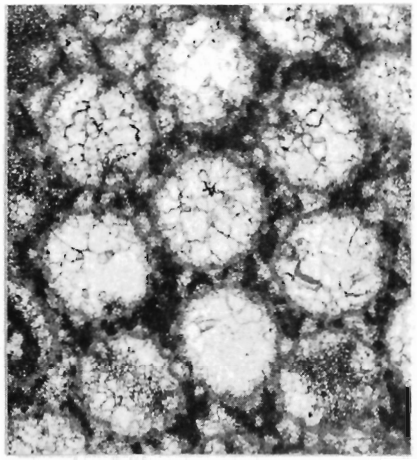

7

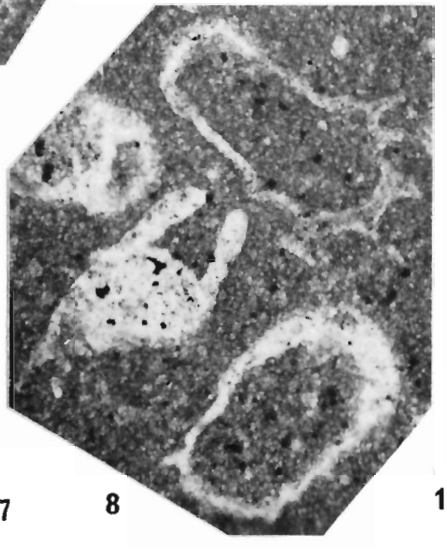

8

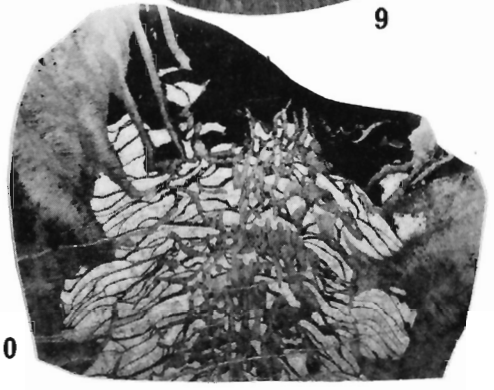

10

Plate 2.6

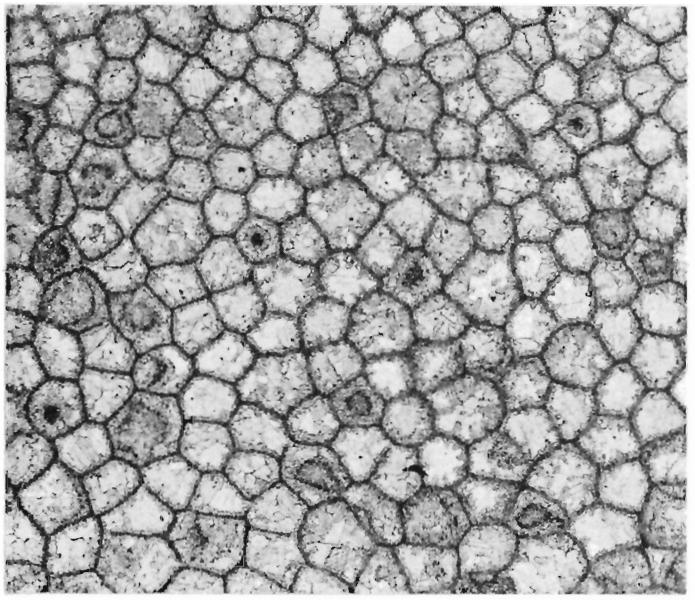

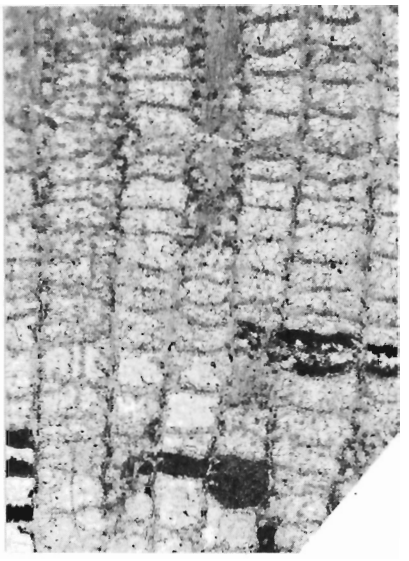

2

3

4

1

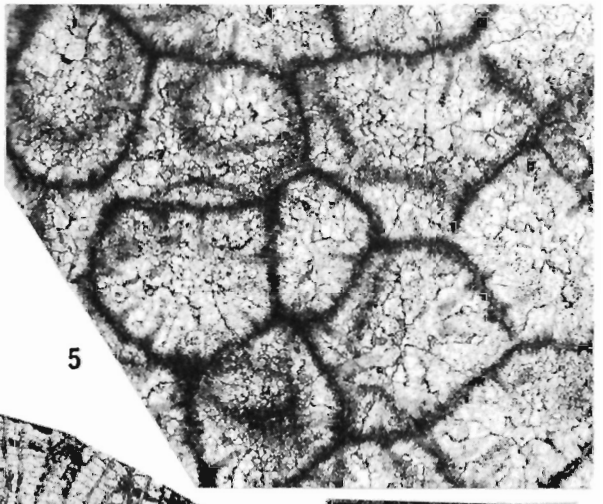

5

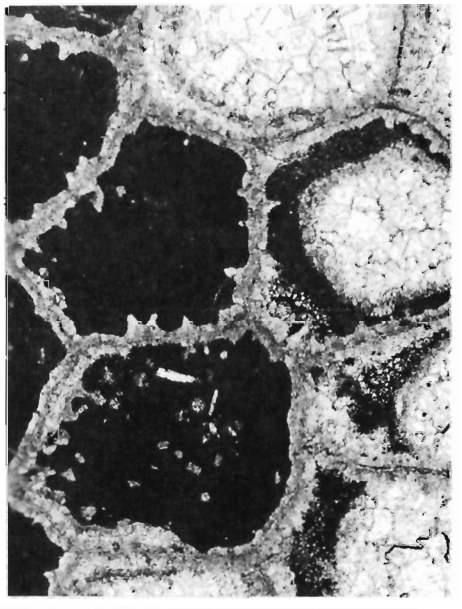

6

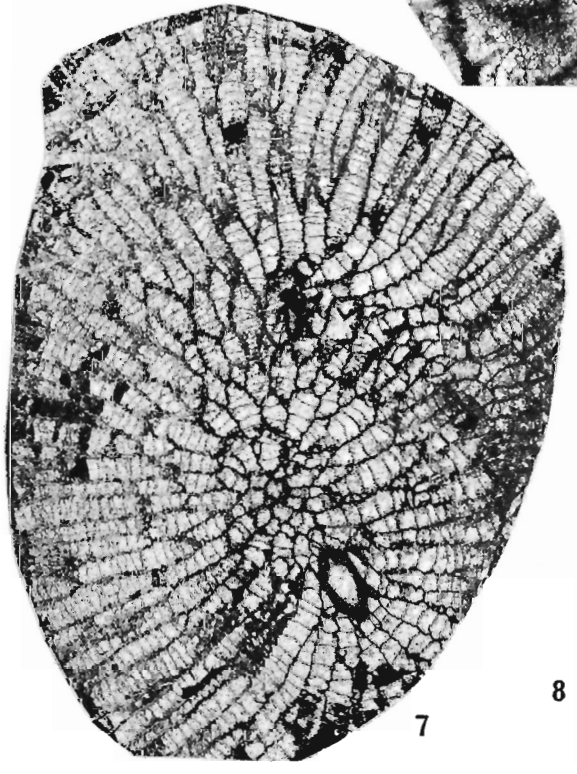

7

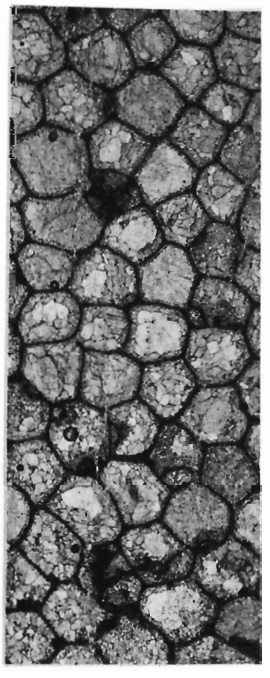

8

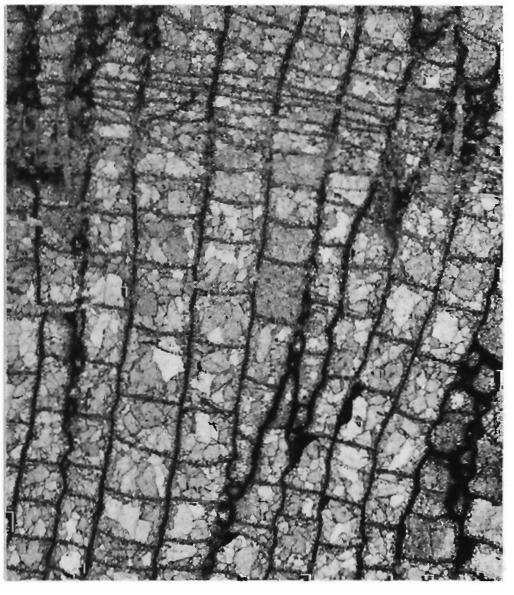

9

Discussion. Coralla with corallites of unequal size and shape similar to the White Head forms are common in the Upper Ordovician rocks of Anticosti Island (Pl. 2.7, fig. 4); Billings (1866) and Twenhofel (1928) reported **P. capax** from this same interval. **P. asper** (d'Orbigny) has smaller corallites with a diameter range of 0.87 to 1.13 mm and closer spaced tabulae. **P. okulitchi** Stearn from the Late Ordovician of Manitoba and Melville Peninsula, District of Keewatin (Bolton et al., 1977, p. 31) is characterized by abundant, large corallites (2.0 to 3.5 mm diameter) and fewer small diameter corallites, both angle and wall pores, and more abundant tabulae.

Types. Hypotype, GSC 53539. Flynn road (road to Irishtown from Percé), Gaspé, Québec (GSC locality 96607); White Head Formation, 32 m below base of Hirnantian mudstone, Upper Ordovician. Hypotype, GSC 53540. Jupiter River road (1958), 4.35 km south of East Branch Oil River crossing, Anticosti Island, Québec (GSC locality 36277); basal interbiohermal beds of member 6, Ellis Bay Formation, Upper Ordovician.

Plate 2.6

Figures 1-7. **Paleofavosites** sp. B. White Head Formation, Upper Ordovician, Grande Coupe, Percé, Québec (GSC locality 27910).

1, 2. Transverse section showing corner and 'solenia-like' pores (left edge, centre of photo), and longitudinal section with some mural pores and abundant spines/squamulae, in rows (left corallite), X5. Figured specimen, GSC 53533.

3, 4. Longitudinal sections showing straight and hooked spines/squamulae, X40. Figured specimen, GSC 53534.

5. Transverse section showing angle pores and a 'solenium', and abundant septal spines, X10. Figured specimen, GSC 53535.

6. Transverse section showing squamulae, X10. Figured specimen, GSC 53536.

7. Longitudinal section through centre of colony illustrating circumrotatory growth, X2. Figured specimen, GSC 53537.

8, 9. **Paleofavosites** sp. B. Transverse and longitudinal sections showing mural corner pores, X5. White Head Formation, Upper Ordovician, Priest Road northwest of Percé, Québec (Lespérance locality 62-L47). Figured specimen, GSC 53538.

Genus **Catenipora** Lamarck, 1816

Type species. **Catenipora escharoides** Lamarck, 1816

Catenipora sp. aff. **C. aequabilis** (Teichert)

Plate 2.7, figures 7, 8

White Head colonies are all small, ranging from spherical (40 mm in diameter) to hemispherical (60 to 110 mm wide and 40 mm to 70 mm high), with corallites radiating from a centre. In transverse sections, corallites are small, subelliptical with a transverse length of 1.3 to 1.6 mm and a mid-width of 0.6 to 1.0 mm (hypotype, GSC 53541) or transverse length of 1.0 to 1.1 mm and mid-width of 0.4 to 0.5 mm (hypotype, GSC 53542), thick walled, arranged in monoserial rank with 1 to 2 corallites per rank, rarely 3, and lacunae accordingly consistently small; septal spines short. In longitudinal section, tabulae are complete, horizontal to very slightly sagging, 9 to 12 per 5 mm in corallite length; at least four vertical rows of spine bases or spheres of poikiloplasm are evident per corallite wall.

Discussion. The White Head species are more consistently restricted in the length of each chain or rank than **C. aequabilis** (Teichert) from the late Middle to early Late Ordovician Bad Cache Rapids Formation of Melville Peninsula, District of Franklin (Bolton et al., 1977, p. 31). **Quepora quebecensis** (Lambe) from the Middle Ordovician Simard beds of Lake St. John, Québec has small corallites, mainly two per lacunae wall, but does range from one to three or more, and 6 to 10 tabulae per 5 mm corallite length. Other species with small corallites and short ranks but with other variable characteristics include the Silurian forms **C. huronensis** (Teichert) and **C. micropora** (Whitfield).

Types. Hypotypes, GSC 53541-53544. GSC locality 27910; White Head Formation, Upper Ordovician.

References

Béland, J. et Vennat, G.
1979: Notes sur les groupes d'Honorat et de Matapédia dans la région de Carleton-St-Omer, Gaspésie, Québec; Commission géologique du Canada, Etude 79-1B, p. 13-15.

Billings, E.
1858: Canadian fossils, containing descriptions of some new genera and species from the Silurian and Devonian formations of Canada; Geological Survey of Canada, Report of Progress for the year 1857, p. 165-192.

Plate 2.7

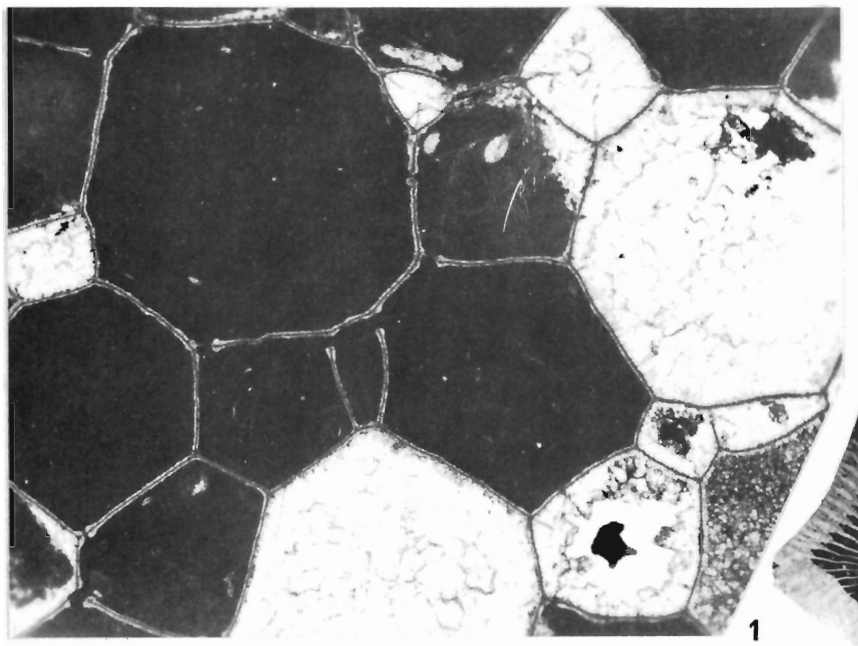
1

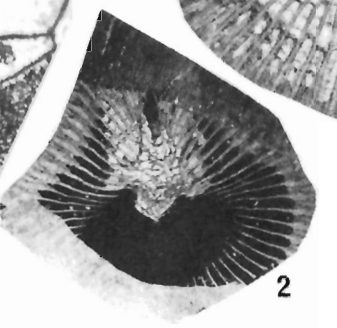
2

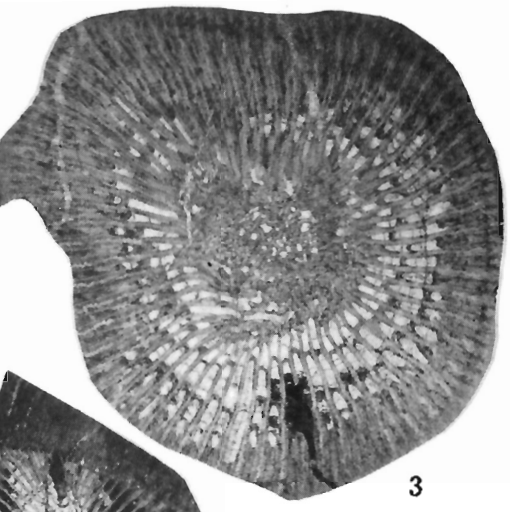
3

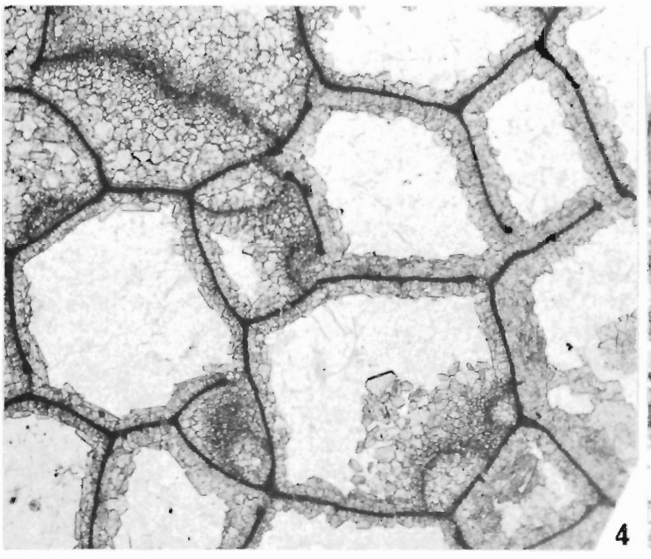
4

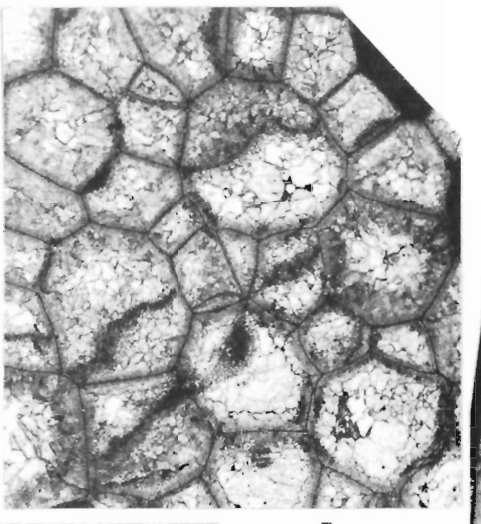
5


6

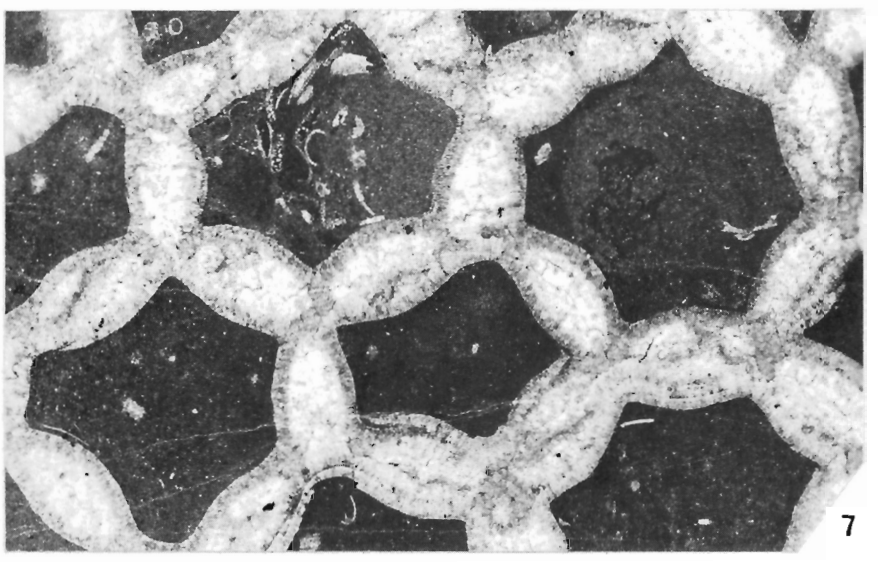
7

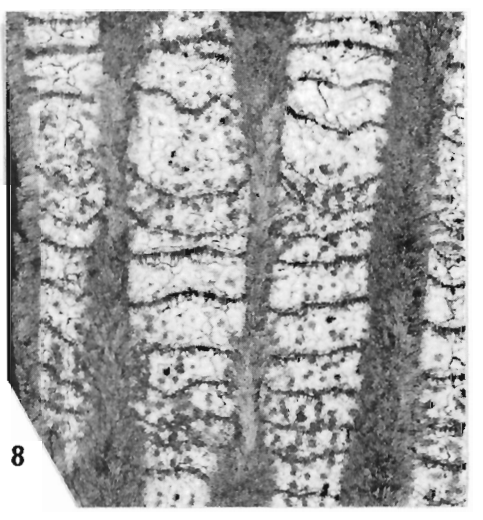
8

Plate 2.7

Figures 1, 4-6. **Paleofavosites capax** (Billings).

1, 5, 6. Transverse section showing corner pores and one wall pore, both with wall swellings, X10, and transverse and longitudinal sections showing variation in corallite diameters and corner pores, X5. White Head Formation, Upper Ordovician, Flynn road, Percé, Québec (GSC locality 96607). Hypotype, GSC 53539.

4. Transverse section showing corner pores with wall swellings, X10. Ellis Bay Formation, Upper Ordovician, Jupiter River road (1958), Anticosti Island, Québec (GSC locality 36277). Hypotype, GSC 53540.

2, 3. **Lobocorallium vaurealensis** (Twenhofel). Transverse sections, X1 and X2. Same horizon and locality as figure 1. Hypotypes, GSC 53546, 53547.

7, 8. **Catenipora** sp. aff. **C. aequabilis** (Teichert). Transverse and longitudinal sections, X10. White Head Formation, Upper Ordovician, Grande Coupe, Percé, Québec (GSC locality 27910). Hypotype, GSC 53541.

Billings, E. (cont.)

1859: Fossils of the Chazy limestone, with descriptions of new species; Canadian Naturalist and Geologist, v. IV, p. 426-470.

1865: Notice of some new genera and species of Palaeozoic fossils; Canadian Naturalist and Geologist, new series, v. II, p. 425-432.

1866: Catalogues of the Silurian fossils of the Island of Anticosti, with descriptions of some new genera and species; Geological Survey of Canada.

Bolton, T.E.

1972: Geological map and notes on the Ordovician and Silurian litho- and biostratigraphy, Anticosti Island, Québec; Geological Survey of Canada, Paper 71-19.

1979: Some Late Ordovician colonial corals from eastern Canada; in Current Research, Part B, Geological Survey of Canada, Paper 79-1B, p. 1-12.

Bolton, T.E. and Nowlan, G.S.

1979: A Late Ordovician fossil assemblage from an outlier north of Aberdeen Lake, District of Keewatin; Geological Survey of Canada, Bulletin 321, p. 1-26.

Bolton, T.E., Sanford, B.V., Copeland, M.J., Barnes, C.S., and Rigby, J.K.

1977: Geology of Ordovician rocks, Melville Peninsula and region, southeastern District of Franklin; Geological Survey of Canada, Bulletin 269.

Bondarenko, O.B.

1963: Tabulata and Heliolitidae of the Tarbagatay Upper Ordovician and Lower Silurian; in The stratigraphy and fauna of the Paleozoic deposits of the Tarbagatay Range (Ordovician, Silurian, Devonian and Lower Carboniferous), All-Union Trust of Aerogeology, USSR. Ministry of Geology and Conservation of Mineral Resources, Moscow State University, p. 97-121.

1977: Evolutionary trends and systematics of Late Ordovician corals of the Family Proheliolitidae; Paleontological Journal, no. 4, p. 34-46.

1978: Polymorphism in Paleozoic tabulatomorphous corals; Paleontological Journal, no. 2, p. 23-35.

Cooper, G.A. and Kindle, C.H.

1936: New brachiopods and trilobites from the Upper Ordovician of Percé, Québec; Journal of Paleontology, v. 10, no. 5, p. 348-372.

Copper, P.

1978: Paleoenvironments and paleocommunities in the Ordovician-Silurian sequence of Manitoulin Island; Michigan Basin Geological Society, Special Papers No. 3, p. 47-61.

1980: Comparison of Late Ordovician coral-stromatoporid communities of Manitoulin and Anticosti Islands (Abstract); Geological Society of America, Abstracts with programs, v. 12, no. 2, p. 29.

Copper, P. and Grawbarger, D.J.

1978: Paleoecological succession leading to a late Ordovician biostrome on Manitoulin Island, Ontario; Canadian Journal of Earth Sciences, v. 15, no. 12, p. 1987-2005.

Cox, I.

1936: Revision of the Genus Calapoecia Billings; National Museum of Canada, Bulletin no. 80, Geological Series No. 53.

Dixon, O.A.
1974: Late Ordovician **Propora** (Coelenterata: Heliolitidae) from Anticosti Island, Québec, Canada; Journal of Paleontology, v. 48, no. 3, p. 568-585.

Flower, R.H. and Duncan, H.M.
1975: Some problems in coral phylogeny and classification; Bulletin American Paleontology, v. 67, no. 287, p. 175-189.

Foerste, A.F.
1924: Upper Ordovician faunas of Ontario and Québec; Geological Survey of Canada, Memoir 138.

1936: Cephalopods from the Upper Ordovician of Percé, Québec; Journal of Paleontology, v. 10, no. 5, p. 373-384.

Hall, R.L.
1975: Late Ordovician coral faunas from north-eastern New South Wales; Royal Society of New South Wales, Journal and Proceedings, v. 108, p. 75-93.

Jull, R.K.
1976: Review of some species of **Favistina**, **Nyctopora**, and **Calapoecia** (Ordovician corals from North America); Geological Magazine, v. 113, no. 5, p. 457-467.

Lambe, L.M.
1900: A revision of the genera and species of Canadian Palaeozoic corals. The Madreporaria Perforata and the Alcyonaria; Geological Survey of Canada, Contributions to Canadian palaeontology, v. IV, pt. I (1899).

1901: A revision of the genera and species of Canadian Palaeozoic corals. The Madreporaria Aporosa and the Madreporaria Rugosa; Geological Survey of Canada, Contributions to Canadian palaeontology, v. IV, pt. II (1900).

Lespérance, P.J.
1968: Ordovician and Silurian trilobite faunas of the White Head Formation, Percé region, Québec; Journal of Paleontology, v. 42, no. 3, pt. 1, p. 811-826.

1968a: Faunal affinities of the trilobite faunas, White Head Formation, Percé Region, Québec, Canada; XXIII International Geological Congress, Report of Proceedings, v. 9, p. 145-159.

1974: The Hirnantian fauna of the Percé area (Québec) and the Ordovician-Silurian boundary; American Journal of Science, v. 274, p. 10-30.

Lespérance, P. and Sheehan, P.M.
1976: Brachiopods from the Hirnantian stage (Ordovician-Silurian) at Percé, Québec; Palaeontology, v. 19, pt. 4, p. 719-731.

Martin, F.
1980: Quelques Chitinozoaires et Acritarches ordoviciens supérieurs de la Formation de White Head en Gaspésie, Québec; Canadian Journal of Earth Sciences, v. 17, no. 1, p. 106-119.

Neuman, R.B.
1968: Paleogeographic implications of Ordovician shelly fossils in the Magog belt of the Northern Appalachian Region; Studies of Appalachian Geology: Northern and Maritime, Interscience, John Wiley and Sons, Inc., New York, p. 35-48.

Oekentorp, K.
1976: Revision und typisiering des Genus **Paleofavosites** Twenhofel, 1914 (Coelenterata, Tabulata); Palaontologische Zeitschrift, v. 50, p. 151-192.

Poole, W.H. and Rodgers, J.
1972: Appalachian geotectonic elements of the Atlantic Provinces and southern Québec; XXIV International Geological Congress, Field Excursion A63-C-63, p. 138-146.

Powell, J.H. and Scrutton, C.T.
1978: Variation in the Silurian tabulate coral **Paleofavosites asper**, and the status of **Mesofavosites**; Palaeontology, v. 21, pt. 2, p. 307-319.

St-Julien, P., Hubert, C., Skidmore, W.B., and Béland, J.
1972: Appalachian structure and stratigraphy in Québec; XXIV International Geological Congress, Field Excursion A56-C56.

Schuchert, C. and Cooper, G.A.
1930: Upper Ordovician and Lower Devonian stratigraphy and paleontology of Percé, Québec. Part I. Stratigraphy and faunas; American Journal of Science, Fifth series, v. XX, no. 117, p. 161-176; Part II. New species from the Upper Ordovician of Percé; ibid., p. 265-288, 365-392.

Sheehan, P.M. and Lespérance, P.J.
1979: Late Ordovician (Ashgillian) brachiopods from the Percé region of Québec; Journal of Paleontology, v. 53, no. 4, p. 950-967.

Steele, H.M. and Sinclair, G.W.
1971: A Middle Ordovician fauna from Braeside, Ottawa Valley, Ontario; Geological Survey of Canada, Bulletin 211.

Stel, J.H.
1978: Environment and quantitative morphology of some Silurian tabulates from Gotland; Scripta Geologica, no. 47.

1979: Studies of the palaeobiology of favositids; Geologisch Instituut, Groningen Nederland, Publicatie Nr. 23g.

Sokolov, B.S.
1955: Paleozoic tabulates from the European part of the U.S.S.R. General problems of classification and history of the development of the tabulates (with characteristics of morphologically close groups); All Soviet Petroleum and Scientific Research in Geology and Prospecting Institute (VNIGRI), Trudy, new series, v. 85.

Sokolov, B.S. and Tesakov, Yu I.
1963: Paleozoic Tabulata of Siberia. Ordovician and Silurian Tabulata of the eastern part of Siberia; USSR Academy of Science, Siberian Branch, Institute of Geology and Geophysics.

Twenhofel, W.H.
1928: Geology of Anticosti Island; Geological Survey of Canada, Memoir 154.

1938: Geology and Paleontology of the Mingan Islands, Québec; Geological Society of America, Special Paper no. 11.

Wilson, A.E.
1948: Miscellaneous classes of fossils, Ottawa Formation, Ottawa-St. Lawrence Valley; Geological Survey of Canada, Bulletin 11.

3.

DEBRIS TORRENTS ACROSS THE ALASKA HIGHWAY NEAR MUNCHO LAKE, NORTHERN BRITISH COLUMBIA

Project 760059

G.H. Eisbacher
Cordilleran Geology Division, Vancouver

Eisbacher, G.H., Debris torrents across the Alaska Highway near Muncho Lake, northern British Columbia, in Current Research, Part C, Paper 80-1C, p. 29-36, 1980.

Abstract

Debris fans along the Rocky Mountain section of the Alaska Highway are the conspicuous result of seasonal springtime floods and rarer storm-triggered debris torrents. Torrents triggered by rainstorms have damaged the Alaska Highway in the summers of 1974, 1975, and 1979. During the storms unimpeded runoff from catchment basins cascaded into torrent runs which are choked with bouldery debris. The debris is derived from steep bluffs along the torrents by processes involving sliding and avalanching of surficial deposits. Potentially destructive debris torrents are different from the seasonal high-water flows in the same channels in that they culminate in surges of debris which often establish new wider tracks commonly involving existing roadbeds. Damage to road structures is particularly great where torrent tracks approach the roadbed at low angles. Flow concentration by artificial diking tends to increase the force of debris torrents.

Introduction

During the early summer months of 1974, 1975, and 1979 the Rocky Mountain section of the Alaska Highway in northern British Columbia was damaged by alpine debris torrents of previously unknown intensity. The Alaska Highway has been open since 1945, and, although closures had occurred before (e.g. 1963), the storms of 1974, 1975, and 1979 were certainly perceived as 'abnormal'. In each case vehicular traffic into the Yukon Territory and Alaska was interrupted at the height of the tourist season. Thus, the debris fans flanking the highway attracted considerable attention. In 1979 the author studied the geological setting of the larger fans in the area and, during the storm of June 30 – July 1, 1979, observed directly the mechanisms which trigger torrent damage along the highway.

Setting of the Debris Fans

The Muncho Lake area (Fig. 3.1) is part of the Muskwa Ranges of the northern Rocky Mountains. This region is underlain by bedrock formations composed of carbonate, quartzite, and calcareous slate of Proterozoic and Paleozoic age. Major bedrock structures trend north-northwesterly. The wide valley that hosts Muncho Lake follows an ancient fault zone separating predominantly slaty-calcareous rocks of the Terminal Range on the west from massive carbonate-quartzite formations of the Sentinel Range on the east. The difference in the dominating lithologies is well reflected in the pattern of vegetation.

On the predominantly slaty formations of the Terminal Range the upper forest limit, as shown on 1:50 000 scale topographic maps, is at about 1500 m and its position varies only slightly . The forests are mature and a thick carpet of underbrush and shrub protects the soil along the steep slopes; tributary creeks flow from incised gullies onto forest-covered fans. In contrast, the carbonate bedrock of the Sentinel Range has an upper forest limit at aobut 1300 m, 200 m lower than in the Terminal Range; it also varies much more than in the Terminal Range depending on geological detail and slope aspect. The upper catchment basins of the Sentinel Range are bare rock slopes which merge downwards with terraces composed of surficial debris. Bedrock ridges above the catchment basins rise to about 1200 m above the floor of the main valley. The bare carbonate slopes of the Sentinel Range favour rapid runoff. This is the main reason for the more

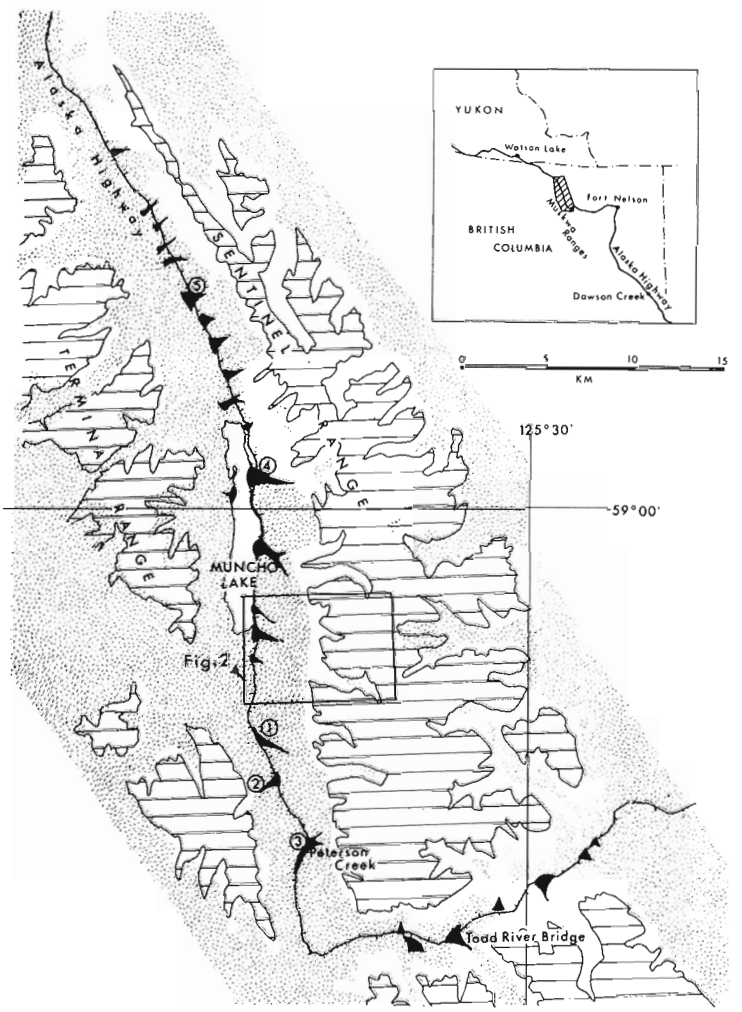

Locality 1 - Figure 3.5; 2 - Figure 3.4; 3 - Figure 3.8 A and B; 4 - Figure 3.7 A and B; 5 - Figure 3.9

Figure 3.1. *Index map showing the location of the active debris fans across the Alaska Highway in the Muncho Lake region. The stippled pattern indicates forest cover. Horizontal ruling outlines terrain above the 1500 m contour. Note the lower forest limit in the Sentinel Range.*

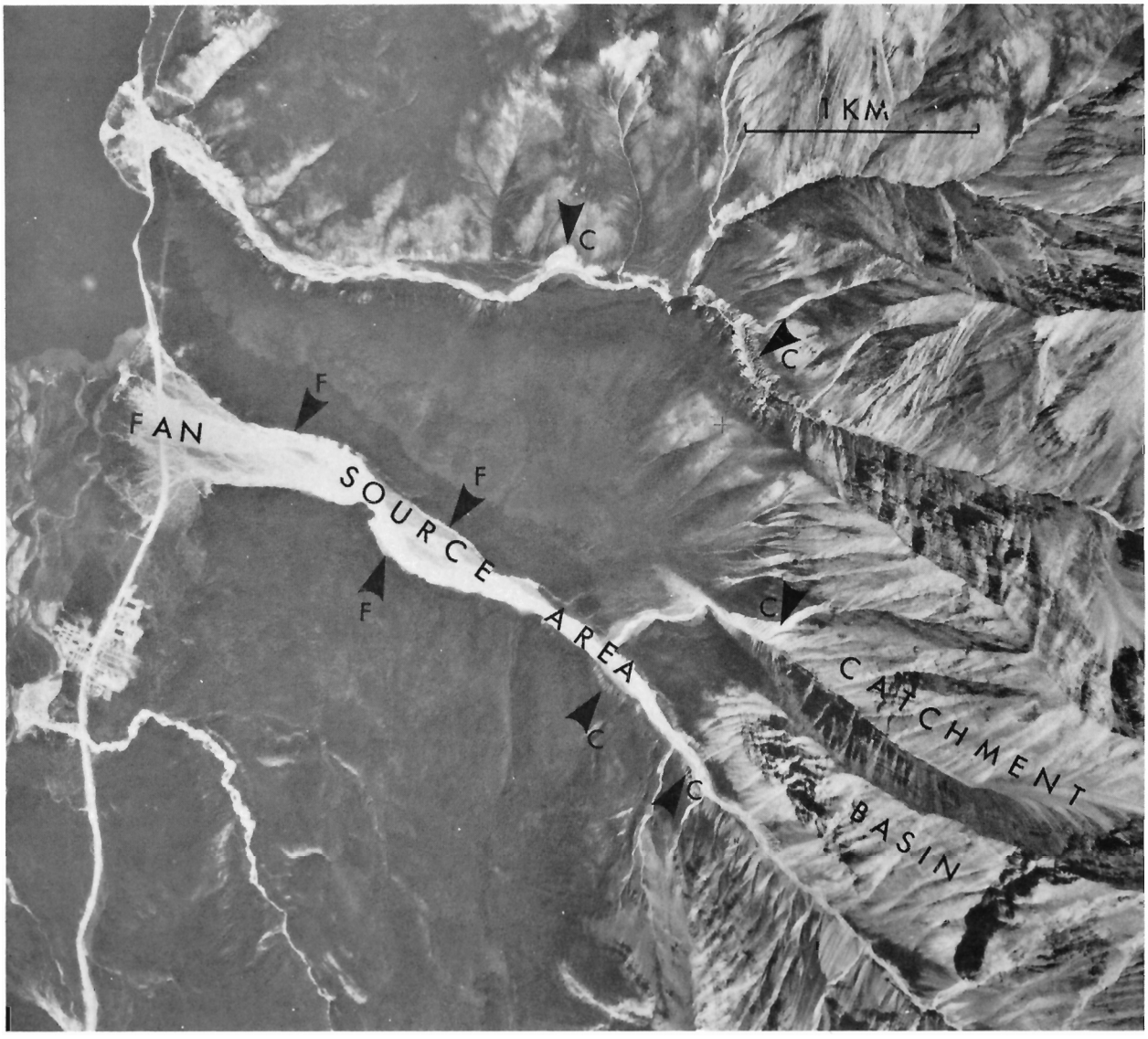

C = erosional scars in well-indurated late Pleistocene ice-contact deposits

F = erosional scars in less indurated inactive fan terraces.

Figure 3.2. *Air photo (EMR A 11484/384) of the south end of Muncho Lake, illustrating the complex transition from catchment basin to the debris sources and the depositional fans.*

obvious fan development in the Sentinel Range if compared to the Terminal Range. The lack or absence of vegetation thus is the subtle control which maintains a geomorphic process which has probably been active intermittently throughout postglacial time since the wasting of the Pleistocene glaciers bared the uplands of the northern Rocky Mountains.

Debris Sources

There are two types of debris sources in the Muncho Lake area: one type of debris is derived from well-indurated late Pleistocene ice-contact deposits and moraine, the other is derived from older debris fan terraces. Ice-contact deposits and moraine are characterized by chaotic to poorly stratified internal structure and very large blocks of bedrock. The terraced fan material is generally well stratified and grainsize tends to be smaller than in the ice-contact debris. The older fan surfaces are generally dissected by the 'active' fan which is the lowest segment of composite fan. What classifies as 'active' and what as 'inactive' segment of a fan complex often comes down to a somewhat arbitrary decision. Density of vegetation is a poor guide in this respect. During the storms of 1974, 1975, and 1979 many fan segments covered with stunted forest were invaded by torrents. It appears, however, that terraces rising 1.5 m and more above the fresh torrent tracks have significant soil development and are not engulfed by recurrent torrents. A 1.5 m elevation above the recent torrent tracks thus is a reasonable boundary outside of which the likelihood of torrent damage can be assumed to be small. This kind of incision of fresh debris tracks into older fans is only found in the upper part of most fans; on the more distal parts of the fans it is rarely possible to delimit 'active' and 'inactive' fan segments,

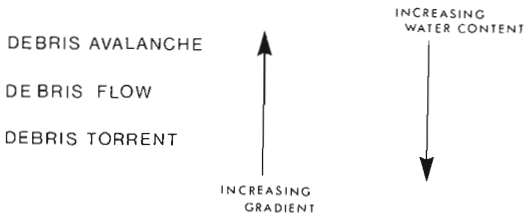

Figure 3.3. *Relationship between the terms debris torrent, debris flow, and debris avalanche, as used in this report.*

Figure 3.4

Typical debris sources situated along both sides of a torrent track incised into an older fan terrace covered thinly by spruce-pine forest (Locality 2 of Fig. 3.1). Debris avalanches choke the torrent run with coarse granular debris. Some of the Carbonate blocks in the bed of the torrent exceed 2 m in diameter.

particularly where debris lobes merge with others before joining the high-gradient braided flood plain along the floor of the valley.

The point sources of debris for the active fans are the erosional scars in fan terraces and ice-contact deposits (Fig. 3.2). The root of the torrent problem is therefore the intermittent accumulation of debris along the lower fan and supply of debris from persistent erosional point sources in the upper fan, mobilized by rapid runoff from the catchment basins.

The Mechanics of the Debris Torrents

Debris transport from the debris source areas to the lower segments of the fan involves three interrelated processes: debris avalanche, debris flow, and debris torrent. The relative importance of each depends on the local gradients and the amount of water partaking in the transport of debris. In simple terms, a debris torrent is the surge like channelized transport of an exceptional volume of bedload. Ridges and waves of debris occasionally emerge above the surface of the torrent, but, unlike debris flows, water still dominates. Debris flows are characterized by channelized debris transport where the mass attains a certain internal stiffness. In debris avalanches, on the far end of the spectrum, granular material tumbles and skips freely through high-gradient chutes or ravines.

The transition between these three modes of debris transport is shown schematically in Figure 3.3. The subtle changes of gradient, flow-velocity, and water content which determine the force of sudden surges of debris down pre-existing channels have been illustrated by Stini (1910), Johnson (1970), Scott and Gravlee (1968), Helley (1969), Shroba et al. (1979), Bergthaler (1975), Bradley and Mears (1980). During the surge stage of torrents the quantity of debris is not only dependant on the flow velocity of the water but is greatly influenced by the availability of debris along the torrent track. The reviews cited above all emphasize the perplexing variations in debris transport and accumulation along individual torrent tracks.

In the Muncho Lake area debris is generally available in abundance; however, the variety of stream profiles, local constrictions, and the short duration of concentrated runoff poses special problems in predicting on which fan what size of boulder will be transported for what distance. It appears from the reconnaissance that most fans in the Muncho Lake area are the result of debris torrents and that clast size decreases relatively regularly down the fans. Nevertheless, massive boulder flows seem to have been mobilized occasionally near bedrock-restricted channel reaches and debris avalanches are common along the upland banks. The best feeling for the geological factors controlling the severity of potential debris pulses can be obtained by following the evolution of the torrents from the catchement basin to points of debris input and onto the fan.

a) Catchment Basin

Most of the high carbonate slopes of the Sentinel Range are dissected by an anastomosing network of steep gullies which, during the early summer, receive meltwater from snowbanks. During rainstorms, the absence of vegetation creates instantaneous runoff which is funneled by the gullies to a point where several gullies combine to form a torrent. There the rushing water generally also encounters the first pockets of debris and depending on the gradient of the bed and the erodibility of debris bedload becomes significant.

b) Debris Source

Ice-contact deposits exposed as well indurated benches and pillars are poorly sorted and contain blocks of carbonate and quartzite up to 3 m in diameter. Randomly interbedded lenses of sand make up a more erodible matrix. In fan terraces the material is poorly indurated but the largest blocks are generally less than 1 m in diameter. The greatest destructive potential of torrents therefore arises in debris derived from ice-contact deposits where such are undercut by torrents in the vicinity of a road structure. Saturated bouldery debris collapses directly into the torrent or avalanches down chutes with characteristic v-shaped cross sections. The chutes tend to expand uphill, thus increasing the potential debris source (Fig. 3.4).

c) Depositional Fans

For most torrent creeks in the Muncho Lake area there are no clear boundaries between the debris source area and

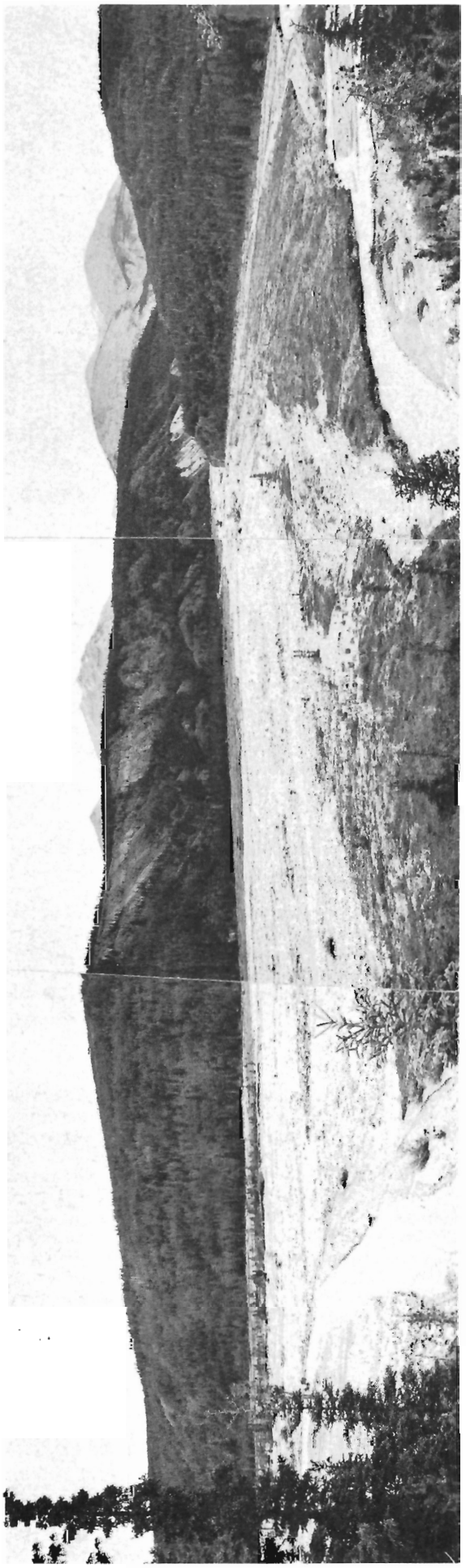

Figure 3.5. *Active debris fan at Locality 1 of Figure 3.1. Note the fresh torrent tracks between 'islands' of thin vegetation. In the background erosional bluffs of debris source terrain and the bare carbonate slopes of the catchment basins in the Sentinel Range.*

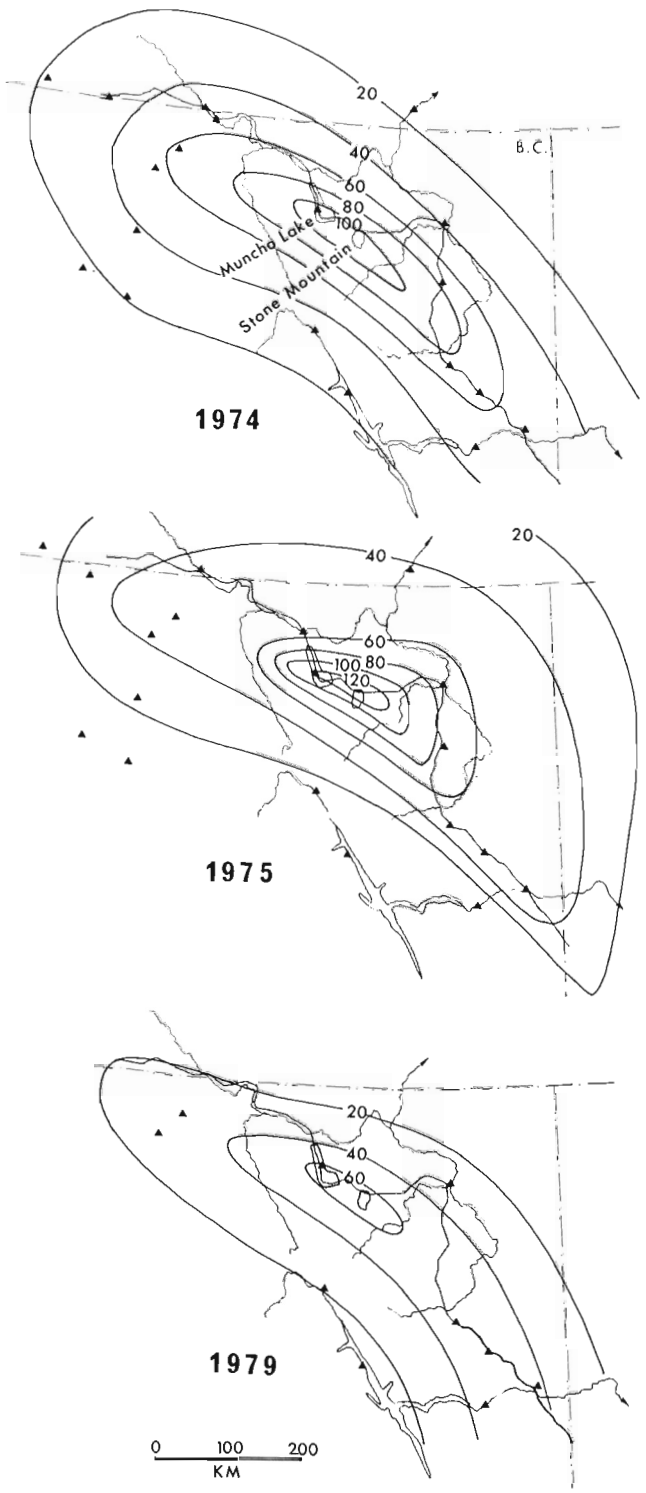

Figure 3.6. *Isohyets (lines of equal rainfall in mm) for the summer rainstorms of July 15-16, 1974, June 25-27, 1975, and June 30-July 1, 1979, along the Alaska Highway (Partly after Stobbe, 1975 and personnel communication). Triangles indicate rain gauges of the Atmospheric Environment Service of Environment Canada. Damage to the Alaska Highway was most severe in an oblong region including Muncho Lake and Stone Mountain provincial parks.*

Figure 3.7

A) Oblique view from the air onto debris fan prograding into Muncho Lake (Locality 4 of Figure 3.1). Photo was taken in summer of 1978. Note the course of the Alaska Highway and the dykes which confine and guide the torrent track towards a bridge underpass. The arrow indicates the sharp bend in the torrent track from where photo 3.7B was taken after the storm of 1979.

B) View of the torrent underpass on the morning of July 2 after passage of the debris torrents. The debris torrents took out the dyke and the elevated section of the highway and avoided the underpass. Stranded travellers for scale.

the aggrading fan. Since the upper fan segments are always incised into older fan terraces the fan head is part of the source area. The most active torrent tracks are immediately below the most conspicuous debris sources. Farther downstream elongated 'islands' of vegetation separate fresh debris tracks (Fig. 3.5). On these islands the pioneer vegetation consists of cottonwoods, followed by pine and spruce. Tree trunks are commonly scarred by the passing of previous torrents. However, none of the scars inflicted in 1974, 1975 and 1979 is more than 1 m above the ground. The debris differs in size down the fan: in the upper part and near point sources blocks of up to 2 to 3 m in diameter are common, in the distal parts of the fans oversize clasts are, in general, less than 0.5 m in diameter. This ubiquitous size grading suggests that truly massive debris flows do not contribute significantly to debris accumulation on the lower fans. The dominant process of deposition is torrents with wide lateral play and limited depth. However, where artificial dikes confine the torrents to narrower channels the full momentum of the debris torrent can be maintained far down the fan.

The Storms of July 15-16, and June 25-27, and June 30-July 1, 1979

Storms with the potential of triggering debris torrents in the Rocky Mountains seem to be similar to the well documented 'torrent' storms along the northern and southern fringes of the Alps (Aulitzky, 1973, p. 38-40). These are known to develop in mixed-air zones where warm humid air moves against colder mountain air. Stobbe (1974) analyzed the meteorological conditions leading up to the 1974 rainstorm along the Alaska Highway. He showed that it began with an atmospheric pressure low near Fort Nelson that was accompanied by local thunderstorms. The uplift of the warm air southwestward against the front of the Rockies, release of latent heat, and a cooler air mass on the west caused the intense rainfall on July 15 and 16, 1974 (Stobbe, 1974).

Approximate isohyets for the three storms outline the remarkable coincidence of the storm centres along the Rocky Mountain section of the Alaska Highway in the region of Muncho Lake and Stone Mountain provincial parks (Fig. 3.6).

Figure 3.8

A) Oblique view from the air onto the upper part of Peterson Creek (Locality 3 in Fig. 3.1). Photo taken in summer 1978. Note the bare carbonate catchment basin, the distinct forest limit, and the incised fan terraces. The active torrent tracks cross the Alaska Highway at a low angle through a wooden bridge and a culvert near the lower right corner of the photo.

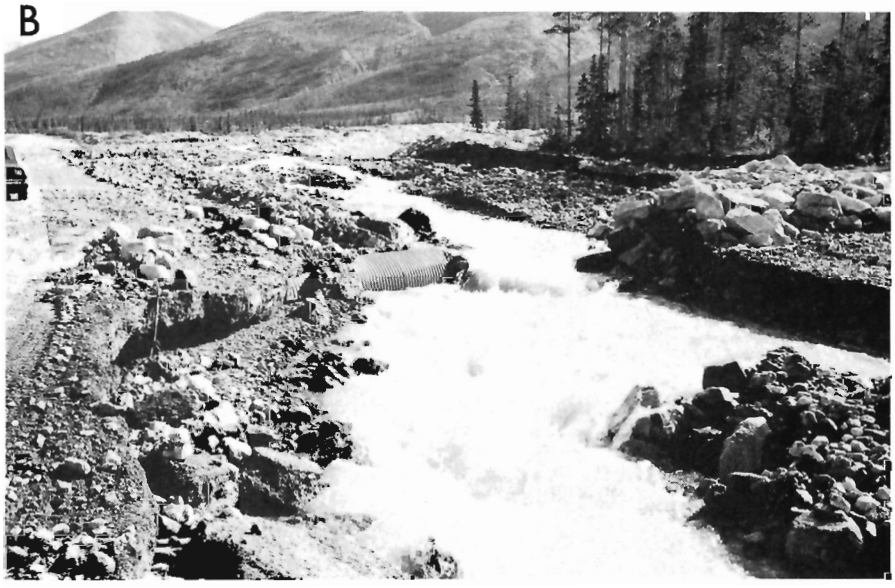

B) View of the new torrent track along the Peterson Creek underpasses on the morning of July 2 after the passage of the torrents. The underpasses were plugged, rendered ineffective and the uphill road ditch was used as the centre of a new track which eventually widened onto the road bed. Blocky debris on the right indicates depth of bebris during maximum torrent flow which was about 1 m.

Figure 3.9

Damage done to roadbed intersecting the highway at high angles (Locality 5 of Fig. 3.1). Note complete plugging of culvert to the left and embankment erosion by overflow.

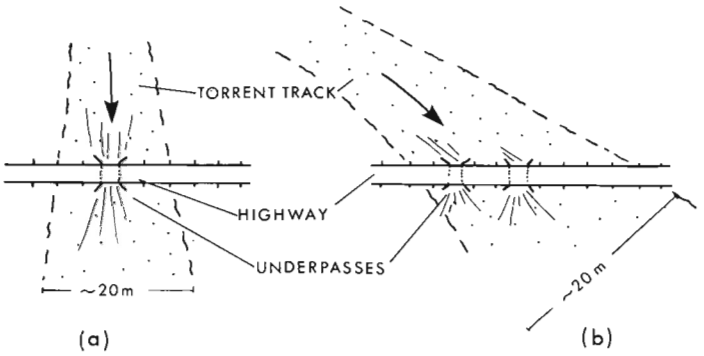

Figure 3.10. *High-angle (a) and low-angle (b) intersection of roadbed and torrent track. In case (b) damage tends to be much greater than in case (a).*

In 1975 and 1979 the focus of damage was somewhat farther to the southeast than in 1974, and the storm of 1979 was less intense than those of 1974 and 1975.

In 1979 the evolution of the torrents in the wake of the storm was observed by the author at Muncho Lake. Short periods of precipitation preceding the storm had occurred at temperatures which were low enough to cause snowfall on adjacent mountains above an elevation of 1800 m. At this time the creeks had passed through the spring flood stage and gone underground on the lower fans. The storm began in the early hours of June 30 and had two stages. Following a period of rainfall amounting to some 30 mm at Muncho Lake the creeks reappeared on the lower fans and turbid water flowed in a shifting network of braided channels. In the upper fan areas gravel was transported by rolling and saltation, accompanied by lateral erosion of low debris banks. Overflow occurred in gaps along the artificial dike system upstream from the Alaska Highway. However, culverts and bridges along the highway were still able to funnel the transported bedload across it. The debris torrents proper were triggered during the second phase of the storm, in the evening of July 1. In the five hours between 1900 and 2400h PDT of July 1, some 23 mm of rain were registered at the Muncho Lake rain gauge. The air was unusually warm and even the highest ridges east of Muncho Lake received all precipitation as rain. The effect of runoff in the catchment basins of the Sentiel Range was felt almost instantaneously and at 2 AM PDT, July 2, sections of the Alaska Highway were reported missing: the debris torrents had broken the confines of some dikes and natural channels, blocked culverts and bridges or simply bypassed them, reinstating a greater width of lateral play. Mobile longitudinal ridges of blocky debris formed in the channels thus triggering vigorous scour along the confining dikes. Low points along the channels were filled by pulsating debris, high points were eliminated by erosion. Erosion and deposition went on side by side. Boulders of up to 50 cm in diameter were pushed along within the chaotic mixture of murky water, sand, and gravel. Apart from minor debris slides and rockfalls along steep highway cuts and a debris flow near Mile Post 405 (east of the area discussed here) no serious slope instabilities were triggered by the rainstorm in the vicinity of the highway[1].

Torrent activity at Muncho Lake subsided as quickly as it had arisen and less intense rainfall beginning later on July 2, amounting to a total of about 30 mm, had no further effects. On July 4 most of the freely flowing water had disappeared again from the surface of the lower fans. On the upper fans the channels ran clear, fed by snow melt. The torrent cycle was complete. One delayed effect of the storm was a rise in the level of Muncho Lake amounting to about 50 cm; the lake level peaked on July 4 and reached to within 5 cm of a paved segment of the Alaska Highway along the southern lakeshore.

Effects on the Alaska Highway

The geological effect of the debris torrents on road structures was studied immediately after the passage of the storm in the morning of July 1, 1979. Prior to the storm the lower segments of some fans had been modified by dikes (See Fig. 3.7). The material for these dikes had been scooped largely from the bottom of natural channels and thus had the composition of torrent bedload. Only locally, coarse riprap quarried form bedrock had been used also. Dikes composed of natural bedload were attacked vigorously by the torrents as soon as the flow was restricted by the dikes (Fig. 3.7B). Several dikes were breached and some were even eroded from the outside in. The destructive impact of the torrents on the highway was a function of the elevation of the roadbed relative to the surface of the fan and the angle between the torrent track and roadbed. Where the roadbed was cut into the fan the only significant damage was accumulation of debris; where the highway surface was elevated above the adjacent fan the torrent carved gashes across the roadbed or, upon reaching the upslope ditches, ran parallel to the roadbed thus scouring it from above (Fig. 3.8A, B). Where the torrent tracks approached the highway at angles close to 90° the main geological effect was plugging of culverts and bridges, giving rise to erosional overflow (Fig. 3.9). Where tracks approached the highway at low angles the roadbed tended to guide the debris torrent for up to 200 m. Therefore the greatest damage from debris torrents was experienced where an elevated section of the road was approached by the debris torrent at a low angle (Fig. 3.10). There, the momentum of the coarse debris was too great to make the required sharp deflection into the artificial underpasses. In these situations a complex pattern of erosion and deposition quickly disrupted the road underpasses and long sections of highway downstream from the crossing were lost (e.g. near Toad River bridge, Peterson Creek, and Mile Post 460). In all cases culverts and bridges, although partially or totally filled with debris were left behind intact. The frequent comment heard from travellers stranded along the highway that 'the bridges were out' was not correct. Bridges and culverts were still in place but the torrents had shifted their course elsewhere or simply widened their bed to a more braided pattern: erosional gashes across the highway alternated with newly accumulated ridges of debris.

The lessons from these observations are the following:

1. Abnormal debris torrents such as those of 1974, 1975, and 1979 are probably the main geologic agents building the debris fans in the Muncho Lake area. The events of 1974, 1975, and 1979 cannot be considered freak 'catastrophies' in the geological sense.
2. Debris torrents tend to flow in braided tracks several tens of metres wide but generally less than 1.5 m deep. Confinement of the torrents by dikes increases their power to erode and transport. Diking systems are effective only with riprap composed of block sizes larger than those found in the natural torrent run.
3. On the fans debris torrents tend to bypass abrupt bends and notches to maintain an overall straight track by filling hollows and eroding edges along the channels.
4. Given a certain lateral play the depth of debris torrents is not great (in general less than 1.5 m). Highway underpasses are efficient when at right angles to the torrent track and when some width of lateral play is allowed for (e.g. several parallel culverts).

[1] During the more intense storms of 1974 and/or 1975 debris slides and avalanches occurred on several slopes facing the main valley.

Economic Impact

Debris torrent activity along the Rocky Mountain Section of the Alaska Highway is a natural geological hazard with considerable impact on this region. The most significant is interruption of traffic into the Yukon Territory. However,the torrents in 1974, 1975, and 1979 had additional significance as they occurred at a time when tourism was at its peak. In the area affected by the destructive torrents a number of restaurant-motel-gas station establishments depend directly on this highly seasonal tourist business. After a preliminary enquiry in 1979 the author estimates that the highway closure, which lasted for a week, meant a total loss of revenue of 50 000 to 100 000 dollars for these people. Secondary effects include a reduced tourist traffic following the re-opening of the highway and an even longer-range bad 'reputation' of the highway caused by exaggerated and even fantastic stories distributed by the media and the travelling public. These effects cannot be directly evaluated. The cost of highway reconstruction in 1974 and 1975 was about 2 000 000 and 1 300 000 dollars respectively (Dept. of Public Works, unpublished reports).

Conclusions

Storm-triggered debris torrents are a significant hazard to be reckoned with along all transportation routes in the northern Rocky Mountains. This hazard was not clearly perceived until the 1974 storm in the Muncho Lake area. Intermittent debris torrents are probably the main reaosn for conspicuous lack of vegetation on debris fans. The three natural factors which contribute most significantly to the torrent problem are: a) unvegetated catchment basins in carbonate bedrock, b) erodible point sources of debris along the lower slopes, and c) abnormal rainstorms such as those of 1974, 1975, and 1979. Experience during the three storms suggests that greatest damage occurs where channelized torrents cross elevated rock sections at low angles. Debris torrent flow is best accommodated by underpasses through roadbeds that cross the torrent tracks at angles close to 90° and that allow for a certain width of flow.

Acknowledgments

The author wishes to thank J. Clague for critical comments on the manuscript. S.T. Stobbe, Atmospheric Environment Sevices, Whitehorse, supplied data on the storms of 1974 and 1975. The gracious hospitality of Frauke and Theo Prystawick, Highland Glen Lodge, Muncho Lake, is gratefully acknowledged.

References

Aulitzky, H.
1974: Endangered Alpine regions and disaster prevention measures; Nature and Environment Series 6, Council of Europe, Strasbourg, 103 p.

Bergthaler, J.
1975: Hochwasseranalyse und Hochwasserprognose bei Wildbächen; Interpraevent (International Symposium), Volume 1, Innsbruck, p. 191-206.

Bradley, W.C. and Mears, A.I.
1980: Calculations of flows needed to transport coarse fraction of Boulder Creek alluvium at Boulder, Colorado: Summary; Geological Society of America Bulletin, Part I., v. 91, p. 135-138.

Helley, E.J.
1969: Field measurement of the initiation of large bed particle motion in Blue Creek near Klamath, California; United States Geological Survey, Professional Paper 562-G, p. G1-G19.

Johnson, A.M.
1970: Physical processes in geology; Freeman, Cooper Co., San Francisco, p. 433-459.

Scott, K.M. and Gravlee, G.C.
1968: Flood surge on the Rubicon River, California – Hydrology, hydraulics and boulder transport; United States Geological Survey, Professional Paper 422-M, p. M1-M40.

Shroba, R.R., Schmidt, P.W., Crosby, E.J., and Hansen, W.R.
1979: Storm and Flood of July 31 – August 1, 1976, in the Big Thompson River and Cache la Poudra River Basins, Larimer and Weld Counties, Colorado – Geologic and geomorphic effecs in the Big Thompson Canyon area, Larimer County; United States Geological Survey, Professional Paper 1115, Part B., p. 87-148.

Stini, J.
1910: Die Muren; Wagner, Innsbruck, 139 p.

Stobbe, S.T.
1975: Alaska Highway rainstorm of July 15-16, 1974; Environment Canada – Atmospheric Environment Service, Internal Report 830, 19 p.

4. STRATIGRAPHY AND PALEONTOLOGY OF THE UPPER YAKOUN FORMATION (JURASSIC) IN ALLIFORD BAY SYNCLINE, QUEEN CHARLOTTE ISLANDS, BRITISH COLUMBIA

Project 750035

H.W. Tipper and B.E.B. Cameron
Cordilleran Geology Division, Vancouver

Tipper, H.W. and Cameron, B.E.B., Stratigraphy and paleontology of the Upper Yakoun Formation (Jurassic) in Alliford Bay Syncline, Queen Charlotte Islands, British Columbia; in Current Research, Part C, Geological Survey of Canada, Paper 80-1C, p. 37-44, 1980.

Abstract

The upper part of Yakoun Formation at Skidegate Inlet, Queen Charlotte Islands comprises sedimentary rocks which enclose abundant pelecypods, belemnites, ammonites, foraminifers, ostracods, and less common gastropods, corals, and radiolaria. Several ammonite faunas provide a basis for dating the beds, namely the Late Bathonian ***Iniskinites*** *fauna, the Bathonian and/or Callovian* ***Seymourites*** *fauna, and the Early Callovian* ***Kepplerites spinosum*** *fauna. Two new microfaunas are also identified and dated by the ammonite fauna, a probable Late Bathonian* ***Pseudolamarckina*** *fauna and the Early Callovian* ***Reinholdella*** *fauna.*

Introduction

A detailed study of the stratigraphy and paleontology of the upper part of the Yakoun Formation was undertaken for brief periods in the summers of 1976, 1978 and 1979 (Tipper, 1975, 1976, 1977; Tipper and Cameron, 1979). The purpose of the present paper is to present preliminary results relating to the strata of the Alliford Bay syncline exposed in Alliford Bay and the east end of Maude Island. We are indebted to Hans Frebold, Ottawa, for identification of new ammonoid faunas collected and for many discussions on the biostratigraphic problems. Identification of the foraminifers is currently underway by Cameron.

Previous Work

The history of geological studies in Queen Charlotte Islands has been adequately described by McLearn (1949), MacKenzie (1916), and Clapp (1914). The early confusion resulting from the inability to separate Jurassic and Cretaceous rocks beacuse of insufficient knowledge of the fossil faunas greatly impeded the work. A major step was taken by MacKenzie (1916) who recognized strata that could be paleontologically dated as Cretaceous and as Jurassic and (?) Triassic separated by a major unconformity. The Jurassic and Triassic rocks were correlated with the Vancouver Group and were divided into two conformable formations, the Yakoun Formation of Middle Jurassic age and the Maude Formation of Early Jurassic and Triassic (?) age.

McLearn in 1921 undertook a detailed study of the Jurassic rocks, particularly the Yakoun Formation (McLearn, 1949). He recognized that there was an upper nonvolcanic marine sedimentary section that contrasted markedly with a predominantly volcanic section lower in the formation. He recognized two distinct ammonoid faunal assemblages and dated the upper one, the **Seymourites** fauna, as Callovian and the lower one, the Stephanoceras fauna, as Bajocian. His measured sections (1949, p. 11-12) clearly illustrate the lithologic differences between the upper and lower parts of the formation.

Sutherland Brown (1968) studied the Yakoun Formation in greater detail throughout Queen Charlotte Islands. He measured the type section on Maude Island but extended it lower than McLearn's section to include volcanic fragmentals previously included in the underlying Maude Formation. He established five members, the upper one, Member E, probably corresponds to McLearn's "sandstone and shale" at the top of the formation. Unfortunately a misidentification of an ammonite found in Member E lead Sutherland Brown to suggest that the entire type section was of Bajocian age. Recent restudy of the fauna, supplemented by new collections, indicates a Late Bathonian fauna as well as the Callovian **Seymourites** fauna of McLearn present within Member E.

Lithology

The sediments of the upper part of Yakoun Formation show no similarity to the volcanics of the lower members nor to the sediments of the lower members which are everywhere more tuffaceous and a minor part of the section (Fig. 4.1). The ammonoid faunas are distinctly different as well. For these reasons it is correct to consider the upper marine sedimentary section as a distinct member of the Yakoun Formation.

The siltstone beds (Y4, Table 4.1, Fig. 4.1) near the top of the section exposed in Alliford Bay are grey to grey-buff, soft, poorly laminated and contain pelecypods, a few ammonites, rare belemnites, rare ostracods, and abundant foraminifers. Some of the macrofossils are contained in small concretions.

The sandstone beds (Y3, Table 4.1, Fig. 4.1) are mainly massive volcanic concretionary sands passing downward into well-bedded sands 10 cm or less in thickness. Generally the bedding is even and planar but on the northest flank of the syncline near Kwuna Point crossbedding suggests a current direction from the north or northeast. The massive sands and the thicker beds below are commonly concretionary with large pelecypods and relativley rare belemnites and ammonites embedded in the concretions. The sands generally weather buff or pale green and the clastic material is volcanogenic. These sandstones are apparently distributed throughout all parts of the syncline. Associated faunas are McLearn's **Seymourites** fauna and the Late Bathonian fauna.

Below the sandstones are a variety of rocks (Y2, Table 4.1, Fig. 4.1). On Robber Point are soft grey siltstones replete with pelecypods, gastropods, ostracods, and foraminifers. Near Kwuna Point rocks consist of volcanic breccia and tuffaceous sandstone. At Fossil Point coarse volcanic sandstones and tuffs outcrop. Although these rocks are generally volcanic-clastics it is not clear whether they were derived from contemporary volcanism or from the earlier Yakoun volcanic rocks. Probably both possibilities are correct and some of these rocks are the last products of Mesozoic marine volcanism in Queen Charlotte Islands.

The base of the upper Yakoun member is marked by a pebble conglomerate composed of closely packed, well-rounded and sorted clasts of volcanic rock derived from the

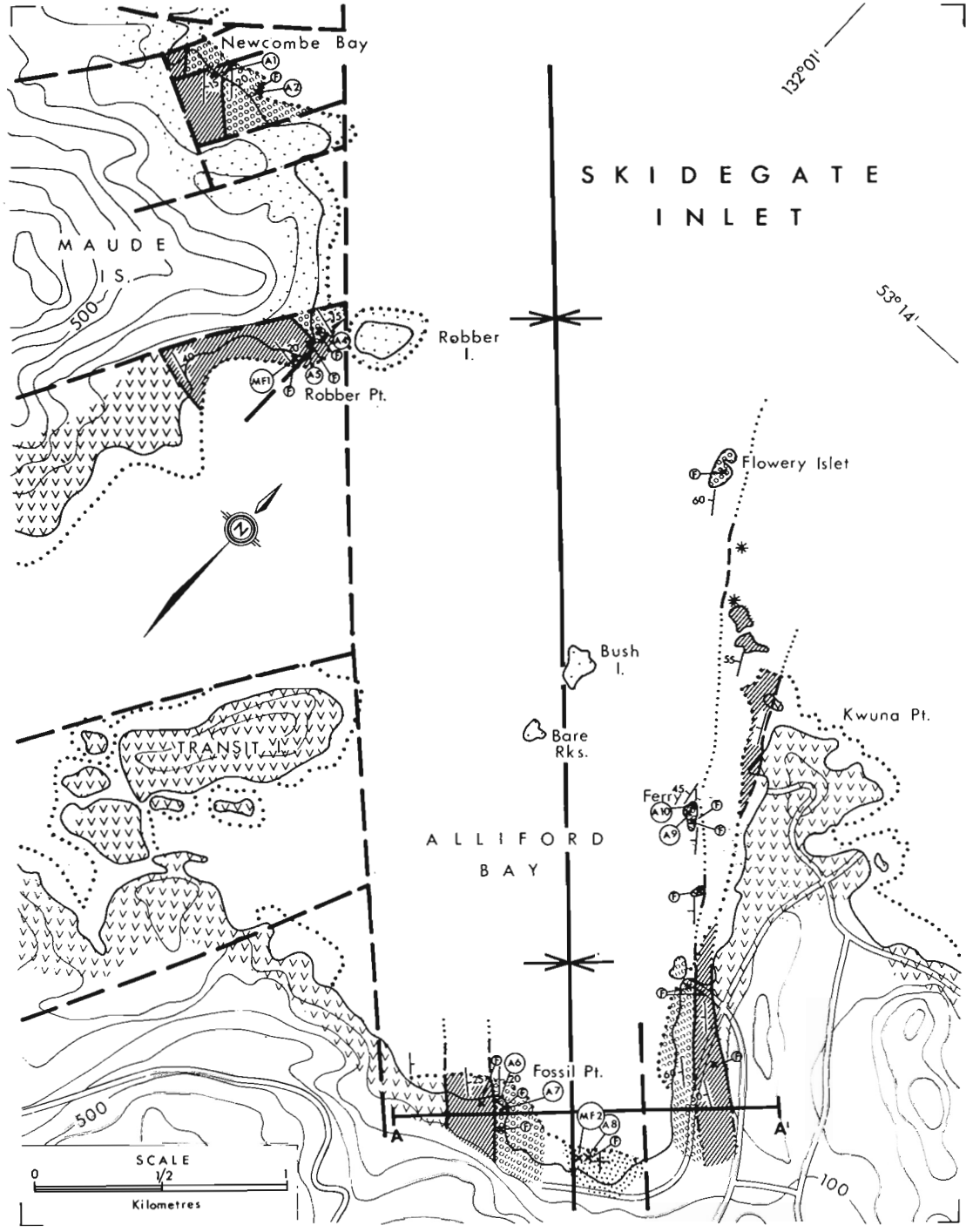

LEGEND

L. CRET

Albian

HAIDA FM.: Green and grey sandstone, silty shale

MIDDLE JURASSIC

UPPER MEMBERS OF YAKOUN FORMATION

Callovian

Y4 Grey shale and siltstone; minor fine sandstone

Bathonian - Callovian

Y3 Buff weathering sandstone, grey sandstone, grey siltstone

Late Bathonian and (?) earlier

Y2 Green weathering coarse sandstone, volcanic breccia and tuff, grey shale and siltstone, pebble conglomerate

LOWER MEMBER OF YAKOUN FORMATION

Middle Bajocian

Y1 Volcanic breccia, tuff, volcanic sandstone; minor volcanic siltstone.

Contacts (defined, approximate, assumed)

Attitudes (inclined, horizontal)

Syncline

Lineaments and faults

Fossil localities

Ammonites A3

Microfossils MF

Macrofossils exclusive of ammonites F

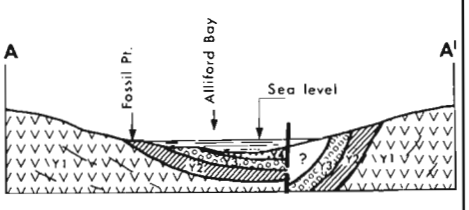

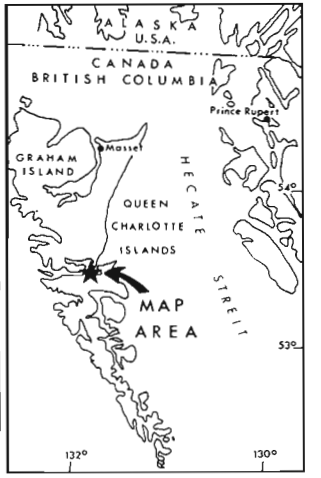

Figure 4.1. *Geology of Alliford Bay Syncline.*

Table 4.1

Distribution of faunas within sections of the upper part of the Yakoun Formation

Age of Map-units	Lithology of Map-units		ALLIFORD BAY			MAUDE ISLAND	
			Ferry Island	Southeast end	Fossil Point	Robber Point	Newcombe Bay
Early Callovian	Y4	grey shale and siltstone	———	*Reinholdella* - MF 2 *Kepplerites* cf. *K. spinosum* (Imlay)	———	———	———
contact not exposed							
Early Callovian ?	Y3	grey siltstone	*Cadoceras* cf. *C. doroschini* (Eichwald)	———	No Ammonites	———	———
		buff sandstone	*Cadoceras* sp. juven.				
		grey sandstone	*Oppelia (Oxycerites) aspidoides* (Oppel)	———	*Oxycerites* sp. indet. *Lytoceras* sp.	———	———
		buff sandstone	*Kepplerites (Seymourites)* sp.	———	*Kepplerites (Seymourites) loganianus* (Whiteaves) *K. (S.) ingrahami* McLearn *K. (S.) newcombii* McLearn *K. (S.)* sp. indet.	*Kepplerites (Seymourites)* sp. *Cadoceras* cf. *C. catostoma* Pompeckj *Cadoceras*? sp. indet.	*Kepplerites (Seymourites) plenus* McLearn *K. (S.)* cf. *K. (S.) abruptus* McLearn *K. (S.) multus* McLearn *K. (S.) gitinsi* McLearn *K. (S.) torrensi* McLearn *K. (S.) penderi* McLearn *K. (S.)* sp. *Cadoceras*? sp. *Phylloceras (Partschiceras) grantzi* Imlay
Late Bathonian ?							
Late Bathonian	Y2	coarse green sandstone / volc. tuff and breccia	Several specimens of *Iniskinites* were collected in 1895 by C. F. Newcombe at Alliford Bay but precise localities were not given.	———		*Iniskinites cepoides* (Whiteaves) *I.* cf. *I. cepoides* (Whiteaves)	*Iniskinites cepoides* (Whiteaves) *I. mclearni* Frebold
		buff concretionary sandstone	No Ammonites	———	No Ammonites	No Ammonites	———
		grey siltstone and shale	No Ammonites	———	———	*Pseudolamarckina* -MFI No Ammonites	———
and ? earlier		sandstone, tuff, pebble congl.	No Ammonites	———	No Ammonites	No Ammonites	———

GSC

lower Yakoun members. The bed is seldom more than a metre thick but in places there are two or more beds separated by fine volcanic breccia.

Origin of the Yakoun Formation

According to Sutherland Brown (1968, p. 75) much of the later volcanism of Yakoun Formation resulted "when a series of vents opened up along a line subparallel and west of the later Sandspit fault". This would be, presumably, a northwest trending line just east of Alliford Bay syncline. This assumption is supported by the meagre evidence in the sediments of current transport from a volcanic highland in the north or northeast. The sediments of the upper Yakoun Formation indicate an entirely volcanic area of provenance.

The sediments of the upper Yakoun Formation were deposited directly on the lower part, apparently without a significant hiatus. The sediments that underlie the Late Bathonian green sandstone evidently filled an irregular basin within a volcanic terrane. Rapid facies changes, varying lithology and differences in thickness all suggest rapid and irregular deposition until a shelf-like surface was attained. Subsequently coarse sand was deposited more or less evenly over a wide area under shallow water conditions wherein a prolific pelecypod fauna thrived. The youngest beds are finer grained, generally siltstone with some shale, but as these are exposed only in part of Alliford Bay, their extent is unknown.

Alliford Bay Syncline and Structural Relations

In Queen Charlotte Islands, Sutherland Brown (1968, p. 156-159) concluded, folds "are of less importance than the faults and may largely be secondary features". The Alliford Bay syncline (Fig. 4.1), although poorly exposed, appears to be a simple structure whose axis trends northwesterly and plunges for the most part gently northwesterly. At the southeast end it may be nearly horizontal or plunge slightly southeasterly. Several normal faults apparently cut the structure but none are of great displacement. The east limb generally dips more steeply than the west limb. These upper members of the Yakoun appear to have been folded with the volcanics of the lower Yakoun but the overlying Cretaceous rocks (Haida Formation) or Robber Island and on islands in

Alliford Bay may or may not have been deformed at the same time. They are at or near the centre of the syncline and have gentle dips or are flat-lying. The upper Yakoun beds are structurally conformable with the lower Yakoun volcanics but, as has been pointed out by many workers, are overlain with angular discordance by the Lower Cretaceous Haida Formation (Sutherland Brown, 1968, p. 68).

The Ammonite Faunas

The ammonites of the Yakoun Formation were described and discussed by McLearn and Frebold. In Geological Survey Bulletin 12, McLearn discussed the "Seymourites" fauna (1949) which he previously described in National Museum of Canada Bulletin 54 (McLearn, 1929). Frebold recently published a report on the Late Bathonian **"Iniskinites** fauna" (1979) and identified and discussed the other ammonid faunas in internal reports. The following is a summation of these reports with additional comments and observations for which Tipper is responsible.

Iniskinites faunas

The late Bathonian **Iniskinites** fauna, the oldest ammonites of this section, has been described by Frebold (1979). The material was collected by several workers, including the authors, but the stratigraphic position of the fauna was established by the present study. The fauna is known in Newcombe Bay and at Robber Point on Maude Island and was collected from some unknown locality in Alliford Bay (Fig. 4.1). On Robber Point it is contained in a coarse green weathering sandstone (Y2) approximately 5 feet below the **Seymourites** fauna. This relationship was recently confirmed in Newcombe Bay. Nowhere has the **Iniskinites** fauna been found associated with the **Seymourites** fauna and it is concluded that in this area the two faunas are mutually exclusive. No other ammonite genera was found associated with **Iniskinites.**

The macrofaunal assemblage of the sandstones of this section generally comprises mature individuals. Seventy five per cent of the ammonites of the **Seymourites** fauna are fully mature when compared with **Seymourites** faunas of the western Cordillera. Belemnites are generally large and apparently mature. The whole sandstone section is characterized by a preponderance of large, mature bivalves. The **Iniskinites** fauna, made up of **Iniskinites cepoides, I.** cf. **I. cepoides,** and **I. mclearni,** are invariably nearly the same size, between 50 and 75 mm in diameter. The writers have seen a total of about 15 specimens obtained from at least three locations in the Alliford Bay syncline. If compared to the **Iniskinites** fauna of Alaska (Imlay, 1975) or of northern Yukon and mainland British Columbia (Frebold, 1978) the Yakoun **Iniskinites** fauna, seems to be immature or juvenile and can be compared, as Frebold did (1979, p. 64), to small or immature forms of **Iniskinites martini** or **I. intermedius** which are known to reach diameters of 125 mm. Because our **Iniskinites** fauna is from a section characterized by a majority of mature forms are all about the same size, and are distributed over a wide area, it is reasonable to suggest that they are fully mature forms and as such are distinctly different from the **Iniskinites** fauna in Alaska, northern Yukon or mainland British Columbia. Its relationship to the **Seymourites** fauna, which here overlies it, also differs to the relationship in Alaska or mainland British Columbia where the two genera occur together.

The Queen Charlotte **Iniskinites** fauna is the most southerly Canadian occurrence of the genus, and considering the possibility of right lateral transport of Queen Charlotte Islands relative to the mainland, its original position, relative to the other **Iniskinites** faunas, may have been much farther south. In Taseko Lakes, Ashcroft, and Harrison Lake map areas to the southeast, **Seymourites** faunas or faunas of the same age are known, but no **Iniskinites** faunas have been reported. The absence of **Iniskinites** could be explained as nondeposition or erosion of Upper Bathonian beds as on Vancouver Island where known Callovian beds rest directly on Triassic rocks.

Frebold (1978) presented evidence that the **Iniskinites** fauna of Alaska, northern Yukon, and mainland British Columbia should be considered Late Bathonian. He subsequently (1979) placed the Queen Charlotte **Iniskinites** in the Late Bathonian. However, if it is a different fauna, as suggested above, and if it is in reality older than the Seymourites fauna, then it could be slightly older than the **Iniskinites** faunas from elsewhere. In Alaska (Imlay, 1953b, p. 50) **Iniskinites** (formerly **Kheraiceras) martini** and **I. intermedius** which is similar to the **Iniskinites** fauna of Queen Charlotte Islands (Frebold, 1979, p. 64), is reported to be among the first species of this genus to appear in the Chinitna Formation. Occurrences of the genus **Iniskinites** are so far only known in Alaska, Northern Yukon, mainland British Columbia and Queen Charlotte Islands.

Seymourites fauna

The age of this fauna in Queen Charlotte Islands was considered by Buckman to be Callovian (in McLearn 1927) and McLearn suggests a correlation with Bathonian-Callovian faunas in East Greenland (McLearn, 1949, p. 17). Species of the Queen Charlotte fauna are known in Alaska (Imlay, 1953b) and some forms on mainland British Columbia are similar to the fauna although preservation is poor. No species from Queen Charlotte Islands have been reported from the Fernie Group of the Canadian Rocky Mountain nor from Western United States (Imlay, 1953a). This seemingly anomalous distribution may be a factor of preservation and collecting but in light of the distribution of the **Iniskinites** fauna (see above) may be of significance. Imlay (1975, p. 15) pointed out that the Alaskan Callovian ammonites have "nothing in common specifically with the western interior of North America and Arctic Canada".

Frebold's determination of the **Iniskinites** fauna as Late Bathonian and the occurrence of **Kepplerites (Seymourites)** with **Iniskinites** in Alaska and mainland British Columbia (Imlay 1953b, p. 50; Frebold, 1978, p. 2) placed the Callovian age of the **Seymourites** fauna in doubt. Clearly some species of **Kepplerites (Seymourites)** must range into Late Bathonian if Frebold's determination is to be accepted. Imlay (1980) described three unnamed species of **Kepplerites** associated with the Late Bathonian. In Alaska several of the Queen Charlotte species apparently have the same range as, or overlap with, **Iniskinites** (Imlay, 1975) but some of them were found above the apparent range of **Iniskinites.** On this Frebold commented as follows: "The age of the beds immediately overlying the beds with the **"Iniskinites** fauna" is uncertain. Imlay (personal communication, 1978) suggested that the upper part of his Alaskan **Catostoma** Zone that does not contain **Iniskinites** may belong to the Early Callovian. The same age may be considered for the beds with **Lilloettia** spp. and **Kepplerites** spp. above the **"Iniskinites** fauna" in the Smithers map area of Britsh Columbia. It would seem possible for the age of the Seymourites fauna, therefore, to be Late Bathonian or Early Callovian or both.

The occurrence of **Cadoceras** cf. **C. catostoma** at Robber Point (Table 4.1) points to the probable correlation with Imlay's Catostoma Zone in Alaska (Imlay, 1975). This occurrence is a single specimen collected by James Richardson in 1872 but the precise location is somewhat in doubt although the presence of **Cadoceras**? sp. indet. collected by the authors suggests the possibility of inclusion with the **Seymourites** fauna. No conclusions should be reached at this time based on a single imprecisely located specimen.

Oxycerites fauna

Although a meagre fauna, consisting of **Oppelia (Oxycerites) aspidoides** (Oppel)., **O. (O.)** sp. undet., and **Lytoceras** sp. undet., the **Oxycerites** fauna is significant in determining the age of the section. **Oxycerites** is known in many areas of the western Cordillera but its age and range have not been established nor have there been many specific identifications. In Alaska one specifically undetermined **Oxycerites** was said to be similar in general appearance to **Oppelia (Oxycerites) aspidoides** (Oppel) with similar suture lines (Imlay 1953b, p. 73). It is recorded as ranging through the middle two thirds of the Tonnie Siltstone Member of the Chinitna Formation overlapping the **Iniskinites** range and coinciding with much of the **Kepplerites (Seymourites)** range. If the Alaskan fauna is similar to the Queen Charlotte fauna in age range, it is probable that there is little, if any, difference in age between the **Oxycerites** and **Seymourites** faunas in Queen Charlotte Islands, a reasonable assumption as they are no more than 3 m apart stratigraphically. Frebold (unpublished internal report) notes, regarding the age of the fauna, that "according to Oppel (1862, p. 148) the species occurs in Europe immediately below the beds with '**Ammonites** macrocephalus' and always in the highest beds of the 'Bathgruppe'".

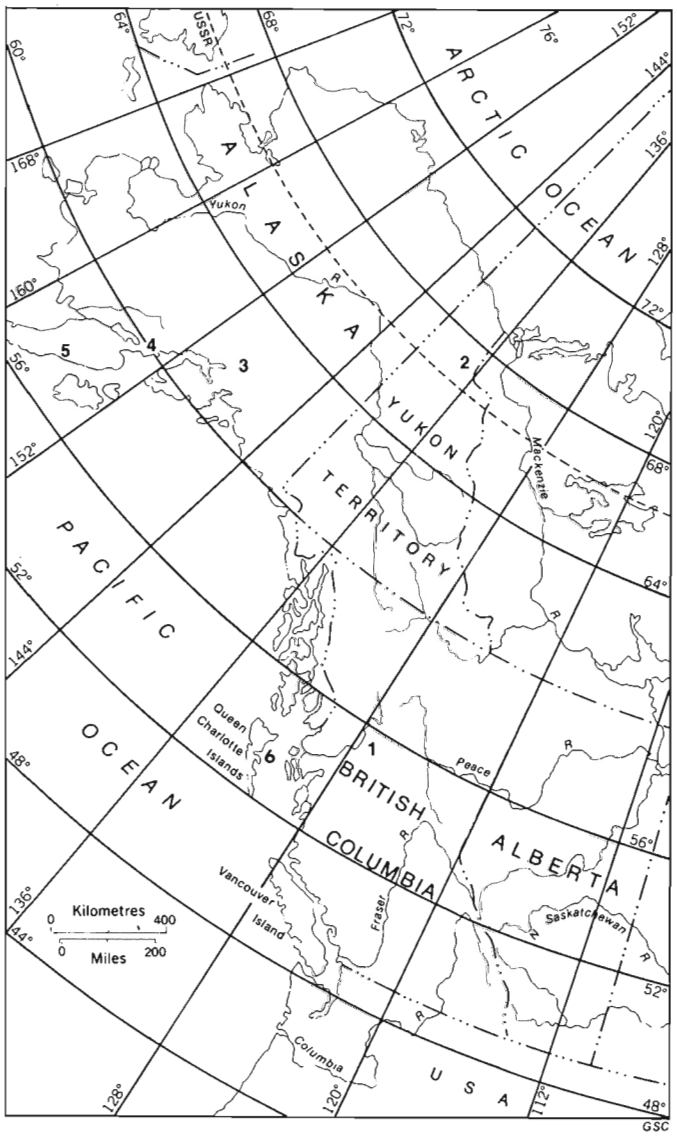

1. Smithers map-area
2. Porcupine River
3. Talkeetna Mountains
4. Tuxedni Bay-Chinitna Bay-Iniskin Bay area
5. Puale Bay-Wide Bay area
6. Queen Charlotte Islands

Figure 4.2. *Locations of* ***Iniskinites*** *occurrences in British Columbia, southern Alaska and northern Yukon.*

Cadoceras fauna

At one locality two specimens of **Cadoceras** were found. One is a juvenile form and the other has affinities to **Cadoceras doroschini** (Eichwald). No age can be assigned with certainty on the basis of these specimens.

Kepplerites spinosum fauna

The stratigraphically highest ammonites found belong to the single species **Kepplerites spinosum** (Imlay). No other ammonites are associated. In southern Alaska the species occurs somewhat above most other species of **Kepplerites,** above all species of **Iniskinites,** but is found associated with **Oxycerites,** some species of **Lilloettia,** and various species of **Cadoceras.** For these reasons this fauna is considered to be no older than Early Callovian.

Other Ammonites

In the British Columbia Provincial Museum in Victoria, there are several specimens, apparently of one species, collected by C.F. Newcombe in 1897 in Alliford Bay. No precise locality is given and the writers were unable to find more of the same species. They are cadoceratids unlike any forms found to date and have not been studied. They probably come from below the **Kepplerites spinosum** fauna.

The Microfaunas

Within the rocks of the upper Yakoun Formation, two distinctive microfossil assemblages are recognized. They were recovered from shale and siltstone exposed at Robber Point and from the southeast end of Alliford Bay. The foraminifers of the Queen Charlotte Islands Jurassic have not been described, consequently for purposes of this report the age assignment of the enclosing rocks is based on the associated or closely associated ammonite faunas.

Pseudolamarckina fauna – MF 1

Approximately 60 species of foraminifers were recovered from the grey siltstone and shale exposed at Robber Point, Maude Island. Approximately 20 m of soft shale are exposed below the more prominent buff concretionary sandstones. Conspicuous elements of the microfauna include species of **Pseudolamarckina, Citharina, Lenticulina, Astacolus, Lingulina s. l., Palmula (Falsopalmula), Tristix, Marginulina** as well as other agglutinating, polymorphinid, and miliolid genera.

Samples from the base of the 20 m shale sequence have yielded only plant debris and a few very thin shelled pelecypods. This is thought to represent marginal marine conditions. Near the top of the shale exposure, however, a great increase in diversity of foraminifers, ostracods, pelecypods, and gastropods is believed to be reflective of a minor marine transgression.

The **Pseudolamarckina** fauna occurs stratigraphically below the **Iniskinites** ammonite fauna of Late Bathonian age and above the Middle Bajocian ammonite faunas which occur lower in the Yakoun Formation on Maude Island. Insofar as Late Bajocian rocks are rare on the Pacific margin and there appears to be stratigraphic continuity between the rocks carrying the **Pseudolamarckina** fauna and the **Iniskinites** fauna, a Late Bathonian age is preferred for the microfauna.

Reinholdella fauna – MF 2

Approximately 70 species of foraminifers were recovered from the grey siltstone and shale sequence at the southeast end of Alliford Bay. Approximately 10 m of strata exposed here represent the youngest Jurassic rocks thus far encountered in the Alliford Bay syncline. The fauna is characterized by species of **Reinholdella, Lenticulina, Astacolus, Citharina, Marginulina, Pseudonodosaria** and others which at the specific level are almost entirely different from species of the same genera occurring in the Bathonian **Pseudolamarckina** fauna.

In addition to the rich microfauna, pelecypods, belemnites and ammonites have been collected. The age of rocks on the basis of the ammonites including **Kepplerites** sp. cf. **K. spinosum** (Imlay) is Early Callovian.

Age and Correlation of the Upper Yakoun

The age of the upper part of Yakoun Formation (i.e. the sedimentary upper member) is at least as old as Late Bathonian and as young as Early Callovian. The youngest guide ammonites in the lower Yakoun are no younger than the top of Humphresianum Zone of the Middle Bajocian (i.e. top of Middle Bajocian) in terms of the Northwest European zonation but this is many metres of volcanic and sedimentary strata below the base of the upper Yakoun. In this interval, represented mainly by volcanic fragmental rocks, there are rare thin beds and lenses with a few brachiopods, belemnites, or pelecypods. Nothing is of significance in suggesting an age assignment but McLearn (1949, p. 16) proposed a time range of late Bajocian through Bathonian on the basis of apparent conformability throughout the formation for this volcanic interval.

Table 4.2

Correlation of the Bathonian-Callovian faunas and formations of Queen Charlotte Islands with those of Alaska, Northern Yukon, and British Columbia

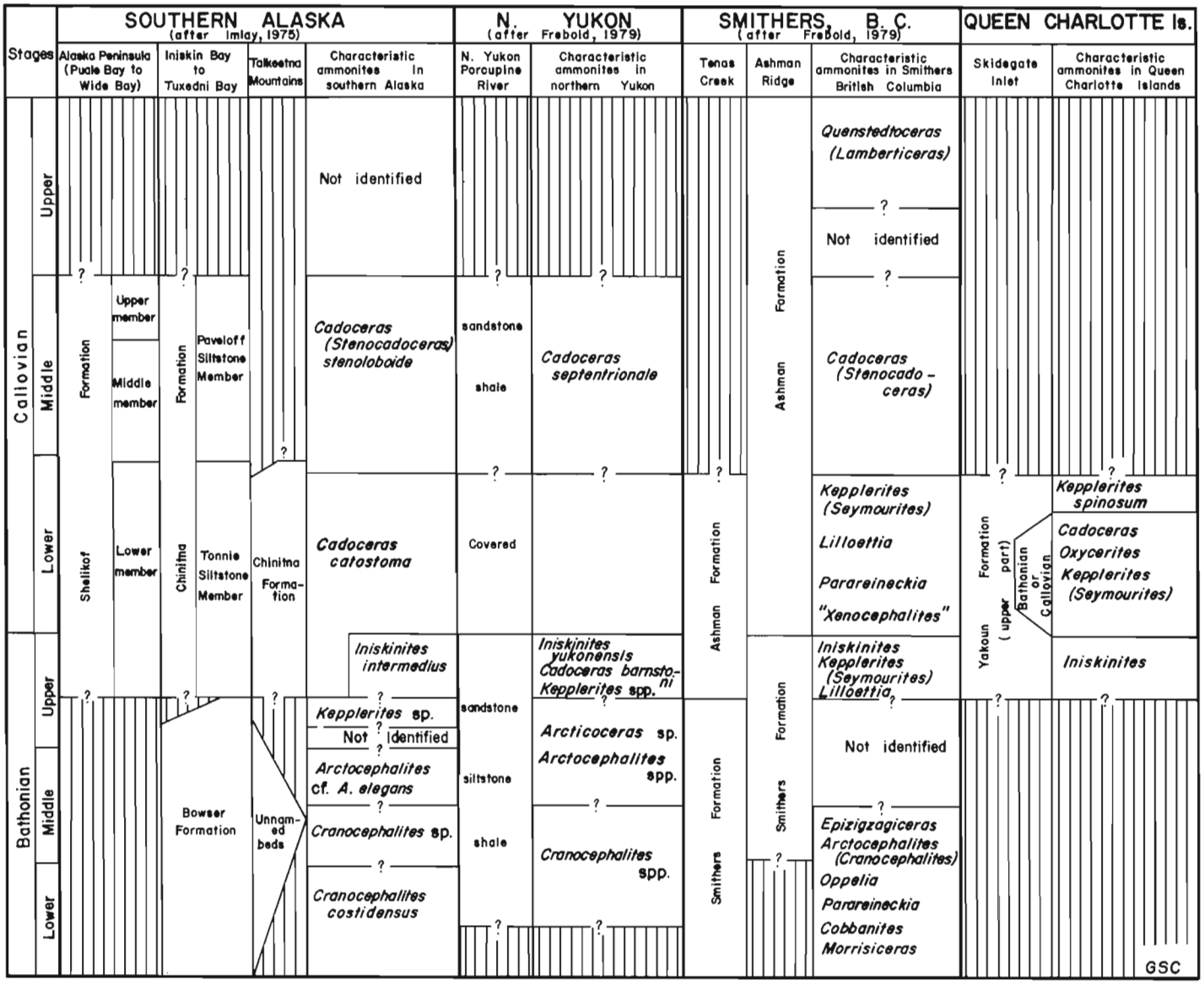

The base of the upper Yakoun is marked by a pebble conglomerate that contrasts markedly with the underlying strata. Although the formation is structurally conformable throughout, this conglomerate could mark an important hiatus of considerable duration. The massively bedded, poorly sorted volcanic sandstones and volcanic fragmental rocks of the lower part of the upper Yakoun suggest rather rapid deposition and the limited distribution of shale and siltstone indicate a relatively short period of accumulation. If the beds of the upper Yakoun below the **Iniskinites** fauna represent a brief period of deposition they could have been deposited within the time span of the **Iniskinites** fauna, that is Late Bathonian.

The **Iniskinites** fauna as already stated is correlated with the **Iniskinites** fauna of southern Alaska, northern Yukon, and mainland British Columbia (Fig. 4.2) and assigned a Late Bathonian age (Frebold, 1978, 1979) although there could be a small discrepancy. This correlates with the **Iniskinites intermedius** subzone of Imlay's **Cadoceras catostoma** zone in southern Alaska. If the **Seymourites** fauna of Queen Charlotte Islands is truly younger than the range of **Iniskinites** then there is a reasonable argument that the **Seymourites** fauna is indeed Callovian, as stated by McLearn (1949). If such were the case it would seem reasonable to correlate the fauna with that of the upper part of Imlay's **Cadoceras catostoma** zone, i.e. above the **Iniskinites intermedius** subzone, and place the base of the Callovian at the top of the subzone. But it is known in Alaska, northern Yukon, and mainland British Columbia that the two genera do occur together hence a Callovian or Bathonian age must be entertained for the Seymourites fauna.

The **Oxycerites** and **Cadoceras** faunas do little to resolve the age problem. Arguments can be made on the basis of their occurrnece in Alaska that they are either Bathonian or Callovian.

The highest fauna known in Queen Charlotte Islands, **Kepplerites spinosum,** occurs above the known range of **Iniskinites** in Alaska and almost into the range of **Pseudocadoceras** which, according to Imlay (1975, p. 13), would start in the upper part of the Lower Callovian. It would seem probable that **Kepplerites spinosum** in Alaska is at least Early Callovian in age. Apparently the species is not abundant and Imlay (1975, p. 14) does not place much reliance on it for an age determination. Imlay's conclusion with regard to the age of the basal beds of the Chinitna Formation in Alaska, with which the upper Yakoun must be correlated, is as follows: "Nonetheless, the basal beds could be older than the **calloviense** zone and even as old as the latest Bathonian provided that the earliest occurrences of **Cadoceras** and **Paracadoceras** in East Greenland are actually latest Bathonian as proposed by Callomon (1959, p. 507-509)."

The upper member of Yakoun Formation can be correlated with parts of the Chinitna and Shelikof formations in Alaska, with parts of the Smithers and Ashman formations on mainland British Columbia, with the "Big Bend section" on Porcupine River, Northern Yukon, and with unnamed beds elsewhere in British Columbia. These correlations are illustrated in Table 4.2

Imlay has pointed out that in southern Alaska the ammonites of these Bathonian-Callovian strata "are dominated by genera characteristic of the Boreal realm, such as **Kepplerites, Cadoceras,** and **Pseudocadoceras,** but include several genera characteristic of the Pacific realm, such as **Xenocephalites, Lilloettia,** and **Parareineckia.** They also include two genera, **Iniskinites** and **Chinitnites. . . .**" (Imlay, 1975, p. 15). Also on the specific level the Callovian ammonites of southern Alaska, British Columbia, Oregon and California have much in common but differ from those in the western interior of North America and Arctic Canada (Imlay, 1975, p. 15). This similarity of faunas almost certainly holds between southern Alaska and mainland British Columbia but the Queen Charlotte Islands faunas display some unique characteristics. In the Queen Charlotte Islands, the Bathonian-Callovian strata have the boreal genera **Kepplerites** and **Cadoceras,** which even on the specific level may be closely related to Alaska and mainland British Columbia faunas. However none of the Pacific realm genera mentioned above is present except **Iniskinites** and on the specific level there appear to be no **Iniskinites** species in common between Queen Charlotte Islands and other areas. Significantly the Yakoun strata alone contain colonial corals (Montastrea? according to Sutherland Brown, 1968, p. 73) which may signify warmer water conditions of deposition in contrast to the beds in Alaska or mainland British Columbia. These faunas may represent a Pacific faunal province as suggested by Imlay (1975, p. 15) but the Queen Charlotte Islands may represent a part that was originally farther south than the other regions and was transported northerly by strike-slip movement as suggested above. If such were the case the juxtaposition of southern Alaska against mainland British Columbia at the latitude of the Smithers area may suggest the amount of offset on one or a family of strike-slip faults; a displacement of 1000 km or more.

References

Callomon, J.H.
1959: The ammonite zones of the Middle Jurassic beds of East Greenland; Geological Magazine, v. 96, no. 6, p. 505-513.

Clapp, C.H.
1914: A geological reconnaissance on Graham Island; Geological Survey of Canada, Summary Report, 1912, p. 12-14.

Frebold, H.
1978: Ammonites from the Late Bathonian "Iniskinites Fauna" of Central British Columbia; Geological Survey of Canada, Bulletin 307.

1979: Occurrence of the Upper Bathonian ammonite genus **Iniskinites** in the Queen Charlotte Islands, British Columbia; in Current Research, Part C, Geological Survey of Canada, Paper 79-1C, p. 63-66.

Imlay, R.W.
1953a: Callovian (Jurassic) ammonites from the United States and Alaska; Part I, Western Interior United States; United States Geological Survey, Professional Paper 249-A.

1953b: Callovian (Jurassic) ammonites from the United States and Alaska; Part 2, Alaska Peninsula and Cook Inlet regions; United States Geological Survey, Professional Paper 249-B.

1975: Stratigraphic distribution and zonation of Jurassic (Callovian) ammonites in southern Alaska; United States Geological Survey, Professional Paper 836.

1980: Middle Jurassic (Bathonian) ammonites from Southern Alaska; United States Geological Survey, Professional Paper 1091.

MacKenzie, J.D.
1916: Geology of Graham Island, British Columbia; Geological Survey of Canada, Memoir 88.

McLearn, F.H.
1927: Some Canadian Jurassic faunas; Royal Society Canada, Transactions 3rd Ser., v. 21, sec. IV, p. 61-73.

McLearn, F.H. (cont.)
1929: Contributions to the stratigraphy and palaeontology of Skidegate Inlet, Queen Charlotte Islands, B.C.; National Museum of Canada, Bulletin 54.

1949: Jurassic formations of Maude Island and Alliford Bay, Skidegate Inlet, Queen Charlotte Islands, British Columbia; Geological Survey of Canada, Bulletin 12.

Sutherland Brown, A.
1968: Geology of the Queen Charlotte Islands; British Columbia Department of Mines and Petroleum Resources, Bulletin 54.

Tipper, H.W.
1975: Taseko Lakes (92C) and Smithers (93L) map-areas, British Columbia; in Report of Activities, Part A, Geological Survey of Canada, Paper 75-1A.

Tipper, H.W. (cont.)
1976: Biostratigraphic study of Mesozoic Rocks in Intermontane and Insular belts of the Canadian Cordillera, British Columbia; in Report of Activities, Part A, Geological Survey of Canada, Paper 76-1A.

1977: Jurassic studies in Queen Charlotte Islands, Harbledown Island and Taseko Lakes area, British Columbia; in Report of Activities, Part A, Geological Survey of Canada, Paper 77-1A.

Tipper, H.W. and Cameron, B.E.B.
1979: Jurassic biostratigraphy of Skidegate Inlet, Queen Charlotte Islands; in Current Research, Part A, Geological Survey of Canada, Paper 79-1A.

THE FORT SMITH RADIOACTIVE BELT, NORTHWEST TERRITORIES

Project 760045

B.W. Charbonneau
Resource Geophysics and Geochemistry Division

Charbonneau, B.W., The Fort Smith radioactive belt, Northwest Territories; in Current Research, Part C, Geological Survey of Canada, Paper 80-1C, p. 45-57, 1980.

Abstract

The Fort Smith Belt is an elongate zone, about 200 km x 50 km, extending from the East Arm of Great Slave Lake southerly into northeastern Alberta. The major feature of the belt is that it is one of the most radioactive regions so far recognized in the Canadian Shield. Potassium, uranium, and thorium are all enriched but the greatest increase is in thorium. The dominant rock type underlying the area is a foliated porphyritic granite. This rock contains an average of about 80 ppm thorium (with areas of tens of square kilometres containing up to 200 ppm) and approximately 11 ppm uranium. In places, dark elongate zones rich in biotite, apatite, and opaque minerals within the porphyritic granite may contain an order of magnitude more uranium and thorium than the porphyry. Radioactive minerals within both the porphyry and the dark zones are principally monazite (containing up to 16% ThO_2) and isolated grains of uraninite. This foliated porphyritic granite is interpreted as being pre- or syntectonic with respect to the Hudsonian event because its foliation parallels that of the surrounding rocks. There has been subsequent deformation.

The second characteristic feature of the Fort Smith Belt is the development of a peripheral zone where eU is enriched relative to eTh correlating mainly with granitoid rocks which surround the thorium-rich area and wherein ratios of eU/eTh exceed 1:2 (compared to the crustal average of 1:4). Uranium may have moved laterally into this marginal area from the thorium-rich porphyry, possibly in a vapour phase. There is a possibility that concentrations of uranium as well as other metals such as Cu, Mo, Zn, Sn, and W could exist in the porphyry and its margin in appropriate chemical and/or structural traps.

The radioactive granitic rocks of the Fort Smith Belt are adjacent to uranium-thorium occurrences in the nearby Proterozoic Nonacho sediments but whether or not a genetic relationship exists between the two situations is uncertain.

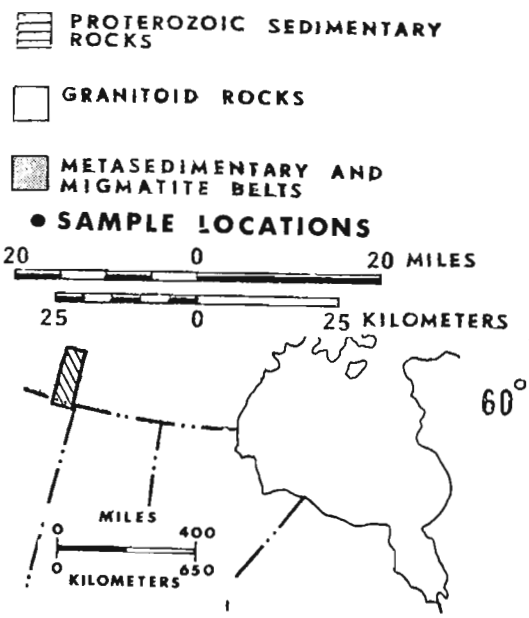

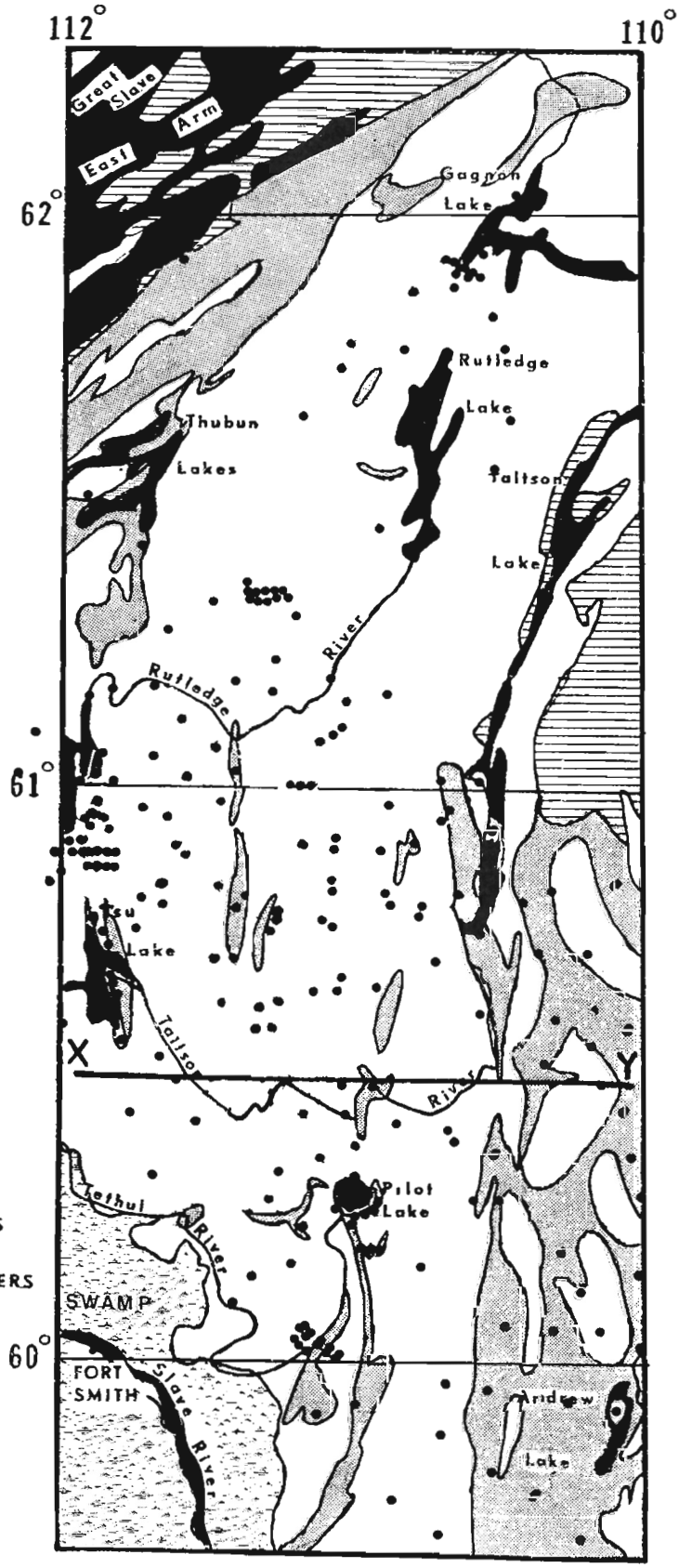

Figure 5.1

The Fort Smith Belt – regional geology and sample sites.

Introduction

An area extending from northeastern Alberta to the East Arm of Great Slave Lake in the Northwest Territories, underlain primarily by granitoid rocks of Archean and/or Proterozoic age, has been recognized as a belt of high radioactivity for several years. Airborne gamma ray spectrometer surveys (Darnley et al., 1971; Darnley and Grasty, 1972) mapped the potassium, uranium and thorium distribution within the area.

Ground investigations were conducted by the Geological Survey of Canada during parts of the 1970, 1973, and 1975 field seasons to determine the cause of the radioelement concentrations and their distribution patterns, and preliminary reports were published by Charbonneau (1971) and Richardson and Charbonneau (1973). Samples collected at 220 sites within the survey area were analyzed in the gamma ray laboratory at the Geological Survey of Canada for K, eU, and eTh. In addition, in three selected areas in situ determinations of K, eU, eTh were made and samples were collected at 100 m intervals along traverses totalling about 30 km.

Figure 5.1 shows the regional geology of the survey area compiled from Stockwell et al. (1968), Henderson (1939), Wilson (1941), and Riley (1960) and the locations of the sites visited during the investigations described in this paper. The area is one of moderate topographic relief with ridges rising to about 100 m above the lakes and marshes. The percentage of outcrop is high but a thin cover of glacial drift is generally present in topographic depressions.

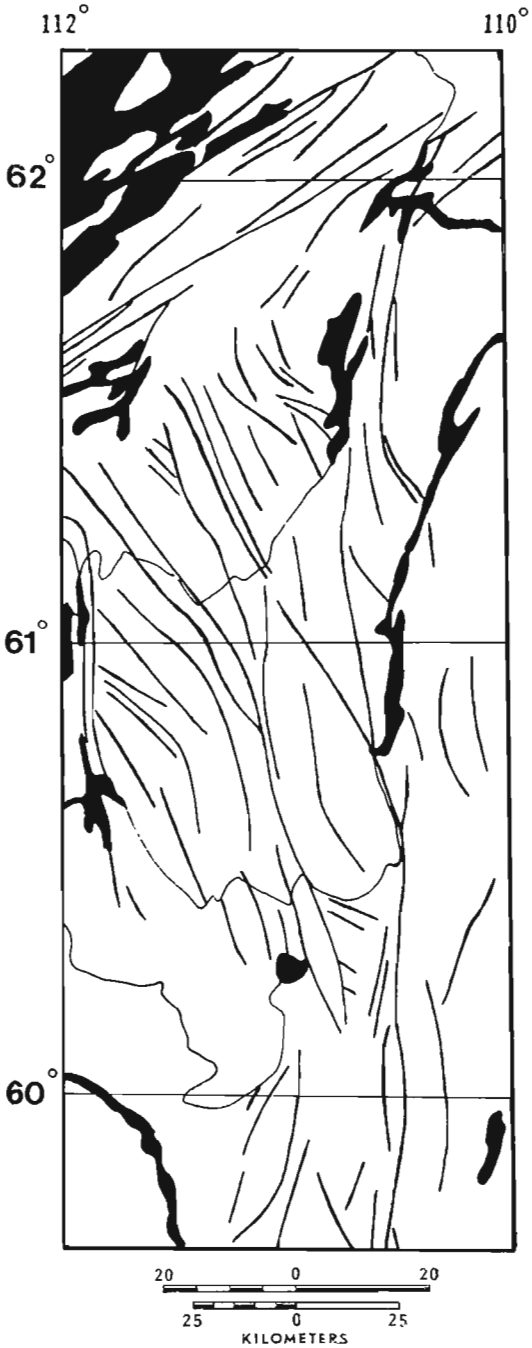

Figure 5.2. Major lineaments from satellite image.

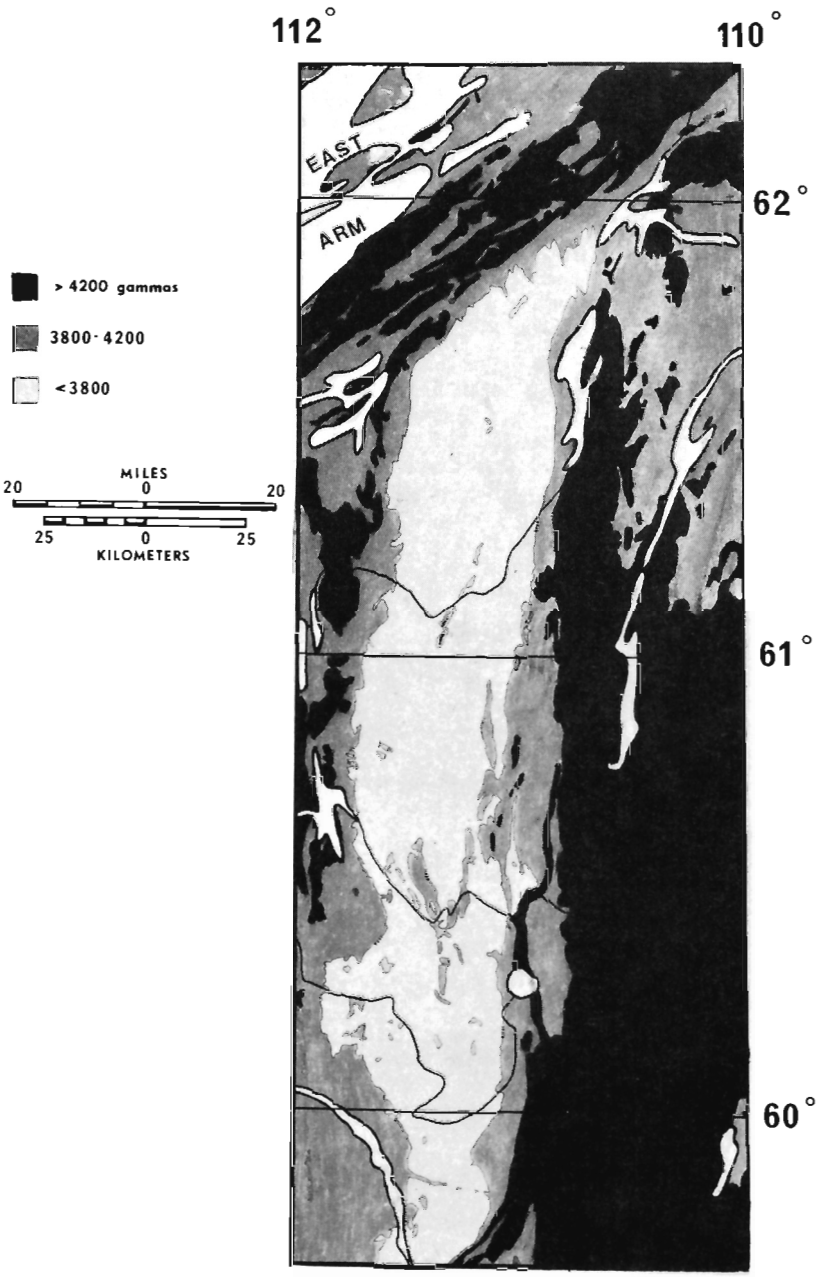

Figure 5.3. Aeromagnetic map of the Fort Smith Belt.

Geology

The oldest formations, metasedimentary and migmatite belts of the Archean Tazin Group, outcrop principally in the northern and eastern parts of the area. All gradations exist from paragneiss to granitoid gneisses and well-foliated granitic porphyries along the central axis of the area. Metamorphism may have reached granulite grade (on the basis of the presence of a garnet-cordierite-sillimanite-spinel assemblage in some of the paragneisses) which was then overprinted by an amphibolite grade metamorphism (Fraser, 1978).

The central axis of the Fort Smith Belt is underlain primarily by granitic rocks. The time of their emplacement is uncertain and more than one period of intrusion and/or granitization may be represented (Bostock, 1980). The concordant relationships of the granitic bodies to the folded enclosing metasedimentary rock suggest that granitic emplacement was pre- or syntectonic. Initial metamorphism and intrusion may have occurred during the Kenoran orogeny (Stockwell et al., 1970) although Archean ages do not appear in the available K-Ar dates. The granitic rocks within the Fort Smith Belt cluster about 1800 Ma on the Isotopic Age Map of Canada (Wanless, 1969), possibly as a result of heating and recrystallization resetting the original age during the Hudsonian orogeny. Pegmatites cutting the gneissic complex of the Tazin Group give Rb-Sr ages in excess of 2500 Ma near Andrew Lake in the southwest part of the survey area (Baadsgaard and Godfrey, 1972).

The Proterozoic sedimentary rocks of the Nonacho Group consist mainly of conglomerates, arkoses, and shales. Diabase dykes in the Fort Smith area generally strike northwesterly. Quartz veins are common, and apparently are of different ages (Henderson, 1939).

Figure 5.2 shows the major lineaments in the Fort Smith Belt and adjacent areas that are visible on Landsat satellite images. Three main periods of faulting have been recognized in the northern part of the area by Reinhardt (1969). The first trends northeastwards and is parallel to the

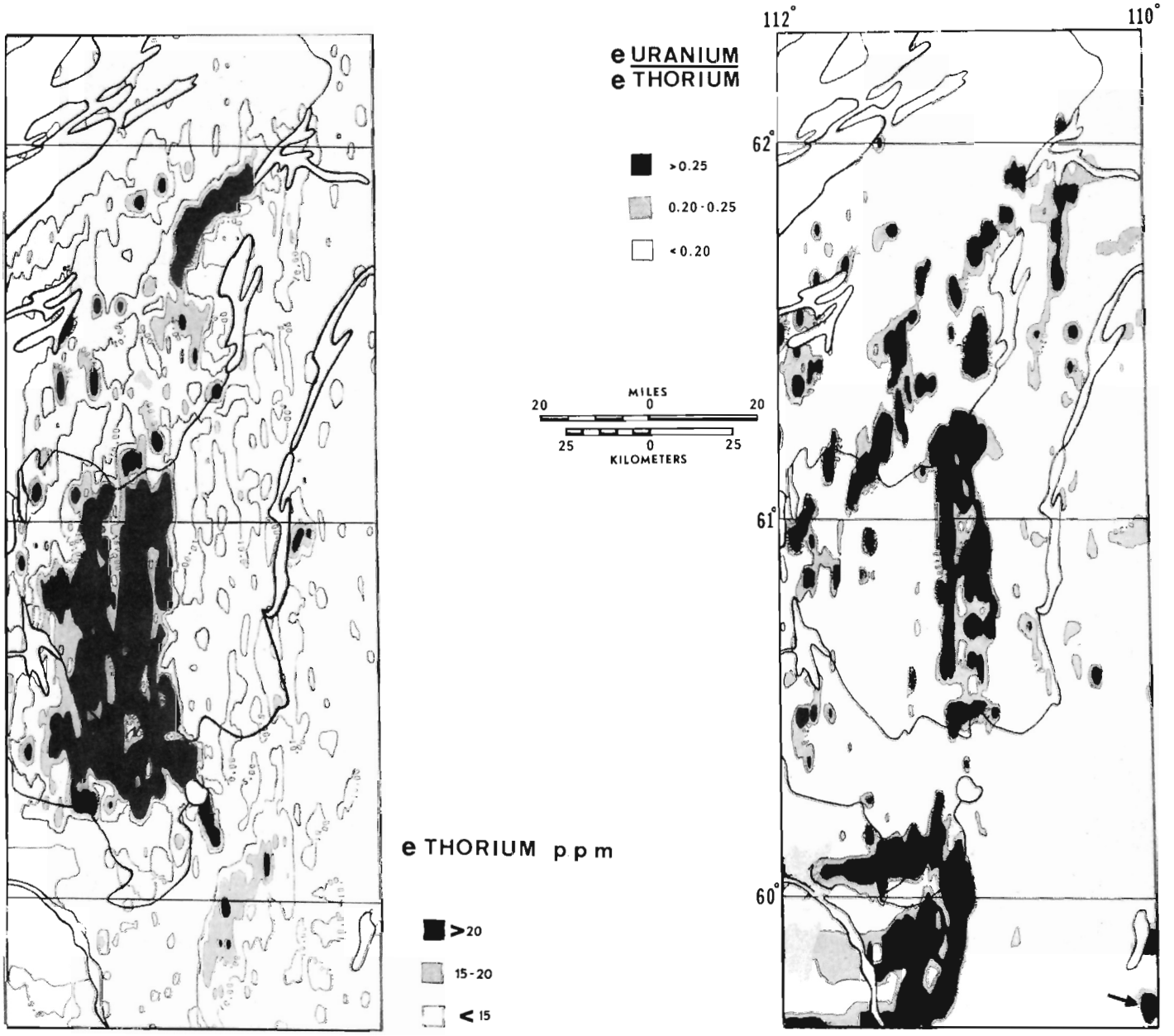

Figure 5.4. Airborne eTh and eU/eTh ratio in the Fort Smith Belt.

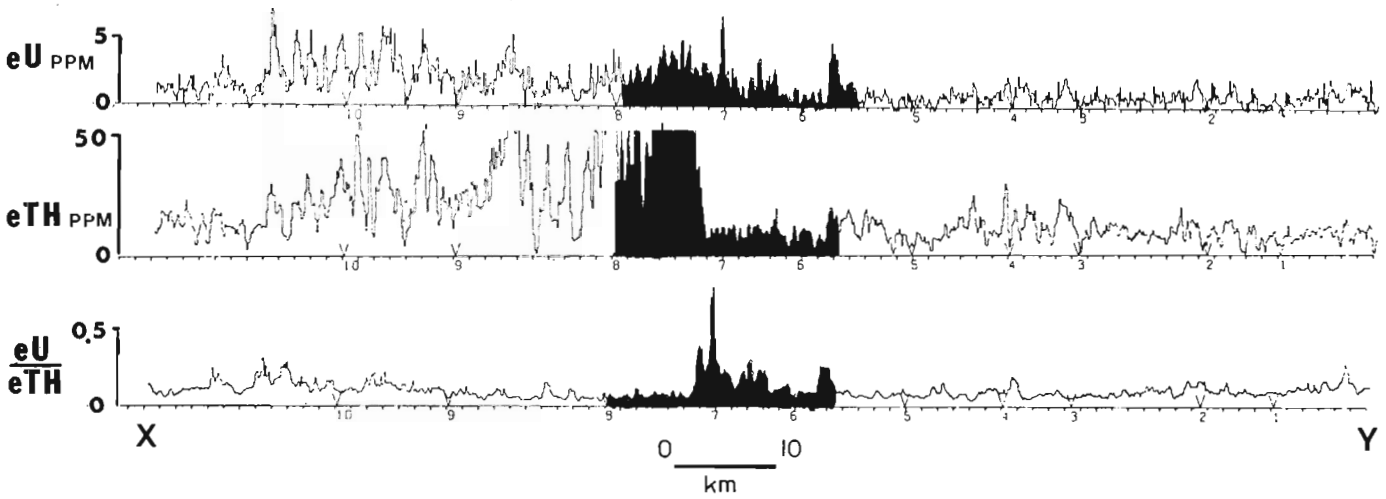

Figure 5.5. *Airborne profile X-Y showing eTh and eU/eTh ratio.*

McDonald fault system. Splays depart from this direction and trend north-south. The second is thought to consist mainly of vertical movements along reactivated major north-eastward striking faults. The third is marked by near-vertical northwestward striking fractures. Observed displacements of magnetic anomalies of less than 1 km indicate relatively small sinistral movements during the third period.

The magnetic anomaly map of Canada (McGrath et al., 1977) shows a strong magnetic low running north-south through the survey area (Fig. 5.3). It is truncated by north-east trending faults that parallel the McDonald Fault. The high magnetic relief on the flanks of the magnetic low correlates with magnetite-bearing metasedimentary gneisses. The northeast trending magnetic high in the northern portion of the map correlates with ferromagnetic gneisses and schists north of the McDonald fault system (MacLaren and Charbonneau, 1968).

Airborne Gamma Ray Spectrometry

Results of the high sensitivity airborne gamma ray spectrometric survey flown in 1970 were compiled and published by Darnley and Grasty (1972). This open file comprises seven contour maps (total count, K, eU, eTh, eU/eTh, eU/K, and eTh/K) and stacked profiles of the seven parameters for each of the east-west flight lines. The airborne system used in this survey was described by Darnley (1973).

Contour maps for the eTh and the eU/eTh ratio are shown in Figure 5.4. The major features shown by the contour maps are: (1) an eTh-rich central belt, (2) a peripheral zone with high eU/eTh ratio, and (3) a terrain exterior to the anomaly with average levels of radioelement concentration. The thorium-rich zone extends southward to about 60°N with a weaker zone extending south of 60°N into northeastern Alberta. The eU/eTh ratio map shows a zone exceeding 0.25 peripheral to the thorium anomaly. Maximum eU/eTh ratios in this zone exceed 0.50 or twice normal crustal levels (Clarke et al., 1966).

These features are illustrated on the east-west profile X-Y shown in Figure 5.5 and located in Figure 5.1. The profile shows eTh values exceeding 50 ppm (full scale) near the middle of the line, decreasing abruptly to 10-15 ppm to the east. Equivalent uranium values range between 3 and 6 ppm across the thorium-rich zone and a short distance beyond, creating a zone of anomalous eU/eTh ratio. The rather sharp eU and eU/eTh peaks near the centre of profile X-Y are the type of feature which could be of economic interest. This interesting section of profile has been darkened to highlight it. In this case the anomaly was underlain by foliated granite with eU values about 10 ppm and eU/eTh ratio values about 2.

The contour map of eU (Fig. 5.6) shows high levels, greater than 3 ppm, coincident with the area of thorium enrichment and extending beyond it to create an adjacent zone with high eU/eTh ratio. While a value of 3 ppm eU is not high for granitic rocks, it should be noted that the airborne spectrometric measurement of radioelement concentration generally underestimates bedrock content in typical Shield terrane by a factor of 2 to 4. Charbonneau et al. (1976) have discussed the relationship between airborne measurements and ground determinations of radioelement contents in bedrock and overburden. The effects of filtering, gridding and contouring airborne data along widely spaced flight lines have also been illustrated by Cameron et al. (1976).

Ground Investigations

Equivalent uranium and thorium profiles have been prepared from 30 km of ground traverses made with a portable gamma ray spectrometer in three areas (A, B, and C in Fig. 5.7). These areas were selected for detailed study because the anomalies typify the radiometric variations in the Fort Smith Belt. These profiles cross a narrow belt with high equivalent uranium and equivalent thorium concentrations (area A), a zone with high equivalent thorium concentration bordered by a high eU/eTh ratio (area B), and an area of high equivalent uranium and equivalent thorium concentrations and high eU/eTh ratio (area C). The profiles are shown in Figures 5.8, 5.10, and 5.11. Each of the ground profiles was produced from in situ analyses made at 100 m intervals, with the spectrometer station located on outcrop if available or on overburden if there was no outcrop near the station. The airborne radiometric maps and profiles presented in Figure 5.8 to 5.11 are in counts per 2.5 seconds. Approximate sensitivities are 26 counts/2.5 second per ppm eU and 11 counts/2.5 second per ppm eTh.

Area A

Three profiles, 4 km in length, cross the narrow thorium anomaly which trends north from Tsu Lake (Fig. 5.8). Five airborne profiles crossing this area (Fig. 5.9) trace the anomaly over a length of about 25 km, with a width of approximately 1 km. Portable spectrometer determinations indicate average concentrations of about 80 ppm eTh and 30 ppm eU in the foliated porphyritic granite of this area. The major radioactive mineral is monazite; sparse grains of uraninite are present.

Area B

In the central part of the survey area, one ground spectrometer profile, 11 km in length (Fig. 5.10) crosses the eastern edge of the monazite-bearing, thorium-rich porphyritic granitoid (Fig. 5.7). The 400 count airborne contour has been shaded in Figure 5.10 to accentuate the edge of the thorium high. In situ analyses of the bedrock indicate eTh concentrations of approximately 180 ppm over a distance of more than 5 km. Equivalent uranium concentrations generally range from 1 to 10 ppm, but occasionally reach 20 ppm. At the edge of the porphyritic mass eTh values drop to 5-15 ppm and eU values increase generally to 5-10 ppm and up to 20 ppm in places, resulting in eU/eTh ratios as high as 1.5 to 2.0. Bedrock having the high eU/eTh ratio is mainly a medium grained, equigranular to faintly foliated pink granite with schlieren of metasediment and gneiss. Uraninite is found in addition to monazite and occasional grains of thorite in the high ratio rocks.

Area C

In the northern part of the survey area, a 7 km ground profile (Fig. 5.11) crosses a complex of foliated porphyritic granitic, granitic, and metasedimentary rocks outlined on the airborne eU map by the 100 count contour (Fig. 5.11). In this complex eU values average about 25 ppm, eTh values average about 50 ppm, and eU/eTh ratios average about 0.5 but locally reach values greater than 2. These rocks contain monazite and uraninite as well as some thorite and have equivalent uranium contents as high as 100 ppm.

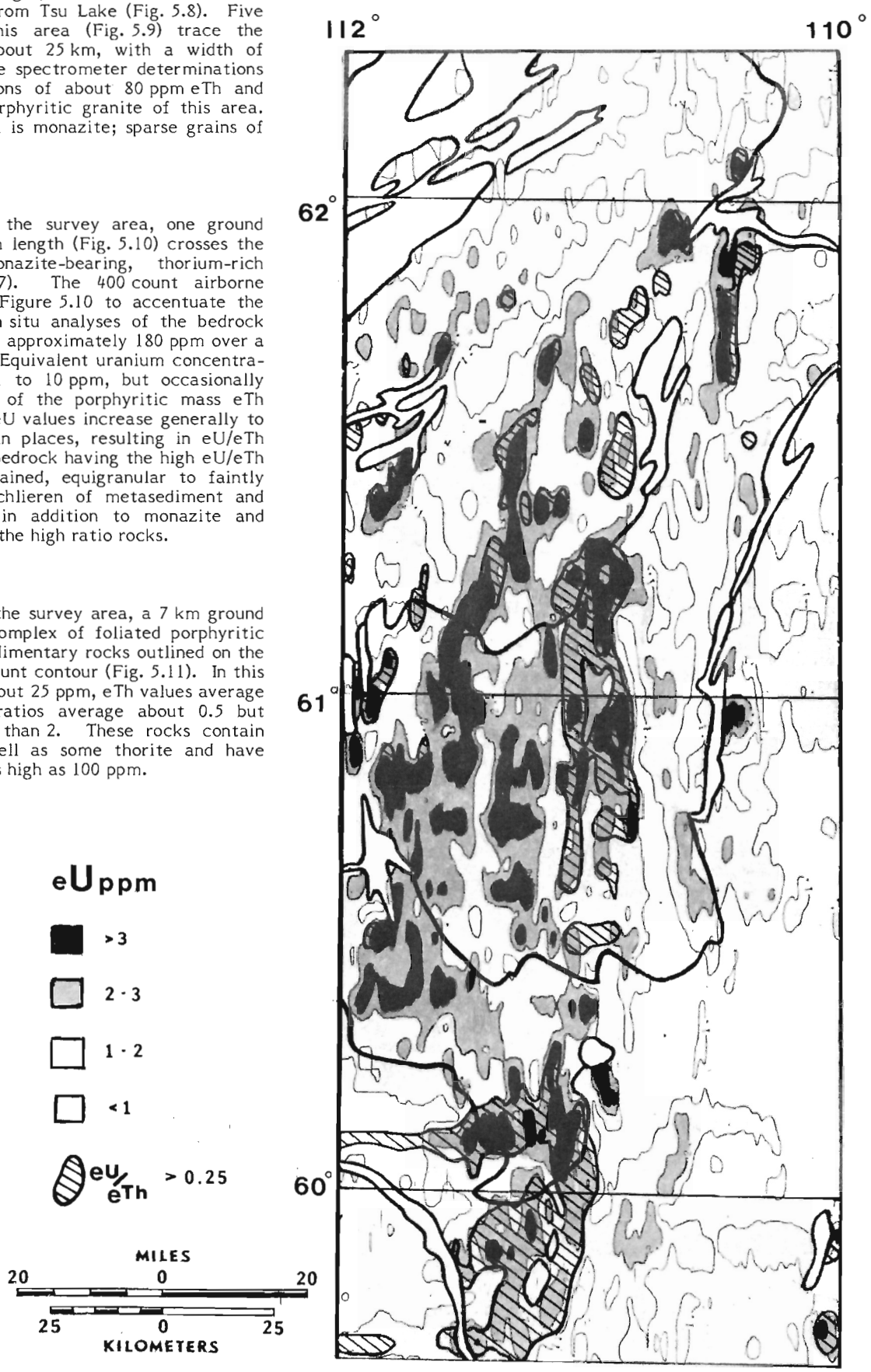

Figure 5.6

Airborne eU with eU/eTh ratio anomaly overlain, Fort Smith Belt.

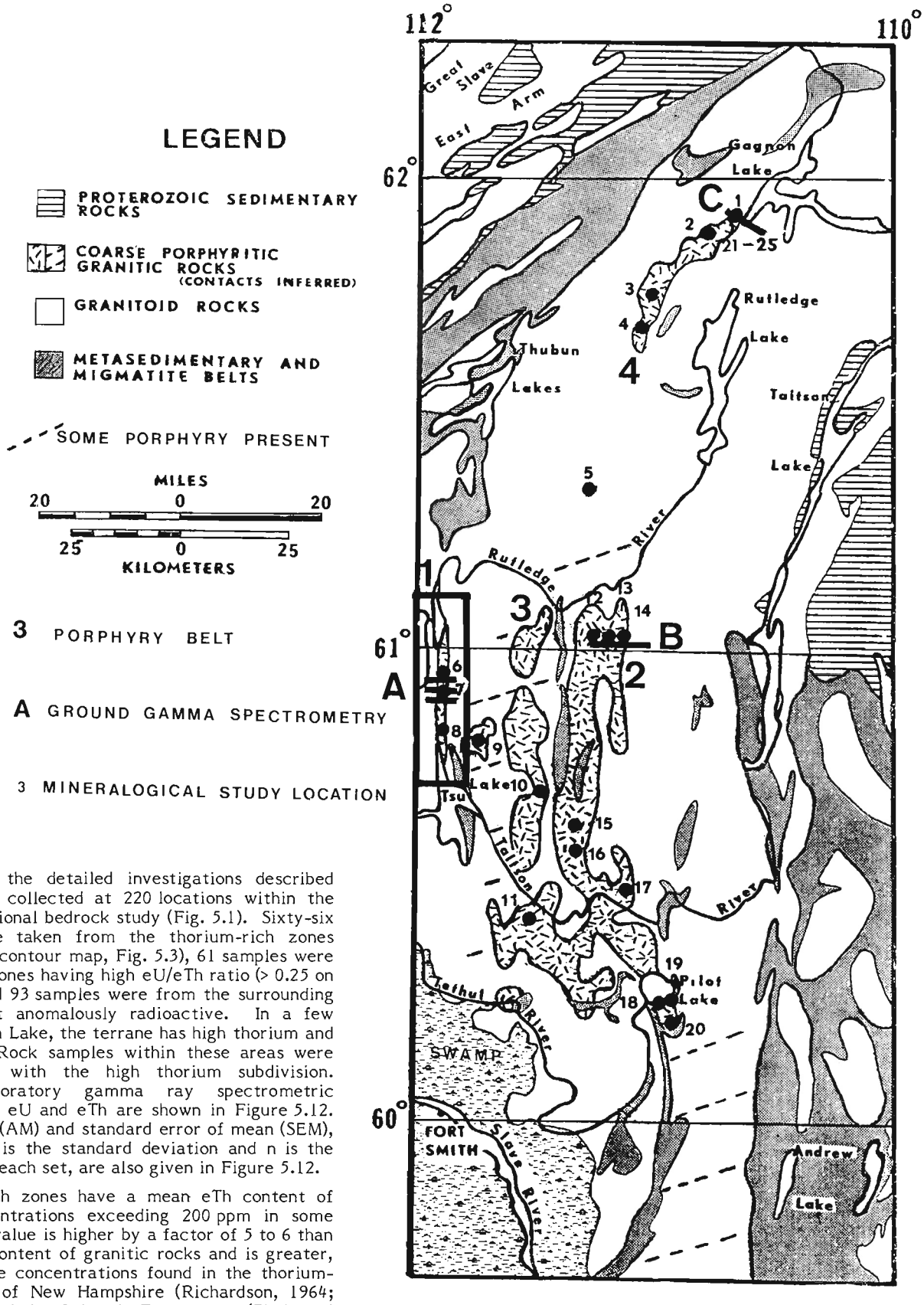

In addition to the detailed investigations described above, samples were collected at 220 locations within the survey area for a regional bedrock study (Fig. 5.1). Sixty-six of the samples were taken from the thorium-rich zones (> 20 ppm eTh on the contour map, Fig. 5.3), 61 samples were from the peripheral zones having high eU/eTh ratio (> 0.25 on the contour map), and 93 samples were from the surrounding terrane which is not anomalously radioactive. In a few localities, e.g. Gagnon Lake, the terrane has high thorium and high eU/eTh ratio. Rock samples within these areas were arbitrarily averaged with the high thorium subdivision. Histograms of laboratory gamma ray spectrometric determinations for K, eU and eTh are shown in Figure 5.12. The arithmetic mean (AM) and standard error of mean (SEM), which is $\sigma/\sqrt{n}$ where σ is the standard deviation and n is the number of samples in each set, are also given in Figure 5.12.

The thorium-rich zones have a mean eTh content of 76.5 ppm with concentrations exceeding 200 ppm in some samples. This mean value is higher by a factor of 5 to 6 than the normal thorium content of granitic rocks and is greater, for example, than the concentrations found in the thorium-rich Conway granite of New Hampshire (Richardson, 1964; Adams et al., 1962) and the Colorado Front range (Phair and Gottfried, 1964). The thorium-rich zones of the Fort Smith area and the peripheral zones with high eU/eTh ratio both

Figure 5.7. Geology and ground gamma ray spectrometry localities and sample sites for study of radioactive accessory minerals, Fort Smith Belt.

contain about 11 ppm eU, while the mean eU/eTh ratio increases from 0.15 in the thorium-rich zones to greater than 0.4 in the peripheral areas. The rocks in the surrounding terrane contain more typical "granitic" levels of thorium (19.9 ppm) and uranium (4.6 ppm), and have an average eU/eTh ratio of 0.23.

Four main zones of thorium-rich porphyritic granitic rocks have been found in the survey area (Fig. 5.7): (1) a thin north-trending zone near the western boundary of the survey area; (2) a larger zone trending north from Pilot Lake to Rutledge River; (3) a zone similar in dimension and parallel to (2) on its west side; and (4) a northeast trending zone southwest of Gagnon Lake in the northern part of the survey area. A portion of the zone near Pilot Lake has been investigated by Cape (1977) who reported radioelement concentrations and petrological characteristics in agreement with those found in this study.

The distribution of the thorium-rich porphyritic granites as shown in Figure 5.7 (patterned plus cross-hatched area) is only an approximation based on the sampling density and on the airborne thorium contour map. Another mass of this rock is located northeast of the survey area on strike with belt (4). This mass which commences just at the boundary of Figure 5.7 near 62°N, 110°W has been described by Maurice and Plant (1979). Chemical analyses of the porphyritic granitoids have been given by Cape (1977) and Maurice and Plant (1979) and the rock compositions are similar to calc-alkaline granite described by Nockolds (1954). The porphyritic granitoid appears to correlate with the Arch Lake granite in northeastern Alberta which was described by Godfrey and Langenberg (1978).

The porphyritic granitoids are generally pinkish in tone and have the composition of granite but may at times approach the composition of quartz monzonite. Mineralogically, they consist of potassium feldspar, plagioclase, quartz, biotite, and accessories. The potassium feldspar is generally idiomorphic microcline or microcline perthite with Carlsbad twinning. These crystals are somewhat deformed, usually crushed at their margins, and range up to 5 cm in length (Fig. 5.13). Some microcline occurs in the ground mass as well as in porphyroclasts. The plagioclase composition averages calcic oligoclase. These grains rarely exceed 5 mm, have a subrounded shape, and are somewhat altered to sericite and epidote. Quartz occurs as isolated grains and in sutured patches. Some vein and lenticular

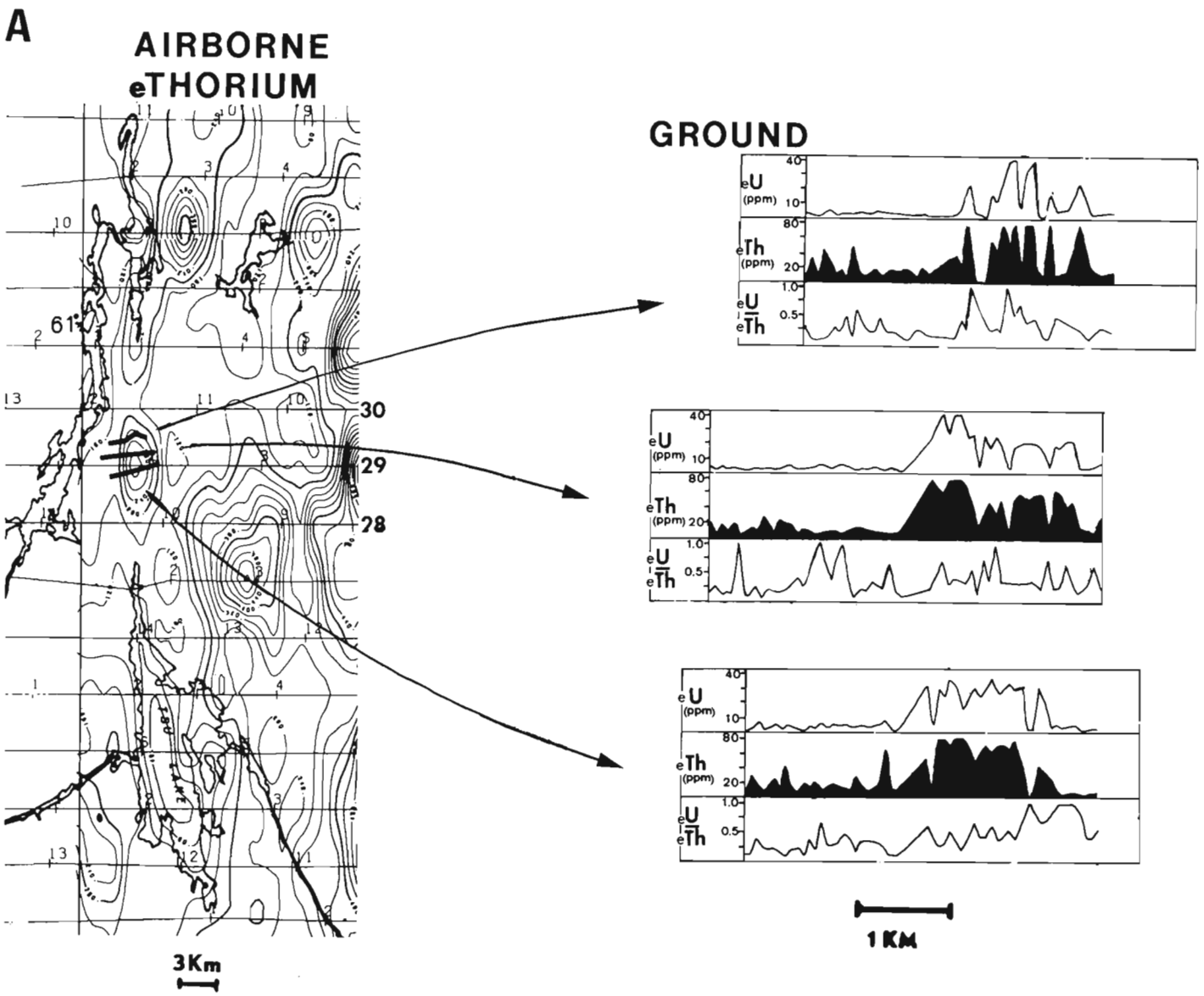

Figure 5.8. Ground gamma ray spectrometry profiles over narrow high eTh belt north of Tsu Lake (Area A, Fig. 5.7).

quartz can be found. Both the plagioclase and quartz are strained. Biotite is brown to greenish and is often altered to chlorite but appears relatively undeformed. Other minerals present are garnet, muscovite, ilmenite, anatase, rutile, hematite, zircon (cyrtolite), rarely fluorite, pyrite and radioactive accessories which are principally monazite and occasional grains of uraninite. The porphyry may contain some altered hypersthene (H.H. Bostock, personal communication).

Narrow elongate dyke-like mafic zones, seldom exceeding 1 m in width and several tens of metres in length, are seen occasionally in the porphyritic rocks. These zones, which may contain an order of magnitude more uranium and thorium than the enclosing porphyry, comprise biotite, garnet, ilmenite, anatase, rutile, hematite and apatite, feldspar and some quartz. The radioactive mineral is monazite. Very rarely a few grains of uraninite are present. These zones may have originally been localized along fractures somewhat similar in style to those described from the East Arm of Great Slave Lake (Badham, 1978). These features in the Pilot Lake area have been considered to be the remnants of heavy mineral sedimentary bands partly digested by igneous activity (Cape, 1977). Similar dark zones in the porphyry mass just outside this study area, northeast of Gagnon Lake (Fig. 5.1) have been described by Maurice and Plant (1979) and ascribed to either intrusive origin or metasedimentary assimilation. Additional dark zones can be found near localities 5 and 7 (Fig. 5.7).

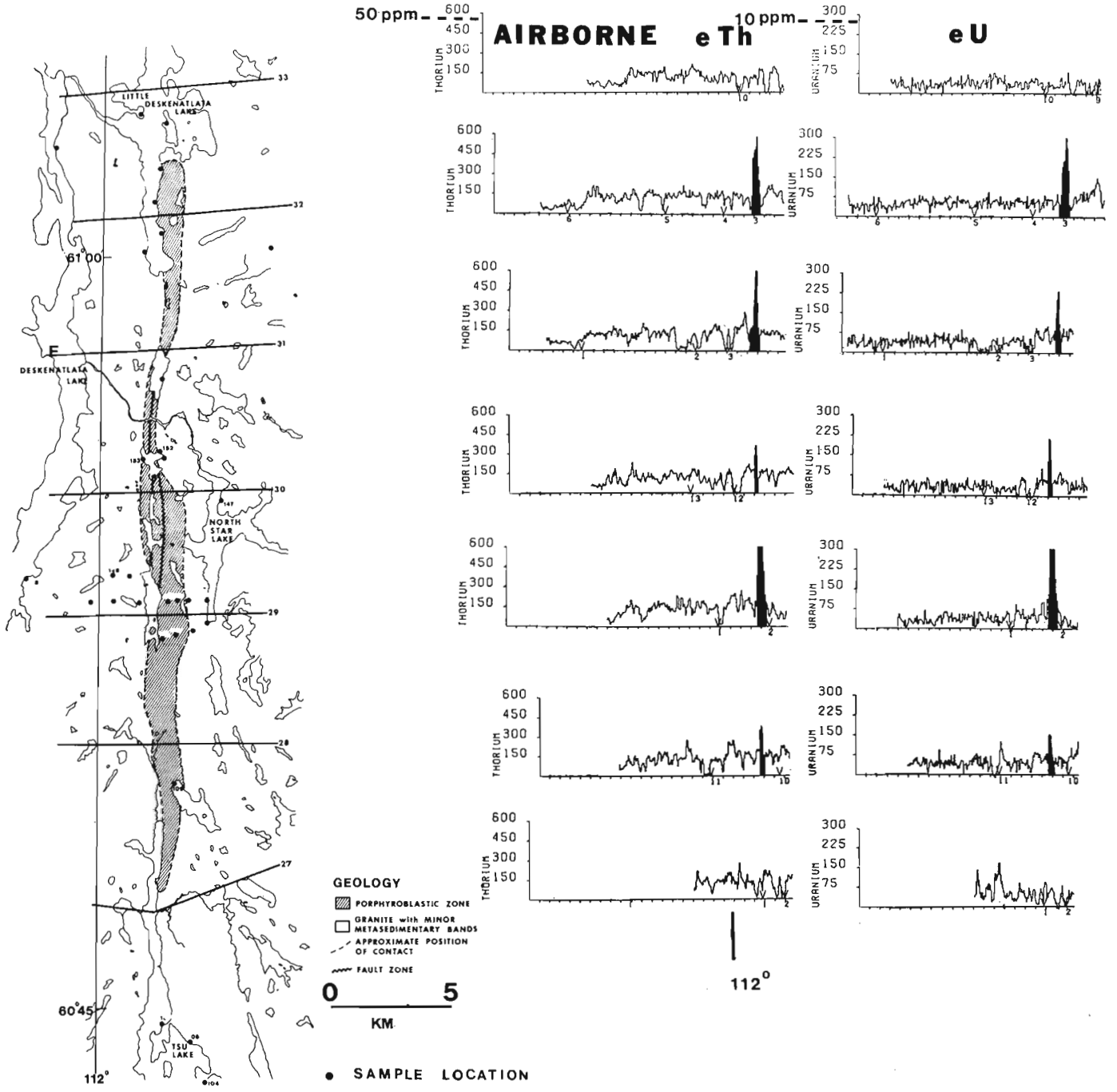

Figure 5.9. *Location of narrow high eTh foliated porphyritic granite belt north of Tsu Lake with locations of sample sites and airborne profile intersections showing eU and eTh.*

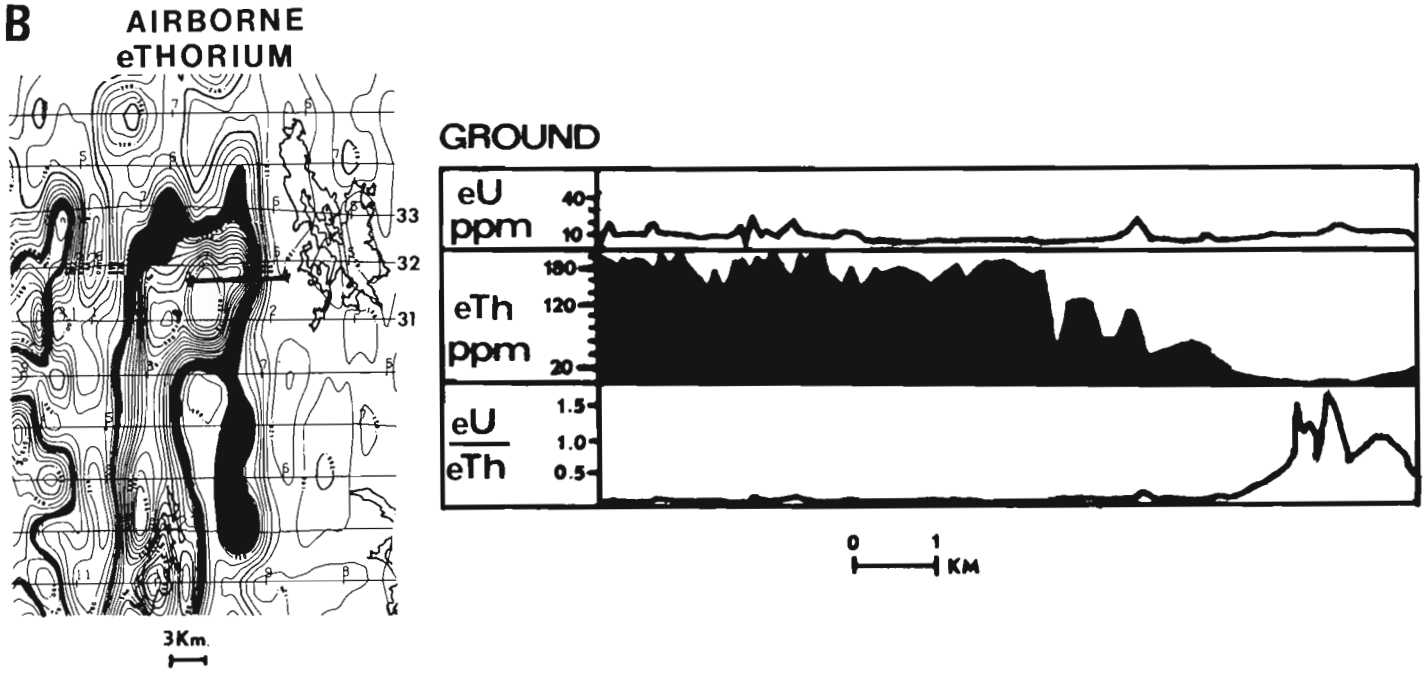

Figure 5.10. *Ground gamma ray spectrometry profile across high eTh foliated porphyritic granite and high eU/eTh ratio marginal zone (Area B, Fig. 5.7).*

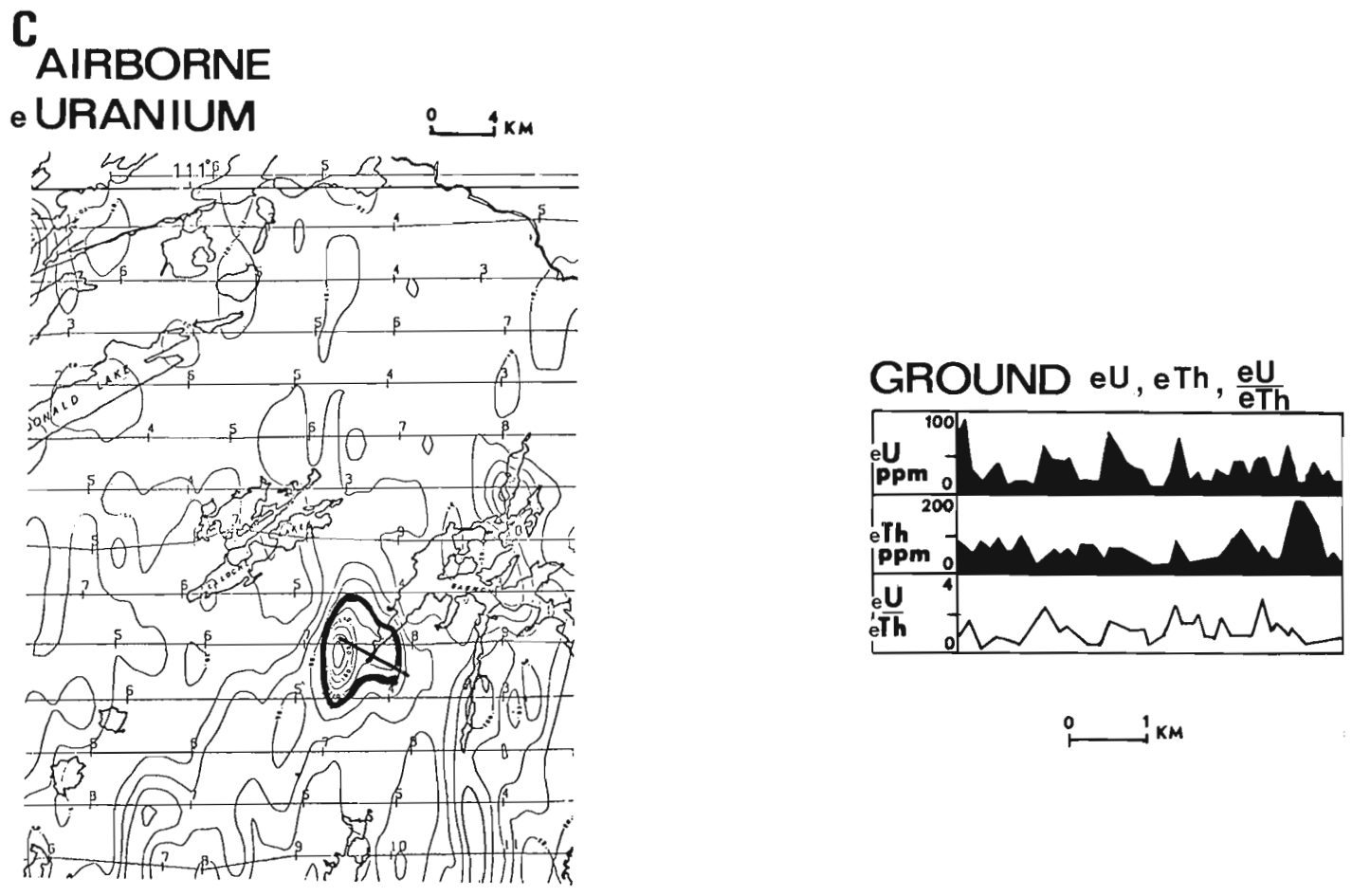

Figure 5.11. *Ground gamma ray spectrometry across high eU and eU/eTh anomaly near Gagnon Lake (Area C, Fig. 5.7).*

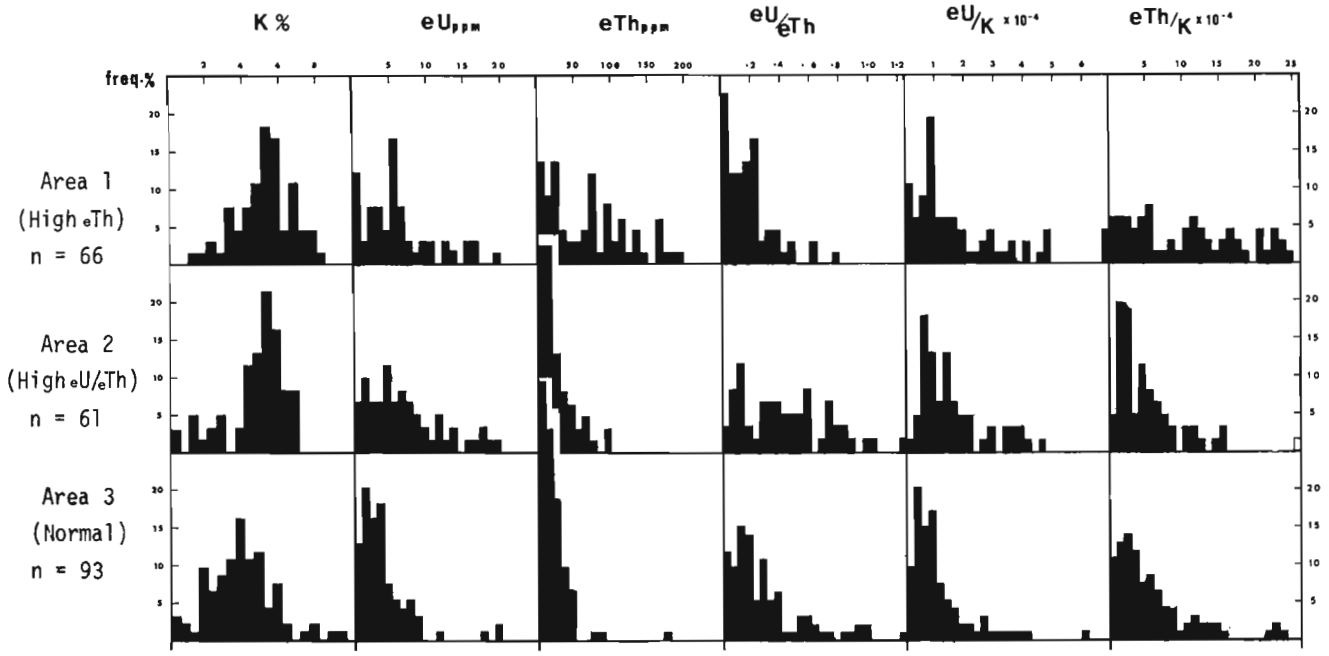

		K%	eU ppm	eTh ppm	eU/eTh	eU/K x 10^{-4}	eTh/K x 10^{-4}
Area 1 (High eTh) n = 66	AM	5.2	11.2	76.5	0.15	2.1	14.4
	SEM	0.2	1.5	10.2			
Area 2 (High eU/eTh n = 61	AM	4.6	10.4	24.2	0.43	2.2	5.2
	SEM	0.2	1.7	2.8			
Area 3 (Normal) n = 93	AM	3.7	4.66	19.9	0.23	1.2	5.3
	SEM	0.1	0.7	2.3			

Figure 5.12. *Histograms of bedrock radioelement concentrations of area 1 (high eTh), area 2 high eU/eTh ratio, area 3 (normal) terranes.*

The peripheral area with high eU/eTh ratio is underlain generally by rocks which are granitic in composition, equigranular to subporphyritic, massive to faintly foliated and/or lineated with minor schlieren of metasediments. It is postulated that these rocks were enriched in uranium by mobilization and migration of uranium outwards from the thorium-rich areas. A vapour phase has been shown to escape from quartz monzonite magma by Whitney (1975). Uranium could have been fractionated in such a vapour and moved outwards to form the zone of marginal eU enrichment characterized by the high eU/eTh ratio. Uraninite has been found in the marginal belt at several locations both within the porphyry and in the wallrocks. Gossans were commonly seen in the contact zone between the porphyry and the wallrocks.

The fact that high eU/eTh ratio anomalies may indicate zones of hydrothermal enrichment of several other metals in addition to uranium has been noted by Bennett (1970). One of his exploration examples was from the Andrew Lake area (southeast corner Fig. 5.1) where molybdenum was associated with high ratio rocks (arrow, Fig. 5.4).

Maurice and Plant (1979) described uranium, copper and zinc enrichment associated with mafic bands in porphyritic rock and with metasediments northeast of 62°N, 110°W. Prominent geochemical (lake sediment) anomalies in U, Cu, Pb, Zn, are known in this area. Unfortunately such coverage is not available for the central axis of the Fort Smith Belt. There is also the possibility that anomalous Sn concentrations in Nonacho conglomerates of 2100 ppm (Maurice and Plant, 1979), may have been derived from the Fort Smith Belt.

The terrain surrounding the thorium-rich areas and the areas with high uranium/thorium ratio is predominantly underlain by granitoid rocks with extensive zones of paragneiss and has near average radioelement concentrations for these rock types. This area, particularly to the east of the thorium-rich zone, is marked by prominent anomalies on the aeromagnetic map (Fig. 5.3). Magnetite is present in many of these rocks, whereas the low magnetic, highly radioactive thorium-rich porphyritic rocks are characterized by ilmenite-anatase-rutile and/or hematite.

Samples of the thorium-rich porphyritic rocks, from 25 locations indicated on Figure 5.7 were examined to identify their radioactive mineralogy. Mineral grains located

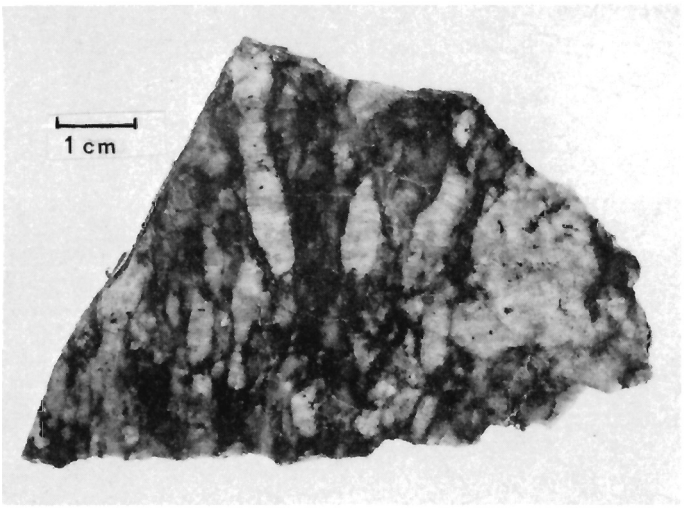

Figure 5.13. *Cut and polished surface of foliated porphyritic granite.*

Table 5.1

Partial Electron Microprobe Analyses of Monazites

Sample Location Figure 7		12			21		20
Analysis	1	2	3	4	5	6	7*
SiO_2	4.5	3.0	0.8	3.2	2.3	3.3	17.3
ThO_2	11.1	4.3	0.0	13.1	10.2	13.1	16.1
UO_2	0.1	0.1	0.0	0.4	0.2	0.7	0.5
La_2O_3	10.3	11.8	10.8	10.7	10.8	9.8	0.4
Ce_2O_3	28.4	33.8	35.5	26.7	28.2	26.0	2.2
Nd_2O_3	10.1	11.7	14.4	7.9	9.3	11.7	1.1
CaO	2.1	0.8	0.3	2.9	2.2	2.8	32.8
P_2O_5	28.0	28.8	28.9	27.7	27.9	28.3	29.0

*Cloudy orange rim of monazite grain

on polished sections by autoradiography were qualitatively analyzed by scanning electron microscopy. This work was performed by G.J. Pringle and A.L. Littlejohn, Geological Survey of Canada.

In all samples, except the one from location 25, the principal radioactive mineral is monazite which occurs as scattered, rounded grains with ThO_2 contents ranging from a trace to approximately 16 per cent, but usually in the range 10-12 per cent ThO_2. The UO_2 content in one case is as high as 0.7 per cent but is commonly less than 0.2 per cent. The monazite grains are frequently altered to a dark orange clouded material that occurs as rims or relicts with higher Si, Th, Ca, P and lower rare earths than the monazite. Section 25 contains few radioactive spots, and all those analyzed are the orange clouded relicts. Table 5.1 contains selected analyses of the monazites, and includes one analysis of the orange rimming material.

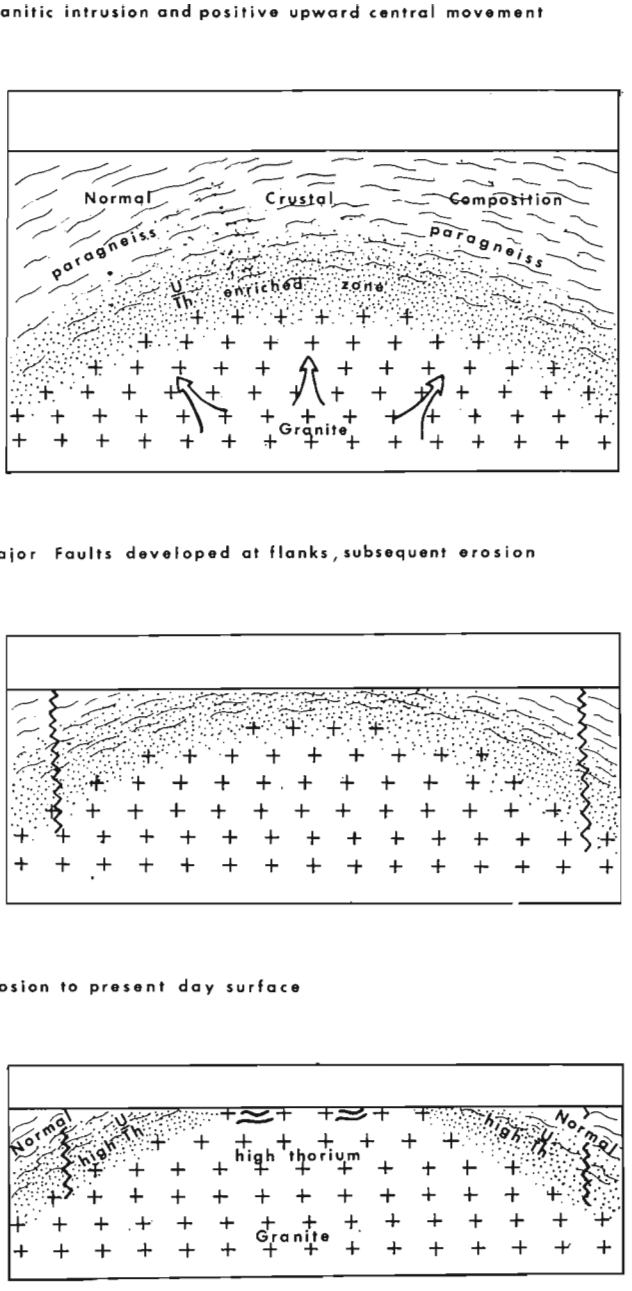

Figure 5.14. *Simplified schematic diagram showing evolution of Fort Smith Belt.*

Sparse grains of uraninite occur in 3 samples, from locations 7, 22 and 24 in Figure 5.7. These have Pb contents of approximately 20 per cent and characteristically have dark circular rims that are in part a mixture of uraninite and chlorite. It should be noted that where high eU/eTh ratio anomalies relate to porphyry (e.g. Gagnon Lake, localities 22, 24, the narrow zone extending north from Tsu Lake, locality 7) the rocks contain uraninite in addition to monazite.

Zircon, present in all sections, is characterized by variable birefringence (cyrtolite). The zircons contain negligible amounts of Th and U, but commonly have Hf as a minor constituent.

Many samples have grains of colourless TiO_2 (anatase) and opaque TiO_2 (rutile). Sphene was not found in any of the sections.

Zircon, anatase, rutile and monazite grains were all confirmed by X-ray diffraction.

In summary, the uranium and thorium contents of the rocks represented by this suite of thin sections are related to (1) an irregular distribution of monazite, (2) the variable thorium content of the monazite, and (3) the presence of uraninite in some samples.

Conclusion

The Fort Smith survey area is one of the most radioactive regions so far recognized in the Canadian Shield. This is a dominantly thoriferous region, but potassium and uranium concentrations are also high. The highest concentration of radioelements is found in a foliated porphyritic granite with mean thorium and uranium concentrations of 76.5 ppm and 11 ppm, respectively. Radioactive minerals in this rock are monazite with variable thorium content and occasional isolated grains of uraninite.

Within the porphyry the highest uranium and thorium concentrations are found in dark biotite-rich bands, high in iron and titanium, and containing apatite, monazite and rarely uraninite.

The pattern of thorium and uranium distribution in the survey area, i.e. the thorium-rich belt with peripheral zones having high eU/eTh ratios, might be explained by a model somewhat analogous to one given by Whitfield et al. (1959). In this model uranium may escape from the intrusion under oxidizing conditions and enter adjacent rocks. Temperature, pressure, H_2O, CO_2 content are all important factors (Whitney, 1975). Figure 5.14 is a schematic illustration of the evolution of the Fort Smith Belt: (1) intrusion of a radioactive granitic body within a metasedimentary and granitoid terrane; (2) uranium enrichment at the granite-country rock boundary; and (3) erosion to present day surface exposing a high thorium granite with a high U/Th margin, within a terrain having normal radioelement concentrations. Late Hudsonian deformation could have helped mobilize some of the uranium into the flank zones of the porphyry.

The margins of the thorium-rich porphyry, where eU/eTh ratios are anomalous, would appear to be a favourable area for uranium exploration. Although much of this area was found to relate to granite and granite with metasedimentary bands containing only moderate levels of uranium and thorium, spotty uraninite concentrations have been found along the western margin of the Fort Smith Belt on the big peninsula in Tsu Lake, in the narrow porphyritic granite belt trending north from Tsu Lake, in porphyry near Gagnon Lake at the northeastern margin of the Fort Smith Belt and in granite marginal to the porphyry in the Rutledge River area (loc. B, Fig. 5.7).

The radioactive rocks of the Fort Smith Belt have been postulated as possible source rocks for some radioactive occurrences in the Nonacho basin (Darnley et al., 1977).

Acknowledgments

Many people contributed to this study, in particular I. Garat, L.D. Jones, and K.L. Ford in the field work component; P.B. Holman for airborne radiometric survey and data compilation, and G.J. Pringle and A.L. Littlejohn for electron microprobe work. One hundred of the two hundred and twenty regional samples, collected by L.J. Kornik of the Geological Survey during a magnetic study in the area, were kindly provided to the author to increase sample density. K.A. Richardson, A.G. Darnley and Y.T. Maurice read the manuscript.

References

Adams, J.A.S., Kline, M.C., Richardson, K.A., and Rogers, J.J.W.
1962: The Conway granite of New Hampshire as a major low-grade uranium resource; Proceedings, National Academy of Sciences, v. 48, no. 11, p. 1898-1905.

Badham, J.P.N.
1978: Magnetite – apatite – amphibole – uranium and silver-arsenide mineralizations in lower Proterozoic igneous rocks, East Arm Great Slave Lake, Canada; Economic Geology, v. 73, p. 1474-1491.

Baadsgaard, H. and Godfrey, J.D.
1972: Geochronology of the Canadian Shield in northeastern Alberta, Andrew Lake area; Canadian Journal of Earth Sciences, v. 4, p. 451-563.

Bennett, R.
1970: Exploration for hydrothermal mineralization with airborne gamma-ray spectrometry; Canadian Institute of Mining and Metallurgy, Special Volume 11, p. 475-478.

Bostock, Hewitt H.
1980: Reconnaissance Geology of the Fort Smith – Hill Island Lake area, Northwest Territories; in Current Research, Part A, Geological Survey of Canada, Paper 80-1A, p. 153-155.

Cameron, G.W., Elliott, B.E., and Richardson, K.A.
1976: Effects of line spacing on contoured airborne gamma-ray spectrometry data; in International Atomic Energy Agency, Symposium on Exploration for Uranium Ore Deposits, Vienna, Austria, 1976, STI/PUB/IAEA-SM-208/2, p. 81-92.

Cape, D.F.
1977: An investigation of the radioactivity of the Pilot Lake area, N.W.T.; Unpublished M.Sc. Thesis, University of Alberta.

Charbonneau, B.W.
1971: Gamma-ray support District of Mackenzie; in Report of Activities, Part A, Geological Survey of Canada, Paper 71-1, pt. A, p. 40-46.

Charbonneau, B.W., Killeen, P.G., Carson, J.M., Cameron, G.W., and Richardson, K.A.
1976: The significance of radioelement concentration measurements made by airborne gamma-ray spectrometry over the Canadian Shield; International Atomic Energy Agency, Symposium on Exploration for Uranium Ore Deposits, Vienna, Austria, 1976, STI/PUB/434, p. 35-53.

Clarke, S.P. Jr., Peterman, A.E., and Heier, K.S.
1966: Abundances of uranium, thorium and potassium; Geological Society of America, Memoir 97, Section 24.

Darnley, A.G.
1973: Airborne gamma-ray survey techniques – present and future; in Uranium Exploration Methods, International Atomic Energy Agency Publication, Vienna, Austria, STI/PUB/334, p. 67-106.

Darnley, A.G. and Grasty, R.L.
1972: Airborne radiometric survey Fort Smith area, N.W.T.; Geological Survey of Canada, Open File 101.

Darnley, A.G., Charbonneau, B.W., and Richardson, K.A.
1977: The distribution of uranium in rocks as a guide to the recognition of uraniferous regions; Symposium on Recognition and Evaluation of Uraniferous Areas, International Atomic Energy Agency, Vienna, Austria, STI/PUB/450, p. 55-86.

Darnley, A.G., Grasty, R.L., and Charbonneau, B.W.
1971: A radiometric profile across part of the Canadian Shield; Geological Survey of Canada, Paper 70-46.

Fraser, J.A.
1978: Metamorphism in the Churchill Province, District of Mackenzie; in Metamorphism in the Canadian Shield, Geological Survey of Canada, Paper 78-10, p. 195-202.

Godfrey, J.D. and Langenberg, C.W.
1978: Metamorphism in the Canadian Shield of northeastern Alberta; in Metamorphism in the Canadian Shield, Geological Survey of Canada, Paper 78-10, p. 129-138.

Henderson, J.F.
1939: Geology, Taltson Lake; Geological Survey of Canada, Map 525A.

Løvborg, L.
1973: Future developments in the use of gamma-ray spectrometry for uranium prospecting on the ground; in Uranium Exploration Methods, International Atomic Energy Agency Publication, Vienna, Austria, p. 141-149.

MacLaren, A.S. and Charbonneau, B.W.
1968: Characteristics of magnetic data over major subdivisions of the Canadian Shield; Geological Association of Canada, Proceedings, v. 19, p. 57-65.

Maurice, Y.T. and Plant, A.G.
1979: Some mineralogical and geochemical characteristics of uranium occurrences in the Nonacho Lake area, District of Mackenzie; in Current Research, Part B, Geological Survey of Canada, Paper 79-1B, p. 179-188.

McGrath, P.H., Hood, P.J., and Darnley, A.G.
1977: Magnetic anomaly map of Canada; Geological Survey of Canada, Map 1255A, 3rd Edition.

Nockolds, S.R.
1954: Average chemical composition of some igneous rocks; Geological Society of America Bulletin, v. 65, p. 1007-1032.

Phair, G. and Gottfried, D.
1964: The Colorado Front Range, U.S.A. as a uranium and thorium province; in The Natural Radiation Environment, J.A.S. Adams, W.M. Lowder, ed., University of Chicago Press, p. 7-38.

Reinhardt, E.W.
1969: Geology, Thubun Lakes, N.W.T.; Geological Survey of Canada, Map 9-1969.

Richardson, K.A.
1964: Thorium, uranium, potassium in the Conway Granite in New Hampshire, U.S.A.; Natural Radiation Environment, J.A.S. Adams, W.M. Lowder, ed., University of Chicago Press, p. 39-50.

Richardson, K.A. and Charbonneau, B.W.
1973: Gamma ray spectrometry investigations 1973; in Report of Activities, Part A, Geological Survey of Canada, Paper 74-1A, p. 371-372.

Riley, G.C.
1960: Geology, Fort Fitzgerald, Alberta; Geological Survey of Canada, Map 12-1960.

Stockwell, C.H., Brown, I.C., Barnes, F.Q., and Wright, G.M.
1968: Geology, Christie Bay, N.W.T.; Geological Survey of Canada, Map 1122A.

Stockwell, C.H., McGlynn, J.C., Emslie, R.F., Sandford, B.V., Norris, A.W., Donaldson, J.A., Fahrig, W.F., and Currie, K.L.
1970: Geology of the Canadian Shield; Chapter 4 in Geology and Economic Minerals of Canada, Geological Survey of Canada, Economic Geology Report 1, p. 44-150.

Wanless, R.K.
1969: Isotopic Age Map of Canada; Geological Survey of Canada, Map 1256A.

Whitfield, J.M., Rogers, J.J.W., and Adams, J.A.S.
1959: The relationship between the petrology and the thorium and uranium contents of some granitic rocks; Geochemica et Cosmochemica Acta, v. 16, p. 248-271.

Whitney, James A.
1975: Vapor generation in a quartz monzonite magma; in Economic Geology, v. 70, no. 2, p. 346-358.

Wilson, J.T.
1941: Fort Smith, N.W.T.; Geological Survey of Canada, Map 607A.

6.

TECTONICS OF THE RICHMOND GULF[1] AREA, NORTHERN QUEBEC – A HYPOTHESIS

Project 770027

F.W. Chandler and E.J. Schwarz[2]
Precambrian Geology Division

Chandler, F.W. and Schwarz, E.J., Tectonics of the Richmond Gulf area, Northern Quebec – a hypothesis; in Current Research, Part C, Geological Survey of Canada, Paper 80-1C, p. 59-68, 1980.

Abstract

The Aphebian Richmond Gulf Graben strikes at a high angle from the Superior Craton toward the convex side of the curved Belcher Foldbelt. Among models of high angle rifts it best fits the aulacogen. Early oceanward fluvio-deltaic sediment transport, as predicted by the model, is absent from the graben. Its record might lie under the Belcher Islands or under a broad circular positive gravity anomaly equidistant from the Belcher Islands and the mainland of Ungava.

Instead, early fluvial sedimentation, and intercalated subaerial basalts (the Richmond Gulf Group) are west-derived, the former from a granitic terrane. Graben formation succeeded this sedimentation. The Richmond Gulf Group is interpreted to be eroded from a pre-rifting thermal dome situated on an Archean continent that continued to the west of the Belcher Islands. Uplift and erosion of these sediments before deposition of carbonates of the succeeding miogeoclinal Nastapoka Group at Richmond Gulf, could have removed intervening seaward-transported fluvio-deltaic clastics.

A volcanic unit, the caprock, within these carbonates is probably correlative with the Eskimo Formation volcanics in the lower part of the Belcher Group. A younger volcanic unit in the Belcher Group, the Flaherty Formation, and associated iron formation and greywacke could record the convergent phase of the orogenic cycle implied above. These younger units have stratigraphic equivalents all or in part in the Sutton Inlier and offshore islands on the east side of Hudson Bay but not at Richmond Gulf.

Consequences of this hypothesis include an explanation for the great arc on the east side of Hudson Bay, further evidence of plate tectonics in the Early Proterozoic and local support for a plate tectonic model for the Circum-Superior Foldbelt.

Introduction

This report discusses briefly the Aphebian geology of the Richmond Gulf area and its regional correlation. It goes on to suggest an explanatory tectonic hypothesis. The rocks considered are part of the Circum-Superior Foldbelt (Fig. 6.1), a structure of which the origin is under debate (Dimroth, 1972; Baragar and Scoates, in press).

The relevance of rigid-plate tectonics to the pre-Mesozoic is disputed (Sutton and Watson, 1974; Dewey and Spall, 1975; Windley, 1973). An important aspect of plate tectonic models is continental rifting, evidence of which is seen in aulacogens (Burke and Dewey, 1973a), sediment-filled cratonic grabens that strike at high angles to craton margins and terminate at bends in adjacent foldbelts that fill re-entrants in the craton margin (Salop and Scheinmann, 1969). Location on the forelands of orogens, away from the maelstrom of compressive tectonics, gives aulacogens a high preservation potential (Burke, 1976, 1977). The graben at Richmond Gulf strikes at a high angle to the margin of the Superior Craton toward a cratonward bend in the Belcher Foldbelt. A model of this structure would contribute to knowledge of the Circum-Superior Foldbelt and the applicability of plate tectonics in the Proterozoic.

Goodwin (1974) saw the Hudson Bay region as the nucleus of accretion of the Canadian Shield, uninterrupted by significant fragmentation about a family of mantle plumes. The arcuate shape of the east coast of Hudson Bay (Fig. 6.2) suggested to Beals (1968) and to Halliday (1968) an origin by meteorite impact. Wilson (1968) considered that Hudson and James bays might be a late Precambrian continental suture, drawing attention to a possible genetic connection with the Cape Smith Belt and the Labrador Trough (Fig. 6.1). He explained the great arc on the east coast of Hudson Bay as a "secondary mountain arc", formed convex toward the foreland, from the folded remains of a basin of sedimentary rocks, at a junction in a series of island arcs. Such arcs (Jacobs et al., 1959, p. 290 et seq.) were regarded as derived from the folding and foreland-directed thrusting of miogeosynclinal sequences.

Gibb (1971), noting a similarity between the shape of the east margin of the Slave Province (Fig. 6.1) and the arc on the east side of Hudson Bay, proposed that the two had been separated by rifting 2.4 Ga ago. Subsequent ocean closure had formed the Churchill Province from Archean microcontinents and new material. Gibb and Walcott (1971) proposed that a Slave-Superior continental collision had formed a suture stretching from the Thompson Nickel Belt in Manitoba, to include the Labrador Trough via the Cape Smith Belt.

Dimroth (1972) objected to a plate tectonic interpretation of the Labrador Trough on several grounds, including the virtual absence of the calc-alkaline igneous suite and the granitic source of many of the sediments of the Trough. Sutton and Watson (1974) believed that rigid-plate tectonics had not developed by the Early Proterozoic (before 1.3 Ga), viewing such terranes as the Churchill Province, as a group of stable nuclei enclosed within mobile belts. Motion on northeast-striking transform faults at the boundaries between these components opened and closed a narrow ocean along another boundary set at an angle to the transforms, so forming the Labrador Trough.

Burke and Dewey (1973b) supported the collision hypothesis for the Circum-Superior Foldbelt using the "triple junction-aulacogen model" to explain sharp bends in the foldbelt, and (Dewey and Burke, 1973) explained the Hudsonian development of the Churchill Province by their

[1] Recently renamed Lac Guillaume Delisle.

[2] Paleomagnetic contribution.

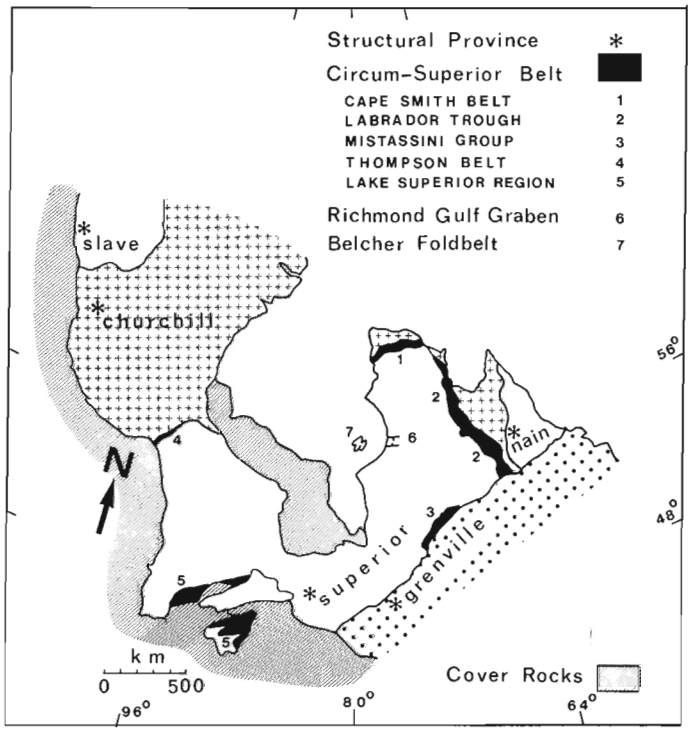

Figure 6.1. *Some Structural Provinces and Subprovinces of the Canadian Shield.*

"Tibetan reactivation model". Following this last paper several gravity studies across the Churchill-Superior Boundary employed the Tibetan reactivation model (Gibb and Thomas, 1976; Kearey, 1976; Thomas and Gibb, 1977). More recently, Baragar and Scoates (in press) supported a plate tectonic origin for the Circum-Superior Foldbelt. The presence of calc-alkaline rocks only in the Lake Superior region of the belt (Fig. 6.1), as well as paleomagnetic restrictions on relative plate movement in the Aphebian between the Slave and Superior provinces, led them to conclude that a wide ocean developed only on the southern margin of the Superior craton.

An important application of paleomagnetism to studies of Proterozoic tectonics is in testing for large-scale relative movement of Archean continental blocks. McGlynn et al. (1975) found a general coherence for the Canadian Archean in the interval 2.2 to 1.8 Ga, but Burke, et. al. (1976) and Cavanaugh and Seyfert (1977) interpreted Aphebian polar wander paths in terms of a Hudsonian collision between the Slave and Superior provinces. McGlynn and Irving (1980) tend to agree with these later views, but caution that the problem is not yet solved.

General Geology

Hudson Bay is bordered on the northwest by the Proterozoic Churchill Structural Province and on the south and east by the Archean Superior Structural Province (Fig. 6.1). Overlying the Hudson Bay coast of the Superior Province and in the Belcher Islands, lie widely distributed Aphebian sedimentary rocks of the Nastapoka Group (Eade, 1966, unit 13b,c; Stevenson, 1968, unit 9b) the Belcher Group (Jackson, 1960; Dimroth et al., 1970) and equivalents (Bostock, 1971). Folding and faulting of these rocks intensifies from gently seaward dipping on the Hudson Bay coast to steeply dipping isoclinal folds in the Belcher Islands. The lower part of these sequences is rich in carbonates and quartz arenites whereas the upper part contains iron formation, abundant greywacke and mafic volcanics.

At Richmond Gulf (Fig. 6.3), these rocks are underlain with angular unconformity by the Aphebian Richmond Gulf Group (Woodcock, 1960; Chandler, 1978, 1979). The latter arkosic rocks are block faulted and confined to an east-striking graben formed in granitic gneiss of the Superior Province.

Stratigraphic Nomenclature

Bell (1879), Eade (1966) and Stevenson (1968) included all of the Aphebian sequence on the east coast of Hudson Bay in the Manitounuk Group. Leith (1910), recognizing an unconformity within the group, divided it into the Richmond Group and overlying Nastapoka Group. Ami (1900) mentioned that Bell (not cited) had already used the last term. Young (1922) pointed out that the term "Richmond Group" was already in use, and advised that it be changed to Richmond Gulf Group.

Woodcock (1960) reported an unconformity within the Richmond Gulf Group and thereupon divided it into the Pachi Group and unconformably overlying Richmond Gulf Formation. The Pachi Group he divided into the Pachi sediments overlain by the Pachi volcanic complex. Stevenson (1968) and Chandler (1978) found no evidence of Woodcock's (1960) unconformity. The appearance of a disconformity is caused by erosion to conglomerate of terrestrial basalt extruded during fluvial sedimentation (see below). The arkosic sediments beneath and overlying the Pachi volcanic complex are clearly separable by 1:25 000 scale mapping (Fig. 6.3) and should retain formational status. Woodcock's (1960) Pachi sediments are therefore renamed the Pachi Formation. The overlying basalt flows (Woodcock's Pachi volcanic complex) form a compact flow unit well exposed in cuestas around Lac Persillon. It is herein named the Persillon Formation. Because Young (1922) had already introduced the name Richmond Gulf Group, Woodcock's use of the name for a formation is invalid. The middle and upper parts of the formation are excellently exposed on 400 m high cliffs forming the east side of Quingaaluk Hill (Fig. 6.3). The basal part overlying the Persillon Formation is well exposed on an oval peninsula 1 km to the northeast of the cliff (Chandler, 1979). It is suggested that the unit be renamed Qingaaluk Formation. Descriptions of the formations within the Richmond Gulf Group were given by Woodcock (1960) and Chandler (1979).

Richmond Gulf Group

The Pachi Formation (Chandler, 1978) is up to 500 m thick but thickness is very varied. For example, only about 20 m were recorded on the central horst (Fig. 6.3). The arkosic formation consists overwhelmingly of sandstone and grit, some pebbly, and coloured mainly green, pink and grey. Local granite-quartzite boulder conglomerate of unknown but probably limited thickness occurs near the base. In good exposure at the northeastern limit of outcrop only 1 m of quartz-granite cobble conglomerate was found 2 m above the base of the unit.

Minor turbidite-like green and grey siltstone units and red mud-cracked siltstone units up to 4 m thick and traceable up to 1 km occur in the formation in the northern part of the area and probably were deposited in shallow lakes, some ephemeral. Dominance of lenticular, cross-stratified sandstone beds, presence throughout the section of sparse, rippled and mud-cracked siltstone lenticles several centimetres thick, and local unimodal paleocurrent directions based on trough crossbeds, suggest a braided fluvial mode of deposition for the bulk of the formation. Measurement of trough crossbeds at the northern margin of the graben show a southward radial paleocurrent pattern. Through the centre and south parts of Richmond Gulf, paleocurrents swing through south to southeast.

Near the base of the formation, to the south of the central horst, at least two columnar-jointed gabbroic sills, the Wiachuan Sill (Woodcock, 1960), with an aggregate thickness of 30 m or more, are prominent.

The Persillon Formation, up to 50 m of subaerial basalt flows and minor interflow clastics, conformably separates the underlying Pachi Formation from the overlying Qingaaluk Formation. It overlaps the Pachi Formation on the northern shoulder of the graben (Woodcock, 1960; Chandler, 1979). Strong hematization of the upper several metres of the formation and concentric "ellipsoidal" structures present on the surface of many outcrops (Woodcock, 1960, p. 28), suggest weathering of columnar joints. Other features of the unit include amygdaloidal zones, lava toes, ropy flow structure, mudcracked red interflow mudstone, and basal pipe vesicles. Amygdules, leaning generally to the east, indicate an eastward flow direction.

The Qingaaluk Formation, like the Pachi, consists mainly of pink arkose and pebbly arkose. The only conglomerate present is a 1 to 2 m thick volcanic cobble conglomerate at the base of the formation. The cobbles may be nearly spherical or very angular. Some were probably derived by spheroidal weathering of columnar joints. Seven kilometres southeast of Persillon Lake the conglomerate is more than 15 m thick. Five per cent of granitic boulders indicate local exposure of the basement. Throughout the area bordering Richmond Gulf, about 80 m of red, mudcracked, rippled, fine grained sandstone and siltstone succeed the conglomerate. Paleocurrents based on numerous trough crossbeds from this unit indicate eastward sedimentary transport with some component toward the southeast in the middle part of the Gulf.

The above redbed member is succeeded by an arkosic sandstone member up to 300 m thick that includes pebbly sandstone. Sedimentary structures and paleocurrent patterns similar to those of the Pachi Formation indicate a braided fluvial mode of deposition. Paleocurrents in the arkosic sandstone, from numerous trough crossbeds, flowed eastward and southeastward in the south part of the Gulf. In the central and western parts, currents flowed southward and southeastward. In some instances, paleocurrents appear to have flowed directly toward locations now occupied by basement horsts and the basement bounding the graben.

A small island isolated in the southwest part of Richmond Gulf (marked "vv" in Fig. 6.3) probably at a stratigraphic level high in the arkosic sandstone member, consists of two columnar basalt flows, the lower unit vesicular and at least 10 m thick, and the upper unit about 15 m thick, separated by one metre of red interflow sediments. Pipe amygdules are present at the base of the upper flow. Air photograph interpretation suggests that similar flows are present at this stratigraphic level 20 km to the south.

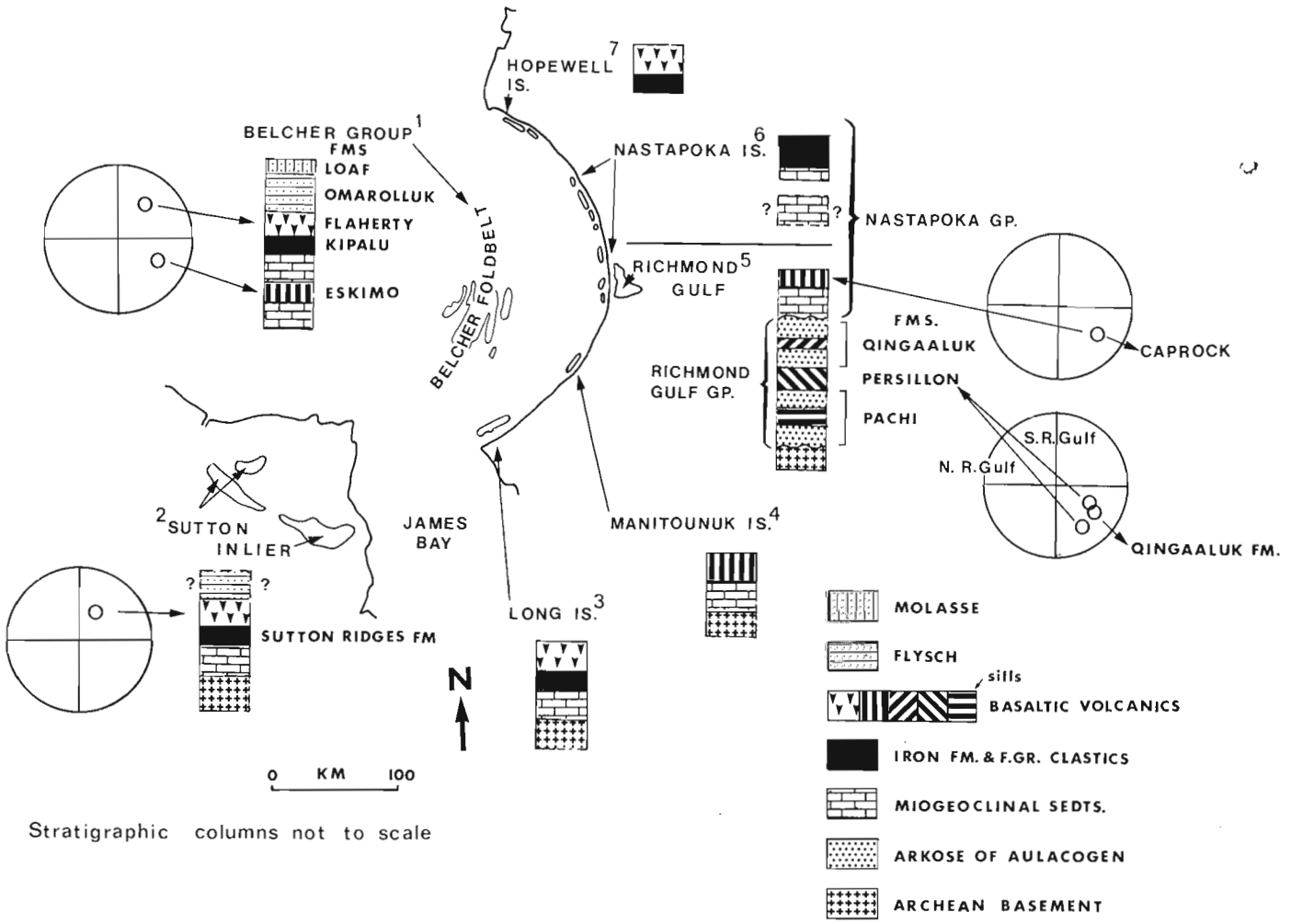

1. *Dimroth et al., 1970;*
2. *Bostock, 1971;*
3. *Low, 1903; Stevenson, 1968;*
4. *Low, 1902;*
5. *Woodcock, 1960; Chandler, 1978, 1979;*
6. *Low, 1903, Stevenson, 1968.*

Figure 6.2. *Stratigraphic and magnetostratigraphic correlation of some Aphebian sequences, Hudson Bay region. Units with similar patterns are interpreted as stratigraphic equivalents.*

The Richmond Gulf Group is folded into a very gentle west-plunging synclinal structure. Within the core of this structure, in the cliffs on the west side of Richmond Gulf, a member is present that is distinguished from the lenticularly-bedded fluvial arkosic sandstone member by its parallel bedding with a continuity measured in hundreds of metres. The member stretches about 9 km north from Castle Peninsula, and pinches out north and southward at the overlying unconformity. It consists of about 70 m of laminated grit and coarse crossbedded feldspathic sandstone with dolomitic matrix and opposed crossbeds, overlain by about 70 m of interlayered sandstone and siltstone on a scale of about one half metre. The sandstone contains numerous planar crossbeds opposed at 180 degrees. The siltstones contain lenticular, wavy and flaser bedding. The unit is probably of tidal marine origin (Fig. 6.1).

Nastapoka Group

The Nastapoka Group overlies the Richmond Gulf Group with gentle angular unconformity, the underlying group having a slightly greater dip to the west. The unconformity surface, which is locally very rugged on a scale of several metres, is generally cut into sandstone of the Qingaaluk Formation, but on Castle Peninsula, rests on an uplifted knob of the granitic basement as well as on the volcanic Persillon Formation. All these units have been bleached and pyritized for some distance beneath the unconformity, the bleached zone at Qingaaluk Hill being about 60 m thick. Copper sulphide and cobalt mineralization are associated with this bleached zone.

On the mainland near Richmond Gulf (Fig. 6.3), the Nastapoka Group consists of a southward-thickening sequence of quartz arenite and carbonate, overlain by basalt. The sedimentary rocks thicken from nothing several kilometres north of the Gulf to about 150 m near the southwest part, and continue southward along the coast to Long Island (Fig. 6.2; Young, 1922). At Richmond Gulf, rock types include supermature quartz arenites and laminated carbonate with oolites, oncolites, stromatolites, tepee structures and edgewise conglomerates composed of laminated carbonate. These features suggest a tidal marine environment for these sediments.

The conformably overlying basalt consists of flows and sills and contains amygdaloidal flow top breccias and ropy flow structure. Woodcock (1960) named the unit the "caprock".

In the Nastapoka Islands, several kilometres west (Fig. 6.3), the group consists in ascending order, of carbonate, carbonate-bearing quartzite, volcanogenic greywacke and intercalated volcanics, topped by iron formation (Low, 1903, p. 9). This sequence bears a strong resemblance to the Kipalu and subjacent Rowatt formations (Fig. 6.2) of the Belcher Group (Dimroth et al., 1970). Minor folding and faulting indicate thrusting from the west (Low, 1903, p. 13, 14).

Structure of the Richmond Gulf and Nastapoka Groups

The Richmond Gulf Group is extensively block-faulted with throws in the order of tens of metres. Normal faults, some listric, step the strata down away from the more or less east-striking, graben-margining faults, and from horsts. Horsts plunge westward and their presence is probably reflected in west-plunging anticlines in the Nastapoka Islands (Fig. 6.3). Dips in the Richmond Gulf Group are usually less than 20 degrees whereas the Nastapoka Group on the mainland dips westward at less than 5 degrees (Woodcock, 1960) and is unfaulted.

On the northern margin of the graben, older units are successively overlapped (Fig. 6.3), the Pachi Formation by the Persillon (Chandler, 1979), the Persillon by the Qingaaluk (Woodcock, 1960). The carbonate-rich sequence underlying the volcanics of the Nastapoka Group thins gradually northward, until several kilometres north of the Gulf the volcanic caprock lies directly upon the granitic basement. At the south margin of the graben, detailed mapping is not yet completed. Nevertheless it is probable that all units of the Richmond Gulf Group are present to the latitude of Petite rivière de la Baleine (Little Whale River), where they are truncated by a prominent east-striking fault (Eade, 1966), south of which carbonates of the Nastapoka Group lie directly upon the granitic basement.

Correlation of Aphebian Sequences in the East Part of Hudson Bay

The segments of Proterozoic supracrustal rocks comprising the Circum-Superior Foldbelt (Fig. 6.1) can be divided into a mainly miogeosynclinal lower part and a mainly eugeosynclinal upper part, separated conformably by a widespread and distinctive Superior-type iron formation (Baragar and Scoates, in press). This stratigraphy is well displayed in the Hudson Bay region by the Belcher Group (Dimroth et al., 1970).

The Belcher Group underlies the Belcher Islands and consists of about 6000 to 9000 m of mutually conformable Aphebian sediments, including twenty to thirty per cent of mafic volcanics and intrusions. The group is separable into a carbonate-rich lower division, including near its base the Eskimo Formation (Fig. 6.2) subaerial plateau basalt (Stirbys, 1975). The overlying second division is dominated by greywacke (Omarolluk Formation) and contains abundant littoral mafic volcanics (Flaherty Formation) and mafic sills. The sequence is terminated by the arkosic Loaf Formation (Dimroth et al., 1970).

Paleocurrents and petrography from the lower division indicate derivation from the Archean Superior Craton that lay to the east. Those of the upper division reflect a western source, and greywacke of the Omarolluk Formation was derived by the erosion of eugeosynclinal volcanics (Barrett, 1975). Bell and Hoffman (1974) thought the lower division to be of shallow water-miogeosynclinal and calc-flysch origin, and the upper division to be of eugeosynclinal origin leading up into an arkosic molasse. A broadly similar view is held by Ricketts (1980).

The Belcher Group is folded into a series of tight anticlines, some isoclinal, and broad synclines with plunge up to 20 degrees, and fold axes concave to the west. Geological and geophysical data indicate that the folding dies out a short distance to the east, but that the rocks beneath Hudson Bay to the west are folded for many miles westward (Jackson, 1960).

Strata correlative with units of the Belcher Group, especially the Kipalu iron formation, are present in several other sequences in the south and east Hudson Bay region (Fig. 6.2). For example, correlation has been made with the Sutton Inlier, Long Island and the Nastapoka (Dimroth et al., 1970) and Hopewell (Lee, 1965) chains of islands.

Dimroth et al. (1970) correlated the caprock volcanic unit of the Richmond Gulf area with argillaceous rocks of the sedimentary Laddie Formation of the Belcher Group. They also correlated the Persillon Formation (Pachi volcanics of Dimroth et al., and of Woodcock, 1960) with the Eskimo Formation of the Belcher Group. The last correlation was endorsed by Ricketts (1980). Other aspects of the correlation of Dimroth et al. include correlation of the Richmond Gulf Group as follows: the Pachi Formation with the carbonates beneath the Eskimo Formation and the Qingaaluk (Richmond Gulf Formation of Dimroth et al., 1970, and of Woodcock, 1960) with the Fairweather Formation (argillite, greywacke, quartzite) immediately overlying the Eskimo.

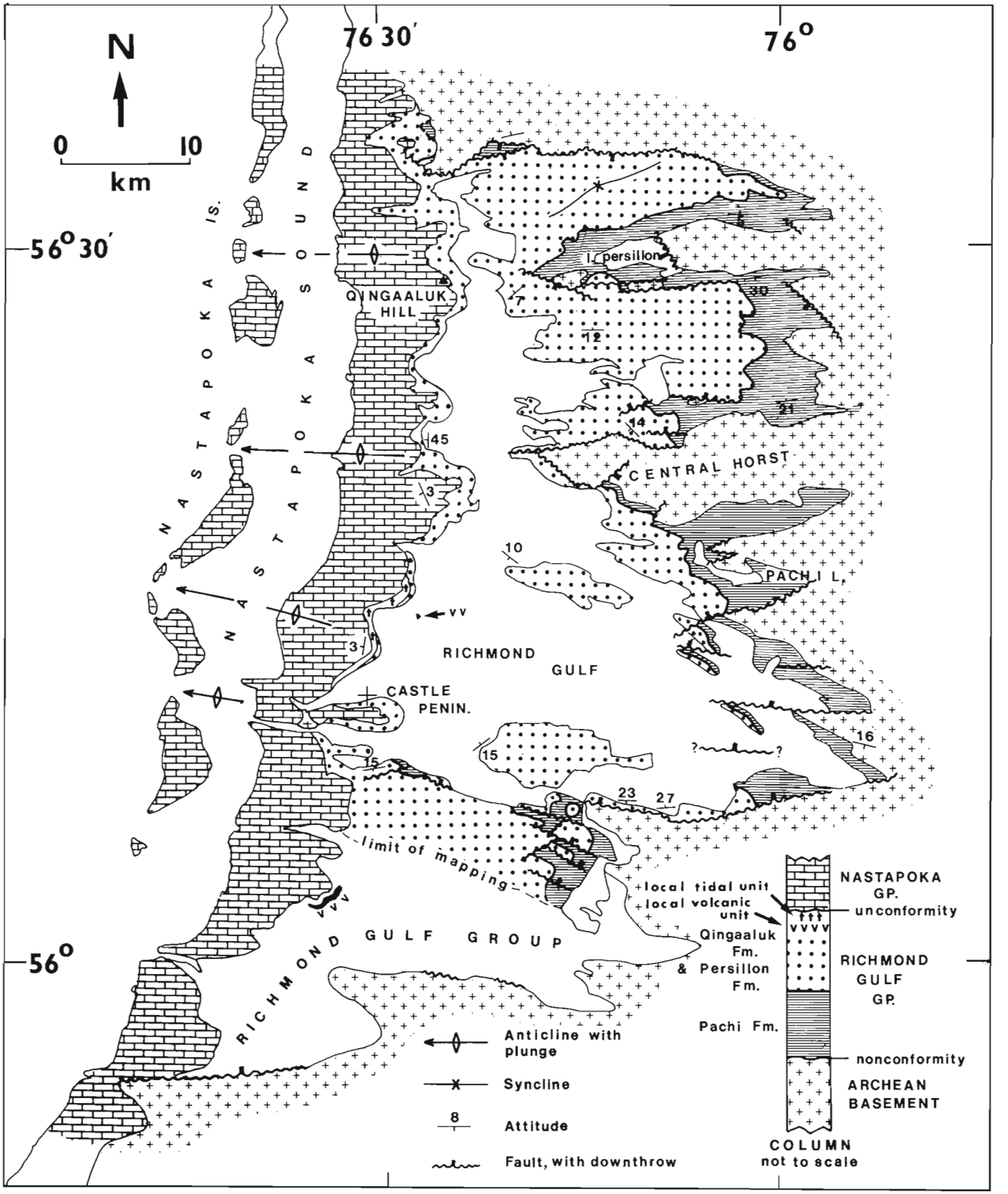

Figure 6.3. *Geology of the Richmond Gulf area.*

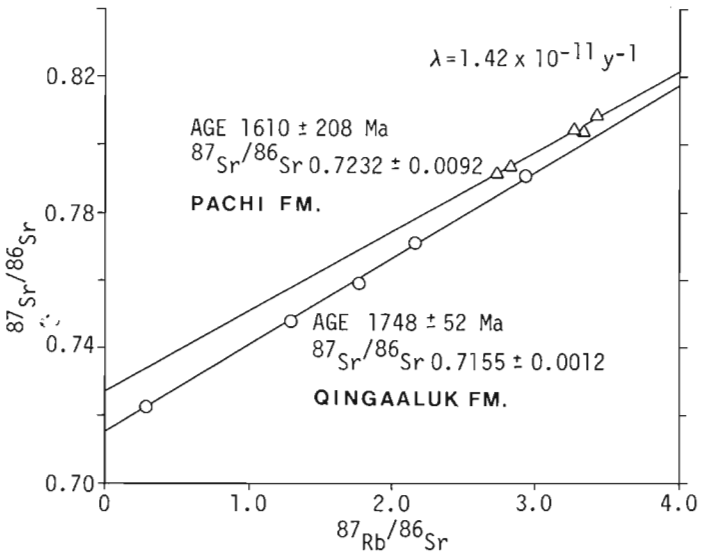

Figure 6.4. *Rubidium-strontium isochrons from the Richmond Gulf Group.*

Relation of the Nastapoka Islands sequence to the Nastapoka Group on the mainland to the east has been uncertain (Woodcock, 1960; Stevenson, 1968), and involved whether or not the Nastapoka Islands sequence was an uplifted stratigraphic equivalent of the mainland rocks or overlay them.

Low (1903) postulated that a thrust fault separated the offshore (Hopewell, Nastapoka and Manitounuk) islands from the mainland. Low's evidence included discovery of thick lean jaspilytes in cliffs on the south shore of Richmond Gulf, which he correlated with those of the Nastapoka Islands. Dimroth et al. (1970) used Low's (1902, p. 77) discovery to support correlation between the underlying Persillon Formation and the Eskimo Formation because of a one metre-thick iron formation overlying the Eskimo. Having visited the cliffs, the first writer considers that the rocks mentioned by Low are likely to be about 80 m of fine grained red sandstone at the base of the Qingaaluk Formation, in an area much block-faulted (Chandler, 1979) and not an iron formation that could be correlated with the iron formation of the Nastapoka Islands.

Thus the writer as well as Stevenson (1968) supports the hypothesis of Leith (1910) that the succession between the mainland and the Nastapoka Islands is continuous and about 300 m of section (Woodcock, 1960) are covered by Nastapoka Sound.

The Eskimo Formation (Stirbys, 1975), the caprock (Woodcock, 1960) and the Persillon Formation all show evidence of subaerial extrusion as plateau basalts. Paleomagnetic studies (Fig. 6.2) indicate that all three are similar in age and distinct from the Flaherty Formation that lies above the Eskimo.

Numerous trough crossbeds indicate paleotransport of the Richmond Gulf Group from a granitic terrane in the northwest to west. The Eskimo Formation is overlain and underlain by a carbonate-dominated succession, and there is no evidence of such a western granitic source in these sediments. On the contrary, paleocurrent patterns in sandstones in the enclosing sequence show transport from the east and interpreted as of marine tidal origin (Barrett, 1975). Carbonates underlie the caprock volcanics and quite probably overlie it, for the top of the missing section under Nastapoka Sound is carbonate (Low, 1903). Thus, the caprock and Eskimo Formation lie within probably similar sequences and are better candidates for correlation.

Paleomagnetism

Independent magnetostratigraphic evidence indicates no considerable time span between the caprock and the Persillon Formation of Richmond Gulf on the basis of essentially single component stable remanent magnetization carried generally by both magnetite and hematite (Schwarz, 1976; Schwarz and Fujiwara, in preparation). The Manitounuk Islands yielded a magnetization direction which differs somewhat from the Richmond Gulf direction, but it is not clear whether this difference is due to a difference in age between the Manitounuk Islands rocks and the Richmond Gulf caprock. Furthermore, Schmidt (1980) showed that the Eskimo volcanics of the Belcher Islands have in part retained a pre-Hudsonian magnetization direction similar to those of the Richmond Gulf and Nastapoka Groups at Richmond Gulf. This suggests a time-stratigraphic correlation between the Eskimo volcanics and the Nastapoka Group caprock and Persillon Formation.

The pre-folding remanence direction reported by Schmidt (1980) for the Flaherty volcanics and the associated Haig diabase intrusives of the Belcher Islands, is significantly different from that of the older Eskimo volcanics and suggests a considerable time span between these volcanic series during which the intercalated sediments (see Fig. 6.1) were probably formed. Also, the Flaherty-Haig pre-folding direction corresponds to the preliminary results for both Sutton Lake basalt and the Tilley Lake redbeds of the Sakami Formation (Schwarz and Freda, 1980; Schwarz and Fujiwara, in press) suggesting that all these are correlative in time. Only three specimen results are reported from Harrison Island of the Hopewell Group and for Long Island, but these are too few and too uncertain to be of help in the correlation of the stratigraphy along the east coast of Hudson Bay. The mean directions of remanent magnetization of the various areas is indicated schematically on Figure 6.2.

Thus magnetostratigraphy supports lithological correlation of the Flaherty volcanics with the sequence in the Sutton Inlier and separation of the iron formation-related volcanics from volcanics such as the Eskimo and Persillon formations and the Richmond Gulf caprock. The magnetic method is not fine enough to decide whether the Persillon Formation or caprock is a correlative of the Eskimo Formation. Geological arguments suggest a caprock-Eskimo correlation.

Geochronology

The age of a high angle continental rift relative to the adjacent foldbelt is important in fitting an appropriate model. Rubidium-strontium ages from later stages in the development of northern parts of the Circum-Superior Foldbelt cluster around 1.8 Ga (Fryer, 1972). Rocks associated with early rifting ought to be significantly older. Dykes interpreted as rift-related (Burke and Dewey, 1973b) have K/Ar ages from 1.96 to 2.29 Ga. Franklin et al. (in preparation) reported lead-isochron ages at 2.1 to 2.25 Ga for galena mineralization in the Mistassini Group. Schimann in Baragar and Scoates (in press) found a Rb/Sr age of 2.15 Ga for volcanics in the Cape Smith Belt (Fig. 6.1).

At Richmond Gulf Hews (1976) got Rb/Sr ages of 1.8 Ga for argillaceous sediments of the Qingaaluk Formation and 1.3 Ga for the Nastapoka Group caprock and the Persillon Formation. A second attempt at dating the fine grained sediments of the Richmond Gulf Group by the Rb/Sr method

at the Geological Survey of Canada yielded 1.61 Ga for the Pachi Formation and 1.75 Ga for the Qingaaluk (Fig. 6.4). The greater age for the overlying unit suggests updating by burial metamorphism. A search for greater ages via the whole rock K/Ar method failed also. The Wiachuan sill yielded 1711 ± 42 Ma and 1787 ± 101 Ma. Mafic dykes cutting the Richmond Gulf Group yielded 1548 ± 60, 1654 ± 46 and 1801 ± 55 Ma. These ages are regarded as inconclusive.

Discussion

Most recent studies have explained the Circum-Superior Foldbelt by the opening and closure of a narrow or wide ocean. The Belcher Group may be a rather complete record of the relevant tectonic cycle from the miogeosynclinal phase through the flysch to the molasse phase. Earlier sediments are probably hidden beneath Hudson Bay and perhaps beneath the Belcher Group. Aphebian strata around the southern and eastern rim of Hudson Bay (Fig. 6.2) are interpreted to be correlative with parts of the Belcher Group. The Richmond Gulf Group, however, is of a facies different from that elsewhere in the region except perhaps the molasse of the Belcher Group (Loaf Formation, Dimroth et al., 1970).

According to plate tectonic theory, location of the Richmond Gulf Group within a graben that strikes at a high angle into the Belcher Foldbelt suggests that it could have formed within one of a family of high angle rifts that form at various stages of orogen development. These include the rifting-related failed arm (Burke, 1978) and its derivative, the aulacogen (Burke, 1977, 1978; Burke and Dewey, 1973b; Hoffman et al., 1974), the post-rifting random rift and the collision-related impactogen (Sengör, 1976; Sengör et al., 1978). Stratigraphic correlations outlined above indicate that the Richmond Gulf Group was deposited before the Belcher Group, thus the failed arm-aulacogen would seem to be the favoured model.

The Aulacogen Model

The geometry of the Richmond Gulf Group lying in a graben striking at a high angle into a foldbelt is characteristic of both the aulacogen and the impactogen. The pronounced salient in the Circum-Superior Foldbelt opposite the point of emergence of the Richmond Gulf Graben from the Superior Craton is strongly suggestive of the former (Salop and Scheinmann, 1969). The great arc of Hudson Bay is similar in plan and scale to the Mackenzie Mountains which were suggested by Burke and Dewey (1973b) to be such an aulacogen-related salient. These salients could be the product of unusually thick miogeoclinal sedimentation of deltaic origin being thrust back onto the foreland during continental collision into the re-entrant left by the original continental fracture at the triple junction. The emergence of the Belcher Group above Hudson Bay in the form of the Belcher Islands may be a topographic expression of this thickening. The unusual preservation of such a wide belt of supracrustals when compared with other supracrustal segments of the Circum-Superior Orogen might indeed be explained by protection within the re-entrant from the rigours of compressive tectonism.

The Richmond Gulf Graben was created by an east-striking set of normal faults, some listric, that broke the Richmond Gulf Group into tilted slabs. Thus it was caused by a tensional tectonic regime, yet there is a paucity of immature conglomerate within the Richmond Gulf Group. This implies that graben formation followed deposition of the group. Further, some local fluvial sediment transport within the Qingaaluk Formation was directly toward graben-bounding faults and basement horsts that even now rise 200 to 300 m above the sediments and lie at a distance of at best a few hundred metres. Thirdly, no evidence was found of faulting before the extensive block-faulting that disrupted all the alluvial sediments of the Richmond Gulf Group. Another curious aspect of the Richmond Gulf Group is its fluvial transport toward the east and southeast as well as eastward flow of the intercalated volcanic Persillon Formation. This is unexpected if the sedimentation in the graben is to be related to the west-transported miogeoclinal sedimentation of the Belcher Group which lies to the west.

An explanation for this apparent inconsistency can be found in the sedimentary effects of the early thermal doming that is the forerunner of continental rifting. Elevations of one kilometre are common on such domes (Burke and Whiteman, 1973) and would give rise to erosion of the dome and centrifugal dispersion of alluvial arkose (Schneider, 1972; Curray, 1980). In the present context such a dome would be centred perhaps a few tens of kilometres to the west of the Belcher Islands and could essentially account for the paleocurrent pattern of the Richmond Gulf Group arkose. The volcanics within the group could be accounted for by incipient crestal rift formation on the dome. Trilete rifting is common on the crest of these thermal domes (Burke, 1978). Inspection of the position of the Churchill-Superior boundary (Fig. 6.1) suggests that the arms of such a hypothetical rift that succeeded in forming an ocean were oriented, one to the north and the other between south and west. An acceptable direction for a failed arm destined to be preserved would be eastward into the Superior Craton at Richmond Gulf. Such a failed arm has the potential to preserve the alluvial clastics of the doming phase.

Modern tectonic theory predicts that following continental rupture several factors combine to cause profound sinking of the adjacent passive margins with concomitant oceanward tilting of the paleoslope (Bott, 1980; Curray, 1980). This would explain the greater westward dip of the Richmond Gulf Group than that of the overlying miogeoclinal Nastapoka Group. The eroded thermal dome would probably be more depressed than adjacent continental margin. This exaggerated depression might contribute to the present depressed circular arc on the east side of Hudson Bay.

The record in the Richmond Gulf Graben is more complex than predicted by the basic model. Deposition of tidal marine clastics is the last record of deposition of the Qingaaluk Formation. Uplift and sculpturing of a jagged unconformity surface beneath the carbonates of the Nastapoka Group followed. Conformity with the Qingaaluk Formation suggests that the tidal clastics preceded the block faulting.

As a result of depression of the Superior continental margin, widespread marine transgression occurred on the faulted clastics of the graben, depositing unfaulted tidal marine carbonates at the base of the Nastapoka Group at Richmond Gulf and probable correlatives elsewhere in the region (Fig. 6.2).

The aulacogen model predicts that as the continental margin sinks a major river may be captured by the failed arm and flow oceanward to build a major delta (Hoffman, 1973; Dewey, 1976; Burke, 1977). Elevation of the Belcher Group as the Belcher Islands above the waters of Hudson Bay offshore from the Richmond Gulf Graben suggests that such a delta might have contributed locally to thickening of the Belcher Group. Mukhopadhyay and Gibb (in press) consider an extensive pear-shaped positive gravity anomaly lying midway between the Belcher Islands and Richmond Gulf and projecting east into the Gulf to be due to local thickening of the Belcher Group to 6 or 7 km. This hypothetical thickening could in part be related to delta formation. Important supporting evidence, a record of seaward fluvial paleocurrents, is absent from the Richmond Gulf Graben.

This could have been removed during erosion of the Qingaaluk Formation at the unconformity beneath the Nastapoka Group. Another contribution to the positive anomaly could be mafic intrusions or volcanics related to graben formation (Burke, 1977).

Evolution to convergent tectonics is seen in the Belcher Group (Bell and Hoffman, 1974) in which flysch, associated volcanics (Flaherty Formation) and iron formation and later molasse were derived from the west. Correlatives of the iron formation are widespread in the islands bordering the eastern Hudson Bay coast (Fig. 6.2). According to the model it is at this stage of convergent tectonics that the miogeoclinal wedge, swollen by local, thick miogeoclinal sedimentation and the inclusion of the large delta formed at the mouth of the failed arm, is forced back into the re-entrant in the passive continental margin that was formed by rifting on two arms of a three-armed rift system. The thickened sedimentary pile, pressed into the re-entrant, is moulded into a salient convex to the foreland continent. Burke and Dewey (1973b) regarded the Mackenzie Mountains as such a salient.

The Impactogen and Random Rift Models

The aulacogen and impactogen have many features in common. However, the latter results from collision and postdates miogeoclinal sedimentation. Consequently, its fill is of the exogeosynclinal phase of orogenic development. Further there is no reason why the thick deltaic sedimentation of the aulacogen should occur and contribute to a bend in the the adjacent foldbelt.

Random rifts (Sengör et al., 1978) may occur at continental margins after initial ocean opening for a variety of reasons. Associated doming will cause erosion of already deposited miogeoclinal strata and deposition of rift-associated clastic wedges on them. The miogeoclinal strata of Richmond Gulf are neither faulted nor thinned by erosion. It seems unlikely that the graben was caused by the impactogen or random rift mechanism.

Future Work

The south margin of the graben at Richmond Gulf is poorly understood. Lead isochron dating of galena mineralization in the Nastapoka Group is in preparation as another approach to setting a minimum age on graben formation. A poorly defined positive gravity anomaly at Richmond Gulf (Earth Physics Branch, open file no. 77-10) could be related to an axial dyke complex. A detailed gravity survey on north-south lines across the Gulf would help to clarify subsurface structure.

The writers gratefully acknowledge critical reviews by A. Bjørlykke, K.L. Currie, R.F. Emslie and J.M. Franklin.

References

Ami, H.M.
1900: Synopsis of the Geology of Canada; Transactions Royal Society of Canada, Section IV, p. 187-225.

Baragar, W.R.A. and Scoates, R.F.J.
The Circum-Superior Belt: A Proterozoic plate margin? in Precambrian plate tectonics, A. Kröner, ed., Elsevier Scientific Publishing Company, Amsterdam. (in press)

Barrett, K.R.
1975: A paleocurrent, paleoslope and provenance study of the Belcher Group; B.Sc. thesis, Brock University, Ontario, St. Catherines, 33 p.

Beals, C.S.
1968: Theories on the origin of Hudson Bay, Part 1; On the possibility of a catastrophic origin for the great arc of eastern Hudson Bay; in Science, History and Hudson Bay, Vol. 2, ed. C.S. Beals, p. 985-998.

Bell, R.
1879: Report on an exploration of the east coast of Hudson's Bay, in 1877; Geological Survey of Canada, Report of Progress, 1877-1878, p. 1C-37C.

Bell, R.T. and Hofmann, H.J.
1974: Investigations of the Belcher Group (Aphebian), Belcher Islands, N.W.T. p. 8, in Program Abstracts, 3rd Circular, Geological Association of Canada, 101 p.

Bostock, H.H.
1971: Geological notes on Aquatuk river map-area, Ontario with emphasis on the Precambrian rocks; Geological Survey of Canada, Paper 70-42, 57 p.

Bott, M.H.P.
1980: Problems of passive margins from the viewpoint of the geodynamics project: A review; Philosophical Transactions of the Royal Society of London, Series A, v. 294, p. 5-16.

Burke, K.
1976: Development of graben associated with the initial ruptures of the Atlantic Ocean; Tectonophysics, v. 36, p. 93-112.

1977: Aulacogens and continental break-up; Annual Review of Earth and Planetary Sciences, v. 5, p. 371-396.

1978: Evolution of continental rift systems in the light of plate tectonics; in Tectonics and Geophysics of Continental Rifts, v. 2, Proceedings of NATO Advanced Study Institute Paleorift Systems with emphasis on the Permian Oslo Rift, p. 1-9.

Burke, K. and Dewey, J.F.
1973a: An outline of Precambrian plate development; in Implications of Continental Drift to the Earth Sciences, v. 2, Academic Press, ed. Tarling, D.M. and Runcorn, S.K., p. 1035-1046.

1973b: Plume-generated triple junctions: Key indicators in applying plate tectonics to old rocks; Journal of Geology, v. 81, p. 406-433.

Burke, K., Dewey, J.F., and Kidd, W.S.F.
1976: Precambrian palaeomagnetic results compatible with contemporary operation of the Wilson cycle; Tectonophysics, v. 33, p. 287-299.

1977: World distribution of sutures – the sites of former oceans; Tectonophysics, v. 40, p. 69-99.

Burke, K. and Whiteman, A.J.
1973: Uplift, rifting and the break-up of Africa; in Implications of Continental Drift to the Earth Sciences, v. 2, Academic Press, ed. Tarling, D.M. and Runcorn, S.K., p. 735-755.

Cavanaugh, M.D. and Seyfert, C.K.
1977: Apparent polar wander paths and the joining of the Superior and Slave provinces during early Proterozoic time; Geology, v. 5, p. 207-211.

Chandler, F.W.
1978: Geological environment of Aphebian Redbeds of the north half of Richmond Gulf, New Quebec, p. 107-110, in Current Research, Part A, Geological Survey of Canada, Paper 78-1A, 588 p.

Chandler, F.W. (cont.)
1979: Geology of the Aphebian supracrustal rocks, Lac Guillaume Delisle, Quebec; Geological Survey of Canada, Open File 600, two bedrock geological maps, scale 1:50 000.

Curray, J.R.
1980: The IPOD programme on passive continental margins; Philosophical Transactions of the Royal Society of London, Series A, v. 294, p. 17-33.

Dewey, J.F.
1976: Ancient plate margins: some observations; Tectonophysics, v. 33, p. 370-385.

Dewey, J.F. and Burke, K.C.A.
1973: Tibetan, Variscan and Precambrian basement reactivation: Products of continental collision; Journal of Geology, v. 81, p. 683-692.

Dewey, J.F. and Spall, H.
1975: Pre-Mesozoic plate tectonics: How far back in Earth history can the Wilson cycle be extended?; Geology, v. 3, p. 422-424.

Dimroth, E.
1972: The Labrador Geosyncline revisited; American Journal of Science, v. 272, p. 487-506.

Dimroth, E., Baragar, W.R.A., Bergeron, R., and Jackson, G.D.
1970: The filling of the Circum-Ungava Geosyncline; in Symposium on Basins and Geosynclines of the Canadian Shield, ed. A.J. Baer, Geological Survey of Canada, Paper 70-40, p. 45-142.

Eade, K.E.
1966: Fort George River and Kaniapiskau River (west half) map areas, New Quebec; Geological Survey of Canada, Memoir 339, 84 p.

Franklin, J.M., Roscoe, S.M., Loveridge, W.D., and Sangster, D.F.
Lead isotope studies in Superior and Southern provinces, Geological Survey of Canada, Paper. (in preparation)

Fryer, B.J.
1972: Age determinations in the Circum-Ungava geosyncline and the evolution of banded iron formations; Canadian Journal of Earth Sciences, v. 9, p. 652-663.

Gibb, R.A.
1971: Origin of the great arc of Eastern Hudson Bay: A Precambrian continental drift reconstruction; Earth and Planetary Science Letters, v. 10, p. 365-371.

Gibb, R.A. and Walcott, R.I.
1971: A Precambrian suture in the Canadian Shield; Earth and Planetary Science Letters, v. 10, p. 417-422.

Gibb, R.A. and Thomas, M.D.
1976: Gravity signature of fossil plate boundaries in the Canadian Shield; Nature, v. 262, p. 199-200.

Goodwin, A.M.
1974: Precambrian belts, plumes and shield development; American Journal of Science, v. 274, p. 987-1028.

Halliday, I.
1968: Theories on the origin of Hudson Bay, part II; Supporting astronomical evidence from three members of the solar system; in Science, History and Hudson Bay, v. 2, ed. C.S. Beals, p. 999-1014.

Hews, P.C.
1976: An Rb-Sr whole rock study of some Proterozoic rocks, Richmond Gulf, Nouveau Quebec; B.Sc. thesis, Carleton University, 64 p.

Hoffman, P.
1973: Evolution of an early Proterozoic continental margin: The Coronation Geosyncline and associated aulacogens of the northwestern Canadian Shield; Philosophical Transactions of the Royal Society of London, Series A, v. 273, p. 547-581.

Hoffman, P., Dewey, J.F., and Burke, K.
1974: Aulacogens and their genetic relation to geosynclines with a Proterozoic example from Great Slave Lake, Canada; in Modern and Ancient Geosynclinal sedimentation, ed. R.H. Dott, Jr., R.H. Shaver, Society of Economic Paleontologists and Mineralogists, Special Publication, No. 19, p. 38-55.

Jackson, G.D.
1960: Belcher Islands, Northwest Territories; Geological Survey of Canada, Paper 60-20, 13 p.

Jacobs, J.A., Russell, R.D., and Wilson, J.T.
1959: Physics and Geology; McGraw-Hill Pub., 424 p.

Kearey, P.
1976: A regional structural model of the Labrador trough, northern Quebec, from gravity studies and its relevance to continent collision in the Precambrian; Earth and Planetary Science Letters, v. 28, p. 371-378.

Lee, S.M.
1965: Nussuaq-Pointe Normand area, New Quebec; Quebec Department of Natural Resources, Geological Report, No. 119, 134 p.

Leith, C.K.
1910: An Algonkian basin in Hudson Bay – a comparison with the Lake Superior basin; Economic Geologist, v. 5, no. 6, p. 227-246.

Low, A.P.
1902: Report on an exploration of the East coast of Hudson Bay from Cape Wolstenholme to the south end of James Bay; Geological Survey of Canada, Summary Report, V. XII, Pt. D, p. 5D-80D.

1903: Report on the Geology and Physical character of the Nastapoka Islands, Hudson Bay; Geological Survey of Canada, Summary Report, V. XIII, Pt. DD, p. 5DD-31DD.

McGlynn, J.C. and Irving, E.
1980: Paleomagnetism of the northwest Canadian Shield and the Slave-Superior comparison, p. 70, in Geological Association of Canada, Halifax '80, Program with Abstracts, v. 5, 94 p.

McGlynn, J.C., Irving, E., Bell, K., and Pullaiah, G.
1975: Paleomagnetic poles and a Proterozoic super-continent; Nature, v. 255, p. 318-319.

Mukhopadhyay Manoj and Gibb, R.A.
Gravity anomalies and deep structure of Eastern Hudson Bay; Tectonophysics. (in press)

Ricketts, B.D.
1980: Sedimentary History of the Belcher Group of Hudson Bay, p. 78; in Halifax '80, Program with Abstracts, v. 5, Geological Association of Canada, 94 p.

Salop, L.I. and Scheinmann, Yu.M.
1969: Tectonic history and structures of platforms and shields; Tectonophysics, v. 7, no. 5-6, p. 565-597.

Schmidt, P.W.
1980: Paleomagnetism of igneous rocks from the Belcher Islands, Northwest Territories, Canada; Canadian Journal of Earth Sciences, v. 17, no. 7, p. 807-822.

Schneider, E.D.
1972: Sedimentary evolution of rifted continental margins; Geological Society of America, Memoir 132, p. 109-118.

Schwarz, E.J.
1976: Paleomagnetism of the Circum-Ungava Belt: in Current Research, Part B, East coast of Hudson Bay, Geological Survey of Canada, Paper 76-1B, p. 37-38.

Schwarz, E.J. and Freda, G.N.
1980: Preliminary paleomagnetic results for Sakami Formation redbeds near La Grande 4, in Current Research, Part C, Geological Survey of Canada, Paper 80-1C; Scientific and Technical Notes.

Schwarz, E.J. and Fujiwara, Y.
Paleomagnetism of the Circum-Ungava Foldbelt II: Proterozoic Rocks of Richmond Gulf and Manitounuk Islands. (in preparation)

Stevenson, I.M.
1968: A geological reconnaissance of Leaf River map-area, New Quebec and Northwest Territories; Geological Survey of Canada, Memoir 356, 112 p.

Sengör, A.M.C.
1976: Collision of irregular continental margins: Implications for foreland deformation of Alpine-type orogens; Geology, v. 4, p. 779-782.

Sengör, A.M.C., Burke, D., and Dewey, J.F.
1978: Rifts at high angles to orogenic belts: tests for their origin and the upper Rhine graben as an example; American Journal of Science, v. 278, p. 24-40.

Stirbys, A.F.
1975: A petrographic and geochemical study of the Eskimo Formation, Belcher Islands, Northwest Territories, unpublished, B.Sc. thesis Brock University, 72 p.

Sutton, J. and Watson, J.V.
1974: Tectonic evolution of continents in early Proterozoic times; Nature, v. 247, p. 433-435.

Thomas, M.D. and Gibb, R.A.
1977: Gravity anomalies and deep structure of the Cape Smith foldbelt, northern Ungava, Quebec; Geology, v. 5, p. 169-172.

Wilson, J.T.
1968: Theories on the origin of Hudson Bay, part III; Comparison of the Hudson Bay Arc with some other features; in Science, History and Hudson Bay, v. 2, ed., C.S. Beals, p. 1015-1033.

Windley, B.F.
1973: Crustal development in the Precambrian; Philosophical Transactions of the Royal Society of London, Series A, v. 273, p. 321-341.

Woodcock, J.R.
1960: Geology of the Richmond Gulf area, New Quebec; Geological Association of Canada Proceedings, v. 12, p. 21-39.

Young, G.A.
1922: Iron-bearing rocks of Belcher Islands, Hudson Bay; Geological Survey of Canada, Summary Report, Part E, 61 p.

7. STRUCTURE, STRATIGRAPHY AND SOME CHEMICAL CHARACTERISTICS OF AN EARLY PROTEROZOIC (BIRIMIAN) VOLCANIC BELT, NORTHEASTERN GHANA

Project 770070

K. Attoh
Precambrian Geology Division

Attoh, K., Structure, stratigraphy and some chemical characteristics of an early Proterozoic (Birimian) volcanic belt, northeastern Ghana; in Current Research, Part C, Geological Survey of Canada, Paper 80-1C, p. 69-80, 1980.

Abstract

The structure of a Birimian volcanic belt at Nangodi in northeastern Ghana is inferred from the distribution of lithologic units, limited evidence for their superposition, and two-dimensional gravity models. Gravity models indicate that the depth to the base of the supracrustal rocks is about 3-4 km. The succession of lithostratigraphic units is: epiclastic sediments interbedded with felsic tuffs, lavas and porphyries, followed by tholeiitic mafic lavas which are overlain by calcalkaline intermediate to felsic tuffs and lavas. The youngest volcanic unit is a calc-alkaline mafic tuff. Manganiferous sediments occur at several stratigraphic horizons within the sequence, but are best developed at the boundary between tholeiitic and calcalkaline volcanic rocks. The volcanic-sedimentary succession is terminated by late orogenic fluviatile sediments. The succession is estimated to be 9000 m thick.

In the Birimian volcanic rocks the ratio of tholeiitic to calcalkaline rocks ranges from 1:1 to 1:1.5 based on the estimated stratigraphic thicknesses of units of the two classes of volcanic rocks in the study area and from the proportion of tholeiitic to calc-alkaline rocks in over a hundred chemical analyses of samples from other early Proterozoic volcanic belts in the West African Shield. Major and trace element chemical characteristics of the volcanic and spatially associated granitic rocks are used to differentiate between postkinematic plutons and plutons comagmatic with the volcanics.

Introduction

The Precambrian shield in West Africa can be subdivided into the three domains or provinces (Fig. 7.1) on the basis of age, and tectonic and lithologic characteristics of the supracrustal rocks. The Libero-Leonian Province (Archean) is exposed in the western part of the shield, and an early Proterozoic province occupies the eastern part of the shield. The Panafrican domain includes late Proterozoic orogenic belts and platform sediments and forms the boundary of the West African craton. There is a change in the lithology at the boundary between Archean and Proterozoic provinces. For example, granulite facies metamorphic complexes and itabiritic iron formations occur only in the Archean province (Hurley et al., 1971), whereas the Proterozoic province is characterized by occurrences of manganese formations.

The Proterozoic province is characterized by north to northeast trending volcanic-sedimentary belts (Birimian) which are exposed in Ivory Coast, Upper Volta, and Ghana. The distribution of the Birimian supracrustal belts is shown in Figure 7.1. The purpose of this report is to present the preliminary results of a project to study the stratigraphy and geochemistry of supracrustal rocks in the West African Shield. The data discussed here were obtained during recent field work in a Birimian volcanic belt located in Nangodi area, northeastern Ghana (Fig. 7.1, Belt 1). Correlation between the stratigraphic classifications used in the reports by Geological Survey of Ghana (GSG) and Bureau des Recherches Géologiques et Minières (BRGM) are discussed in the light of the stratigraphic relations established for the Nangodi volcanic belt.

Problems in Stratigraphic Classification of Birimian Supracrustal Rocks

The definitive report on Birimian stratigraphy is by Junner (1954) and recent work in Ghana differs only in detail (e.g. Asihene and Barning, 1975). In the above reports, Birimian rocks have been classified into older, predominantly epiclastic rocks (Lower Birimian) and younger, predominantly volcanic rocks (Upper Birimian) in southwestern Ghana. A recent study in southwestern Ghana has shown that the sedimentary rocks referred to as Lower Birimian are typical of flysch-type turbidite deposits (Trashliev, 1974). The Upper Birimian volcanic rocks have been less well studied and little lithostratigraphic information is available. Indeed, in Ghana, it has not been demonstrated that the "Upper Birimian" volcanics are everywhere younger than the "Lower" Birimian sediments.

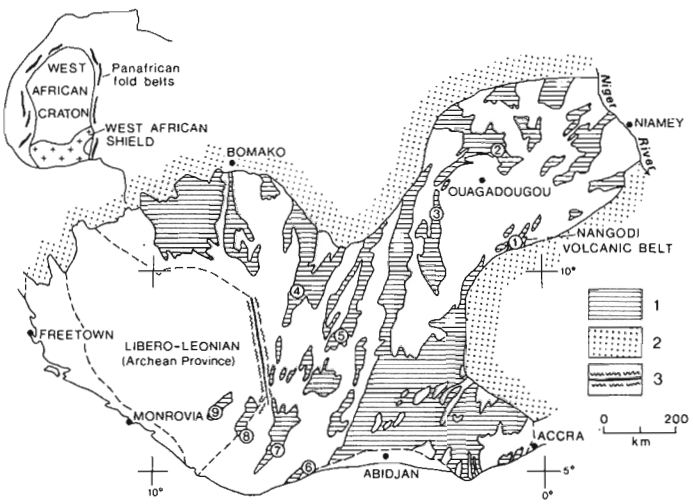

1. *Birimian volcanic sedimentary belts (numerical labels refer to belts from which chemical data are available),*
2. *Late Proterozoic platform sediments,*
3. *Approximate boundary between Proterozoic and Archean shields; partly marked by Sassandra fault zone.*

Figure 7.1. *West African Shield showing the distribution of Proterozoic volcanic-sedimentary belts.*

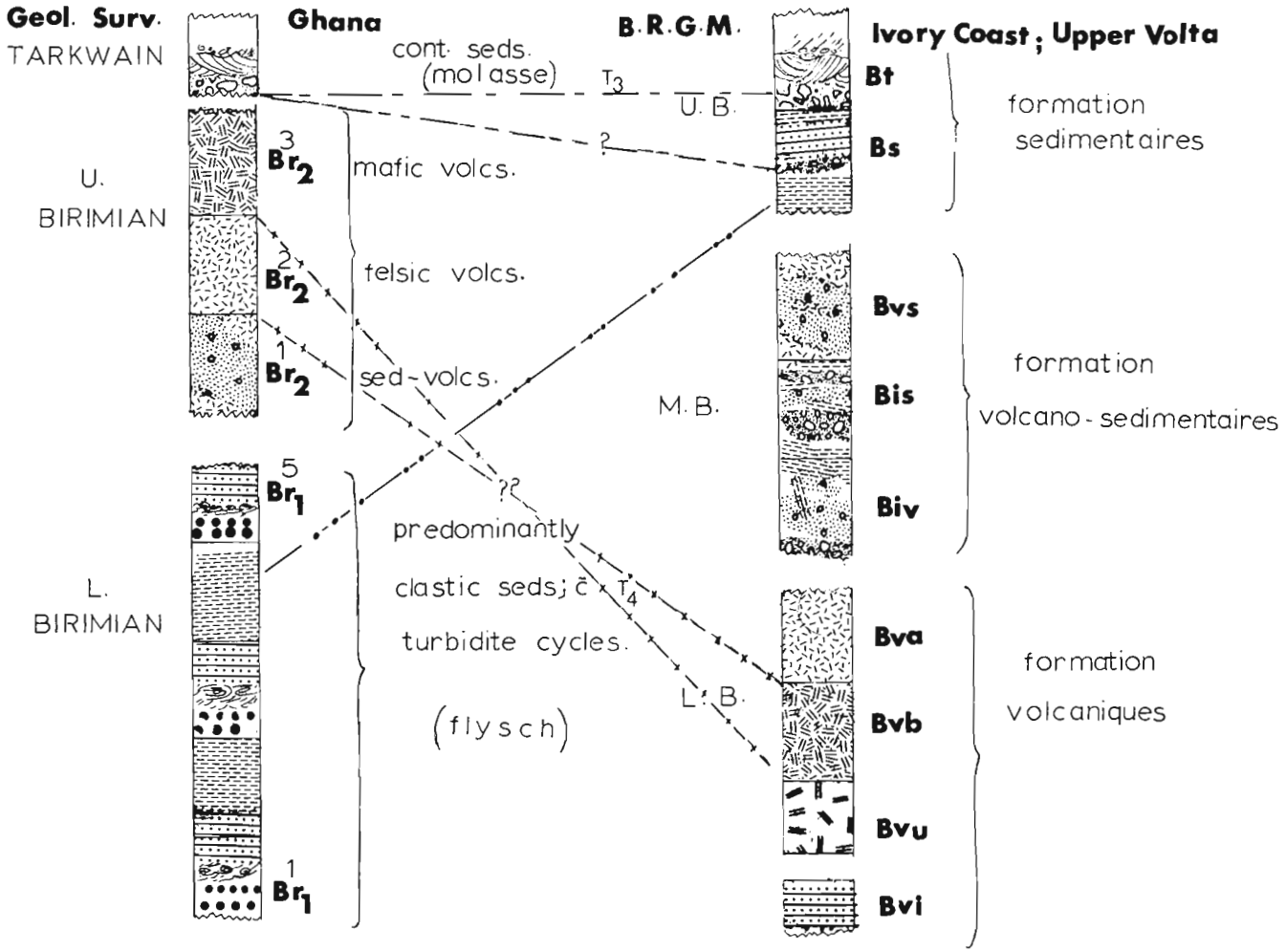

Bvu	= *ultrabasic volcanics*	*Bvb*	= *basic volcanics*
Bva	= *acid volcanics*	*Bvs*	= *mixed volcanics and sediments*
Biv	= *undifferentiated volcanic-sedimentary unit*	*Bs*	= *sediments (turbidites)*
Bis	= *volcanic sedimentary unit (sediments dominant)*	*Bt*	= *continental sediment with conglomerates considered to be equivalent to Tarkwaian in Ghana*
$Br_1^1 \ldots Br_1^5$	= *subdivisions, of Lower Birimian*	$Br_2^1 \ldots Br_2^3$	= *subdivisions of Upper Birimian by Geological Survey of Ghana*

Figure 7.2. *Correlation between stratigraphic classifications of the Birimian supracrustal rocks as presently used by Geological Survey of Ghana and Bureau de Reserches Geologiques et Minières (in Ivory Coast and Upper Volta).*

The stratigraphic scheme for the Birimian adopted by Francophone geologists working in Cote d'Ivoire and Haute Volta which contrasts strongly with that used in Ghana, is summarized in Papon (1973), Blanchot et al. (1972) and reviewed by Bessoles (1977). As adopted by BRGM and used on their maps, the Birimian stratigraphic succession consists of a lower formation volcanique, a middle formation volcano-sedimentaire, and an upper formation sedimentaire. The BRGM sequence is the reverse of the stratigraphic order used by the Geological Survey of Ghana and the controversy is illustrated in Figure 7.2. There is little evidence to support the stratigraphic order implied in either of the two schemes, and both stratigraphic columns shown in Figure 7.2 are more conceptual than factual. For example, the sequence used by BRGM is based on Tagini's (1971) concept of Birimian stratigraphy which was based on the presumed similarity between Alpine and Birimian volcanic successions. Recent structural and stratigraphic studies in the Birimian have shown that neither of the stratigraphic sequences in Figure 7.2 are generally valid (see review by Bessoles, 1977, p. 302-305).

Another difference between the BRGM and GSG stratigraphic schemes concerns the sediments that occur at the top of the Birimian sequences (Fig. 7.2). In Ghana, because a basal conglomerate marks the angular unconformity at the base of the Tarkwaian, the original definition of the Birimian by Junner (1954) excluded the Tarkwain type sediments. The BRGM, however, considers these as part of the Birimian succession because the belts of the "formation sedimentaire" are structurally conformable with the underlying Birimian volcanic-sedimentary sequence.

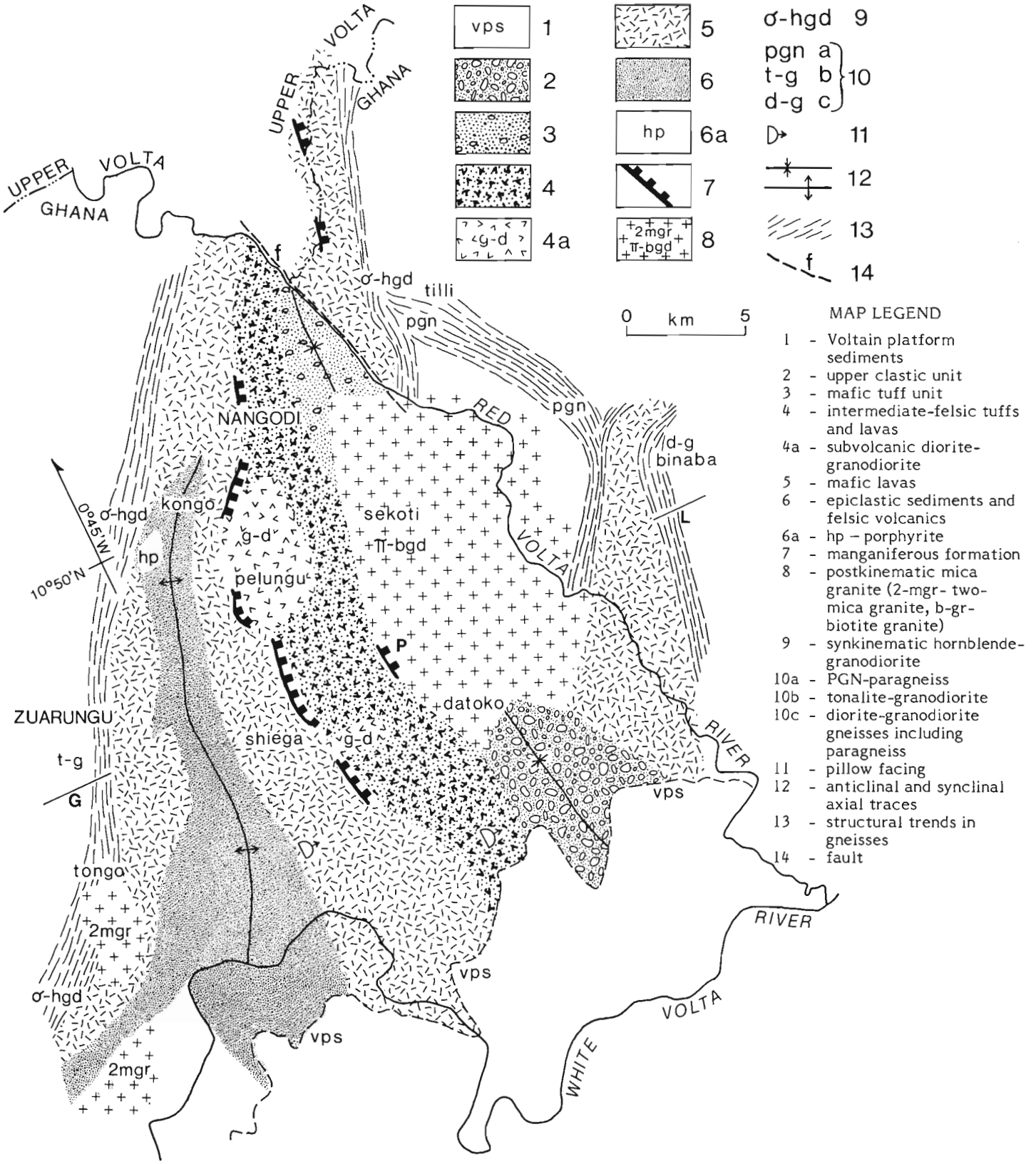

Figure 7.3. *Geological map of the Nangodi volcanic belt.*

A - *gravity profile along G.P.L. (Fig. 7.3) and computed sub-surface distribution of supracrustal rocks with the indicated density contrast.*

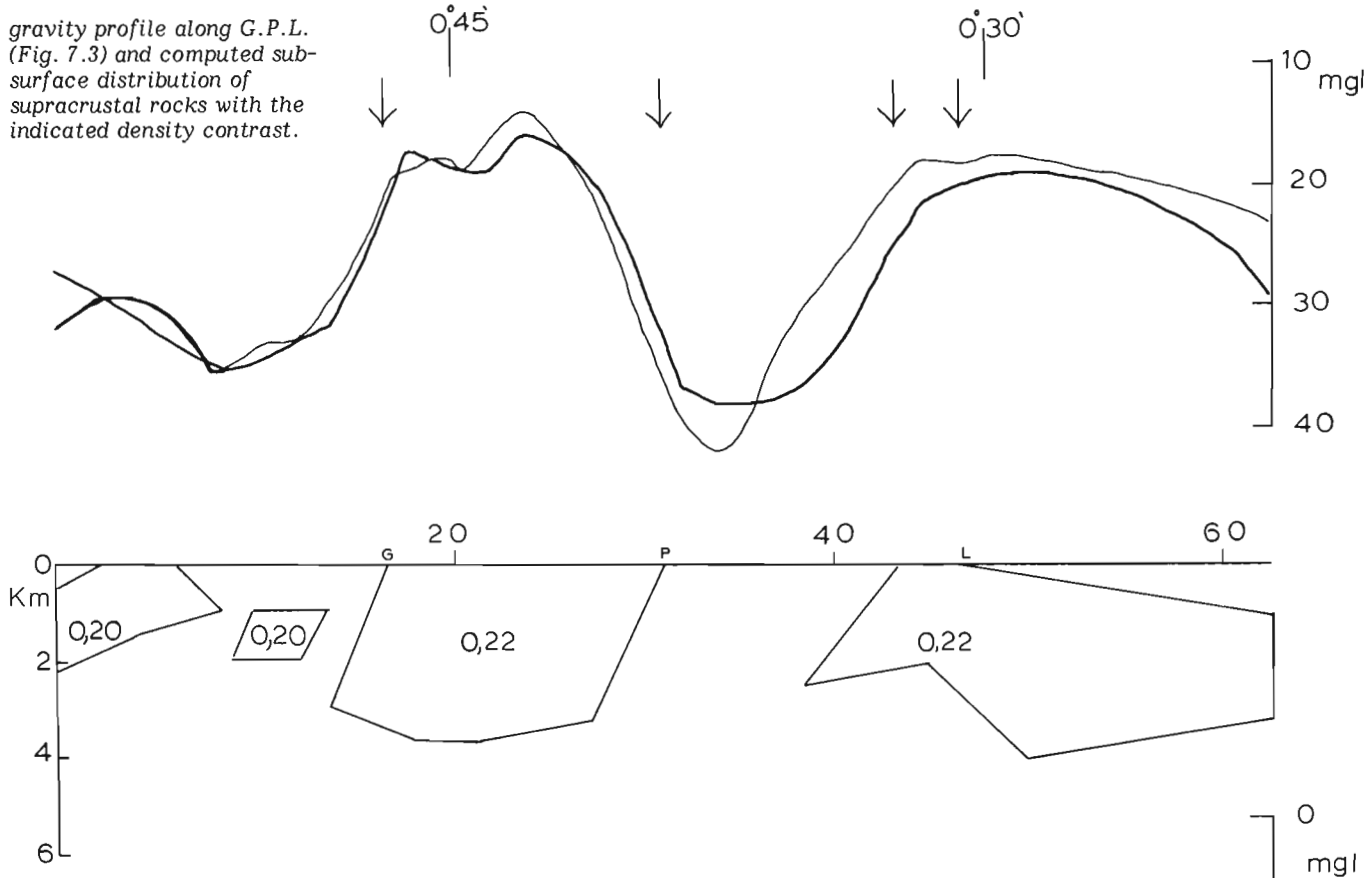

B - *detail gravity profiles along G.P. showing the computed structures.*

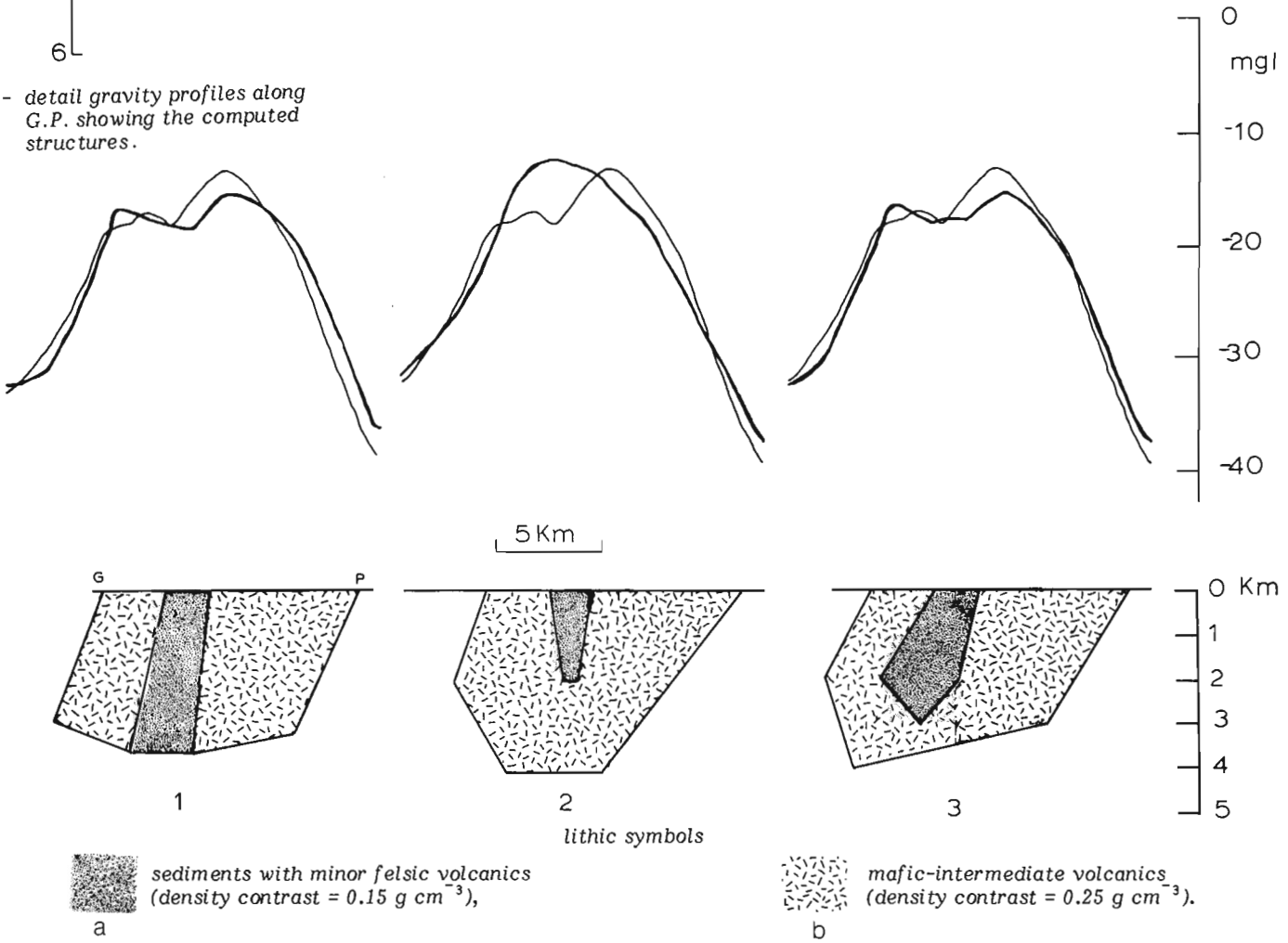

Figure 7.4. *Bouguer gravity models for the Nangodi volcanic belt; observed (thin line), computed (thick line).*

Structure of the Birimian Volcanic Belt in the Nangodi area

The Nangodi volcanic belt is located in northeastern Ghana (Fig. 7.1) close to the Upper Volta border. The geological map of the area is shown in Figure 7.3, from which the distribution of the lithic units would permit a unique solution to the structure if the stratigraphic relations were known, or vice versa. As only limited critical stratigraphic data are available in the Nangodi area, several possible solutions of the structure exist and it is difficult, if not impossible, to choose between the different interpretations. However an additional constraint can be imposed on the structure by the interpretation of the available Bouguer gravity data.

A hand-contoured Bouguer gravity map compiled by Prucha (1972) at 1:250 000 scale shows a 'high' centred along the Nangodi volcanic belt and a "low" over the granitic pluton outcropping near Sekoti. A profile constructed along 10°45'N (G.P.L. in Fig. 7.3) is shown in Figure 7.4A. A variety of plausible subsurface mass-distribution models could account for the observed gravity anomaly associated with the volcanic belt. Values of density contrasts were assumed to be similar to actual measurements in other greenstone belts (Gibb and Thomas, 1980). The granite body with the lowest gravity values was chosen for background so that all density contrasts would have positive values. From two-dimensional models of the Bouguer gravity data the following interpretations of the structure can be made:

a. About 3-4 km of supracrustal rocks having average density contrasts (0.20-0.22 g cm^{-3}, with respect to the background) would account for the observed gravity anomaly (Fig. 7.4A).

b. An overturned fold corresponding to the anticlinorium shown on Figure 7.3 accounts well for the observed profile. In particular, the asymmetrical double peak in the observed profile is best explained by a 3 to 4 km thick fold core (Fig. 7.4B, model 1). The fold core corresponds with the sedimentary unit and the anticlinal structure is compatible with the geological facing and vergence data (Fig. 7.3).

c. If a synclinal structure is assumed in which about 2 km of mafic volcanics underlie about 2 km of sediments, the two-dimensional gravity model does not account for the anomaly (Fig. 7.4B, model 2). An overturned syncline with considerable thickening of the sedimentary unit would account for the observed profile (Fig. 7.4B, model 3), but the facing of the east limb of the synclinal structure is not compatible with the sparse facing direction available.

Other subsurface intrusive bodies of appropriate density contrast could be invoked to account for the profile, but such models cannot be tested. It is therefore concluded that with the available data, the overturned anticline (Fig. 7.4B, model 1) is the best interpretation of the structure.

Stratigraphy of Birimian Supracrustal Rocks in the Nangodi Area

Sedimentary Unit

Sedimentary rocks occupy the core of the anticlinal structure shown in Figure 7.3 and represent the lowest part of the Birimian succession in the Nangodi belt. The unit comprises epiclastic sediments and minor felsic lavas, tuffs and porphyrites. The clastic sediments include greywacke, shale, fine grained tuffaceous sediments and rare, intraformational conglomerate beds in which the pebble-size, rounded clasts consist of finely laminated sediments. Primary structures include bedding, convolute lamination and graded bedding. Thin siliceous sediments with Fe-Mn rich layers are present locally and ash beds occur in the tuffaceous sediments. The felsic lavas associated with wacke sediments are plagioclase-phyric rhyolites. The thin beds are commonly folded into tight isoclines. The porphyrite is an amphibole-phyric dacite that ranges in texture from aphyric to coarsely porphyritic. The estimated thickness of the sedimentary unit is at least 1800 m (Fig. 7.5).

The contact between the volcanic-sedimentary belt and foliated granodiorite is exposed about 2 km west of Kongo (Fig. 7.3). At the contact the sediments are metamorphosed to a hornblende schist and are injected by granodioritic material. Angular blocks of metasediment are enclosed in the granodiorite rock and clearly indicate that the hornblende granodiorite is intrusive into the sediments. The nature of the basement on which the sediments accumulated is not known.

Mafic Volcanic Unit

The mafic volcanic rock, which forms the prominent hills in the area, occurs on both limbs of the anticlinorium (Fig. 7.3) and overlies the sedimentary unit. Chert beds and rare pillow structures provide the only evidence of stratification in the mafic volcanic unit. The chert beds, considered to be siliceous chemical sediments, occur as discontinuous thin beds. Pillow structures with thin selvages and no internal structure were observed in only one locality. The pillowed flow occurs at the base of the mafic volcanic unit. Felsic feldspar porphyries occur in the unit and, at one locality west of Tongo, a differentiated mafic flow consists of felsic rocks near the top.

Manganese Formation

The best developed manganiferous rocks occur more or less continuously along the contact between the mafic volcanic unit and the overlying intermediate-felsic volcanic unit (Fig. 7.3). The manganese formation is a black Mn-oxide rock interbedded with siliceous sediments. The unit is characterized by disharmonic soft sediment folding. Manganiferous rocks also occur in the sedimentary unit and near the top of the intermediate-felsic volcanic unit (Fig. 7.5). The manganiferous rocks at the different stratigraphic levels are lithologically similar and each probably marks a hiatus in volcanism or clastic sedimentation.

Intermediate-Felsic Volcanic Unit

Intermediate-felsic lavas and lithic tuffs overlie the mafic volcanic unit (Fig. 7.3, 7.5). Fragmental textures are well preserved and consist of porphyritic felsic volcanic rock fragments in a dark chlorite-rich matrix. Pillow structures with interpillow hyaloclastic tuff breccia occur at one locality south of Datoko. Rhyolite lava flows and welded tuffs have been identified in the unit. The unit which includes clastic sediments is estimated to be between 2000 and 2500 m thick.

A Mafic Tuff Unit

In the core of the syncline north of Sekoti (Fig. 7.3) is the youngest volcanic rock in the area. The distinctive fragmental texture consists of leucocratic fragments in a mafic, amphibole-rich matrix. The matrix is tightly crenulated, producing a set of S-surfaces which enhance the fragmental texture. Primary layering is preserved as alternating fine and coarse grained layers in the amphibole crystal tuffs. Plagioclase-rich sediments (greywacke tuff) are associated with the unit. The unit is estimated to be about 500 m thick.

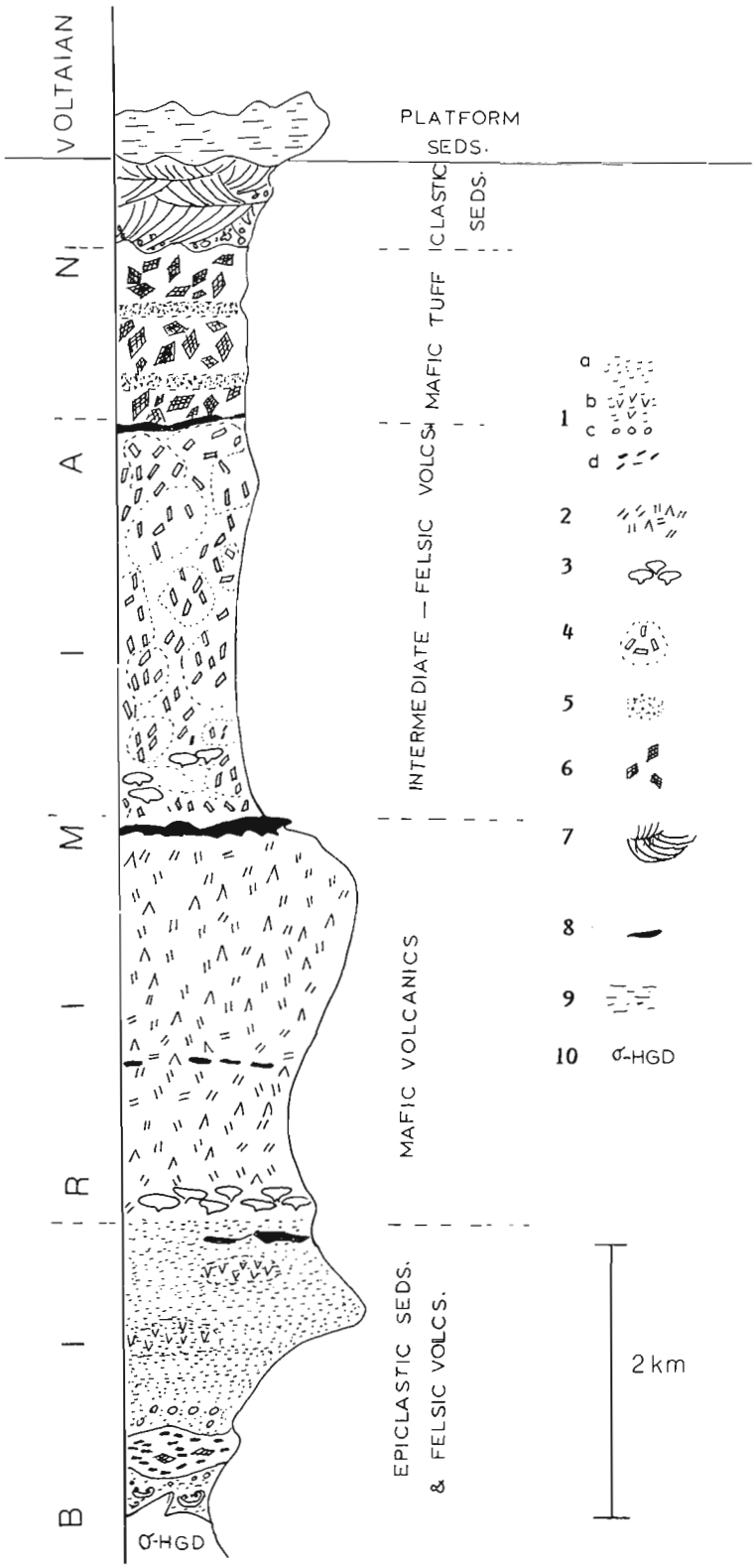

1a - fine laminated tuffaceous and clastic sediments
1b - felsic lavas
1c - conglomerate
1d - porphyrite
2 - mafic lavas (massive)
3 - pillow lavas
4 - lithic tuffs
5 - greywacke tuff
6 - crystal tuff
7 - cross-bedded sediments
8 - manganiferous formation
9 - platform sediments
10 - synkinematic granodiorite

Figure 7.5. *Stratigraphic column for the Nangodi volcanic belt.*

Upper Clastic Sedimentary Unit

The crossbedded arenites and rudites of this unit are exposed just south of Datoko. The clasts include rounded mafic volcanic rock fragments in a silty matrix. Crossbedding in scour channel deposits is well developed and a fluviatile origin is indicated. Junner (1954) did not include clastic sediments with similar sedimentary features in the original classification of Birimian rocks. However in the Nangodi area the fluviatile clastic sedimentary unit is considered to represent the terminal part of the Birimian volcanic-sedimentary succession for the following reasons. The upper clastic unit is structurally conformable with the underlying volcanic succession and occurs in the core of the synclinal structure which can be traced into the mafic tuffs (Fig. 7.3) and both the upper clastics and the underlying volcanics are unconformably overlaid by flat-lying Late Proterozoic platform sediments (Voltaian). The unconformity implied by the presence of mafic volcanic rock fragments in the upper clastic sediments does not appear to represent a major time break, instead, the upper clastics are interpreted as late-orogenic sediments belonging to the underlying volcanic and sedimentary sequence.

Chemical Characteristics of Birimian Volcanic Rocks

With few exceptions (eg. Murray, 1960) there is a dearth of chemical data on Birimian volcanic rocks in Ghana. The chemical characteristics discussed here are based on analyses of the "least altered" samples. The selection was based on a "cut-off limit" of 3.8 per cent of total volatile components ($H_2O + CO_2$). This criterion assumes that the high values of volatile components indicate alteration. In many cases evidence for alteration in the form of calcite veins, and altered feldspars can be seen in hand specimens and in thin section (see review of some criteria by Gélinas et al., 1977).

The following discussion assumes that the selected volcanic rocks have preserved their primary chemical characteristics with respect to the major elements used in the classification (SiO_2, Al_2O_3, FeO, MgO, CaO, K_2O and Na_2O) and this assumption is extended to the trace element concentration. Primary trace elements characteristics can be used to infer volcano-tectonic environments (Pearce and Cann, 1973) and the nature of the source of the volcanogenic material and have been used in petrogenetic models for Archean volcanic rocks (Arth and Hanson, 1975; Jahn et al., 1974).

Major Element Chemistry

The Birimian volcanic rocks are classified according to the scheme of Irvine and Baragar (1971). Figure 7.6a is the silica alkali diagram (SiO_2 vs K_2O) where it can be seen that all the samples including the potash-rich postkinematic granites plot in the subalkali field. The AFM diagram (Fig. 7.6b) shows that both tholeiite and calc-alkali trends occur in Nangodi volcanic rocks. An iron-enrichment trend is present but not as extreme as has been observed in some oceanic and ridge tholeiites (Carmichael et al., 1974, p. 373-426). The absence of alkali-enriched rocks in part reflects the fact that the fragmental felsic rocks are highly altered and have been excluded from the samples plotted. The Al_2O_3 vs normative plagioclase diagram also shows the distribution of the samples in tholeiite and calc-alkali fields (Fig. 7.6c). It should be noted that the occurrence of both tholeeitic and calc-alkali suites in the same Archean volcanic belt is already well documented (Baragar, 1972).

On colour index (CI) vs normative plagioclase diagram (Fig. 7.6d), the sample clusters correspond closely with the map units of the volcanic rocks. In addition the rocks which

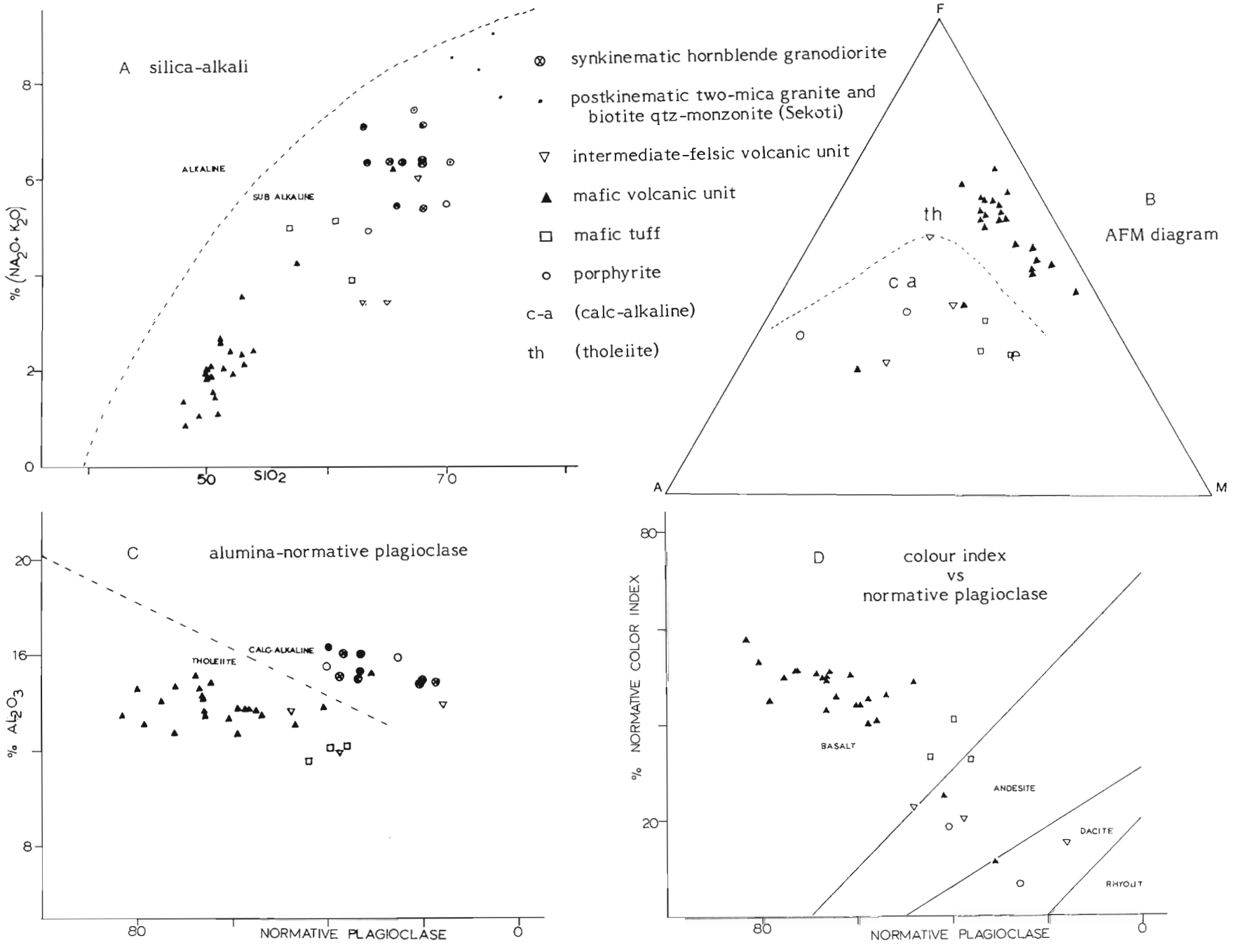

Figure 7.6. *Major element chemical characteristics of Nangodi volcanic rocks.*

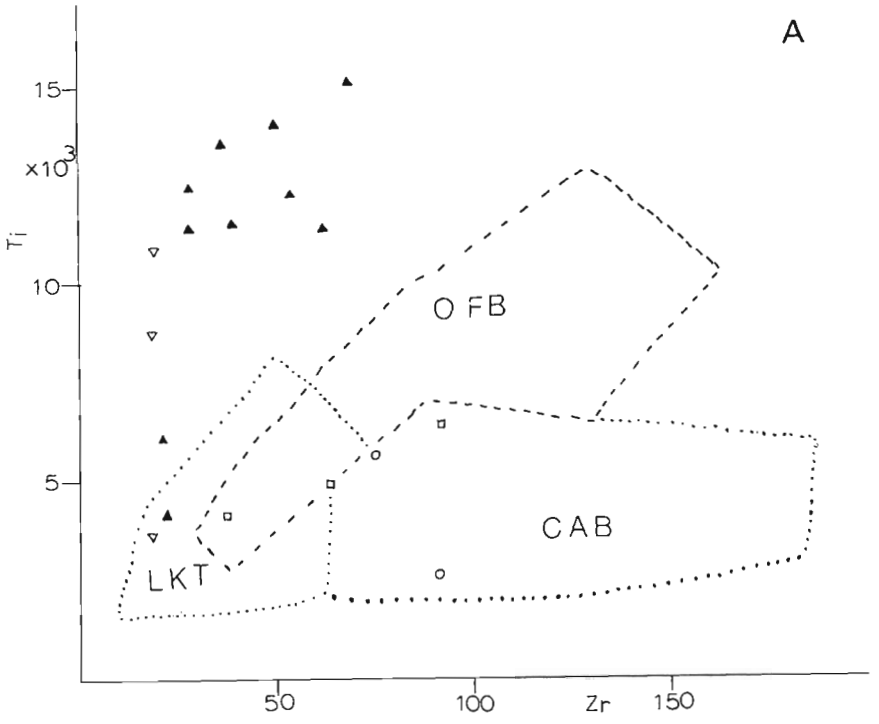

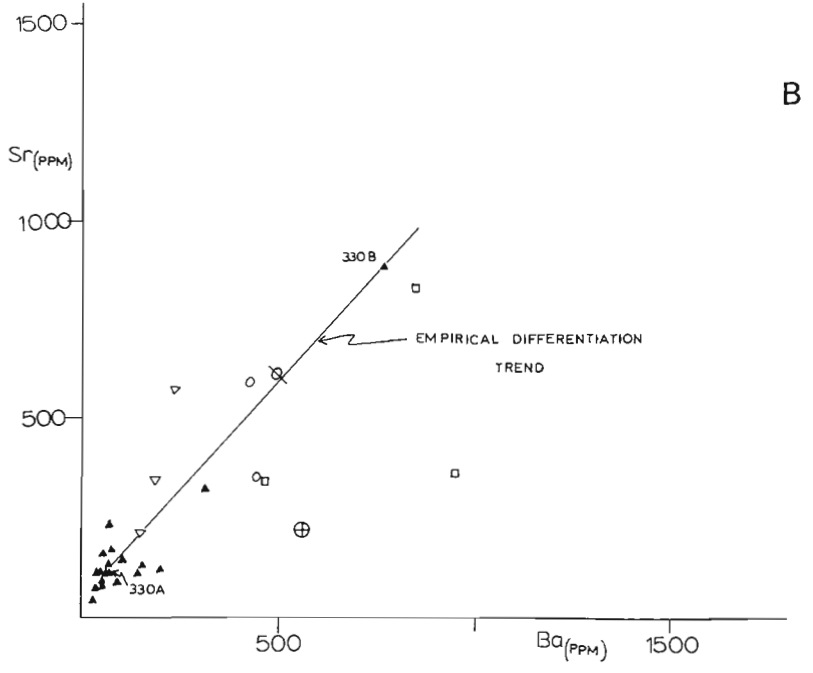

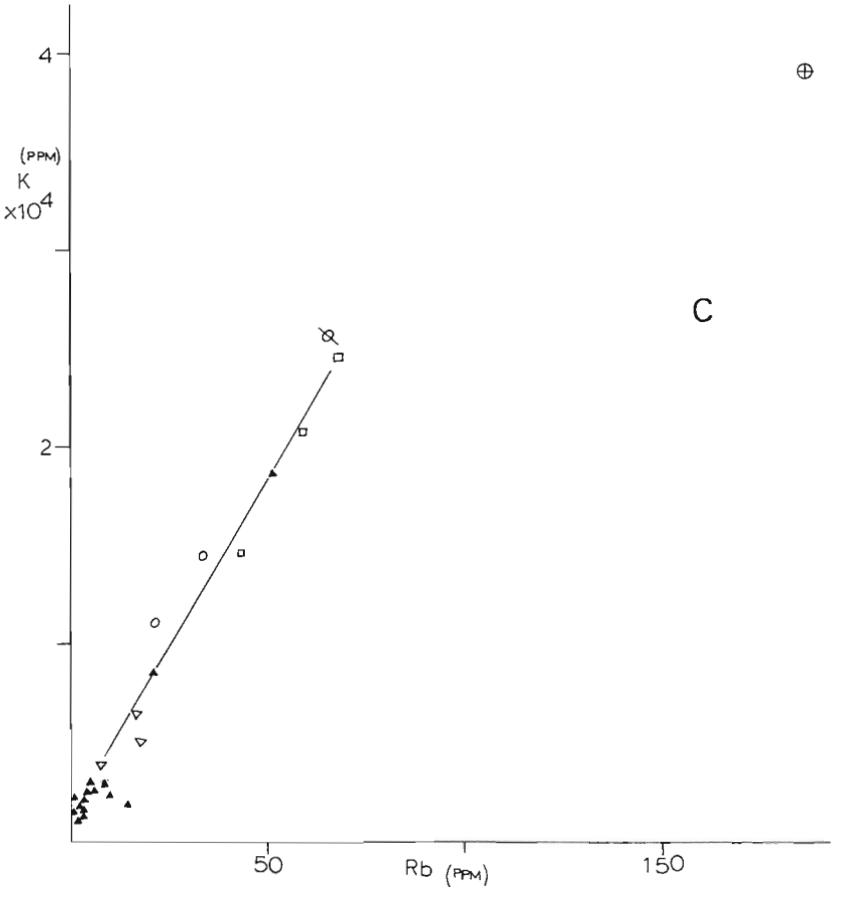

Figure 7.7. *Trace element chemical characteristics of Nangodi volcanic rocks.*
A - Ti vs Zr *B - Sr vs Ba* *C - K vs Rb*

Symbols (See also Fig. 7.6)

⊗ *synkinematic granodiorite*

⊕ *postkinematic mica-granite (Tongo)*

OFB = ocean floor basalts

LKT = low potassium tholeiites

CAB = calc-alkaline basalts

plot in the tholeiitic field are characterized by low quartz-normative values and only two samples from the tholeiite unit are olivine normative (and these have less than 1% olivine in the norm). Samples from the intermediate-felsic volcanic unit are calc-alkaline, have high quartz normative values (22-33%) and the normative plagioclase compositions are characterized by Ab>An. The calc-alkaline basalt samples are from the mafic tuff unit and are characterized by high Or in the normative mineralogy. Samples from the hornblende porphyrite body plot in the calc-alkaline dacite or andesite field.

Trace Element Chemistry

Ti-Zr concentrations are plotted in Figure 7.7a. The clear separation between calc-alkaline and tholeiite suites conforms with the major element data and is explicable from the petrographic observation that ilmenite is a common phase in the mafic volcanic rocks. If the Ti-Zr concentrations are compared with modern volcanic rocks (Pearce and Cann, 1973) the tholeiitic rocks from the Nangodi volcanic belt are higher in titatium than low potassium tholeiites (LKT) and ocean floor basalts (OFB).

Sr-Ba concentrations are plotted in Figure 7.7b. The low Sr and Ba concentration in the tholeiite is comparable to other ancient volcanic rocks (Arth and Hanson, 1975). An empirical differentiation trend shown on the diagram is based on two samples taken from a differented flow. A crude trend exists in the distribution of all analyzed rocks which in general conforms with the postulated differentiation. The proposed differentiated trend would correspond to Sr/Ba obtained by 10-15 per cent partial melting of a tholeiite (Arth and Hanson, 1975). It is suggested that the volcanic-related granitic rocks should plot close to the differentiation trend while unrelated plutonic rocks could plot off the trend. In Figure 7.7b it can be seen that the syn-late-kinematic amphibole-bearing granodioritic rocks in the Nangodi belt conform well to the trend, while the samples from the postkinematic two-mica granites (Fig. 7.3) do not.

K-Rb concentrations are shown in Figure 7.7c. The low concentrations of K and Rb in the mafic volcanic unit are similar to data from Archean volcanic terranes (eg. Arth and Hanson, 1975). The trend from mafic to felsic volcanic rocks lies crudely along the empirical differentiation trend, while the sample from postkinematic granite is very high in potassium and rubidium.

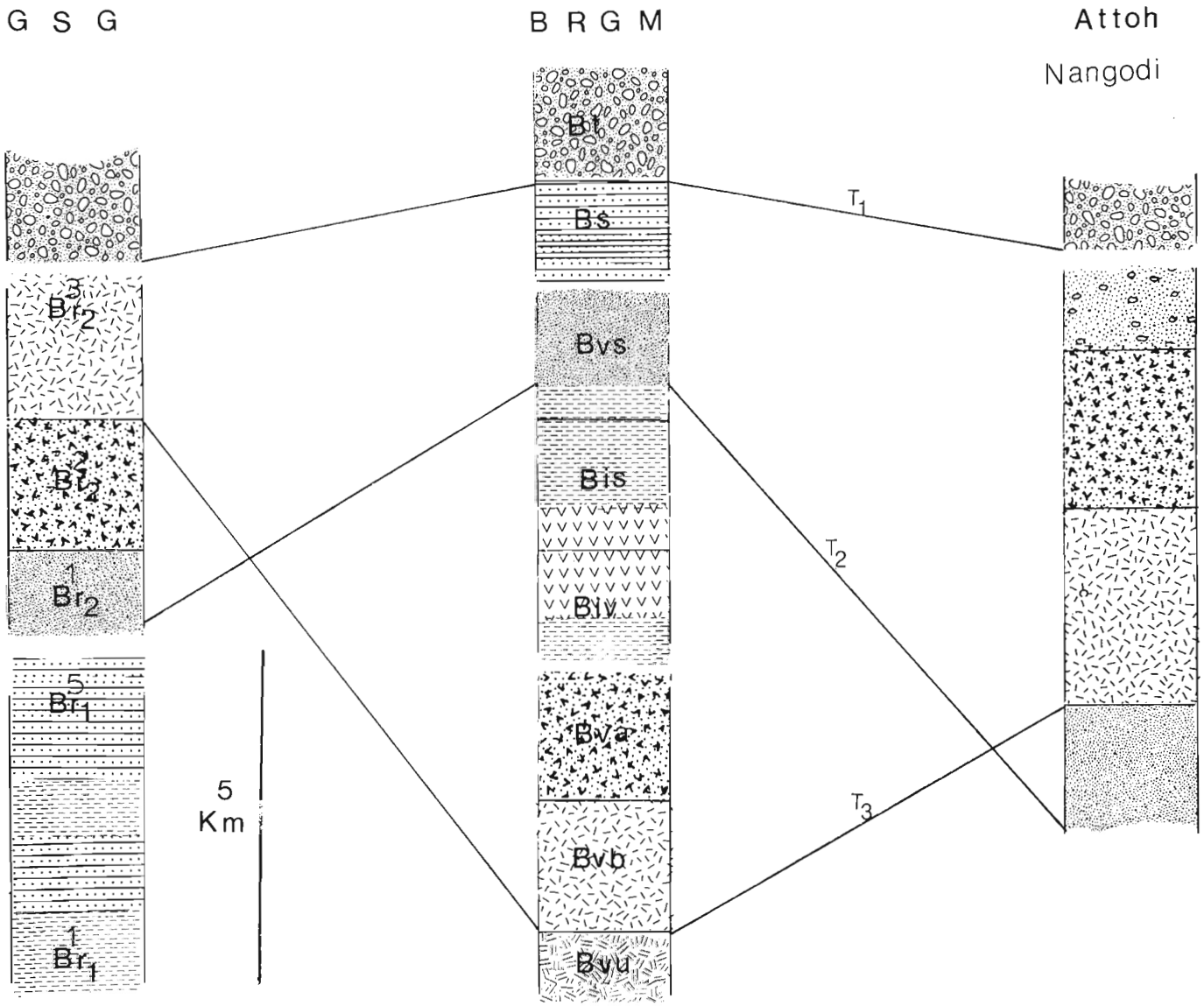

Figure 7.8. *Correlation of the volcanic stratigraphy in northeastern Ghana (Fig. 7.5, this study) with the stratigraphic classifications used by BRGM and GSG. (See Fig. 7.2 and 7.3 for unit symbols).*

Regional Chemical Characteristics and Possible Lithostratigraphic Correlations Between Birimian Volcanic-Sedimentary Belts

Chemostratigraphic Considerations

Ninety-six chemical analyses of Birimian volcanic rocks have been compiled from BRGM reports (Alsac, 1968, 1969a, b; Papon, 1973; Doucellier, 1963). Volcanic belts for which chemical analysis data are available are shown on Figure 7.1 (belts 2-9). An AFM plot of all analyses available from the volcanic belts again shows both tholeiitic and calc-alkaline trends (Fig. 7.9a). Of the available analyses about 45 per cent belong to the tholeiitic suite and 55 per cent are calc-alkaline. The calc-alkaline series shows a more complete differentiation trend than the truncated iron-enrichment trend of tholeiitic rocks.

The estimated proportions of rock types based on the chemical classification scheme of Irvine and Baragar (1971) are shown in Figure 7.9b. The ultramafic rocks are high-Mg basalts and constitute about 5 per cent of the samples analyzed. Komatiites have not yet been reported from the Birimian, although ultramafic rock units associated with mafic volcanics have been mapped in some belts, for example, Blanchot et al. (1972) show ultramafic units in belt 3 (Fig. 7.1). Tholeiitic rocks are dominantly quartz-tholeiitic basalts which form about 91 per cent of the tholeiitic suite (Fig. 7.9b). Of the calc-alkaline suite, andesite is the dominant rock type, constituting about 40 per cent. Calc-alkaline basalts make up about 9 per cent and dacite, rhyodacite and rhyolite together represent 48 per cent of the calc-alkaline samples. The proportion of tholeiite to calc-alkaline volcanic rocks from other Birimian volcanic belts is similar to the proportion of tholeiitic to calc-alkaline rocks in the Nangodi volcanic belt based on the thicknesses of the various units (Fig. 7.5). If the sample distribution in the various belts is representative of the proportions of rock types present then the Nangodi volcanic belt may be considered to be a typical Birimian volcanic belt.

Correlation between Birimian Volcanic-Sedimentary Belts

It has been shown that the various Birimian volcanic belts have similar chemical characteristics and lithologic associations, therefore it seems reasonable to attempt to correlate between the lithostratigraphic units which occur in the various belts. Although the possibility of lithostratigraphic correlation between the various volcanic belts is limited by the nature of volcanism, the repetition of chemically and lithologically similar volcanic units and lack of long distance continuity of some volcanic units, an attempt is made in order to rationalize the various lithostratigraphic sequences which are claimed to be representative of the Birimian.

In Figure 7.8, the lithostratigraphic sequence established for the Nangodi volcanic belt is compared with stratigraphic schemes used by the GSG and BRGM and the differences are quite evident. For example, the mafic volcanic unit in Nangodi belt occurs above a sedimentary unit while such a unit does not appear in the stratigraphic sequences used by both GSG and BRGM. The correlation indicated by T_3 and T_2 (Fig. 7.8) are clearly impossible. Nonetheless, the attempted correlation serves the purpose of testing the validity and usefulness of the conceptual stratigraphic schemes which have been proposed for the Birimian volcanic belts (Fig. 7.2). The correlation of actual lithostratigraphic sequences with the succession in the Nangodi belt (Fig 7.5) is at present impossible because the stratigraphic succession in the other belts is not as well known. It must be concluded that the existence of a typical or representative Birimian sequence cannot be justified at present.

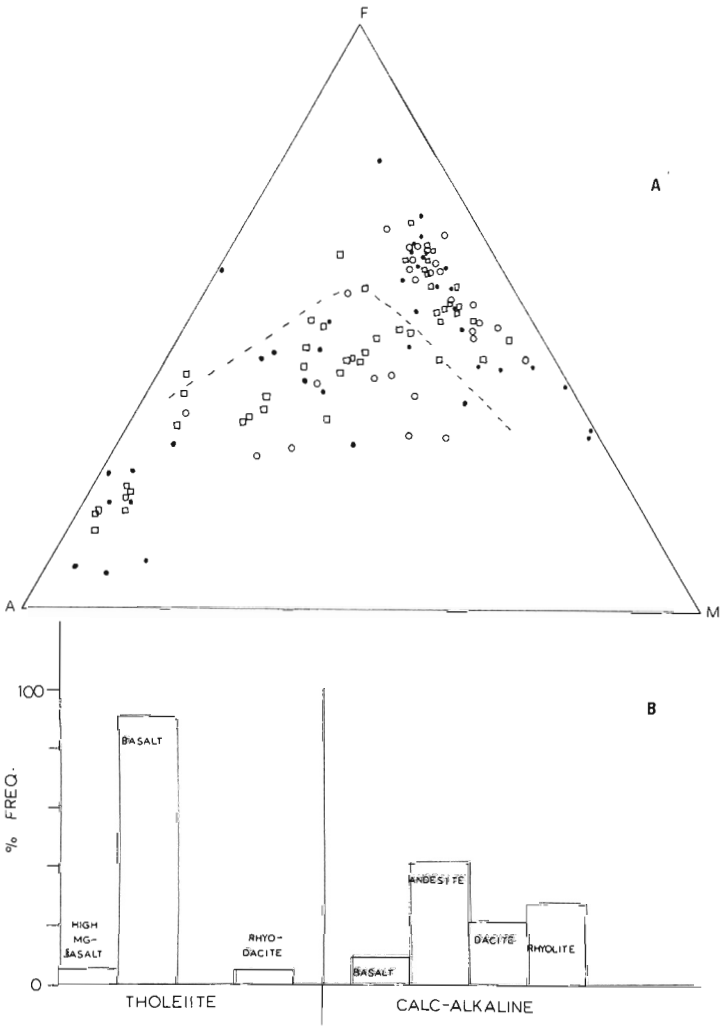

A - AFM diagram symbols:
o Nangodi volcanic belt, from belt 2, 3, 4, 5
, from belts 6, 7, 8, 9

B - frequency distribution of rock types (excluding the Nangodi volcanic belt).

Figure 7.9. *Chemical characteristics of early Proterozoic volcanic rocks in the West African Shield.*

Age of Birimian Volcanics

The age of the Birimian volcanics is poorly known. In Ghana, the Proterozoic age assigned to the Birimian is based on Rb-Sr isochrons constructed from analyses of mixed samples of granitic and sedimentary rocks (eg. Kolbe et al., 1967). Similar Rb-Sr isochrons have been reported on samples from Ivory Coast (see review Bessoles, 1977, p. 254, 301). The Rb-Sr ages reported on samples of two-mica granite (quartz-monzonite) which are everywhere intrusive (postkinematic) into older plutonic and the Birimian supracrustal rocks range from 1870 to 1940 Ma. K-Ar analyses of amphiboles from metabasites gave 2105-2135 Ma and U-Pb analyses of synkinematic granitic rocks gave 2100-2160 Ma. (Papon, 1973; Bessoles, 1977).

Two K-Ar ages (2087 ± 138 and 2223 ± 283 Ma) obtained for this study represent the only direct age determination on Birimian volcanic rocks in Ghana. The amphibole analyzed for the younger age (2087 Ma) was obtained from a dacite porphyry (HP in Fig. 7.3) and occurs as euhedral crystals with oscillating zoning and is distinctively

titaniferous. For the older age (2223 Ma) the amphibole was obtained from the mafic tuff unit which is the youngest volcanic unit in the Nangodi succession (Fig. 7.5). Even though the K-Ar ages are interpreted as thermal (metamorphic) events the agreement with the U-Pb ages on zircons from synkinematic granites is quite significant. However, because Birimian volcanic rocks have not been dated by U-Pb and Rb-Sr methods, much of the published geochronologic data and the K-Ar ages reported here are of limited use in the correlation problems outlined. Nonetheless, the available age data can be used to set a minimum age for the Birimian volcanic-sedimentary rocks. An upper limit for the age of the Birimian volcanics is based on the age of emplacement of the synkinematic granitic rocks and the thermal event recorded by the oldest K-Ar age. The available data suggest that the lithologic associations comprising the Birimian volcanic belts developed before 2200 Ma ago.

Conclusions

In this report it has been shown that the lithological and chemical characteristics of the Nangodi volcanic belt are similar to those in other early Proterozoic volcanic belts in the West African Shield. It has also been shown that the conceptual stratigraphic schemes previously proposed for the Birimian volcanic-sedimentary rocks are not valid for the Nangodi area. Furthermore lithostratigraphic data at present are not available to justify a representative stratigraphic succession of Birimian volcanic-sedimentary belts and to correlate lithologic sequences in the West African Shield. Therefore the present usage of the term "Birimian" to refer to the post-Archean-early Proterozoic volcanic sedimentary belts with the implied common stratigraphic sequence such as shown in Figure 7.2 as well as to refer to the structural province in which the rocks occur has little value and should be abandoned. Instead it is proposed that the term "Birimian" be used only to refer to the early Proterozoic lithologic association such as those described in the Nangodi area and the sequence of supracrustal rocks of early Proterozoic (older than 2200 Ma) in the Nangodi area be referred to as Nangodi Group.

Acknowledgments

The field work on which this report is based was supported by the Gold Export Levy Fund, Ministry of Lands and Mineral Resources (Government of Ghana). I was assisted in the field by Nii Adzei Akpor and I have benefitted from discussion on Birimian volcanic rocks with Drs. W.R.A. Baragar, K.D. Card and M.B. Lambert. I wish to thank Dr. M.D. Thomas (Earth Physics Branch, E.M.R.) for his interest and instruction on gravity modelling. The opportunity to work on Birimian volcanic rocks at G.S.C. was made possible by an N.S.E.R.C. visiting fellowship, for which I am grateful. I wish to thank Drs. Baragar, Card and Henderson for reading various versions of the manuscript.

References

Alsac, C.
1968: Étude des caractères magmatiques de formation volcanique de la region de Poura (Haute Volta); Bureau de recherches géologiques et minières, G4514B.

1969a: Études des caractères magmatiques des roches éruptives du Précambrien de la région de Boundiali (Côte d'Ivoire); Bureau de recherches géologiques et minières, G4514C.

1969b: Études des caractères magmatiques des métavolcanites de Katiola (Côte d'Ivoire); Bureau de recherches géologiques et minières, G4514D.

Arnould, M.
1961: Étude géologique des migmatiques et des granites précambriens du nord-est de la Côte d'Ivoire de la Haute Volta méridionale; Bureau de recherches géologiques et minières, Mémoire 3.

Arth, J.G. and Hanson, G.N.
1975: Geochemistry and origin of early Precambrian crust of northeastern Minnesota; Geochimica et Cosmochimica Acta, v. 39, p. 325-362.

Asihene, K.A.B. and Barning, K.
1975: A contribution to the stratigraphy of the Birimian system of Ghana, West Africa; Geological Survey of Ghana, Report 75/5.

Baragar, W.R.A.
1972: Some physical and chemical aspects of Precambrian volcanic belts of the Canadian Shield; in The Ancient Lithosphere, ed., E. Irving, Earth Physics Branch, Department of Energy, Mines and Resources, Publication 42, p. 129-140.

Bessoles, B.
1977: Le craton ouest africain – Geologie de l'Afrique; Bureau de recherches géologiques et minières, Mémoire 88.

Blanchot, A., Dumas, J-P, et Papon, A.
1972: Carte géologique de la partie méridionale de l'Afrique de l'ouest; Bureau de recherches géologiques et minières, publication.

Carmichael, I.S.E., Turner, F.J., and Verhoogen, J.
1974: Igneous petrology; McGraw-Hill Book Co., 739 p.

Doucellier, J.
1963: Contribution à l'étude des formations crystallines et métamorphiques du centre de nord de la Haute Volta; Bureau de recherches géologiques et minières, Mémoire 10.

Gélinas, L., Brooks, P., Perrault, G., Carignan, J., Trudel, P., and Grasso, F.
1977: Chemostratigraphic division within the Abitibi volcanic belt Rouyn-Noranda District; in Volcanic Regimes in Canada, ed., W.R.A. Baragar, L.C. Coleman, and J.M. Hall, Geological Association of Canada Special Publication 6.

Gibb, R.A. and Thomas, M.D.
1980: Density determinations of basic volcanic rocks of the Yellowknife Supergroup by density measurements in mine shafts; Geophysics, v. 45, p. 18-31.

Hurley, P.M., Leo, G.W., White, R.W., and Fairbairn, H.W.
1971: Liberian age province in Liberia and Sierra Leone; Geological Society of America Bulletin, v. 82, p. 3483-3490.

Irvine, T.N. and Baragar, W.R.A.
1971: A guide to chemical classification of common volcanic rocks; Canadian Journal of Earth Sciences, v. 8, p. 523-548.

Jahn, B-M, Shih, C-Y, and Murthy, V.R.
1974: Trace element geochemistry of Archean volcanic rocks; Geochimica et Cosmochimica Acta, v. 30, p. 611-627.

Junner, N.R.
1954: Notes on the classification of the Precambrian of West Africa; XIX International Geological Congress, Algiers, No. 20, p. 114-117.

Kolbe, P., Pinson, W.H., and Sand, J.M.
1967: Rb-Sr study of the country rocks of the Bosumtwi Crater, Ghana; Geochimica et Cosmochimica Acta, v. 31, p. 869-875.

Murray, R.J.
1960: The geology of the Zuarungu 1/2° field sheet; Geological Survey of Ghana, Bulletin 25.

Papon, A.
1973: Géologie et Minéralisation du sud-ouest de la Côte d'Ivoire; Bureau de recherches géologiques et minières, Mémoire 80.

Pearce, J.A. and Cann, J.R.
1973: Tectonic setting of basic volcanic rocks determined using trace element analyses; Earth and Planetary Science Letters, v. 19, p. 290-300.

Prucha, A.M.
1972: Bouguer gravity map of the Gambaga sheet; Geological Survey of Ghana, Open File Report.

Tagini, B.
1971: Equisse structurale de la Côte D'Ivoire – essai de géotectonique régionale; SODEMI, ABIDJAN, 302 p.

Trashliev, S.A.
1974: Cycles of Birimian flysch from southwestern Ghana; Bulletin Geological Institute (series: stratigraphy and lithology), Bulgaria Academy of Sciences, v. XXIII, p. 151-158.

8.

SUMMARY OF CONODONT BIOSTRATIGRAPHY OF THE BLUE FIORD AND BIRD FIORD FORMATIONS (LOWER-MIDDLE DEVONIAN) AT THE TYPE AND ADJACENT AREAS, SOUTHWESTERN ELLESMERE ISLAND, CANADIAN ARCTIC ARCHIPELAGO

Project 680101

T.T. Uyeno and Gilbert Klapper[1]
Institute of Sedimentary and Petroleum Geology, Calgary

Uyeno, T.T. and Klapper, G., Summary of conodont biostratigraphy of the Blue Fiord and Bird Fiord formations (Lower-Middle Devonian) at the type and adjacent areas, southwestern Ellesmere Island, Canadian Arctic Archipelago; in Current Research, Part C, Geological Survey of Canada, Paper 80-1C, p. 81-93, 1980.

Abstract

Conodonts of the Blue Fiord Formation in sections located 2.5 km and 30 km (near Sor Fiord) east of the type section in southwestern Ellesmere Island, are assignable to (in ascending order): ***dehiscens***, ***gronbergi***, ***inversus***, *and* ***serotinus*** *zones (approximately Pragian-Zlichovian boundary to Dalejan stages, Lower Devonian). The upper part of the underlying Eids Formation in this area also contains conodonts of the* ***dehiscens*** *Zone. The Blue Fiord Formation is diachronous as it has yielded conodonts of Eifelian age on Grinnell Peninsula, Devon Island, and on Cornwallis and Bathurst islands.*

The Bird Fiord Formation at its type section, also on southwestern Ellesmere Island, yielded conodonts that are either long-ranging or new, and thus cannot be so precisely dated. Brachiopods from the upper part of the formation, however, are assignable to the ***Warrenella kirki*** *Zone which, in Nevada, coincides with part of the conodont* ***kockelianus*** *Zone (late Eifelian). The Bird Fiord Formation is similarly diachronous, and on Bathurst Island it has been regarded as Eifelian to Givetian in age.*

A new genus, ***Steptotaxis****, is introduced.*

Introduction

The Blue Fiord Formation and the overlying Bird Fiord Formation were named by McLaren (in Fortier et al., 1963, p. 318-328) for 1159 m and 900 m, respectively, of strata exposed in the vicinity of Blue Fiord on southwestern Ellesmere Island (see Fig. 8.1). The Blue Fiord Formation was originally divided by McLaren (op. cit.) into two units, informally designated as the limestone and shale (lower) member (732 m thick), and the overlying brown limestone (upper) member (427 m). Kerr and Thorsteinsson (1972) similarly divided the Bird Fiord Formation into a lower member, consisting of limestone and shale that are variably quartzose and green weathering, and an upper member, consisting of sandstone that is partly calcareous and mainly of red or green colour. The thicknesses of the individual Bird Fiord members were not given. The type sections for these formations were subsequently selected by McLaren (in Kerr and Thorsteinsson, 1972).

The material on which the present study is based was collected by Uyeno in 1969 from the Blue Fiord Formation exposed along creeks located 2.5 km east of the type section, and from the type section of the Bird Fiord Formation (section 1 on Fig. 8.1; see also Uyeno and McGregor, 1970, section 5; base of section at UTM Zone 16X, 518000 E, 8574500 N and the top of section at UTM Zone 16X, 518750 E, 8569000 N; these are approximately equivalent to lat. 77°14.2'N, long. 86°16.5'W, and lat. 77°11.1'N, long. 86°14.5'W, respectively), and from the Blue Fiord Formation by Klapper and A.E.H. Pedder in 1971 from the Sor Fiord section, located some 30 km east of the type section (section 2 on Fig. 8.1; base of section at lat. 77°17'12"N, long. 85°07'00"W, and top of section at lat. 77°15'48"N, long. 85°03'30"W). The collection from the Bird Fiord Formation at the type section is supplemented by three samples collected by R. Thorsteinsson in 1979 (loc. 1-3, Fig. 8.1).

The conodont faunas summarized herein are discussed more extensively by Uyeno (in preparation) and by Klapper (in Pedder and Klapper, in preparation). In this paper, Uyeno is responsible for the identification of conodonts from the type area of the Blue Fiord and Bird Fiord formations, and Klapper for the Eids and Blue Fiord formations at Sor Fiord. A part of this paper is based on the unpublished Sor Fiord manuscript prepared by Klapper in 1978.

The Ordovician through Lower Devonian conodont succession found in two wells located near the present study area (designated on Fig. 8.1), has been studied previously by Uyeno and Barnes (in Mayr et al., 1978).

Incidental to the main thrust of this paper, we note the presence of two-hole echinoderm ossicle **Gasterocoma? bicaula** Johnson and Lane in both the Blue Fiord and Bird Fiord formations at their type area (section 1 of Fig. 8.1). It ranges almost throughout the Blue Fiord Formation (from the **dehiscens** to **serotinus** Zones), and in the Bird Fiord it occurs at GSC loc. 83767. As noted elsewhere, the interval at and near the latter locality cannot be as precisely dated, but may possibly be of Eifelian age.

Previous Conodont Studies

Insofar as is known, this is only the second report on conodonts from the Bird Fiord Formation. The studies on conodonts from the Blue Fiord Formation, or strata that at least have been mapped as such by others, are more extensive and include the following:

Klapper (1969, Fig. 3) described conodonts from three samples collected by A.R. Ormiston in 1961 from the lower part of what was then mapped as Blue Fiord Formation (30, 45, and 90 m above the base of the formation) at Sutherland River, Devon Island. These collections, which are now referred to the Disappointment Bay Formation (Thorsteinsson, in preparation), with **Polygnathus foveolatus** Philip and Jackson (= **P. inversus** Klapper and Johnson of the present paper) and **Steptotaxis glenisteri** were regarded as Early Devonian, Emsian (Klapper, 1969, Fig. 4).

Uyeno (in McGregor and Uyeno, 1972, p. 13-16) described conodonts from the Blue Fiord and Bird Fiord formations on the east side of Young Inlet, northeastern

[1] Department of Geology, University of Iowa, Iowa City, Iowa, 52242.

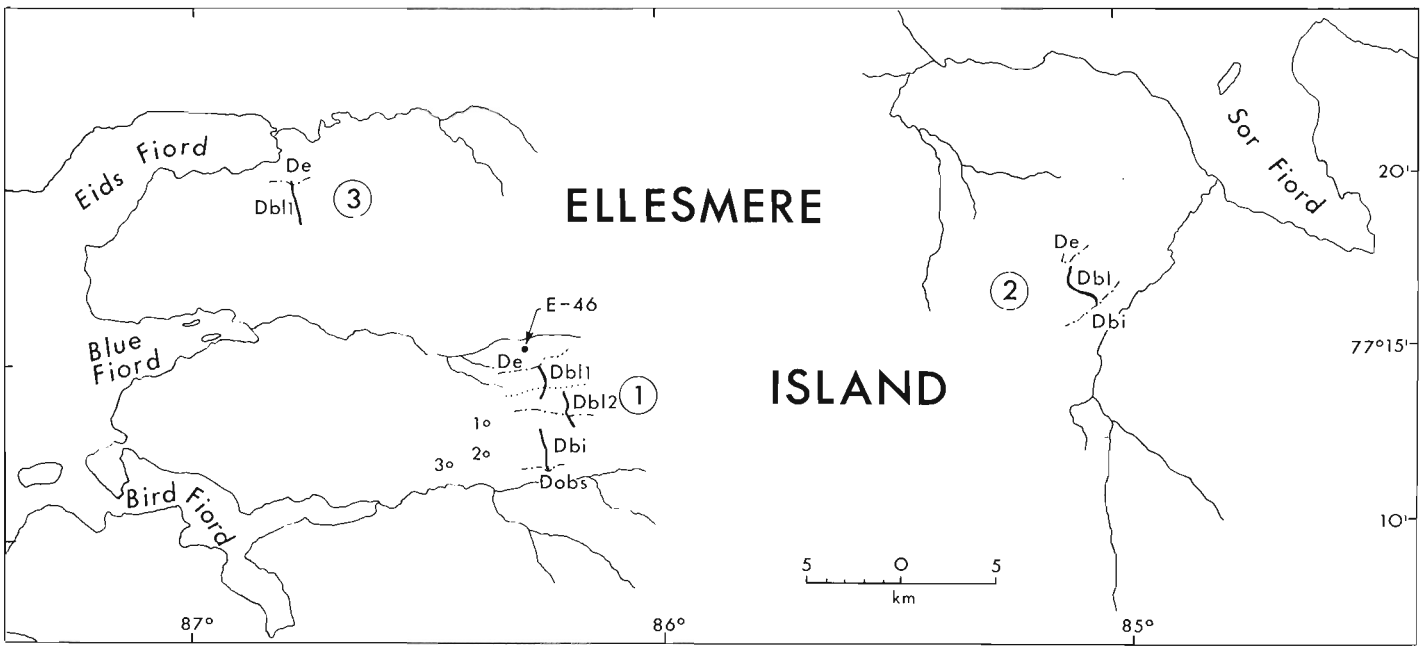

De = Eids Fm. Dbi = Bird Fiord Fm.
Db11 = limestone and shale (lower) member
Db12 = brown limestone (upper) member, Blue Fiord Fm.
Dobs = Strathcona Fiord Fm., Okse Bay Group.
= formational contact = intraformational contact
(after Kerr and Thorsteinsson, 1972).

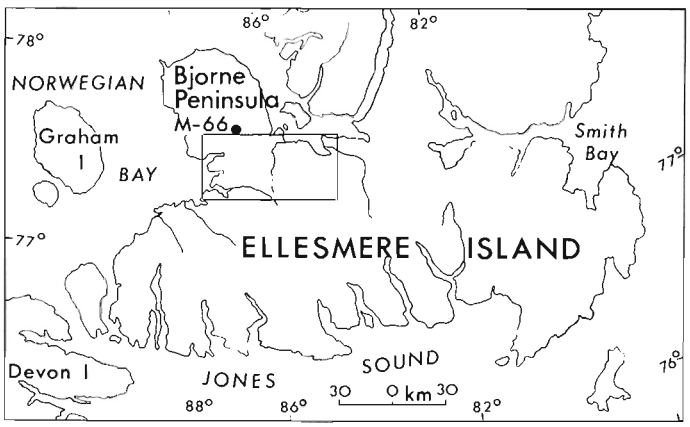

Figure 8.1. *Index map showing the locations of (1) the Blue Fiord Formation exposed along creeks located 2.5 km east of the type section, and the type section of the Blue Fiord Formation, and (2) the Eids and Blue Fiord formations at the Sor Fiord section. The section of the Blue Fiord Formation near Eids Fiord, studied by Weyant (1975), is shown as (3). Three small circles mark the locations of R. Thorsteinsson's Bird Fiord collections (see Appendix: 1 = C-76076, 2 = C-76075, and 3 = C-76074). Two well-sites shown are E-46 = Panarctic ARCO et al. Blue Fiord E-46, and M-66 = Panarctic Tenneco et al. CSP Eids M-66 (see Mayr et al., 1978). Small scale map shows the geographic position of the enlarged map.*

Bathurst Island (see Kerr, 1974, section 20, p. 6, 111-114). The entire suite of Blue Fiord collections, from the intervals of 5 to 274 m above the base of the formation (total thickness of formation at this section is 276 m), was tentatively regarded as Eifelian. A similar fauna, also dominated by **Icriodus,** was found in the highest bed of the Blue Fiord Formation at Rookery Creek, west-central Cornwallis Island (in an undescribed collection made by R. Thorsteinsson in 1976; GSC loc. C-63567). This fauna is similarly regarded as Eifelian in age. In collections made by Ormiston in 1962 from 134 m and 147 m above the base of the Blue Fiord Formation at Twilight Creek on Bathurst Island (located some 35 km southwest of the Young Inlet section; see Ormiston, 1967, p. 144-146, and Kerr, 1974, section 25, p. 118), **Icriodus norfordi** Chatterton occurs in small faunas similarly regarded as Eifelian (Klapper and Johnson, 1980, p. 444, Table 7). These beds are the source of the types of **Deltadechenella bathurstensis** Ormiston (1967, p. 105). **Icriodus norfordi** was illustrated (Klapper and Johnson, 1980, Pl. 3, fig. 25, 26) from the nearby Warner River section (Ormiston, 1967, p. 36, Fig. 2; a sample from 107 m above the base of the Blue Fiord Formation, which also contains **Scutellum depressum** Cooper and Cloud). The Bird Fiord conodonts from the Young Inlet section were tentatively dated as Eifelian-Givetian, with the boundary placed approximately in the lower part of the formation.

In undescribed collections made by Kerr from Kerr's member C_1, high in the Blue Fiord Formation at Grove Lake on Grinnell Peninsula, Devon Island (GSC loc. C-22892), Klapper identified **Eognathodus bipennatus** (Bischoff and Ziegler) of the robust kind previously illustrated by Bultynck (1970, Pl. 19, fig. 1) and species of **Icriodus,** together indicative of an Eifelian age.

Weyant (1975) illustrated and listed conodonts from the lower 530 m (entirely within the lower limestone and shale member) of the Blue Fiord Formation, from a section southeast of the head of Eids Fiord (section 3 on Fig. 8.1). The specimens illustrated in lower view and identified by Weyant (1975, Pl. 1, fig. 39, 41) as **Polygnathus foveolatus** from 156 m above the base of the formation, compare most closely with **P.** aff. **P. perbonus** (Philip). **Steptotaxis glenisteri** (Klapper) was illustrated from 156 m and 158 m above the base of the formation (Weyant, 1975, Pl. 1, fig. 31, 33, 34). Weyant (op. cit.) concluded that the conodont fauna of the lower part of the Blue Fiord Formation at this section is Emsian in age, a conclusion with which we agree.

The important sequence of **Polygnathus** found in the Eids and Blue Fiord formations in the Sor Fiord section was summarized by Klapper and D.B. Johnson (1975, Fig. 4), and Blue Fiord conodonts from this section were listed in Table 5 and 6 by Klapper and J.G. Johnson (1980).

Table 8.1

Correlation of Lower and Middle Devonian conodont zones with stages in Europe (from Klapper and Johnson, 1980, Text-fig. 1)

CONODONT ZONES	STAGES	
kockelianus	Eifelian	Couvinian
australis		
costatus costatus		
patulus	Emsian	?
serotinus		Dalejan
inversus/laticostatus		Zlichovian
gronbergi		
dehiscens		Pragian
kindlei	?	

Note: A lower part of the Pragian and the uppermost parts of the Eifelian-Couvinian are not shown. Leading contenders for the Lower-Middle Devonian boundary, under consideration by the International Subcommission on Devonian Stratigraphy, are levels corresponding to the bases of the Couvinian and Eifelian Stages, or approximately the bases of the **patulus** Zone and the upper part of the **patulus** Zone, respectively. the **partitus** Zone was introduced by Weddige, Werner, and Ziegler (1979, p. 161) for the informal upper part of the **patulus** Zone of Klapper, Ziegler, and Mashkova (1978, p. 107), an action which thus restricted the scope of the **patulus** Zone. In this paper, however, we continue to use the **patulus** Zone in the unrestricted sense.

The Blue Fiord Formation in the subsurface of Cameron and Vanier islands, was examined for lithofacies interpretation and conodont biostratigraphy (Uyeno and Mayr, 1979). While no consistent paleoecological relationship was found between the conodont faunas and the lithofacies of the enclosing rocks, the age of the formation was found to range from the probable **gronbergi-inversus** zones through **serotinus** Zone to the **patulus** and/or **costatus costatus** zones. The correlation of the conodont zones mentioned in this paper with stages in Europe is shown on Table 8.1.

In the Strathcona Fiord section, located 11 km southwest of Strathcona Fiord (see Trettin, 1978, p. 116, Fig. 66 and section 11, Fig. 7), the upper beds of the Blue Fiord (GSC loc. C-26496) yielded only **Pandorinellina expansa** (Uyeno and Mason). As noted on Figures 8.2 and 8.3, this is a long-ranging species, extending from about mid-part of the Blue Fiord Formation to the upper part of the overlying Bird Fiord Formation. The accompanying brachiopods were questionably dated as Emsian by J.G. Johnson, D.G. Perry, and R.E. Smith. (This section was sampled for conodonts by Uyeno, see Uyeno and McGregor, 1970, section 6.)

Incidental to the study of the conodonts of the underlying Eids Formation in the subsurface of northwestern Victoria Island, conodonts from the Blue Fiord Formation outcropping on the larger of the nearby Princess Royal Islands were illustrated and listed by Uyeno (in Mayr et al., 1980, p. 215, Pl. 32.1, fig. 53-55). These include **Polygnathus inversus** and **Pandorinellina** sp., the latter in all probability being the same as that found in this study (Fig. 8.2, GSC loc. 83742).

Previous Age Determinations of the Blue Fiord and Bird Fiord Formations and Their Correlatives
(based on other than conodont faunas)

McLaren (in Fortier et al., 1963, p. 322, 324, 326, 328) considered the Blue Fiord and Bird Fiord formations in the type area as Middle Devonian in age, and tentatively suggested correlations with the Eifelian and Givetian stages, respectively.

Ormiston (1967), on evidence of trilobite studies, regarded the Blue Fiord on northern Bathurst Island (principally at Twilight Creek) as Eifelian in age, and suggested that older (Emsian?) beds are present in units that were mapped earlier as Blue Fiord Formation and located east of Bathurst Island [specifically at Sutherland River, Devon Island, and Goose Fiord, Ellesmere Island; localities with **Prodrevermannia sverdrupi** (Tolmachoff); Ormiston, 1967, p. 19, 58, Fig. 5; 1975, p. 394]. The beds at Sutherland River are now referred to the Disappointment Bay Formation, and those at Goose Fiord require further refinement for correct assignment (Thorsteinsson, in preparation, Table 1). Ormiston (1967, p. 23) further suggested that the Eifelian-Givetian boundary may be within the basal 60 m of the Bird Fiord Formation at Twilight Creek, thus indicating a Givetian age for the remainder of the formation. In central Bathurst Island, some 45 km southwest of Twilight Creek, the lower two-thirds of the Bird Fiord Formation was considered to be of probable late Eifelian age (Johnson and Perry, 1976, p. 617). At that locality, the Blue Fiord Formation is missing and the Bird Fiord rests directly on the Eids Formation.

In Ormiston's collection of Disappointment Bay fossils (specifically, those from 30 m above the base of the formation; the conodonts identified by Klapper, 1969, cited earlier) from Sutherland River, Devon Island, J.G. Johnson (in Harper et al., 1967, p. 430, footnote) noted the presence of **Phragmostrophia** sp. He also identified **P.** sp. aff. **P. merriami** Harper et al. in McLaren's collection (in Fortier et al., 1963, p. 320; GSC loc. 26513) from the Blue Fiord Formation, about 180 m above the base of the formation, on the south side of Eids Fiord, southwestern Ellesmere Island. Johnson (op. cit.) concluded that both collections are Emsian in age.

Correlation of Blue Fiord and Bird Fiord Polygnathus Sequence

The **Polygnathus** sequence of the Blue Fiord and Bird Fiord formations is given far greater weight for correlation than the other conodonts, because species of the genus form an integral part of the zonation of the upper part of the Lower Devonian (and, incidental to this study, the lower part of the Middle Devonian) in western North America (Klapper, 1977a) and in Europe (Weddige and Ziegler, 1977; Klapper, 1977b; Klapper et al., 1978). The **Polygnathus** species are widespread in the Northern Hemisphere and Australia, whereas some of the non-**Polygnathus** species used in the zonation in Europe (Weddige and Ziegler, 1977, Fig. 1) are unknown in North America (see also Klapper and Johnson, 1980). Similarly, two of the numerically dominant conodonts in these formations, **Pandorinellina exigua exigua** (Philip) and **P. expansa**, are unknown in Europe, and four others, **Pelekysgnathus** n. sp. and **Steptotaxis** n. spp. A, B, and C, are new. **Ozarkodina linearis** (Philip) is also unknown in Europe.

Polygnathus dehiscens Philip and Jackson (Pl. 8.1, fig. 1-4), which occurs near the top of the Eids Formation at Sor Fiord (GSC loc. C-12504), and in the lower 141 m of the lower member of the Blue Fiord Formation at its type area (GSC loc. 83722 and 83725), is the nominal species of the **dehiscens** Zone (Fahraeus, 1971; Klapper, 1977a, p. 41-42).

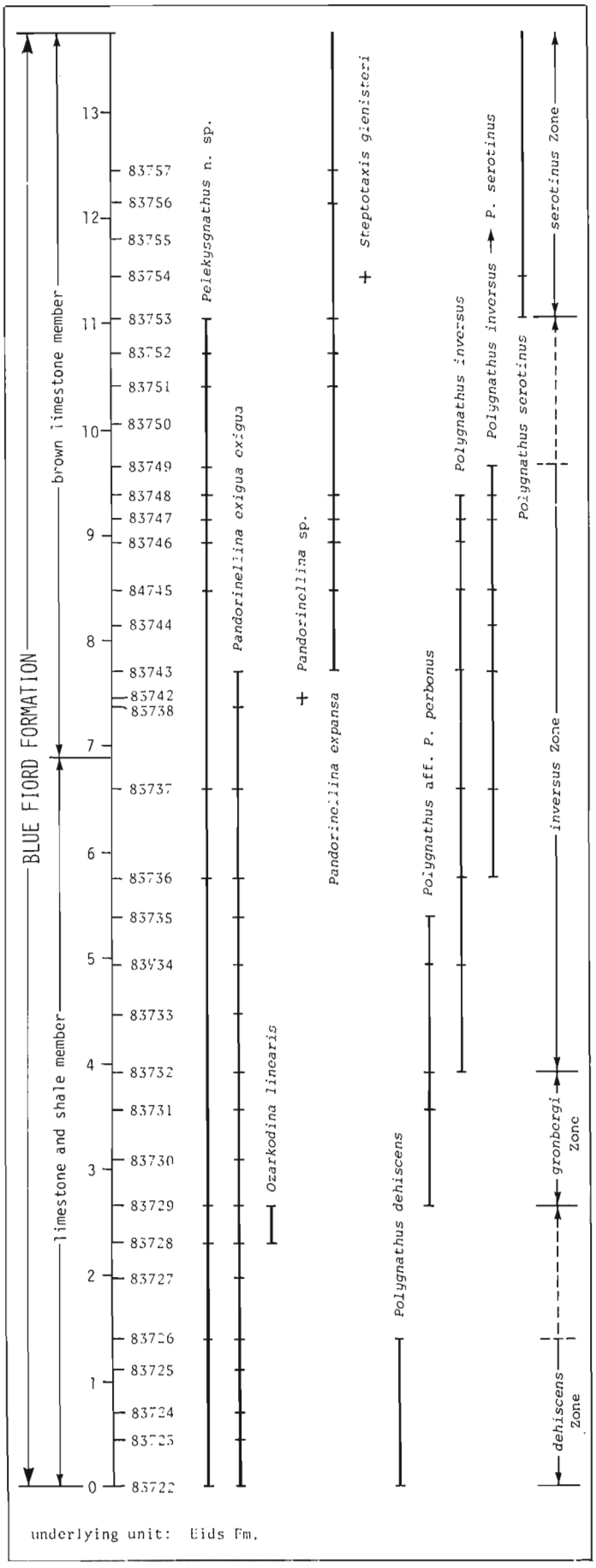

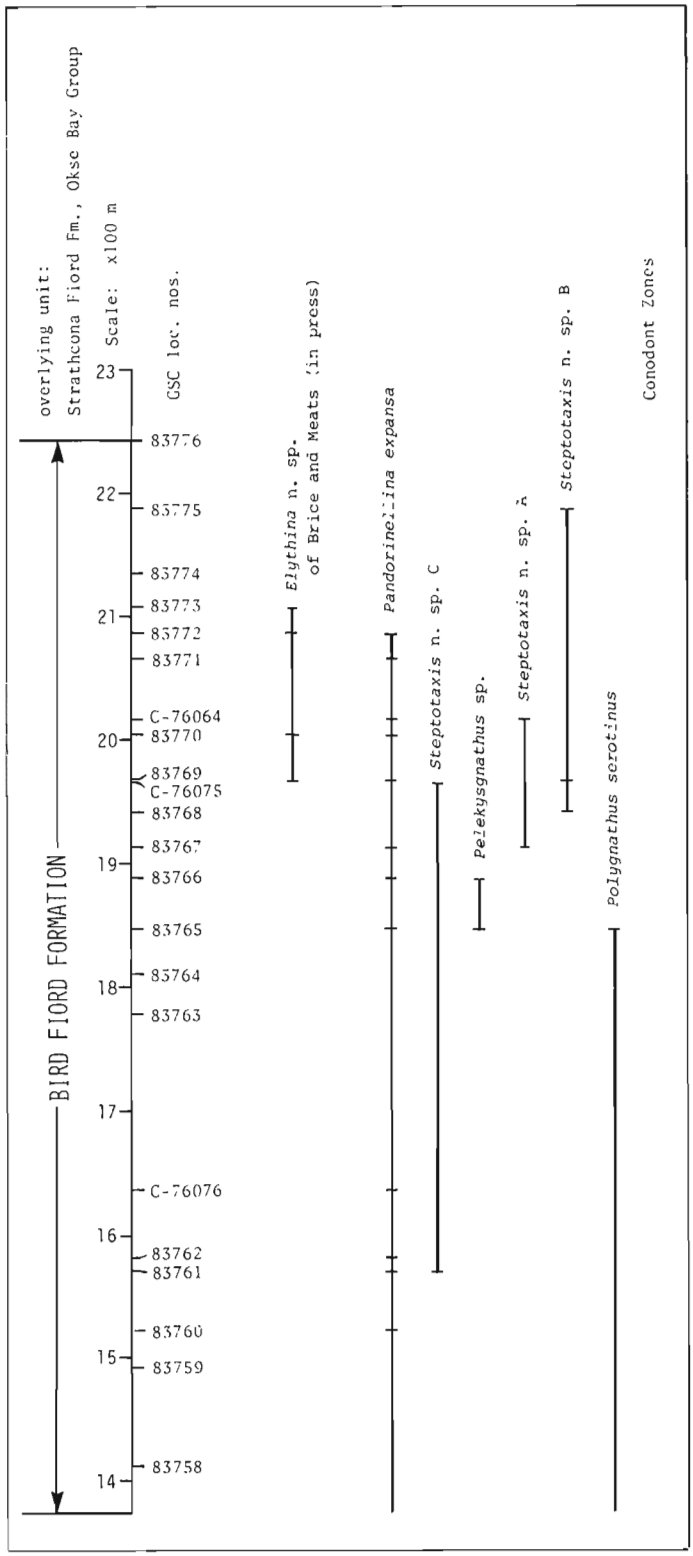

Figure 8.2. *Conodont distribution and zonation of the Blue Fiord Formation exposed along creeks located 2.5 km east of the type section, and of the Bird Fiord Formation at its type section.*

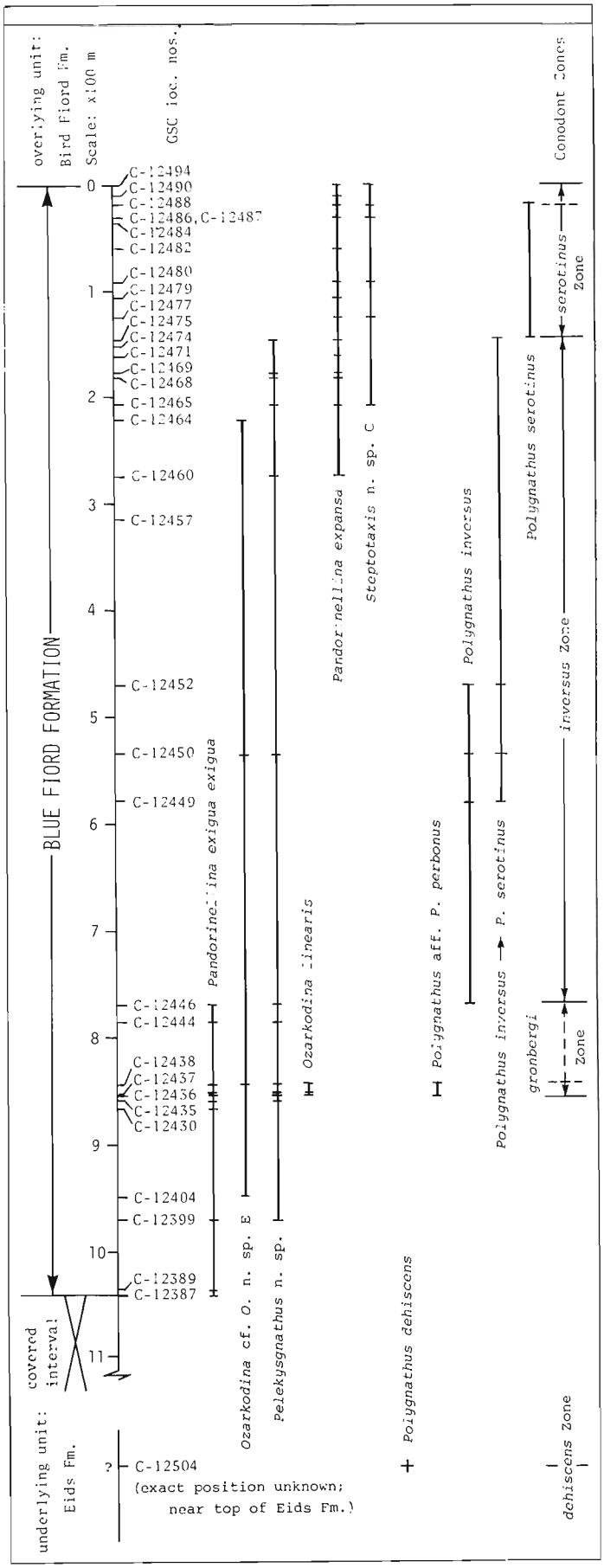

Figure 8.3. *Conodont distribution and zonation of the Blue Fiord Formation at the Sor Fiord section.*

The species ranges as high as the lower part of the **gronbergi** Zone in Nevada, Alaska, and in the Khodzha-Kurgan section in the Zeravshan Range, central Asia (Klapper and Johnson, 1980, Table 5).

Polygnathus aff. **P. perbonus** (Pl. 8.1, fig. 5, 6; Pl. 8.3, fig. 11, 12) ranges in the type area of the lower member of the Blue Fiord Formation from 267 to 539 m above the base of the formation, and at Sor Fiord from 846 to 852 m below the top of the formation. It is tentatively identified herein in the lower member of the Blue Fiord Formation at southeast of Eids Fiord (Weyant, 1975, Pl. 1, fig. 39, 41; section 3 of Fig. 8.1 herein). **Polygnathus** aff. **P. perbonus** occurs within the **gronbergi** Zone in Nevada (Klapper, 1977a, p. 42), but within the **inversus** Zone in the type Cranswick Formation, northern Yukon Territory (Pedder and Klapper, 1977, p. 231). The range of **P.** aff. **P. perbonus** is entirely below the first occurrence of **P. inversus** at Sor Fiord, and at the type area, the two species have a common occurrence in two samples, at the levels of 393 and 495 m above the base of the Blue Fiord Formation (GSC loc. 83732, 83734). This suggests that the levels of **P.** aff. **P. perbonus** below the first occurrence of **P. inversus** at these sections may represent the **gronbergi** Zone by inference of stratigraphic position. The **gronbergi** Zone, on evidence of the zonally-restricted nominal species, has been identified in the upper Zlichovian Chýnice Limestone in the Barrandian area (Klapper, 1977b). **Polygnathus gronbergi** occurs with the tantaculite **Nowakia barrandei** Bouček and Prantl in the Harz Mountains (Klapper and Johnson, 1975, p. 71) and in the Schönau Limestone of the Kellerwald, Germany (Weddige and Ziegler, 1977, p. 71).

As noted earlier, there is some overlap in the ranges of **Polygnathus** aff. **P. perbonus** and **P. inversus** in the Blue Fiord Formation at the type area. **P. inversus** (see Pl. 8.1, fig. 7-12; Pl. 8.3, fig. 6, 13) is joined by a morphologically transitional form between **P. inversus** and **P. serotinus** (referred to as **P. inversus → P. serotinus** in the stratigraphic part of the paper, as for example, on Figures 8.2 and 8.3, but as **"P. inversus,** transitional to **P. serotinus"** in the Systematics and on explanations to Pl. 8.1, fig. 13-16, Pl. 8.3, fig. 4, 5) at 574 m above the base of the Blue Fiord (GSC loc. 83736) and the overlap continues to the 939-m level (GSC loc. 83748). The transitional form continues upward to the 966-m level (GSC loc. 83749). At Sor Fiord, **Polygnathus inversus** and **P. inversus → P. serotinus** range from 770 to 469 m and from 579 to 147 m below the top of the Blue Fiord Formation, respectively. **Polygnathus inversus** is the nominal species of the inversus Zone (Klapper, 1977a, p. 42) and ranges as high as the lowest part of the **serotinus** Zone.

The **inversus** Zone is equivalent to strata that, in central Europe, contain the **laticostatus** Zone (or Fauna; see Weddige and Ziegler, 1977, p. 71-73; Klapper, 1977a, p. 35). **Polygnathus laticostatus** and **P. inversus** occur jointly in Nevada and in the Harz Mountains, Germany, in a sample with the tentaculite, **Nowakia cancellata** (Richter) (Klapper and Johnson, 1975, p. 71). The **laticostatus** Zone occurs in the Barrandian area of Czechoslovakia in the lower part of the Suchomasty Limestone at levels with **Nowakia elegans** (Barrande) and higher with **N. cancellata** (Klapper et al., 1978, p. 105, Fig. 1, 2). The Zlichovian-Dalejan boundary is drawn at the **elegans-cancellata** zonal boundary, according to the proposal of Chlupáč (1976a, Fig. 1; 1976b, p. 180, 182), and this falls within the **laticostatus** Zone.

Polygnathus inversus occurs elsewhere in the Canadian Arctic Archipelago in the Disappointment Bay Formation at Sutherland River, Devon Island (Klapper, 1969, Pl. 6, fig. 19-30; also in undescribed collections of Uyeno, see Uyeno and McGregor, 1970, section 4), in the Blue Fiord Formation at Weatherall Bay, northeastern Melville Island (undescribed collections of Uyeno, see McGregor and Uyeno, 1969, section 2), and on the larger of the princess Royal Islands (Uyeno in Mayr et al., 1980, Pl. 32.1, fig. 53, 54).

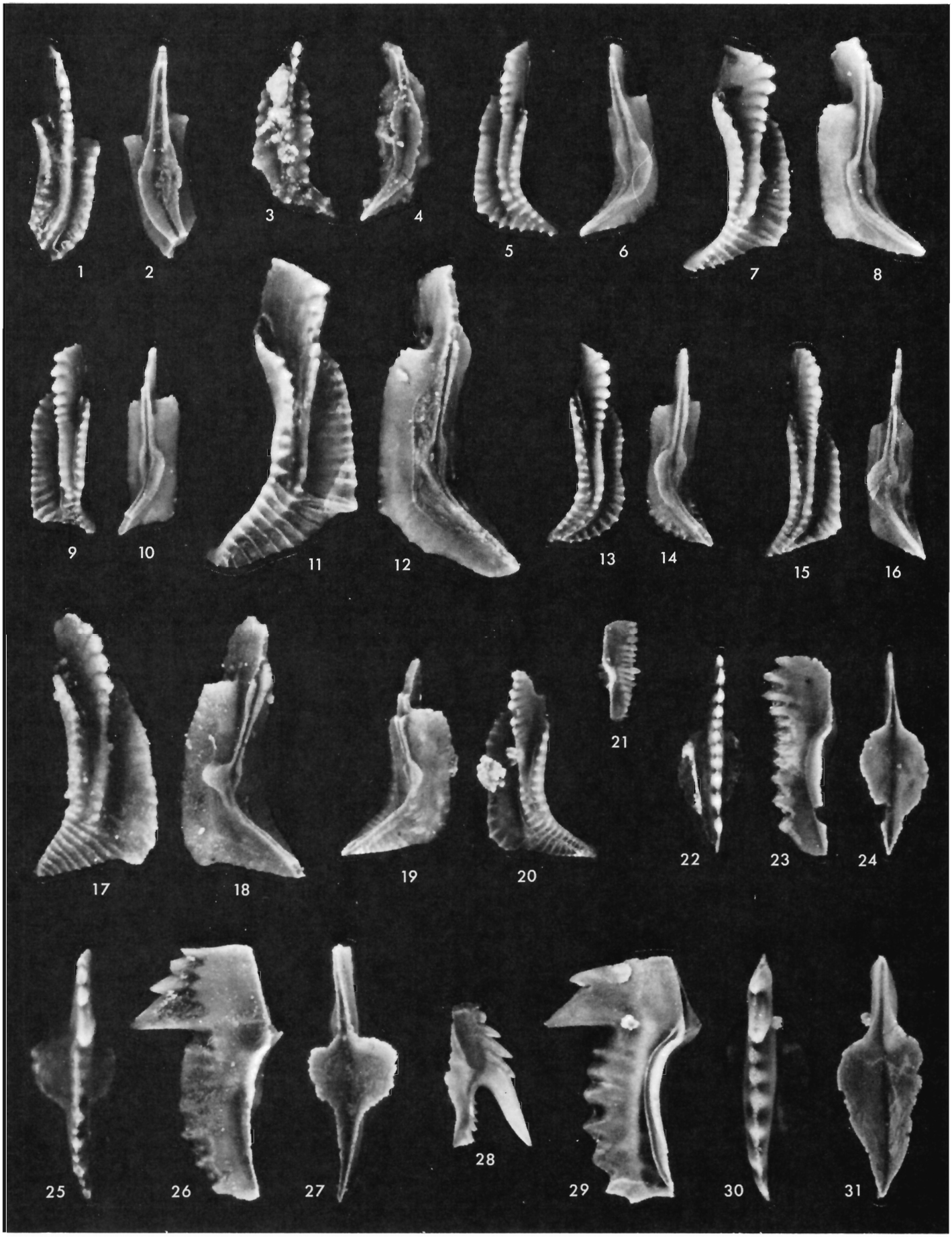
1
2
3
4
5
6
7
8
9
10
11
12
13
14
15
16
17
18
19
20
21
22
23
24
25
26
27
28
29
30
31

The species has its other occurrences in the Stuart Bay Formation at Young Inlet, northeastern Bathurst Island (Uyeno in McGregor and Uyeno, 1972, Pl. 5, figs. 13, 14), and Twilight Creek, northern Bathurst Island (undescribed collections made by Ormiston in 1962 and by Uyeno in 1969).

Polygnathus serotinus Telford (Pl. 8.1, fig. 17-20) occurs in two collections in the Blue Fiord Formation near the type section (at 1104 and 1144 m above the base of the formation, GSC loc. 83753 and 83754), and in a third collection from about midway in the Bird Fiord Formation at 469 m above the base of the formation (GSC loc. 83765). At Sor Fiord the species occurs at 147 m and 18 m below the top of the Blue Fiord Formation (GSC loc. C-12475 and C-12488). **P. serotinus** is the nominal species of the **serotinus** Zone, but ranges as high as the **costatus costatus** Zone. The Sor Fiord specimens appear to represent early phyletic forms of the species, however, because the anterior outer margin is relatively low for **P. serotinus.** Furthermore, in the collection at 147 m, **P. serotinus** is accompanied by **P. inversus → P. serotinus,** the latter also occurring in the **inversus** Zone in Nevada (Klapper and Johnson, 1975, p. 73, Pl. 3, fig. 19-22, 24-31). Thus, this evidence suggests that the collections at 147 m and 18 m below the top of the Blue Fiord Formation at Sor Fiord are within the **serotinus** Zone. Although the upper range of **P. inversus → P. serotinus** is below the first occurrence of **P. serotinus** at the Blue Fiord type area, it is very probable, too, that the upper part of the upper member of the Blue Fiord Formation is similarly within the **serotinus** Zone. **P. serotinus** has been reported previously from the Blue Fiord Formation from the subsurface on Cameron Island (Uyeno and Mayr, 1979, Pl. 38.1, fig. 47, 48).

The **serotinus** Zone is identified in the Barrandian area in the Suchomasty and Třebotov limestones (Dalejan) at levels within the **Nowakia richteri** Zone and in the lowest part of the **N. holynensis** Zone (Klapper, 1977b; Klapper et al., 1978, Fig. 1, 2).

In the absence of indicators of the overlying zones, the occurrence of **Polygnathus serotinus** in the Bird Fiord Formation is difficult to assess. As noted earlier, the species ranges elsewhere into the overlying **patulus** and **costatus costatus** zones. That this occurrence is possibly of Eifelian age is suggested by the presence higher in the section, between 591 to 732 m above the base of the formation (GSC loc. 83769 to 83773, Fig. 8.2) of **Elythina** n. sp. of Brice (name in press, and carried here in open nomenclature; identified by A.W. Norris). According to Norris (personal communication), **Elythina** n. sp. "...is placed by Brice [and Meats] (in press) within the **Warrenella kirki** Zone. In Nevada the **W. kirki** Zone occurs within Johnson's (1977, fig. 2) Interval 17 which is within the conodont **kockelianus** Zone of Eifelian, early Middle Devonian age". The Emsian-Eifelian boundary cannot be placed accurately here, but may fall near the base of the Bird Fiord Formation at its type section.

To summarize the conodont evidence, the entire Blue Fiord Formation, at the section immediately east of the type section and at Sor Fiord, and the lower member of the formation just south of Eids Fiord, all on southwestern Ellesmere Island, and the formation outcropping on the larger of the Princess Royal Islands, are late Early Devonian in age (**dehiscens** to **serotinus** zones, approximately Pragian-Zlichovian boundary to Dalejan). The lower 125 m of the Disappointment Bay Formation at Sutherland River on Devon Island is of similar age (**inversus** Zone) (Klapper, 1969, Fig. 4; revised figure based on undescribed collections of Uyeno, see Uyeno and McGregor, 1970, section 4). The Blue Fiord Formation in the subsurface of Cameron and Vanier islands (located northwest of Bathurst Island) ranges in age from late Early to early Middle Devonian (**gronbergi-inversus** zones through the **patulus** and/or **costatus costatus** zones). In contrast, the formation on the east side of Young Inlet and at Twilight Creek, northern Bathurst Island, and the upper part of the formation at Grove Lake, Grinnell Peninsula, Devon Island, and at Rookery Creek, west-central Cornwallis Island, are early Middle Devonian (Eifelian), confirming the original dating of McLaren (in Fortier et al., 1963, p. 612) and Ormiston (1967) on the basis of brachiopods and trilobites.

The Bird Fiord Formation at its type section on southwestern Ellesmere Island is probably of late Early to early Middle Devonian age (Dalejan? to Eifelian). The formation outcropping on the east side of Young Inlet, northern Bathurst Island, is entirely within the Middle Devonian, probably Eifelian to Givetian age, thus again confirming McLaren's (in Fortier et al., 1963, p. 615) and Ormiston's (1967) original dating.

Plate 8.1

All figures x50. Unless otherwise noted, all specimens from the Blue Fiord Formation, from section located 2.5 km east of the type section.

Figures 1-4. **Polygnathus dehiscens** Philip and Jackson.
1,2, GSC 64481, upper and lower views of Pa element, GSC loc. 83722;
3,4. GSC 64482, upper and lower views of Pa element, GSC loc. 83726.

Figures 5,6. **Polygnathus** aff. **P. perbonus** (Philip).
GSC 64483, upper and lower views of Pa element, GSC loc. 83729.

Figures 7-12. **Polygnathus inversus** Klapper and Johnson.
7-10, GSC 64484 and 64485, upper and lower views of two Pa elements, GSC loc. 83736;
11,12. GSC 64486, upper and lower views of Pa element, GSC loc. 83737.

Figures 13-16. **Polygnathus inversus** Klapper and Johnson, transitional to **P. serotinus** Telford.
13,14, GSC 64487, upper and lower views of Pa element, GSC loc. 83743;
15,16. GSC 64488, upper and lower views of Pa element, GSC loc. 83749.

Figures 17-20. **Polygnathus serotinus** Telford.
17,18, GSC 64489, upper and lower views of Pa element, GSC loc. 83754;
19,20. GSC 64490, lower and upper views of Pa element, Bird Fiord Formation, type section, GSC loc. 83765.

Figure 21. **Pandorinellina** sp.
GSC 64491, lateral view of Pa element, GSC loc. 83742.

Figures 22-24. **Ozarkodina linearis** (Philip).
GSC 64492, upper, lateral, and lower views of Pa element, GSC loc. 83729.

Figures 25-27. **Pandorinellina exigua exigua** (Philip).
GSC 64493, upper, lateral, and lower views of Pa element, GSC loc. 83722.

Figures 28-31. **Pandorinellina expansa** Uyeno and Mason.
28, GSC 64494, lateral view of Pb element, GSC loc. 83746;
29,31. GSC 64495, lateral, upper, and lower views of Pa element, Bird Fiord Formation, type section, GSC loc. 83765.

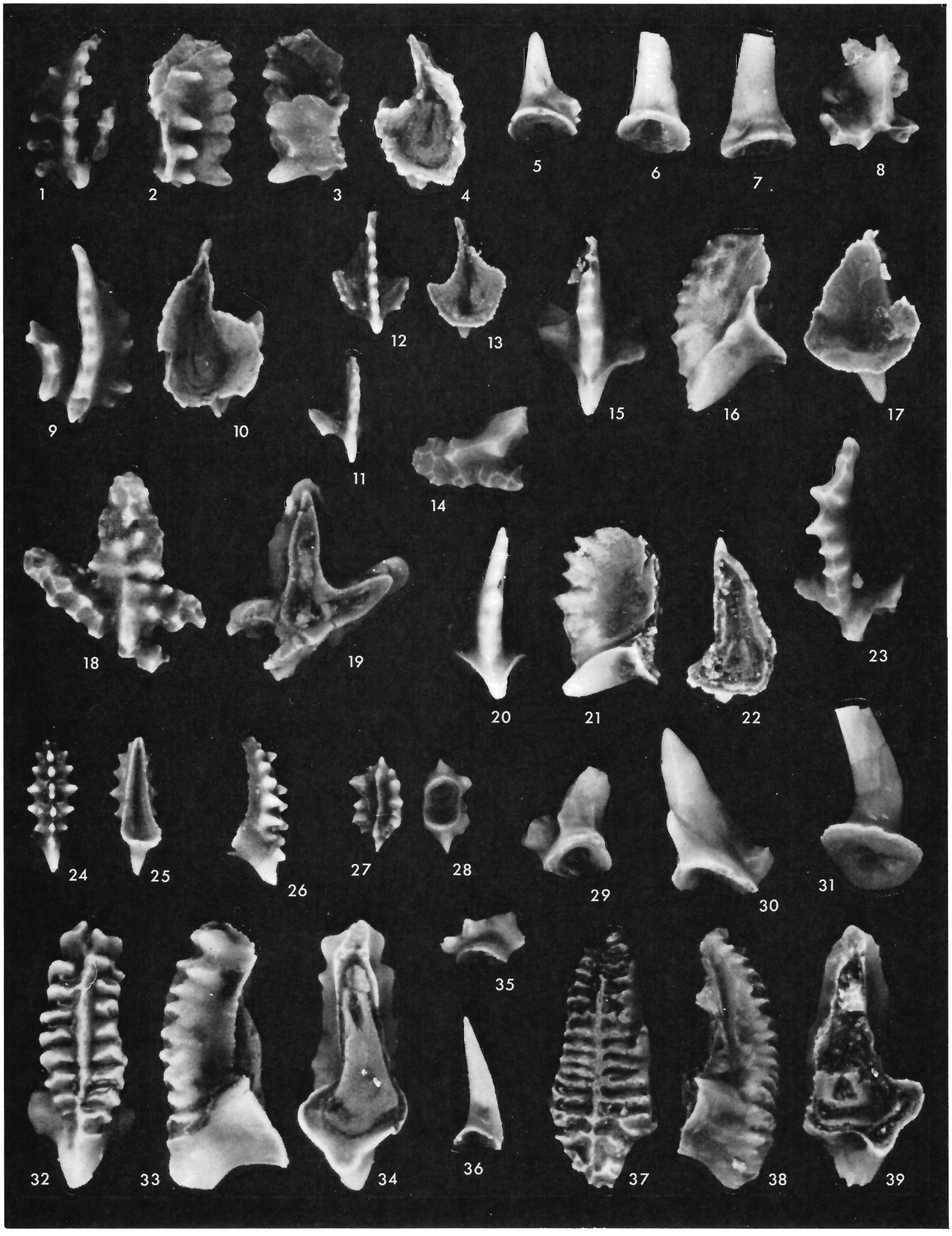
1
2
3
4
5
6
7
8
9
10
11
12
13
14
15
16
17
18
19
20
21
22
23
24
25
26
27
28
29
30
31
32
33
34
35
36
37
38
39

Plate 8.2

All figures x50. Unless otherwise noted, all specimens from the Bird Fiord Formation. (All Bird Fiord collections from the type section, except Figures 1-7, 9, 10, 14, 18, and 19).

Figures 1-11. **Steptotaxis** n. sp. A.
- 1-4, GSC 64496, upper, outer lateral, inner lateral, and lower views of I element, GSC loc. C-76074;
- 5, GSC 64497, lateral view of S_{2b} element, GSC loc. C-76074;
- 6, GSC 64498, lateral view of M_2 element, GSC loc. C-76074;
- 7, GSC 64499, lateral view of S_{2a} element, GSC loc. C-76074;
- 8, GSC 64500, upper view of S_{2c} element, GSC loc. 83767;
- 9,10, GSC 64501, upper and lower views of I element, GSC loc. C-76074;
- 11. GSC 64502, upper view of I element, GSC loc. 83767.

Figures 12,13. **Steptotaxis glanisteri** (Klapper)
GSC 64503, upper and lower views of I element, Blue Fiord Fm., section 2.5 km east of the type section, GSC loc. 83754.

Figures 14,18,19. **Steptotaxis** n. sp. C.
- 14, GSC 64504, upper view of S_{2c} element, GSC loc. C-76075;
- 18,19. GSC 64505, upper and lower views of I element, GSC loc. C-76075.

Figures 15-17. **Pelekysgnathus** sp.
GSC 64506, upper, lateral, and lower views of I element, GSC loc. 83767.

Figures 20-23. **Pelekysgnathus** n. sp.
- 20-22, GSC 64507, upper, lateral, and lower views of I element, Blue Fiord Fm., section at 2.5 km east of the type section, GSC loc. 83722;
- 23. GSC 64508, upper view of I element, Blue Fiord Fm., section at 2.5 km east of the type section, GSC loc. 83737.

Figures 24-39. **Steptotaxis** n. sp. B.
(all from GSC loc. 83769 unless otherwise noted)
- 24,25, GSC 64509, upper and lower views of I element;
- 26, GSC 64510, lateral view of I element;
- 27,28, GSC 64511, upper and lower views of S_{2c} element;
- 29, GSC 64512, lateral view of S_{2b} element;
- 30, GSC 64513, lateral view of S_{2b} element;
- 31, GSC 64514, lateral view of M_2 element;
- 32-34, GSC 64515, upper, lateral, and lower views of I element, GSC loc. 83768;
- 35, GSC 64516, lateral view of S_{2c} element;
- 36, GSC 64517, lateral view of S_{2a} element;
- 37-39. GSC 64518, upper, lateral, and lower views of I element, GSC loc. 83775.

Systematic Paleontology

Genus **Polygnathus** Hinde, 1879

Type species: **Polygnathus dubius** Hinde, 1879

Polygnathus inversus Klapper and Johnson

Plate 8.1, figures 7-16; Plate 8.3, figures 4-6, 13

Polygnathus inversus Klapper and D.B. Johnson, 1975, p. 73, Pl. 3, figs. 15-39
[synonymy through 1974]

Polygnathus inversus Klapper and Johnson, in Klapper and J.G. Johnson, 1980, p. 453
[synonymy through 1979]

Remarks. In the original description of **Polygnathus inversus** from Nevada, a transition between that species and **P. serotinus** Telford (= **P.** sp. nov. D of Klapper and Johnson, 1975, p. 73 and explanation of Pl. 8.3) was suggested on the evidence of a substantial number of specimens with lower surface features of intermediate aspect. Such specimens (e.g., Klapper and Johnson, 1975, Pl. 3, fig. 19-22, 24-31, as well as several hundred unfigured Nevada specimens; Pl. 8.1, fig. 13-16, Pl. 8.3, fig. 4, 5 herein) have an incipient development of a shelf-like protuberance on the outer side of the pit, but the protuberance characteristic of **P. serotinus** is more distinctly demarcated and smaller (e.g. Pl. 8.1, fig. 17-20). Futhermore, the pit itself in **P. serotinus** is smaller than in the transitional form. In the lower stratigraphic range of the transitional form in the Blue Fiord sections of this paper (e.g., GSC loc. 83743, Fig. 8.2; GSC loc. C-12449, C-12450, C-12452, Fig. 8.3) the anterior outer margin is about at the same height as the inner margin, as in the transitional forms from Nevada and in agreement with the diagnosis of **P. inversus.** In the higher stratigraphic range of the transitional form in the Blue Fiord sections (e.g., GSC loc. 83749, Fig. 8.2; GSC loc. C-12475, Fig. 8.3) the anterior outer margin is somewhat higher than the inner margin, but not so markedly higher as is characteristic of **P. serotinus.** These higher transitional forms thus compare with **P. declinatus** Wang (1979, p. 401-402, Pl. 1, fig. 12-20), but as the Blue Fiord Formation shows a sequence of transitional forms between **P. inversus** and **P. serotinus,** we do not favour formal designation of individual morphotypes within the sequence. Rather, we prefer to express the observed transition by designating the specimens as **"P. inversus,** transitional to **P. serotinus"** or, as has been done in the stratigraphic part of this paper, simply as **"P. inversus → P. serotinus".**

Genus **Steptotaxis** new genus

Type species. **Pelekysgnathus pedderi** Uyeno and Mason, 1975

Derivation of name. steptos, Gr. = crowned, taxis, Gr. = arrangement, for the diagnostic coronellan element of the apparatus.

Diagnosis. Multielement conodont genus in which the composition of the apparatus is like that of **Pelekysgnathus,** except that a coronellan element is present in the S_2 position in addition to acodinan elements.

Remarks. The multielement genus **Pelekysgnathus** Thomas (1949) is characterized by an apparatus consisting basically of three kinds of skeletal elements: pelekysgnathan in the I position, acodinan in the S_2 position, and a weakly costate or unornamented cone, the base of which is circular to elliptical in cross section, in the M_2 position (Klapper and Philip, 1972, p. 101-102). In contrast, all species assigned with certainty to the genus **Steptotaxis** include coronellan, as well as

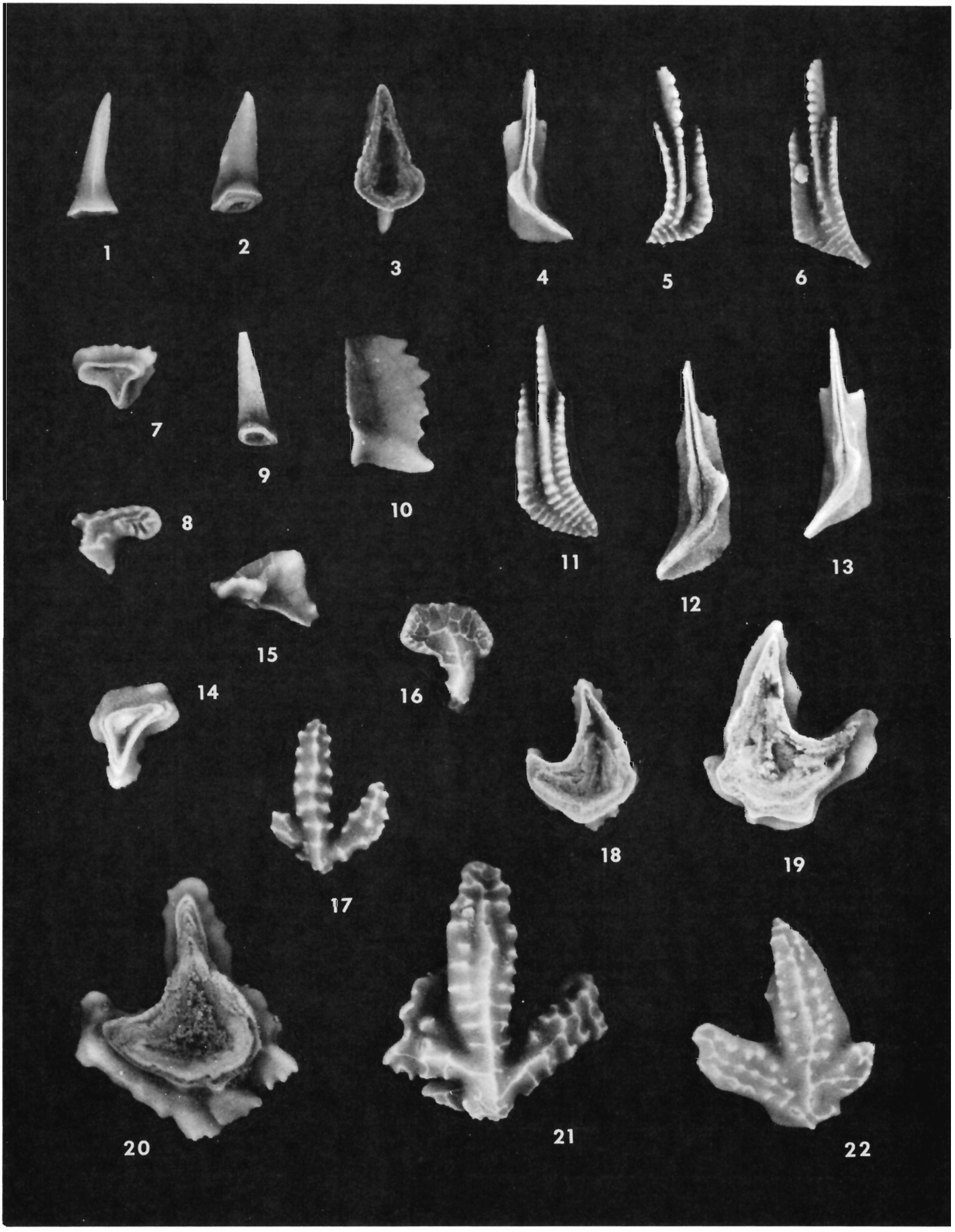
1
2
3
4
5
6
7
9
10
11
12
13
8
15
16
14
18
19
17
20
21
22

acodinan elements in the S_2 position. Thus, we revise **Pelekysgnathus** herein to exclude those species represented by apparatuses which include coronellan elements and refer the following instead to **Steptotaxis: Pelekysgnathus pedderi** Uyeno and Mason (1975), **P. uyenoi** Chatterton (1979), and **P. glenisteri** Klapper (1969). The coronellan element was illustrated when the first two were originally described, whereas the apparatus of **P. glenisteri** was illustrated by Klapper and Philip (1972). In addition, **Steptotaxis** includes the three species cited in open nomenclature and illustrated in the present paper (Pl. 8.2, 8.3).

Besides the presence of the distinctive coronellan element, **Steptotaxis** may be distinguished from **Pelekysgnathus** in that the main process of the I element in all but one of the species is characterized by icriodontan denticulation. The principal exception is **Steptotaxis** n. sp. A, in which the denticulation of the main process is a single row of nodes, but some specimens of **S. uyenoi** also show this development in common with I elements of **Pelekysgnathus.** Furthermore, in contrast with **Pelekysgnathus,** I elements of **Steptotaxis** characteristically have two well-developed lateral processes directed anteriorly, which have denticulation like that of the main process. Again there is one exception, namely **Steptotaxis** n. sp. B, which lacks such processes.

Plate 8.3

All figures x40. All specimens from the Blue Fiord Formation, from the Sor Fiord section.

Figures 1,2,7-9,14-22. **Steptotaxis** n. sp. C.
- 1, GSC 53495, lateral view of M_2 element, GSC loc. C-12487;
- 2, GSC 53496, lateral view of S_{2a} element, basal funnel preserved, GSC loc. C-12487;
- 7,8, GSC 53499, lower and upper views of S_{2c} element, posterior toward the bottom, GSC loc. C-12465;
- 9, GSC 53497, lateral view of S_{2a} element, GSC loc. C-12488;
- 14-16, GSC 56150, lower, lateral, and upper views of S_{2c} element, posterior toward the bottom in figs. 14, 16, anterior platform to left and posterior cusp to right in fig. 15, basal plate preserved (fig. 14), GSC loc. C-12487;
- 17,18, GSC 56149, upper and lower views of I element, basal plate preserved, GSC loc. C-12465;
- 19,22, GSC 56152, lower and upper views of I element, basal plate preserved, GSC loc. C-12465;
- 20,21, GSC 56154, lower and upper views of I element, basal plate preserved, GSC loc. C-12487.

Figures 3,10. **Pelekysgnathus** n. sp.
GSC 56160, lower and lateral views of I element, basal plate preserved, GSC loc. C-12438.

Figures 4,5. **Polygnathus inversus** Klapper and Johnson, transitional to **P. serotinus** Telford.
GSC 53489, lower and upper views of Pa element, GSC loc. C-12452.

Figures 6,13. **Polygnathus inversus** Klapper and Johnson.
GSC 53493, upper and lower views of Pa element, GSC loc. C-12450.

Figures 11,12. **Polygnathus** aff. **P. perbonus** (Philip).
GSC 53494, upper and lower views of Pa element, GSC loc. C-12437.

Some I elements of **Steptotaxis** species (e.g., **S. pedderi, S.** n. sp. C) resemble those of **Pedavis** Klapper and Philip, but the latter genus has a modified sagittodontan S_2 element and a strongly costate M_2 element.

Sannemannia was proposed by Al-Rawi (1977, p. 58-59) with **S. pesanseris** Al-Rawi as the designated type species. **Sannemannia** included **Pelekysgnathus glenisteri** and **P. furnishi** Klapper (1969) in Al-Rawi's proposal. The genus was diagnosed strictly in terms of morphology of the I element, with no account taken of the then indicated multielement taxonomy of **Pelekysgnathus glenisteri** and **P. furnishi,** discussed by Klapper and Philip (1972, p. 102). The multielement association of the type species of **Sannemannia** is unclear, because **S. pesanseris** was originally based on a single specimen of an I element. Subsequently, Hans P. Schönlaub recovered well-preserved I elements of **S. pesanseris** from the type stratum at the type locality in the Frankenwald, Germany; included in Schönlaub's collections is one S_{2c} element that differs radically from coronellan elements of **Steptotaxis** (we are grateful to Dr. Schönlaub for sharing these data and to Dr. W. Ziegler for providing SEM pictures of Schönlaub's specimens of **S. pesanseris**). Furthermore, the I element of **S. pesanseris** has a single row of nodes on the main process and shows no trace of the icriodontan denticulation that is characteristic of all but one of the species of **Steptotaxis.** Thus, we restrict **Sannemannia** herein to the type species and do not include the species listed under the genus by Klapper (in Klapper and Johnson, 1980, p. 455), but which are instead referred to **Steptotaxis,** as discussed above.

There remains the problem of the generic assignment of **Pelekysgnathus furnishi.** As yet, we have not found a coronellan element in the apparatus of this species, but the denticulation of the main process of the I element is incipiently icriodontan (Klapper and Philip, 1972, p. 102) and thus may be transitional with that of **Steptotaxis glenisteri.** At present, we can only assign **P. furnishi** to **Steptotaxis** with question.

Range. As presently understood, **Steptotaxis** ranges from the **dehiscens** Zone (in an undescribed collection from the Eids Formation at Vendom Fiord, southwestern Ellesmere Island) to at least as high as the **pedderi** faunal unit in Canada (i.e., approximately **australis** Zone).

Appendix

Included in this study are three collections from the Bird Fiord Formation near its type section, made by R. Thorsteinsson in 1979. These are:

C-76076 = UTM Zone 16X, 515,600 mE, 8,571,625 mN;

C-76075 = UTM Zone 16X, 515,500 mE, 8,570,000 mN; and

C-76074 = UTM Zone 16X, 513,500 mE, 8,569,375 mN.

References

Al-Rawi, D.
1977: Biostratigraphische Gliederung der Tentaculiten-Schichten des Frankenwaldes mit Conodonten und Tentaculiten (Unter- und Mittel-Devon; Bayern, Deutschland); Senkenbergiana Lethaea, v. 58, p. 25-79.

Brice, D.
Brachiopods du Devonien Inférieur et Moyen des Formations Blue Fiord et Bird Fiord des Îsles Arctiques Canadiennes; Geological Survey of Canada, Bulletin 326. (in press)

Bultynck, P.
1970: Révision stratigraphique et paléontologique (brachiopodes et conodontes) de la coupe type du Couvinien; Louvain, Université catholique, Institut géologique, Mémoires, v. 26.

Chatterton, B.D.E.
1979: Aspects of late Early and Middle Devonian conodont biostratigraphy of western and northwestern Canada; in Western and Arctic Canadian biostratigraphy, eds. C.R. Stelck and B.D.E. Chatterton, Geological Association of Canada, Special Paper 18, p. 161-231 [imprint 1978].

Chlupáč, I.
1976a: The oldest goniatite faunas and their stratigraphical significance; Lethaia, v. 9, p. 303-315.

1976b: The Bohemian Lower Devonian stages and remarks on the Lower-Middle Devonian boundary; Newsletters on Stratigraphy, v. 5, p. 168-189.

Fåhraeus, L.
1971: Lower Devonian conodonts from the Michelle and Prongs Creek formations, Yukon Territory; Journal of Paleontology, v. 45, p. 665-683.

Fortier, Y.O. et al.
1963: Geology of the north-central part of the Arctic Archipelago, Northwest Territories (Operation Franklin); Geological Survey of Canada, Memoir 320.

Harper, C.W., Jr., Johnson, J.G., and Boucot, A.J.
1967: The Pholidostrophiinae (Brachiopoda; Ordovician, Silurian, Devonian); Senckenbergiana lethaea, v. 48, p. 403-461.

Hinde, G.J.
1879: On conodonts from the Chazy and Cincinnati Group of the Cambro-Silurian, and from the Hamilton and Genesee-Shale divisions of the Devonian, in Canada and the United States; Geological Society of London Quarterly Journal, v. 35, p. 351-369.

Johnson, J.G.
1977: Lower and Middle Devonian faunal intervals in central Nevada based on brachiopods; in Western North America: Devonian, eds. Murphy, M.A., Berry, W.B.N., and Sandberg, C.A.; University of California, Riverside Campus Museum Contribution 4, p. 16-32.

Johnson, J.G. and Perry, D.G.
1976: Middle Devonian brachiopods from the Bird Fiord Formation of Bathurst Island, Arctic Canada; Canadian Journal of Earth Sciences, v. 13, p. 615-635.

Kerr, J.W.
1974: Geology of Bathurst Island group and Byam Martin Island, Arctic Canada (Operation Bathurst Island); Geological Survey of Canada, Memoir 378.

Kerr, J.W. and Thorsteinsson, R.
1972: Geology, Baumann Fiord, District of Franklin; Geological Survey of Canada, Map 1312A.

Klapper, G.
1969: Lower Devonian conodont sequence, Royal Creek, Yukon Territory and Devon Island, Canada, with a section on Devon Island stratigraphy by A.R. Ormiston; Journal of Paleontology, v. 43, p. 1-27.

Klapper, G. (cont.)
1977a: (with contributions by D.B. Johnson) Lower and Middle Devonian conodont sequence in central Nevada; in Western North America: Devonian, eds. Murphy, M.A., Berry, W.B.N., and Sandberg, C.A.; University of California, Riverside Campus Museum Contribution 4, p. 33-54.

1977b: Lower-Middle Devonian boundary conodont sequence in the Barrandian area of Czechoslovakia; Časopis pro mineralogii a geologii, v. 22, p. 401-406.

Klapper, G. and Johnson, D.B.
1975: Sequence in conodont genus **Polygnathus** in Lower Devonian at Lone Mountain, Nevada; Geologica et Palaeontologica, v. 9, p. 65-83.

Klapper, G. and Johnson, J.G.
1980: Endemism and dispersal of Devonian conodonts; Journal of Paleontology, v. 54, p. 400-455.

Klapper, G. and Philip, G.M.
1972: Familial classification of reconstructed Devonian conodont apparatuses; in Symposium on conodont taxonomy, eds. Lindström, M. and Ziegler, W., Geologica et Palaeontologica, v. SB1, p. 97-114.

Klapper, G., Ziegler, W., and Mashkova, T.V.
1978: Conodonts and correlation of Lower-Middle Devonian boundary beds in the Barrandian area of Czechoslovakia; Geologica et Palaeontologica, v. 12, p. 103-116.

Mayr, U., Uyeno, T.T., and Barnes, C.R.
1978: Subsurface stratigraphy, conodont zonation, and organic metamorphism of the lower Paleozoic succession, Bjorne Peninsula, Ellesmere Island, District of Franklin; in Current Research, Part A, Geological Survey of Canada, Paper 78-1A, p. 393-398.

Mayr, U., Uyeno, T.T., Tipnis, R.S., and Barnes, C.R.
1980: Subsurface stratigraphy and conodont zonation of the lower Paleozoic succession, Arctic Platform, in southern Arctic Archipelago; in Current Research, Part A, Geological Survey of Canada, paper 80-1A, p. 209-215.

McGregor, D.C. and Uyeno, T.T.
1969: Mid-Paleozoic biostratigraphy of the Arctic Islands (58 F, 69 A, 78 H); in Report of Activities, Part A, Geological Survey of Canada, Paper 69-1A, p. 134-135.

1972: Devonian spores and conodonts of Melville and Bathurst islands, District of Franklin; Geological Survey of Canada, paper 71-13.

Ormiston, A.R.
1967: Lower and Middle Devonian trilobites of the Canadian Arctic Islands; Geological Survey of Canada, Bulletin 153.

1975: Siegenian trilobite zoogeography in Arctic North America; Fossils and Strata, no. 4, p. 391-398.

Pedder, A.E.H. and Klapper, G.
1977: Fauna and correlation of the type section of the Cranswick Formation (Devonian), Mackenzie Mountains, Yukon Territory; in Report of Activities, Part B, Geological Survey of Canada, Paper 77-1B, p. 227-234.

Thomas, L.A.
1949: Devonian-Mississippian formations of southeast Iowa; Geological Society of America Bulletin, v. 60, p. 403-437.

Thorsteinsson, R.
(with contributions by T.T. Uyeno) Stratigraphy and conodonts of Upper Silurian and Lower Devonian rocks in the environs of the Boothia Uplift, Canadian Arctic Archipelago, Part I, Contributions to Stratigraphy; Geological Survey of Canada, Bulletin 292. (in preparation)

Trettin, H.P.
1978: Devonian stratigraphy, west-central Ellesmere Island, Arctic Archipelago; Geological Survey of Canada, Bulletin 302.

Uyeno, T.T. and Mason, D.
1975: New Lower and Middle Devonian conodonts from northern Canada; Journal of Paleontology, v. 49, p. 710-723.

Uyeno, T.T. and Mayr, U.
1979: Lithofacies interpretation and conodont biostratigraphy of the Blue Fiord Formation in the subsurface of Cameron and Vanier islands, Canadian Arctic Archipelago; in Current Research, Part A, Geological Survey of Canada, paper 79-1A, p. 233-240.

Uyeno, T.T. and McGregor, D.C.
1970: Silurian-Devonian biostratigraphy of the Arctic Islands, District of Franklin; in Report of Activities, Part A, Geological Survey of Canada, Paper 70-1A, p. 110-110b.

Wang, C.
1979: Some conodonts from the Sipai Formation in Xiangzhou of Guangxi; Acta Palaeontologica Sinica, v. 18, p. 395-408.

Weddige, K., Werner, R., and Ziegler, W.
1979: The Emsian-Eifelian boundary, an attempt at correlation between the Eifel and Ardennes regions; Newsletters on Stratigraphy, v. 8, p. 159-169.

Weddige, K. and Ziegler, W.
1977: Correlation of Lower/Middle Devonian boundary beds; Newsletters on Stratigraphy, v. 6, p. 67-84.

Weyant, M.
1975: Sur l'âge du member inférieur de la Formation Blue Fiord dans le Sud-Ouest de l'île Ellesmere (Archipel Arctique Canadien) d'après les conodontes; Newsletters on Stratigraphy, v. 4, p. 87-95.

9. QUELQUES CORAUX DU TRIAS ET DU JURASSIQUE DU CANADA

Convention de recherche 760042

L. Beauvais[1] et T.P. Poulton
Institut de géologie sédimentaire et pétrolière, Calgary

Beauvais, L. et Poulton, T.P., "Quelques coraux du Trias et du Jurassique du Canada"; en Recherche en cours, partie C, Commission géologique du Canada, Etude 80-1C, p. 95-101, 1980.

Résumé

Un genre nouveau, Coelomeandra, est décrit ainsi que trois espèces nouvelles. C. kochi n. sp. et Pseudisastraea cassiarensis n. sp. proviennent de bancs de la région de Bowser Lake (Colombie-Britannique) dont l'âge est probablement triassique supérieur. Ampakabastraea microcalix n. sp. et Isastraea nantuacumensis Beauvais proviennent de bancs probablement bajociens, du groupe de Laberge, situés au sud du territoire du Yukon.

Avant-propos

Les coraux triassiques du Canada proviennent de plusieurs localités situées dans les parties occidentales de la Cordillère, jusqu'à la latitude 61°N (Tozer, 1970). Plusieurs espèces ont été décrites jusqu'à présent (p.e. Clapp et Shimer, 1911; Smith, 1927; Tozer, 1970). Quelques coraux triassiques se trouvent dans d'épais bancs bioclastiques (Tozer, 1970).

Les coraux sont peu communs dans les roches sédimentaires jurassiques des régions occidentales du Canada, qui sont, d'autre part, très fossilifères localement. Deux espèces seulement ont été décrites jusqu'à présent – Astrocoenia irregularis Whiteaves (1884, p. 246, pl. 33, fig. 1) et Kraterostrobilis bathys Crickmay (1930, p. 40, pl. 2, figs. g, h, i, j). Le présent rapport est le premier résultat d'une étude des spécimens des coraux jurassiques présents dans les collections de la Commission géologique du Canada.

La plupart des coraux jurassiques trouvés au Canada se présentent sous forme de petites colonies isolées dans des grès ou des roches argileuses dont la faune dominante est composée de mollusques. En Amérique du Nord, on ne trouve de récifs jurassiques que dans le golfe du Mexique (Imlay, 1965).

On ne rencontre pas de coraux dans les roches triassiques et jurassiques des régions arctiques de l'Amérique du Nord. On peut en récolter dans le Trias supérieur (Karnien à Norien supérieur) au sud du territoire du Yukon (Tozer, 1970). À l'exception des travaux de Whiteaves (1884) et de Crickmay (1930), les espèces jurassiques les plus septentrionales furent décrites par Wells (1942) et Imlay (1956) dans le Bajocien des Pryor Mountains du Wyoming et du Montana aux États-Unis. Les espèces les plus septentrionales connues sont les espèces décrites ici, elles proviennent du groupe de Laberge du territoire du Yukon du Sud, ainsi que du Jurassique inférieur et moyen (Bajocien inférieur) de la région de Cook Inlet au sud de l'Alaska (Imlay, 1965, p. 1035). Ainsi, la rareté des faunes coralliennes dans le Trias et le Jurassique du nord de l'Amérique du Nord est conforme avec la transition du domaine téthytien ou pacifique au domaine boréal, transition reconnue dans quelques autres groupes d'invertébrés (p. e., Tozer, 1970; Imlay, 1965).

La présence dans le Jurassique moyen de Madagascar, du Maroc, et de l'Inde (voir descriptions des espèces) des deux espèces jurassiques décrites ici indique probablement une répartition générale de quelques espèces de coraux dans des domaines de faunes non boréales (voir aussi Beauvais, 1976). De plus, ces découvertes permettent de corroborer l'hypothèse du transport vers le nord d'une faune qui provient généralement des localités du sud.

Les spécimens décrits ici, et ceux du sud de l'Alaska, proviennent des régions occidentales de la Cordillère et furent peut-être transportés depuis des latitudes lointaines, au sud où ils étaient déposés dans le Mésozoïque, vers le nord, au moyen de failles transcurrentes (p. e., Tozer, 1970; Monger et Price, 1979).

Localités, stratigraphie et âges

57186. La même que C-18178.

83428. coll. N.G. Koch pour Dome Petroleum Co., 1968. Côté ouest du Delta Peak, Bowser Lake (west-half) map-area, Cassiar District, Colombie-Britannique; lat. 56°38.75'N, long. 129°35.5'W. Aucun fossile caractéristique n'a été trouvé avec les coraux. Cette localité est située dans une région compliquée, riche en affleurements du Trias supérieur (au sud de la carte géologique de Monger, 1977, p. 261, fig. 52.4) et J.W.H. Monger (com. pers.) croit que les coraux sont probablement d'âge du Trias supérieur.

C-18178. coll. D.J. Tempelman-Kluit, 1972. Cañon d'un affluent du Nordenskiold River, 1.6 km environ au nord du Mt. Vowles, Aishihik Lake map-area, Territoire du Yukon du Sud, lat. 61°28'N, long. 130°09'W. Les coraux proviennent de la partie supérieure du groupe de Laberge; aucun fossile pouvant caractériser l'âge n'a été trouvé avec les coraux, mais la localité renferme des bivalves trigoniidées qui sont probablement du Jurassique moyen, et peut-être, plus précisément, du Bajocien moyen (Poulton, in Tempelman-Kluit, 1974, p. 96). La présence dans les bancs des coraux décrits ici, d'Isastraea nantuacumensis et d'Ampakabastraea microcalix, rend possible cette détermination d'âge.

[1] Département de Paléontologie, Laboratoire de Paléontologie des Invertébrés, Université Pierre et Marie Curie, Paris, France. ER 154 du CNRS.

Description systématique

Tous les spécimens sont conservés dans la collection de la Commission géologique du Canada, 601, rue Booth, Ottawa, Ontario, Canada.

MADRÉPORAIRES

SOUS-ORDRE ARCHAEOCOENIIDA
Alloiteau 1952 emend. Beauvais 1979

Famille Tropiphyllidae Beauvais 1979

Genre Coelomeandra nov. gen.

Espèce-type

Coelomeandra kochi nov. sp., probablement du Trias supérieur, Bowser Lake (W 1/2) area, Colombie-Britannique.

Caractères du genre

Colonie cério-méandroïde, d'apparence subplocoïde. Rares calices polygonaux isolés. Séries plus ou moins longues et plus ou moins sinueuses à centres calicinaux parfaitement distincts, réunis par des septes de vallée. Les séries sont délimitées par une muraille septothécale formée par le bord externe des éléments radiaires qui s'incurve et se soude au bord externe voisin pour former un type de muraille qu'Alloiteau avait appelé archéothèque. Endothèque très abondante, formée de dissépiments horizontaux et de planchers infundibuliformes, donnant, en section longitudinale, un aspect sinusoïdal analogue à ce que l'on observe chez le genre Clausastraea et montrant, en section transversale, une disposition en anneaux concentriques dont le plus interne ressemble à une pseudomuraille parathécale, délimitant un pseudo-calice circulaire, ce qui donne à la colonie son aspect subplocoïde. Pas de périthèque. Éléments radiaires: sont des septes subcompacts, légèrement perforés au bord interne (trabécules dissociées formant de véritables épines septales visibles sur les planchers); ils ne sont pas confluents, à l'exception des septes de vallée qui sont des lames biseptales. Microstructure: les septes sont constitués de trabécules simples, bien centrées, peu nombreuses. Pas de columelle ni de synapticules.

Rapports et différences

La microstructure des éléments radiaires et de la muraille de ce genre est identique à celle de Coelocoenia Laube (1865), du Trias de St-Cassiar, Tirol, genre redécrit par Cuif en 1972. La disposition concentrique de l'endothèque rappelle celle du genre Diplocoenia chez qui l'on observe, comme ici, une véritable muraille septothécale et une pseudo muraille interne, toutefois chez Diplocoenia il n'existe pas de planchers. L'endothèque de Coelomeandra rappelle celle du genre Clausastraea. La forme méandroïde de la colonie est tout à fait particulière à ce genre nouveau.

Derivatio nominis

Le genre est voisin de Coelocoenia mais possède une forme méandroïde.

Coelomeandra kochi nov. gen., nov. sp.

Pl. 9.1, fig. 1

Matériel et provenance

Holotype GSC 64472 et paratype GSC 64473 de la localité GSC 83428. Probablement du Trias supérieur, Bowser Lake (west half) map-area, Colombie-Britannique.

Derivatio nominis

L'espèce est dédiée au Dr. N.G Koch qui a récolté ces spécimens.

Dimensions des spécimens figurés

Largeur des séries = 6 à 12 mm; diamètre des pseudo-calices = 5 à 6 mm; distance des centres calicinaux = 10 à 15 mm; nombre de septes par calices = 30 à 35 (15 à 22 arrivant dans le pseudo-calice).

Description de spécimens figurés

Le polypier est colonial, massif, cério-méandroïde. Les calices, rarement isolés, sont le plus souvent réunis en séries plus ou moins longues et plus ou moins sinueuses à centres parfaitement distincts et fréquemment réunis par des septes de vallée qui sont des lames biseptales. Pas de périthèque entre les séries qui sont unies directement par une muraille septothécale plus ou moins épaisse, formée de trabécules identiques à celles des éléments radiaires dont le bord externe s'incurve pour former une structure qu'Alloiteau avait désignée sous le nom d'archéothèque. Endothèque très abondante constituée par de larges dissépiments, nombreux, alignés sur un même plan horizontal dans la région externe des polypiérites et constituant, au centre de ceux-ci, de véritables planchers infundibuliformes; en section verticale, l'ensemble de l'endothèque présente un aspect sinusoïdal rappelant l'endothèque du genre Clausastraea; en section transversale, les dissépiments et planchers sont disposés en

---

PLANCHE 9.1

Coelomeandra kochi nov. gen., nov. sp.

Figure 1. a = section transversale X2, montrant la disposition en anneaux concentriques des dissépiments endothécaux de l'holotype GSC 64472.

b et c = sections longitudinales X10, montrant (b) l'alignement horizontal des dissépiments dans la région externe des polypiérites et (c) leur inflexion infundibuliforme au centre des calices, les deux du paratype GSC 64473.

d = section transversale d'un septe X66, montrant (en noir) les centres de calcification, du paratype GSC 64473.

e = section transversale dans la région centrale d'un calice X20, montrant les trabécules du bord interne dissociées, du paratype GSC 64473.

f et g = sections transversales X20, dans la région murale montrant la structure trabéculaire de la muraille, du paratype GSC 64473.

Ampakabastraea microcalix nov. sp.

2. a = section transversale X10 de l'holotype GSC 64475.

b = section transversale du paratype GSC 64476 X10.

1a

1d

1b

1f

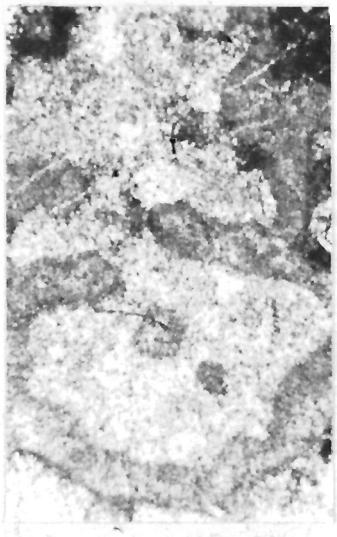

1e

1c

2a

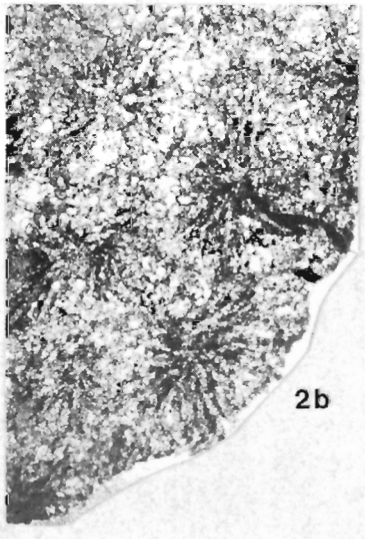

2b

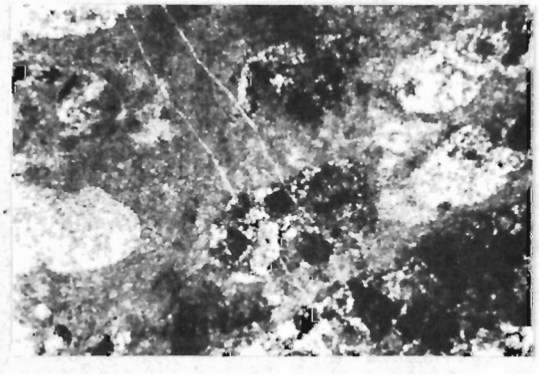

1g

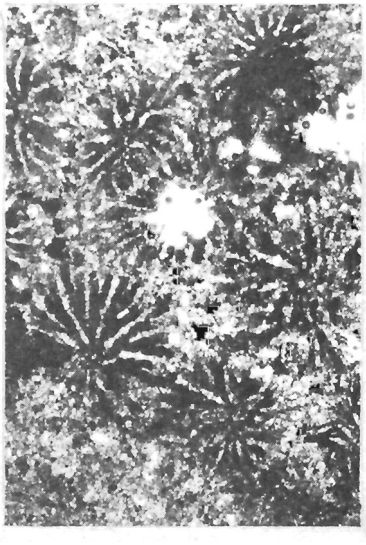

anneaux concentriques, l'anneau le plus interne simulant une muraille parathécale interne qui confère à la colonie une apparence plocoïde analogue à ce qui est observé chez le genre Diplocoenia. L'espace circulaire ainsi délimité au centre des calices est appelé "pseudo-calice" (voir Beauvais, 1964, p. 179). Les éléments radiaires sont des septes non confluents, rarement subconfluents à l'exception des septes de vallée qui sont des lames biseptales. Ils sont subcompacts, formés de trabécules simples, bien centrées, peu nombreuses, pouvant se dissocier au bord interne en épines septales, bien visibles, en section verticale, sur les planchers. Bord distal denté. Gemmation intracalicinale, se produisant dans la région périphérique des calices, entre la muraille et l'anneau le plus interne de l'endothèque. Pas de columelle. Pas de synapticules.

SOUS-ORDRE FUNGIIDA Verrill 1965

Famille Andemantastraeidae Alloiteau 1952

Genre Ampakabastraea Alloiteau 1958

Espèce-type

Ampakabastraea ampakabensis Alloiteau, 1958, Bathonien d'Ampakabo, Madagascar.

Ampakabastraea microcalix nov. sp.

Pl. 9.1, fig. 2; pl. 9.2, fig. 1

Matériel et provenance

Holotype GSC 64475, de la localité GSC C-18178 ainsi que le paratype GSC 64476; les autres spécimens non figurés de la localité GSC 57186. Du Jurassique moyen, probablement du Bajocien moyen; Aishihik Lake map-area, territoire du Yukon du Sud.

Derivatio nominis

Allusion au diamètre peu élevé des calices.

Dimensions des spécimens figurés

Diamètre des calices = 1, 5 à 3, 5 mm; distance des centres calicinaux = 1, 5 à 4 mm; nombre de septes par calice = 22 à 36; densité septale = 4 par 1 mm.

Description

Colonie cérioïde, massive, en forme de massue. Les calices sont petits, serrés, polygonaux, irréguliers, ils se multiplient à la fois par bourgeonnement intra- et intercalicinal, ne se disposent jamais en séries. Ils sont peu profonds. Les éléments radiaires (probablement des costo-septes) sont compacts, droits ou un peu flexueux, libres, disposés en symétrie radiaire, en systèmes inégaux. Ils sont non ou subconfluents parfois, mais rarement, ils peuvent être confluents et subthamnastérioïdes. Leur bord distal est armé de dents aigües, très fines, égales et équidistantes. Les faces latérales sont ornées de granules spinuleux alignés en files verticales mais ne se soudant pas en carènes. Endothèque peu abondante. Rares synapticules. Columelle plus ou moins développée et variable: parfois lamellaire et située dans le prolongement d'un S_1, parfois pariétale et formée de plusieurs tigelles, parfois encore, constituée d'une seule tigelle. Pas de pali. Muraille septo-synapticulaire, visible en plaque mince, paraissant souvent absente en surface.

Rapports et différences

Cette espèce se distingue des autres Ampakabastraea par la petite taille de ses calices, par sa densité septale plus élevée et par la présence d'une muraille.

Répartition géographique et stratigraphique

L'espèce se rencontre aussi dans le Bathonien de Madagascar (collection Collignon conservée à l'Institut de Paléontologie, Muséum national d'histoire naturelle de Paris, n°629; inédit).

SOUS-ORDRE FAVIIDA Vaughan et Wells 1943

Famille Montlivaltiidae Dietrich 1926 emend. Alloiteau 1952 et Beauvais 1979

Genre Isastraea M. Edw. et Haime 1851

Espèce-type

Astraea helianthoides Goldfuss 1826. De l'Oxfordien supérieur d'Heidenhein, Würtemberg.

Isastraea nantuacumensis Beauvais

Pl. 9.2, fig. 2

1885 Isastraea richardsoni M.Edw. et Haime in Koby, p. 286, pl. 85, fig. 11

1966 Isastraea nantuacumensis Beauvais, p. 1005, pl. VII, fig. 3 et pl. VIII, fig. 1

1970 Isastraea nantuacumensis Beauvais, p. 41

1972 Isastraea nantuacumensis Beauvais, p. 20, pl. B, fig. 3.

Matériel et provenance

Hypotype GSC 64478, de la localité GSC C-18178 et hypotype GSC 64479 de la localité GSC 57186. Du Jurassique moyen, probablement du Bajocien moyen, Aishihik Lake map-area, territoire du Yukon du Sud.

PLANCHE 9.2

Ampakabastraea microcalix nov. sp.

Figure 1. a = face calicifère de l'holotype GSC 64475 X1.

b = face calicifère du paratype GSC 64476 X45.

Isastraea nantuacumensis BEAUVAIS

2. a = face calicifère X1, hypotype GSC 64478.

b = face calicifère X1, hypotype GSC 64479.

c et d = sections transversales X10, hypotype GSC 64478.

Pseudisastraea cassiarensis nov. sp.

3. Holotype GSC 64480. Partie de la face calicifère X1.

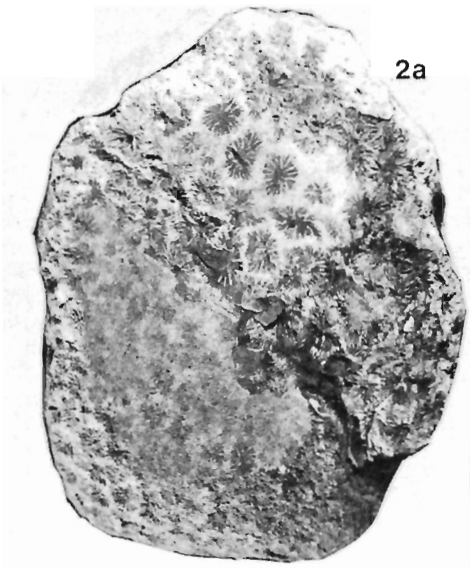
2a


1a

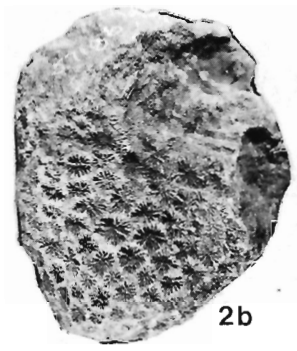
2b


2c

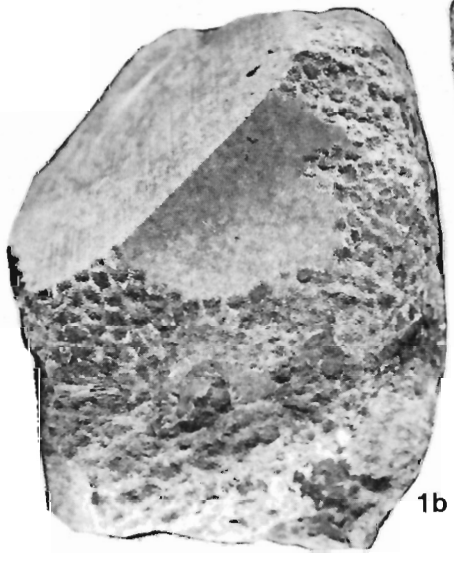
1b


3


2d

Dimensions des spécimens figurés	Hypotype GSC 18178	Hypotype GSC 57186
Diamètre des calices	2, 5 à 7 mm	3, 5 à 6, 5 mm
Distance des centres calicinaux	3 à 6 mm	4 à 7 mm
Nombre de septes	25 à 42	30 à 37
Densité septale	5 par 2 mm	4 à 5 par 2 mm

Description

Colonie massive, cérioïde. Les polypiérites sont polygonaux, peu profonds, unis directement par leur muraille et se multipliant par gemmation intercalicinale, parfois par fissiparité. Les éléments radiaires sont compacts, plus ou moins épais, non confluents, parfois subconfluents, souvent épais au bord interne, disposés en symétrie radiaire, en systèmes très inégaux; la disposition septale étant également très variable d'un calice à l'autre. Le bord distal est cassé mais quelques dents sont néanmoins observables par places. Les faces latérales sont également difficilement observables, elles sont ornées de carènes verticales. L'endothèque est peu abondante, formée de quelques dissépiments minces, localisés dans la région périphérique des chambres interseptales. Columelle absente ou pariétale faible. Muraille septo-parathécale avec quelques synapticules.

Rapports et différences

Par leurs dimensions, la rareté de l'endothèque, et l'épaisseur des septes, ces spécimens peuvent être rattachés à l'espèce bajocienne qui fut décrite par Koby en 1885 sous le nom d'Isastraea richardsoni M. Edw. et Haime et pour laquelle une espèce nouvelle a été créée (Beauvais, 1966, p. 1005).

Répartition géographique et stratigraphique

Cette espèce a été rencontrée dans le Bajocien de Nantua (Ain) et de Denariaz, près de Ste-Croix (Suisse), dans le Bajocien du Maroc et dans le Bathonien inférieur de St-Gaultier (Inde) (voir synonymie).

Famille Faviidae Gregory 1900

Genre Pseudisastraea Alloiteau 1958

Espèce-type

Isastraea parva Gregory 1900. Du Bathonien de Cutch, Inde.

Pseudisastraea cassiarensis nov. sp.

Pl. 9.2, fig. 3

Matériel et provenance

Holotype GSC 64480, de la localité GSC 83428. Probablement du Trias supérieur, Bowser Lake (west half) map-area, Colombie-Britannique.

Derivatio nominis

De la région de sa provenance: Cassiar District, Colombie-Britannique.

Dimensions de l'holotype

Longueur de la colonie = 180 mm; largeur de la colonie = 145 mm; épaisseur de la colonie = 60 mm; diamètre des calices = 3, 5 à 6, 5 mm; distance des centres calicinaux = 3 à 7 mm; nombre de septes par calice = 25 à 50.

Description de l'holotype

Grande colonie massive, de forme plus ou moins lamellaire, fixée par sa face inférieure qui est subplane. La face calicifère est légèrement convexe. La colonie est cérioïde. Les calices polygonaux, plus ou moins profonds, se multiplient par bourgeonnement intercalicinal, mais on peut observer de rares cas de bourgeonnement intracalicinal. Les éléments radiaires sont compacts, non ou subconfluents, à bord interne légèrement épais. Ils sont souvent réunis, au centre du calice, entre eux et à la columelle, par de larges dissépiments; ils sont disposés sans symétrie nette et en systèmes non discernables. La columelle est pariétale, faible, formée par une ou deux tigelles plus ou moins aplaties. La muraille est septo-parathécale, plus ou moins élevée. L'endothèque est formée de dissépiments épars dans tout le lumen. Pas de synapticules. Le bord distal et les faces latérales des septes n'ont pas pu être observés. En section transversale on peut toutefois distinguer, sur les faces latérales, quelques granules spinuleux épais.

Rapports et différences

Le spécimen est très recristallisé mais les caractères que l'on peut y observer sont ceux du genre Pseudisastraea Alloiteau. La seule espèce jusqu'à présent connue de ce genre, P. parva (Gregory), possède des calices deux fois plus petits et un nombre d'éléments radiaires deux fois moindres.

Références

Alloiteau, J.

1952: Madréporaires post-paléozoïques; in Piveteau J., Traité de Paléontologie, t.I, p. 539-782. Paris, Masson édit.

1958: Monographie des Madréporaires fossiles de Madagascar; Annales géologiques de Madagascar, fasc. XXV, 218 p., 38 pl. Paris.

Beauvais, L.

1964: Étude stratigraphique et paléontologique des formations à Madréporaires du Jurassique supérieur du Jura et de l'Est du Bassin de Paris. Mémoires de la Société géologique de France, nov. sér., t. XLIII, fasc. 1, mém. n°100, 288 p., 38 pl.

1966: Révision des Madréporaires du Dogger de la collection Koby; Eclogae geologicae Helvetiae, v. 59, n°2, p. 989-1024, pl. I-XV.

1970: Étude de quelques polypiers bajociens du Maroc; Service géologique du Maroc, Notes, t. 30, n°225, p. 39-50, 1 pl.

1972: Contribution à l'étude de la faune bathonienne dans la vallée de la Creuse (Inde). Madréporaires; Annales de paléontologie, Invertébrés, t. LVIII, fasc. 1, p. 35-87, pl. A-E.

Beauvais, L. (suite)
1976: Paleobiogeography of the Middle Jurassic Corals; in Historical Biogeography, Plate Tectonics, and the Changing Environment, Gray, J. and Boucot, A.J.; Oregon State University Press, 1979.

1979: Sur la taxinomie des Madréporaires mésozoïques; 3rd International Symposium on Fossil Cnidarians, Varsovie, Sept. 1979, 16 p., 3 tabl. (sous presse).

Clapp, C.H. and Shimer, H.W.
1911: The Sutton Jurassic of Vancouver Group; Proceedings of Boston Society of Natural History, v. 34, p. 425-438.

Crickmay, C.H.
1930: The Jurassic rocks of Ashcroft, British Columbia; University of California Publications in Geological Sciences, v. 19, p. 23-74.

Cuif, J.P.
1972: Recherches sur les Madréporaires du Trias. I. Famille des Stylophyllidae; Muséum national d'histoire naturelle, 3°sér., n°97, Bulletin Sciences de la Terre 17, p. 211-291.

Gregory, J.W.
1900: Jurassic fauna of Cutch; India, Geological Survey, Palaeontologica Indica, sér. IX, vol. 2, 195 p., pl. 2-27.

Imlay, R.W.
1956: Marine Jurassic exposed in Bighorn Basin Pryor Mountains and northern Bighorn Mountains, Wyoming and Montana; American Association of Petroleum Geologists, Bulletin, v. 40, p. 577-584.

1965: Jurassic marine faunal differentiation in North America; Journal of Paleontology, v. 39, p. 1023-1038.

Koby, F.
1881-1887: Monographie des Polypiers jurassiques de la Suisse; Société paléontologique de Suisse, Mémoires, 582 p., 130 pl.

Laube, G.
1865: Die Fauna der Schitchten von St-Cassian; Oesterreichische akademie der wissenschaften, Denkschriften, 1 Abt., v. 24, p. 223-266, pl. I-X.

Monger, J.W.H.
1977: Upper Paleozoic rocks of northwestern British Columbia; Geological Survey of Canada, Paper 77-1A, p. 255-262.

Monger, J.W.H. et Price, R.A.
1979: Geodynamic evolution of the Canadian Cordillera - progress and problems; Canadian Journal of Earth Sciences, v. 16, p. 770-791.

Smith, J.P.
1927: Upper Triassic marine invertebrate faunas of North America; United States Geological Survey Professional Paper 141.

Tempelman-Kluit, D.J.
1974: Reconnaissance geology of Aishihik Lake, Snag and part of Stewart River map-areas, west-central Yukon; Geological Survey of Canada, Paper 73-41.

Tozer, E.T.
1970: Marine Triassic Faunas; in Geology and Economic Minerals of Canada, Geological Survey of Canada, Economic Geology Report 1, p. 633-640.

Vaughan, T.W. et Wells, J.W.
1943: Revision of the suborders, families and genera of Scleractinia; Geological Society of America, Special Paper, n°44, 363 p., 51 pl.

Wells, J.W.
1942: A new species of Coral from the Jurassic of Wyoming; American Museum Novitates, n°1161, American Museum of Natural History, 2 p., 1 pl.

Whiteaves, J.F.
1884: Mesozoic fossils, vol. 1, Part III - On the fossils of the coal-bearing deposits of the Queen Charlotte Islands collected by Dr. G.M. Dawson in 1878; Geological and Natural History Survey of Canada.

10. GAMACHIGNATHUS, A NEW MULTIELEMENT CONODONT GENUS FROM THE LATEST ORDOVICIAN, ANTICOSTI ISLAND, QUÉBEC

Project 770077

A.D. McCracken[1], G.S. Nowlan, and C.R. Barnes[2]
Institute of Sedimentary and Petroleum Geology, Ottawa

*McCracken, A.D., Nowlan, G.S., and Barnes, C.R., **Gamachignathus**, a new multielement conodont genus from the latest Ordovician, Anticosti Island, Québec; in Current Research, Part C, Geological Survey of Canada, Paper 80-1C, p. 103-112, 1980.*

Abstract

*The multielement conodont genus, **Gamachignathus** n. gen. has been identified from the Late Ordovician Vauréal and Ellis Bay formations of Anticosti Island, Québec. The apparatus of **Gamachignathus** includes paired cordylodiform, gothodiform, keislognathiform, hibbardelliform, cyrtoniodiform, falodiform, prioniodiform, and modified prioniodiform elements. Two species are presently known: **Gamachignathus ensifer** n. sp. (the type species) and **G. hastatus** n. sp. Associated conodont data indicate that **Gamachignathus** first appears in the Richmondian, flourishes in the Gamachian (post-Richmondian), and is known to extend to within 2 m of the Ordovician-Silurian boundary on Anticosti, as defined by conodonts. **Gamachignathus** is also known from Late Ordovician strata of western United States (Hanson Creek Formation, Nevada; Ely Springs Dolomite, California) and northwestern and eastern Canada (Road River Formation, Yukon Territory; Matapedia Group, Québec, respectively). The genus has an apparatus plan similar to genera of the relatively warm water North American Midcontinent Province (e.g. **Oulodus, Aphelognathus**), but in element morphology appears to be more closely related to genera of the cooler water North Atlantic Province (e.g. **Amorphognathus, Prioniodus**). The appearance of **Gamachignathus** in the outer margins of the Midcontinent Province may reflect a cooling of the marine environment as a result of the Late Ordovician glaciation.*

INTRODUCTION

Excellent exposure and apparently continuous sedimentation on Anticosti Island make it one of the prime study areas in North America of the Ordovician-Silurian boundary. In the course of intensive investigations of the conodont faunas of the island, a significant new Late Ordovician conodont genus **Gamachignathus** has been recovered. Since the initial discovery, the genus has been recognized from other parts of North America.

Anticosti Island, situated in the Gulf of St. Lawrence (Fig. 10.1) lies in that part of the St. Lawrence Platform referred to as the Anticosti Basin, comprising a Lower Ordovician to Lower (Middle?) Silurian succession. This basin includes the Lower and Middle Ordovician strata of the Mingan Islands, and the autochthonous Cambrian to Lower and Middle Ordovician sediments of western Newfoundland and the Cambrian rocks of the southeast coast of Labrador. The basin is bordered by the Canadian Shield to the north and the Appalachian Orogen to the south and east.

Anticosti Island is underlain by Ordovician and Silurian limestones and shales with a total thickness (including subsurface) that varies from 900 m in the northwest to 3300 m in the southeast (Roliff, 1968). The subsurface is known from a number of drillholes, some of which have been faunally assessed by Riva (1969). The strata lack any major structural complications and dip at less than 2° to the southwest. The Upper Orodivician is represented by a thick sequence (approximately 1300 m including about 900 m in the subsurface) of shales and limestones including the Macasty Formation, the overlying Vauréal Formation and lower part of the Ellis Bay Formation. Sedimentation was apparently continuous into the Lower Silurian which is represented by the upper part of the Ellis Bay, Becscie, Gun River, Jupiter and Chicotte formations, the latter being late Llandovery and/or possibly early Wenlock in age (Bolton, 1972). Lithologic evidence suggests a shallow water shelf environment with a land area to the east or northeast.

Previous studies of the strata of Anticosti Island have been reviewed by Bolton (1972). The Ordovician-Silurian boundary has been placed by most previous workers within or at one of the boundaries of the Ellis Bay Formation.

The conodonts from all formations on Anticosti Island are presently under investigation. Preliminary results were recently presented (McCracken and Barnes, 1978; Nowlan et al., 1979; Uyeno et al., 1979) and some of the detailed studies are now completed and have been accepted for publication as a Bulletin of the Geological Survey of Canada (in press) in which Nowlan and Barnes and McCracken and Barnes describe the conodonts from the Vauréal Formation and the Ellis Bay Formation, respectively. The purpose of this report is to document the discovery of an important new Late Ordovician multielement conodont genus, **Gamachignathus.** The genus and its two known species **(G. ensifer** n. sp., type species; **G. hastatus** n. sp.) are believed to have potential as indicators of latest Ordovician (post-Richmondian) strata. McCracken and Barnes propose the re-establishment of the Gamachian Stage (Schuchert and Twenhofel, 1910; Twenhofel, 1928) for this stratigraphic interval.

The Ordovician conodont faunas of the exposed (upper) part of the Vauréal Formation include many of the key taxa indicative of Fauna 12 (Sweet et al., 1971; Sweet and Bergström, 1976) and the **Amorphognathus ordovicicus** Zone (Bergström, 1971) of the North American Midcontinent and North Atlantic provinces, respectively. These taxa include: **Amorphognathus ordovicicus** (Branson and Mehl), **Belodina profunda** (Branson and Mehl), and **Plegagnathus dartoni** (Stone and Furnish) as well as species of **Aphelognathus, Oulodus,** and **Plectodina.** In addition, several new species of simple cone genera **(Panderodus, Staufferella)** are present. Most of the fauna of the Vauréal Formation persists into the Ellis Bay, but in reduced abundance. The fauna of the Ellis Bay Formation although generally similar to that of the Vauréal has some significant differences, including the great abundance of the specimens of the two new species of **Gamachignathus.** These comprise 45 per cent of the total

[1] Department of Geology, University of Western Ontario, London, Ontario, N6A 3K7.

[2] Department of Earth Sciences, University of Waterloo, Waterloo, Ontario, N2L 3G1.

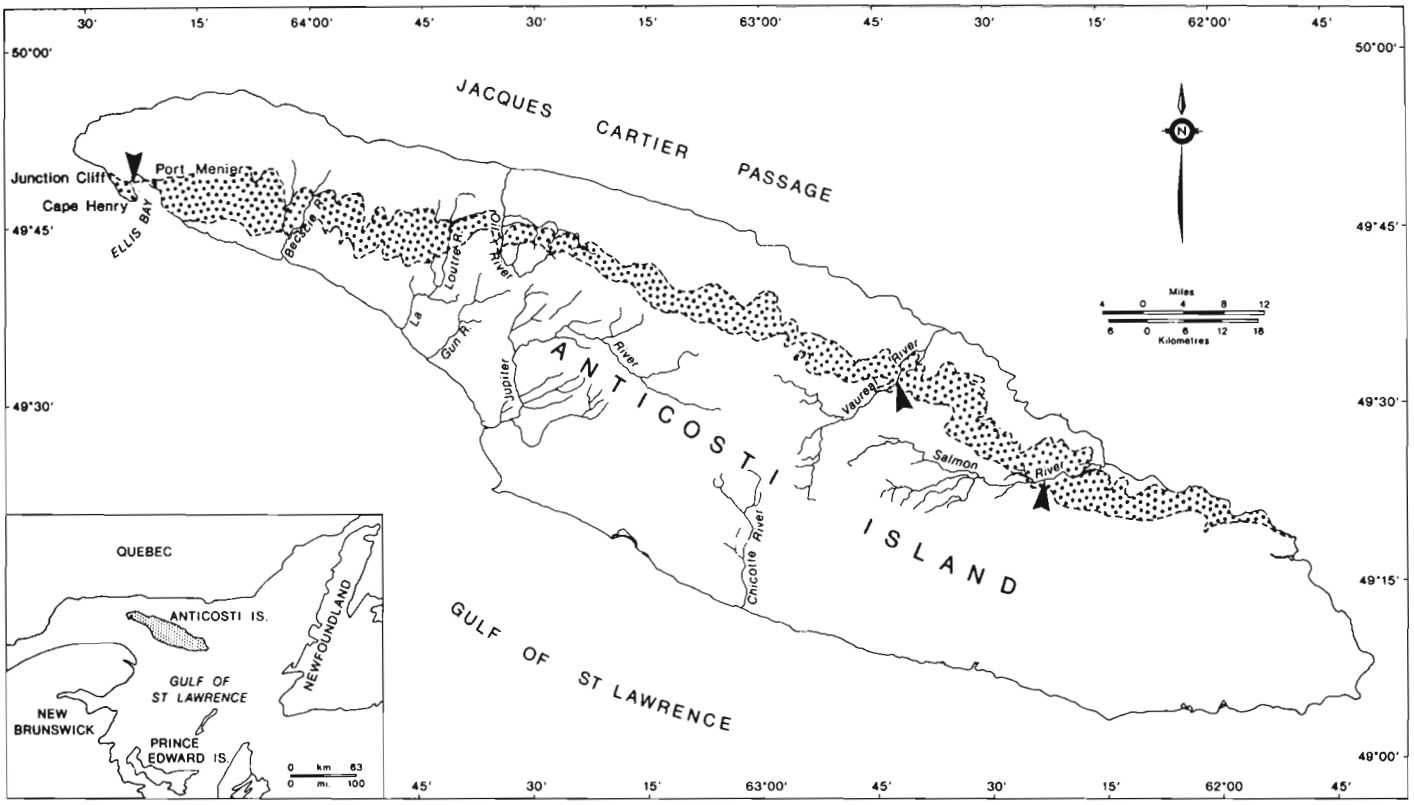

Figure 10.1. *Index map of Anticosti Island showing the distribution of the Ellis Bay Formation (stippled) and locations of sections studied (arrows). Sections studied include those on the west and east sides of Cape Henry and the east side of Ellis Bay, and along the Vauréal and Salmon rivers. The Vauréal Formation outcrops to the north of the Ellis Bay Formation and was examined at the west end of the island, and on the Oil, Vauréal and Salmon rivers.*

fauna in the type Ellis Bay section. McCracken and Barnes will formally propose a new conodont fauna (Fauna 13) representing Gamachian (post-Richmondian, Late Ordovician) time.

Elements of **Gamachignathus** are also known from unpublished collections elsewhere. **G. ensifer** is reported from the Hanson Creek Formation, central Nevada (Ross et al., 1979; see synonymy herein) and the upper member of the Ely Springs Dolomite in the Funeral Mountains, California (A.G. Harris, personal communication, 1979). Recent collections from the Road River Formation in the Ogilvie Mountains, Yukon Territory (by A.D. McCracken) contain elements of **Gamachignathus**, as well as **"Prioniodus ferrarius** Knüpfer" sensu Thompson and Satterfield (1975). This fauna was recovered about 3 m below beds containing graptolites that are suggestive of the **Glyptograptus persculptus** Zone, presently regarded as indicating earliest Silurian age. The **"P. ferrarius"** fauna from the Edgewood Group (and its lateral equivalents) in Missouri was described by Thompson and Satterfield (1975). Unpublished study of topotype material from the Edgewood Group by the authors suggests that the generic identification of **"P. ferrarius"** is probably valid. Its occurrence with **Gamachignathus** in the Road River Formation suggests that it is also a latest Ordovician species.

Occurrence of **Gamachignathus** in the platformal strata of Anticosti Island prompted one of us (G.S. Nowlan) to examine strata of equivalent age in deeper water facies in the Gaspé Peninsula, Québec. A few preliminary samples were collected from the Matapedia Group in southern Gaspé Peninsula in 1978. Two of these samples yielded abundant elements of **Gamachignathus.** The Matapedia Group is a poorly fossiliferous sequence of thin bedded calcareous siltstone and limestone. Alcock (1935) recovered a few shelly fossils which indicated a late Ordovician age, the fauna being similar to that recovered from Upper Ordovician strata in Percé, Québec (White Head Formation; Lespérance, 1974). The preliminary results from the conodont samples encouraged a systematic collection of the Matapedia Group of southern Gaspé and White Head Formation of southeastern Gaspé which was undertaken at the time of writing.

All of these occurrences of **Gamachignathus** are located in strata that accumulated in areas marginal to the North American midcontinent during the late Ordovician. These probably preserve the record of latest Ordovician deposition during a major late Ordovician regression presumed to be related to the continental glaciation in North Africa (Beuf and Biju-Duval, 1966; Allen, 1975).

SYSTEMATIC PALEONTOLOGY

The systematic paleontology of this paper has been co-ordinated with the monographs of McCracken and Barnes, and Nowlan and Barnes to be published as a Bulletin of the Geological Survey of Canada to avoid duplication. The former report contains a full account of the Ordovician-Silurian conodont paleontology of the Ellis Bay Formation, Anticosti Island. The writers have also used the traditional style of element nomenclature to retain continuity with the above studies, together with the new system of nomenclature proposed by Barnes et al. (1979). The reader is referred to that paper for a more extensive discussion of this system, and of the structure and evolution of Ordovician conodont apparatuses.

All specimens are deposited in the National Type Fossil Collection, Geological Survey of Canada (GSC), Ottawa, Ontario.

Genus GAMACHIGNATHUS n. gen.

Type species. **Gamachignathus ensifer** n. sp.

Etymology. The prefix is in honour of Oliver Louis Gamache (1784-1854) who made his home at Ellis Bay – then called Gamache Bay. Twenhofel (1928) described Gamache as a smuggler chieftain but according to MacKay (1979), Gamache had deliberately made himself a reputation as a figure of terror to protect his home against unwanted visitors. It was believed by some that he was in league with the devil and had drawn ships onto the surrounding reefs with false beacons to secure their cargoes. The suffix is from the Greek "gnathos" meaning "jaw".

Diagnosis. Apparatus of **Gamachignathus** n. gen. consists of eight paired morphotypes. The ramiform complex includes elements of an asymmetrical to symmetrical transition series (i.e. cordylodiform, gothodiform, keislognathiform, hibbardelliform; = a-1, a-2, b, c elements). The other elements are cyrtoniodiform, falodiform, prioniodiform, and modified blade-like prioniodiform (= e-1, e-2, f, and g). Posterior process (where present) has hindeodellid type of denticulation which may be overgrown in large specimens.

Remarks. Two new species of **Gamachignathus** are recognized in the Anticosti material, G. ensifer and G. hastatus. The apparatuses of both species of Gamachignathus have two element positions that are each occupied by two element types (or morphotypes, sensu Barnes et al., 1979). The a position has both cordylodiform (a-1) and gothodiform (a-2) elements (the latter being asymmetrical with an antero-lateral costa). The other (e position) is represented by cyrtoniodiform (e-1) and falodiform (e-2) elements. By comparison with other Ordovician conodont apparatuses, it is unusual to have all of these elements in a single species. Other genera that have the prioniodid type of apparatus (sensu Sweet and Bergström, 1970) or Type IV apparatus (sensu Barnes et al., 1979) may have up to seven morphotypes. However, in some there appears to be a subdivision of element positions. For example, **Oulodus ulrichi** (Stone and Furnish), with a Type IVB apparatus, has two forms of both the a and e elements (Barnes et al., 1979, p. 138). The a position is represented by cordylodiform (a-1) and eoligonodiniform (a-2) elements: the difference being a modification of the antero-lateral margin (denticulated process in the latter). The e position has cyrtoniodiform elements with or without a peg-like denticle on the anterior margin of the cusp (e-1, e-2, respectively). The relationship between the a-1 and a-2, and e-1 and e-2 elements of **Gamachignathus** is considered analogous to the above example. The gothodiform element (a-2) of **Gamachignathus** differs from the cordylodiform (a-1) in possessing a sharp antero-lateral costa. The cyrtoniodiform (e-1) and falodiform (e-2) elements likewise differ, the latter bearing a denticulated anterior process. Thus, both forms of elements are comparable to each other and to the other elements of the **Gamachignathus** apparatus in terms of colour, size, distribution, etc. The similarity in morphology and occurrence support the proposed apparatus plan.

This subdivision of position to contain two similar morphotypes could represent sexual dimorphism (cf. Jeppsson, 1972) or intraspecific variation. However, the former explanation is considered speculative, and the latter is not supported by element distribution. All elements consistently co-occur: thus, a subspecies interpretation does not apply to the Anticosti material.

The apparatus of **Gamachignathus** has similarities to genera that have a Type IVA or IVB apparatus plan (Barnes et al., 1979). **Gamachignathus** has an apparatus similar to Type IVB genera of the North American Midcontinent Province (e.g. **Aphelognathus, Oulodus**) in that it lacks the d morphotype (tetraprioniodiform element). However, the morphology of the elements of **Gamachignathus** is more comparable to Type IVA genera of the North Atlantic Province. Such genera (e.g. **Amorphognathus, Prioniodus**) have a ramiform complex or first transition series (sensu Barnes et al., 1979) that is represented by cordylodiform, keislognathiform (or gothodiform), hibbardelliform and tetraprioniodiform elements (= a, b, c, and d morphotypes). Elements of the first transition series of Type IVA apparatuses are distinguished by aborally directed lateral processes (where present) and a posterior process with a hindeodellid type of denticulation. This is in contrast to the outwardly directed lateral processes and subdued posterior process found in the first transition series of Type IVB genera. Thus, the genus **Gamachignathus** is believed to have greater affinities to genera from the North Atlantic Province than those from the Midcontinent Province. The appearance of **Gamachignathus** in the Midcontinent Province and its domination in the more offshore environments (as shown by the distribution in the Ellis Bay Formation) may reflect a cooling of the marine environment as a result of the Late Ordovician-Early Silurian glaciation that was centred in North Africa (Beuf and Biju-Duval, 1966; Allen, 1975).

When compared to known genera, **Gamachignathus** is most similar to **Prioniodus** (senior subjective synonym of **Baltoniodus**, Fåhraeus and Nowlan, 1978). During the evolution of **Prioniodus**, the e element has been either a falodiform (cf. **P. navis** Lindström) or oistodiform (cf. **P. gerdae** Bergström) element, the difference between these elements is the form of the anterior cusp margin. There are, however, morphologic differences between these elements of **Prioniodus** species and the falodiform and cyrtoniodiform elements of **Gamachignathus**. The prioniodiform (f) element of **Gamachignathus** has closer similarities to **P. variabilis** Bergström and older species than it does to the younger species **P. gerdae** Bergström. The modified, blade-like, prioniodiform (g) elements of **Gamachignathus** differ from the equivalent element in **Prioniodus** in that the antero-lateral or lateral process is not aborally directed. They also lack the well developed platform-like posterior and postero-lateral processes found in **P. gerdae**. The posterior process is more blade-like and the postero-lateral area has only a basal flare. In this respect, the modified prioniodiform element of **Gamachignathus** is more similar to that of older species of **Prioniodus**. Species of **Gamachignathus** appear to have more in common with older species of **Prioniodus** than younger species but this is based only on the two prioniodiform elements. The evolutionary relationships of **Gamachignathus** are obscure.

GAMACHIGNATHUS ENSIFER n. sp.

Plate 10.1, figures 1-17

Aphelognathus? n. sp. Ross, Nolan, and Harris, 1979 (in part), p. C11, fig. 7, a, b, e, f (only).

Exochogognathus keislognathoides Pollock, Rexroad, and Nicoll. Ross, Nolan, and Harris, 1979, p. C11, fig. 7ℓ.

Distomodiform elements Ross, Nolan, and Harris, 1979, p. C11, fig. 7, h, i.

Etymology. From the Latin, "ensifer" meaning "sword-bearing", in reference to the shape of the cusp and denticles.

Diagnosis. A species of **Gamachignathus** in which cusp and denticles are laterally compressed with sharp edges, cusp is relatively short and broad in cyrtoniodiform (e-1), falodiform (e-2), and prioniodiform (f) elements. Posterior process of elements has hindeodellid style of denticulation which is commonly overgrown. Keislognathiform (b) and hibbardelliform (c) elements have lateral flanges on cusp. Falodiform element lacks well developed posterior process but has a curved, denticulated anterior process. Anterior process of prioniodiform element is similar to that of falodiform element. Anterior edge of cusp on modified, blade-like, prioniodiform (g) element extends to denticulated lateral process. This element is blade-like with small gap between cusp and first denticle of anterior process.

Description. Cusp and denticles are laterally compressed with sharp edges. Denticulation of lateral and posterior process, if present, is of hindeodellid style. This is commonly subdued by overgrowth with development of triangular tips, especially in cyrtoniodiform, prioniodiform and modified prioniodiform elements. Most elements have deep basal cavity that does not extend into cusp. Cavity extends under all processes and anticusps. White matter occurs in cusp and denticles; boundary is generally cloudy. Relatively coarse striations are present on the lower part of the posterior face of the cusp and base on gothodiform and hibbardelliform (Plate 10.1, fig. 14) elements; finer striations are likewise present on the cordylodiform elements. Striations are either rare or absent on other elements of apparatus.

Cordylodiform (a-1) and gothodiform (a-2) elements: Cusp is proclined basally, erect distally. Anterior edge continues along anticusp to produce flat inner basal face. Angle between anticusp and posterior process is about 60-70°. Basal cavity is conical with slight oral inflection of tip into cusp. Cordylodiform elements have outer lateral face that is narrowly rounded. Gothodiform elements have base with outer lateral costa that extends as ridge to aboral margin. Ridge forms nearly planar antero-lateral face on anticusp. Posterior to ridge, base is slightly concave. Anterior margin of element is less convex than that of cordylodiform element.

Keislognathiform (b) element: Cusp is proclined basally, erect distally and twisted so that inner and outer edges are antero- and postero-laterally situated, respectively. Cusp and posterior process are inclined and flexed to the inner side, respectively. Anterior face of cusp is convex. Sharp lateral edges of cusp extend aborally to processes as flanges. Posterior face has sharp ridge extending to base of denticles. Lateral processes diverge at low angle. Extremely asymmetrical forms have inner and outer lateral processes bowed such that aboral margin is concave and convex, respectively. Inner lateral process is adenticulate for greater part of length. Proximal denticle of both processes is subparallel with cusp, confluent for most of length, and is incorporated into cusp in some specimens. Distally, denticles are inclined towards cusp, reclined towards posterior. Denticles are long, discrete and slender. Basal cavity is deep. White matter occurs in cusp and denticles as well as in the posterior and lateral edges of main cusp.

Hibbardelliform (c) element: Element is symmetrical and has cusp ornamentation, denticulation, and white matter distribution similar to that of keislognathiform element.

Cyrtoniodiform (e-1) and falodiform (e-2) elements: Cusp is lanceolate, broad, high, and tapers abruptly to sharp point. Edges develop into keels in larger forms. Cusp is slightly flexed to inner side and is unornamented. Cyrtoniodiform element has recurved cusp. Anterior margin of cusp is convex, and in some, anticusp is proclined. Outer face of cusp is more broadly convex than inner face. Anticusp is about one-third length of cusp. In lateral view, angle between anterior and aboral margin of anticusp is between 25-45°. Posterior process is straight, commonly broken near cusp. Aboral angle of process and base is between 120-140°. Basal cavity is shallow. Base is narrowly flared on inner face; maximum flare occurs posterior to cusp axis. Outer face of base is slightly concave or planar. White matter continues along part of anticusp margin. Falodiform element has reclined cusp. Anterior process is directed aborally and laterally. Process is flexed such that outer lateral face is convex, inner lateral face is concave. Process has four or more denticles. Denticles are short, triangular, basally confluent and inclined towards cusp. In small specimens, denticles are more discrete. Posterior process, if present, may bear a small germ denticle. On some larger specimens a long reclined denticle is incorporated into cusp for most of its length. Flare of base is expanded beneath cusp, variable in outline. Elements with circular flare have narrow cavity beneath anterior process. Elements with subcircular flare have anterior process that is more broadly excavated. Posterior process, if present, is shallowly excavated.

Prioniodiform (f) element: Element has cusp similar to cyrtoniodiform element but with short costa on inner face.

PLATE 10.1

All specimens are from the Ellis Bay Formation except figures 10 and 15 which are from the Matapedia Group. All specimens are paratypes unless otherwise noted.

Figures 1-17 - **Gamachignathus ensifer** n. gen., n. sp.

1. Inner lateral view, cordylodiform (a-1) element, X 100, GSC 60047.
2. Outer lateral view, gothodiform (a-2) element, X 100, GSC 60049.
3. Posterior view, markedly asymmetrical keislognathiform (b) element, X 80, GSC 60051.
4. Posterior view, slightly asymmetrical keislognathiform (b) element, X 120, GSC 60053.
5. Posterior view, hibbardelliform (c) element, X 130, GSC 60055.
6. Lateral view, hibbardelliform (c) element, X 100, GSC 60056.
7. Inner lateral view, cyrtoniodiform (e-1) element, X 90, GSC 60057.

8, 12. Inner lateral and oral views, falodiform (e-2) element, X 90, GSC 60060.

9, 13. Holotype, antero-lateral and oral views, prioniodiform (f) element, X 90, GSC 60063.

10. Hypotype, antero-lateral view, prioniodiform (f) element, X 70, GSC 60800.
11. Lateral view, modified prioniodiform (g) element, X 60, GSC 60072.
14. Striations on posterior surface, hibbardelliform (c) element, X 1100, GSC 60055.
15. Hypotype, lateral view, modified prioniodiform (g) element, X 80, GSC 60801.

16, 17. Lateral and oral views, modified prioniodiform (g) element, X 50, GSC 60071.

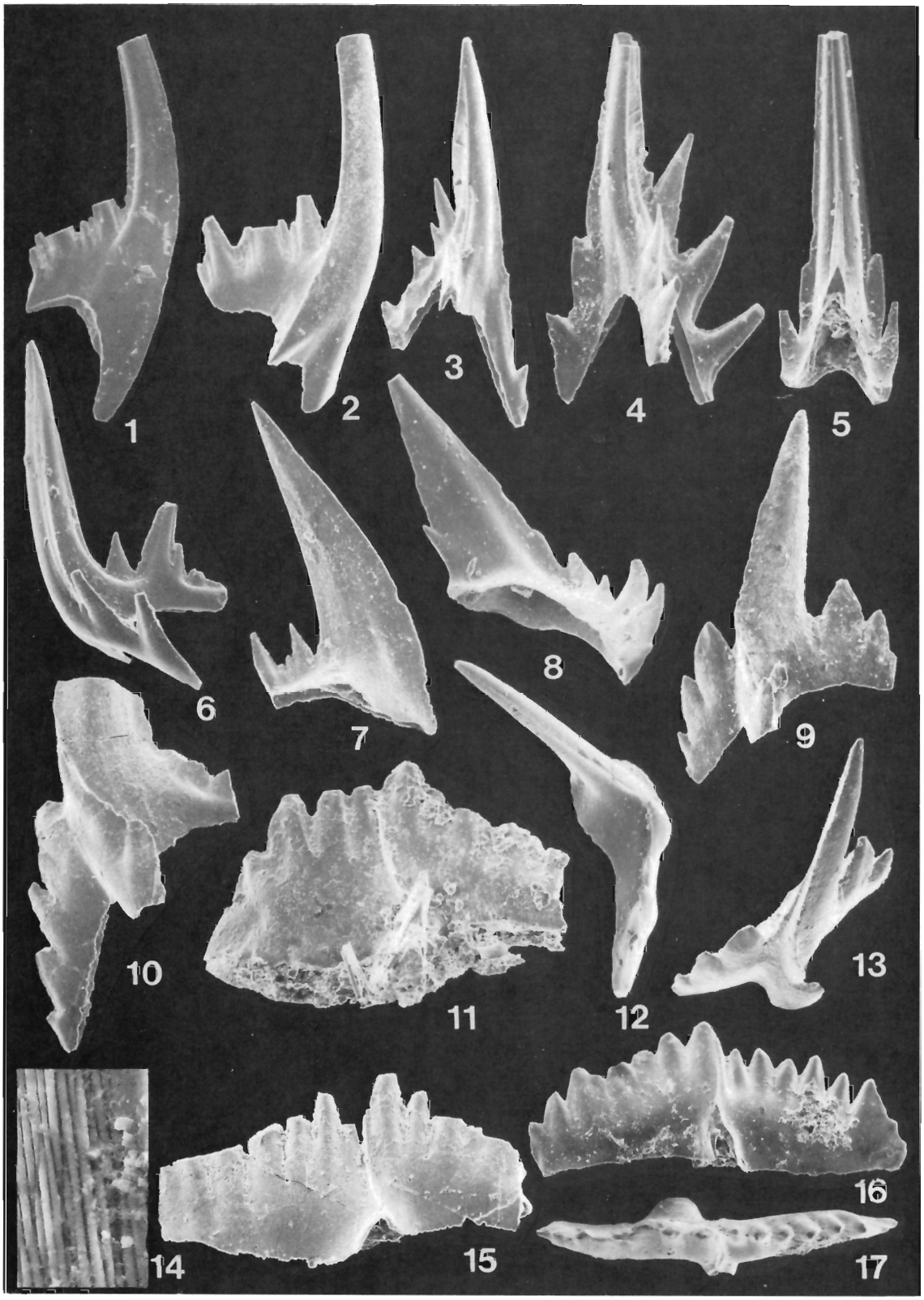
1
2
3
4
5
6
7
8
9
10
11
12
13
14
15
16
17

Cusp is directed slightly out of plane of processes. Anterior edge of cusp continues as denticulated anterior process. Sharp lateral inflection of process is present at base of cusp. Anterior process is strongly directed aborally so that it is out of plane of other processes. Other two processes are posteriorly bowed and only slightly deflected aborally. Denticulation of anterior process is similar to that of falodiform element. Denticles of lateral process are curved towards posterior. Broad flare is present on inner face of base. White matter is present along full length of anterior edge, as well as in cusp and denticles.

Modified, blade-like, prioniodiform (g) element: Element has straight anterior process, laterally and aborally bowed posterior process, and denticulated outer lateral process. Cusp is higher and wider than denticles, and flexed laterally so that anterior edge extends across base to outer lateral process. Denticles are triangular in outline and confluent for most of length in large specimens. In large forms, they number 6 to 8 on each process. Denticles decrease gradually in size to ends of processes, being higher on posterior process. Base is high beneath cusp. Oral margin of processes is aborally directed. Basal cavity is deep, well excavated. Base is flared on inner lateral face immediately posterior to cusp. Opposite face is inwardly concave. Junction of outer lateral process and base is slightly expanded. Lateral process is commonly broken at junction, rarely preserved with one or more triangular denticles.

Remarks. The elements of the ramiform complex (first transition series) of **G. ensifer** n. sp. show certain differences compared to previously described form species. As mentioned in the generic discussion, they have the general morphology of some North Atlantic Province species. There are some similarities to the corresponding elements of species of **Icriodella** and **Distomodus** which are present in the Silurian conodont fauna of the Ellis Bay Formation. This again may indicate a close affinity to some North Atlantic Province genera. The cyrtoniodiform (e-1) elements are distinguishable from other form species of **Cyrtoniodus.** In particular, most other form species have discrete denticles on the posterior process. The falodiform (e-2) element differs from others in that there is little or only minor development of a posterior process, the anterior process is long and bowed, and the base is not laterally compressed.

The prioniodiform (f) element is similar in general morphology to **"Prioniodus ferrarius** Knupfer" s.f. (= sensu formo) found in the Upper Ordovician of Missouri and Illinois (Satterfield, 1971; Thompson and Satterfield, 1975). This identification is questionable because it lacks the typical development of the anterior process, and the holotype is from strata considered by Knupfer (1967) to be Llanvirn to Llandeilo in age. The anterior process of **"P. ferrarius"** s.f., like that of the holotype does, however, originate high on the anterior margin of the element whereas on the prioniodiform element of **G. ensifer**, it originates from low on the base and is more aborally directed. **"P. ferrarius"** also differs from this element of **G. ensifer** in that the denticles are discrete and the cusp is shorter and more antero-posteriorly compressed. In addition, the other processes of **"P. ferrarius"** s.f. are more laterally situated and hence the element is more blade-like. The equivalent processes on the prioniodiform element of **G. ensifer** are laterally and posteriorly directed. **P. girardeauensis** Satterfield s.f. has a more typical prioniodiform shape but it differs from elements of **G. ensifer** for the same morphological reasons as **"P. ferrarius"** s.f.

Although **"P. ferrarius"** s.f. is blade-like it differs from the modified prioniodiform (g) element. The processes of the latter are antero-posteriorly situated and the element has a morphology that is more comparable to form species of **Aphelognathus.** It differs from these form species in that the sharp, slightly offset anterior edge of the cusp continues aborally to a denticulated lateral process.

One element recovered by Nowlan and Barnes from the Vauréal Formation is probably part of **G. hastatus.** The differences between the elements of **G. ensifer** and **G. hastatus** n. sp. are discussed within the description of the latter species.

Material. Elements from the Ellis Bay Formation: cordylodiform (a-1) – 278; gothodiform (a-2) – 89; keislognathiform (b) – 404; hibbardelliform (c) – 46; cyrtoniodiform (e-1) – 325; falodiform (e-2) – 109; prioniodiform (f) – 217; modified prioniodiform (g) – 426. Elements from the Vauréal Formation: a-28; b-23; c-12; e-1-8; e-2-0; f-6; g-6.

Types. Type numbers are followed by sample numbers in parentheses. Figured holotype GSC 60063 (E36); figured paratypes, GSC 60047 (E36), 60049 (S25), 60051 (V12), 60053 (E36), 60055 (E07), 60056 (V12), 60057 (E36), 60060 (E36), 60071 (E36), 60072 (E44); unfigured paratypes, GSC 60048 (E07), 60050 (S25), 60052 (E06), 60054 (E36), 60058 (E36), 60059 (S25), 60061 (E36), 60064 (E07), 60065 (E36), 60066 (E34), 60067 (E32), 60068 (E36), 60069 (E36), 60070 (E36); figured hypotypes 60800, 60801.

PLATE 10.2

All specimens are from the Ellis Bay Formation and are paratypes unless otherwise noted.

Figures 1-16 - **Gamachignathus hastatus** n. gen., n. sp.

1. Outer lateral view, cordylodiform (a-1) element, X 70, GSC 60073.
2. Outer lateral view, gothodiform (a-2) element, X 70, GSC 60075.
3. Posterior view, markedly asymmetrical keislognathiform (b) element, X 80, GSC 60078.
4. Posterior view, markedly asymmetrical keislognathiform (b) element with extensive basal sheathing, X 90, GSC 60077.
5. Posterior view, hibbardelliform (c) element, X 195, GSC 60079.
6. Inner lateral view, cyrtoniodiform (e-1) element, X 90, GSC 60080.

7, 10. Outer lateral and aboral views, falodiform (e-2) element, X 140, GSC 60082.

8, 11. Inner lateral and oblique oral views, falodiform (e-2) element, X 160, GSC 60799.

9. Antero-lateral view, prioniodiform (f) element, X 150, GSC 60083.
12. Holotype, postero-lateral (inner) view, prioniodiform (f) element, X 120, GSC 60084.

13, 16. Lateral and oblique oral views, modified prioniodiform (g) element, X 80, GSC 60087.

14. Striations on posterior surface, keislognathiform (b) element, X 1100, GSC 60076.
15. Lateral view, modified prioniodiform (g) element, X 90, GSC 60085.

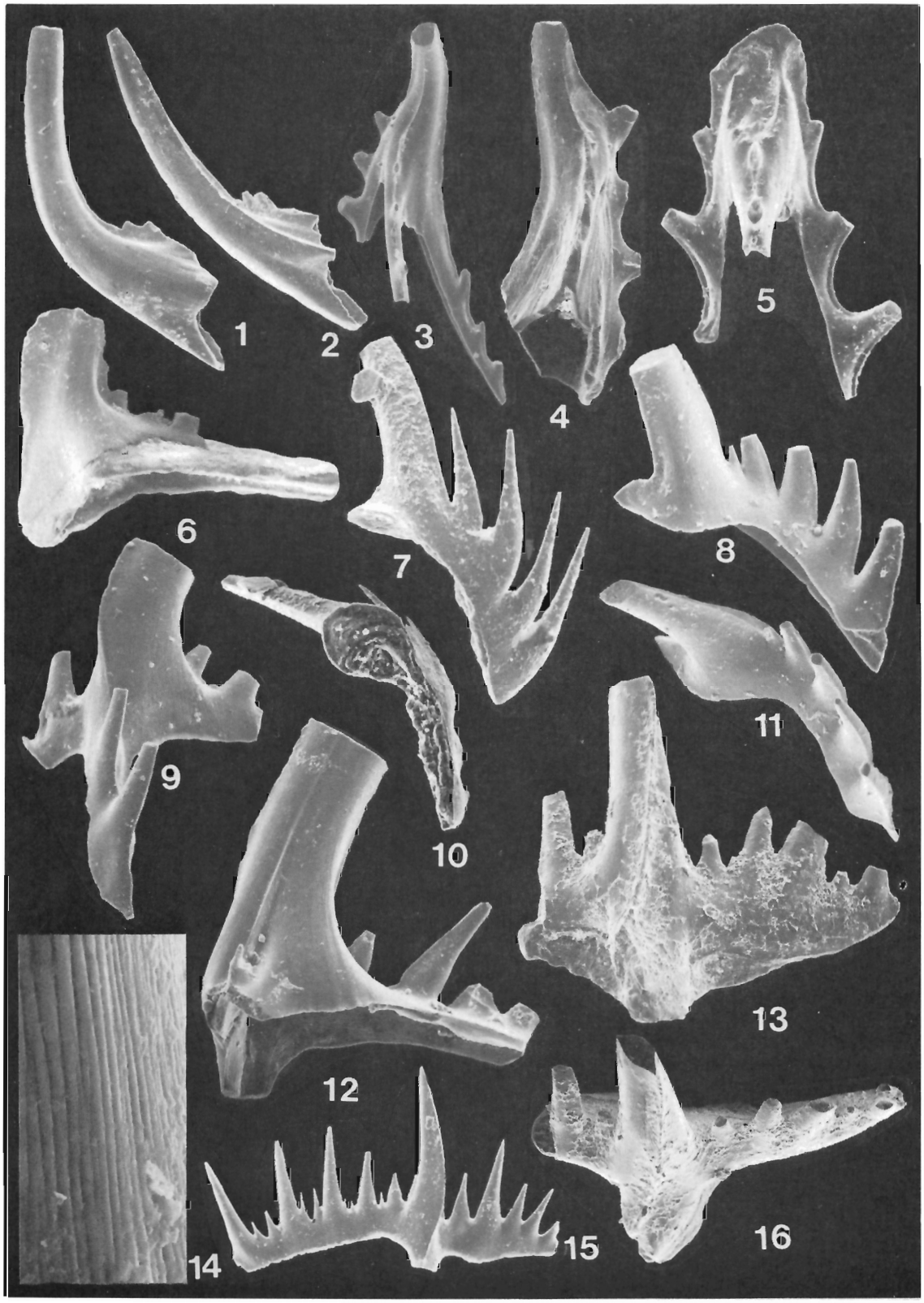
1
2
3
4
5
6
7
8
9
10
11
12
13
14
15
16

The localities and stratigraphic position of the type specimens, all from the six members of the Ellis Bay Formation (Bolton, 1972) (except hypotypes, which are from the Matapedia Group, Gaspé) are as follows. Samples E02, E06, E07 (all from Member 1), and E09 (Member 2) are from 9.3 m, 1 m, 0.7 m below, and 2.7 m above the base of Member 2, respectively, at the Junction Cliff section. Samples E16, E26 (both from Member 3), E32, E34, E36 (all from Member 4), and E44 (Member 6) are from the West Cliff section on the west side of Ellis Bay. Sample E16 is from 4 m above the base of Member 3; E26, E32, E34, and E36 are from 3.5 m below, 4.5 m, 11.5 m, and 15.5 m above the upper boundary of Member 3, respectively. Sample E44 is from 1.5 m above the base of Member 6. Sample V12 (Member 2?) is from the Vauréal River section, 20.5 m below the bioherms of Member 4. Samples S21 and S25 are from the Natural Bridge section on Salmon River, 1 m above and 0.6 m below the lower and upper boundaries of Member 5, respectively. The two specimens from the Matapedia Group were collected on Highway 132, 5 km west of Matapedia, Québec (GSC Locality 96052).

GAMACHIGNATHUS HASTATUS n. sp.

Plate 10.2, figures 1-16

Etymology. From the Latin "hastatus" meaning "armed with a spear", in reference to the shape of the cusp and denticles.

Diagnosis. A species of **Gamachignathus** in which cusp and denticles are long and slender with subcircular cross-section. Posterior process of elements has hindeodellid style of denticulation, which may be overgrown. In large specimens, keislognathiform (b) and hibbardelliform (c) elements have lateral costae on cusp. Falodiform (e-2) element has weakly developed, adenticulate posterior process but has curved, denticulated anterior process. Anterior process of prioniodiform (f) element is similar to that of falodiform element. Anterior edge of cusp on modified, blade-like, prioniodiform (g) element extends to lateral process. This element has gap between proximal anterior process denticle and cusp.

Description. Elements are similar to those of **G. ensifer** n. sp. but differ in that cusp and denticles are long and narrow. Cusp cross-section is subcircular basally and is only slightly laterally compressed distally. Posterior face of cusp of all ramiform complex (first transition series) elements has shallow groove at proximal end. Denticulation of posterior process is of hindeodellid style although subdued in some specimens. Denticles are longer, narrower, and more subcircular, and base of element is generally lower than in elements of **G. ensifer**. White matter occurs in cusp and denticles. Presence of striations is same as for **G. ensifer**. Differences between individual elements and comparable elements of **G. ensifer** are as follows.

Cordylodiform (a-1) and gothodiform (a-2) elements: Cusp is more proclined and anticusp is more reclined than representatives of **G. ensifer**. Gothodiform element differs form same element of **G. ensifer** in that ridge on base is more posteriorly situated and antero-lateral face of anticusp is convex.

Keislognathiform (b) element: Cusp has lateral costae that extend along its length to base of denticles on lateral processes. These denticles are widely separated. Larger, more asymmetrical forms have pronounced lateral twist and flexure of cusp and anterior portion of element, respectively. On such forms, white matter boundary is above proximal denticle of both lateral processes resulting in oblique boundary. Extensive basal sheathing is present on larger forms.

Hibbardelliform (c) element: Element is symmetrical with cusp ornamentation, denticulation and white matter distribution similar to keislognathiform element. Proximal denticles of lateral processes are commonly present as small nodes. Posterior process is straight.

Cyrtoniodiform (e-1) and falodiform (e-2) elements: Cyrtoniodiform element differs from equivalent element of **G. ensifer** in that basal flare is more broadly convex. Falodiform element is not known to have as variable a basal flare.

Prioniodiform (f) element: Cusp has anterior and posterior costae that extend for its full length. Anterior costa extends to anterior process and has sharp lateral inflection at base of cusp. Inner face has costa that extends to base of denticles on lateral process; costa diminishes distally. Denticles are long, narrow, and triangular. Hindeodellid style of denticulation on processes, if present, is not preserved.

Modified, blade-like, prioniodiform (g) element: Element is known only from small and medium sized specimens; if large specimens do occur, they are indistinguishable from those of **G. ensifer**. The differences between the smaller elements of **G. hastatus** and those of similar size in **G. ensifer** include the following. Cusp is long, narrow, ellipsoidal in cross-section with anterior and posterior costae. Denticles are long, triangular, confluent only at bases on anterior process; posterior process has hindeodellid style of denticulation. Anterior costae of cusp extends to inverted V-shaped excavation in aboral margin of base (i.e. broken process or narrow flare). Basal cavity is shallow, widely excavated and flared on inner lateral face immediately posterior to cusp.

Remarks. The keislognathiform and hibbardelliform (b and c) elements of **G. hastatus** n. sp. are similar to **"Trichonodella asymmetrica** (Knüpfer)" s.f. as illustrated by Thompson and Satterfield (1975). Both of the above elements of **G. hastatus** have narrowly diverging lateral processes with nearly erect denticles. They also have an anterior face of the cusp and lateral processes that are planar. **"T. asymmetrica"** s.f. differs in that the denticles on the lateral processes are more inclined towards the cusp, the cusp ornamentation is more subdued and the proximal ends of the lateral processes are more anterior than is the base of the cusp.

The other elements of **G. hastatus** are similar in general morphology to those of **G. ensifer** n. sp. and thus cannot be compared with other form species. Both f and g elements of **G. hastatus** also differ from **"Prioniodus ferrarius** Knüpfer" s.f. and **P. girardeauensis** Satterfield s.f. in that the cusp and denticles are long and narrow rather than short and robust.

Material. Elements from the Ellis Bay Formation: cordylodiform (a-1) – 52; gothodiform (a-2) – 1; keislognathiform (b) – 149; hibbardelliform (c) – 19; cyrtoniodiform (e-1) – 45; falodiform (e-2) – 26; prioniodiform (f) – 91; modified prioniodiform (g) – 45. A single element has been recovered from the Vauréal Formation by Nowlan and Barnes.

Types. Type numbers are followed by sample numbers in parentheses. Figured holotype GSC 60084 (S21); figured paratypes, GSC 60073 (S21), 60075 (V12), 60076 (E36), 60077 (E06), 60078 (E36), 60079 (E36), 60080 (E02), 60082 (E16), 60083 (E36), 60085 (E36), 60087 (E26), 60799 (S25); unfigured paratypes, GSC 60074 (E36), 60081 (E09), 60086 (E02).

The geographic and stratigraphic location of samples is given under **G. ensifer.**

ACKNOWLEDGMENTS

C.R. Barnes and G.S. Nowlan gratefully acknowledge financial support, through operating grants and post-doctoral scholarship respectively, for this study from the National Research Council of Canada. The collection of samples from Anticosti Island was made possible through co-operation of the following: P. Levac, Governor of Anticosti Island; N. Renière, Bureau de l'Intendant, Anticosti; A.A. Petryk, A.H. Sikander, and P.O. Simard of the Direction Générale de l'Energie, Ministère des Richesses Naturelles, Québec; and T.E. Bolton of the Geological Survey of Canada. A.D. McCracken acknowledges financial support from N.R.C. operating grants of A.C. Lenz, University of Western Ontario, London, Ontario and J.A. Legault, University of Waterloo, Waterloo, Ontario for field support in the northern Yukon. D.J. Kennedy, University of Waterloo, kindly provided conodont samples from the Edgewood Group in Missouri. The SEM photographs were taken by D. Walker, Geological Survey of Canada, Ottawa. M. Maziarz of the University of Waterloo drafted the figure.

An earlier draft of this paper was critically read by S.M. Bergstrom, Ohio State University and C.B. Rexroad, Indiana Geological Survey.

REFERENCES

Alcock, F.J.
1935: Geology of the Chaleur Bay region; Geological Survey of Canada, Memoir 183.

Allen, P.
1975: Ordovician glacials of the central Sahara; in Ice Ages: Ancient and Modern; A.E. Wright and F. Moseley, ed. Geological Journal Special Issue No. 6, p. 275-285.

Barnes, C.R., Kennedy, D.J., McCracken, A.D., Nowlan, G.S., and Tarrant, G.A.
1979: The structure and evolution of Ordovician conodont apparatuses; Lethaia, v. 12, p. 125-151.

Bergström, S.M.
1971: Conodont biostratigraphy of the Middle and Upper Ordovician of Europe and eastern North America; Geological Society of America, Memoir 127, p. 83-161.

Beuf, S. and Biju-Duval, B.
1966: Ampleur des glaciations 'Siluriens' au Sahara; Institut Français du Pétrole, Revue, v. 21, p. 363-381.

Bolton, T.E.
1972: Geologic map and notes on the Ordovician and Silurian litho- and biostratigraphy, Anticosti Island, Québec; Geological Survey of Canada, Paper 71-19.

Fåhraeus, L.E. and Nowlan, G.S.
1978: Franconian (Late Cambrian) to Early Champlainian (Middle Ordovician) conodonts from the Cow Head Group, Western Newfoundland; Journal of Paleontology, v. 52, no. 2, p. 444-471.

Jeppsson, L.
1972: Some Silurian conodont apparatuses and possible conodont dimorphism; Geologica et Palaeontologica, v. 6, p. 51-69.

Knüpfer, J.
1967: Zur fauna und biostratigraphie des Ordoviziums (Gräfenthaler Schichten) in Thüringen; Freiberger Forschungshefte, C220 Paläontologie), 119 p.

Lespérance, P.J.
1974: The Hirnantian fauna of the Percé area (Québec) and the Ordovician-Silurian boundary; American Journal of Science, v. 274, p. 10-30.

MacKay, D.
1979: Anticosti: the untamed island; McGraw-Ryerson Ltd., 160 p.

McCracken, A.D. and Barnes, C.R.
1978: Conodont faunas across the Ordovician-Silurian boundary, Ellis Bay Formation, Anticosti Island, Québec; Geological Society of America, Abstracts with Programs, v. 10, p. 233, 234.

Conodont biostratigraphy and paleoecology of the Ellis Bay Formation, Anticosti Island, Québec; Geological Survey of Canada, Bulletin 329. (in press)

Nowlan, G.S., McCracken, A.D., and Barnes, C.R.
1979: Conodont biostratigraphy of the Vauréal and Ellis Bay formations, Anticosti Island, Québec, and its relation to the Ordovician-Silurian boundary; Geological Association of Canada, Programme with Abstracts, v. 4, p. 69.

Nowlan, G.S. and Barnes, C.R.
Late Ordovician conodonts from the Vauréal Formation, Anticosti Island, Québec; Geological Survey of Canada, Bulletin 329. (in press)

Riva, J.
1969: Middle and Upper Ordovician graptolite faunas of St. Lawrence Lowlands of Québec and of Anticosti Island; American Association of Petroleum Geologists, Memoir 12, p. 513-556.

Roliff, W.A.
1968: Oil and gas exploration – Anticosti Island, Québec; Proceedings of the Geological Association of Canada, v. 19, p. 31-36.

Ross, R.J., Jr., Nolan, T.B., and Harris, A.G.
1979: The Upper Ordovician and Silurian Hanson Creek Formation of central Nevada; United States Geological Survey, Professional Paper 1126-C.

Satterfield, I.R.
1971: Conodonts and stratigraphy of the Girardeau Limestone (Ordovician) of southeast Missouri and southwest Illinois; Journal of paleontology, v. 45, p. 265-273.

Schuchert, C. and Twenhofel, W.H.
1910: Ordovicic-Siluric section of the Mingan and Anticosti Islands, Gulf of St. Lawence; Bulletin of the Geological Society of America, v. 21, p. 677-716.

Sweet, W.C. and Bergström, S.M.
1970: The generic concept in conodont taxonomy; Proceedings of the North American Paleontological Convention, September 1969, Part C, p. 157-173.

Sweet, W.C. and Bergström, S.M. (cont.)
1976: Conodont biostratigraphy of the Middle and Upper Ordovician of the United States midcontinent; in M.G. Bassett, ed., The Ordovician System: proceedings of a Palaeontological Association symposium, Birmingham, September 1974, University of Wales Press and National Museum of Wales, Cardiff, p. 121-151.

Sweet, W.C., Ethington, R.L., and Barnes, C.R.
1971: North American Middle and Upper Ordovician conodont faunas; Geological Society of America, Memoir 127, p. 163-193.

Thompson, T.L. and Satterfield, I.R.
1975: Stratigraphy and conodont biostratigraphy of strata contiguous to the Ordovician-Silurian boundary in eastern Missouri; Missouri Geological Survey, Report of Investigations 57, Part 2, p. 61-108.

Twenhofel, W.H.
1928: Geology of Anticosti Island; Geological Survey of Canada, Memoir 154, 481 p.

Uyeno, T.T., Fåhraeus, L.E., and Barnes, C.R.
1979: Lower Silurian conodont biostratigraphy, Anticosti Island, Québec; Geological Association of Canada, Programme with Abstracts, v. 4, p. 84.

11. TWO CAMBRIAN STRATIGRAPHIC SECTIONS NEAR GATAGA RIVER, NORTHERN ROCKY MOUNTAINS, BRITISH COLUMBIA

Project 650024

W.H. Fritz
Institute of Sedimentary and Petroleum Geology, Ottawa

Fritz, W.H., Two Cambrian stratigraphic sections near Gataga River, northern Rocky Mountains, British Columbia; in Current Research, Part C, Geological Survey of Canada, Paper 80-1C, p. 113-119, 1980.

Abstract

Two new sections near the east edge of the Rocky Mountain Trench provide control between six previously studied Cambrian sections centred 40 km to the east and eight published Cambrian sections in the Kechika and Cassiar mountains (across the Trench) to the northwest. The Lower Cambrian, above a folded and faulted base, contains abundant quartzite and correlates with the Gog Group in the southern Canadian Rocky Mountains. These strata do not resemble the Atan Group of equivalent age west of the Trench. The latest Lower Cambrian, Middle Cambrian, and part of the Upper Cambrian in the sections consist of clean carbonates that probably represent large carbonate buildups similar to those comprising numerous peaks to the south (Spectre Peak, etc.). If so, the carbonate belongs to a complex of carbonate buildups in outer detrital strata that is flanked to the south (Ospika River) by shelf carbonates, to the east by inner detrital deposits, and to the west by outer detrital shale(?).

Correlation to diamictites faulted against one of the sections suggests that both are underlain by a late Proterozoic(?) succession that may contain tillites (s.l.). If tillites are indeed present, a large sub-Cambrian unconformity exists in this area, and all or nearly all of the Miette Group or its equivalent has been eroded along the eastern side of the Trench. This eastern succession provides a striking contrast when compared to the thick Miette equivalent (Ingenika Group) immediately west of the Trench. The abrupt change in late Proterozoic and Cambrian strata on either side of the Trench is attributed to major right lateral movement on the Rocky Mountain Trench Fault in post-Cambrian time.

Introduction and Acknowledgments

Numerous sections on either side of the Rocky Mountain Trench (Fig. 11.1, either side of Kechika and Finlay rivers) have been described recently (Gabrielse, 1975; Fritz, 1972, 1978, 1979a, 1980) to provide a general knowledge of Cambrian stratigraphy in north-central British Columbia. The sections west of the Trench (Fig. 11.1, sections 1C to 8C) were measured in 1977 and 1979 in conjunction with Operation Dease, which was directed to H. Gabrielse. Most of the sections east of the Trench (Fig. 11.1, 2R to 6R) were measured in 1978 in conjunction with Operation Liard, which was headed by G.C. Taylor, and the remaining sections (Fig. 11.1, 1R and two sections beyond southern border of Fig. 11.1) were measured in 1971 while assisting Operation Finlay, which was guided by H. Gabrielse.

The sections presented in this paper (Fig. 11.1, 7R, 8R) are the results of continued co-operation with Operation Dease in 1979, and assistance on the outcrop by M.E. Fortin. The sections are of importance because they are located between the two main areas of stratigraphic control and are close to the eastern edge of the Rocky Mountain Trench. The base of section 7R is at lat. 58°9'45", long. 125°57'0", and the top is at lat. 58°9'15", long. 125°57'45". The base of section 8R is lat. 57°57'45", long. 125°31'15", and the top is at lat. 57°57'45", long. 125°31'45". All map co-ordinates are given to the nearest 15 minutes.

Stratigraphic Nomenclature

No formal nomenclature is available for the Cambrian strata in the two sections, and none is contemplated until more regional control is available. In describing strata in the two sections, the oldest map unit is referred to as the "Lower Cambrian quartzite succession" and the overlying map unit to the "late Lower Cambrian to Upper Cambrian carbonate succession". Each stratigraphic unit within a succession is given a number-letter designation followed by the section number. The first number refers to the position of the stratigraphic unit above the succession's lowest exposure in the section, and the letter refers to the succession (Q=Lower Cambrian clastic succession, C=late Lower Cambrian to Upper Cambrian carbonate succession).

The Cambrian strata in section 7R were previously mapped (Taylor and Stott, 1973) as two informal and unnamed formations within the Atan Group. Reasons for discouraging the use of Atan Group east of the Rocky Mountain Trench have been stated (Fritz, 1978, p. 15; 1979a, p. 109; 1980), and will be discussed further in this paper.

Stratigraphic Section 7R

Lower Cambrian Quartzite Succession, Stratigraphic Units 1-Q7 to 4-Q7, 519+ m

The lowest exposed unit (1-Q7, 95 m^{+}) is composed of light grey to light brown weathering quartzite in thick, blocky beds. Fresh surfaces are light brown and the quartzite is mainly medium- and coarse-grained. Crossbeds located 3, 26, 27, and 28 m above the lowest outcrop indicate current directions from S10°W, S10°E, N10°E, and S30°W, respectively. **Skolithos** sp. is present in beds 1.5, 7.5, and 34 m above the lowest outcrop.

Unit 2-Q7 (68 m) contains three-fourths light brown, medium light brown, and rust weathering fine grained quartzite. The quartzite is in thin, wavy beds and fresh surfaces are light brown. Burrowed quartzite beds are present at various horizons. The remaining one-fourth of the unit is interbedded siltstone that is dark grey on weathered and fresh surfaces.

Medium grey weathering limestone in medium and thin beds predominates in unit 3-Q7 (72 m). The limestone is medium to medium dark grey on fresh surface and finely

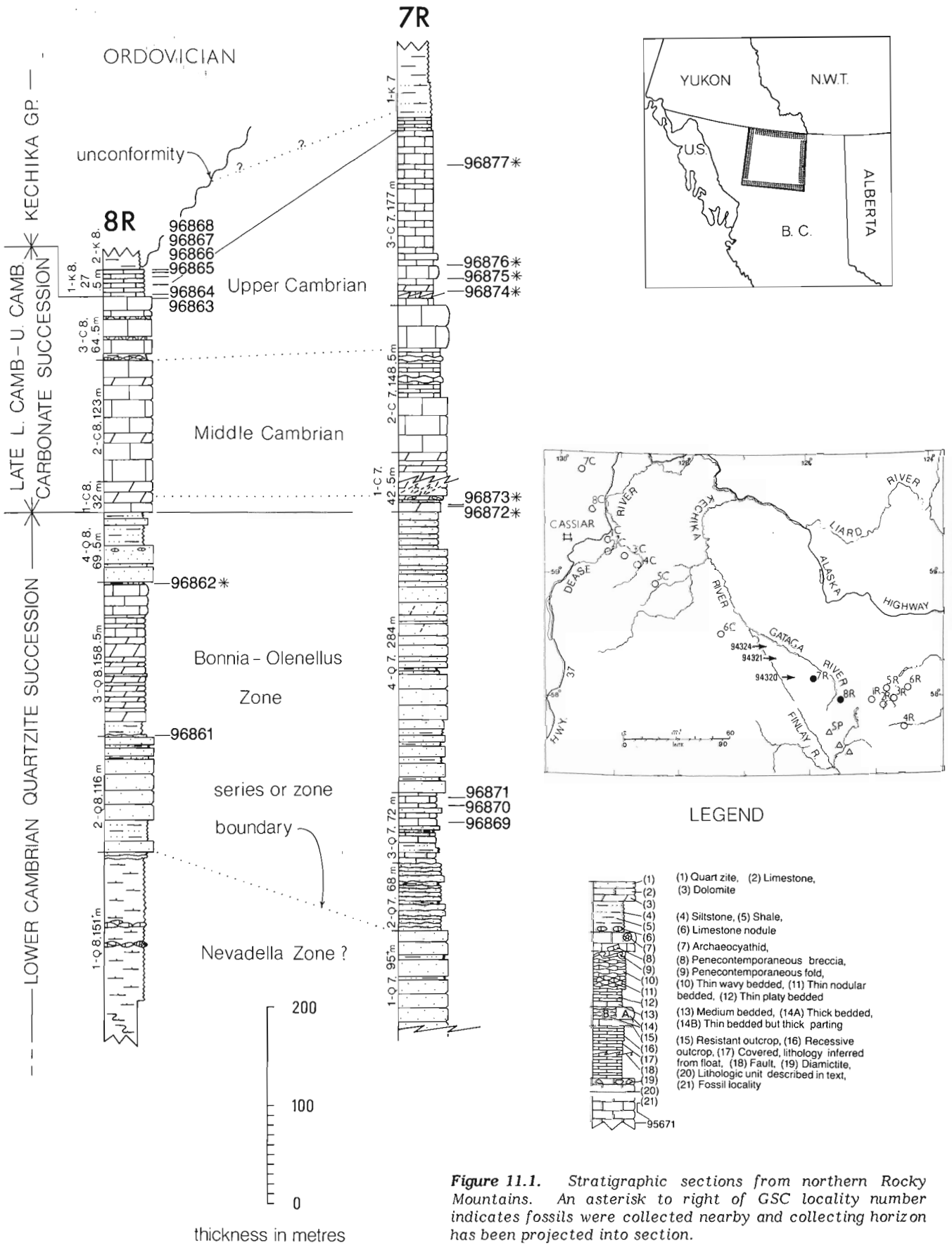

Figure 11.1. *Stratigraphic sections from northern Rocky Mountains. An asterisk to right of GSC locality number indicates fossils were collected nearby and collecting horizon has been projected into section.*

crystalline. Sparse, large (3 mm) crystals are scattered through the limestone in the lower part of the unit. Light orange to silvery weathering siltstone is present 12 to 21 m and 32 to 34.5 m above the base, and fine grained quartzite is present 34.5 to 38.5 m and 52 to 57 m above the base.

A thick unit (4-Q7, 284 m) of light brownish grey weathering and unweathered quartzite is present at the top of the Lower Cambrian quartzite succession. The quartzite is mainly thick- and medium-bedded and fine- to medium-grained. Crossbeds are abundant, and, of the 33 measured, approximately half indicate currents from either the south or south-southwest and nine indicate currents from the north or north-northwest. Some (one third) medium brownish grey weathering siltstone is present in the lower 73 m of the unit. **Skolithos** sp. is present 87.5, 148.5, and 217 m above the base.

Late Lower Cambrian to Upper Cambrian Carbonate Succession, Stratigraphic Units 1-C7 to 3-C7, 368 m

Cream weathering and fresh dolomite in thin to thick beds predominate in this basal unit (1-C7, 42.5 m) of the carbonate succession. The interval 9 to 17.5 m above the base contains thin and medium beds of quartzite (9-15 m) with possible penecontemporaneous folds, and a thick dolomite bed (15-17.5 m) containing penecontemporaneous limestone breccia. Above the breccia bed the unit is extensively fractured and faulted, but the total thickness of the unit is not inconsistent with thicknesses noted at nearby exposures. Local float from interbeds located low in this unit and near the section contain late Lower Cambrian trilobites (GSC loc. 96872, 96873). As these are rare limestone localities in an otherwise mainly barren dolomite unit, their positions are recorded on Plate 11.1, figure 4.

Unit 2-C7 (148.5 m) is composed of medium light grey weathering and fresh limestone in thick to massive beds (0-56 m, 106.5 to 148.5 m) and in thick to thin beds (56 to 106.5 m). Limestone in the thick to massive beds is finely crystalline and in the thin and medium beds it is fine- to coarse-grained.

The succeeding unit (3-C7, 177 m) contains limestone similar to that present in the middle of the underlying unit (2-C7, 56 to 106.5 m interval). Because the limestone in unit 3-C7 is thin- to thick-bedded and lacks the massive beds present in the lower and upper parts of unit 2-C7, it is less resistant and at section 7R the exposures are only fair. Better exposures of unit 3-C7 were inspected northwest of the section (Pl. 11.1, fig. 3). There the thick beds form light grey, discontinuous ribs between talus covered intervals underlain by thin and medium bedded limestone. While inspecting these beds, GSC localities 96874 to 96877 were collected on the first ridge northwest of section 7R. These collecting horizons are projected into section 7R in Figure 11.1.

Lower Kechika Group

This group underlies the more subdued topography at the top of section 7R. The basal 13 m consists of medium blue grey weathering limestone that weathers to thin plates with bright orange partings. Fresh limestone surfaces are dark grey and finely crystalline. The limestone is overlain by 21 m of light yellow brown weathering siltstone that is medium light grey and slightly limy. Overlying the siltstone is an unmeasured succession of medium light grey weathering, silvery shale that is soft and is medium grey on fresh surface. The basal 14.5 m of this shale is interbedded with siltstone (one-half) similar to that in the beds immediately below.

Stratigraphic Section 8R

Lower Cambrian Quartzite Succession, Stratigraphic Units 1-Q8 to 4-Q8, 495+ m

Unit 1-Q8 (151^{+} m) is exposed in a highly folded core of an anticline. The unit is composed of silvery light brown weathering shale of which the upper, least disturbed 151 m was measured. Below the base of the measured section (below point "a", Pl. 11.1, fig. 6), the unit contains some thick beds of light grey weathering and fresh limestone with archaeocyathids. Similar limestone in small (11 cm x 25 cm) pods is present 54 m and 74 m above the base of the section. Archaeocyathids are also present in the 54 m pod horizon. Orange brown weathering, fine grained sandstone occupies the upper 6 m of the unit.

Unit 2-Q8 (116 m) contains cream to light orange weathering and fresh quartzite in thick beds. Crossbeds are common (Pl. 11.1, fig. 2) and the quartzite is fine- to coarse-grained. Of the 19 crossbeds measured in the interval 38 to 90 m above the base, most (14) indicate currents from the southwest. Interval 11 to 32 m and one-sixth of interval 93 to 116 m contains siltstone. **Skolithos** sp. is present 84 m and 90 m above the base.

Cream and light grey weathering dolomite predominates in unit 3-Q8 (158.5 m). The dolomite is in thin to thick beds and is finely crystalline. Brownish grey and orange weathering siltstone occupies the basal 16 m of the unit, and light grey weathering and fresh limestone in thick beds is present in the upper 34 m.

The uppermost unit (4-Q8, 69.5 m) in the Lower Cambrian quartzite succession is composed of quartzite and siltstone. Resistant light brown weathering and fresh quartzite in thick beds occupies the lower (0-37 m) part of the unit. The quartzite is fine- and medium-grained and contains some limestone pods in the top 1.5 m. The upper part of the unit (37-69.5 m) is composed of light brownish grey to light greenish grey weathering very fine grained sandstone and siltstone that are light greenish grey on fresh surfaces. Bedding in the upper part is thin to very thin except for some medium and thick beds of very fine grained quartzite.

Late Lower Cambrian to Upper Cambrian Carbonate Succession, Stratigraphic Units 1-C8 to 3-C8, 219.5 m

The basal unit (1-C8, 32 m) in this succession is mainly composed of cream weathering and fresh dolomite in thick beds. Medium light grey limestone (0-9.5 m) is present in the lower part of the unit. The limestone and the overlying dolomite are finely crystalline, and both are planar laminated.

Unit 2-C8 (123 m) contains light grey weathering and unweathered limestone in thick beds. The beds exhibit irregular laminae that parallels the parting surfaces, and the limestone is finely crystalline. Some (5 per cent) cream weathering and fresh dolomite is present in medium and thick interbeds.

The highest unit (3-C8, 64.5 m) consists of medium light grey weathering and unweathered limestone in thick beds. The limestone is marked by laminae similar to those in the unit below, and fresh limestone surfaces are dense. A subordinate amount (10 per cent) of olive grey shale containing limestone nodules is interbedded with the limestone.

Lower Kechika Group

The basal unit (1-K8, 27.5 m) of the Kechika Group is composed of medium grey, thin bedded limestone that weathers to plates with orange, pink, or medium grey parting surfaces. The limestone is planar laminated and fresh surfaces are dark grey and finely crystalline.

The next overlying unit (2-K8, unmeasured) consists of light brownish grey weathering shale that is light grey on fresh surface.

Late Proterozoic Strata

East of section 8R, and faulted against the anticline upon which the section is located, are unmeasured strata that correlate with the diamictite-bearing succession directly underlying the Cambrian in section 1R and 2R (Fritz, 1979a, p. 108, Fig. 13.2). A stream that originates in a cirque (Pl. 11.1, fig. 6) immediately south of section 8R exposes the diamictite-bearing map unit 0.5 km east of the section for a distance of 1 km along its banks (Pl. 11.1, fig. 5). It is estimated that diamictite and quartzite in thick, irregular interbeds comprises 30 per cent of the succession, and the remaining 70 per cent is composed of shale. Prominent clasts in the diamictite are composed of medium grey limestone that is dark grey on fresh surface and is finely crystalline. These clasts average 6 cm in diameter and weather in relief above a medium brown weathering mudstone matrix that is dark grey on fresh surface and slightly limy. The quartzite is composed of fine to coarse quartz grains that are light brown on both weathered and unweathered surfaces. The shale is recessive and outcrops at numerous stream cuts where fresh surfaces are black; slightly weathered surfaces exhibit a faint iridescent sheen. Moderately weathered shale is a bright rust colour, and flakes of shale (local float) that have undergone still more weathering are medium dark grey.

Age of Gataga River Sections

All of the fossils from in and just above the Lower Cambrian quartzite succession in sections 7R and 8R belong to the late Lower Cambrian **Bonnia-Olenellus** Zone. The older collections (GSC loc. 96869 to 96871, 96861) contain **Olenellus,** a genus that ranges through the zone. GSC locality 96862 contains **Proleostracus,** sp. indicating a medial position within the zone. The collections from just above the Lower Cambrian quartzite succession (GSC loc. 96872, 96873) contain a latest Lower Cambrian assemblage that includes **Bonnia** sp., **Goldfieldia**? sp., **Ogygopsis batis**? Walcott, **Olenoides**? sp., **Syspacephalus** sp., and **Zacanthopsis** sp.

Except for GSC localities 96872 and 96873, strata in the lower and middle part of the late Lower to Upper Cambrian carbonate succession in section 7R and 8R are barren. A collection (GSC loc. 96863) near the top of the succession in section 8R contains **Acmarhachis** sp., **Comanchia**? sp. and **Olenaspella** sp., and is tentatively placed high in the Dresbachian Stage (early Upper Cambrian). Collections from the upper part of the succession in section 7R (GSC loc. 96874 to 96877) contain **Plethometopus** sp., and the lowest of these collections (GSC loc. 96874) also contains **Euptychaspis**? sp. These collections belong to the late Upper Cambrian Trempealeauan Stage.

Fossils from the lower Kechika Group in section 8R (GSC loc. 96864 to 96868) belong to the Dresbachian and Franconian stages of the Upper Cambrian. GSC location 96864 contains **Glyptagnostus**? sp. and **Stenambon**? sp., GSC location 96865 contains unidentified trilobite fragments and GSC locality 96866 contains **Cernuolimbus**? sp., **Pseudagnostus**? sp., and **Tholifrons**? sp. and are placed in the Dresbachian Stage. GSC location 96867 (trilobite fragments) and GSC location 96968 containing **Brabbia**? sp. and **Hungaia**? sp. are placed in the Franconian Stage.

Two nearby sections provide some insight as to the thickness of the incomplete Lower Cambrian quartzite succession in sections 7R and 8R, and to the age of strata in intervals that have thus far proved barren. One of the nearby sections (Fig. 11.1, section 1R; Gabrielse, 1975, section 1; Fritz, 1979a, section 1) is located 27 km east of section 8R and a short distance northwest of Mount Lloyd George. The second (Fig. 11.1, section 2R; Fritz, 1979a, section 2) is located 37 km east of section 8R near Mount Smythe. A comparison of the Lower Cambrian quartzite succession in the present sections with that in the nearby sections suggests

Plate 11.1 (opposite)

Figure 1. View looking south at Cambrian strata in section 7R. Lower Cambrian quartzite succession is between points "a" and "d"; carbonate unit (3-Q7) within succession is between points "b" and "c". Late Lower Cambrian to Upper carbonate succession is between points "d" and "e". Composite of GSC photos 203474-C, 203474-D.

2. Crossbedding in fine- to coarse-grained sandstone, Lower Cambrian quartzite succession, section 8R, unit 2-Q8, 228 m above base of section (above "a" in fig. 6).
GSC photo 203474-A.

3. View looking northwest at late Lower Cambrian to Upper Cambrian carbonate succession, location is along strike and 2 km northwest of section 7R. Medium light grey ribs are thick beds and lenses of finely crystalline limestone, recessive intervals are underlain by thin and medium beds of fine- to coarse-grained limestone. GSC photo 203474-E.

4. View looking west at late Lower Cambrian to Upper Cambrian carbonate succession, first ridge northwest of section 7R. Latest Lower Cambrian GSC fossil localities 96872 and 96873 are approximately located at "a". Localities are in local float 5 m (96872) and 7 m (96873) above the base of the late Lower Cambrian to Upper Cambrian carbonate succession. GSC photo 203474-B.

5. View looking north at late Precambrian diamictite-bearing succession 0.5 km west of section 8R. Black shale is exposed at "a", resistant interbeds of diamictite and quartzite are at "b" and "c". GSC photo 203474-T.

6. View looking northwest at Cambrian strata in section 8R. Lower Cambrian quartzite succession is between points "a" and "d"; carbonate unit 3-Q8 within succession is between points "b" and "c". Most of late Lower Cambrian to Upper Cambrian succession is between points "d" and "e" (top of succession is short distance behind ridge crest at "e"). Archaeocyathids are present in limestone interbeds below base of section at "f". GSC fossil locality 96861 is 0.25 m above contact between units 2-Q8 and 3-Q8 at "b". GSC photo 203474-S.


d
c
b
a
e
1


2


3

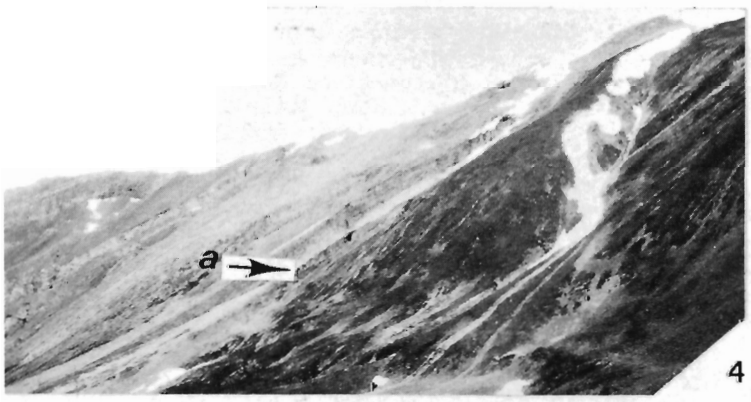
a
4

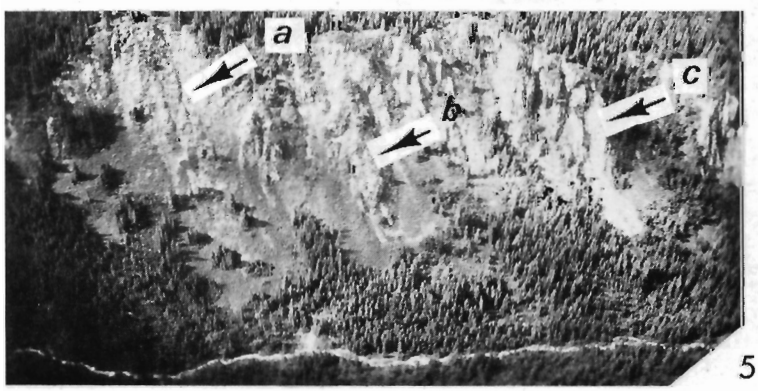
a
b
c
5

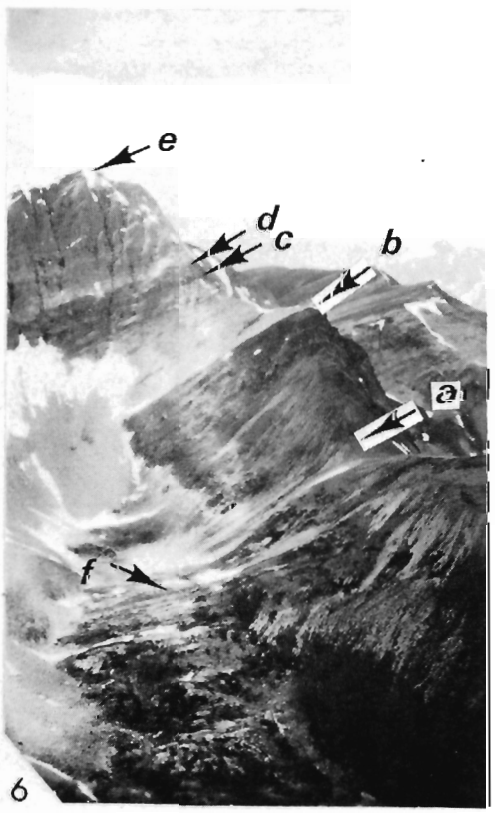
e
d
c
b
a
f
6

the thickness of the Lower Cambrian in sections 7R and 8R should be in the order of twice (600 m) that exposed. A lithological correlation between the Mount Lloyd George (1R) section and section 8R indicates the mentioned archaeocythid-bearing shale located below the base of section 8R (below point "a", Pl. 11.1, fig. 6) belongs to the **Nevadella** Zone.

A comparison of the late Lower Cambrian to Upper Cambrian carbonate succession in sections 7R and 8R with that in the nearby sections 1R and 2R (Fritz, 1979a, section 1, unit 9 and section 2, unit 7) suggests that only a minor thickness of the succession in sections 7R and 8R belongs to the Lower Cambrian. A considerable thickness in sections 7R and 8R probably belongs to the Middle Cambrian, and the Middle and Upper Cambrian carbonate in sections 7R and 8R can be presumed to interfinger laterally to the east with shale and siltstone of that age in the mentioned nearby sections.

Reference to isolated fossil localities nearby provides additional insight as to the age and interpretation of barren strata in sections 7R and 8R. Three collections (GSC loc. 94320, 94321, 94324) of Middle Cambrian fossils submitted by H. Gabrielse in 1976 from west and northwest of section 7R (Fig. 11.1, between Kechika and Gataga rivers) contain Middle Cambrian fossils, and thus support the assumption that a considerable part of the late Lower to Upper Cambrian carbonate succession belongs to the Middle Cambrian.

Middle Cambrian fossils are also present in large carbonate buildups 31 km south of section 8R. Spectre Peak (Fig. 11.1, SP; Fritz, 1979a, Pl. 13.3, fig. 6) is formed of one of several large carbonate buildups that are aligned in a northwesterly direction and surrounded by dark shale. Fossils from the Spectre Peak carbonate buildup (GSC loc. 95646, 95647) belong to the **Bathyuriscus-Elrathina** Zone (?) and to the **Bolaspidella** Zone (Fritz, 1979a, p. 108).

A latest Lower Cambrian trilobite and archaeocyathid collection (GSC loc. 70472) located 55 km north of section 7R is anomalous when compared with data from the present sections. The collection was submitted by G.C. Taylor from a locality on the north side of the West Toad River (lat. 58°39'30", long. 125°52'39"). The writer (Fritz, 1967) tentatively assigned the trilobites to the latest Lower Cambrian and noted that the archaeocyathids were not from the same horizon because they were contained in a different rock type. It should be added here that no archaeocyathids are known to be associated with trilobites that young in the North American Cordillera. Taylor and Stott (1973, p. 16) reported the trilobites and archaeocyathids as part of a single collection, however, and showed the archaeocyathids to extend into still younger rocks (op. cit., Fig. 1).

The location of the same latest Lower Cambrian trilobite fauna in section 7R (GSC loc. 96872, 96873) provides an opportunity to assess this fauna relative to other fossils in a continuous section. In section 7R no archaeocyathids were seen with the trilobites and none were seen in younger strata. Equivalent strata in section 8R are also barren of archaeocyathids. The only ones seen are in unit 1-Q8, which is far below the West Toad River trilobite level. These findings suggest that the archaeocyathid ranges given by Taylor and Stott may reflect a tectonic position in which the older ones were faulted against and above the latest Lower Cambrian trilobites at the West Toad River locality. The belief that the high archaeocyathids position was stratigraphic rather than tectonic may have been responsible for the correlation (Taylor and Stott, 1973, p. 14) of strata that are here assigned to the late Lower Cambrian to Upper Cambrian carbonate succession to the older, archaeocyathid-bearing Atan Group in the Cassiar Mountains.

Correlation

The Lower Cambrian quartzite succession in section 7R and 8R is not fully exposed, but correlation with nearby sections 1R and 2R provides information on the remaining strata and demonstrates the close resemblance in both age and lithology to the Gog Group of the southern Canadian Rocky Mountains. Illustration of Gog sections (Fritz, 1980) near Mount Robson, northeast of Williston Lake, and near Mount Lloyd George (section 1R) provides evidence that there may be physical continuity of the Gog into the northern Rocky Mountains. Fossils from the succession in sections 7R and 8R provide an age correlation with the carbonate Rosella Formation (upper Atan Group) in the Cassiar Mountains and the carbonate and siltstone Sekwi Formation in the Mackenzie Mountains.

The late Lower Cambrian to Upper Cambrian carbonate succession in sections 7R and 8R is believed to belong to large carbonate bodies (possibly bioherms or patch reefs surrounded by outer detrital clastics. The clean carbonate in these sections resembles that in other large bioherms nearby (i.e. Spectre Peak), while laterally equivalent strata in sections 1R to 4R belong mainly to the outer detrital facies. The complex of "bioherms" and outer detrital strata extends southward to Pesika Creek (Gabrielse, 1975, Fig. 3, section 2) and then changes facies in the Middle Cambrian at Ospika River (loc. cit., sections 3 to 5) to the middle carbonate facies. The Upper Cambrian changes into the middle carbonate facies a considerable distance farther south. The carbonate in section 7R is equivalent in age to the Hota (=Peyto) Formation through Lynx Group in the high Rocky Mountains. To the east, Middle Cambrian strata in the complex (sections 1R to 4R) changes laterally within a short distance to inner detrital strata (sections 5R, 6R). To the west, it can be assumed that the outer detrital strata does not contain "bioherms" because of a deeper water environment.

The younger age of the late Lower Cambrian to Upper Cambrian carbonate succession in sections 7R and 8R indicate that a physical continuity is unlikely between the northern Rocky Mountain strata and the older, clean platform carbonates composing the Rosella Formation (upper Atan Group) in the Cassiar Mountains. Formations in the Mackenzie Mountains that correlate with this succession in section 7 are part of the uppermost Sekwi Formation (Sekwi upper contact is diachronous), the Rockslide Formation, and parts of the Rabbitkettle and Broken Skull formations. If one accepts the supposition that the succession in sections 7R and 8R represents one of many bioherms within an outer detrital slope complex, then there is close similarity between this complex and the Rockslide Formation, with the exception that Rockslide bioherms are much smaller (Fritz, 1979b, Pl. 15.1, fig. 6).

Although the basal Cambrian contact is not exposed at sections 7R and 8R, correlation with sections 1R and 2R indicates an unconformity exists between the Cambrian and the diamictite-bearing succession exposed a short distance east of section 8. The writer (Fritz, 1972, p. 211) has suggested that the diamictite may be a tillite (s.l.), and, if so, the succession belongs to a late Precambrian glacial and glacial marine deposit that can be traced throughout the Cordillera (Stewart, 1972). From the United States (Park and Cannon, 1943) the tillite is next seen in the nearby Columbia Mountains (Little, 1960) and again near Monkman Pass (Slind and Perkins, 1966; Stelck et al., 1978). The present occurrence is midway between the Monkman Pass tillite and tillite exposures in the Mackenzie Mountains (Eisbacher, 1978). From the Mackenzie Mountains the tillite is next exposed northward into the Wernecke Mountains and possibly westward into Alaska (Yeo, 1980). If the tillite correlation is applied in the present area, it follows that all, or nearly all of

the Miette Group or equivalent strata were eroded before Cambrian time. The thin late Precambrian succession, be it tillite or otherwise, presents a striking contrast when compared to the thousands of metres of late Precambrian strata (Ingenika Group) that occupy a position between the tillite level and the base of the Cambrian immediately west of the Rocky Mountain Trench (Mansy and Gabrielse, 1978). This abrupt thickness change is attributed to a 400 to 450 km right lateral displacement along the Tintina-Rocky Mountain Trench Fault (Read, 1980, Fig. 3; Tempelman-Kluit, 1979, Fig. 17, Fig. 21).

An alternate age for the diamictite-bearing succession has been offered by Taylor and others (1979, p. 227), who state that the diamictite "could be of Early Cambrian age". This seems unlikely because of the angular relationship between the white (basal?) Cambrian quartzite and the diamictite at section 2R (Fritz, 1979a, Pl. 13.1, fig. 1), because diamictites of this type are not known to the writer in the Lower Cambrian elsewhere, and because no trace fossils have been found in the diamictite-bearing succession near section 8R or at sections 1R and 2R.

References

Eisbacher, G.H.
1978: Re-definition and subdivision of the Rapitan Group, Mackenzie Mountains; Geological Survey of Canada, Paper 77-35.

Fritz, W.H.
1967: Geological Survey of Canada internal paleontology report, number C4-1967-WHF.

1972: Cambrian biostratigraphy, western Rocky Mountains, British Columbia (83 E, 94 C, 94 F); in Report of Activities, Part A, Geological Survey of Canada, Paper 72-1A, p. 209-211.

1978: Upper (carbonate) part of Atan Group, Lower Cambrian, north-central British Columbia; in Current Research, Part A, Geological Survey of Canada, Paper 78-1A, p. 7-16.

1979a: Cambrian stratigraphy in the northern Rocky Mountains, British Columbia; in Current Research, Part B, Geological Survey of Canada, Paper 79-1B, p. 99-109.

1979b: Cambrian stratigraphic section between South Nahanni and Broken Skull rivers, southern Mackenzie Mountains; in Current Research, Geological Survey of Canada, Paper 79-1B, p. 121-125.

1980: Two new formations in the Lower Cambrian Atan Group, Cassiar Mountains, north-central British Columbia; in Current Research, Part B, Geological Survey of Canada, Paper 80-1B, p. 219-225.

Gabrielse, H.
1975: Geology of Fort Grahame, east half map area, British Columbia; Geological Survey of Canada, Paper 75-33.

Little, H.W.
1960: Nelson map area, west half, British Columbia; Geological Survey of Canada, Memoir 308.

Mansy, J.L. and Gabrielse, H.
1978: Stratigraphy, terminology and correlation of Upper Proterozoic rocks in Omineca and Cassiar Mountains, north-central British Columbia; Geological Survey of Canada, Paper 77-19.

Park, C.F. Jr. and Cannon, R.S. Jr.
1943: Geology and ore deposits of the Metaline Quadrangle, Washington; U.S. Geological Survey, Professional Paper 202.

Read, B.C.
1980: Lower Cambrian archaeocyathid buildups, Pelly Mountains, Yukon; Geological Survey of Canada, Paper 78-18.

Slind, O.L. and Perkins, G.D.
1966: Lower Paleozoic and Proterozoic sediments of the Rocky Mountains between Jasper, Alberta and Pine River, British Columbia; Bulletin of Canadian Petroleum Geology, v. 14, no. 4, p. 442-468.

Stelck, C.R., Burwash, R.A., and Stelck, D.R.
1978: The Vreeland High: a Cordilleran expression of the Peace River Arch; Bulletin of Canadian Petroleum Geology, v. 26, no. 1, p. 87-104.

Stewart, J.H.
1972: Initial deposits in the Cordilleran Geosyncline: evidence of a late Precambrian (<850 m.y.) continental separation; Geological Society of America Bulletin, v. 83, p. 1345-1360.

Taylor, G.C. and Stott, D.F.
1973: Tuchodi Lakes map-area, British Columbia; Geological Survey of Canada, Memoir 373.

Taylor, G.C., Cecile, M.P., Jefferson, C.W., and Norford, B.S.
1979: Stratigraphy of Ware (east half) map area, north-eastern British Columbia; in Current Research, Part A, Geological Survey of Canada, Paper 79-1A, p. 227-231.

Tempelman-Kluit, D.J.
1979: Transported cataclasite, ophiolite and granodiorite in Yukon: evidence of arc-continent collision; Geological Survey of Canada, Paper 79-14.

Yeo, G.M.
1980: The late Proterozoic Rapitan glaciation in the northern Cordillera; Geological Association of Canada, Program with Abstracts, v. 5, p. 88.

12. SURFICIAL GEOLOGY: PAPINEAUVILLE-WAKEFIELD REGION, QUÉBEC

Project 740068

S.H. Richard
Terrain Sciences Division

Richard, S.H., Surficial geology: Papineauville-Wakefield region, Québec; in Current Research Part C, Geological Survey of Canada, Paper 80-1C, p. 121-128, 1980.

Abstract

Pitted outwash valley trains found at and above the marine limit in all the main valleys of the Laurentian Highlands within the study area may be part of the St. Narcisse moraine system.

New radiocarbon dates relating to the deglaciation chronology and the marine limit of the western Champlain Sea along the northern rim of the basin show that ice retreat from the Laurentian Highlands between Montreal and Ottawa was not a synchronous event but rather that the western part of this area was deglaciated and inundated by the Champlain Sea earlier than the eastern part between Lachute and Montebello. A ^{14}C date of 10 100 ± 130 years (GSC-2189) for shells from the lowest marine beach of the Champlain Sea north of Ottawa River relates to the last stand of the sea.

Introduction

Preliminary results of field work on the Quaternary deposits and terrain features of the Buckingham map area (National Topographic System 31 G/NW) are presented here. Field investigations were carried out during the summer and fall of 1978; geological data were obtained by systematic road traversing and examination of all accessible exposures through Quaternary sediments.

Previous Work

Studies of the bedrock geology and mineral resources of parts of the study area were carried out by Wilson (1924), Faessler (1948), Mauffette (1949a, b), Béland (1954), and Hogarth (1962, 1970). Wilson (1946) incorporated earlier works on the bedrock geology of the Ottawa and St. Lawrence lowlands. The most recent compilation of bedrock geology is provided by Douglas (1978). Investigations and mapping of the surficial geology of parts of the Buckingham map area were carried out by Antevs (1925, 1928), Buckley (1968, 1970), Gadd (1973, 1976), Lajoie (1974), Romanelli (1975a, b), Rust and Romanelli (1975), Fransham et al. (1976a, b), Richard (1976b, c), Vincent (1976a, b), and Taylor (1979). The soils of Papineau, Hull and Gatineau counties were mapped by Lajoie (1962, 1967).

Distribution and Chronology of Quaternary Sediments

Unconsolidated Quaternary sediments of Papineauville-Wakefield region (Fig. 12.1) consist mainly of glacial and ice-marginal glaciofluvial deposits abandoned by the Laurentide Ice Sheet and of marine sediments deposited during submergence of low parts of the area by the Champlain Sea. Six new radiocarbon dates on marine shells recovered from some of the highest and oldest of these sediments relate to the deglaciation chronology for the area and the first penetration of marine waters into the western Champlain Sea along the northern rim of the basin. One ^{14}C date on marine shells recovered from the lowest and youngest marine beach of the Champlain Sea north of Ottawa River relates to the last stand of the Champlain Sea in the lowland.

Surficial Geology

Most unconsolidated Quaternary deposits in the Buckingham map area are found in Ottawa Valley and in its tributary valleys from the north. Throughout the Precambrian basement uplands bedrock outcrops in the form of bare hilly knobs and ridges and numerous small basins filled by lakes and bogs. Figure 12.1 shows the general area discussed in this report.

Till Deposits

In the Laurentian Highlands (Bostock, 1969), glacial deposits abandoned by the Laurentide Ice Sheet occur mainly as a discontinuous mantle of lodgment and melt-out till, bouldery and gravelly to sandy in texture, covering the floors and lower sides of valleys and depressions developed between the bedrock hills and knobs forming the major part of the Highlands. A thin discontinuous mantle or veneer of till also commonly covers the top and flanks of the bedrock hills and ridges. In the Ottawa Valley lowland, north of Ottawa River, lodgment and melt-out till deposits are nearly nonexistent on the surface below marine limit; if some of this till has been deposited by Laurentide ice, the deposits must be very patchy over the bedrock and lie buried under marine sediments.

Glaciofluvial Deposits

Glaciofluvial deposits produced at the ice margin by glacial meltwater during retreat of the wasting Laurentide Ice Sheet are found in the major river valleys and their main tributaries in the Laurentian Highlands at, above, and north of marine limit. They occur as fairly thick (~10 m) bodies of well sorted and bedded, bouldery, cobbly gravel and sand in the form of pitted outwash plains, outwash fans, pitted and nonpitted valley trains, pitted kame terraces, and kames. In the Petite Nation Valley, the main ice-frontal glacial outwash bodies are commonly pitted and extend between Lac Simonet and the southern shore of Lac Simon. In Lièvre Valley, a well developed pitted outwash train extends 17 km downvalley from the northern edge of the map area to the northwestern end of Lac de l'Argile. A well developed pitted outwash fan and kame terrace are present in Ruisseau du Prêtre valley, a small tributary to Lièvre River, and similar pitted outwash valley trains of coarse sand and gravel occur in Blanche Valley north of Lac Blanche, and south of Lac Long near Mayo. Small tributary valleys draining into Gatineau River from the east contain pitted outwash trains at and above marine limit; examples are found near Wilson's Corners and near Lac Sainte-Marie. Within Gatineau Valley marine limit lies north of the study area so no outwash bodies are present.

Just north of the Ottawa Valley lowland meltwater deposits were found below marine limit north of Buckingham and Papineauville, resting on bedrock and rising above the marine clay plain surface. The upper part of these bouldery sand and gravel deposits was reworked into marine beaches during the postglacial submergence of the area. More information on two such deposits in Lièvre Valley north of Buckingham can be found in Taylor (1979).

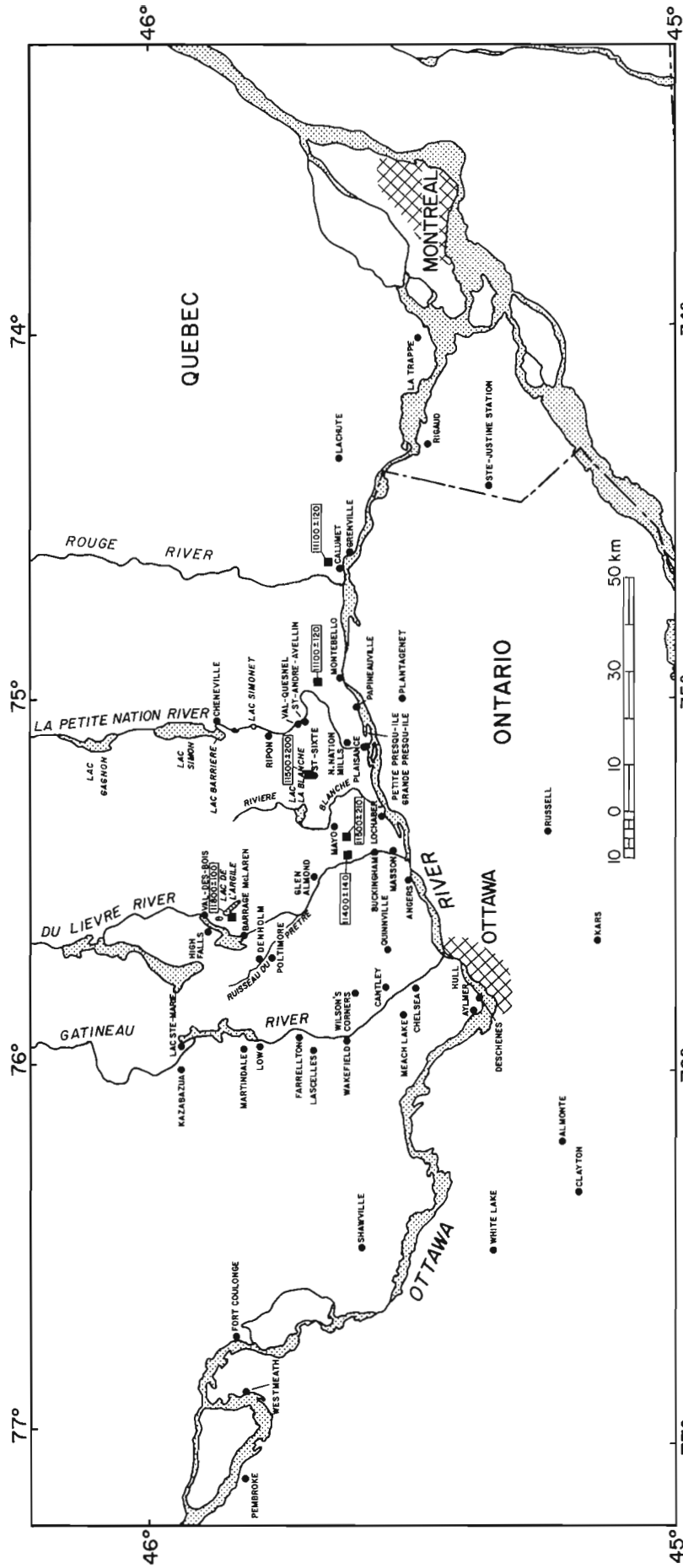

Figure 12.1. Map showing localities where new radiocarbon dates relating to deglaciation chronology and Champlain Sea marine limit have been obtained along the northern rim of the basin between Ottawa and Montreal.

Marine Deposits

Marine sediments deposited by the Champlain Sea, following the withdrawal of Laurentide ice, make up about 20 to 25 per cent of the land surface of the map area. The most important of these in area and thickness are grey, massive, calcareous, fossiliferous, blocky marine clay and silt. They are best developed in Ottawa Valley between Papineauville and Chelsea and in the Laurentian Highlands where their deposition was restricted to valleys of the Petite Nation, Blanche, Lièvre and Gatineau rivers and their main tributaries. In the Ottawa Valley lowland, these primary marine deposits form gently sloping clay plains varying in elevation from ca. 105 m near Papineauville and Plaisance to ca. 115 m near Buckingham and Quinnville. In the valleys of the Laurentian Highlands, the clay fill surface varies from ca. 185 to 190 m in the north to ca. 115 to 120 m in the south, burying all bedrock topography and pre-Champlain Sea glacial deposits lying at lower elevations, except where they have been exhumed. Above these elevations, valley walls and isolated hillslopes below marine limit consist mainly of washed bare Precambrian bedrock.

In valleys of the Laurentian Highlands, the clay is grey, blocky, massive, and contains marine fossils. In Ottawa Valley, the marine clay is grey, blocky, and massive, but the upper part of the unit shows horizontal laminations consisting of thin red bands alternating with grey bands; marine fossils are rare.

In some areas of the Laurentian Highlands, sand mantles the marine clay valley fills. The best developed marine deltaic sand plains are found in the Petite Nation Valley between Chénéville and Saint-André-Avellin, in the Blanche Valley north of Lac la Blanche, and in Lièvre Valley between Denholm and Poltimore. In the Ottawa Valley lowland, the lowest and youngest marine sand deltas deposited by Petite Nation and Lièvre rivers are at North Nation Mills, 4 km north of Plaisance, at ca. 128 to 106 m and at Buckingham at ca. 122 to 107 m.

Post-Champlain Sea Deposits

In the Ottawa Valley lowland, below ca. 92 m a.s.l., nonfossiliferous alluvial channel and terrace sand deposits were identified near Lochaber, Plaisance, and Papineauville.

Table 12.1

Champlain Sea radiocarbon dates relating to marine limit along the northern rim of the basin between Ottawa and Montreal

Laboratory Dating No.	Date (years B.P.)	Locality	Elevation (m a.s.l.)	Material
GSC-2769	11 800 ± 100	Val-des-Bois, Papineau County	180	Marine shells in beach sands
GSC-2863	11 500 ± 200	Saint-Sixte, Papineau County	145	Marine shells in offshore clay
GSC-2878	11 500 ± 210	Mayo, Papineau County	182	Marine shells in offshore clay
GSC-2763	11 400 ± 140	Buckingham, Papineau County	180	Marine shells in offshore clay
GSC-2590	11 100 ± 120	Montebello, Papineau County	167	Marine shells in beach gravels and sands
GSC-2703	11 100 ± 120	Calumet, Argenteuil County	160	Marine shells in beach sands

Late-Glacial History

Ice Retreat

Apart from the flat-topped, kettled, glacial outwash valley trains and deltas, there are no other frontal glacial deposits, except for a 1 km long transverse and arcuate till ridge separating Lac Simon from Lac Barrière. This ridge is at the southern end of Lac Simon, lying on the north, proximal side of the well developed pitted glacial outwash plain and delta damming Lac Simon in Petite Nation Valley. It is believed to be the same morainal ridge identified and mapped by Parry and Macpherson (1964, p. 238) and by LaSalle and Elson (1975) at the western end of the 320 km long St. Narcisse moraine system. The impressive bodies of coarse waterlaid materials extending down the main valleys of the Laurentian Highlands are also similar to those described by these authors as forming the St. Narcisse moraine system between Saint-Siméon and Lac Simon: "the moraine system...includes till ridges, ice-contact stratified drift, outwash deltas built into the Champlain Sea and well developed valley trains" (LaSalle and Elson, 1975, p. 622).

Minimum Age for Ice Retreat

Several radiocarbon dates on marine shells (collected by the author) have been obtained relating to the deglaciation chronology of the Laurentian Highlands between Montreal and Ottawa (Table 12.1; Fig. 12.1).

A radiocarbon date of 11 800 ± 100 years (GSC-2769) indicates that Lièvre Valley had become ice free as far north as Lac de l'Argile by that time, Blanche Valley by 11 500 ± 210 years ago (GSC-2878), Saint-Sixte Valley by 11 500 ± 200 years ago (GSC-2863), and Rouge Valley by 11 100 ± 120 years ago (GSC-2703). A date of 11 100 ± 120 years (GSC-2590) obtained from the highest marine beach deposit found in the Montebello area provides a minimum age for deglaciation of the southern part of the Laurentide Uplands.

Radiocarbon dates obtained previously for marine shells recovered from undisturbed, high level marine sediments at or near the marine limit show that the lower reaches of Gatineau Valley were ice free as far north as Cantley by ca. 12 200 years ago (GSC-1646; Lowdon and Blake, 1973) and as far north as Martindale by ca. 11 900 years ago (GSC-1772; Lowdon and Blake, 1973).

This chronology supports the contention of Hillaire-Marcel (1974, p. 413) that the western parts of the Laurentian Highlands between Saint-Sixte and Ottawa, where valleys are deeper and wider, lost their ice cover earlier than the eastern parts between Lachute and Montebello, where valleys are fewer, smaller, and narrower. It does not support the pattern and chronology of deglaciation of the Laurentide Ice Sheet presented by Prichonnet (1977, p. 340) for this area.

Correlations

Since no datable material was recovered from the core of any ice-frontal outwash valley trains or from the Lac Simon moraine, none of these ice marginal deposits can be dated directly and consequently it is not known whether deposition was synchronous. If their formation is not synchronous, it is likely that ice-marginal deposits of Gatineau and Lièvre valleys are older than those found in valleys farther east, since the radiocarbon dates on marine deposits in these two western valleys are older. If, however, they could be shown to correlate with the St. Narcisse moraine system, as suggested by Parry and Macpherson (1964) and by LaSalle and Elson (1975) for the Lac Simon moraine, they would then all be roughly contemporaneous and would have been formed 10 600 to 11 000 years ago, which is the age of formation of the St. Narcisse moraine system, as given by LaSalle and Elson (1975) and Ochietti (1976, 1977).

Champlain Sea

The highest marine deltaic and beach deposits in Petite Nation Valley lie at 210 m a.s.l. northeast of Chénéville; 210 m a.s.l. in Blanche and Blanche Est valleys; and up to 197 m a.s.l. in Lièvre Valley, 2 km south of High Falls. The elevations of the upper level reached by marine waters were determined by locating the elevation of the highest marine features (measured with Abney level) between two adjacent contours on topographic maps.

Marine Fauna. The penetration of marine waters into Ottawa Valley was soon followed by the arrival of a marine fauna, and fossil remains of both the macrofaunas and the microfaunas that lived near the northern rim of the western Champlain Sea have been found in all major valleys of the Buckingham map area (see Table 12.2).

Table 12.2

Shells, foraminifera, and ostracodes recovered from marine sediments of the Buckingham map area

Locality	Date	Elevation (m a.s.l.)	Material	Macrofauna	Microfauna	Identification and Reference
3 km NW of Ripon, Papineau Co.	-	190	Marine clay	**Hiatella arctica** (Linné)	-	S.H. Richard
5 km NE of Val-Quesnel, Papineau Co.	-	145	Marine clay	**Portlandia arctica** (Gray)	-	M.F.I. Smith, National Museum of Natural Sciences
1.5 km NE of Saint-Sixte, Papineau Co.	11 500 ± 200 (GSC-2863)	145	Marine clay	**Portlandia arctica, Macoma balthica** (Linné)	-	M.F.I. Smith, National Museum of Natural Sciences
4.5 km E of Saint-Sixte, Papineau Co.	-	148	Marine clay	**Macoma balthica, Hiatella arctica, Balanus** sp.		S.H. Richard
3 km SW of Mayo, Papineau Co.	11 500 ± 210 (GSC-2878)	182	Marine clay	**Macoma balthica, Hiatella arctica**	**Elphidium excavatum** (Terquem), **Protelphidium orbiculare** (Brady), **Elphidium asklundi** (Brotzen), **Guttulina** sp.	C.G. Rodrigues, University of Windsor (Foraminifera), S.H. Richard (Macrofauna)
1.2 km N of Mayo, Papineau Co.	-	155	Marine clay	**Portlandia arctica**	**Elphidium excavatum** (Terquem)	C.G. Rodrigues (Foraminifera), S.H. Richard (Macrofauna)
6 km N of Buckingham, Papineau Co.	11 400 ± 140 (GSC-2763)	180	Stony marine clay or diamicton	**Macoma balthica, Hiatella arctica**	**Elphidium excavatum** (Terquem), **Protelphidium orbiculare** (Brady)	C.G. Rodrigues (Foraminifera), S.H. Richard (Macrofauna)
5 km NNW of Buckingham, Papineau Co.	10 700 ± 100 (GSC-2621)	146	Stony marine clay	**Portlandia arctica, Macoma balthica, Hiatella arctica, Mytilus edulis** (Linné)	**Protelphidium orbiculare** (Brady), **Elphidium asklundi** (Brotzen), **Elphidium excavatum** (Terquem), **Elphidium subarcticum** (Cushman), **Eoeponidella pulchella** (Parker), **Islandiella helenae** (Feyling-Hanssen and Buzas), **Cassidulina reniforme** (Nørvang), **Guttulina** sp.	C.G. Rodrigues (Foraminifera), S.H. Richard (Marine shells), J-S. Vincent in Lowdon and Blake, 1978, p. 5.

Table 12.2 (cont.)

Locality	Date	Elevation (m a.s.l.)	Material	Macrofauna	Microfauna	Identification and Reference
5 km S of Val-des-Bois, Papineau Co.	11 800 ± 100 (GSC-2769)	180	Marine sand	**Macoma balthica**	-	S.H. Richard
5 km N of Montebello, Papineau Co.	11 100 ± 120 (GSC-2590)	167	Marine sand and gravel	**Hiatella arctica**, **Balanus hameri**, **Macoma balthica**, **Mytilus edulis**	-	S.H. Richard
2.7 km N of Calumet, Argenteuil Co.	11 100 ± 120 (GSC-2703)	160	Marine sand	**Macoma balthica**, **Hiatella arctica**	-	S.H. Richard
1 km NE of North Nation Mills, Papineau Co.	-	118	Marine sand and gravel	**Macoma balthica**, **Hiatella arctica**, **Portlandia arctica**, **Balanus hameri**, **Mytilus edulis**	-	S.H. Richard
3 km NE of Buckingham, Papineau Co.	-	118	Marine sand	**Macoma balthica**	**Cassidulina reniforme** (Nørvang), **Elphidium excavatum** (Terquem), **Islandiella helenae** (Feyling-Hanssen and Buzas), **Protelphidium orbiculare** (Brady), **Elphidium asklundi** (Brotzen), **Guttulina lactea** (Walker and Jacob) Ostracodes: **Heterocyprideis sorbyana** (Jones), **Eucytheridea punctillata** (Brady)	C.G. Rodrigues, (Foraminifera and ostracodes), S.H. Richard (Marine shells)
3.5 km N of Deschênes, Gatineau Co.	10 100 ± 130 (GSC-2189)	94	Marine sand and gravel	**Hiatella arctica**, **Macoma balthica**	-	S.H. Richard

In Gatineau Valley, marine fossils from Champlain Sea sediments have been reported upon by Antevs (1928), Mauffette (1949a), Sabourin (1965), Buckley (1968, 1970), Bickel (1970), Gadd in Lowdon and Blake, 1975, Romanelli (1975a, b), Rust and Romanelli (1975), Vincent (1976a), and Richard (1976b). Marine assemblages of both macrofaunal and microfaunal species have been recovered at various elevations up to 195 m a.s.l. near Meach Lake, Cantley, Wakefield, Lascelles, Farrellton, and Martindale (Fig. 12.1).

Table 12.2 shows that specimens of the arctic species **Portlandia arctica** (Gray) are present in all valleys of the Laurentian Highlands in the study area and that this species characterizes the marine clay filling the floor of these former fiords. A preliminary reconnaissance sampling of the Champlain Sea clays and sands carried out at five localities revealed the presence of the following microfaunal species (identification by C.G. Rodrigues, now with University of Windsor): **Protelphidium orbiculare** (Brady), **Elphidium asklundi** (Brotzen), **Elphidium excavatum** (Terquem), **Elphidium subarcticum** (Cushman), **Islandiella helenae** (Feyling-Hanssen and Buzas), **Cassidulina reniforme** (Nørvang), **Eoeponidella pulchella** (Parker), **Guttulina lactea** (Walker and Jacob). The species **Elphidium excavatum** has been recovered at all five sites sampled for microfauna. Feyling-Hanssen (1972) provided a detailed study of this species and found that today it commonly dominates arctic assemblages. It is a good paleoecological indicator and when found in high numbers it provides strong evidence for an arctic environment. **Cassidulina reniforme** (Nørvang) flourishes today in arctic environments; a detailed discussion of its fossil record is found in Feyling-Hanssen et al. (1971). **Islandiella helenae**, a circumpolar species, was studied by Feyling-Hanssen and Buzas (1976), who determined that it is essentially an arctic species. In a recent study, Cronin (1979) found that "the abundance of **Elphidium incertum, E. subarcticum, E. excavatum clavata** and **Protelphidium orbiculare** provides strong evidence for a shallow cold-water environment in the Champlain Sea".

A date of 10 700 ± 100 years (GSC-2621) obtained for **Hiatella arctica** shells (Table 12.2; Taylor, 1979, p. 38; Lowdon and Blake, 1978, p. 5) provides strong evidence that arctic-subarctic environmental conditions were still in existence at this time along the northern margin of the western Champlain Sea. This date can be compared with a ^{14}C date of 10 900 ± 100 years (GSC-2312) obtained by Cronin (1976; Lowdon and Blake, 1976, p. 6-7) for a marine faunal assemblage recovered near Kars, 25 km south of Ottawa, providing strong evidence for the existence of similar frigid-subfrigid conditions in that part of the sea.

Radiocarbon Chronology. Radiocarbon dates listed in Table 12.1 relate to the chronology of the Champlain Sea. These indicate that Lièvre Valley was occupied by 11 800 ± 100 years ago (GSC-2769), Blanche Valley by 11 500 ± 200 years ago (GSC-2878), Saint-Sixte Valley by 11 500 ± 200 years ago (GSC-2863), an unnamed valley north of Montebello by 11 100 ± 120 years ago (GSC-2590), and Rouge Valley by 11 100 ± 120 years ago (GSC-2703). This apparently is somewhat later than in Almonte and Gatineau River areas (Richard, 1978) and is further proof that marine limit is not synchronous in the Champlain Sea basin (Parry and Macpherson, 1964, p. 247; Gadd et al., 1972, p. 14). It should be noted, however, that the Blanche and Saint-Sixte Valley shells are from clay (Table 12.1) and consequently do not closely date inundation.

Last Stand of the Champlain Sea. The beaches and nearshore sand deposits representing the last and lowest shoreline of the western Champlain Sea along the northern rim of the basin, north of Ottawa River, were found at ca. 94 m a.s.l. near Aylmer (Richard, 1978, p. 25-26), at ca. 76 m near Papineauville, and at ca. 70 m in the east near La Trappe, Deux-Montagnes County (Richard, 1976a, p. 208). These gradually decreasing elevations from west to east show that the final retreat of the Champlain Sea from Ottawa Valley took place through an eastward shoreline migration downvalley from the Ottawa area towards the Montreal area. Only the Aylmer site has been dated – 10 100 ± 130 years (GSC-2189; Richard, 1978, p. 25-26).

Post-Champlain Sea Events

Regression of the Champlain Sea was followed by a phase of channel downcutting by the early Ottawa River. Between Gatineau and Papineauville, this channelling phase produced several generations of now abandoned river channels, bluffs, and erosional terraces cut into the marine clay plains below 92 m elevation.

River incision through the soft clay continued until the degrading early Ottawa River exposed underlying glacial drift and bedrock on each channel floor. The more resistant materials stopped downcutting, causing successive abandonment. Downstream from glacial drift or bedrock exposures, the surfaces of erosional clay terraces commonly are mantled by a thin cover of alluvial sand derived from the exhumed material.

Following this phase of channel and terrace downcutting, massive slope failures and mass movements have taken place in the marine clays. They occur in three main areas: 1) in the main river valleys of the Laurentian Highlands, especially along the banks of Lièvre River between Glen Almond and Barrage McLaren and of Gatineau River between Wakefield and Kazabazua; 2) along the uppermost and highest abandoned river-cut bluff of the early Ottawa River, especially between Buckingham and Masson, and at Angers; and 3) along the lowermost and still active river-cut bluff of the present day Ottawa River, where the most spectacular of these have produced two islands – Grande Presqu'île and Petite Presqu'île – in the middle of the river between Plaisance and Papineauville (Crawford, 1961, p. 205-207; Lajoie, 1974, p. 424). This interpretation of the formation of the islands differs from that presented by Gadd (1976, p. 1-2). In all three types of settings where landslides have occurred since retreat of the Champlain Sea, i.e. during the last 10 000 years, slope failures in the sensitive marine clays have resulted in the production of hummocky aprons and fans of tilted or slumped clay and sand blocks on the floor of abandoned or active river channels.

Following deglaciation in the highlands and land emergence in the lowlands, marshes and peat bogs developed in poorly drained swales of undulating ground moraine, of recently ice-freed rock basins, and of the abandoned river channel floors.

Conclusions

The main points made in this paper are:

1. Ice frontal glacial outwash deposits indicating the former position of an active ice margin are present at and north of the marine limit in all valleys of the Laurentian Highlands within the Buckingham map area. These well developed pitted valley trains and outwash deltas may be part of the St. Narcisse moraine system of LaSalle and Elson (1975).

2. New radiocarbon dates relating to the deglaciation chronology show that ice retreat from the Laurentian Highlands between Montreal and Ottawa was not a synchronous event and that the western part of this area was deglaciated and occupied by the Champlain Sea earlier than the eastern sector between Lachute and Montebello.

3. The Champlain Sea flooded the area up to an elevation of at least 205 to 210 m in the eastern part of the area and up to at least 195 to 198 m in the western part. This invasion occurred as early as 12 200 years ago in Gatineau Valley but may have been as late as 11 100 years B.P. north of Calumet in Rouge Valley.

Acknowledgments

The author is indebted to R.J. Fulton who critically reviewed the original manuscript and contributed many useful suggestions incorporated in the revised version. J. Taylor ably assisted in the field and contributed an independent detailed study of two Pleistocene sections exposed in Lièvre Valley near Buckingham which was used for a B.Sc. Thesis at Carleton University. I wish to thank C.G. Rodrigues, University of Windsor, and P. Jones, Carleton University, Ottawa, who accompanied the author in the field to sample sections for marine microfossils and for their laboratory work on the identification of the foraminifers and ostracodes of the Buckingham area. Thanks are extended to Dr. W. Blake, Jr. who supervised the processing of the shell samples submitted to the Geological Survey of Canada Radiocarbon Dating Laboratory. The author is thankful to Mrs. M.F.I. Smith, National Museum of Natural Sciences, Ottawa, who kindly identified the marine shells submitted to the Museum.

References

Antevs, E.
1925: Retreat of the last ice sheet in eastern Canada; Geological Survey of Canada, Memoir 146, 138 p.

1928: The Last Glaciation, with Special Reference to the Ice Retreat in Northeastern North America; American Geographical Society, Research Series, No. 17, New York, 202 p.

Béland, R.
1954: Preliminary report on Wakefield area, Gatineau County, Quebec; Quebec Department of Mines, Preliminary Report, No. 298, 7 p.

Bickel, E.D.
1970: Pleistocene non-marine mollusca of the Gatineau valley and Ottawa areas of Quebec and Ontario, Canada; Sterkiana, no. 38, 50 p.

Bostock, H.S.
1969: Physiographic regions of Canada; Geological Survey of Canada, Map 1254A, scale 1:5 000 000.

Buckley, J.T.
1968: Geomorphological map of the Gatineau Park; in Report of Activities, Part B, Geological Survey of Canada, Paper 68-1B, p. 79.

1970: Surficial deposits and land forms, Gatineau Park and vicinity; Geological Survey of Canada, Open File 36.

Crawford, C.B.
1961: Engineering studies of Leda clay; in Soils in Canada, ed. R.F. Leggett; Royal Society of Canada, Special Publication no. 3, University of Toronto Press, p. 205-207.

Cronin, T.M.
1976: An arctic foraminiferal fauna from Champlain Sea deposits in Ontario; Canadian Journal of Earth Sciences, v. 13, no. 12, p. 1678-1682.

1979: Late Pleistocene benthic foraminifers from the St. Lawrence Lowlands; Journal of Paleontology, v. 53, no. 4, p. 781-814.

Douglas, R.J.W. (co-ordinator)
1978: Geology, Rivière Gatineau, Quebec-Ontario; Geological Survey of Canada, Map 1334A, scale 1:1 000 000.

Faessler, C.
1948: Région du lac Simon, comté de Papineau, Québec; Ministère des Mines de la Province de Québec, Rapport géologique nº. 33, 33 p.

Feyling-Hanssen, R.W.
1972: The foraminifer **Elphidium excavatum** (Terquem) and its variant forms; Micropaleontology, v. 18, no. 3, p. 237-254.

Feyling-Hanssen, R.W. and Buzas, M.
1976: Emendation of **Cassidulina** and **Islandiella helenae** new species; Journal of Foraminiferal Research, v.6, no. 2, p. 154-158.

Feyling-Hanssen, R.W., Jørgensen, J.A., Knudsen, K.L., and Andersen, A-L.L.
1971: Late Quaternary foraminifera from Vendsyssel, Denmark and Sandnes, Norway; Geological Society of Denmark, Bulletin 21, p. 67-317.

Fransham, P.B., Gadd, N.R., and Carr, P.A.
1976a: Geological variability of marine deposits, Ottawa-St. Lawrence Lowlands; in Report of Activities, Part A, Geological Survey of Canada, Paper 76-1A, p. 37-41.

1976b: Sensitive clay deposits and associated landslides in the Ottawa Valley; Geological Survey of Canada, Open File 352.

Gadd, N.R.
1973: Distribution of marine deposits, Ottawa-St. Lawrence Basin; in Report of Activities, Part A, Geological Survey of Canada, Paper 73-1A, p. 183.

1976: Surficial geology and landslides of Thurso-Russell map-area, Ontario; Geological Survey of Canada, Paper 75-35, 7 p.

Gadd, N.R., LaSalle, P., Dionne, J-C., Shilts, W.W., and McDonald, B.C.
1972: Quaternary geology and geomorphology, southern Quebec; XXIV International Geological Congress, Guidebook, Field Excursion A44-C44, 70 p.

Hillaire-Marcel, C.
1974: La déglaciation au nord-ouest de Montréal: données radiochronologiques et faits stratigraphiques; Revue de géographie de Montréal, vol. XXVIII, nº 4, p. 407-417.

Hogarth, D.D.
1962: A guide to the geology of the Gatineau-Lièvre district; Canadian Field Naturalist, v. 76, no. 1, p. 1-55.

1970: Geology of the southern part of Gatineau Park, National Capital Region; Geological Survey of Canada, Paper 70-20, 8 p, Map 7-1970.

Lajoie, P-G.
1962: Étude pédologique des comtés de Gatineau et de Pontiac, Québec; Ministère de l'Agriculture du Canada, p. 77-79, 84-85, carte.

Lajoie, P-G. (cont.)
1967: Étude pédologique des comtés de Hull, Labelle et Papineau (Québec); Ministère de l'Agriculture du Canada, p. 15-16, 28-29, 90-93, cartes.

1974: Les coulées d'argile des basses-terrasses de l'Outaouais, du Saint-Laurent et du Saguenay; Revue de géographie de Montréal, vol. XXVIII, nº 4, p. 419-428.

LaSalle, P. and Elson, J.A.
1975: Emplacement of the St. Narcisse Moraine as a climatic event in eastern Canada; Quaternary Research, v. 5, p. 621-625.

Lowdon, J.A. and Blake, W., Jr.
1973: Geological Survey of Canada radiocarbon dates XIII; Geological Survey of Canada, Paper 73-7, 61 p.

1975: Geological Survey of Canada radiocarbon dates XV; Geological Survey of Canada, Paper 75-7, 32 p.

1976: Geological Survey of Canada radiocarbon dates XVI; Geological Survey of Canada, Paper 76-7, 21 p.

1978: Geological Survey of Canada radiocarbon dates XVIII; Geological Survey of Canada Paper 78-7, 20 p.

Mauffette, P.
1949a: Notes sur la découverte de sédiments fossilifères de la mer Champlain dans les régions de Val-des-Bois, de Martindale et de Farrellton, P.Q.; Annales de l'Acfas, vol. 16, p. 100-103.

1949b: Preliminary report on Val-des-Bois map area, Papineau and Gatineau counties, Quebec; Quebec Department of Mines, Preliminary Report no. 223, 10 p.

Ochietti, S.
1976: Dépôts et faits quaternaires du Bas-St-Maurice, Québec (2e partie); in Report of Activities, Part C, Geological Survey of Canada, Paper 76-1C, p. 217-220.

1977: Stratigraphie du Wisconsinien de la région de Trois-Rivières-Shawinigan, Québec; Géographie physique et Quaternaire, vol. XXXI, nº 3-4, p. 307-322.

Parry, J.T. and Macpherson, J.C.
1964: The St. Faustin-St. Narcisse moraine and the Champlain Sea; Revue de géographie de Montréal, v. XVIII, no. 2, p. 235-248.

Prichonnet, G.
1977: La déglaciation de la vallée du St-Laurent dans la région de Montréal et l'invasion marine contemporaine; Géographie physique et Quaternaire, vol. XXXI, nº 3-4, p. 323-345.

Richard, S.H.
1976a: Surficial geology mapping: Valleyfield-Rigaud area, Quebec (31 G/1, 8, 9); in Report of Activities, Part A, Geological Survey of Canada, Paper 76-1A, p. 205-208.

1976b: Surficial geology, Wakefield, Quebec (31 G/12 (S 1/2, W of Gatineau River)); Geological Survey of Canada, Open File 369.

1976c: Surficial geology, Thurso, Ontario and Quebec (31 G/11 (W 1/2, Ontario part)); Geological Survey of Canada, Open File 368.

1978: Age of Champlain Sea and "Lampsilis Lake" episode in the Ottawa-St. Lawrence Lowlands; in Current Research, Part C, Geological Survey of Canada, Paper 78-1C, p. 23-28.

Romanelli, R.
1975a: The Champlain Sea episode in the Gatineau River valley and Ottawa area; Canadian Field-Naturalist, v. 89, no. 4, p. 356-360.

1975b: Environmental history of Champlain Sea deposits in the Gatineau Valley, Quebec; unpublished Ms.Sci. Thesis, Geology Department, University of Ottawa, 119 p.

Rust, B.R. and Romanelli, R.
1975: Late Quaternary subaqueous outwash deposits near Ottawa, Canada; in Glaciofluvial and Glaciolacustrine Sedimentation, ed. A.V. Jopling and B.C. McDonald; Society of Economic Paleontologists and Mineralogists, Special Publication 23, p. 177-192.

Sabourin, R.J.E.
1965: Bristol-Masham area, Pontiac and Gatineau counties, Quebec; Quebec Department of Natural Resources, Geological Report no. 110, 44 p.

Taylor, J.
1979: A detailed study of Pleistocene deposits of the Buckingham area, Quebec; unpublished B.Sc. Thesis, Geology Department, Carleton University, Ottawa, 86 p.

Vincent, J-S.
1976a: Dépôts meubles du secteur sud de la carte de Wakefield (31 G/12), Ontario et Québec; Commission géologique du Canada, Dossier public 371.

1976b: Dépôts meubles du secteur sud de la carte de Thurso (31 G/11), Ontario et Québec; Commission géologique du Canada, Dossier public 370.

Wilson, A.E.
1946: Geology of the Ottawa-St. Lawrence Lowland, Ontario and Quebec; Geological Survey of Canada, Memoir 241, 62 p.

Wilson, M.E.
1924: Arnprior-Quyon and Maniwaki areas, Ontario and Quebec; Geological Survey of Canada, Memoir 136, 152 p.

13. TRIASSIC CONODONTS FROM THE PAVILION BEDS, BIG BAR CREEK, CENTRAL BRITISH COLUMBIA

Project 500029

M.B. Rafek[1]
Institute of Sedimentary and Petroleum Geology, Calgary

Rafek, M.B., Triassic conodonts from the Pavilion Beds, Big Bar Creek, central British Columbia; in Current Research, Part C, Geological Survey of Canada, Paper 80-1C, p. 129-133, 1980.

Abstract

A fauna containing ***Epigondolella primitia*** *Mosher, 1970,* ***Epigondolella abneptis*** *(Huckriede, 1958),* ***Neogondolella bifurcata*** *(Budurov and Stefanov, 1972),* ***Neogondolella excentrica*** *Budurov and Stefanov, 1972, and* ***Neogondolella polygnathiformis*** *(Budurov and Stefanov, 1965) from the Triassic of central British Columbia is herein described and its stratigraphic implications discussed.*

Introduction

During the course of Triassic research in western Canada a suite of 25 samples was collected at the Venables Creek locality "Stop 5-3" (Campbell et al., 1976, p. 104) together wtih 10 samples from a limestone outcrop one-half mile (0.8 km) south of Venables Creek, along the Trans-Canada Highway. A further suite of 110 samples was collected from the "next high roadcuts (of) probable Triassic limestone . . . . before . . . . Spences Bridge Group", at 27.6 miles (44.4 km) south of Cache Creek along the Trans-Canada Highway to the township of Spences Bridge (Campbell et al., 1976, p. 105) (see Fig. 13.1).

Furthermore, 20 samples were collected on the south-western slope of Mount Kostering from an isolated outcrop, the strata of which have been assigned to the Pavilion beds (Trettin, 1980) (see Fig. 13.1). An additional three samples from this locality were obtained from H. Trettin of the Geological Survey of Canada.

Although all 165 samples collected by the author proved barren [with the exception of two (VC1 and VC) from Venables Creek, which contained sponge spicules, fish teeth and scales], one of the three samples obtained from H. Trettin yielded identifiable conodonts. This sample, collected by J.H.W. Monger, is from GSC locality C-54823 – Yalakom River area, southwestern slope of Mount Kostering, about 3.8 km east of the Big Bar ferry (Trettin, 1980). As the presence of these conodonts has already been recorded (Trettin, 1980), the objective of this report is to illustrate and discuss the significance of the fauna.

Furthermore, it should be mentioned that dilute (10 per cent) hydrofluoric acid was used to digest the samples since the slightly metamorphosed rocks did not react with acetic acid.

Conodont Fauna

Upper Triassic conodonts have been previously reported from the vicinity of this sample. Okulitch and Cameron (1976) reported conodonts from rocks assigned to the Nicola, Cache Creek, and Mount Ida groups of south-central British Columbia. They recovered **Epigondolella primitia** Mosher, 1970, and **Epigondolella abneptis** (Huckriede, 1958) from argillites near an outcrop assigned to the Cache Creek Group (GSC locality 86351) and **E. primitia** and **Neogondolella polygnathiformis** (Budurov and Stefanov, 1965) also from rocks which were previously assigned to the Cache Creek Group, but were suspected to be of Triassic age (Preto in Okulitch and Cameron, 1976) (GSC locality 86350). Both samples are from the Vernon map area. In addition, they recovered **N. polygnathiformis** from strata assigned to the Nicola Group in the Bonaparte Lake map area.

Conodont elements recovered from the present sample belong to the form genera **Epigondolella** and **Neogondolella** (Plate 13.1). The conodonts are fractured and black, of colour alteration index of 5 (Epstein et al., 1977), suggesting that they have been subjected to a considerably high temperature (300°-400°C).

The neogondolellids present are **Neogondolella bifurcata** (Budurov and Stefanov, 1972), which ranges from the Pelsonian (Middle Anisian) to Ladinian, **N. excentrica** Budurov and Stefanov, 1972, which has been reported mainly from Lower Fassanian (Lower Ladinian) strata and **N. polygnathiformis** with a reported age range of middle Late Ladinian – middle Late Karnian.

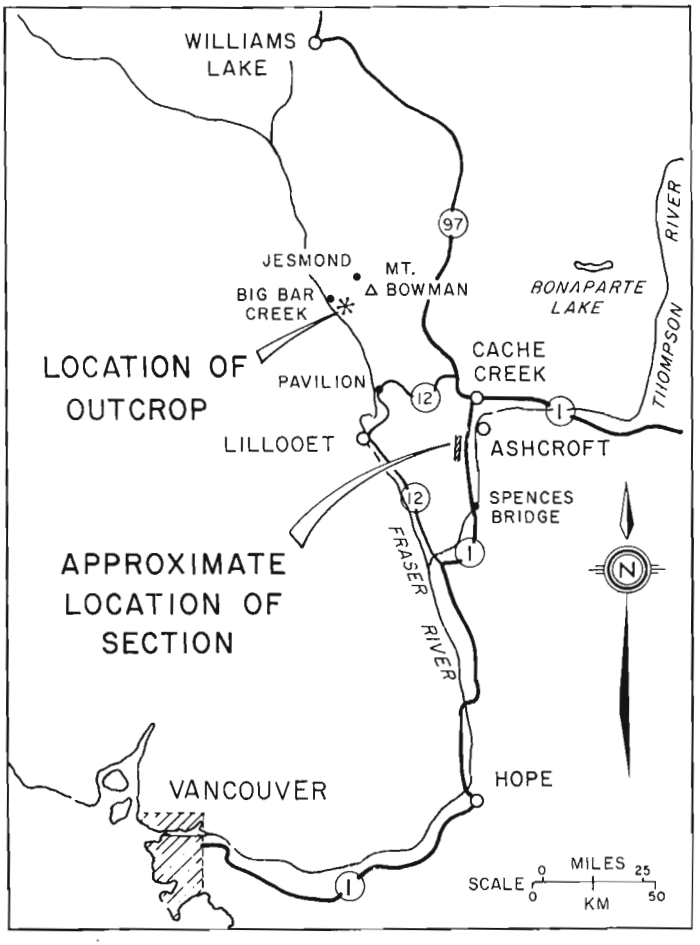

Figure 13.1. *Location of outcrops in study area.*

[1] Department of Geology, University of New Brunswick, Fredericton, New Brunswick E3B 5A3

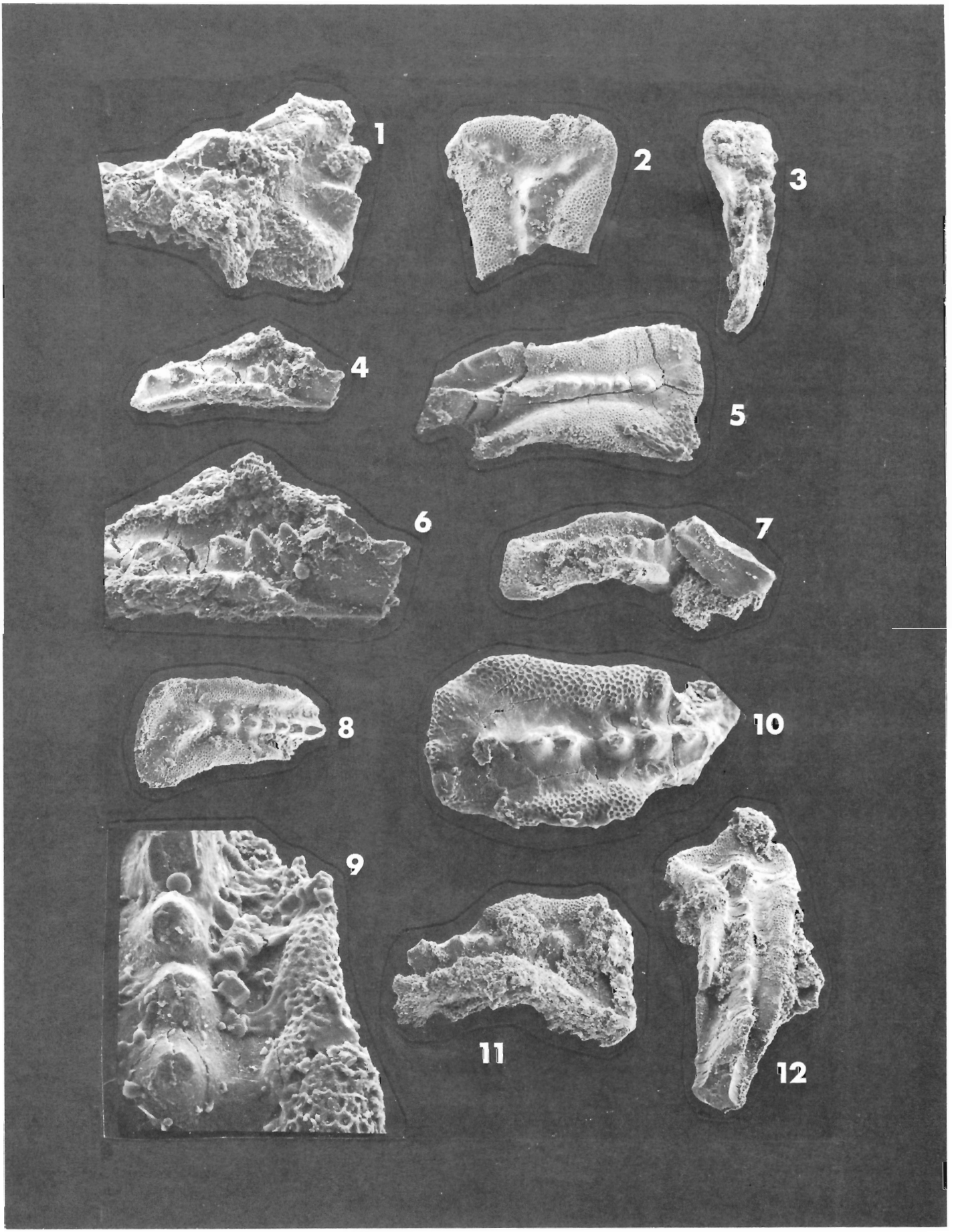
1
2
3
4
5
6
7
8
9
10
11
12

The epigondolellids present are **Epigondolella abneptis** and **E. primitia. Epigondolella abneptis** ranges from Lower – Middle Norian, while **E. primitia** is a guide fossil for the Karnian/Norian boundary (Mosher, 1970).

Discussion

In northeastern British Columbia **Neogondolella excentrica** occurs in the uppermost part of the Toad Formation in association with other Middle Triassic elements (Rafek, in preparation). The occurrence of this distinctive Middle Triassic indicator together with **Epigondolella primitia,** elsewhere known only from the Upper Triassic, is somewhat unsettling, and remains an unsolved problem.

Neogondolella bifurcata has been reported from the Upper Anisian of Bulgaria (lowermost Illyrian conodont Zone AIII-alpha), and from the Middle Triassic Muschelkalk facies of Poland and West Germany (Trammer, 1975; Rafek, 1977). It has as yet to be recovered from strata of the Middle Triassic Toad Formation of northeastern British Columbia (Rafek, in preparation).

Systematic Paleontology

All designated specimens are deposited in the collection of the Geological Survey of Canada, Ottawa (prefix GSC). All specimens illustrated were photographed using the scanning electron microscope and are coated with gold.

PLATE 13.1

(unless otherwise stated, magnification x 64)

Figure

1. **Epigondolella abneptis** (Huckriede) (x 120) (GSC 64678). Upper view of broken remains of posterior margin is crenulated.
2. **Neogondolella bifurcata** (Budurov and Stefranov) GSC 64679). Upper view of specimen illustrates forked carina.
3. **Neogondolella polygnathiformis** (Budurov and Stefanov) (x 32) (GSC 64680). Upper view.

4,6. **Epigondolella primitia** Mosher (GSC 64681).

4. Upper view of posterior end of incomplete specimen.
6. Detail of antero-lateral platform margin illustrating nodes.
5. **Neogondolella polygnathiformis** (Budurov and Stefanov) (GSC 64682). Upper view.
7. **Neogondolella polygnathiformis** (Budurov and Stefanov) (GSC 64683). Upper view of specimen with broken blade.

8,9. **Neogondolella excentrica** (Budurov and Stefanov) (GSC 64684).

8. Upper view of incomplete specimen illustrates curved carina.
9. Detail of antero-lateral platform margin; note the absence of nodes (x 130).
10. **Epigondolella** cf. **E. primitia** Mosher (x 130) (GSC 64685). Upper view of specimen with nodes along the antero-lateral margin.
11. **Neogondolella polygnathiformis** (Budurov and Stefanov) (GSC 64686). Upper view.
12. **Neogondolella polygnathiformis** (Budurov and Stefanov) (GSC 64687). Upper view.

Order Conodontophorida

Superfamily Gondolellacea Lindström, 1970

Family Gondolellidae Lindström, 1970

Genus **Epigondolella** Mosher, 1968

Type species **Polygnathus abneptis** Huckriede, 1958

Epigondolella abneptis (Huckriede, 1958)

(Plate 13.1, figure 1)

Polygnathus n. sp. indet. Diebel, 1956, p. 436, Plate 5, fig. 3a, b.

Polygnathus abneptis Huckriede, 1958, p. 156, Plate 11, fig. 33?, Plate 12, fig. 30-36, Plate 14, fig. 1-3, 5, 12-14, 16-22, 26, 27, 32, 47-58; Budurov and Vrabljanski, 1966, Plate 4, fig. 22; Spassov, 1967, p. 29, Plate 1, fig. 12-14; Budurov and Pevny, 1970, Plate 17, fig. 13, 14.

Gladigondolella abneptis (Huckriede), Nogami, 1968, p. 122, Plate 8, fig. 1-7, ?8; Hayashi, 1968, p. 68, Plate 2, fig. 6, 7, 8.

Gladigondolella abneptis echinatus Hayashi, 1968, p. 68-69, Plate 2, fig. 1.

Epigondolella abneptis (Huckriede), Mosher, 1968, p. 936, Plate 118, fig. 22-30; Mosher, 1970, Plate 110, fig. 14, 15, 18, 20, 21; Sweet et al., 1971, Plate 1, fig. 18, 27.

Tardongondolella abneptis (Huckriede), Bender, 1970, p. 531, Plate 59, fig. 21; Kozur and Mostler, 1971, Plate 2, fig. 7, 9; Okulitch and Cameron, 1976, Plate 1, fig. 2, 5-6.

Remarks: One incomplete specimen, identified by crenulations on the posterior margin of platform.

Epigondolella primitia Mosher, 1970

(Plate 13.1, figures 4, 6)

Gladigondolella abneptis Nogami, 1968, Plate 8, fig. 8.

Epigondolella primitia Mosher, 1970, p. 740, Plate 110, fig. 7-13, 16, 17; Mosher, 1973, p. 161, Plate 18, fig. 1-5, 7-11; Metcalfe et al., 1979, p. 743, Plate 97, fig. 8, 9, 12-20; Sweet in Ziegler, 1977, p. 193-194, **Epigondolella** Plate 2, fig. 3a-c.

Tardogondolella abneptis Bender, 1970, Plate 58, fig. 29, 30.

Tardogondolella nodosa nodosa (Hayashi), Kozur and Mostler, 1971, Plate 2, fig. 10, 11, 13.

Epigondolella n. sp., Sweet et al., 1971, Plate 1, fig. 8, 40.

Remarks: Only incomplete specimens recovered.

Epigondolella cf. **E. primitia** Mosher, 1970

(Plate 13.1, figure 10)

Remarks: The specimen has only slight crenulations along the antero-lateral margin of the platform, illustrating the link to its "polygnathiformis" ancestor (Mosher, 1970).

Genus **Neogondolella** Bender and Stoppel, 1965

Type species **Neogondolella mombergensis** (Tatge)

Neogondolella bifurcata (Budurov and Stefanov, 1972)

(Plate 13.1, figure 2)

Paragondolella bifurcata Budurov and Stefanov, 1972, p. 843, Plate 1, fig. 1-25, Plate 22, fig. 1-9.

Gondolella bifurcata (Budurov and Stefanov), Trammer, 1975, Plate 25, fig. 6a-b.

Neogondolella bifurcata (Budurov and Stefanov), Sweet in Ziegler, 1975, p. 219.

Remarks: Only one incomplete specimen recovered. Forked carina at the posterior end provides positive identification. Reported from the Illyrian of Bulgaria, Pelsonian of Poland and the Middle Triassic of West Germany and France.

Neogondolella excentrica Budurov and Stefanov, 1972

(Plate 13.1, figures 8, 9)

Neogondolella excentrica Budurov and Stefanov, 1972, p. 840, Plate 4, fig. 9-28; Budurov and Stefanov, 1973/74, p. 300, Plate 1, fig. 13, 14, 31-34; Budurov and Stefanov, 1975, p. 16, Plate 3, fig. 3-8, 20-21; Bupta and Rafek, 1976, p. 209, Plate. 2, fig. 1a-b; Sweet in Ziegler, 1975, p. 225-226.

Gondolella excentrica (Budurov and Stefanov), Trammer, 1975, Plate 25, fig. 4-5.

Remarks: One incomplete specimen recovered, illustrating a curved posterior carina. Anterior platform margins lack nodes. Occurs in Lower Fassanian of Bulgaria, Poland, Turkey and the Middle Triassic of West Germany and France.

Neogondolella ploygnathiformis (Budurov and Stefanov, 1965)

(Plate 13.1, figures 3, 5, 7, 11, 12)

Gondolella polygnathiformis Budurov and Stefanov, 1965, p. 118, Plate 3, fig. 3-7; Burdurov and Vrabljanski, 1966, Plate 5, fig. 3, 4, 8.

Paragondolella polygnathiformis (Budurov and Stefanov), Mosher, 1968, p. 939, Plate 118, fig. 9-17, 19; Mosher, 1970, Plate 110, fig. 3, 6; Flügel and Ramovš, 1970, Plate 1, fig. 1-3; Sweet et al., 1971, Plate 1, fig. 11.

Metapolygnathus communisti Hayashi, 1968, p. 72, Plate 3, fig. 11.

Metapolygnathus linguiformis Hayashi, 1968, p. 72, Plate 3, fig. 9.

Metapolygnathus noah Hayashi, 1968, p. 72, Plate 3, fig. 10.

Neogondolella palata Bender, 1970, p. 519, Plate 58, fig. 6, 7, 11, 17.

Metapolygnathus polygnathiformis (Budurov and Stefanov), Mosher, 1973, p. 164, Plate 20, fig. 7, 12; Eicher and Mosher, 1974, p. 736, Plate 1, fig. 27, 28, 30, 34, 39, 40, Plate 2, fig. 6; Okulitch and Cameron, 1976, Plate 1, fig. 1; Metcalfe et al., 1979, p. 745, Plate 97, fig. 1-5.

Neogondolella polygnathiformis (Budurov and Stefanov), Gupta and Rafek, 1976, p. 211, Plate 1, fig. 8a, b; Sweet in Ziegler, 1973, v. 1, p. 145-146, Neogondo Plate 1, fig. 8.

Remarks: Eight specimens recovered have typical squared-off posterior platform margin and where free blade is preserved it is high. Occurs in Early Karnian of Bulgaria and late Early Karnian and middle Late Karnian of Canada.

Acknowledgments

The Natural Sciences and Engineering Council of Canada and the Department of Geological Sciences, University of Saskatchewan, Saskatoon are gratefully acknowledged for providing financial support and research facilities. I wish to express my gratitude to W.W. Nassichuk, H.P. Trettin and T.T. Uyeno for their support and encouragement throughout the study. H.P. Trettin made samples available; T.T. Uyeno read an initial draft of the manuscript. The Institute of Sedimentary and Petroleum Geology is acknowledged for facilities and support provided during the course of the project. I also wish to express my thanks to N. Holmlund for field assistance.

References

Bender, H.
1970: (Preprint 1967): Zur Gliederung der mediterranen Trias II. Die Conodontenchronologie der mediterranen Trias; Annuaire géologique des pays helléniques, v. 19, p. 465-540.

Bender, H. and Stoppel, D.
1965: Perm-Conodonten, Bundesanstalt für bodenforschung, Geologisches Jahrbuch, v. 82, p. 331-357.

Budurov, K. and Penvy, J.
1970: Über die Anwesenheit von Trias-Conodonten in den Westkarpaten; Práce Geologiczne, v. 51, p. 165-171.

Budurov, K. and Stefanov, S.
1965: Gattun **Gondolella** aus der Trias Bulgariens; Bulgarska akademiia na naukite, Geologichiski institut 'Strashimir Dimitrov', Seriia paleontologiia, v. 7, p. 115-127.

1972: Plattform-Conodonten und ihre Zonan in der mittleren Trias Bulgariens; Mitteilungen der Gesellschaft der Geologie – und Bergbaustudenten in Wien, v. 21, p. 829-852.

1973/74: Die triassischen Conodonten in manchen Bohrungen Nordbulgariens; Sofia, Faculté de Géologie et Géographie, Annuaire, Livre 1, 66, p. 299-301.

1975: Middle Triassic conodonts from drillings near the town of Knezha; Bulgarian Academy of Sciences, Paleontology, Stratigraphy and Lithology, v. 3, p. 11-18.

Budurov, K. and Vrabljanski, B.
1966: Beitrag zur Stratigraphie des Karbonaten Paläozoikums und der Trias aus Kräiste und ihre Conodontenfauna; Institut scientifique des recherches géologiques, Bulletin, v. 3, p. 165-182.

Campbell, R.B., McMillan, W.J., Mountjoy, E.W.,
Okulitch, A.V., Preto, V.A.G., and Read, P.B.
1976: Geology of Canadian Cordillera between Edmonton and Vancouver; Guidebook to field excursion C-11, Geological Association of Canada, Annual Meetings, Edmonton, Alberta.

Diebel, K.
1956: Conodonten in der Oberkreide von Kamerun; Geologie, v. 5, p. 424-450.

Eicher, D.B. and Mosher, L.C.
1974: Triassic conodonts from Sinai and Palestine; Journal of Paleontology, v. 48, p. 727-739.

Epstein, A.G., Epstein, J., and Harris, L.D.
1977: Conodont color alteration – an index to organic metamorphism; United States Geological Survey, Professional Paper 995.

Flügel, H. and Ramovš, A.
1970: Zur Kenntnis der Amphiclinenschichten Sloweniens; Geoloski Vjesnik, v. 23, p. 21-37.

Gupta, V.J. and Rafek, M.B.
1976: Middle and Upper Triassic conodonts from the Himalaya; Chayanica Geologica, v. 2, p. 196-214.

Hayashi, S.
1968: The Permian conodonts in chert of the Adoyama formation, Ashio Mountains, central Japan; Earth Science, v. 22, p. 63-77.

Huckriede, R.
1958: Die conodonten der mediterranen Trias und ihr stratigraphischer Wert; Palaontologische Zeitschrift, v. 32, p. 141-175.

Kozur, H. and Mostler, H.
1971: Probleme der Conodontenforschung in der Trias; Geologie und Palaontologie Mitteilungen Innsbruck, v. 1, p. 1-19.

Lindstrom, M.
1970: A suprageneric taxonomy of the conodonts; Lethaia, v. 3, p. 427-445.

Metcalfe, I., Koike, T., Rafek, M.B., and Haile, N.S.
1979: Triassic conodonts from Sumatra; Palaeontology, v. 22, p. 737-746.

Mosher, L.C.
1968: Triassic conodonts from western North America and Europe and their correlation; Journal of Paleontology, v. 42, p. 895-946.

1970: New conodont species as Triassic guide fossils; Journal of Paleontology, v. 44, p. 737-742.

1973: Triassic conodonts from British Columbia and the northern Arctic Islands; Geological Survey of Canada, Bulletin 222, p. 141-193.

Nogami, Y.
1968: Trias-Conodonten von Timor, Malaysien und Japan; Kyoto University, Faculty of Science, Series of Geology and Mineralogy, v. 34, p. 115-136.

Okulitch, A.V. and Cameron, B.E.B.
1976; Stratigraphic revisions of the Nicola, Cache Creek, and Mount Ida groups, based on conodont collections from the western margin of the Shuswap Metamorphic Complex, south-central British Columbia; Canadian Journal of Earth Sciences, v. 13, p. 44-53.

Rafek, M.B.
1977: Platform conodonts form the Middle Triassic Upper Muschelkalk of West Germany and Northeastern France; unpublished Ph.D. thesis, Institute of Paleontology, University of Bonn, Federal Republic of Germany.

Spassov, U.
1967: Paleozoic and Triassic conodont fauna from West Macedonia; Geological Institute of the Socialist Republic of Macedonia, v. 12, p. 23-32.

Sweet, W., Mosher, L.C., Clark, D., Collinson, J., and Hasenmüller, W.
1971: Conodont biostratigraphy of the Triassic; Geological Society of America, Memoir 127, p. 441-465.

Trammer, J.
1975: Stratigraphy and facies development of the Muschelkalk in the southwestern Holy Cross Mountains; Acta Geologica Polonica, v. 25, p. 179-216.

Trettin, H.P.
1980; Permian rocks of the Cache Creek Group in the Marble Range, Clinton area, British Columbia; Geological Survey of Canada, Paper 79-17.

Ziegler, W. (ed.)
1973: Catalogue of conodonts, vol. 1; Schweizerbart'sche Verlagsbuchhandlung, Stuttgart.

1975: Catalogue of conodonts, vol. 2; Schweizerbart'sche Verlagsbuchhandlung, Stuttgart.

1977: Catalogue of conodonts, vol. 3; Schweizerbart'sche Verlagsbuchhandlung, Stuttgart.

MINNES COAL, NORTHEASTERN BRITISH COLUMBIA

Project 780039

D.F. Stott and D.W. Gibson
Institute of Sedimentary and Petroleum Geology, Calgary

Stott, D.F. and Gibson, D.W., Minnes Coal, northeastern British Columbia; in Current Research, Part C, Geological Survey of Canada, Paper 80-1C, p. 135-137, 1980.

Abstract

Recent field and laboratory work within the Carbon Creek coal basin of northeastern British Columbia indicates that the thick coal-bearing rock succession (1100 m) may be mainly part of the Minnes Group and not the Gething Formation as formerly interpreted. Evidence now suggests that the coal-bearing strata represent a sequence that extends downward from within the lower Gething Formation, through the Cadomin Formation, and into the Minnes Group, the last including an unnamed unit at the top, the underlying Monach and Beattie Peaks formations, and the uppermost beds of the Monteith Formation. The succession contains in excess of 100 seams of coal varying in rank between high volatile and medium volatile bituminous, and ranging in thickness from a few centimetres to 4.3 m.

The consequences of this new interpretation thus increase the stratigraphic range and areal distribution of coal-bearing rocks not only in the Carbon Creek basin, but also in adjacent areas of the British Columbia Foothills.

Regional relationships reveal that, although facies belts within the Minnes Group may persist laterally for great distances along a north-south depositional trend, marked facies changes may occur within a few kilometres eastward across that trend.

The occurrence of important coal deposits in the strata of Carbon Creek basin of northeastern British Columbia (Fig. 14.1) is of current interest, not only in that area of the Foothills but, because of broader implications, it may also be of economic significance in other areas. The seams occur within a thick succession of Lower Cretaceous strata which have generally been assumed to be part of the Gething Formation, but which are now interpreted to be mainly part of the older Minnes Group.

Coals of the Carbon Creek area were discovered in 1911 by Cowper Rochfort, David Barr and George McAllister who subsequently acquired 10 square miles for development. Senator Patrick Burns became involved at an early stage and controlling interest eventually was held by the Burns Foundation. J.D. Galloway (1924), Mathews (1947) and Hughes (1964, 1967), of the British Columbia Department of Mines, examined the property at various times. Later, the property was acquired by Utah Mines Limited who made extensive investigations both by surface mapping and drilling between 1971 and 1976.

The nomenclatural problems related to the Lower Cretaceous succession were outlined by Stott (1967, p. 19) and will not be treated in any detail here, except where they relate to an understanding of the stratigraphy. Mathews (1947) divided the succession in Carbon Creek area into two parts: the lower or "Marine Bullhead" containing the Monteith, Beattie Peaks and Monach formations and the upper or "Nonmarine Bullhead", equivalent in part to the Gething Formation of Peace River but also including older beds. Stott (1967, p. 19; 1973) recommended that Mathews' three newly defined formations and an overlying unnamed coal-bearing unit[1] be included in the Minnes Group and that younger conglomerate and conglomeratic sandstone and succeeding coal-bearing strata be assigned to the Cadomin and Gething formations within a restricted Bullhead Group. Subsequent stratigraphic investigations have demonstrated the validity of the six-fold division of the sandy succession occurring above Jurassic Fernie shales in the region of Carbon Creek.

According to Mathews (1947, p. 19), the coal deposits "are confined to the continental beds of the Bullhead group". His continental beds included the Gething Formation and extended downward to the top of his newly defined Monach Formation. Mathews did not indicate the precise stratigraphic position of the seams, although he did state (p. 13) that seams

> "...occur in the continental beds as little as 300 feet (91 m) above their base, and several seams are known in the lower 2000 feet (610 m) of the succession, but thick seams are most common in the upper part of the coal measures..."

Hughes (1964), who examined the geology of Pine Valley and surrounding area, implied and later stated (1967, p. 87) that most of the mineable seams of that region occurred within the Gething Formation, but also recorded coal in underlying formations. The thick coal seams within the type Gething at Peace River were described by McLearn (1918, 1923), McLearn and Irish (1944), and Stott (1968, 1973). It was, therefore, assumed by some, including the writers, that the similar thick coal-bearing succession of the Carbon Creek basin also formed part of the Gething Formation.

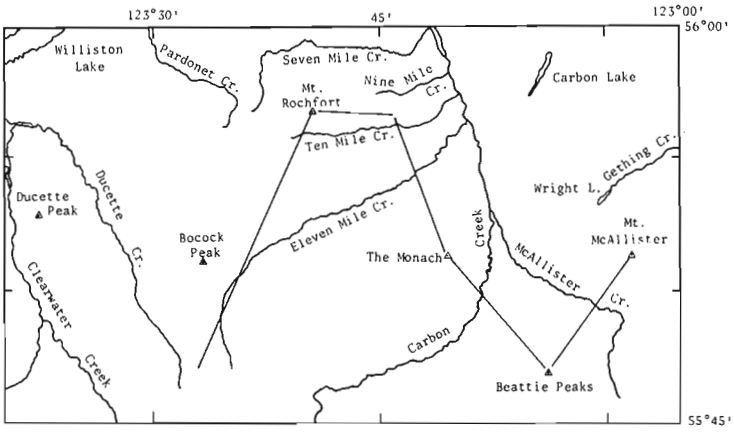

Figure 14.1. *Map showing location of line of section across Carbon Creek basin.*

[1] Definition of this unnamed formation, in accordance with the North American Code of Stratigraphic nomenclature, will be published shortly by Stott.

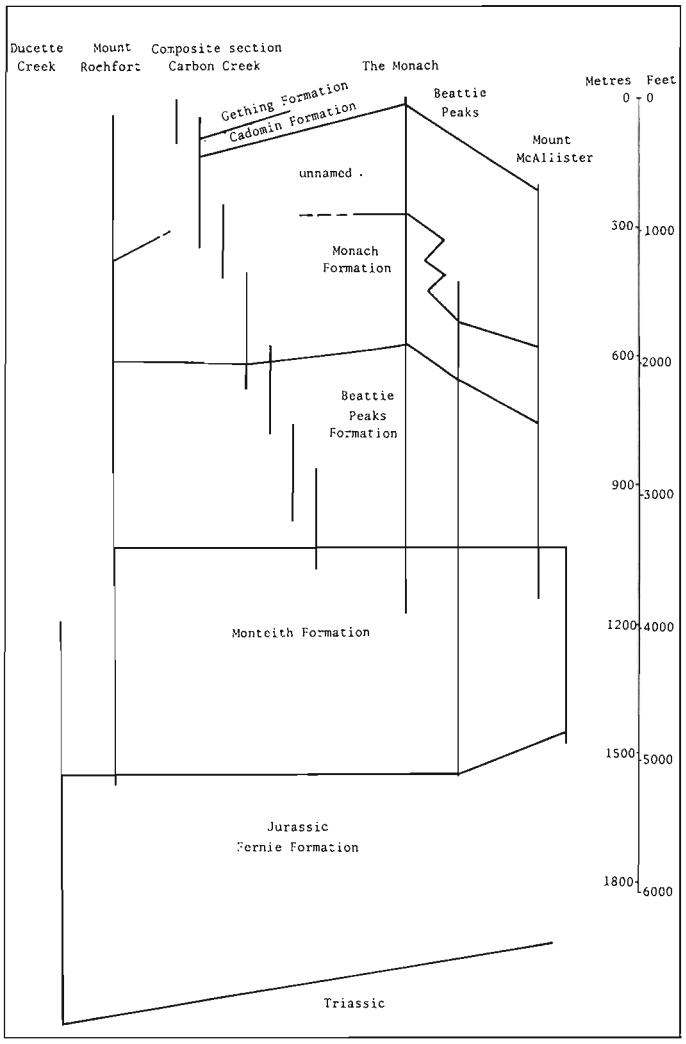

Figure 14.2. *Schematic diagram of Minnes Group illustrating thicknesses and stratigraphic relationships within Carbon Creek basin, northeastern British Columbia. (Based on descriptions by Gibson and Stott to be published shortly.)*

During a recent meeting (February 1980) held at Qualicum Beach, British Columbia, of coal geologists involved with the study and exploration of coal-bearing strata in the northeastern part of the province, R. Karst of the British Columbia Ministry of Mines and Petroleum Resources suggested that the thick coal-bearing succession in the Carbon Creek basin might not all be part of the Gething Formation and could possibly comprise part of the Minnes Group. Additional questions concerning regional relationships developed in discussions with R. Anderson of Utah Mines Limited. As a result the writers re-examined and re-evaluated field, subsurface, and laboratory data within and adjacent to the Carbon Creek basin and have concluded that most coal-bearing successions in the basin probably occur within the Minnes Group and not within the Gething Formation as previously assumed. Recently acquired lithologic samples from the Carbon Creek basin and adjacent areas are now being analyzed for their microfaunal content in order to support or disprove the new interpretation. The results of this work will be reported at a later date.

The consequences of this new interpretation of major coal occurrences within the Minnes Group of the Carbon Creek basin thereby increases the stratigraphic range and areal distribution of potential coal-bearing rocks not only in the basin but also in adjacent areas of British Columbia Foothills.

Regional stratigraphic investigations by Stott show the occurrence of thin coals throughout much of the Minnes Group, and have resulted in the development of a basic stratigraphic framework for that group (Stott, 1975b, in preparation). Recent studies by Karst (1978) and Gibson (in preparation) of cores taken by Utah Mines Limited within the Carbon Creek basin document the occurrence of numerous coal seams within a stratigraphic succession having a composite thickness of at least 1100 m (3600 ft). This work now provides a well defined geological setting for the coals of the Carbon Creek basin.

Recent observations within the Carbon Creek basin by Stott show the Cadomin Formation as occupying a more restricted area around the axis of the Carbon Creek syncline than previously assumed (Stott, 1969, 1975a, b), with a small area in the middle occupied by strata of the Gething Formation. Those beds are underlain, both to the east and west, by a continuous succession of the Minnes Group, ranging downward from the unnamed upper unit, through the Monach and Beattie Peaks formations to the basal Monteith Formation. The very low bedding attitudes within the central part of the syncline and the apparent lack of major structural complications appear to preclude the presence of any great thickness of Gething strata. Accordingly, many of the test holes drilled by Utah Mines Limited between 1971 and 1976 in the basin were in all probability spudded within the area underlain only by Minnes strata. Some of the holes were spudded only in the central area of the syncline where the surface bedrock is assigned to the Gething and Cadomin formations.

Gibson (in preparation) has completed a detailed examination of many cores from the boreholes, and with the co-operation of staff of Utah Mines Limited, has established a detailed correlation of the strata penetrated within Carbon Creek basin. The succession appears to correlate with surface sections measured and described by Stott (in preparation) on Mount Rochfort and surrounding ridges, Beattie Peaks, Mount McAllister and elsewhere adjacent to the basin (Fig. 14.1, 14.2). It now appears that the strata represent a sequence that extends downward from within the lower Gething Formation, through the Cadomin conglomerate, into the Minnes Group including the unnamed unit, Monach and Beattie Peaks formations, into the uppermost beds of the Monteith Formation. It is apparent also that the composite thickness of 1100 m (3600 ft), recorded from the cores, equates closely with the measured thickness of the upper Minnes interval determined from surface sections in the vicinity of Mount Rochfort and other nearby peaks.

The composite section, as reported by Karst (1978) and Gibson (in preparation), based on core from the Carbon Creek basin, contains in excess of 100 seams of coal ranging in thickness from a few centimetres to 4.3 m (14 ft), with 61 of those seams being greater than 0.3 m (1 ft) in thickness and 10 seams ranging between 0.9 and 4.3 m (3-14 ft) thick. The coal grades in rank between high volatile bituminous at the base of the Gething Formation (as now defined by the writers) to medium volatile bituminous near the base of the cored succession.

The conclusion reached from these studies indicates that at Carbon Creek the thickest seams were encountered in the upper part of the succession and that numerous thin seams occur through much of what now appears to be Minnes strata. Within the Minnes, coal is most abundant in strata equivalent to the "unnamed unit" but occurs as well within beds correlated with the Monach and Beattie Peaks formations.

Regional relationships reveal that, although facies belts within the Minnes Group persist laterally for great distance along a north-south depositional trend, marked changes occur within a few kilometres, in the eastward direction across that trend. Thus, although the Beattie Peaks Formation is dominantly marine mudstone and siltstone in an easterly belt extending from south of Goodrich Peak to north of Sikanni Chief River, it changes from that lithology at Mount McAllister and Mount Frankroy on the eastern side of Carbon Creek basin to sandier strata which contain nonmarine beds with thin coals at Mount Rochfort and in the cores from the area west of Carbon Creek. Similarly, marine sandstone of the Monach Formation thickens westward across the region and, on Mount Rochfort and in the coal property of Carbon Creek includes nonmarine intervals of coal-bearing rocks. Therefore, although only the "unnamed unit" appears to be coal-bearing throughout the region, parts of the Monach and Beattie Peaks formations also contain coal along the western side of Carbon Creek basin.

South of Pine River similar facies changes are evident and all the Minnes succession above the Monteith sandstone becomes increasingly continental toward the Monkman Pass map area (Stott, 1975a). In the southern area, the Beattie Peaks and Monach formations are not recognized and no marine strata are evident in the upper half to two-thirds of the group. A nonmarine unit with traces of coal occurs within the Monteith Formation at Mount Stephenson and on ridges west of Goodrich Peak in Pine Pass map area, and a few minor nonmarine shaly units occur within the Monteith at Mount Minnes.

The character of the Minnes Group north of Peace River was described in earlier reports by Stott (1967, 1969). In that region marine strata of the Beattie Peaks are still recognized. Beds equivalent to the Monach Formation and the "unnamed unit" were included in Units 2 and 3 respectively of strata included in the "Beattie Peaks and ?Younger Beds". Current studies assign Unit 2 to the Monach Unit and Unit 3 to the "unnamed unit". Only the latter appears to contain thin coals in that region.

The occurrence and recognition of potential economic coal deposits in the Minnes Group of the Foothills belt, especially in the area of the Carbon Creek basin, may be of economic interest in view of recent coal exploration developments in northeastern British Columbia. Strata of the Minnes Group occupy a large area of the surface bedrock of the Foothills belt. The distribution of the Minnes has been mapped on a reconnaissance basis within Dawson Creek, Pine Pass, and Monkman Pass map areas[1] (Stott, 1975a). It has been found also to the north in the Halfway and Trutch map areas (Stott, 1969). Although the coals within the Minnes are generally thin and perhaps of limited lateral extent, the Minnes succession, attaining a maximum thickness of 2100 m (7000 ft) and extending over many hundreds of square kilometres within the Foothills of northeastern British Columbia, is a potential target for coal exploration.

References

Galloway, J.D.
1924: Carbon River field; British Columbia Minister of Mines, Annual Report 1923, p. 140-141.

Hughes, J.E.
1964: Jurassic and Cretaceous strata of the Bullhead succession in the Peace and Pine River Foothills; British Columbia Department of Mines and Petroleum Resources, Bulletin 51, 73 p., 6 pls.

1967: Geology of the Pine Valley, Mount Wabi to Solitude Mountain, northeastern British Columbia; British Columbia Department of Mines and Petroleum Resources, Bulletin 52, 137 p., 6 pls.

Karst, R.H.
1978: Vitrinite reflectance as a correlation tool in the Carbon Creek coal measures (93 O/10,15); in Geological Fieldwork, British Columbia Department of Mines and Petroleum Resources, p. 73-77.

Mathews, W.H.
1947: Geology and coal resources of the Carbon Creek – Mount Bickford map-area, 1946; British Columbia Department of Mines, Bulletin 24, 27 p.

McLearn, F.H.
1918: Peace River section, Alberta; Geological Survey of Canada Summary Report 1917, pt. C, p. 14-21.

1923: Peace River Canyon coal area, British Columbia; Geological Survey of Canada, Summary Report 1922, pt. B, p. 1-46.

McLearn, F.H. and Irish, E.J.W.
1944: Some coal deposits of the Peace River Foothills, British Columbia; Geological Survey of Canada, Paper 44-15.

Stott, D.F.
1967: The Fernie and Minnes strata north of Peace River Foothills of northeastern British Columbia; Geological Survey of Canada, Paper 67-19, pt. A, 58 p.

1968: Lower Cretaceous Bullhead and Fort St. John Groups between Smoky and Peace Rivers, Rocky Mountain Foothills, Alberta and British Columbia; Geological Survey of Canada, Bulletin 152, 279 p.

1969: Fernie and Minnes strata north of Peace River, Foothills of northeastern British Columbia; Geological Survey of Canada, Paper 67-19, pt. B, 132 p.

1973: Lower Cretaceous Bullhead Group between Bullmoose Mountain and Fetsa River, Rocky Mountain Foothills, northeastern British Columbia; Geological Survey of Canada, Bulletin 219, 228 p.

1975a: Geological maps of parts of northeastern British Columbia and northwest Alberta. Compiled by D.F. Stott and G.C. Taylor. Wapiti (83 L) – Monkman Pass (93 T) – Pine Pass (93 O) – Dawson Creek (93 P); Geological Survey of Canada, Open File Report 286.

1975b: The Cretaceous System in northeastern British Columbia; in The Cretaceous System in the Western Interior of North America; W.G.E. Caldwell, ed., The Geological Association of Canada, Special Paper no. 13, p. 441-467.

[1] Mapping was done on a reconnaissance scale and as a second priority to the stratigraphic study. The authors recognize that errors may occur within the maps, owing to widely spaced observations, lack of adequate topographic maps and the availability of only poor quality photos at the time of the original work. Additions and/or corrections would be appreciated.

SCIENTIFIC AND TECHNICAL NOTES
NOTES SCIENTIFIQUES ET TECHNIQUES

PRELIMINARY PALEOMAGNETIC RESULTS FOR SAKAMI FORMATION REDBEDS NEAR LA GRANDE 4, QUÉBEC

Project 730160

E.J. Schwarz and G.N. Freda
Precambrian Geology Division

The belt of Proterozoic rocks (Circum-Ungava Belt) surrounding the eastern part of the Archean Superior Province have been the subject of a number of paleomagnetic studies (Fujiwara and Schwarz, 1975; Park, 1977; Schmidt, 1980; Seguin, 1977; Schwarz and Fujiwara, in preparation). Along the east coast of Hudson Bay, the results suggest that the lower volcanic series (Eskimo Formation) of the Belcher Islands is contemporaneous with the volcanics and redbeds (Nastapoka, Richmond Gulf, and Pachi groups) of Richmond Gulf and the Manitounuk Islands between Richmond Gulf and Poste de la Baleine (Schmidt, 1980; Schwarz and Fujiwara, in preparation). The Manitounuk Islands, Belcher Islands, Hopewell Islands and Cape Smith show the presence of a secondary magnetization (southwest, steeply down) which was probably acquired during the Hudsonian orogeny (Fujiwara and Schwarz, 1974; Schmidt, 1980; Schwarz and Fujiwara, in press). Results available from the Labrador Trough on the east side of the Superior Province are highly complex and their interpretation is uncertain (Park, 1977; Seguin, 1977).

The Superior Province carries Proterozoic sediments in several fault bounded basins. These rocks are essentially undeformed and of interest in uranium exploration. A paleomagnetic study of these rocks would provide useful results which might correlate with the results already available for

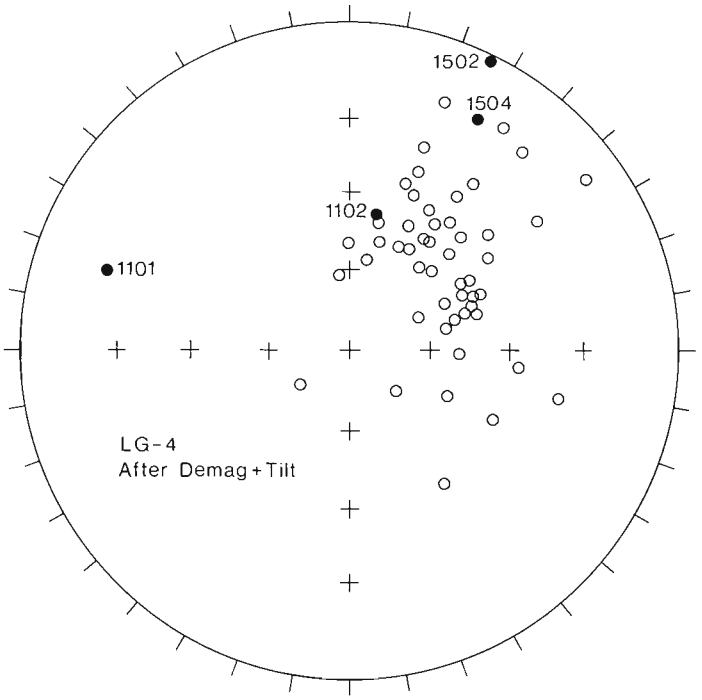

Figure 1. *All core directions after alternating field and/or thermal testing of stability of natural remanent magnetization. Beds rotated to horizontal. Open and closed symbols indicate directions up and down respectively (latter are indicated by site number followed by specimen number).*

Table 1

La Grande 4

	NRM							AFTER DEMAG				
SITE	N	n	D	I	K	α95	AF	T	D	I	K	α95
10	5	5	36	-42	63	9.7		620-670	37	-54	61	9.9
11	5	2	30	-38	45	38	300		28	-49	64	31
12	5	5	34	-51	15	20		660-670	35	-63	35	13
13	6	6	52	-15	14	18		660-670	41	-36	23	14
14	6	6	29	-97	46	10		660-670	21	-64	111	6.4
15	6	3	50	-26	8.2	46	300	670	63	-57	516	5.4
16	6	6	62	-57	12	20		660-670	63	-61	15	18
17	5	5	49	-63	5.7	35		660-670	50	-62	9.8	26
18	5	5	85	-38	7.6	30		660-670	66	-53	5.1	37
TILTED BEDS: Mean												
All Sites		9	59	-33	10	17			53	-47	20	12
All Samples		43	60	-34	6.7	9.2			64	-48	11	6.9
Pole Position			126.3°W		9.5°N							
AFTER TILT CORRECTION:												
All Sites		9	47	-43	17	13			45	-56	41	8.1
All Samples		43	48	-44	8.6	7.9			45	-56	14	5.9
Pole Position			108°W		9.7°N							

From: Scientific and Technical Notes in Current Research, Part C; Geol. Surv. Can., Paper 80-1C.

the Circum-Ungava Belt. From each of nine sites, 5 or 6 oriented drill cores were collected from the lower part (red silty sandstones) and middle part (orange coarse grained sandstones) of the Sakami Formation northwest and north of La Grande 4 in the James Bay Power project area. Each core yielded at least 2 specimens which were subjected to alternating field and thermal testing. The averaged results (Table 1) show that the magnetization direction is highly stable to testing in fields up to 600 oe and temperatures up to 670°C, hematite being the dominant remanence carrier in most cases. Rotating the beds to horizontal improves the grouping of directions noticeably suggesting that the magnetization was probably acquired during deposition while the faulting controlling the basins was still active. The tilt-corrected pole position comes to 108°W, 10°N, 9°, 6° (43 cores). This position is near Schmidt's (1980) results for the Haig intrusives and Flaherty volcanics which overlie the Eskimo volcanics in the Belcher Islands. The Sakami Formation would thus be younger than the Richmond Gulf volcanics and redbeds.

Acknowledgment

We thank the Société de Développement de la Baie James for their full co-operation in the field work stage of this study.

References

Fujiwara, Y. and E.J. Schwarz
1975: Paleomagnetism of the Circum-Ungava Belt (I): Cape Smith Komatiitic Basalts; Canadian Journal of Earth Sciences, v. 12, no. 10, p. 1785-1793.

Park, J.K.
1977: A reconnaissance paleomagnetic survey of the central Labrador Trough, Quebec; Canadian Journal of Earth Sciences, v. 14, p. 159-174.

Schmidt, P.W.
1980: Paleomagnetism of igneous rocks from the Belcher Islands, Northwest Territories, Canada; Canadian Journal of Earth Sciences, v. 17, p. 807-822.

Schwarz, E.J. and Fujiwara, Y.
Paleomagnetism of the Circum-Ungava Fold-belt II: Proterozoic rocks of Richmond Gulf and Manitounuk Islands. In: Proterozoic Basins in Canada, F.H.A. Campbell (Editor), Geol. Survey Canada, Special Paper. (in preparation).

Seguin, M.K.
1977: Paleomagnetism of metavolcanics and meta-gabbros of the north-central Labrador Trough; Acta. Cient. Venezolana, v. 20, p. 322-327.

LANTHANITE-(Nd), A NEW MINERAL FROM CURITIBA, PARANÁ, BRAZIL

Projects 680023 and 550101

A.C. Roberts[1], G.Y. Chao[2], and F. Cesbron[3,4]
Central Laboratories and Technical Services Division

Lanthanite-(Nd) is the neodymium-predominant member of the lanthanite group of rare-earth carbonate minerals, having the general formula $(RE)_2(CO_3)_3 \cdot 8H_2O$. The mineral name was assigned using the nomenclature for rare-earth minerals proposed by Levinson (1966). Both the mineral and its name were approved by the Commission on New Minerals and Mineral Names, I.M.A. Type material is presently preserved in the National Mineral Collection, Geological Survey of Canada, Ottawa, and in the Mineralogical Collection of the P. and M. Curie University, Paris.

Lanthanite-(Nd) occurs near Curitiba, Paraná, Brazil, as bright pink platy crystals in recent carbonate-rich sediments. Detailed data on occurrence, locality, and paragenesis are reported in Coutinho (1955) and in Cesbron et al. (1979). Mineralogical data have been reported previously by Coutinho (1955), Ansell et al. (1976) and Cesbron et al. (1979). This note presents, in tabular form, a compilation of pertinent mineralogical data obtained to date on lanthanite-(Nd); data not previously published are marked with an asterisk. We are extremely grateful to Carlos do Prado Barbosa, who provided nearly all the lanthanite-(Nd) which was examined by Roberts, Ansell, Pringle, and Chao, and to the Société Rhône-Poulenc for the rare-earth analysis.

Table 1

Crystallographic Data for Lanthanite-(Nd)

Crystal System	Orthorhombic mmm
a	9.476 (4) Å
b	16.940 (8) Å
c	8.942 (4) Å
*a:b:c	0.5594 : 1 : 0.5279
Space Group	Pbnb (56)
Cell Volume	1435.4 Å^3
Z	4
G (meas.)	2.81 (3) (by Berman balance)
*G (calc.)	2.816 for analytical formula

Table 2

Chemical Data for Lanthanite-(Nd)

	wt.%[1]	
Nd_2O_3	21.84	
La_2O_3	19.44	
Pr_2O_3	5.18	
Sm_2O_3	4.10	Analytical Formula:
Gd_2O_3	1.69	$(Nd_{0.397}La_{0.365}Pr_{0.096}Sm_{0.072}Gd_{0.029}$
Eu_2O_3	1.64	$Eu_{0.028}Dy_{0.007}Y_{0.006})_2(CO_3)_3 \cdot 8H_2O$
Dy_2O_3	0.44	Theoretical Formula:
Y_2O_3	0.22	$(Nd,La)_2(CO_3)_3 \cdot 8H_2O$
Ce_2O_3	0.03	with Nd>La
ThO_2	0.03	*Chemical Refractive Energy[2]
CO_2	22.15	= 0.2004 for analytical formula
H_2O	22.75	
Total	99.51	

[1] Relative proportions of rare earths determined by wet assay, total percentage of rare earths determined on 39 mg handpicked crystals; separate handpicked sample used to determine H_2O (by Penfield method) and CO_2.

[2] Constants from Mandarino (1976).

Table 3

Physical and Morphological Properties of Lanthanite-(Nd)

Occurrence:	as veneers of bright pink micaceous crystals in calcareous sandy clay sediments of the Curitiba formation of recent age (for more information see Cesbron et al., 1979).
Opacity:	transparent, but turns a dull milky white on exposure to the elements
Lustre:	vitreous to pearly
*Streak:	white
Hardness:	between 2.5 and 3
*Fluorescence:	nonfluorescent in both long- and short-wave ultraviolet light
Chemical Tests:	vigorous effervescence in dilute HCl
Morphological Characteristics:	well formed orthorhombic crystals are rare and do not exceed 2 mm in length; flattened on [010]; cleavage {010} perfect, {101} very good; forms present are {001}, {010}, {100}, {101}, {122} and {121}; (010) often shows striations due to twinning on [101]

[1] Associated authors are H.G. Ansell and G.J. Pringle.

[2] Department of Geology, Carleton University, Ottawa, Ontario, K1S 5B6.

[3] Laboratoire de Mineralogie-Cristallographie associé au C.N.R.S., Université P.-et M. Curie, 4 place Jussieu, 75230 Paris Cedex 05, France.

[4] Associated authors are M.C. Sichère, H. Vachey, J.P. Cassedanne and J.O. Cassedanne; the last two are at the Institut de Géosciences U.F.R.J. et Conseil national de Recherches, Rio de Janeiro, Brésil.

From: Scientific and Technical Notes in Current Research, Part C; Geol. Surv. Can., Paper 80-1C.

Table 4

X-ray Powder Data for Lanthanite-(Nd)

I/I_o	dÅ obs.	dÅ calc.	hkl	I/I_o	dÅ obs.	dÅ calc.	hkl
100	8.50	8.47	020	12	2.440	2.438	043
52	4.741	4.739	200	13	2.424	2.425	260
56	4.473	4.471	002	8	2.388	2.387	062
28	4.233	4.235	040	9	2.368	2.369	400
34	4.139	4.135	220	21	2.282	2.282	420
32	3.953	3.954	022	10	2.234	2.235	004
7	3.868	3.867	140	7	2.202	2.203	342
7	3.829	3.827	041	26	2.167	2.168	303
63	3.252	3.252	202			2.168	243
7	3.160	3.157	240	6	2.161	2.161	024
10	3.075	3.074	042	9	2.132	2.132	262
58	3.038	3.035	222	6	2.107	2.107	124
14	3.004	3.004	151	27	2.093	2.093	402
7	2.980	2.978	301	13	2.068	2.067	440
		2.977	241	9	2.050	2.053	352
7	2.926	2.925	142	29	2.032	2.032	422
7	2.846	2.843	103	18	2.022	2.023	253
12	2.823	2.824	060	16	2.013	2.014	441
9	2.810	2.810	321	11	1.978	1.977	044
12	2.707	2.706	160	19	1.966	1.967	224
15	2.691	2.692	061	6	1.936	1.935	144
6	2.638	2.635	331	23	1.876	1.876	442
30	2.579	2.579	242	12	1.825	1.826	353
6	2.551	2.550	312	8	1.812	1.812	423
6	2.531	2.532	340				

Guinier-de Wolff Nonius camera ($Cu\ K\alpha$, radiation), quartz added as an internal standard; indexed with a = 9.476Å, b = 16.940Å, c = 8.942Å.

Table 5

Optical Properties* of Lanthanite-(Nd)

Colour in transmitted light	colourless
Character	biaxial
Sign	negative
α	1.532(1)
β	1.590(1)
γ	1.614(1)
2V meas.	61°
2V calc.	63.5°
X	=b
Y	=c
Z	=a
Physical Refractive Energy(Kp)	0.2059 for G. (meas.)
1-(Kp/Kc)	0.0274[1]

Optical properties determined on two different crystals (previously oriented on a precession camera) using a spindle stage and a sodium vapour lamp as an illuminator, immersion liquids checked immediately after a match with an Abbé refractometer

[1] Classification of Mandarino (1979) indicates excellent compatability.

Table 6

Thermal Behaviour of Lanthanite-(Nd)

TGA/DTG maxima (heating rate 300°C/hour)	DTA maxima (heating rate 600°C/hour)	Interpreted Reaction
90°C	119°C	continuous loss of eight H_2O molecules
483°C	500°C	loss of two CO_2 molecules
677°C	766°C	loss of one CO_2 molecule

References

Ansell, H.G., Pringle, G.J., and Roberts, A.C.
1976: A hydrated neodymium-lanthanum carbonate from Curitiba, Parana, Brazil; in Current Research, Part B, Geological Survey of Canada, Paper 76-1B, p. 353-355.

Cesbron, F., Sichère, M.C., Vachey, H., Cassedanne, J.P., and Cassedanne, J.O.
1979: La lanthanite à europium de Curitiba, Paraná, Brésil; Bulletin de Minéralogie, v. 102, p. 342-347.

Coutinho, J.M.V.
1955: Lantanita de Curitiba, Parana; Univ. Sao Paulo, Fac. filosof., ciencias e letras, Bol. no. 186, Mineralogia no. 13, p. 119-126.

Levinson, A.A.
1966: A system of nomenclature for rare-earth minerals; American Mineralogist, v. 51, p. 152-158.

Mandarino, J.A.
1976: The Gladstone-Dale relationship. Part I: Derivation of new constants; Canadian Mineralogist, v. 14, p. 498-502.

1979: The Gladstone-Dale relationship. Part III: Some general applications; Canadian Mineralogist, v. 17, p. 71-76.

A PORTABLE WIND GENERATOR FOR FIELD USE

Project 770035

P. Egginton
Terrain Sciences Division

Introduction

A small wind generator was constructed to facilitate, by battery warming and charging, the extended use of soil temperature recorders in a study of slope processes at North Henik Lake, District of Keewatin.

Long term recorders are used in geomorphic process work to provide continuous information. Many of these can run for periods of 1 to 6 months if a suitable power source is available. Unfortunately acid or gel batteries, the most common power sources, discharge rapidly in cold temperatures. Discharge efficiencies at given temperatures for various batteries are available from most battery manufacturers. For example, a typical automotive battery rated at 50 ampere hours (at the 20 hour rate) might be expected to provide 150 A for 8 minutes at 27°C or for 4 minutes at -18°C, giving a service of 20 and 10 ampere hours, respectively; in other words only 50 per cent of the rated discharge is available at the lower temperature. From this it is clear that warming a battery that is in use in a low temperature environment can extend its serviceable life and/or the period between charging.

Conventional equipment and fuel available for charging and warming are bulky and expensive. Small wind generators provide an alternative power source. They are an attractive alternative particularily in areas above treeline as the sparse vegetation offers little resistance to wind passage, thus high towers are not necessary to tap the wind as an energy source.

This paper describes a low cost (less than $50) system used for charging and warming batteries.

Construction

The type of field work demanded that the generator be both portable and durable. These factors limited the windmill size, output, and degree of sophistication. On the basis of past field experience durability implies simplicity.

Generator. A Sturmey-Archer hub (ac) generator, readily available from bicycle speciality stores, was tested as a possible power source for the wind generator. One advantage of using this generator is that it produces a current regardless of the direction of generator rotation. A four watt Motorolla rectifier (MDA970-1) was used to make the generated current compatible with the battery (dc).

Generator voltage varies with the resistance, and for a given resistance it varies with generator rpm (Fig. 1). At 2700 rpm with a resistance of 1256 ohms the generator delivers 53 mA at 75 volts. Even at lower (200-300) rpm a useful potential is achieved. Since only a low current at six volts is required to trickle charge, the hub generator was selected for use.

Charging. As voltage varies with the rpm of the generator (Fig. 1), for charging purposes a 5000 ohm potentiometer was introduced to the system to facilitate the manual regulation of the voltage at the required six volts.

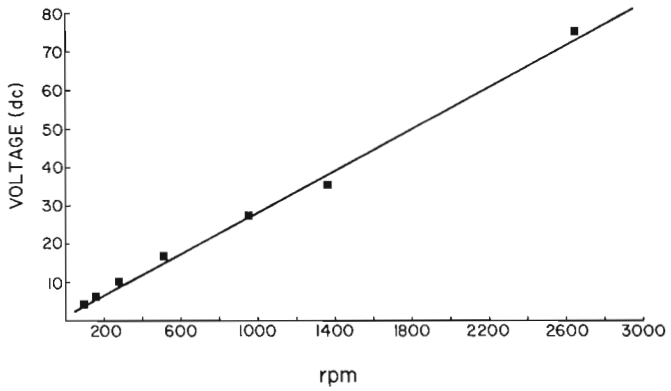

Figure 1. *Voltage produced by the hub generator, at various rpm at a fixed resistance of 1256 ohms, after being rectified.*

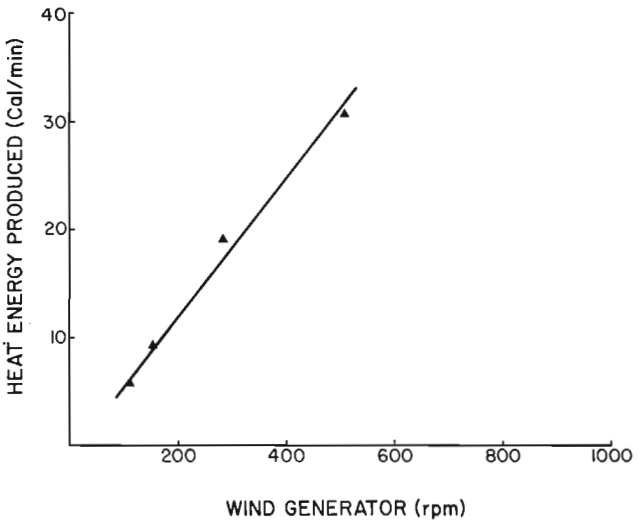

Figure 2. *Heat produced by the heating coil with the generator operating at various speeds.*

Warming. The battery warmer consisted of a well insulated box containing the battery and a heating coil, the latter being a 14 m length of enamel coated copper wire (0.0002 mm diameter) which was coiled inside the box. The thermal output of the heating coil with the generator operating at various speeds was determined in the laboratory. The heating coil was placed in a known quantity of water and the temperature change over time was recorded as a current was applied from the generator operating at a fixed speed. The heat produced varied with generator speed in a linear fashion over the rpm range investigated. At about 500 rpm 30 cal/min are produced (Fig. 2). This is sufficient heat to keep a 1000 cm^3 box, insulated with 10 cm of polyurethane, 12°C above external box temperature, assuming heat loss is only by conduction.

Windpower. One advantage of using the hub generator as a power source is that blades or arms can be attached directly to the hub, thereby avoiding gear or pulley systems. This is a definite bonus in terms of simplicity and ease of construction.

A vertical axis wind-generator was constructed but later abandoned in favour of a simpler multiblade design. The hub generator has a cogging action and some torque is required at low wind speed to initiate rotation.

From: Scientific and Technical Notes in Current Research, Part C; Geol. Surv. Can., Paper 80-1C.

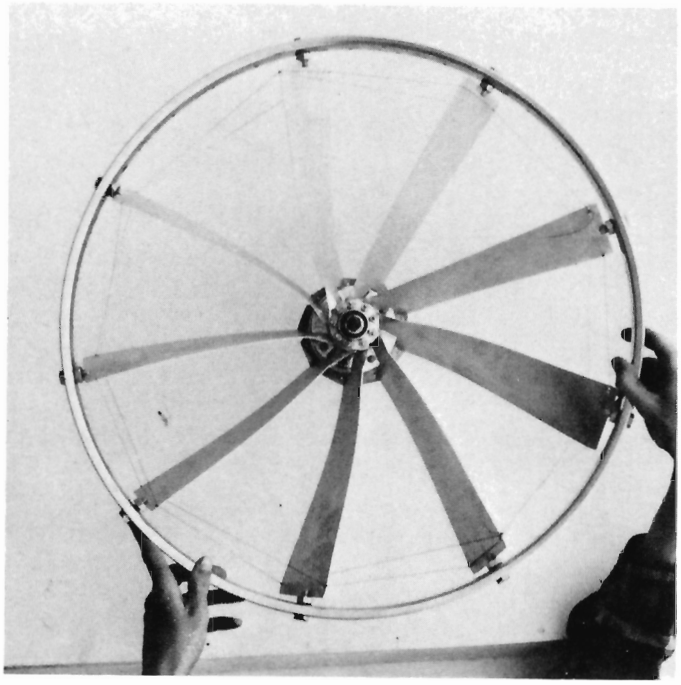

Figure 3. *A close up of the wind generator showing the blades mounted between split bolts on a bicycle rim. The blade pitch, once set, is fixed by a nylon line.*

The specific blade design was chosen arbitrarily. The blades were constructed form 1.0 mm thick aluminum sheet and were fixed to the hub by means of bolts. The blades are 20 cm in length and were temporarily attached to a 60 cm bicycle rim by a series of split bolts. This simple jig permitted the blades to be set at any desired pitch, in this case one of 20 degrees (Fig. 3). Nylon line was used as a webbing to secure the blades in position before the jig was removed.

For field use the wind generator was bolted to a 2.5 cm diameter, 1.5 m high mast (Fig. 4). The system was rigid; the wind generator could not swing into the wind; this was not a great disadvantage as the generator used operated irrespective of the direction of rotation. Further, the wind generator was oriented directly into prevailing winds which were frequent enough for warming or charging purposes.

For comparison, two similar systems incorporating the hub generator into a wind generator design have been described by Trunk (1974).

Operation and Evaluation

Performance. The wind generator starts in a 5 km/h wind and produces 6 to 12 volts at aobut 150 to 350 rpm, corresponding to a wind speed to 15 to 30 km/h (Fig. 1, 5). It is most efficient at wind speeds below 45 km/h; in higher winds one blade steals air from another preventing the system from reaching a higher rate of rotation. For example, on the basis of lower wind speed performance (Fig. 5) the generator may be expected to turn at about 850 rpm in winds of 70 km/h; however, only 700 rpm is achieved. This stealing feature, common to all multiblade systems, effectively prevents over-reving. But for this feature, centrifugal forces at high rpm could tear the system apart. The hub is sturdy and the wind generator survived winds in excess of 90 km/h in the field without the addition of a feathering mechanism.

Battery Warming. Extensive field tests on the battery warmer were not carried out. The purpose of the warmer

Figure 4. *The wind generator in operation, trickle charging uninsulated six volt batteries, North Henik Lake, District of Keewatin.*

was merely to add as much heat as possible to the battery box during the early spring when night temperatures dipped well below freeezing. The batteries, which had a 6 L volume, were covered with styrofoam, placed in a steel container, and covered with vermiculite. The thermal conductivity of the insulation, which was of uneven thickness, was not determined.

In one case over a 36 hour period when air temperatures did not rise above 0°C, battery box temperatues of 15°C were maintained. During this period winds were in excess of 50 km/h and the skies were clear. The ability of the battery warmer alone to maintain such temperatures is highly suspect. The external surface of the battery box was undoubtedly warmed by solar radiation. External surface temperatures of the box were not measured, nor is the contribution of heat released by the chemical reaction within the battery known.

On a seasonal basis the output from the wind generator undoubtedly helped to maintain battery box temperature several degrees above external air temperature. It is clear, however, that a higher output generator or an extremely well insulated box is necessary if substantial heating is required.

Battery Charging. Typically the wind generator was left attached to the battery warmer. When periodic visits to the site indicated that the potential of the battery had dropped, the generator was manually switched to charge the battery. The potentiometer was addjusted to ensure that a constant six volts was delivered to the battery. Charging took place over a 3 to 4 hour period while other field work was carried out in the area. The output was checked to ensure that it remained steady at the required six volts; few adjustments to the potentiometer were required as the winds commonly remained constant over the charging period.

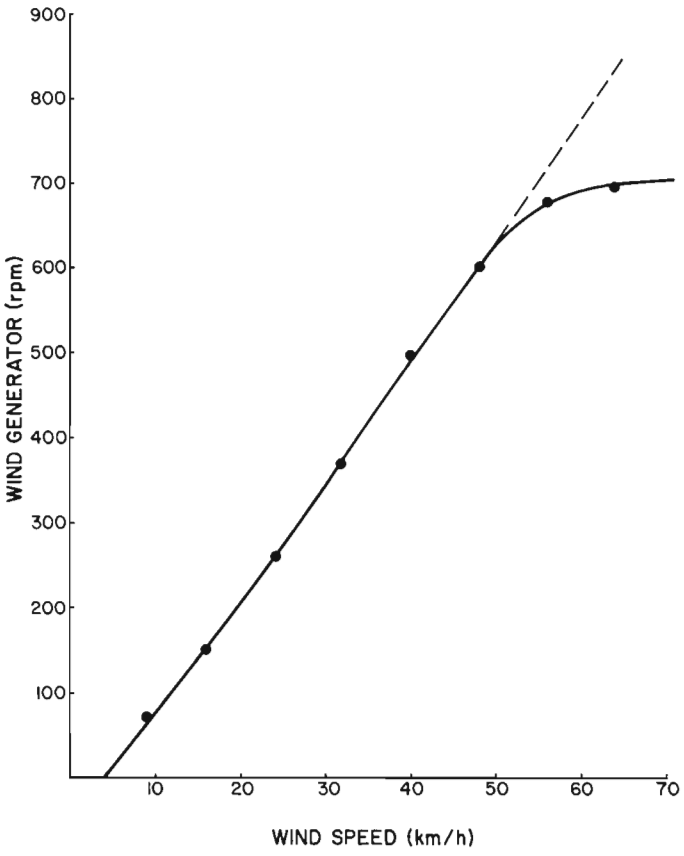

Figure 5. *Generator rpm as a function of wind speed (solid line) under a fixed load. The point where the dashed line and solid line diverge indicates the wind speed and generator rpm at which the blades begin to 'steal' significant quantities of air from each other (see text). Note that a wind of approximately 5 km/h is required for wind generator start up.*

Summary and Future Design Considerations

The wind generator proved useful for charging and marginally so for warming batteries. A larger output generator or better insulation is required for more effective warming.

A simple multiblade design was used for the wind generator. Systems incorporating a vertical axis and/or dual or tri-blade designs would be more efficient but somewhat more complex as they would require feathering mechanisms. For most purposes the fixed multiblade is probably a better choice, particularly in view of the cogging action of the generator used.

The system could be improved greatly by the addition of a regulator such as that used in automobiles. The wind generator could then charge the battery directly on demand. Excess output could be used to power a battery warmer, although if the battery is constantly trickle charged and if only low amperage demands are made on the battery, the warmer may be superfluous.

Acknowledgments

The author would like to thank personnel of the Electrical Methods Section, Resource Geophysics and Geochemistry, for their useful suggestions and comments during the early planning and construction of the wind generator.

References

Trunk, E.
1974: Free power from the wind; in Handbook of Homemade Power, Bantam Books, Inc., New York, p. 140-141.

A DEPENDABLE SHALLOW-WATER BOTTOM-MOUNTED CURRENT METER SYSTEM

Project 780027

John R. Harper[1] and Randolph Kashino[2]
Cordilleran Geology Division, Vancouver

Introduction

The coastal region has always provided a unique and challenging environment for installation, operation, and recovery of scientific instrumentation. This is particularly the case with measuring nearshore currents where instrumentation must discriminate wave-, tide-, and wind-induced currents as well as being capable of surviving in such a dynamic environment. Recent refinements of electromagnetic current meters (Appell, 1977; Heldebrant et al., 1978; Huntley, 1979) have provided a sensor capable of withstanding the rigors of the nearshore zone and of recording vector-averaged currents. This paper describes the unique deployment of a self-contained electromagnetic current meter for use in measuring wave-, wind-, and tide-induced currents in relatively shallow water (<12 m).

Acknowledgments

The current meter installation/recovery was sponsored by the Geological Survey of Canada through a contract to Dobrocky Seatech of Victoria, British Columbia. Ian Webster from Seatech suggested the unique idea of jetting the instrument into the bottom. The skipper and crew of the Fisheries vessel Pillar Rock provided invaluable support during the project as did diver Jim Dempsey.

Current Meter Description

The main features of the current meter (Marsh-McBirney, Model 585; Fig. 1, Table 1) are: (1) a two-dimensional electromagnetic sensor for resolving the x-y components of the current, (2) an electronic compass for resolving the x-y co-ordinates to north-south, east-west components, and (3) an internal microprocessor which controls data collection and permits teletype interfacing with the meter. Deployments of up to 270 days are possible.

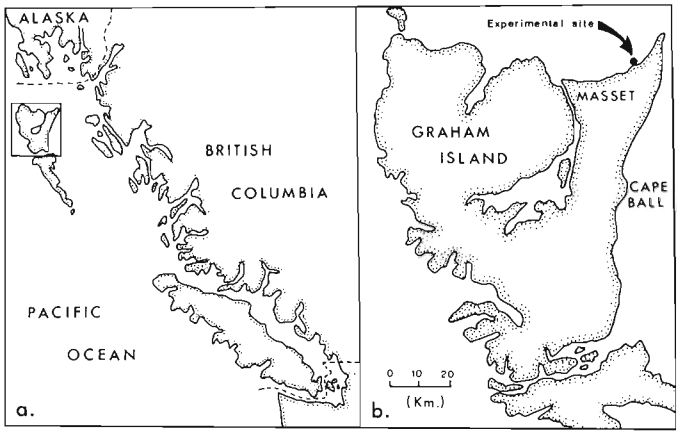

Figure 2. Locations maps of (a) Graham Island (Queen Charlotte Islands) and (b) the experimental site north of Graham Island.

The flexibility in programming sampling rate is especially well suited to shallow-water applications. The meter takes one velocity and direction sample per second, electronically averages the samples for the entire "on-time", and records the average on magnetic tape. This recorded average is then a vector average of the combined tide-, wind-, and wave-induced currents. Oscillatory wave motion is filtered out, but any net current produced by the waves is included in the vector average. The meter can be programmed to a raw data output and in fact, the manufacturer offers a wave data package which allows the meter to measure wave heights and to discriminate the direction of maximum orbital velocity (i.e. wave orthongonal direction) (Mulcahy, 1978). In its standard configuration, the meter offers a valuable tool for measuring the combined effects of wave-, wind-, and tide-induced currents on bottom sediment transport.

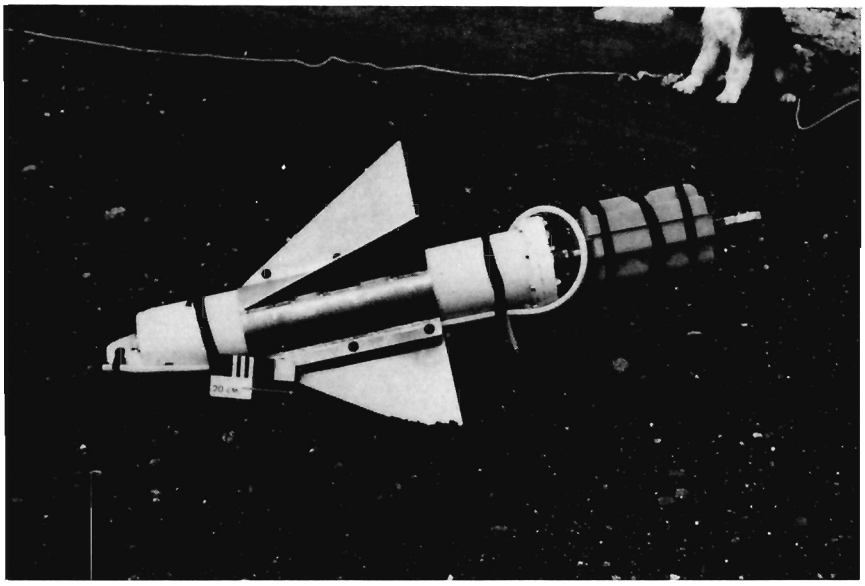

Figure 1. Photograph of meter prior to deployment showing lateral stability fins. The electromagnetic sensor has been covered to prevent damage during installation.

Table 1

Current Meter Specifications

PHYSICAL DIMENSIONS:		
Total Length	1.48	m
Pressure Case Length	0.97	m
Pressure Case Diameter	0.18	m
Sensor Diameter	0.10	m
Sensor Weight	41.	kg
Sensor Weight in Water	18.	kg
SENSITIVITY (MANUFACTOR SUPPLIED):		
Resolution	0.2	cm/sec
Range	±305	cm/sec

[1] Woodward-Clyde consultants, 16 Bastion Square, Victoria, B.C. V8W 1H9

[2] Dobrocky Seatech Ltd., 130 Kingston St., Victoria, B.C.

From: Scientific and Technical Notes in Current Research, Part C; Geol. Surv. Can., Paper 80-1C.

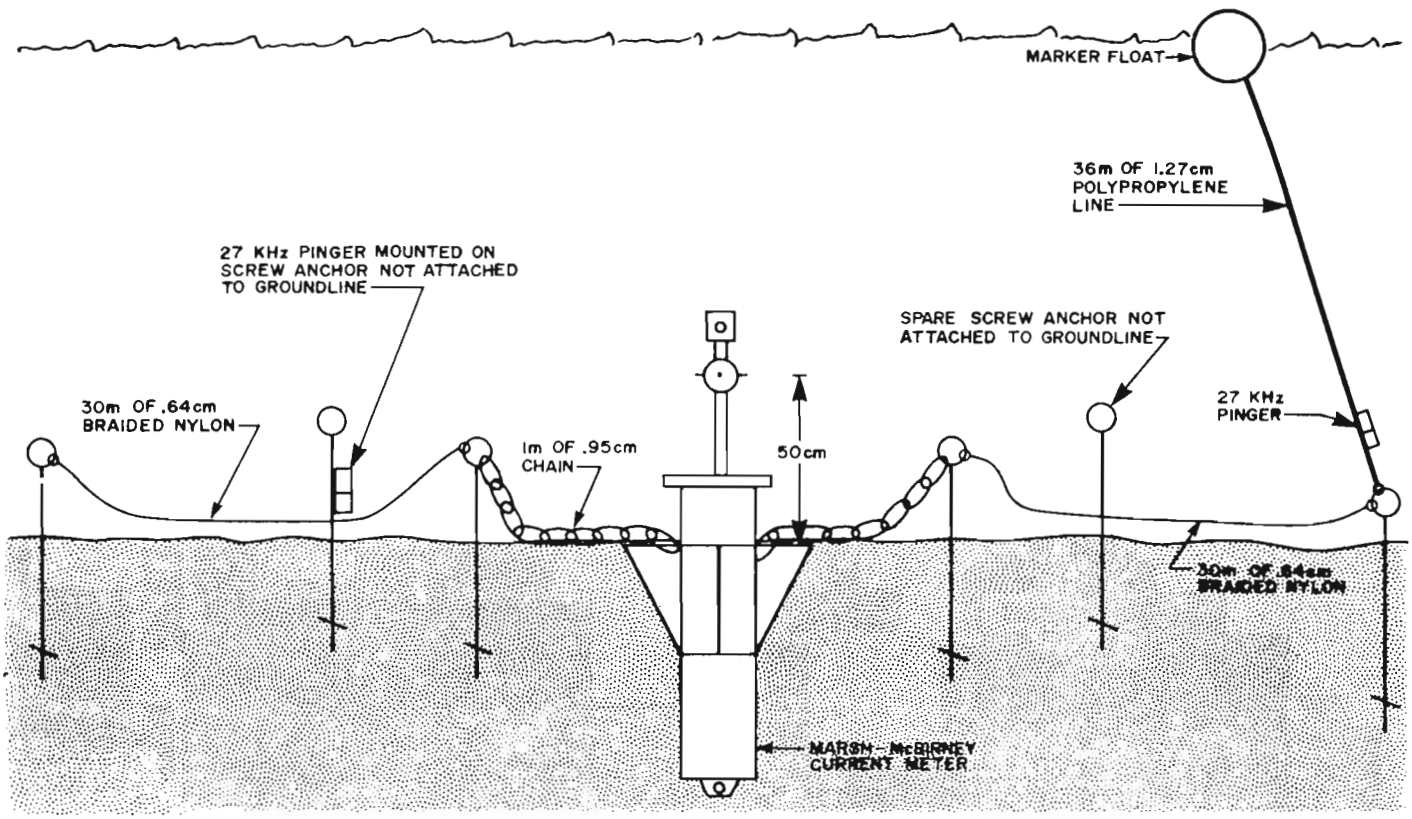

Figure 3. *Schematic diagram (the dimensions are not drawn to scale) of the deployment configuration.*

Deployment and Recovery

The experimental site was located on the northeastern shore of the Queen Charlotte Islands, British Columbia (Fig. 2). Earlier studies with seabed drifters suggested a net onshore sediment transport, and offshore sediment textures (cobble and boulder lags) indicate that sands deposited onshore were ultimately derived from offshore (Harper, 1980a, b). However, the onshore transport mechanism (that is, waves, winds or tides) was uncertain, and the experiment was a response to that problem.

The experimental site was in 12 m of water, 1.9 km from the shore. The bottom is composed of shelly fine sand with gravel-size shell fragments. Unfortunately no wave data were available for the area; simple hindcasting calculations suggest maximum wave heights may exceed 7 m, and significant wave heights frequently exceed 3 m. The site is also subject to Pacific swell propagating into Dixon Entrance.

The meter installation is schematically illustrated in Figure 3 and pictured in Figure 4. The meter was hydraulically jetted into the sand bottom to a depth of 0.82 m using a surface-powered pump. Fins on the meter provided additional lateral stability (Fig. 1), and the meter was secured via chains (Fig. 3, 4) to two 1.2 m long screw anchors (used in phone and light pole installations). Ground lines, two underwater pingers and a surface buoy were also installed to aid in diver relocation. Deployment of the current meter required 3.8 diver-hours (a diver hour is the amount of bottom time required to complete the work assuming only one diver is working).

The meter was recovered after 30 days (9 February to 10 March, 1980) in good condition. Divers reattached the surface float to the meter and also added a bouyancy float to provide lift to the meter. By exposing the fins, and lifting on the securing chains the meter was pulled form the bottom and eventually raised to the surface. Recovery of the meter required 1.3 diver hours.

At the time of recovery the current meter sensor was found to be free of seaweed fouling. A small, 10 cm deep scour depression on the south side of the meter was observed during recovery, and was probably produced by a net southerly current just prior to recovery.

Discussion

Unfortunately due to an electronic malfunction in the current meter recording mechanism, no currents were recorded. However the deployment itself proved successful and warrants further discussion. The current meter installation and recovery is of note because: (1) it was performed without the use of sophisticated equipment and the boat required no special preparation (sea state permitting, the operation could be performed from a large inflatable boat); (2) the meter configuration was stable and flow was unobstructed by tripod legs and (3) the sensor, located at 0.5 m above the bottom, provides an accurate measure of near-bottom currents.

The mooring configuration proved secure despite the meter location in a high wave energy region. Simple calculations indicate that the not uncommon 3 m high waves would

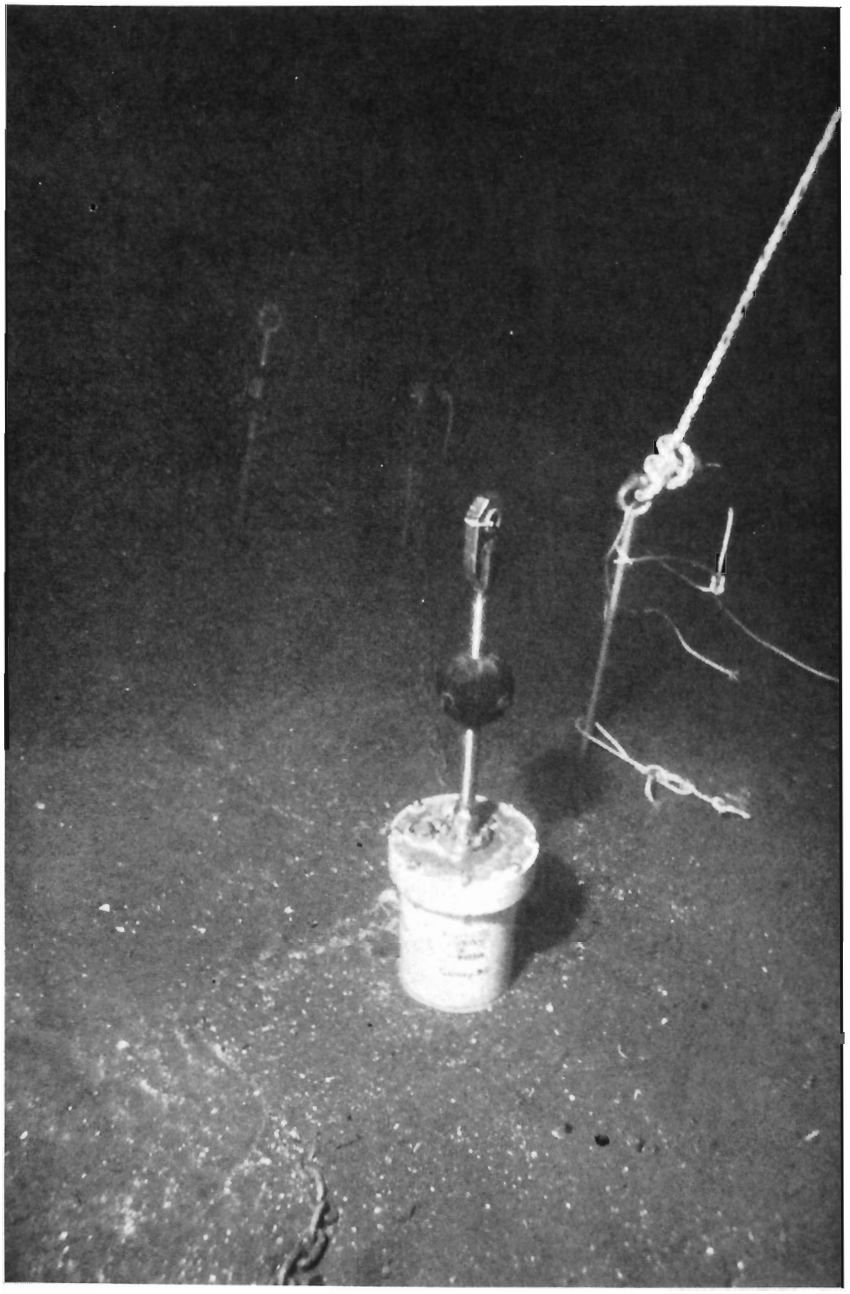

Figure 4. *Underwater photograph of the final installation showing the substrate, current meter sensor, and screw anchors. The screw anchor with line attached was used for locating the meter during installation and was removed immediately after the installation. Sensor is 10.2 cm (4 inches) in diameter.*

generate maximum bottom velocities of 0.87 m/s (1.7 knots) and that 7 m waves could generate bottom currents up to 2.0 m/s (3.9 knots). The stability of the mooring was due to the small size of the exposed portion of the meter. The total exposed cross-sectional area of the meter (Fig. 4) was 348 cm^2 whereas that of the buried portion was 2847 cm^2 (including fins) giving a low exposed: unexposed ratio (1:8). This advantageous exposure ratio allows the weight of the mooring configuration to be minimized; in this case, the weight of the meter in addition to the strength provided by the sediment was sufficient to secure the meter. The attachment of two screw anchors was prudent but proved unnecessary. The end result is a very secure, low-weight configuration which makes the system well suited to deployment in remote areas of limited logistical support.

No operational difficulties were encountered during this deployment or recovery, however changes in substrate elevations are a potential problem. Large changes of bottom elevation, which may occur quickly in the nearshore zone, could bury or alternately completely expose the meter, and caution should be exercised in use of this technique in areas where bottom changes are likely to exceed 0.5 m.

Summary

The bottom-mounted current meter system described herein is particularly well suited to shallow water high energy environments. Averaging algorithms of the meter allow reliable data collection in oscillatory flows, unlike conventional rotor or vane current meters, and the system combines the reliability of an electromagnetic current sensor (no moving parts and high sensitivity) with a unique yet functional deployment technique. By hydraulically jetting the meter into the bottom, only a small portion, primarily the sensor, is exposed to wave and/or current forces.

References

Appell, G.F.
1977: Performance of advanced ocean current sensors; Proceedings of Oceans '77 Conference, Los Angeles, California. (Marine Technology Society). Paper 30E.

Harper, J.R.
1980a: Coastal processes on Graham Island, Queen Charlotte Islands, B.C.; Geological Survey of Canada, in Current Research, Part A, Paper 80-1A, p. 13-18.

1980b: Coastal processes on Graham Island, Queen Charlotte Islands, B.C. (abstract); Geological Society of America, Cordilleran Section Meeting, Corvallis, Oregon.

Heldebrant, K.E., Test, L.S., and Micheland, E.D.
1978: The development and testing of current meters for long-term deployment on the continental shelf; Proceedings of Oceans '78 Conference, Washington, D.C. (Marine Technology Society), p. 308-314.

Huntley, D.A.
1979: Electromagnetic flowmeters in nearshore field studies; National Research Council, Workshop on Instrumentation for Currents and Sediments in the Nearshore Zone, p. 47-60.

Mulcahy, M.
1978: A solid state water current meter for wave direction sensing; Sea Technology, v. 19, no. 7, p. 14-16.

RADIOCARBON DATING OF DRIFTWOOD; INTER-LABORATORY CHECKS ON SAMPLES FROM NORDAUSTLANDET, SVALBARD

Project 570148

W.Blake, Jr.
Terrain Sciences Divison

Introduction

An important facet of the work of any radiocarbon dating facility is the cross-checking of samples between laboratories. It is customary, when a laboratory begins operation, to determine the age of a number of samples that have been dated previously in other institutions. A group of such inter-laboratory checks was duly reported in the first list of results produced by the Geological Survey of Canada Radiocarbon Dating Laboratory (Table 1 in Dyck and Fyles, 1962). Over the years a number of other samples have been cross-dated, and these have been reported in our annual compilations of age determinations (see especially the GSC-1802 series on a 25 000 year-old log from British Columbia (Lowdon and Blake, 1979).

Obviously a log provides the best material for cross-checking purposes, as then it is possible to supply identical samples to each laboratory. A good example is the dendrochronologically dated pieces (spanning about 10 years each) of bristlecone pine, **Pinus aristata**, which have been analyzed by the radiocarbon laboratories at the University of Arizona, Tucson, the University of California at San Diego, La Jolla, and the University of Pennsylvania, Philadelphia (Ralph et al., 1973). Shells or peat are less suitable materials as the peat may not be homogeneous and a collection of shells may contain individuals of different ages. Nevertheless, in all four examples listed below, good agreement was obtained, and the first three results show that determinations made early in the life of three different laboratories (Yale, Isotopes, and Saskatchewan), during the first decade of radiocarbon dating, have stood the test of time very well indeed.

Examples of Previous Cross-Checks

1. Peat moss (**Scorpidium scorpioides**; identified by M. Kuc) from Rossendale, Manitoba, originally dated by Yale University at 12 400 ± 420 years (Y-165; Preston et al., 1955), was recollected in 1969 by J.A. Elson and re-dated at 12 100 ± 160 years (GSC-1319; Lowdon et al., 1971).
2. **Portlandia arctica** shells (collected by J.G. Fyles and identified by F.J.E. Wagner) from the ground surface at Peel Point, Victoria Island, Northwest Territories, originally dated at 12 400 ± 320 years (I (GSC)-18; Walton et al., 1961), were re-dated at 12 600 ± 140 years (GSC-1707; Lowdon and Blake, 1976).
3. A single piece of charred **Quercus** sp. wood (collected by A. Dreimanis and identified by R.J. Mott) from clay exposed along the shore of Lake Huron at Blackwell, Ontario, originally dated by the Saskatchewan Research Council Laboratory at 4650 ± 200 years (S-24; McCallum and Dyck, 1960), was re-dated at 4660 ± 60 years (GSC-2186; Lowdon et al., 1977).
4. A single piece of **Picea** sp. wood (collected by A.V. Morgan and identified by L.D. Farley-Gill) from the sand overlying the Two Creeks forest bed, Wisconsin, originally dated by the University of Waterloo at 11 860 ± 110 years (Wat-57; Morgan and Morgan, 1979), was re-dated at 11 810 ± 100 years (GSC-2166; Lowdon and Blake, 1979). Both determinations correspond closely with the average age of the Two Creeks forest bed, given as 11 850 ± 100 years (Broecker and Farrand, 1963).

From: Scientific and Technical Notes in Current Research, Part C; Geol. Surv. Can., Paper 80-1C.

Data on Svalbard Driftwood

Unfortunately, such good agreement is not always the rule, as the results listed in Table 1 show. Following my field work in 1966 in northern Nordaustlandet, Svalbard, several sets of samples were sent to Gakushuin University, Tokyo, Japan, for dating. Many of the samples dated were pieces of driftwood logs which had been collected in association with a concentration of pumice on a particularly well developed raised beach. Earlier, several age determinations on driftwood associated with the same pumice horizon in northwestern Nordaustlandet had been carried out at the Institute of Physics, University of Uppsala, Sweden; the results ranged from 6330 ± 110 years (U-107) to 7030 ± 120 years (U-112; cf. Olsson, 1959, 1960; Blake, 1961; the differences from the published dates are the result of conversion to the NBS oxalic acid standard: I.U. Olsson personal communication, 1966). As the results started to accumulate, it became apparent that some determinations differed by a considerable amount from the earlier grouping; hence sample 8 (1958), a piece of wood that had been dated previously in Uppsala, was submitted to Gakushuin. The result (first line of Table 1) was not encouraging. Because the National Museum of Canada, Ottawa, was also purchasing some of its radiocarbon age determinations on archeological materials from Gakushuin at the time (cf. Wilmeth, 1969), a program of cross-checking was initiated.

Results and Discussion

The first two age determinations, GSC-1117 and -1345, were based on separate collections from the same log, made in 1958 and 1966, respectively; the results were discussed in detail in Lowdon et al. (1971). The discrepancy between GSC-1117 and GSC-1345 may well be because the parts of the log used for dating were not identical; however, the difference is no more significant than the varying results obtained for GSC-1345 when the same gas was counted in three different counters (Lowdon et al., 1971). These two determinations plus seven others (the exception is GSC-1728) all relate to the pumice horizon referred to earlier. All nine GSC determinations range between 6000 and 7000 years, i.e., only a slightly larger range than was the case with the original group of six dates from Uppsala (a seventh determination in Uppsala, to check a potential mix-up in the original group, gave a similar result: 6700 ± 70 years (U-618; Olsson et al., 1969; Blake, 1970). The Gakushuin dates vary over a much greater range, 3000 years instead of 1000. As reported in Lowdon et al. (1971), the fact that small amounts of carbon from previous samples were discovered at times to be adhering to the walls of the stainless steel 'reaction tubes' (K. Kigoshi, personal communication, 1969) may be the cause of the discrepancy between the Gakushuin age determinations and those run by Uppsala and the Geological Survey of Canada. Although a few of the results, such as GaK-1210 and GaK-1414, agree reasonably well with the GSC determinations, most do not (the Gakushuin determinations are quoted with a 1σ error term, the GSC values are given with 2σ).

From a theoretical point of view it is possible to have driftwood of various ages concentrated on a particular raised beach by means of a slight transgression or because of a balance between the rate at which the eustatic rise of sea level is proceeding and the rate at which the land is rebounding following removal of the ice load (cf. Blake, 1970, 1975). If we assume that all the driftwood reaches its destination with a minimum of delay, however, a considerable vertical interval (as much as several metres) on the beaches would be represented by wood that had drifted ashore over a 3000 year period, a much smaller interval for wood spanning only 1000 years. The less time that is represented by such an event, the more easily it can be accommodated. A transgression of the magnitude necessary to concentrate

Table 1

Radiocarbon age determinations on driftwood, northeastern Svalbard

Location	Co-ordinates	Approximate sample elevation (m)	Species[1]	Field sample No.	Gakushuin University Dating No.	Gakushuin Age[2] (uncorrected)	GSC Age[2,3] (uncorrected)	GSC Age[2,3] (corrected)	$\delta^{13}C$ ‰	GSC Dating No.
Vestre Tvillingneset	80°02.5'N,18°08'E	8	**Larix** sp.	8(1958)	GaK-1909	6910 ± 140	6180 ± 100	6240 ± 100[4]	-21.2	GSC-1117
	80°02.5'N,18°08'E	8	**Larix** sp.	193-66	GaK-1409	5350 ± 170	6340 ± 80	6390 ± 80[5]	-22.0	GSC-1345
East side Zordragerfjorden	80°26'N,22°50'E	12	**Populus** sp.	149-66	GaK-1415	4260 ± 90	6340 ± 70	6350 ± 70	-24.8	GSC-1521
	80°26'N,22°50'E	12	**Larix** sp.	148-66	GaK-1210	6450 ± 100	6570 ± 70	6580 ± 70	-24.1	GSC-1556
	80°23.5'N,22°50'E	13	**Pinus sylvestris**	152-66	GaK-1214	7330 ± 100	6960 ± 110	6990 ± 110	-22.8	GSC-1691
Søre Repøya	80°24.5'N,24°09'E	17	**Larix** sp.	182-66	GaK-1209	8220 ± 110	7900 ± 80	7940 ± 80	-22.4	GSC-1728
East side Zordragerfjorden	80°26'N,22°50'E	11.5	**Picea** sp.	146-66	GaK-1413	4950 ± 130	6270 ± 80	6290 ± 80	-23.5	GSC-1824
	80°26'N,22°50'E	12	**Picea** sp.	150-66	GaK-1337	5690 ± 120	5990 ± 80	6030 ± 80	-22.7	GSC-1951
	80°26'N,22°50'E	12	**Larix** sp.	147-66	GaK-1414	5800 ± 120	6030 ± 70	6010 ± 70	-26.2	GSC-2220
West side Rijpfjorden	80°07'N,21°52'E	14	**Picea** sp.	100-66	GaK-1215	5070 ± 100	6140 ± 60	6150 ± 60	-24.4	GSC-2441

[1] Identification of wood samples by R.J. Mott and L.D. Farley-Gill, Quaternary Paleoecology Laboratory, Geological Survey of Canada.

[2] All age determinations from both Gakushuin University (Kigoshi and Endo, 1963) and the Geological Survey of Canada are based on the Libby half-life for ^{14}C (quoted as 5570 ± 30 years or 5568 ± 30 years) and 0.95 of the activity of the NBS oxalic acid standard. Ages are quoted in conventional radiocarbon years before present where 'present' is taken to be 1950. All GSC finite age determinations are based on the 2σ criterion; i.e., there is a 95% probability that the correct age in conventional radiocarbon years lies within the stated limits of error; Gakushuin University dates are based on the 1σ criterion (68% probability). $^{13}C/^{12}C$ ratios were determined as follows: GSC-1117 to GSC-1728, Isotopes, Inc.; GSC-1824 and GSC-1951, Geological Survey of Canada; GSC-2220 and GSC-2441, University of Waterloo.

[3] From January 1963 through December 1972 all radiocarbon age determinations reported by the GSC quoted an age error calculated by using the following five factors: counting error of sample, background, and standard; the error in the half-life; and an error term to account for the average variation of ±1.5% in the ^{14}C concentration of the atmosphere during the past 1100 years, based mainly on the work of Willis et al. (1960) on tree rings from **Sequoia gigantea** and the work of Dyck (1965, 1966, 1967) on tree rings from Douglas fir **(Pseudotsuga menziesii).** More recent work on bristlecone pine **(Pinus aristata)** has extended the period covered by dated tree rings back to approximately 7500 years, and it has now become apparent that the variations in the ^{14}C concentration of the atmosphere are as large as 15% during this interval (Olsson, 1970; Damon et al., 1973). Thus, as of January 1973, the correction for fluctuations of atmospheric ^{14}C is no longer being applied to GSC radiocarbon age determinations (Lowdon and Blake, 1973), and all dates utilized in the present paper have been recalculated. This change does not affect the resultant date, but it reduces the error term assigned, hence the discrepancy between two of the dates discussed here and the values which have been published previously (cf. GSC-1117 and -1345; Lowdon et al., 1971).

[4] Uppsala age determination U-107: 6330 ± 110 years (recalculated from original value of 6200 ± 100 years; Olsson, 1960; Lowdon et al., 1971).

[5] Quebec age determination (as inter-laboratory check) QU-10: 6100 ± 210 years (P. LaSalle, personal communication, 1974).

material differing in age by 3000 years onto a single raised beach would have been a fairly major geological event. This event would have taken place some 4170 to 4350 years ago, according to the youngest Gakushuin date, but there is no record of a significant rise in sea level at this time in the diatom stratigraphy of low-lying lakes in northwestern Nordaustlandet (Häggblom, 1963; Hyvärinen, 1969).

In conclusion, the value to inter-laboratory checks cannot be overemphasized. As the examples given here illustrate, such checks are useful both to show that different laboratories are able to achieve identical results (and they may be using quite different analytical procedures and counting methods) and to help a laboratory pinpoint a source of error when the results do not agree.

Acknowledgments

The writer's participation in the Stockholm University Svalbard Expedition 1966 was sponsored by the Arctic Institute of North America with the approval and financial support of the U.S. Office of Naval Research under contract N00014-70-A-0219-0001 (subcontract ONR-377(1966)). Major funding for the expedition, led by Professors V. Schytt and G. Hoppe, came from the Swedish Natural Science Research Council. Norsk Polarinstitutt aided with logistical support. I am indebted to my colleagues R.J. Mott and L.D. Farley-Gill for identifying the driftwood, to J.A. Lowdon and associates for carrying out the age determinations, and to Lowdon and D.A. Hodgson for providing helpful comments on the manuscript.

References

Blake, W., Jr.
1961: Radiocarbon dating of raised beaches in Nordaustlandet, Spitsbergen, in Geology of the Arctic, ed. G.O. Raasch; Proceedings of the First International Symposium on Arctic Geology, Calgary, Alberta (January 1960); University of Toronto Press, p. 133-145.
1970: Studies of glacial history in Arctic Canada. I. Pumice, radiocarbon dates, and differential postglacial uplift in the eastern Queen Elizabeth Islands; Canadian Journal of Earth Sciences, v. 7, p. 634-664.
1975: Radiocarbon age determinations and postglacial emergence at Cape Storm, southern Ellesmere Island, Arctic Canada; Geografiska Annaler, Series A, v. 57A, p. 1-71.

Broecker, W.S. and Farrand, W.R.
1963: Radiocarbon age of the Two Creeks Forest Bed, Wisconsin; Geological Society of America Bulletin, v. 74, p. 795-802.

Damon, P.E., Long, A., and Wallick, E.I.
1973: Dendrochronologic calibration of the carbon-14 time scale; 8th International Conference on Radiocarbon Dating (Lower Hutt, New Zealand, October 1972), Proceedings, v. 1, p. A28-A43.

Dyck, W.
1965: Secular variations in the C^{14} concentration of Douglas fir tree rings; Proceedings of the 6th International Conference on Radiocarbon and Tritium Dating (Pullmann, Washington, 1965); U.S. Atomic Energy Commission, Conf-650652, p. 440-451.
1966: Secular variations in the ^{14}C concentration of Douglas fir tree rings; Canadian Journal of Earth Sciences, v. 3, p. 1-7.
1967: The Geological Survey of Canada radiocarbon dating laboratory; Geological Survey of Canada, Paper 66-45, 45 p.

Dyck, W. and Fyles, J.G.
1962: Geological Survey of Canada radiocarbon dates I; Radiocarbon v. 4, p. 13-26.

Häggblom, A.
1963: Sjöar på Spetsbergens Nordostland; Ymer 1963, no. 1-2, p. 76-105.

Hyvärinen, H.
1969: Trullvatnet: a Flandrian stratigraphic site near Murchisonfjorden, Nordaustlandet, Spitsbergen; Geografiska Annaler, Series A, v. 51A, p. 42-45.

Kigoshi, K. and Endo, K.
1963: Gakushuin natural radiocarbon measurements II; Radiocarbon, v. 5, p. 109-117.

Lowdon, J.A. and W. Blake, Jr.
1973: Geological Survey of Canada radiocarbon dates XIII; Geological Survey of Canada, Paper 73-7, 61 p.
1976: Geological Survey of Canada radiocarbon dates XVI; Geological Survey of Canada, Paper 76-7, 21 p.
1979: Geological Survey of Canada radiocarbon dates XIX; Geological Survey of Canada, Paper 79-7, 58 p.

Lowdon, J.A., Robertson, I.M., and Blake, W., Jr.
1971: Geological Survey of Canada radiocarbon dates XI; Radiocarbon, v. 13, p. 255-324.
1977: Geological Survey of Canada radiocarbon dates XVII; Geological Survey of Canada, Paper 77-7, 25 p.

McCallum, K.J. and Dyck, W.
1960: University of Saskatchewan radiocarbon dates II: American Journal of Science, Radiocarbon Supplement, v. 2, p. 73-81.

Morgan, A.V. and Morgan, A.
1979: The fossil Coleoptera of the Two Creeks forest bed, Wisconsin; Quaternary Research, v. 12, p. 226-240.

Olsson, I.U.
1959: Uppsala natural radiocarbon measurements I; American Journal of Science, Radiocarbon Supplement, v. 1, p. 87-102.
1960: Uppsala natural radiocarbon measurements II; American Journal of Science, Radiocarbon Supplement, v. 2, p. 112-128.
1970: Explanation of Plate IV; in Radiocarbon variations and absolute chronology, ed. I.U. Olsson; Proceedings of the 12th Nobel Symposium (Uppsala, Sweden, 1969); Wiley Interscience Division, New York, London, Sydney; Almqvist and Wiksell, Stockholm, p. 625-626.

Olsson, I.U., El-Gammal, S., and Göksu, Y.
1969: Uppsala natural radiocarbon measurements IX; Radiocarbon, v. 11, p. 515-544.

Preston, R.S., Person, E., and Deevey, E.S.
1955: Yale natural radiocarbon measurements II; Science, v. 122, p. 954-960.

Ralph, E.K., Michael, H.N., and Han, M.C.
1973: Radiocarbon dates and reality; MASCA Newsletter, v. 9, p. 1-20.

Walton, A., Trautman, M.A., and Friend, J.P.
1961: Isotopes, Inc., radiocarbon measurements I; Radiocarbon, v. 3, p. 47-59.

Willis, E.H., Tauber, H., and Münnich, K.O.
1960: Variations in the atmospheric radiocarbon concentration over the past 1300 years; American Journal of Science, Radiocarbon Supplement, v. 2, p. 1-4.

Wilmeth, R.
1969: Canadian archaeological radiocarbon dates; National Museum of Canada, Bulletin 232, Contributions to Anthropology VII: Archaeology, p. 68-126.

WHOLE ROCK Rb-Sr STUDIES IN THE GRENVILLE PROVINCE OF SOUTHEASTERN ONTARIO AND WESTERN QUEBEC – A SUMMARY REPORT

DSS Contract OSU78-00052

Keith Bell[1] and John Blenkinsop[1]
Precambrian Geology Division

Introduction

The Hastings Basin, within the Central Metasedimentary Belt of the Grenville Province, is an area in which the metamorphic grade is considerably lower than in the surrounding regions. For this reason, it has become an attractive area for both field and laboratory studies. Some of the questions that have been addressed include the identification of basement to the Grenville Supergroup, and relative timing of plutonism, deformation, and metamorphism.

The Central Metasedimentary Belt in southeastern Ontario includes intrusions of igneous rocks of different compositions. Although most rocks show various degrees of cataclasis and/or metamorphic recrystallization, parts of some igneous bodies have primary igneous textures preserved. Detailed mapping in the eastern Hastings Basin (Moore and Thompson, 1972, in press) has demonstrated that a major unconformity separates a younger psammite and pelite sequence (the Flinton Group) from older volcanic, sedimentary, and plutonic rocks. It was hoped that a whole rock Rb-Sr study from this area would answer questions concerning: (i) the existence of basement to the supracrustals; (ii) the age(s) of magmatic activity; (iii) the petrogenesis of the igneous bodies based on their initial Sr isotope ratios; and (iv) the age of the Flinton Group, which overlies both the Grenville Supergroup and plutons that intrude it.

Collections were made from several well-exposed bodies whose field relationships were known. Included among them were the Addington, Deloro, Elzevir, Hinchinbrooke, Mazinaw Lake, Mellon Lake, Moira Lake, Northbrook, Skootamatta, Weslemkoon, and White Lake plutons. Also included in the study was a suite from the Loranger syenite in Quebec. In addition, collections were made from the Tudor volcanics, the Radcliffe hybrid gneiss, and two suites each of Flinton Group pelites and possible basement granulites.

Results and Discussion

Analytical procedures have been described elsewhere (Bell et al., 1977). Errors are given at the two sigma level, and all ages quoted have been calculated using the decay constants recommended by Steiger and Jager (1977). Initial $^{87}Sr/^{86}Sr$ ratios have been adjusted to an Eimer and Amend value of 0.7080. The results reported here supersede those given in Davidson et al. (1979).

Table 1 summarizes the Rb-Sr weight ratios of almost 200 samples analyzed during the course of this study. In general the Rb-Sr ratios tend to conform to rock type. For example, the granodioritic plutons such as the Elzevir, Mellon Lake and Northbrook bodies tend to have Rb-Sr ratios less than 1, whereas the more potassic, granitic bodies, such as the Addington and Mazinaw Lake plutons, typically have ratios between 1 and 6. The greatest spread in Rb-Sr ratio, from about 1 to 20, is shown by samples collected from the Deloro stock; these include both peralkaline and granophyric material. In some cases, such as the Hinchinbrooke gneiss and the White Lake pluton, the Rb-Sr ratios were so restricted in range (less than 0.05) that no further work was attempted on these bodies.

The whole rock Rb-Sr isochron data are summarized in Table 2. For most of the isochrons, it was necessary to exclude some of the points in order to obtain an acceptable MSWD (mean square of weighted deviates, Brooks et al., 1972). The practice of excluding those points that do not fit the isochron is not uncommon in Rb-Sr geochronology, especially when the samples are from high-grade metamorphic terranes. In almost all cases the samples omitted were those with higher Rb-Sr ratios. There are only two cases (one of the two granulite suites, and the samples from the Loranger syenite) where all data have been used.

Table 1

Ranges of Rb-Sr weight ratios for the suites studied

	Unit	Range	No. of Samples
possible basement	Barry's Bay, "west suite"	0.04 - 0.37	6
	Barry's Bay, "south suite"	0.03 - 0.23	5
	Radcliffe hybrid gneiss	0.01 - 0.41	11
	Tudor metavolcanics	0.01 - 3.3	19
older granodiorite plutons	Elzevir	0.08 - 0.92	16
	Hinchinbrooke	0 - 0.05	12
	Mellon Lake	0.04 - 1.0	10
	Northbrook	0.07 - 0.26	12
	Weslemkoon	0.06 - 0.16	11
	White Lake	0.05 - 0.09	8
granitic plutons	Addington	1.2 - 5.4	11
	Mazinaw Lake	0.92 - 5.7	7
	Deloro	0.6 - 20	27
	Loranger	0.07 - 0.33	10
	Moira Lake	0.01 - 3.6	8
	Skootamatta	0.01 - 0.29	10
	Flinton pelite 1	1.3 - 2.7	5
	Flinton pelite 2	0.29 - 1.7	5

[1] Department of Geology, Carleton University, Ottawa K1S 5B6

From: Scientific and Technical Notes in Current Research, Part C; Geol. Surv. Can., Paper 80-1C.

Table 2

Summary of isochron data

Unit	Age (Ma)	Initial Ratio*	Comments
Barry's Bay, "west suite"	1430 ± 20	0.7032 ± 0.0001	6 points; MSWD:1.0
Barry's Bay, "south suite"	1090 ± 90	0.7034 ± 0.0002	4 of 5 points; MSWD:0.7
Radcliffe hybrid gneiss	1020 ± 70	0.7041 ± 0.0007	4 of 5 points; MSWD:1.3
Tudor metavolcanics	1250 ± 90	0.7029 ± 0.0004	7 of 13 points; low Rb-Sr MSWD:1.6
Elzevir	1240 ± 50	0.7020 ± 0.0005	4 of 5 points; MSWD:0.7
Mellon Lake	1120 ± 90	0.7019 ± 0.0006	5 of 7 points; MSWD:2.0
Northbrook	1030 ± 120	0.7032 ± 0.0008	4 of 5 points; MSWD:0.5
Addington	1060 ± 30†	0.7068 ± 0.0014†	3 of 6 points; MSWD:0.3
Mazinaw Lake	1185 ± 25	0.699 ± 0.002	4 of 5 points; MSWD:0.4
Loranger	1120 ± 60	0.7030 ± 0.0005	5 points; MSWD:1.9
Skootamatta	1020 ± 50	0.7032 ± 0.0003	4 of 5 points; MSWD:2.4

* adjusted to Eimer and Amend $^{87}Sr/^{86}Sr = 0.7080$

† tentative value

The important findings to date are as follows:

i) An age of 1430 ± 20 Ma obtained from six samples of a granulite lying less than 8 km to the west of the westerly margin of the Grenville Supergroup, near Barry's Bay. This age is in general agreement with some other values from the Ontario Gneiss Segment (Krogh et al., 1968; Krogh and Davis, 1969; Davis et al., 1970; Krogh et al., 1971), and from the Central Granulite Terrain (Barton and Doig, 1973). For the present we prefer to regard this date as corresponding to a metamorphic event, although much further work is required before this interpretation can be accepted.

ii) Basic and intermediate volcanism during the early stages of the deposition of the Grenville Supergroup at about 1250 Ma ago. The new Rb-Sr isochron age is in good agreement with an earlier U-Pb age of 1286 ± 15 Ma (Silver and Lumbers, 1966) on zircons from the Tudor Formation.

iii) Early granodioritic magmatism at about 1240 ± 50 Ma (the Elzevir pluton). Similarity in both initial $^{76}Sr/^{86}Sr$ ratios and age between the Elzevir pluton and the Tudor volcanics could be used as evidence in support of a cogenetic relationship. Again both U-Pb (Silver and Lumbers, 1966) and Rb-Sr ages agree well within analytical uncertainties.

iv) Extensive plutonism between 1250 and 1050 Ma ago. There is some indication from the isotopic data that the Loranger syenite and the Addington granite may well reflect periods of magmatism at about 1100 Ma, subsequent to the emplacement of the Elzevir and related plutons.

v) Relatively low initial $^{87}Sr/^{86}Sr$ ratios of about 0.7020 ± 0.0008, consistent with values from other plutons of Proterozoic age (Bell et al., 1979). These ratios do not reflect any significant continental component of the type to be expected from the reworking of old continental crust. Only the provisional initial ratio from the Addington pluton of 0.7068 ± 0.0014 is significantly higher than the remainder, and if valid may point to either a more complex history or even a different origin, perhaps one that involved crustal reworking.

vi) A possible maximum depositional age of about 1100 Ma for the Flinton Group, since the latter contains clasts of Northbrook-like material (Psutka, 1976) and clasts derived from the Addington pluton, and is not cut by any of the granitoid bodies.

Conclusion

At least three events at about 1430 Ma, 1250 Ma and perhaps 1100 Ma are indicated by the isotopic data. If the granulites north of Barry's Bay are considered older than the Grenville Supergroup, then the latter was deposited after about 1400 Ma. Extensive plutonism and basic volcanism started at about 1250 Ma and ended at about 1100 Ma. Late-stage pegmatites (Silver and Lumbers, 1966) and plutons (Krogh and Hurley, 1968) at about 1000 Ma marked the final period of igneous activity associated with the Grenville Province.

References

Barton, J.M. Jr. and Doig, R.
1973: Time-stratigraphic relationships east of the Morin anorthosite pluton, Quebec; American Journal of Science, v. 273, p. 376-384.

Bell, K., Blenkinsop, J., and Strong, D.F.
1977: The geochronology of some granitic rocks from eastern Newfoundland and its bearing on Appalachian evolution; Canadian Journal of Earth Sciences, v. 14, p. 456-476.

Bell, K., Blenkinsop, J., and Watkinson, D.H.
1979: Geochronology of alkalic complexes, Ontario; Ontario Geological Survey, Miscellaneous Paper 87, p. 69-78.

Brooks, C., Hart, S.R., and Wendt, I.
1972: Realistic use of the two-error regression treatments as applied to rubidium-strontium data; Reviews of Geophysics and Space Physics, v. 10, p. 551-577.

Davidson, A., Britton, J.M., Bell, K., and Blenkinsop, J.
1979: Regional synthesis of the Grenville Province of Ontario and western Quebec; in Current Research, Part B, Geological Survey of Canada, Paper 79-1B, p. 153-172.

Davis, G.L., Krogh, T.E., Hart, S.R., Brooks, C., and Erlank, A.J.
1970: The age of metamorphism in the Grenville Province, and the age of the Grenville Front; Carnegie Institute of Washington Yearbook 68, p. 307-314.

Krogh, T.E. and Davis, G.L.
1969: Geochronology of the Grenville Province; Carnegie Institute of Washington Yearbook 67, p. 224-230.

Krogh, T.E. and Hurley, P.M.
1968: Strontium isotope variations and whole rock isochron studies in the Grenville Province of Ontario; Journal of Geophysical Research, v. 73, p. 7107-7125.

Krogh, T.E., Davis, G.L., Aldrich, L.T., Hart, S.R., and Steuber, A.
1968: Geological history of the Grenville Province; Carnegie Institute of Washington Yearbook 66, p. 528-536.

Krogh, T.E., Davis, G.L., and Frarey, M.J.
1971: Isotopic ages along the Grenville Front in the Bell Lake area, southwest of Sudbury, Ontario; Carnegie Institute of Washington Yearbook 69, p. 337-339.

Moore, J.M., Jr. and Thompson, P.H.
1972: The Flinton Group, Grenville Province, eastern Ontario; 24th International Geological Congress, Proceedings, Section 1, p. 221-229.

The Flinton Group: A late Precambrian metasedimentary succession in the Grenville Province of eastern Ontario; Canadian Journal of Earth Sciences. (in press)

Psutka, J.F.
1976: Provenance of the plutonic pebbles in the Kaladar metaconglomerate and geology of the associated metasediments; unpublished B.Sc. thesis, Carleton University, Ottawa, Ontario, 62 p.

Silver, L.T. and Lumbers, S.B.
1966: Geochronological studies in the Bancroft – Madoc area of the Grenville Province, Ontario; Geological Society of America, Special Publication 87, p. 156.

Steiger, R.H. and Jager, E.
1977: Subcommission on Geochronology: Convention on the use of decay constants in geo- and cosmochronology; Earth and Planetary Science Letters, v. 36, p. 359-362.

BASE METAL AND URANIUM CONCENTRATIONS IN TILL, NORTHERN BOOTHIA PENINSULA, DISTRICT OF FRANKLIN

Project 750071

Arthur S. Dyke
Terrain Sciences Division

Introduction

Till samples from the northern half of Boothia Peninsula have been analyzed for base metal and uranium contents. Twenty-two samples collected in 1974 were analyzed for Cu, Pb, Zn, Co, Ni, and U; 280 samples collected in 1978 were analyzed for these elements plus Cr, Mo, Mn, and Fe. Shilts and Klassen (1976) have reported on the uranium content of the 1974 samples.

This note presents contour maps and histograms for each element and relates findings to the local geology to the extent possible.

Method

In two areas, samples were collected at 1 to 2 km intervals during ground traverses; elsewhere samples were collected at roughly 10 km intervals during helicopter traverses.

Most samples were collected 10 to 20 cm beneath the unvegetated surfaces of active mudboils, a technique developed during extensive drift prospecting in central District of Keewatin (Shilts, 1973; Klassen and Shilts, 1977). Because of cryoturbation (mudboiling) of till, material near the surface is as little weathered as material just above the permafrost table. Blebs and streaks of oxidized material occur throughout the active layer, but in most cases these were avoided.

The clay fractions (<2 μm) of the samples were separated by centrifugation at the Geological Survey of Canada Sedimentology Laboratory. Shilts (1975) has found that this is the best size fraction for trace element analysis

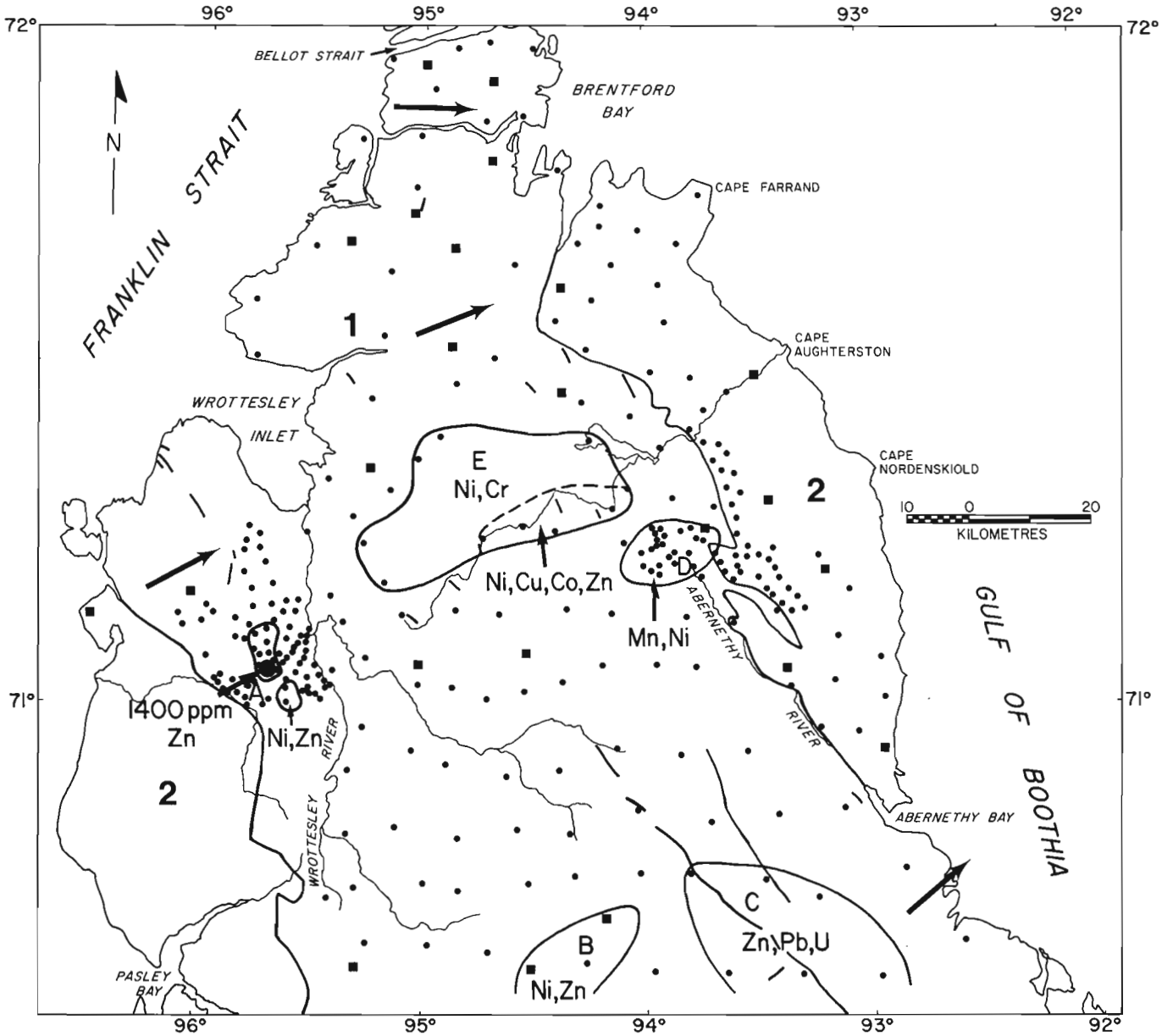

Figure 1. *Areas with concentration of anomalous samples; most persistent anomalies noted (see Table 2). Arrows show generalized ice flow directions during last glacial maximum. Squares are 1974 samples, dots are 1978 samples. Area 1 is Precambrian gneiss, Area 2 is lower Paleozoic carbonate rock. Precambrian/Paleozoic contact and dykes are shown by heavy black lines.*

From: Scientific and Technical Notes in Current Research, Part C; Geol. Surv. Can., Paper 80-1C.

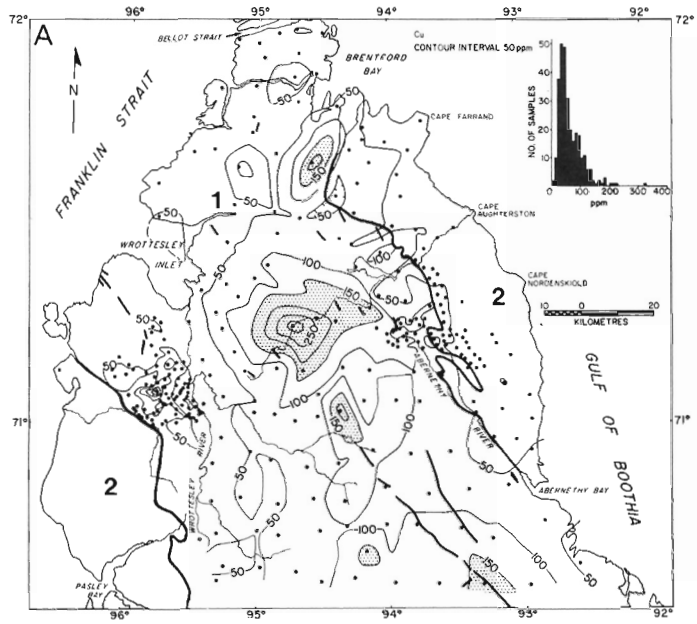
A
Co
CONTOUR INTERVAL 50 ppm
FRANKLIN STRAIT
BELLOT STRAIT
BRENTFORD BAY
CAPE FARRAND
CAPE AUGHERSTON
CAPE NORDENSKIOLD
WROTTESLEY INLET
GULF OF BOOTHIA
ABERNETHY BAY
PASLEY BAY
NO. OF SAMPLES
ppm
KILOMETRES

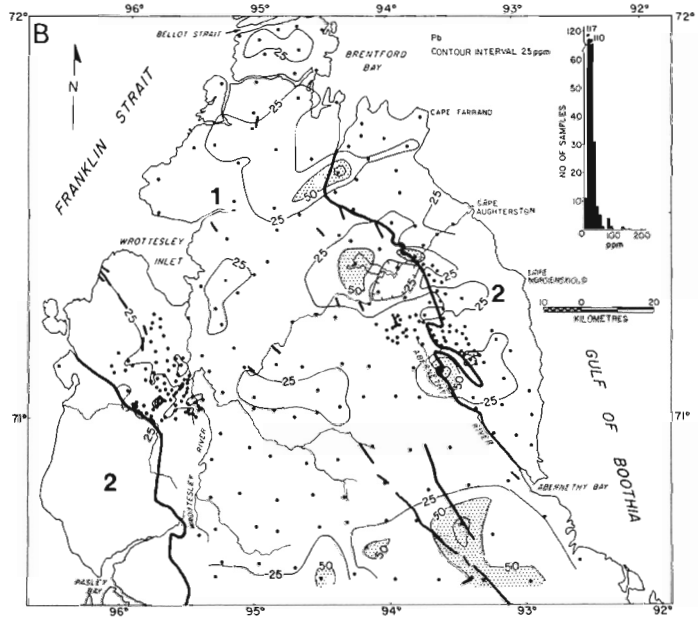
B
Pb
CONTOUR INTERVAL 25 ppm
FRANKLIN STRAIT
BELLOT STRAIT
BRENTFORD BAY
CAPE FARRAND
CAPE AUGHERSTON
CAPE NORDENSKIOLD
WROTTESLEY INLET
GULF OF BOOTHIA
ABERNETHY BAY
PASLEY BAY
NO. OF SAMPLES
ppm
KILOMETRES

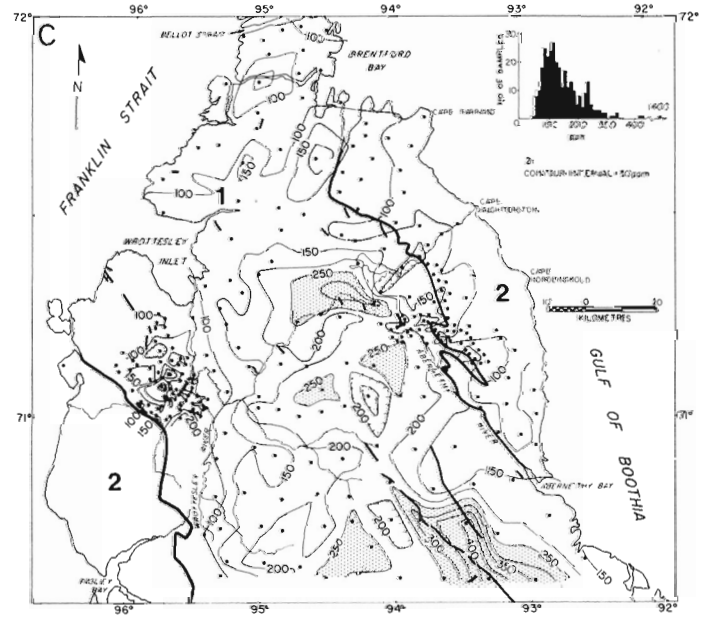
C
Zn
CONTOUR INTERVAL 50 ppm
FRANKLIN STRAIT
BELLOT STRAIT
BRENTFORD BAY
CAPE FARRAND
CAPE AUGHERSTON
CAPE NORDENSKIOLD
WROTTESLEY INLET
GULF OF BOOTHIA
ABERNETHY BAY
PASLEY BAY
NO. OF SAMPLES
ppm
KILOMETRES

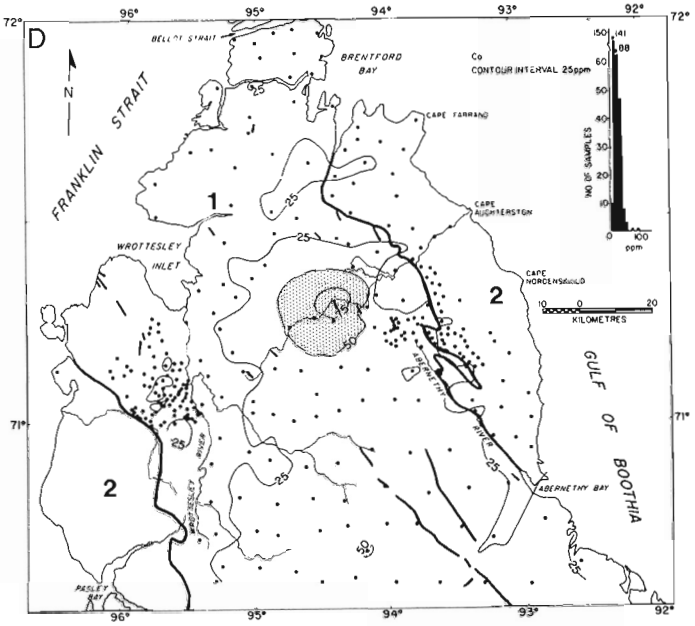
D
Co
CONTOUR INTERVAL 25 ppm
FRANKLIN STRAIT
BELLOT STRAIT
BRENTFORD BAY
CAPE FARRAND
CAPE AUGHERSTON
CAPE NORDENSKIOLD
WROTTESLEY INLET
GULF OF BOOTHIA
ABERNETHY BAY
PASLEY BAY
NO. OF SAMPLES
ppm
KILOMETRES

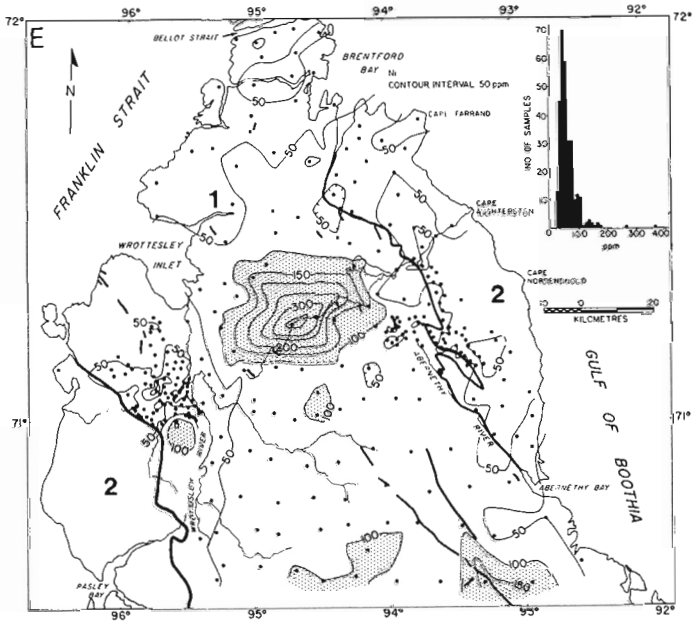
E
Ni
CONTOUR INTERVAL 50 ppm
FRANKLIN STRAIT
BELLOT STRAIT
BRENTFORD BAY
CAPE FARRAND
CAPE AUGHERSTON
CAPE NORDENSKIOLD
WROTTESLEY INLET
GULF OF BOOTHIA
ABERNETHY BAY
PASLEY BAY
NO. OF SAMPLES
ppm
KILOMETRES

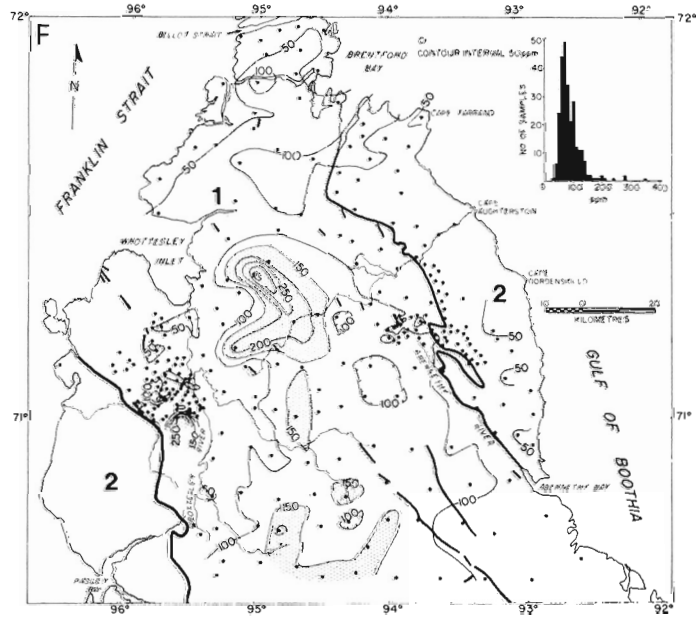
F
Cr
CONTOUR INTERVAL 50 ppm
FRANKLIN STRAIT
BELLOT STRAIT
BRENTFORD BAY
CAPE FARRAND
CAPE AUGHERSTON
CAPE NORDENSKIOLD
WROTTESLEY INLET
GULF OF BOOTHIA
ABERNETHY BAY
PASLEY BAY
NO. OF SAMPLES
ppm
KILOMETRES

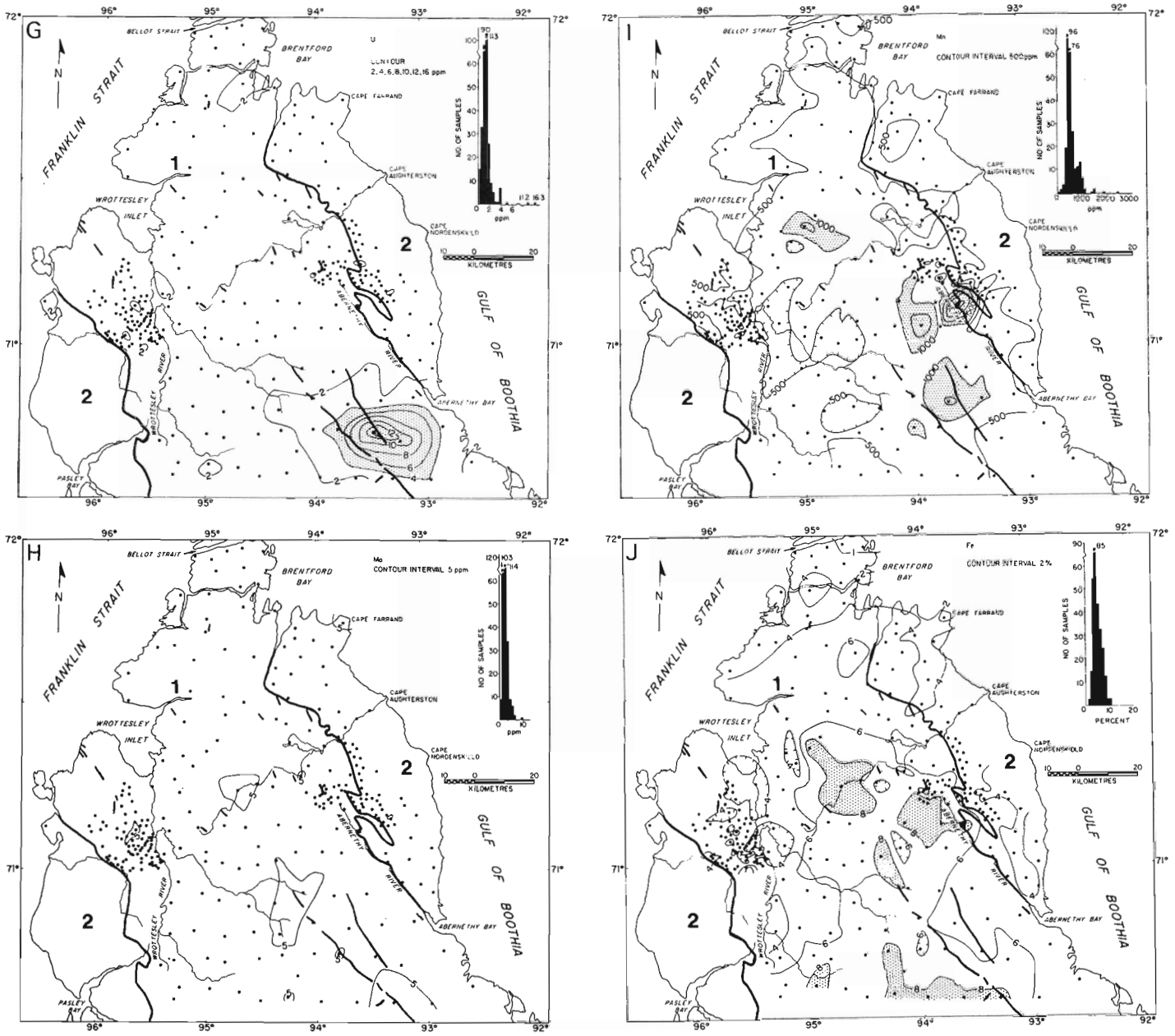

A - Cu	*F - Cr*
B - Pb	*G - U*
C - Zn	*H - Mo*
D - Co	*I - Mn*
E - Ni	*J - Fe*

Figure 2. *Maps and histograms of concentrations in the <2 μm fraction of till samples from northern Boothia Peninsula. Shaded areas are anomalies except for map of Fe, where high background is shaded. Area 1 is Precambrian gneiss, Area 2 is lower Paleozoic carbonate rock. Precambrian/Paleozoic contact and dykes are shown by heavy black lines.*

Table 1

Background values in calcareous versus granitic (shield-derived) tills and most anomalous values

Element	Calcareous till (ppm)	Granitic till (ppm)	Highest value (ppm)
Cu	<50	50-150	325
Pb	<25	<50 but most <25	136
Zn	<150	150-250	1400
Co	<25	25-50	92
Ni	<50	50-100	370
Cr	<100	100-150	350
Mn	<500	<500-1000	2600
U	<4	<4	16.3

Table 2

Anomalies and number of samples yielding anomalous values in the five areas shown in Figure 1

Area	No. samples in area	Anomalies (no. samples)				
A	13	Ni(7),	Zn(5),	Cr(2),	Pb(1),	Cu(1)
B	3	Ni(3),	Zn(3),	Pb(2),	Cr(1),	Co(1)
C	6	Zn(5),	Pb(3),	U(3),	Ni(2),	Cu(1)
D	22	Mn(8),	Ni(5),	Zn(3),	Cu(1),	Cr(1)
E	10	Ni(9),	Cu(4),	Cr(4),	Co(3),	Zn(3),
		Pb(1),	Mn(1)			
Total anomalies in areas A, B, C, D, E = 83						
Total anomalies in study area = 114						

because the clay minerals have scavenged cations released by weathering of sulphide particles. Trace element concentrations were measured by Bondar-Clegg and Co. Ltd., Ottawa, using LaForte reverse aqua-regia extraction for base metals and nitric acid extraction for uranium.

Regional Geology

The study area contains two major bedrock units (Fig. 1). The largest is the Boothia Horst, composed of intensely folded and steeply dipping, north striking gneiss of Precambrian age. The gneiss consists of alternating mafic and felsic bands; the former, in particular, form lengthy rusty bands (gossans). The gneiss is intruded by northwest-southeast trending diabase dykes; two dykes in the southeast part of the study area outcrop nearly continuously for 30 to 60 km, and in fact continue south of the study area. Other information on the Precambrian rocks is given in Blackadar (1967).

The gneiss is flanked on the northeast and southwest by lower Paleozoic sediments that dip away from the axis of the horst. These sediments are mostly limestone and dolostone, but minor sandstone occurs. Christie (1973) provides stratigraphic information.

The Boothia Uplift, which produced the Boothia Horst and flanking fold belts, was intermittently active from late Precambrian to Tertiary time. Late Cretaceous or early Tertiary sediments occur on the down dropped side of a fault south of Wrottesley Inlet (Kerr and de Vries, 1977).

During the height of the last glaciation, Laurentide ice flowed vigorously eastward across the northern part of the study area and less vigorously northeastward across the central and southwestern part of the area (Fig. 1). The ice flow pattern was more complex during deglaciation, but this lasted only a few centuries and caused little redistribution of till (Dyke, 1979).

Till overlying the western carbonate bedrock and the western and northern parts of the gneiss is highly calcareous and fine textured. Over the central and eastern part of the gneiss the till is weakly calcareous to noncalcareous and coarse textured. Gneissic components were carried only a short distance beyond the northeastern contact of the Shield, so the till over the eastern carbonate bedrock is also fine textured and highly calcareous.

Geochemistry

Anomalously high concentrations of all metals except Mo and Fe occur in parts of the study area (Fig. 2). The boundaries between background and anomalous values were determined by inspection of the histogram accompanying each map, and anomalies are shaded on the maps. This is overly simplistic because in fact background values are lower in areas of highly calcareous till than in areas of granitic till (Fig. 2)[1]. These differences are summarized in Table 1, where the highest values obtained are given as well.

Five areas have anomalous concentrations of five or more metals (Fig. 1). In a total of 114 anomalous values (total of 2932 measurements), 83 anomalies fall in these five areas (Table 2). Only the most persistent anomalies are noted on Figure 1.

In the vicinity of area A, most till is highly calcareous because it was derived from the carbonate bedrock to the west. The samples with highest trace element concentrations, however, came from small pockets of locally derived gneissic till. The local till occurs on the lower slopes of a Tertiary fault scarp (Kerr and de Vries, 1977) that forms the western side of Wrottesley Valley and was emplaced during a brief period of northward ice flow during deglaciation (Dyke, 1979). Trains of decreasing values projecting about 10 km down-ice from the most anomalous samples are apparent on the maps of Zn, Cu, and Ni (Fig. 2).

The wide spacing of samples in areas B, C, D, and E makes it unlikely that the highest values have been located. More detailed sampling should allow location of peak values and delineation of glacial dispersal trains. The anomalous samples are all from gneissic tills. No detailed information on the bedrock geology of these areas is available. However, location of the Zn, Pb, and U anomalies near the large dykes of area C is notable.

Conclusion

Samples from five well defined areas of northern Boothia Peninsula have concentrations of several metals considerably in excess of background concentrations. These high concentrations may reflect economic mineralization or variations in metal levels in the bedrock. A small, densely sampled area (A of Fig. 2) shows distinct peaks of Zn, Cu, and Ni with down-ice dispersal trains of decreasing values; Zn reaches values of 1400 ppm. Four areas of widely spaced samples are worthy of closer inspection. All anomalous samples are of till derived from gneiss in an area of known ice flow history.

[1] Background correction for carbonate was applied by Bondar-Clegg and Co. Ltd., so the differences are probably real.

References

Blackadar, R.G.
1967: Precambrian geology of Boothia Peninsula, Somerset Island, and Prince of Wales Island, District of Franklin; Geological Survey of Canada, Bulletin 151, 61 p.

Christie, R.L.
1973: Three new Lower Paleozoic formations of the Boothia Peninsula Region, Canadian Arctic Archipelago; Geological Survey of Canada, Paper 73-10, 31 p.

Dyke, A.S.
1979: Glacial geology of northern Boothia Peninsula, District of Franklin; in Current Research, Part B, Geological Survey of Canada, Paper 79-1B, p. 385-394.

Kerr, J.W. and de Vries, C.D.S.
1977: Structural geology of Somerset Island and Boothia Peninsula, District of Franklin; in Report of Activities, Part A, Geological Survey of Canada, Paper 77-1A, p. 107-111.

Klassen, R.A. and Shilts, W.W.
1977: Uranium exploration using till, District of Keewatin; in Report of Activities, Part A, Geological Survey of Canada, Paper 77-1A, p. 471-477.

Shilts, W.W.
1973: Drift prospecting; geochemistry of eskers and till in permanently frozen terrain: District of Keewatin, Northwest Territories; Geological Survey of Canada, Paper 72-45, 34 p.

1975: Principles of geochemical exploration for sulphide deposits using shallow samples of glacial drift; Canadian Mining and Metallurgical Bulletin, May 1975, p. 1-8.

Shilts, W.W. and Klassen, R.A.
1976: Drift prospecting in the District of Keewatin – uranium and base metals; in Report of Activities, Part A, Geological Survey of Canada, Paper 76-1A, p. 255-257.

NATIVE COPPER ON SUPERIOR SHOAL, ONTARIO

Projects 700059 and 750098

R.V. Kirkham and J.M. Franklin
Economic Geology Division

Superior Shoal is a shallow submerged area in the central part of Lake Superior, about 80 km south of Terrace Bay, Ontario. Dolph King, retired fisherman in Rossport, has reported recovering pieces of native copper in his nets while fishing on the Shoal.

The first author had the exceptional opportunity to join the Cousteau Expedition from September 18-24, 1980 on Lake Superior. His primary objective was to obtain geological information about the shoal, and attempt to investigate the reported occurrence of native copper.

Bad weather did not permit scuba or submersible dives on the shoal, but dredge samples, including mud, sand, rounded glacially transported material, and angular blocks of sandstone and basalt (in varying proportions) were collected from five localities. The angular samples are relatively fresh, and are interpreted to be from bedrock. The general findings and interpretation of this material will be presented elsewhere, but the discovery of native copper in one block is reported here.

At 48°03.8'N latitude and 87°08.31'W longitude, and at a depth of approximately 18 m (10 fathoms) a single, angular block, weighing 2.65 kg (Fig. 1) was recovered by the dredge from a steep rocky slope. The sample has a dark grey surface, and is slightly porphyritic amygdaloidal basalt with a pronounced weathered rim, 1.0- to 1.5-cm thick, on all but one side, and a relatively fresh centre. The fresh interior is purple-grey. The rock is ophitic and contains approximately 20 per cent of 0.5- to 2-mm long plagioclase laths, and about 20 per cent of irregular 0.1- to 12-mm diameter amygdules. Most of the large amygdules are filled with white sparry calcite. The outer rims of the large amygdules and most small amygdules contain dark green, Fe-rich chlorite, and subround grains of native copper, 0.1 to 1 mm in diameter. Trace amounts of chalcocite and digenite were identified by X-ray. The copper is most common in small amygdules and near the walls of large amygdules, and is clearly an early cavity filling. A representative fresh sample, 6.7 cm long and weighing 143 g, removed from the central part of the block, contains 0.23 per cent copper (analyzed by atomic absorption spectroscopy, Central Laboratories and Technical Services Division, GSC).

This sample confirms native copper at Superior Shoal; obviously more work is required to determine its extent.

The opportunity provided by the Cousteau Society to visit and sample Superior Shoal is gratefully acknowledged. The hard work and enthusiasm of the officers and crew on board the **R.V. Calypso** enabled us to recover these samples.

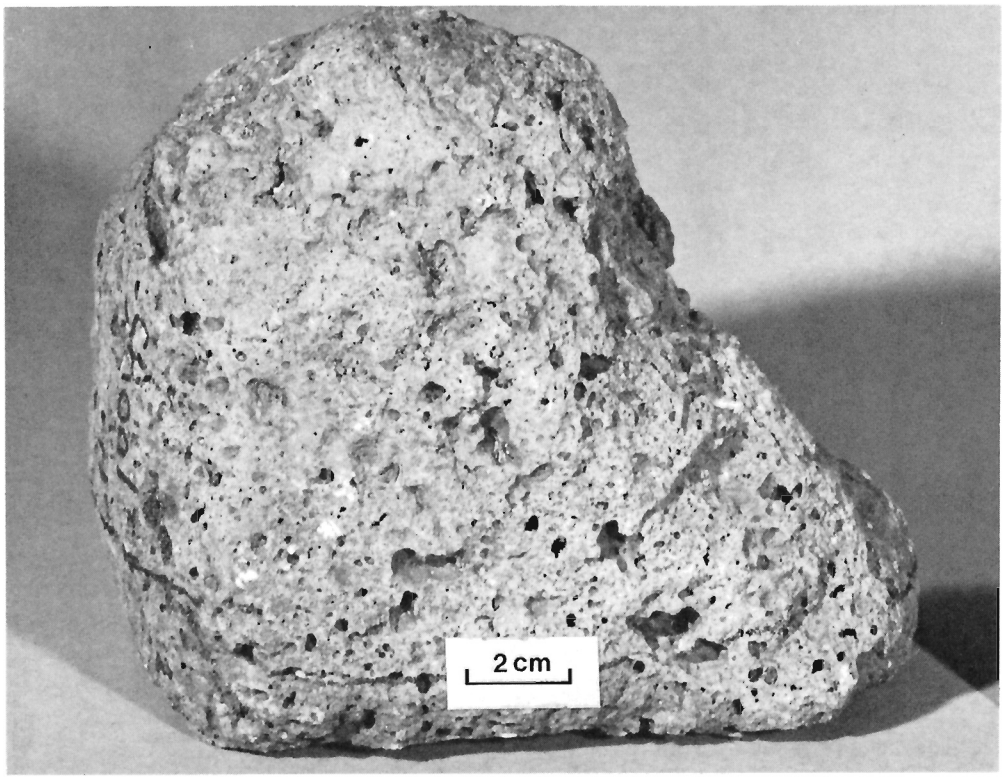

Figure 1. *Dredged sample of amygdaloidal basalt from Superior Shoal. Calcite has been leached from the amygdules near the surface of the sample. (GSC 203641-D)*

From: Scientific and Technical Notes in Current Research, Part C; Geol. Surv. Can., Paper 80-1C.

RUBIDIUM-STRONTIUM AND URANIUM-LEAD ISOTOPIC AGE STUDIES

ÉTUDES DES DATATIONS ISOTOPIQUES PAR LES MÉTHODES RUBIDIUM-STRONTIUM ET URANIUM-PLOMB

RUBIDIUM-STRONTIUM AND URANIUM-LEAD ISOTOPIC AGE STUDIES, REPORT 3

Analytical results presented and discussed by W.D. Loveridge and geological discussions and interpretations by A.J. Baer, J.H. Bourne, E.M. Cameron, I.F. Ermanovics, T. Frisch, R.A. Frith, J. Guha, J.B. Henderson, M.B. Lambert, W.D. Loveridge, J.C. McGlynn, W.H. Poole, M. Schau, D. Shaw, and R.I. Thorpe.

Loveridge, W.D., Rubidium-strontium and uranium-lead isotopic age studies. Report 3; in Current Research, Part C, Geological Survey of Canada, Paper 80-1C, p. 161-246, 1980.

Abstract

Rubidium-strontium whole rock isochron ages and initial $^{87}Sr/^{86}Sr$ ratios and uranium-lead ages on zircon from suites of samples selected from localities across Canada are presented. A description of the geological problem and interpretation of the measured age is included with each paper. Laboratory age determination methods and techniques are described or referenced.

This collection of geochronological papers honours Dr. R.K. Wanless, retired Head of the Geochronology Section, under whose leadership and guidance the Section operated from 1952 to 1979. All the geochronological work presented in this report was completed under his aegis.

Note: Where reference is to be made to a geological interpretation of an age determination reported herein, the appropriate author should be cited, for example:
Poole, W.H., 1980: Rb-Sr of the Shunacadie pluton, central Cape Breton Island, Nova Scotia; in Loveridge, W.D., Rubidium-strontium and uranium-lead isotopic age studies, Report 3; in Current Research, Part C, Geological Survey of Canada, Paper 80-1C, p. *165-169*, 1980.

CONTENTS

INTRODUCTION

W.D. Loveridge

The following papers present the results of 19 rubidium-strontium isotopic age studies predominantly on whole rock samples, and 5 uranium-lead isotopic age studies on zircon concentrates. These age determination projects are joint research studies by field geologists of the Geological Survey of Canada and members of the staff of the Geochronology Section, typically initiated by the field geologists in an attempt to solve specific geological problems. In most cases the results are known to the geologist in question but not to the geological community at large. In some instances preliminary reference has been made in scientific reports to the resultant ages but the analytical data and other details have not been published.

Over the years the Geochronology Section has accumulated a number of such unpublished studies. This current group of papers is the first in a series to be presented in coming editions of "Current Research, Part C". It is our intention to bring out all of the currently inactive, unpublished age determinations in this manner in a complete form including all relevant analytical data plus a description of the geological problem by the scientist who initiated the study. If, however, this is not possible the age and analytical data of some studies may be presented unsupported by geological discussion.

Rb-Sr Whole Rock Isochron Studies

The analytical work leading to the Rb-Sr age results published in this collection of papers was performed from 1963 to 1979. Analytical procedures have progressed and been modified over the years, but are based on those described by Wanless and Loveridge (1972). The analytical uncertainty to be associated with the isotopic ratios has also changed with time, and is listed individually in each data table.

All whole rock isochron data were subjected to regression analysis using the program published by Brooks et al. (1972). The published ages and initial $^{87}Sr/^{86}Sr$ ratios and their associated errors (95% confidence interval) are those determined by the York 1 portion of the program. The value obtained for the Mean Square of Weighted Deviates (MSWD) from the McIntyre portion of the program is used to classify the linear array of experimental points as an isochron or an errorchron. In the terminology of Brooks et al. (1972) an errorchron is the result of regression of data that possess scatter in excess of experimental error whereas the data points forming an isochron are collinear within experimental error. Thus the excess scatter of points forming an errorchron is attributable not to lack of laboratory precision, but to inherent properties of the rocks under investigation.

Brooks et al. (1972, p. 557) pointed out that the uncertainties associated with errorchron results at a given confidence interval contain none of the predictive aspects that characterize true confidence intervals. For an isochron with error figures given at the 95 per cent confidence level, 19 of 20 repeats should fall within those error figures. This is not the case with an errorchron; it is possible that no repeats would fall within the stated error limits. Therefore the error limits associated with errorchrons may be indicative of the uncertainty in the age and initial ratio results, but are by no means definitive. For this reason the error limits associated with errorchron results are mentioned only in the text but omitted from the introductory statement and diagrams to prevent inadvertent misuse by the casual reader.

The ^{87}Rb decay constant used in this series of papers is $1.42 \times 10^{-11} a^{-1}$ as recommended by the IUGS Subcommission on Geochronology (Steiger and Jaeger, 1977). Previously published Rb-Sr ages referred to in these papers have been adjusted to this constant.

Uranium-Lead Age Studies on Zircon Concentrates

The preparation of zircon concentrates and analytical procedures for uranium-lead age determination work is discussed by Sullivan and Loveridge in the following paper in this volume. The uranium-lead results presented in this group of papers were determined during the period 1975 to 1980 and are either concordant or consist of two to four analytical points defining a chord, the upper intercept of which, with the concordia curve, determines the geological age. The analytical points defining the two point chords are sufficiently close to the concordia curve in these studies to define the upper intercept age with the desired precision.

The concordia intercept ages are calculated by a computer program which first determines the parameters of the chord through a least squares linear regression and then finds the intercepts by an iterative method. The uncertainties associated with concordia intercept ages of two point chords are determined from the error envelope defined by the analytical uncertainties associated with the individual analytical points. However, the uncertainties associated with concordia intercept ages of chords derived from three or more analytical points are based on the standard error of the slope of these chords. These uncertainties are determined from the intersection with concordia of hypothetical chords with slopes equal to that of the original chord plus and minus its standard error, projected from a point which is the average of the analytical points.

The uranium decay constants used are: ^{238}U, $1.55125 \times 10^{-10} a^{-1}$ and ^{235}U, $9.8485 \times 10^{-10} a^{-1}$ as recommended by the IUGS Subcommission on Geochronology (Steiger and Jaeger, 1977). Descriptions of zircon concentrates are by R.K. Wanless and R.W. Sullivan compiled by R.D. Stevens.

I would particularly like to thank R.D. Stevens for critically reading all papers in this section and for his unflagging support and assistance in preparing this collection of papers.

References

Brooks, C., Hart, S.R., and Wendt, I.
1972: Realistic use of two error regression treatments as applied to rubidium-strontium data; Reviews of Geophysics and Space Physics, v. 10, no. 2, p. 551-577.

Steiger, R.H. and Jaeger, E.
1977: Subcommission on Geochronology: Convention on the use of decay constants in geo- and cosmochronology; Earth and Planetary Science Letters, v. 36, no. 3, p. 356-362.

Wanless, R.K. and Loveridge, W.D.
1972: Rubidium-strontium isochron age studies, Report 1; Geological Survey of Canada, Paper 72-23.

URANIUM-LEAD AGE DETERMINATIONS ON ZIRCON AT THE GEOLOGICAL SURVEY OF CANADA: CURRENT PROCEDURES IN CONCENTRATE PREPARATION AND ANALYSIS

R.W. Sullivan and W.D. Loveridge

The procedures in use at the Geological Survey of Canada for the preparation of zircon concentrates and the extraction and isotopic analysis of uranium and lead are continually being modified and upgraded as new instrumentation and techniques become available. Contributions of other workers in the field, especially Krogh (1973), and the advent of clean air systems and ultra pure reagents have allowed us to reduce sample sizes and associated lead contamination or "blank" levels by a factor of 10^3 over the past ten years. The following analytical procedures are those currently in use in our laboratories.

Zircon concentrates are prepared in the mineral separation laboratory using standard procedures of crushing, sieving, Wilfley table and heavy liquid techniques, and by separation of the more magnetic minerals from the zircon using a Frantz isodynamic separator. The samples are further purified, as required, in the geochronology laboratory using a froth flotation technique that effectively removes sulphide mineral impurities. Selected size fractions, prepared by sieving through nylon screens, are passed through a Frantz separator to obtain relatively magnetic versus nonmagnetic pairs, and finally hand picking is employed, as required, to obtain a pure zircon and/or to select a specific type of zircon based on physical characteristics.

The zircon fractions selected for analysis are washed in a warm mixture of pure HCl (6N) and HNO_3 (6N) for 30 minutes to dissolve any remaining sulphide impurities and to remove lead contamination from the crystal surfaces. The acid treatment is followed by washings with pure H_2O and air drying with pure acetone.

The chemical procedure consists of dissolving the zircon in a teflon crucible inside a stainless steel pressure vessel similar to the design of Krogh (1973). All reagents are ultra-pure and prepared in either teflon or quartz isothermal distillation apparatus. Refined cleaning procedures and chemical techniques are utilized to minimize lead contamination. Critical procedures are carried out in class 100 clean air environments. The teflon crucibles are thoroughly cleaned and just before loading are pretreated twice in an oven at 240°C overnight (14 hours) with a charge of 2 ml pure HF and a drop of ULTREX HNO_3. The zircon samples are dissolved in 2 to 3 ml of pure HF and 1 drop of ULTREX HNO_3 by heating the pressure vessel for 14 hours in an oven at 240°C. The solutions are slowly evaporated to dryness; the crucibles are re-loaded into the vessels with a charge of 3 ml of 1 N HCl and heated again overnight at 240°C. This procedure completely dissolves the zircons, resulting in a clear solution in 1 N HCl.

The lead and uranium are extracted and purified using ion-exchange elution chromatography with columns made from shrinkable teflon tubing similar in design to that of Krogh (1973), and charged with BIO RAD anion exchange resin AG1x8, 100-200 mesh, which has been previously cleaned and pretreated. Separate columns are used for lead and uranium, and prepared fresh for each sample. Four zircon samples are usually processed together, along with a total reagent and procedure blank.

Isotope dilution techniques using ^{208}Pb and ^{235}U tracers (spikes) are employed to determine the lead and uranium concentrations, with a separate unspiked lead analysis used to provide the isotopic composition of the lead. In detail, the sample solution is aliquoted into three parts by weight: an unspiked lead cut, a spiked lead and uranium cut, and a reserve portion. Each lead aliquot is passed through a resin column pretreated with 1 N HCl which is then washed with 5 ml of 1 N HCl. The sorbed lead is then eluted with 3 ml of 6 N HCl into a teflon dish where it is evaporated to dryness for mass spectrometer analysis. The spiked uranium is extracted from the eluted spiked lead sample solution plus the associated washing by evaporating to near dryness, adding 2 ml of 6 N HCl and passing through a second resin column (pretreated with 6 N HCl). This column is washed with 5 ml of 6 N HCl and the uranium is eluted with 3 ml of water into a teflon dish where it is evaporated to dryness with one drop of ULTREX HNO_3. The blank solution is aliquoted and spiked with ^{206}Pb and processed in the same way as the spiked lead solution. The spike solutions are stored in quartz bottles with teflon mininert valves and dispensed by weight using plastic needles and syringes. Sample sizes are currently 5 mg or less of zircon and contamination lead levels range from 0.5 to 2 ng, generally accounting for less than two per cent of the lead in each analysis. Common lead levels are more variable but generally comprise less than two per cent of the radiogenic lead for zircons of Archean age. Typical error limits at the 95 per cent confidence level are: $^{207}Pb/^{206}Pb \pm 0.25\%$, $^{206}Pb/^{238}U$ and $^{207}Pb/^{235}U \pm 0.7\%$.

Uranium and lead analyses are performed on the Geological Survey of Canada, fifteen inch radius of curvature, 90° mass spectrometer. Lead samples are analyzed using the silica gel – phosphoric acid technique, whereas uranium samples are mounted on the rhenium filament with tantalum pentoxide and phosphoric acid. Ion currents are amplified by an electron multiplier, detected by a vibrating reed electrometer and measured with an integrating digital voltmeter. A mini computer receives and stores the output of the digital voltmeter for further processing. Corrections are applied to the raw data for instrumental baselines, average fractionation as determined on standards, and non linearity of the electron multiplier. A computer program has been developed to calculate elemental and age parameters from the measured isotopic compositions. The isotopic compositions assumed for the common lead corrections are based on model lead compositions (Stacey and Kramers, 1975) of age equivalent to the upper concordia intercept age of the chord defined by the sample points in question.

References

Krogh, T.E.
1973: A low-contamination method for hydrothermal decomposition of zircon and extraction of U and Pb for isotopic age determinations; Geochimica et Cosmochimica Acta, v. 37, p. 485-494.

Stacey, J.S. and Kramers, J.D.
1975: Approximation of terrestrial lead isotope evolution by a two stage model; Earth and Planetary Science Letters, v. 26, p. 207-221.

1. Rb-Sr AGE OF SHUNACADIE PLUTON, CENTRAL CAPE BRETON ISLAND, NOVA SCOTIA

Isochron Age = 574 ± 11 Ma
$^{87}Sr/^{86}Sr$ initial = 0.7055 ± 0.0004

The results of isotopic analyses on five whole rock samples are presented in Table 1 and displayed on an isochron diagram, Figure 1. Four of the five points are collinear yielding an isochron age of 574 ± 11 Ma, initial $^{87}Sr/^{86}Sr$ of 0.7055 ± 0.0004 and low MSWD of 0.12. Sample number 3 falls considerably below the line defined by the other four points.

The initial $^{87}Sr/^{86}Sr$ ratio is somewhat higher than is usually found for mantle derived rocks of this age and may indicate crustal contamination or some other mechanism of strontium isotopic homogenization.

Geological Setting and Interpretation
by W.H. Poole

Geological Setting

Granitic rocks are plentiful in central and southeastern Cape Breton Island. Most have intruded Precambrian volcanic and sedimentary rocks and are nonconformably overlain by Middle Devonian to Pennsylvanian, post-Acadian successor basin clastic and carbonate strata. Their relations to Cambrian and Lower Ordovician are generally less certain. Some of those few that clearly cut these strata have yielded Devonian Rb-Sr isochron ages (e.g. Gillis Mountain pluton) but the majority have yielded Hadrynian-Cambrian ages (Cormier, 1972).

The Shunacadie pluton[1] underlies the upland surface of central and western Boisdale Hills in central Cape Breton Island, southeast of St. Andrews Channel of Bras d'Or Lake. The pluton is 19 km long, 6 km wide in the southwest and narrows northeasterly (Fig. 2). The Shunacadie pluton has not been mapped or studied in detail. Weeks (1954) and Kelley (1967) referred to its variable composition of quartz monzonite, granodiorite, granite, syenite and diorite with biotite and/or hornblende, and generally medium grain. The pluton clearly has

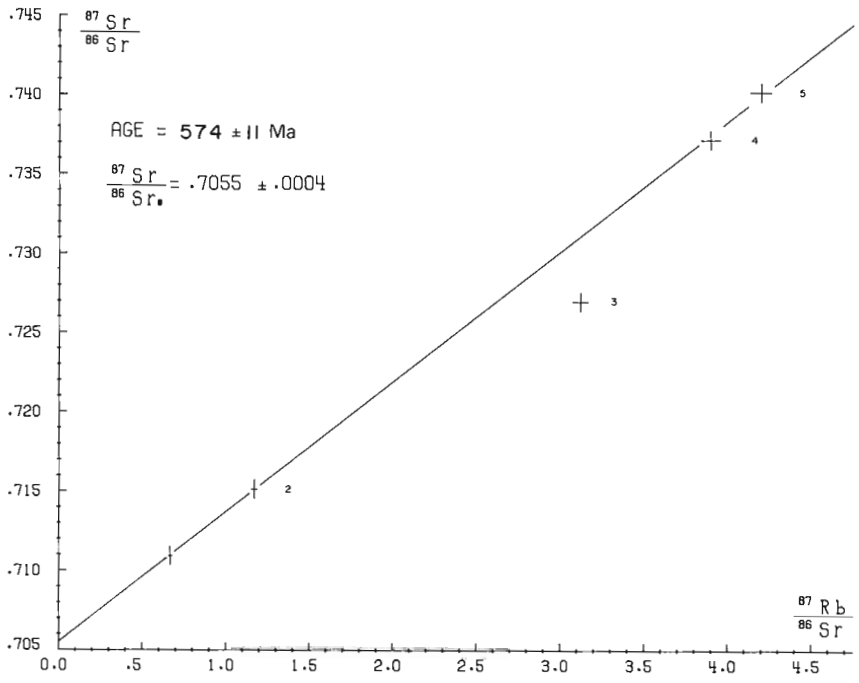

Figure 1. *Rb-Sr isochron, Shunacadie pluton, central Cape Breton Island, Nova Scotia.*

Table 1

Analytical data, whole rock samples, Shunacadie pluton, central Cape Breton Island, Nova Scotia

Sample No.	Rb ppm	Sr ppm	$^{87}Sr/^{86}Sr$ unspiked	$^{87}Sr/^{86}Sr$ spiked	$^{87}Sr/^{86}Sr$ average	$^{87}Rb/^{86}Sr$
1	55.09	238.4	0.7108	0.7110	0.7109 ± 0.0011	0.669 ± 0.020
2	78.05	192.7	0.7152	0.7149	0.7151 ± 0.0011	1.173 ± 0.035
3	* 70.16	65.06	0.7274	0.7265	0.7269 ± 0.0011	3.122 ± 0.094
4	135.7	100.75	0.7374	0.7369	0.7371 ± 0.0011	3.900 ± 0.117
5	141.1	97.22	0.7408	0.7395	0.7401 ± 0.0011	4.202 ± 0.126

*Average of two determinations

[1] The name "Shunacadie" is herein applied to the pluton, and is derived from the name of the village on the coast of St. Andrews Channel about 7 km southwest of the edge of Figure 2.

From: Rb-Sr and U-Pb Isotopic Age Studies in Current Research, Part C
Geol. Surv. Can., Paper 80-1C

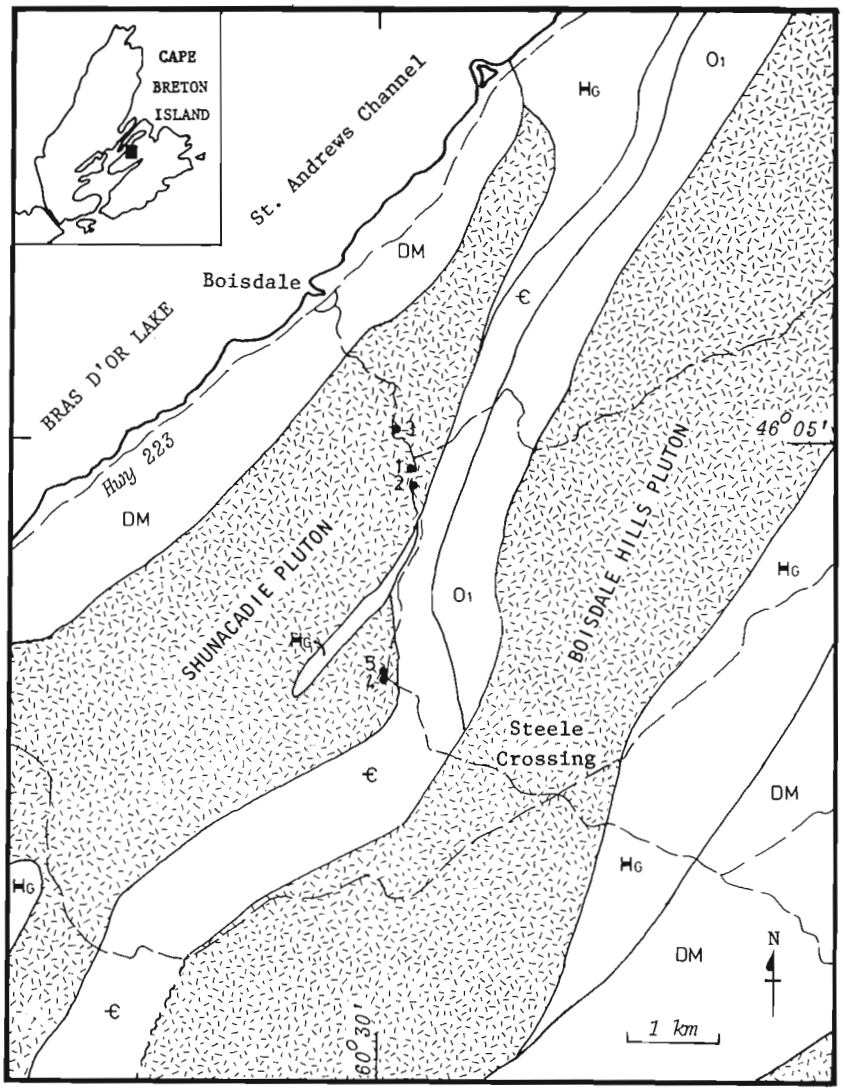

Devonian and Mississippian
DM Red and grey sandstone, conglomerate, siltstone

Lower Ordovician
O1 Grey shale

Middle and Upper Cambrian
€ Mafic volcanics, shale, siltstone, sandstone

Helikian (?)
HG George River Group: schist, slate, gneiss, marble, quartzite

Granitic rocks

Figure 2

Location of samples within Shunacadie pluton, Boisdale Hills, central Cape Breton Island, Nova Scotia. Geology generalized from Bell and Goranson (1938), Kelley (1967), and Hutchinson (1952).

intruded Hadrynian or older (Helikian?) George River Group schist, gneiss, quartzite, slate and marble (Bell and Goranson, 1938; Kelley, 1967; Helmstaedt and Tella, 1972, 1973). Hadrynian calc-alkaline felsic and mafic volcanic rocks (Helmstaedt and Tella, 1973) occur in the Coxheath Hills about 3 km east of Figure 2 and they underlie a considerable area of the terrain in southeastern Cape Breton Island (Weeks, 1954). A narrow belt of more than 1000 m of Middle Cambrian to Lower Ordovician volcanic and sedimentary rocks (Hutchinson, 1952) separates the Shunacadie pluton from the somewhat similar Boisdale Hills pluton to the southeast (Fig. 2). The Middle Cambrian rocks comprise calc-alkaline (Helmstaedt and Tella, 1973) or bimodal alkaline-subalkaline (Keppie and Dostal, 1980) mafic and felsic volcanics and some sedimentary rocks of shallow marine origin (Bourinot Group) and overlying shallow marine siltstone, shale and sandstone (MacMullin Formation). These strata unconformably overlie the George River Group with a low-angle relationship (Bell and Goranson, 1938; Hutchinson, 1952; Helmstaedt and Tella, 1972, 1973). The disconformably overlying Upper Cambrian and Lower Ordovician strata are deeper water, marine, grey and black shale. Unconformably overlying all these units are folded and faulted but unmetamorphosed Devonian and Mississippian coarse clastic strata (McAdam Lake and Grantmire formations) which contain clasts of all older rocks.

The age of the plutonic rocks in the Boisdale Hills is an unresolved question. Bell and Goranson (1938) assigned the Shunacadie and Boisdale Hills plutons a late Precambrian or very early Paleozoic age because the plutonic rocks seemed spatially related to the George River Group and the Hadrynian volcanics in Coxheath Hills, and they did not find any igneous rocks cutting the Cambrian and Ordovician sedimentary rocks. Further, they remarked on the less metamorphosed character of "Precambrian(?)" volcanics (now known to be Middle Cambrian; Hutchinson, 1952) where they overlie the George River Group along St. Andrews Channel and on the volcanic pebbles in the overlying Middle Cambrian sedimentary rocks. Hutchinson (1952) and Weeks (1954) stated that the Shunacadie pluton intruded the Cambrian strata, and assigned a Devonian age to the pluton. Independent evidence that the granitic rocks are not Devonian resulted from the early Rb-Sr studies of Fairbairn et al. (1960). Feldspar and biotite yielded ages from 460 to 527 Ma[1], i.e. middle Ordovician to late Cambrian, and certainly not Devonian. Subsequently, ages from K-Ar minerals and Rb-Sr whole rock isochrons (Wanless et al., 1968; Cormier, 1972) supported the belief that the granitic rocks of plutons in the Boisdale and Coxheath hills are not Devonian.

[1] K-Ar and Rb-Sr ages quoted from published papers have been calculated or recalculated using the new constants recommended by Steiger and Jäger (1977). The time scale used in this report is that of Armstrong (1978), constructed using the new constants.

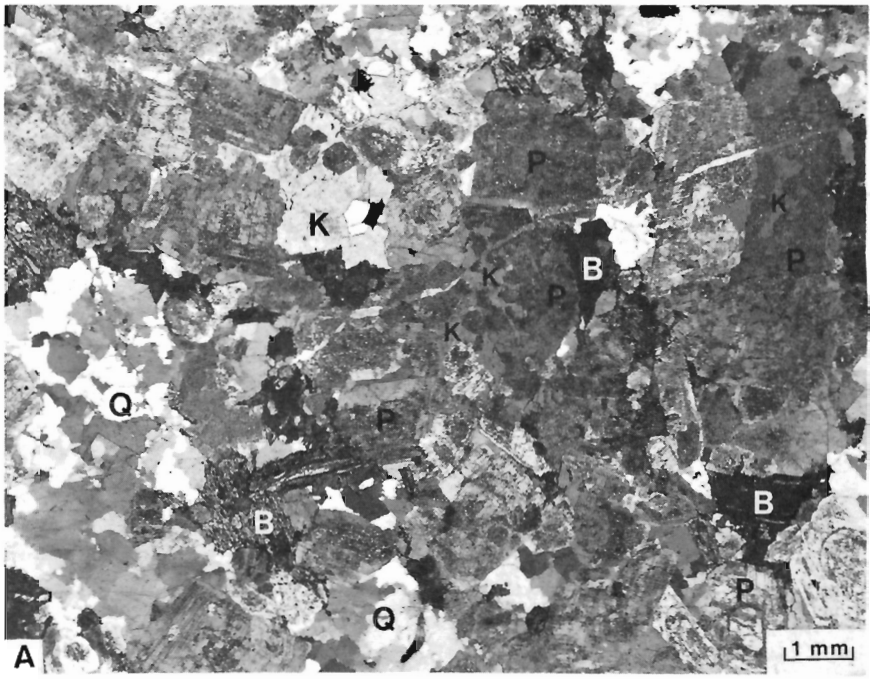

A. Medium grained, massive biotite tonalite with saussuritized plagioclase (P), interstitial potash feldspar (K) partly replacing plagioclase, quartz with mosaic texture (Q), and biotite almost completely altered to chlorite, sphene and calcite (B). Sample 1. (GSC Photo 203617-H)

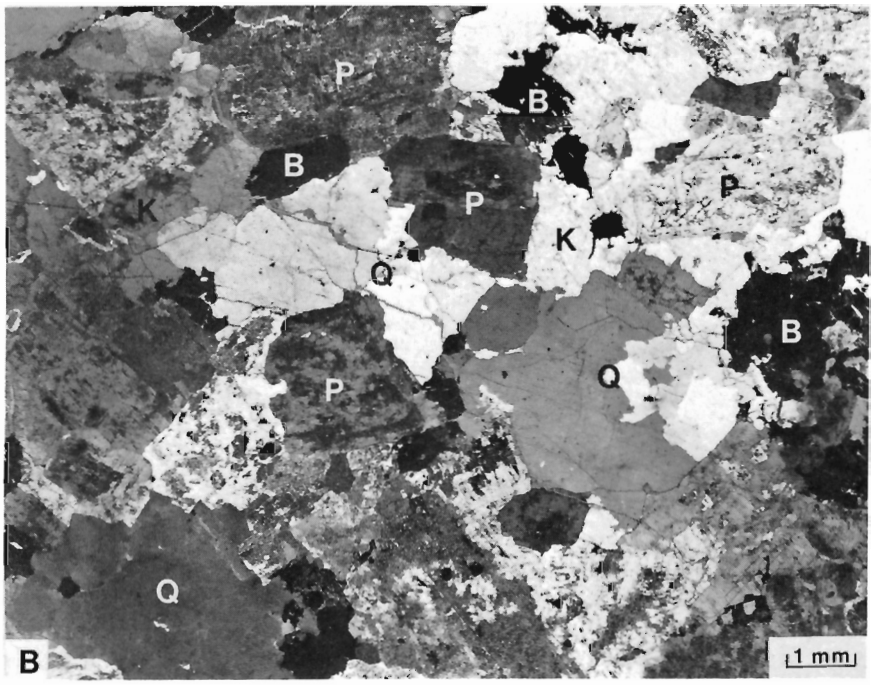

B. Coarse grained, massive biotite granite with partly saussuritized plagioclase (P), perthitic potash feldspar (K), quartz with some mosaic texture (Q), and biotite altered to chlorite and sphene (B). Trace of hornblende occurs with biotite. Sample 5. (GSC Photo 203617-G)

Figure 3. *Photomicrographs of Shunacadie pluton.*

Helmstaedt and Tella (1972, 1973) argued from field relations, age determinations and from chemistry of the Hadrynian and Cambrian volcanics and of the plutonic rocks that most of the plutonic rocks are Hadrynian. They argued for a low-angle unconformity at the base of the Middle Cambrian strata, in part from the locally intense metamorphism and recrystallization of George River rocks and Coxheath volcanics and in part from the presence of pebbles of diorite, monzonite, granodiorite, granite and contact metamorphosed George River slate in the basal Middle Cambrian on Long Island in St. Andrews Channel, 6 km northeast of Figure 2. However, they also argued that some of the granite in the Boisdale Hills (how much is unknown) is younger than the Middle Cambrian strata (and almost certainly younger than the Lower Ordovician strata), because exposures of hornfelsed equivalents of these rocks have been found locally, thus confirming Hutchinson's (1952) observations.

Two major questions remain:

1. Do granitic rocks which seem to be pre-Middle Cambrian make up most of the plutonic terrane in the Boisdale Hills? Are they younger than or the same age as Hadrynian volcanics, or are some older than the volcanics but younger than George River rocks? Are these granitic rocks the same age as the metamorphism of the George River rocks?
2. Where are the granitic bodies which locally have hornfelsed the lower Paleozoic strata in the Boisdale Hills, how do they differ lithologically from the pre-Middle Cambrian granitic rocks, and what is their age?

Our present isochron deals only with the pre-Middle Cambrian granitic rocks.

Interpretation

Within the Shunacadie pluton, the only other published isotopic ages are those of Fairbairn et al. (1960) briefly referred to above. From the same outcrop of our sample 4, biotite yielded an age of 527 Ma by K-Ar and 460 Ma by Rb-Sr, and potash feldspar an age of 476 Ma by Rb-Sr. These ages span the Late Cambrian-Middle Ordovician period.

A number of isotopic ages have been determined on the Boisdale Hills pluton. Biotite from granodiorite collected on the road 0.7 km southwest of the east edge of Figure 2 yielded a K-Ar age of 502 ± 20 Ma (Wanless et al., 1968, p. 127-129) and granodiorite collected about 1.2 km to the northeast, just beyond the east edge of Figure 2, yielded a Rb-Sr biotite-whole rock age of 508 ± 70 Ma with an initial $^{87}Sr/^{86}Sr$ ratio of 0.7198 ± 0.002 (Cormier, 1972). From a granite quarry (Long Island quarry) along highway 223, 5 km north-northeast of the northeast corner of Figure 2, Cormier (1972) produced a 7-point Rb-Sr isochron of 563 ± 20 Ma with an initial $^{87}Sr/^{86}Sr$ ratio of

Table 2

Sample numbers and localities, Shunacadie pluton, Boisdale Hills, central Cape Breton Island, Nova Scotia

Sample Number			Locality		
This work	Field	Rock type	Latitude	Longitude	N.T.S.
1	PB63-44	Biotite tonalite, grey with abundant orange feldspar, medium grained, massive (Fig. 3A)	46°04'50"	60°29'41"	11 K/1
2	PB63-46	Hornblende-biotite granodiorite, grey with light orange-pink and light green feldspars, medium grained, massive	46°04'43"	60°29'44"	11 K/1
3	PB63-39	Altered granodiorite, light grey with light orange and light yellow-green feldspars, medium grained, massive	46°05'05"	60°29'51"	11 K/1
4	PB63-55	Biotite granite, with orange-pink perthite and light greenish-grey plagioclase, coarse grained, massive	46°03'37"	60°29'55"	11 K/1
5	PB63-54	Biotite granite, with orange-pink perthite and light greenish-grey plagioclase, coarse grained, massive (Fig. 3B)	46°03'37"	60°29'55"	11 K/1

0.7042 ± 0.0017. He concluded that the granite was pre-Early Cambrian. Poole during 1979 found that the granite in the quarry lacked zircons and was in fact a granophyre with associated porphyritic rhyolite suggesting a close relation to volcanic rocks, presumably Hadrynian. A further 6 km to the northeast, near George River station, Cormier (1972) produced a less satisfactory, 2-point whole rock plot from syenite of 552 ± 70 Ma with an initial $^{87}Sr/^{86}Sr$ ratio of 0.7010 ± 0.002.

And finally, from syenodiorite and granite cutting the Hadrynian Coxheath volcanics some 5 km east of the east edge of Figure 2, hornblende yielded a K-Ar age of 593 ± 28 Ma (Wanless et al., 1968) and a potash feldspar-whole rock pair yielded a Rb-Sr age of 569 ± 70 Ma with an initial $^{87}Sr/^{86}Sr$ ratio of 0.7060 ± 0.002 (Cormier, 1972).

Samples for the isochron reported here were collected in 1963 from the Shunacadie pluton along 3 km of the Bourinot Road between 1.5 and 4.5 km southeast of Boisdale. The analyzed samples range in composition from tonalite to granite and are equigranular, massive and variably altered (Table 2). Zircon, apatite, sphene and iron ore are accessories common to all samples. Sample 1 (Fig. 3A) is a tonalite with orange, altered feldspar consisting of subhedral plagioclase (60%) with fine, weak albite twinning and zoning, altered to coarse white mica and calcite; interstitial potash feldspar partly replacing plagioclase (2%); quartz (24%) consisting of equant anhedra comprising interlocking sutured and strained subgrains; and chlorite with sphene, calcite and iron ore (14%) from mafic minerals, mainly, if not all, biotite. Sample 2 is a granodiorite, much less altered than sample 1. Plagioclase (57%) is strongly zoned, in part oscillatory, and saussuritized to white mica, epidote group and calcite; potash feldspar (11%) is interstitial microperthite with some microcline twinning; quartz (22%) is similar to sample 1; and biotite (7%) and green hornblende (3%) are markedly altered.

Sample 3 is a granodiorite, texturally like samples 1 and 2 but more intensely altered. Plagioclase (46%) is a chalky, light yellow-green unzoned saussurite which is bent and broken; potash feldspar (8%) is interstitial; quartz (36%) is equant, strained and internally mosaic textured like samples 1 and 2; and the mafic mineral, presumably biotite, has been completely altered to bent chlorite, sphene and iron ore (10%).

Samples 4 and 5 (Fig. 3B) are distinctly different from the other three and were collected about 15 m apart. They are pink, coarse grained, massive, altered granites with coarse orange-pink perthite, light greenish grey plagioclase, grey quartz and biotite. Plagioclase (oligoclase, 31-36%) is partly saussuritized with white mica and epidote, well twinned and zoned and some crystals are bent and broken. Perthite (20-25%) has some microcline twinning. Like the other samples, quartz (40-42%) consists of strained and sutured internal subgrains, biotite (3-5%) is pleochroic brown and reddish brown to light yellow and most crystals are thoroughly altered to chlorite and sphene. Traces of green hornblende are also present. Sample 4 contains accessory allanite (confirmed by A.C. Roberts by X-ray diffraction).

In summary, samples 1, 2 and 3 are altered medium grained biotite (hornblende) granodiorites and tonalite and samples 4 and 5 are altered coarse grained biotite (hornblende) granites. Sample 3 is markedly more altered. The rocks have been mildly deformed but not to the point of tectonically flattened quartz grains. Although samples 1, 2 and 3 differ modally from samples 4 and 5 and are separated by a short narrow belt of George River rocks (Fig. 2) in this small part of the pluton, the two groups have the same minerals, alteration effects, and deformational effects. It seems reasonable to suppose that they are the same age and had the same initial $^{87}Sr/^{86}Sr$ ratio during intrusion.

The Rb-Sr regression line through samples 1, 2, 4 and 5 yields a high-quality isochron of 574 ± 11 Ma with an initial

$^{87}Sr/^{86}Sr$ ratio of 0.7055 ± 0.0004 over a range of $^{87}Rb/^{86}Sr$ of 0.6 to 4.2 and with a MSWD of 0.12. Sample 3 plots far off the line and can be disregarded with confidence because of the markedly more intense alteration of the sample.

I conclude therefore that the age derived from the four samples is dependable. If the Hadrynian-Cambrian boundary is accepted at about 575 Ma, then the sampled part of the Shunacadie pluton is latest Hadrynian or earliest Cambrian in age.

The sampled granitic rocks may be the same age as or slightly younger than the Hadrynian volcanics but they are clearly older than the Middle Cambrian Bourinot volcanics. The isochron supports the general conclusions of Cormier (1972) and Helmstaedt and Tella (1972, 1973) that most plutonic rocks of the Boisdale Hills are latest Hadrynian-earliest Cambrian and it follows that the contacts between Middle Cambrian rocks and these plutonic rocks must be either unconformities or faulted unconformities (see Helmstaedt and Tella, 1973, Fig. 2; Keppie, 1979). Contacts with the unlocated post-Lower Ordovician, presumed granitic, intrusives would of course be intrusive or faults.

The Shunacadie isochron of 574 ± 11 Ma is very much like Cormier's (1972) 563 ± 20 Ma isochron on part of the Boisdale Hills pluton, and the K-Ar hornblende 593 ± 28 Ma age (Wanless et al., 1968) and the Rb-Sr potash feldspar whole rock 569 ± 70 Ma age (Cormier, 1972) on the Coxheath Hills pluton. It therefore seems probable that these three plutons are the same age in so far as geochronological methods can determine at present. The biotite ages of 502 ± 20 Ma by K-Ar and 508 ± 70 Ma by Rb-Sr biotite whole rock on the Boisdale Hills pluton (Wanless et al., 1968; Cormier, 1972) appear to suggest that uplift and cooling (perhaps also associated with local intrusion of granites) through the argon blocking and strontium immobility temperatures occurred in the late Early Ordovician or early Middle Ordovician. At this time, allochthons were moving from the Iapetus ocean northwestward toward the St. Lawrence Platform as evidenced by the coarse Iapetus-derived clastics of the Lower Ordovician Tourelle Formation in northern Gaspé Peninsula (Hiscott, 1978). Contemporaneous uplift of the Avalon zone is suggested by the fact that in the Avalon zone, Lower Ordovician strata occur in eastern Newfoundland, Cape Breton Island, and southern New Brunswick, and in each area are the youngest units of the Cambro-Ordovician platformal sequence. The lack of Middle and Upper Ordovician strata can be explained by uplift.

References

Armstrong, R.L.
1978: Pre-Cenozoic Phanerozoic time scale – computer file of critical dates and consequences of new and in-progress decay-constant revisions; in Contributions to the Geologic Time Scale, ed. G.V. Cohee, M.F. Glaessner and H.D. Hedberg; American Association of Petroleum Geologists, Studies in Geology No. 6, p. 73-91.

Bell, W.A. and Goranson, E.A.
1938: Sydney sheet (west half), Cape Breton and Victoria counties, Nova Scotia; Geological Survey of Canada, Map 360A with marginal notes.

Cormier, R.F.
1972: Radiometric ages of granitic rocks, Cape Breton Island, Nova Scotia; Canadian Journal of Earth Sciences, v. 9, no. 9, p. 1074-1086.

Fairbairn, H.W., Hurley, P.M., Pinson, W.H. Jr., and Cormier, R.F.
1960: Age of the granitic rocks of Nova Scotia; Bulletin Geological Society of America, v. 71, no. 4, p. 399-414.

Helmstaedt, H. and Tella, S.
1972: Structural history of pre-Carboniferous rocks in parts of eastern Cape Breton Island; in Report of Activities, Part A, April to October, 1971; Geological Survey of Canada, Paper 72-1, Part A, p. 7-10.

1973: Pre-Carboniferous structural history of S.E. Cape Breton Island, Nova Scotia; Maritime Sediments, v. 9, no. 3, p. 88-99.

Hiscott, R.N.
1978: Provenance of Ordovician deep-water sandstones, Tourelle Formation, Quebec, and implications for initiation of the Taconic orogeny; Canadian Journal of Earth Sciences, v. 15, no. 10, p. 1579-1597.

Hutchinson, R.D.
1952: The stratigraphy and trilobite faunas of the Cambrian sedimentary rocks of Cape Breton Island, Nova Scotia; Geological Survey of Canada, Memoir 263, 124 p.

Kelley, D.G.
1967: Baddeck and Whycocomaugh map-areas with emphasis on Mississippian stratigraphy of central Cape Breton Island, Nova Scotia (11 K/12 and 11 F/12); Geological Survey of Canada, Memoir 351, 65 p.

Keppie, J.D., compiler
1979: Geological map of the Province of Nova Scotia; Nova Scotia Department of Mines and Energy.

Keppie, J.D. and Dostal, J.
1980: Paleozoic volcanic rocks of Nova Scotia; in Proceedings, The Caledonides of the USA, I.G.C.P. Project 27, Caledonide Orogen, ed. D.R. Wones; Department of Geological Sciences, Virginia Polytechnic Institute and State University, Memoir 2, p. 249-256.

Steiger, R.H. and Jäger, E., compilers
1977: Subcommission on Geochronology: convention on the use of decay constants in geo- and cosmochronology; Earth and Planetary Science Letters, v. 36, no. 3, p. 359-362.

Wanless, R.K., Stevens, R.D., Lachance, G.R., and Edmonds, C.M.
1968: Age determinations and geological studies, K-Ar isotopic ages, report 8; Geological Survey of Canada, Paper 67-2, part A, 141 p.

Weeks, L.J.
1954: Southeast Cape Breton Island, Nova Scotia; Geological Survey of Canada, Memoir 277, 112 p.

2. Rb-Sr AGE OF SOME GRANITIC ROCKS BETWEEN LUDGATE LAKE AND NEGRO HARBOUR, SOUTHWESTERN NEW BRUNSWICK

Isochron Age = 526 ± 13 Ma
$^{87}Sr/^{86}Sr$ initial = 0.7045 ± 0.0007

The isotopic results obtained for 7 whole rock samples are presented in Table 1 and depicted on an isochron diagram in Figure 1. The insert in the isochron diagram shows the samples with low $^{87}Rb/^{86}Sr$ in greater detail. Samples 1 to 4 plus 6 and 7 form a good isochron of age 526 ± 13 Ma, initial $^{87}Sr/^{86}Sr$ of 0.7045 ± 0.0007 and low MSWD of 0.54. The parameters of this isochron are biased heavily toward the two aplite samples, 6 and 7, which have very high Rb/Sr ratios. A calculation was made to determine the isochron parameters of the four samples with the lowest Rb/Sr ratios (samples 1 to 4) for purposes of comparison with the six point isochron. The results, age 546 ± 75 Ma and initial $^{87}Sr/^{86}Sr$ ratio 0.7041 ± 0.0017, are indistinguishable within the statistical uncertainty, from the six point isochron parameters. The MSWD of the four point isochron is 2.1 indicating satisfactory fit of the experimental data to the calculated isochron. Both initial $^{87}Sr/^{86}Sr$ ratios 0.7045 and 0.7041 are consistent with mantle derivation of these rocks but do not preclude a short period of crustal residence.

The results for sample 5, confirmed by a replicate analysis, fall considerably below either of the above two isochrons and yield an age of 439 ± 17 Ma when calculated with an assumed initial $^{87}Sr/^{86}Sr$ ratio of 0.7045.

Geological Setting and Interpretation
by W.H. Poole

Geological Setting

A belt of granitic rocks as much as several kilometres wide extends for 50 km southwesterly from the St. John River near Saint John, to Negro Harbour, where the belt passes under Bay of Fundy. Alcock (1959) and Perry and Alcock (1960) mapped these granitic rocks as one elongate body intrusive into the Hadrynian and older strata and overlain by Pennsylvanian strata. The altered and deformed character of the granitic rocks in part led these authors to assign them a Proterozoic or earlier age (see also Potter et al., 1979). A suite of samples was collected in 1965 along the belt to determine the age of the granitic rocks by the Rb-Sr whole rock method.

More recent mapping by Ruitenberg and associates (1975a, b, c; 1979) subdivided the granitic belt within this Rb-Sr study area into four plutons with different although uncertain assigned ages. The geology portrayed by Ruitenberg and associates is not accepted by all recent workers and controversy continues (Rast and Grant, 1973; Currie, 1975; Rast and Currie, 1976). Despite these uncertainties, Figure 2 has been drawn from the work of Ruitenberg and associates so that the results of the Rb-Sr study can be viewed in terms of their pluton subdivisions. They believed that two of their plutons, the Red Head and Musquash, are Ordovician and earlier (?); a third, the Lepreau pluton, is Late Silurian and later (?); and a fourth, one of the Chance Harbour intrusions, is Mississippian and earlier (?). The seven analyzed whole rock samples used in this study are scattered through the four plutons (Fig. 2, Table 2). If Ruitenberg and associates are correct, these specimens should not yield an isochron, while if the original interpretation of Alcock (1959) and Perry and Alcock (1960) is correct, they might yield an isochron.

Most granitic rocks within the Red Head, Musquash and Lepreau plutons of the belt consist of altered hornblende-biotite granodiorite and quartz diorite. They are generally grey-green to pinkish, medium grained, equigranular, and either massive or weakly foliated. Plagioclase is green to yellow-green from saussuritization; potash feldspar is pink to orange-pink and commonly microperthitic; quartz is strained and partly recrystallized; and hornblende and biotite are altered to chlorite, epidote and sphene. The average of 46 modal analyses of thin sections of the Red Head and Lepreau plutons (Ruitenberg et al., 1979, appendices B-6 and B-7) is 26% quartz, 43% plagioclase, 13% potash feldspar, 12% combined chlorite, biotite and hornblende, and 6% combined additional alteration and accessory minerals. The average plots within the granodiorite field. The Chance Harbour pluton differs by being mainly a pink to orange, medium to coarse grained leucogranite (Ruitenberg et al., 1979).

The Red Head and Lepreau plutons, according to Ruitenberg et al. (1979), cut Hadrynian Coldbrook volcanics although some "intrusive" contacts are in dispute and may be thrust faults. The Lepreau pluton has intruded the Red Head pluton, and the Musquash pluton has intruded the Helikian(?) Green Head Group (Ruitenberg et al., 1979). All plutons are faulted against Pennsylvanian and Triassic strata.

Sample 1 (Chance Harbour pluton) is a tonalite consisting of 28% unstrained quartz, 55% planar-oriented euhedral to subhedral andesine-oligoclase, well zoned and in part oscillatory, 5% clear poikilitic potash feldspar and 12% combined green hornblende and highly altered biotite. Sample 1 was collected near the mapped border of the intrusion, and is lithologically unlike most rocks in the Chance Harbour intrusions as described by Ruitenberg et al. (1979). Sample 2 (Lepreau pluton) is an undeformed augite-bearing quartz diorite, atypical of the Lepreau and should be used with caution. Sample 3 (Lepreau pluton) is a massive granodiorite with 35% strained but not polygonized quartz, 41% saussuritized plagioclase, 20% slightly clouded microperthitic potash feldspar and 4% biotite partly altered to chlorite, epidote and sphene. Sample 4 (Red Head pluton) is a foliated granodiorite with 32% highly strained quartz with mortar texture, 40% saussuritized, fractured and bent plagioclase, and 20% microperthitic and fractured potash feldspar. Mafic minerals have been completely altered to chlorite, epidote and sphene. The rock has a close-spaced fracture cleavage. Sample 5 (Musquash pluton) is a massive granodiorite with 29% quartz, 45% saussuritized plagioclase rimmed by clear albite, 17% microperthitic potash feldspar and 9% mafic minerals completely altered to chlorite, sericite, epidote and sphene. And finally, samples 6 and 7 (Chance Harbour pluton) are both pink aplites from outcrops containing dioritic inclusions and epidote-chlorite stringers. They are petrographically similar: 39-41% weakly strained and unstrained quartz, 30-33% partly clouded, well twinned, weakly zoned oligoclase-albite, 27-28% potash feldspar some of which is microperthitic, and less than 1% chlorite, sphene and iron ore. Both aplite samples plot within the granite B field.

From: Rb-Sr and U-Pb Isotopic Age Studies in Current Research, Part C
Geol. Surv. Can., Paper 80-1C

Table 1

Analytical data, whole rock samples, granitic rocks between Ludgate Lake and Negro Harbour, southwestern New Brunswick

Sample No.	Rb ppm	Sr ppm	$^{87}Sr/^{86}Sr$ unspiked	$^{87}Sr/^{86}Sr$ spiked	$^{87}Sr/^{86}Sr$ average	$^{87}Rb/^{86}Sr$
1	46.75	405.9	0.7067	0.7054	0.7061 ± 0.0011	0.333 ± 0.010
2	72.84	213.0	*0.7131	0.7122	0.7127 ± 0.0011	0.990 ± 0.030
3	109.2	144.9	*0.7217	0.7207	0.7212 ± 0.0011	2.182 ± 0.065
4	88.46	*113.7	0.7218	*0.7205	0.7211 ± 0.0011	2.253 ± 0.068
5	145.4	58.81	0.7488	0.7497	0.7493 ± 0.0011	7.158 ± 0.215
6	177.9	* 11.62	*1.0369	*1.0383	1.0376 ± 0.0015	44.33 ± 1.33
7	171.2	* 4.644	*1.5023	*1.4984	1.5003 ± 0.0019	106.7 ± 3.2

*Average of two determinations

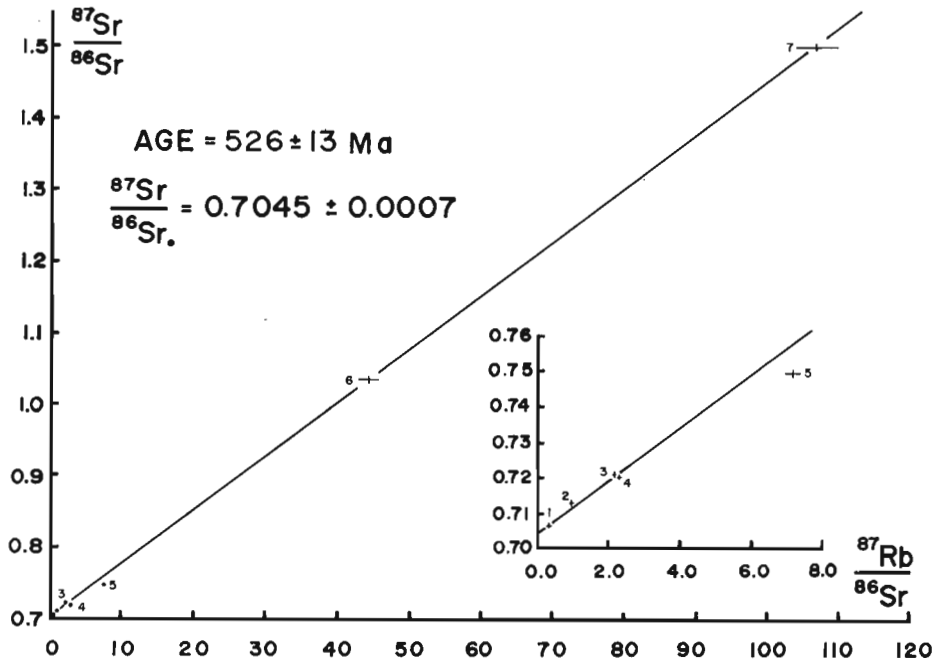

Figure 1. *Rb-Sr isochrons of some granitic rocks between Ludgate Lake and Negro Harbour, southwestern New Brunswick.*

ages related to an intrusive event at the Hadrynian-Cambrian boundary (or earlier).

In a more recent Rb-Sr study not yet complete (W.J. Olszewski and H.E. Gaudette, personal communication, 1980) a seven-point isochron of grey and pink granite samples collected along highway 1 about 8 km west of Ludgate Lake, presumably from the Musquash pluton, yielded an age of 615 ± 37 Ma with an initial $^{87}Sr/^{86}Sr$ ratio of 0.7056 ± 0.0032. This late Hadrynian age may well be the age of intrusion.

In our Rb-Sr study, samples 1, 2, 3 and 4 yielded an isochron (MSWD of 2.1) of 546 ± 75 Ma with a low initial ratio of 0.7041 ± 0.0017 and a narrow range of $^{87}Rb/^{86}Sr$ of 0.3 to 2.2. The 4 points on the isochron are reasonably collinear, but the samples were collected from three plutons as mapped by Ruitenberg et al. (1975a, b; 1979). As described and commented upon above, sample 1 is not characteristic of a Chance Harbour intrusion and sample 2 is an augite-bearing quartz diorite, quite atypical of the Lepreau pluton. Thus the significance of the age is uncertain.

Interpretation

Only one K-Ar age has been produced from the four plutons within the study area. Ruitenberg et al. (1979, p. 61) quoted an age, prepared by M. Shafiquallah, of 493 ± 15 Ma[1] on biotite from the Musquash pluton. The age is essentially the same as the 488 to 495 ± 20 Ma age range of four biotites and 517 ± 20 Ma age of one hornblende from the Fairville granite exposed on trend to the northeast in the City of Saint John (Wanless et al., 1970, p. 69; 1972, p. 68; 1973, p. 83). All these ages centre on Late Cambrian and Early Ordovician. Since the Cambrian and Lower Ordovician sequence near Saint John bears no evidence of an episode of folding and uplift during the Cambrian and Early Ordovician interval, such as to be expected to accompany intrusion of such large plutons, these K-Ar ages are probably cooling

A regressed line through samples 1, 2, 3, 4, 6 and 7 yielded as isochron (MSWD of 0.54) of 526 ± 13 Ma with a low initial ratio of 0.7045 ± 0.0007. Samples 6 and 7 consist of aplite from the Chance Harbour intrusion. The aplite may be the same age as the intrusion, and have had the same initial $^{87}Sr/^{86}Sr$ ratio, but we cannot be sure. Samples 6 and 7 have relatively high $^{87}Rb/^{86}Sr$ ratios compared with the samples 1, 2, 3 and 4, and thus the 526 Ma age is essentially that of the aplites alone.

Both of these ages centre on Cambrian. The 546 ± 75 Ma age from samples 1, 2, 3 and 4 using the error limits encompasses a 621 to 471 Ma range, i.e. from late Hadrynian to early Middle Ordovician. The 526 ± 13 Ma age from samples 1, 2, 3, 4, 6 and 7 encompasses Middle and Late Cambrian. As argued above, the Cambrian-Lower Ordovician

[1] K-Ar ages quoted from published papers have been recalculated using the new constants recommended by Steiger and Jäger (1977). The time scale used in this report is that of Armstrong (1978), constructed using the new constants.

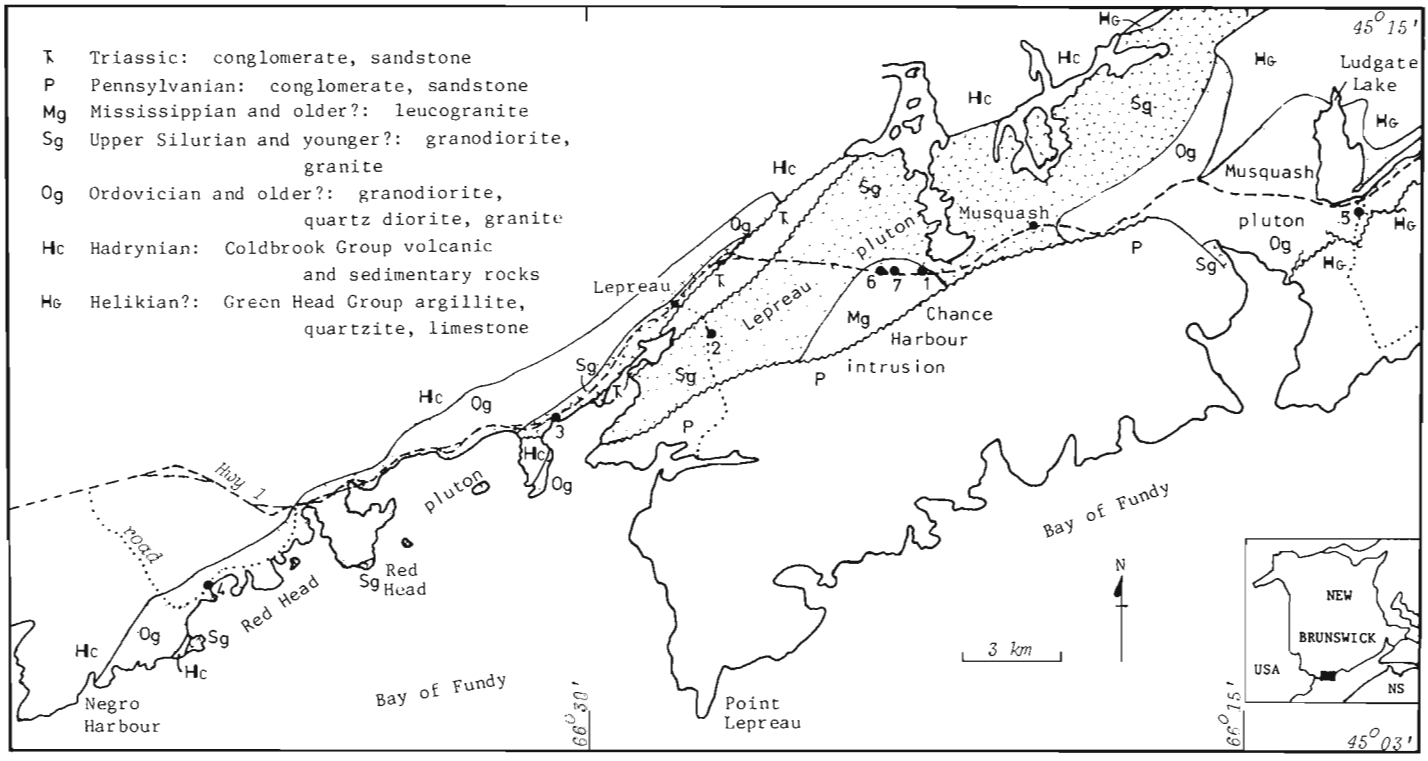

Figure 2. *Locations of samples from granitic rocks, southwestern New Brunswick. Geology after Ruitenberg et al. (1975a, b, c; 1979).*

Table 2

Sample numbers and localities, some granitic rocks between Ludgate Lake and Negro Harbour, southwestern New Brunswick

Sample No. This work	Field	Pluton	Rock Type	Location Latitude	Longitude	N.T.S.
1	PB65-245	Chance Harbour	Hornblende-biotite tonalite, grey, medium grained, foliated, non-cataclastic	45°10'48"	66°22'29"	21 G/1
2	PB65-227	Lepreau	Hornblende-biotite quartz diorite, grey, medium grained, massive, augite-bearing	45°09'55"	66°27'03"	21 G/1
3	PB65-222	Lepreau	Biotite granodiorite, orange-pink, medium grained, massive	45°08'23"	66°30'45"	21 G/2
4	PB65-212	Red Head	Chloritic granodiorite, green-grey with orange-pink feldspar, medium grained, foliated	45°05'43"	66°38'35"	21 G/2
5	PB65-254	Musquash	Chloritic granodiorite, green-grey with orange-pink feldspar, medium grained, massive	45°11'43"	66°12'23"	21 G/1
6	PB65-242	Chance Harbour	Aplite, pink, fine grained, massive	45°10'52"	66°23'21"	21 G/1
7	PB65-243	Chance Harbour	Aplite, pink, fine grained, massive	45°10'50"	66°23'07"	21 G/1

sequence near the City of Saint John lacks internal evidence of folding and uplift within this period. I conclude that the plutons were emplaced probably in the late Hadrynian or very early Cambrian, perhaps as synvolcanic intrusions related to the extensive Hadrynian Coldbrook Group. Cambrian volcanic rocks which could be co-genetic with the plutons, however, do occur here and there within the Cambrian strata of the Avalon zone of the Canadian Appalachian belt. One locality is at Beaver Harbour on the west edge of Figure 2 (Helmstaedt, 1968). Nevertheless, it seems entirely possible that the Red Head, Lepreau and the one Chance Harbour intrusion in the study area are of late Hadrynian age. A similar but stronger conclusion can be made for the Musquash pluton from the isochron of Olszewski and Gaudette (see above). It seems therefore that from these data the age assignment of Alcock (1959) and Perry and Alcock (1960) is probably correct as opposed to the age assignments of Ruitenberg et al. (1975a, b, c; 1979).

Our Musquash sample, number 5, an altered granodiorite, plotted far off the regressed lines of our isochrons. A replicate analysis confirmed that the analysis is not spurious. An age line through sample 5 with an assumed initial $^{87}Sr/^{86}Sr$ ratio of 0.7045 of one of our isochrons yielded an age of 439 Ma (mid-Silurian). We have no explanation for this disparity.

References

Alcock, F.J.
1959: Geology, Musquash area, Charlotte, Kings and Saint John Counties, New Brunswick; Geological Survey of Canada, Map 1084A.

Armstrong, R.L.
1978: Pre-Cenozoic Phanerozoic time scale – computer file of critical dates and consequences of new and in-progress decay-constant revisions; in Contributions to the Geologic Time Scale, ed. G.V. Cohee, M.F. Glaessner and H.D. Hedberg; American Association of Petroleum Geologists, Studies in Geology No. 6, p. 73-91.

Currie, K.L.
1975: Studies of granitoid rocks in the Canadian Appalachians; in Report of Activities, April to October 1974; Geological Survey of Canada, Paper 75-1A, p. 265-270.

Helmstaedt, Herwart
1968: Structural analysis of the Beaver Harbour area, Charlotte County, New Brunswick; University of New Brunswick, unpublished Ph.D. thesis.

Perry, S.C. and Alcock, F.J.
1960: Geology, St. George area, Charlotte County, New Brunswick; Geological Survey of Canada, Map 1094A.

Potter, R.R., Jackson, E.V., and Davies, J.L., compilers
1979: Geological map, New Brunswick; New Brunswick Department of Natural Resources, Map Number N.R.-1, Second Edition.

Rast, N. and Currie, K.L.
1976: On the position of the Variscan front in southern New Brunswick and its relation to Precambrian basement; Canadian Journal of Earth Sciences, v. 13, p. 194-196.

Rast, N. and Grant, R.H.
1973: The Variscan Front in southern New Brunswick; in Geology of New Brunswick, ed. N. Rast; Field Guide to Excursions, New England Intercollegiate Geological Conference, p. 4-11.

Ruitenberg, A.A., Giles, P.S., Venugopal, D.V.,
Buttimer, S.M., McCutcheon, S.R., and Chandra, J.
1975a: Saint George, east half; in Geological Maps to accompany report 'Geology and Mineral Deposits of Caledonia Area'; New Brunswick Department of Natural Resources.

1975b: Musquash, west half; in Geological Maps to accompany report 'Geology and Mineral Deposits of Caledonia Area'; New Brunswick Department of Natural Resources.

1975c: Musquash, east half; in Geological Maps to accompany report 'Geology and Mineral Deposits of Caledonia Area'; New Brunswick Department of Natural Resources.

1979: Geology and mineral deposits of Caledonia area; New Brunswick Department of Natural Resources, Memoir 1, 213 p.

Steiger, R.H. and Jager, E., compilers
1977: Subcommission of Geochronology: convention on the use of decay constants in geo- and cosmochronology; Earth and Planetary Science Letters, v. 36, no. 3, p. 359-362.

Wanless, R.K., Stevens, R.D., Lachance, G.R., and
Delabio, R.N.
1970: Age determinations and geological studies, K-Ar isotopic ages, report 9; Geological Survey of Canada, Paper 69-2A, 78 p.

1972: Age determinations and geological studies, K-Ar isotopic ages, report 10; Geological Survey of Canada, Paper 71-2, 96 p.

1973: Age determinations and geological studies, K-Ar isotopic ages, report 11; Geological Survey of Canada, Paper 73-2, 139 p.

3. Rb-Sr AGES OF THE "SUGAR" GRANITE AND LOST LAKE GRANITE, MIRAMICHI ANTICLINORIUM, HAYESVILLE MAP AREA, NEW BRUNSWICK

A) "Sugar" granite
Isochron Age = 498 ± 19 Ma
$^{87}Sr/^{86}Sr$ initial = 0.7034 ± 0.0029

B) Lost Lake granite
Errorchron Age = 444 Ma
$^{87}Sr/^{86}Sr$ initial = 0.7070

The "Sugar" granite: Eight whole rock samples and one biotite from the "Sugar" granite were isotopically analyzed. The results are listed in Table 1A and depicted in an isochron diagram, Figure 1. Five of the eight whole rock samples define an isochron of age 498 ± 19 Ma, initial ratio 0.7034 ± 0.0029 and MSWD 1.13. The other three samples, A3, A4 and A7 fall below this line. An errorchron age of 484 ± 33 Ma, intercept 0.7039 ± 0.0052 and MSWD 4.85 is obtained if all eight samples are included in the regression analysis. The biotite-whole rock age for sample A8 is 378 ± 31 Ma with a high initial ratio of 0.7409 ± 0.0094. The low initial ratio of 0.7034 for the whole rock isochron is compatible with a mantle derivation for rocks of this age and is indicative of a primary origin for the "Sugar" granite.

The Lost Lake granite: Isotopic compositions were determined for five whole rock samples and one muscovite from the Lost Lake granite. The results are listed in Table 1B and depicted on the isochron plot of the "Sugar" granite, Figure 1. The four whole rock samples with $^{87}Rb/^{86}Sr$ ratios less than 11 form an errorchron of age 444 ± 72 Ma, initial $^{87}Sr/^{86}Sr$ ratio of 0.7070 ± 0.0049 and MSWD 11.52. Separate anlayses were performed on two splits of whole rock sample B5 which were not included in the errorchron regression due to its extremely high $^{87}Rb/^{86}Sr$ ratio. The high isotopic ratios of this sample allow calculation of an age which is only minimally affected by the choice of initial $^{87}Sr/^{86}Sr$ ratio. The ages determined for the two splits are 412 ± 12 and 411 ± 13 Ma, assuming an initial ratio of 0.707, equivalent to the errorchron initial ratio. The muscovite-whole rock age for sample B4 is 424 ± 24 Ma with initial ratio 0.7110 ± 0.0036.

Geological Setting and Interpretation
by W.H. Poole

Geological Setting

The granitic rocks of western Hayesville map area (21 J/10) in central New Brunswick have intruded sedimentary and volcanic strata of Early and Middle Ordovician age, equivalent to and correlative with the Tetagouche Group some 80 km on trend to the northeast in the Bathurst district (Skinner, 1974). These strata can be divided into two mappable units. The lower unit consists of quartzose and pelitic sedimentary rocks which locally at the top contain brachiopods and conodonts of late Early Ordovician age (Neuman, 1971, 1972; Nowlan, in press). The metamorphic level, usually that of slate, grades locally northwesterly through cordierite-andalusite to sillimanite of the amphibolite facies. The quartzose and aluminous nature of the strata led Poole (1963, 1967) to speculate that they were deposited in a para-platformal depositional environment upon an underlying, unexposed older basement of Hadrynian or earlier age. The younger unit consists in the Hayesville area of mafic volcanics, manganiferous and ferruginous slate and chert, graptolitic graphitic slate and chert, overlain by a thick assemblage of greywacke and slate. The graptolites are of Middle Ordovician (Caradocian) age. In the southeastern part of Hayesville map area, Silurian greywacke and slate of the Fredericton Synclinorium are faulted against the Ordovician strata (Poole, 1963). Detritus in the Silurian greywacke includes fragments of mafic volcanic rocks, deformed quartz, some plagioclase and a variety of sedimentary rocks, much of which could have been derived from the Ordovician terrane. The Ordovician and Silurian rocks have been folded into major anticlines and synclines, and many of the strata are steeply overturned (Poole, 1963; Anderson and Poole, 1959; Crouse, 1979a, b, c).

The granitic rocks were separated by Poole (1963) into an older, presumed Upper Ordovician or Lower Silurian, cataclastic and partly recrystallized assemblage, and a younger, Devonian non-cataclastic assemblage, containing as one member the epizonal Burnthill muscovite-biotite granite associated with molybdenite, wolframite, cassiterite and fluorite.

The western half of the Hayesville map area has recently been remapped (Fig. 2) and the results published at a more detailed scale of 1 inch to 1/4 mile (Crouse, 1979a, b, c). Crouse confirmed the existence of Poole's younger granites, the Burnthill granite and the Nashwaak granite, but he subdivided Poole's older granites into three types, two of Ordovician age and the third of Devonian age (Crouse's Lost Lake granite).

A Rb-Sr study was carried out to determine the age of magmatic crystallization of the old granites (as then envisioned by Poole). The superimposed deformation, attendant alteration and recrystallization were hoped to be either essentially the "same" age as that of emplacement or if considerably younger, to be insufficient to chemically homogenize the isotopes and reset the Rb-Sr clock. Samples were collected from two areas and since the petrography of the rocks is quite different in each, the resulting Rb-Sr plots will be considered separately, firstly the "Sugar" granite and then the Lost Lake granite.

1. "Sugar" granite The "Sugar" granite, a field name used informally by Poole during mapping, is an elongate body about 10 km long and 2.5 km wide in southwestern Hayesville map area and adjacent Juniper map area (St. Peter, 1979c). It trends northwest athwart the northeasterly grain of the Miramichi Anticlinorium (Fig. 2). Along its northeast side, the granite has intruded the lower, quartzose and pelitic unit of the Ordovician rocks, the pelitic members of which consist of sillimanite-muscovite-biotite schist. The granite in turn was intruded by the Devonian Nashwaak granite along its southwest side and southeast end. The "Sugar" granite (Table 2A) is light pink to light grey, weathers deeply to a light honey brown, and has a distinctive fine grained granular

From: Rb-Sr and U-Pb Isotopic Age Studies in Current Research, Part C Geol. Surv. Can., Paper 80-1C

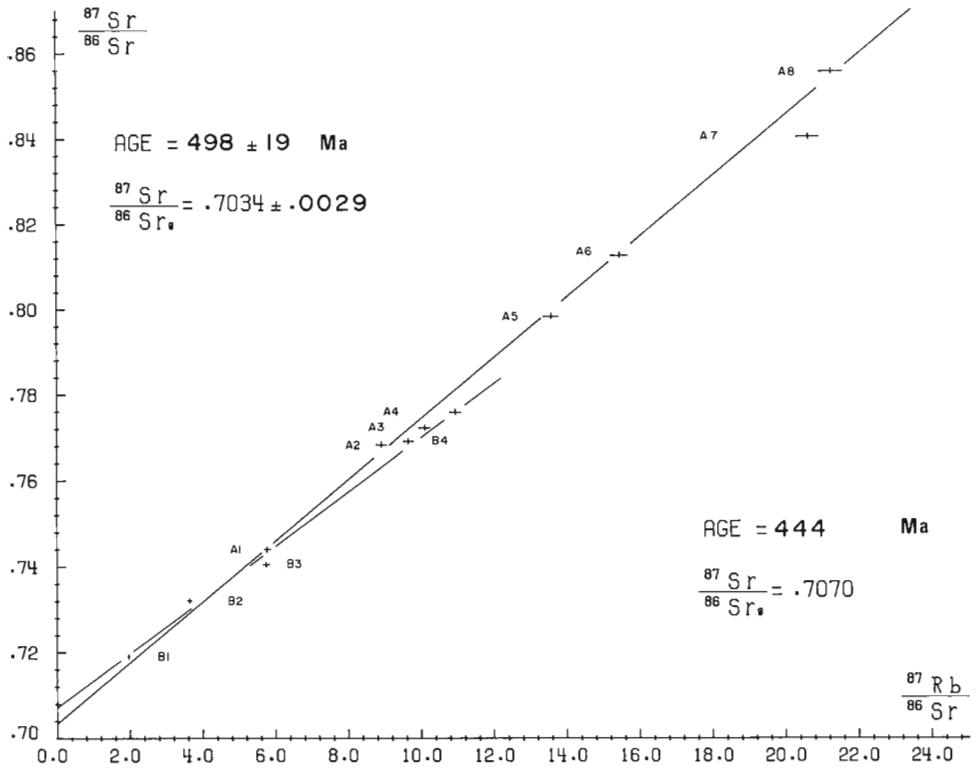

Figure 1. *Rb-Sr isochron diagram, "Sugar" granite and Lost Lake granite, Hayesville map area, New Brunswick.*

or sugary texture (Fig. 3). Discontinuous streaks of dark brown to black biotite "dust" define a wavy foliation. In thin sections, the rock exhibits allotriomorphic granular mosaic texture and lacks evidence of strain and alteration except for minor alteration of biotite. Most minerals are anhedral and equidimensional, from 0.2 to 1.0 mm in diameter with some to 2 mm. Potash feldspar displays microcline twinning and some larger, possibly relict crystals are perthitic. Plagioclase (oligoclase) has well developed albite twinning, is weakly zoned, and only slightly altered to white micas. Biotite is pleochroic dark brown to light yellow and slightly altered to chlorite. Point counts of two thin sections of typical granite yielded 39% quartz, 20-30% microcline, 30-40% oligoclase, 1-2% biotite, and a trace of muscovite and accessories. The granite appears to have been cataclastically deformed and completely recrystallized to produce a granoblastic texture.

2. Lost Lake granite The Lost Lake granite (Crouse, 1979a, b) within northwestern Hayesville map area is a body 16 km long and varies from 3 km wide north of the Burnthill granite in the east to 11 km wide at the west edge of Hayesville map area (Fig. 2). It extends 7 km farther southwest into Juniper map area (St. Peter, 1979a, b). The granite body trends northeasterly parallel to the Miramichi Anticlinorium. In Hayesville map area, Crouse (1979a, b) separated the Lost Lake granite from a cataclastic, pink to grey medium to coarse grained granite and granodiorite which he considered to be of Ordovician age. Since Crouse believed the Lost Lake granite to be Devonian, the contact therefore must be intrusive. Poole (1963) considered both the Lost Lake granite and Crouse's Ordovician granite to be of Late Ordovician or Early Silurian age. The Lost Lake granite is clearly cut by the Burnthill granite of Devonian age (Poole 1963; Crouse 1979a, b). Crouse further subdivided his Lost Lake granite into two intergradational phases: a central phase he described as pink, medium to coarse grained, equigranular to subporphyritic, biotite-muscovite granite with minor garnet-biotite-muscovite pegmatite, and a bordering phase he described as light grey to light pink, massive to weakly foliated, medium grained, equigranular biotite granite with minor pegmatite. All the samples collected for the Lost Lake granite Rb-Sr study fall within Crouse's central phase. However, samples B1 (Fig. 4), B3 and B4 (Table 2B) are grey medium grained biotite granodiorite and biotite-muscovite granite lacking visible foliation on the outcrop but as seen in thin sections are deformed more severely than the Burnthill and Nashwaak granites. Biotite is reddish brown, altered to chlorite and opaques, and bent, and some associated muscovite is bent. Quartz is highly strained and polygonized. Plagioclase is oligoclase, albite-twinned, zoned, and some crystals are bent and broken, and the cores altered to sericite. Potash feldspar displays microcline twinning. Sample B1 (Fig. 4) has 28% quartz, 44% oligoclase, 14% microcline and 13% biotite, and Sample B4 has 27% quartz, 35% oligoclase, 25% microcline, 5% altered biotite and 8% muscovite. Sample B2 is a biotite augen granodiorite, more intensely deformed than samples B1, B3 and B4. Sample B5 is a deformed pink garnetiferous aplite. Sample B6 is like B1, B3 and B4.

Interpretation

1. "Sugar" granite Sample A8 yielded a K-Ar age of biotite of 366 ± 14 Ma[1] (Wanless et al., 1973, p. 79-82), which falls on the Devonian-Mississippian boundary. This age seems to be low by at least 5% because biotite from a sample of the younger Nashwaak granite about 1 km southeast of the "Sugar" granite and about 1.5 km southeast of sample locality A8 yielded a K-Ar age of 386 ± 16 Ma, that is, about the boundary between Middle and Late Devonian (Wanless et al., 1972, p. 71). Furthermore, biotite, muscovite and hornblende from schist, granite and amphibolite along the Plaster Rock-Renous highway in Tuadook Lake map area next north of Hayesville map area yielded five K-Ar ages ranging from 384 ± 16 to 394 ± 16 Ma (Wanless et al., 1972, p. 73-76). Similarly a Rb-Sr plot of biotite and whole rock analyses of sample A8 yielded 378 ± 31 Ma with a very high initial $^{87}Sr/^{86}Sr$ ratio of 0.7409. All these dates are interpreted as cooling ages associated with intrusion and uplift of Devonian (Acadian) granites, the K-Ar method yielding the age when the rocks cooled to the temperature at which the minerals began retaining argon and the biotite-whole rock Rb-Sr method yielding an age when the strontium isotopes became immobile.

The Rb-Sr regression lines yield ages ranging from 498 ± 19 to 484 ± 33 Ma depending upon which samples are used to control the lines. All samples, A1 to A8, are of the same lithology and character, and petrographically there is no reason to discard one sample or another from the plot.

[1] All K-Ar and Rb-Sr ages quoted from published papers, as well as those presented here, have been calculated or recalculated using the new constants recommended by Steiger and Jäger (1977). The time scale used in this report is that of Armstrong (1978), constructed using the new constants.

Table 1A

Analytical data, biotite and whole rock samples, "Sugar" granite

Sample No.	Rb ppm	Sr ppm	$^{87}Sr/^{86}Sr$ unspiked	$^{87}Sr/^{86}Sr$ spiked	$^{87}Sr/^{86}Sr$ average	$^{87}Rb/^{86}Sr$
A1	136.5	68.39	*0.7438	0.7443	0.7440 ± 0.0011	5.779 ± 0.173
A2	170.8	55.45	0.7678	0.7686	0.7682 ± 0.0012	8.919 ± 0.268
A3	331.0	99.13	0.7693	0.7687	0.7690 ± 0.0012	9.666 ± 0.290
A4	182.7	48.26	0.7765	0.7751	0.7758 ± 0.0012	10.96 ± 0.33
A5	193.7	*41.27	0.7991	*0.7972	0.7982 ± 0.0012	13.59 ± 0.41
A6	186.5	34.70	0.8114	0.8136	0.8125 ± 0.0012	15.47 ± 0.46
A7	249.2	34.94	0.8392	0.8415	0.8403 ± 0.0013	20.65 ± 0.62
A8	*242.8	33.03	0.8552	0.8558	0.8555 ± 0.0013	21.28 ± 0.64
A8 biotite	169.1	8.99	3.4609	3.8863	3.6736 ± 0.2130	544.6 ± 16.3

*Average of two determinations

Table 1B

Analytical data, muscovite and whole rock samples, Lost Lake granite

Sample No.	Rb ppm	Sr ppm	$^{87}Sr/^{86}Sr$ unspiked	$^{87}Sr/^{86}Sr$ spiked	$^{87}Sr/^{86}Sr$ average	$^{87}Rb/^{86}Sr$
B1	146.1	214.4	0.7191	0.7189	0.7190 ± 0.0011	1.972 ± 0.059
B2	137.9	109.6	0.7321	0.7321	0.7321 ± 0.0011	3.643 ± 0.109
B3	*245.9	*123.8	0.7405	*0.7405	0.7405 ± 0.0011	5.751 ± 0.173
B4	267.6	76.59	0.7721	0.7720	0.7721 ± 0.0011	10.12 ± 0.30
B4 muscovite	647.9	6.84	2.4412	2.2926	2.3669 ± 0.074	274.2 ± 8.2
B5 (A)	330.7	2.93	2.6212	2.6268	2.6240 ± 0.0028	327.2 ± 9.8
B5 (B)	*376.7	2.80	2.9965	2.9797	2.9881 ± 0.0084	390.1 ± 11.7

*Average of two determinations

The relatively high range of $^{87}Rb/^{86}Sr$ ratios, from about 6 to 21, reflects the potassic nature of the granite. Samples A1, A2, A5, A6 and A8 define an isochron (MSWD of 1.13) of 498 ± 19 Ma with a low initial $^{87}Sr/^{86}Sr$ ratio of 0.7034 ± 0.0029. By including samples A3 and A4 (A4 was collected far from the other samples), the regression line becomes an errorchron of 496 ± 35 Ma (MSWD of 3.90) and when sample A7 is added, the line is another errorchron of 484 ± 33 Ma (MSWD of 4.85), both with similar low initial ratios of 0.7025 ± 0.0052 and 0.7034 ± 0.0052, respectively.

The isochron age of 498 ± 19 Ma centres on late Early Ordovician (Arenig) and the two errorchrons on late Early Ordovician and early Middle Ordovician. The "Sugar" granite thus is the same age as the volcanic rocks in the Tetagouche Group. A few thin, altered siliceous ash beds are intercalated in the calcareous strata bearing Arenigian brachiopods at Lower Birch Island in eastern Hayesville map area (Poole, 1963) at the top of the lower unit of the Tetagouche Group. Most of the volcanic rocks in the Tetagouche Group northeast of Hayesville map area appear to lie between the Arenigian horizon and the Caradocian graptolitic black slate and chert horizon, that is about Llanvirnian and Llandeilian. The "Sugar" granite is thus probably a subvolcanic pluton and the volcanic envelope and cap, if the granite rose to that level, have been eroded away.

The age of the deformation and recrystallization of the "Sugar" granite is uncertain. If the metamorphic minerals of the bordering sillimanite schist were produced during intrusion of the "Sugar" granite magma, then they should have become deformed during deformation followed by recrystallization of the granite. But the metamorphic minerals are not deformed. Therefore, the granite may have been emplaced as a hot solid which underwent deformation and recrystallization during emplacement. If on the other hand, the granite was deformed and recrystallized at its present level and at a lower temperature, then the metamorphic minerals of the bordering schist must be genetically related to the younger, Devonian granite although hornfels and not schist is the characteristic contact metamorphic rock bordering the Devonian granites in Hayesville map area and most if not all other areas of the Miramichi Anticlinorium. Thus a hot solid emplacement of the granite is an attractive hypothesis, and is partly supported by the unusual northwesterly cross-trend of the granite, and the moderate outward dips of the concordant bordering schist.

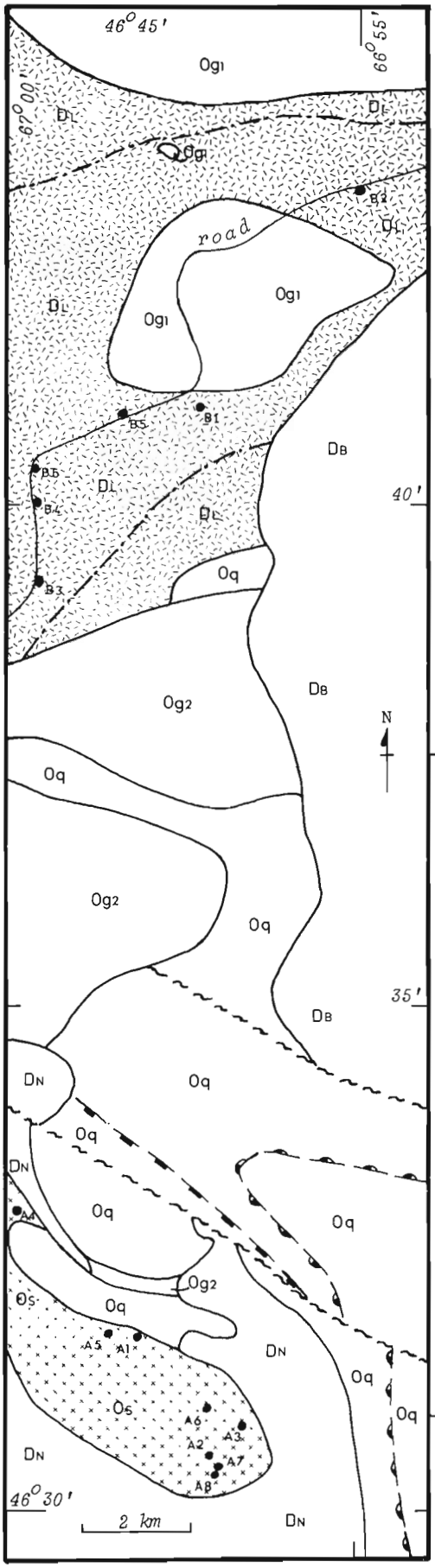

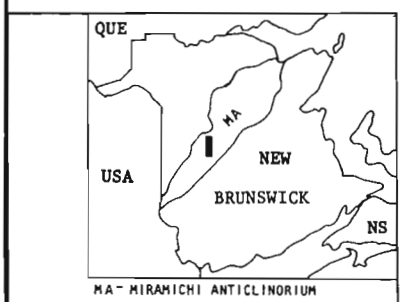

Devonian

- D_B Burnthill granite
- D_N Nashwaak granodiorite
- D_L Lost Lake granodiorite

Ordovician

- Og_1 feldspar augen granite
- Og_2 foliated biotite granite
- O_S "Sugar" granite
- O_q quartzite, slate; metamorphic equivalents

cordierite-andalusite isograd

sillimanite isograd

Figure 2. *Location of samples from the "Sugar" granite and the Lost Lake granite, western Hayesville map area, New Brunswick. Geology after Crouse (1979a, b, c).*

Deformation and recrystallization of the "Sugar" granite could conceivably have occurred in the late Middle or Late Ordovician during the Taconian Orogeny (Poole, 1967) if the lack of deformation of the metamorphic minerals in the bordering sillimanitic schist is overlooked or explained otherwise. If such thorough recrystallization could be expected to have homogenized the strontium isotopes and reset the Rb-Sr clock, then the isochron age should have been about 450-460 Ma, some 8 per cent younger than the 496 Ma isochron. This alternative seems improbable.

A question which arises is whether the proposed solid emplacement of the "Sugar" granite in Arenigian to Llandeilian time should be reflected in the Tetagouche stratigraphic record by an episode of deformation and uplift. An unconformity has not been observed within the Tetagouche Group and its equivalents in the Miramichi Anticlinorium although conglomerate has been noted here and there about this stratigraphic level (below the Caradocian graptolitic rocks) in the Napadogan map area, next south of the Hayesville map area (Anderson and Poole, 1959) and in nearby parts of Hayesville map area (Potter 1968; Crouse, 1979c). Neuman (1967) reported an unconformity in the Shin Pond area of Maine, 150 km west-southwest of the "Sugar" granite between older pelitic, quartzose and tuffaceous strata (equivalent of the lower Tetagouche Group) and younger tuff and tuffaceous sandstone bearing Arenigian brachiopods (equivalent of the upper Tetagouche Group) (Neuman, 1971, 1972). The possibility exists therefore that an unconformity does separate the two units of the Tetagouche Group and the fact that it has not been observed in the Hayesville and Napadogan map areas may be attributed to the lack of a significant widespread conglomerate above the unconformity and to the lack of exposure of the contact itself. Curiously, the strata immediately above the Arenigian calcareous slate at Lower Birch Island consist of red ferruginous and manganiferous slate and chert overlain by the Caradocian slate and chert; both rocks are probably of quiet deep water origin and are quite unlike those to be expected above an unconformity occasioned by deformation and uplfit.

A similar 7-point Rb-Sr isochron age of 479 ± 14 Ma with a similar low initial $^{87}Sr/^{86}Sr$ ratio of 0.7030 ± 0.0060 was obtained from a light pink, medium to coarse grained, schistose augen granite in samples from several bodies as much as 40 km apart in northeastern Miramichi Anticlinorium centred about 85 km northeast of the "Sugar" granite (Fyffe et al., 1977). These authors interpreted the age as indicating emplacement during Early Ordovician (although on Armstrong's (1978) time scale, 479 Ma is Llanvirnian of the early Middle Ordovician) and that the granite was "consanguineous with extensive felsic volcanic rocks of the Tetagouche Group" (Fyffe et al., 1977, p. 1689). They presumably believed that the penetrative deformation, alteration and a later deformation did not modify the isotopic ratios, or that these superimposed processes occurred in the Early Ordovician (or early Middle Ordovician). Nevertheless, the 479 ± 14 Ma isochron is sufficiently like our 498 ± 19 Ma isochron to indicate that early Ordovician plutonism was a widespread event in the Miramichi Anticlinorium.

2. Lost Lake granite Sample B6, not part of the Rb-Sr study, yielded a K-Ar age of biotite of 394 ± 18 Ma and sample B4 yielded a K-Ar age of muscovite of 363 ± 16 Ma (Wanless et al., 1973, p. 79-82). Sample B4 muscovite and whole rock yielded a Rb-Sr age of 424 ± 24 Ma with an initial $^{87}Sr/^{86}Sr$ ratio of 0.7110 in this present study. The K-Ar ages 394 and 363 Ma span the Middle and Late Devonian and are presumably Acadian cooling ages. The Rb-Sr muscovite age of 424 Ma, on the other hand, centres on latest Silurian, but using the ±24 Ma analytical error, spans Silurian and Early Devonian.

Table 2A

Sample numbers and localities, "Sugar" granite,
southwestern Hayesville map area, New Brunswick

Sample No. This work	Sample No. Field	Rock type	Locality Latitude	Locality Longitude	N.T.S.
A1	5-33-1/PB	Biotite granite, fine grained, foliated	46°31'46"	66°58'05"	21 J/10
A2	5-20-4/PBK	Biotite granite, fine grained, foliated	46°30'35"	66°57'04"	21 J/10
A3	5-32-1/PB	Biotite granite, fine grained, foliated	46°30'51"	66°56'36"	21 J/10
A4	5-24-3/PB	Biotite granite, fine to medium grained, foliated	46°33'01"	66°59'51"	21 J/10
A5	5-33-4/PB	Biotite granite, fine grained, foliated	46°31'48"	66°58'32"	21 J/10
A6	5-19-1/PBM	Biotite granite, fine grained, foliated	46°31'01"	66°57'06"	21 J/10
A7	5-20-3/PBK	Biotite granite, fine to medium grained, foliated	46°30'26"	66°56'58"	21 J/10
A8	5-35-2/PB	Biotite granite, fine grained, foliated (Fig. 3)	46°30'23"	66°56'59"	21 J/10

Table 2B

Sample numbers and localities, Lost Lake granite,
northwestern Hayesville map area, New Brunswick

Sample No. This work	Sample No. Field	Rock Type	Locality Latitude	Locality Longitude	N.T.S.
B1	5-30-4/PB	Biotite granodiorite, medium grained, deformed (Fig. 4)	46°40'59"	66°57'14"	21 J/10
B2	5-30-2/PB	Biotite augen granodiorite, intensely deformed	46°43'13"	66°54'52"	21 J/10
B3	6-47-1/PB	Biotite granodiorite, medium grained, weakly deformed	46°39'15"	66°59'35"	21 J/10
B4	5-30-6/PB	Biotite-muscovite granite, medium to coarse grained, slightly deformed	46°40'02"	66°59'41"	21 J/10
B5	6-47-2/PB	Garnetiferous biotite-muscovite aplite, slightly deformed	46°40'52"	66°58'18"	21 J/10
B6	5-30-5/PB	Biotite-muscovite granodiorite, medium to coarse grained, slightly deformed	46°40'24"	66°59'39"	21 J/10

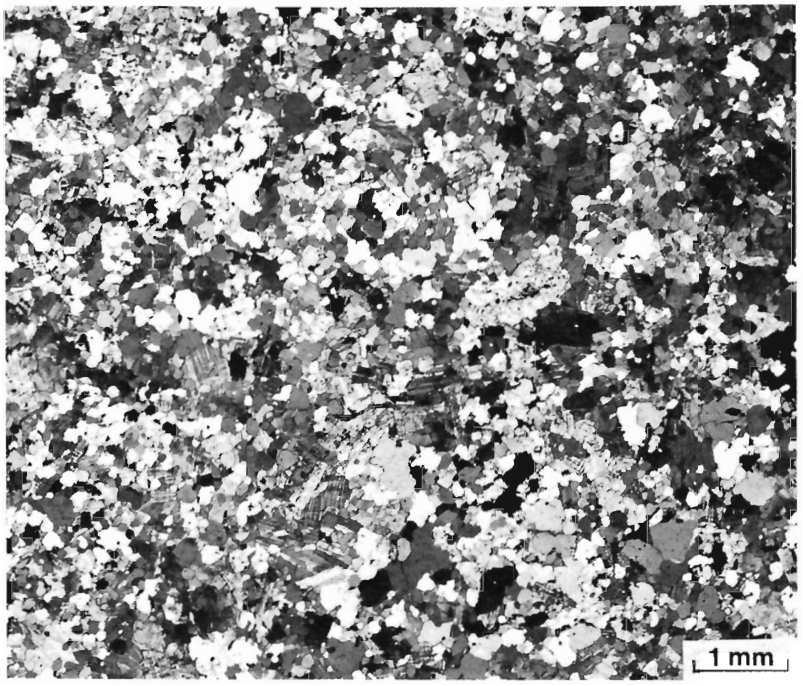

Figure 3. Photomicrograph of typical "Sugar" granite showing fine grained allotriomorphic granular mosaic (granoblastic) texture of undeformed albite, microcline, quartz and biotite. Sample A8. (GSC Photo 203617)

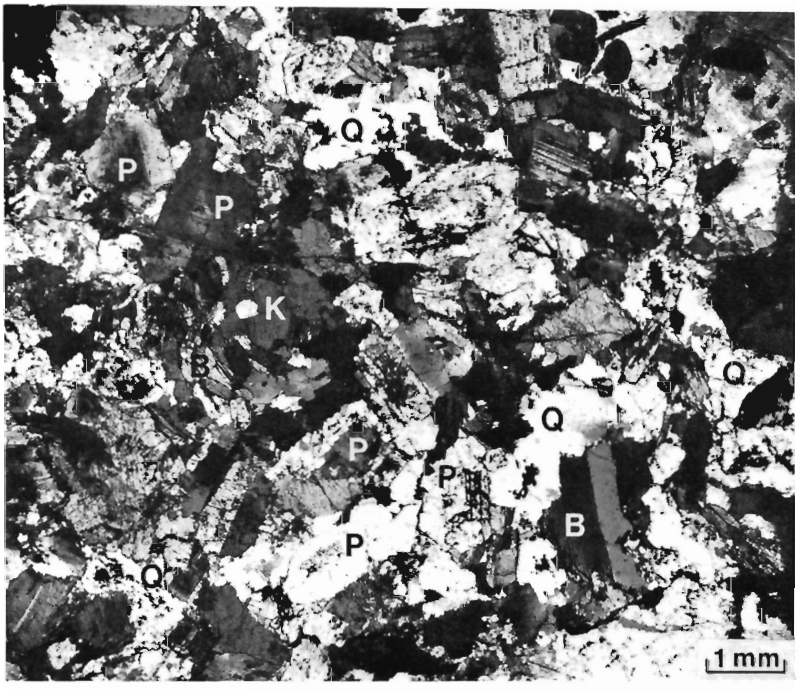

Figure 4. Photomicrograph of Lost Lake granite. Medium grained biotite granodiorite with deformed and partly recrystallized quartz (Q), zoned oligoclase (P) with altered cores, minor potash feldspar (K) and bent and altered biotite (B). Sample B1. (GSC Photo 203617A)

The Rb-Sr regression line through samples B1 through B4 is unfortunately an errorchron with a large MSWD of 11.52. The 444 Ma age has a large error of ±72 Ma, although the initial $^{87}Sr/^{86}Sr$ ratio of 0.7070 is moderately low. Compared with the "Sugar" granite, the Lost Lake granite's age appears to be younger, the initial ratio is higher and the scatter of plotted analyses is much greater despite the fact that the Lost Lake granite has undergone much less deformation and recrystallization.

Samples B1, B3 and B4 are lithologically very similar: grey, medium to coarse grained biotite (muscovite) granodiorite and granite with relatively mild deformational features, whereas sample B2 is a biotite augen granodiorite with intense deformational features. A regression line through samples B1, B3 and B4 yields an errorchron (MSWD of 9.32) of 448 ± 65 Ma with an initial $^{87}Sr/^{86}Sr$ ratio of 0.7058 ± 0.0049, almost the same age as that for all four samples B1 through B4.

Two splits of samples B5, a deformed garnetiferous aplite yielded Rb-Sr whole rock ages of 412 ± 12 and 411 ± 13 Ma based on an assumed initial $^{87}Sr/^{86}Sr$ ratio of 0.707. The aplite has very high rubidium and low strontium, and is quite unlike samples B1, B3 and B4. The 411 Ma age centres on early Early Devonian.

The errorchron ages of 444 and 448 Ma fall upon the Ordovician-Silurian boundary although with the error, the age could be some time between Late Cambrian and Late Devonian. Thus the errorchrons do not provide a satisfactory age of the Lost Lake granite and further geochronological study must be undertaken.

References

Anderson, F.D. and Poole, W.H.
1959: Geology of Woodstock-Fredericton, York, Carleton, Sunbury and Northumberland Counties, New Brunswick; Geological Survey of Canada, Map 37-1959.

Armstrong, R.L.
1978: Pre-Cenozoic Phanerozoic time scale – computer file of critical dates and consequences of new and in-progress decay-constant revisions; in Contributions to the Geologic Time Scale, ed. G.V. Cohee, M.F. Glaessner, and H.D. Hedberg; American Association of Petroleum Geologists, Studies in Geology No. 6, p. 73-91.

Crouse, Gregory
1979a: Parts of Burnthill and Clearwater Brooks, Victoria, Carleton and York Counties (K-14); New Brunswick Department of Natural Resources, Plate 79-32.

1979b: Lower part of Burnthill Brook, Carleton and York Counties (K-15); New Brunswick Department of Natural Resources, Plate 79-33.

1979c: Mouth of McKiel and Burnthill brooks, York County (K-16); New Brunswick Department of Natural Resources, Plate 79-34.

Fyffe, L.R., Irrinki, R.R., and Cormier, R.F.
1977: A radiometric age of deformed granitic rocks in north-central New Brunswick; Canadian Journal of Earth Sciences, v. 14, no. 7, p. 1687-1689.

Neuman, R.B.
1967: Bedrock geology of the Shin Pond and Stacyville quadrangles, Penobscot County, Maine; United States Geological Survey, Professional Paper 524-I, 37 p.

1971: An early Middle Ordovician brachiopod assemblage from Maine, New Brunswick and northern Newfoundland; in Paleozoic Perspectives: a Paleontological Tribute to G. Arthur Cooper, ed. J.T. Dutro, Jr.; Smithsonian Contributions Paleobiology, no. 3, p. 113-124.

1972: Brachiopods of Early Ordovician volcanic islands; 24th International Geological Congress, 1972, Section 7, p. 297-302.

Nowlan, G.S.
Some Ordovician conodont faunules from the Miramichi Anticlinorium, New Brunswick; Geological Survey of Canada, Bulletin. (in press)

Poole, W.H.
1963: Geology of Hayesville, New Brunswick; Geological Survey of Canada, Map 6-1963.

1967: Tectonic evolution of Appalachian region of Canada; in Collected Papers on Geology of the Atlantic Region, Hugh Lilly Memorial Volume, ed. E.R.W. Neale and H. Williams; Geological Association of Canada, Special Paper No. 4, p. 9-51.

Potter, R.R.
1968: Geology of the Burnt Hill area with special reference to the ore controls in the vicinity of the Burnt Hill tungsten mine; Carleton University, unpublished Ph.D. thesis.

Skinner, Ralph
1974: Geology of the Tetagouche Lakes, Bathurst and Nepisiguit Falls map-areas, New Brunswick, with emphasis on the Tetagouche Group; Geological Survey of Canada, Memoir 371, 133 p.

St. Peter, Clinton
1979a: Upper part, North Branch, Southwest Miramichi River, Victoria and Carleton Counties (J-14); New Brunswick Department of Natural Resources, Plate 79-2.

1979b: Part of Beadle and McKiel Brooks, Carleton and York Counties (J-15); New Brunswick Department of Natural Resources, Plate 79-3.

1979c: Juniper Station – McKiel Lake, Carleton and York Counties (J-16); New Brunswick Department of Natural Resources, Plate 79-4.

Steiger, R.H. and Jäger, E., compilers
1977: Subcommission on Geochronology: convention on the use of decay constants in geo- and cosmochronology; Earth and Planetary Science Letters, v. 36, no. 3, p. 359-362.

Wanless, R.K., Stevens, R.D., Lachance, G.R., and Delabio, R.N.
1972: Age determinations and geological studies, K-Ar isotopic ages, report 10; Geological Survey of Canada, Paper 71-2, 96 p.

1973: Age determinations and geological studies, K-Ar isotopic ages, report 11; Geological Survey of Canada, Paper 73-2, 139 p.

4. Rb-Sr AGE OF GRANITIC ROCKS IN OPHIOLITE, THETFORD MINES-BLACK LAKE AREA, QUEBEC

Isochron Age = 466 ± 13 Ma
$^{87}Sr/^{86}Sr$ initial = 0.7172 ± 0.0011

The results of isotopic analyses on seven whole rock samples are listed in Table 1 and depicted on an isochron plot, Figure 1. The seven analytical points form an isochron of age 466 ± 13 Ma, initial $^{87}Sr/^{86}Sr$ 0.7172 ± 0.0011 and MSWD 1.11. The $^{87}Rb/^{86}Sr$ ratios of five of the samples fall within a somewhat limited range from 2.4 to 5.6 but sample numbers 6 and 7 have $^{87}Rb/^{86}Sr$ ratios of 24.3 and 38 respectively. Because analytical points with high Rb/Sr ratios such as these commonly fall below isochrons established using points with lower ratios, and because of the great disparity in Rb/Sr ratio between these two samples and the other five, a second regression was performed using only the results of the five samples with lower Rb/Sr. The results of this regression, isochron age 469 ± 48 Ma, initial $^{87}Sr/^{86}Sr$ 0.7170 ± 0.0028, MSWD 1.21, are in excellent agreement with the seven point isochron results. This is a strong indication that the two samples with the higher Rb/Sr ratios are coeval and cogenetic with the other five.

The high initial $^{87}Sr/^{86}Sr$ ratio for the isochron indicates a secondary origin for the granites. The time of original separation from the mantle of the precursors of these bodies may be as great as several hundred million years prior to the 466 Ma indicated by the isochron. Or, alternatively, the granitic bodies have been metasomatized which may have resulted in the addition of relatively radiogenic strontium from an external source.

Geological Setting and Interpretation
by W.H. Poole

Geological Setting

The ultramafic rocks of the Thetford Mines area are interpreted as parts of an intensely deformed, partly dismembered ophiolite suite of Early Ordovician or earlier age, obducted in late Early Ordovician time (St-Julien and Hubert, 1975; Laurent, 1975). The ophiolite structurally overlies unfossiliferous Caldwell Group quartz-sericite and quartz-sericite-chlorite schist, quartzite, and pillowed metabasalt (Riordon, 1954). The Caldwell is presumed to be Cambrian and/or Early Ordovician (St-Julien, 1972; Laurent, 1975), or Early Cambrian (St-Julien and Hubert, 1975). The ophiolite is conformably or unconformably overlain to the southeast by the St. Daniel Formation consisting of polymictic mélange, slate and sandstone, succeeded farther southeast by the graptolitic Middle Ordovician Magog Group slate, sandstone, chert and acidic tuff which is believed to be laterally equivalent to calc-alkaline volcanics of island arc affinity (Ascot and Weedon formations) several kilometres farther southeast (St-Julien and Hubert, 1975).

The age of the ophiolite suite is uncertain. The suite is clearly pre-Middle Ordovician and older than the undated St. Daniel Formation. Generally, most authors have presumed an Early Ordovician and/or Cambrian age based on stratigraphic and regional relations in Quebec and Newfoundland. Laurent and Vallerand (1974) prepared a $^{40}Ar/^{40}K$ isochron plot from six K-Ar analyses of whole rock amphibolite from three localities along about 70 km of the ultramafic belt. The amphibolites "are directly associated with the asbestos-bearing peridotites of Thetford Mines and Asbestos" (Laurent and Vallerand, 1974, p. 53). The plot yielded an age of 561 Ma[1], from which the authors speculated that "perhaps a significant part of the ophiolitic complexes...formed in Middle Cambrian time". A Middle Cambrian (or earlier) age of the ophiolites was accepted by Laurent in later papers (Laurent, 1975; Laurent and Hébert, 1977) but the geochronological data have not been published in full.

A minimum age of the Thetford Mines ophiolites can be obtained from the age of the many granitic and dioritic bodies associated with the peridotite and gabbro (Riordon, 1954). The light coloured bodies of quartz monzonite, granite, pegmatite, and albitite (De, 1961, 1972) form rootless, irregular, generally elongate bodies commonly less than a kilometre long and half as wide. The bodies contain inclusions of peridotite, are bordered by serpentinite altered to chlorite, diopside, talc and anthophyllite, and show petrographic evidence of metasomatism, including development of rodingitic assemblages at the contact (De, 1961, 1972). The granitic bodies clearly have intruded the ophiolite, and equally clearly they have been deformed with the ophiolite.

The granitic bodies seem quite out of place within the ophiolite, and no firm model for them has emerged within the plate-tectonic evolutionary models. Riordon (1954) believed them to be of Ordovician age, apparently because of their close association with the ophiolite. Lamarche (1972) favoured an Ordovician age, and an origin by magmatic differentiation and liquid immiscibility. St-Julien and Hubert (1975) believed the granitic bodies to be of Ordovician age. Laurent (1975) regarded the bodies as manifestations of the calc-alkaline island arc volcanism which produced the Ascot and Weedon formations farther southeast. If the bodies are related to mid-Ordovician subduction and island arc volcanism, they would be expected to have intruded the ophiolite some time between about 460 and 490 Ma. If they are products of differentiation during original formation of the ophiolite at or near a mid-oceanic ridge, they would have been emplaced between 490 and 575 Ma, or even earlier.

Samples analyzed for the Rb-Sr isochron were collected from a single tabular granitic body on the south wall, 1000 level, of British Canadian No. 1 pit about a half kilometre south of the village of Black Lake as the pit and village existed in 1965 (Fig. 2, Table 2).

[1] All K-Ar and Rb-Sr ages quoted from published papers, as well as those presented here, have been calculated or recalculated using the new constants recommended by Steiger and Jäger (1977). The time scale used in this report is that of Armstrong (1978), constructed using the new constants.

From: Rb-Sr and U-Pb Isotopic Age Studies in Current Research, Part C
Geol. Surv. Can., Paper 80-1C

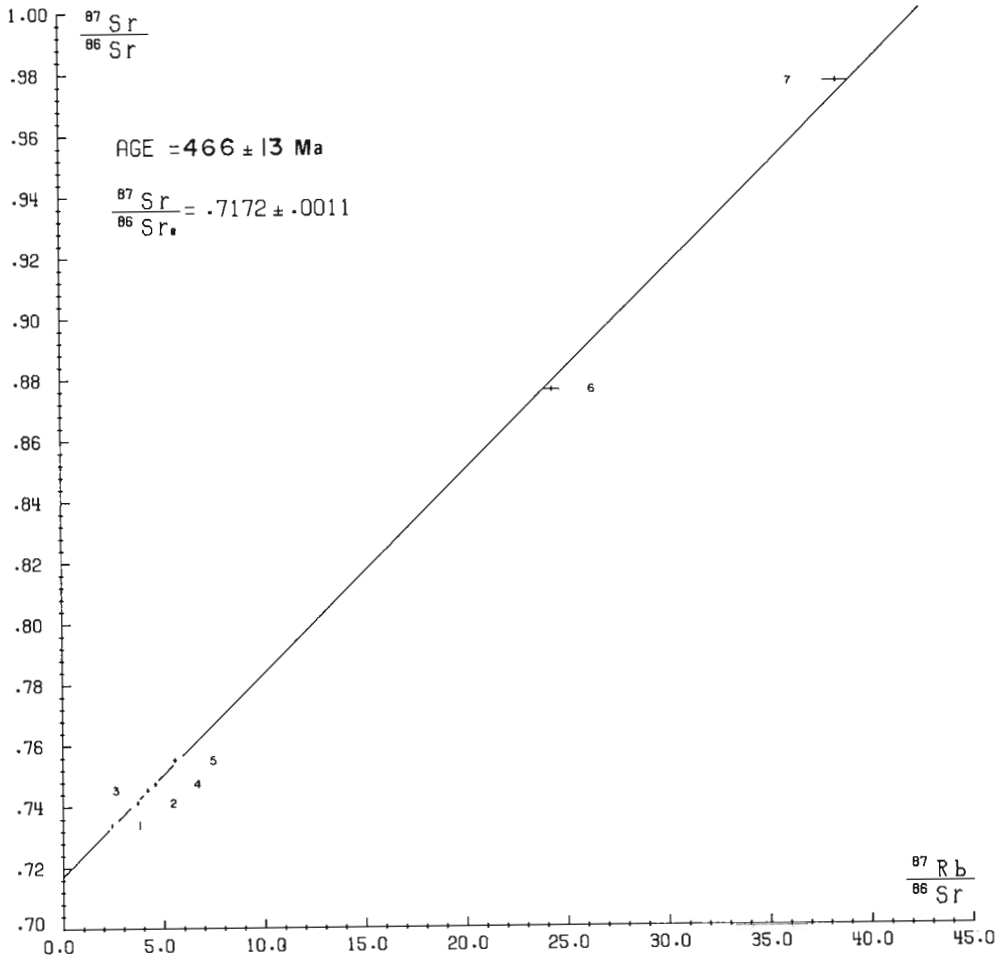

Figure 1. *Rb-Sr isochron for granitic rocks in ophiolite, Thetford Mines-Black Lake area, Quebec.*

Table 1

Analytical data, whole rock samples, granitic rocks in ophiolite, Thetford Mines-Black Lake area, Quebec

Sample No.	Rb ppm	Sr ppm	$^{87}Sr/^{86}Sr$ unspiked	$^{87}Sr/^{86}Sr$ spiked	$^{87}Sr/^{86}Sr$ average	$^{87}Rb/^{86}Sr$
1	162.2	192.2	0.7335	0.7343	0.7339 ± 0.0011	2.443 ± 0.073
2	147.3	114.3	0.7411	0.7410	0.7411 ± 0.0011	3.731 ± 0.112
3	151.1	103.6	0.7450	0.7457	0.7453 ± 0.0011	4.223 ± 0.127
4	135.2	85.10	0.7477	0.7469	0.7473 ± 0.0011	4.600 ± 0.138
5	153.0	79.48	0.7546	0.7556	0.7551 ± 0.0011	5.573 ± 0.167
6	367.0	* 43.64	*0.8752	*0.8764	0.8758 ± 0.0013	24.35 ± 0.73
7	352.6	* 26.54	*0.9756	*0.9775	0.9765 ± 0.0015	38.46 ± 1.15

*Average of two determinations

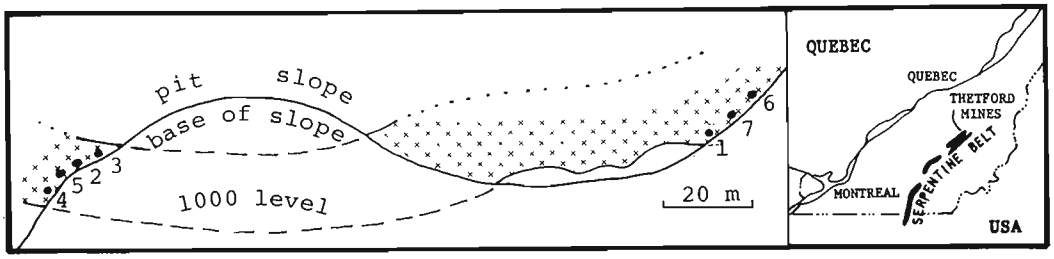

Figure 2. *Location of samples in granitic body within peridotite, British Canadian No. 1 pit, south wall, 1000 level in 1965, Thetford Mines-Black Lake area, Quebec.*

Table 2

Sample numbers and localities, British Canadian No. 1 pit, Thetford Mines-Black Lake area, Quebec

Sample No. This work	Sample No. Field	Rock Type	Locality Latitude	Locality Longitude	N.T.S.
1	PB65-84	Biotite-muscovite granite	46°02'14"	71°21'16"	21 L/3
2	PB65-79	White granite	46°02'14"	71°21'16"	21 L/3
3	PB65-78	Feldspathic pegmatite and grey granite	46°02'14"	71°21'16"	21 L/3
4	PB65-81	White granite	46°02'14"	71°21'16"	21 L/3
5	PB65-80	Pegmatite with muscovite books	46°02'14"	71°21'16"	21 L/3
6	PB65-86	Pegmatite with muscovite books	46°02'14"	71°21'16"	21 L/3
7	PB65-85	Pegmatite with muscovite books	46°02'14"	71°21'16"	21 L/3

Interpretation

K-Ar ages on muscovites from two samples collected by Jacques Béland from granitic bodies in the Thetford Mines-Black Lake area have yielded 486 and 490 Ma (Leech et al., 1963, p. 78-79). The 486 Ma sample was almost certainly collected from the same body which was sampled by Poole for the present isochron. The rock is a white, foliated, coarse grained, pegmatitic granite in which the feldspars are clouded, fractured and bent, the quartz strained and recrystallized, and the muscovite coarse and bent but unaltered. The 490 Ma sample was from Granite Hill, 5.4 km northeast of the first sample. The rock is a light grey-buff, foliated, medium grained granite in which the feldspars are sericitized, quartz is strained and recrystallized, and muscovite is straight, unaltered and cuts across bent and chloritized biotite. The muscovites are evidently younger than some of the deformation, and taken on face value, the granitic bodies are of early Middle Ordovician age or older. The 486 and 490 Ma ages are anomalously old when compared to three other K-Ar ages ranging from 327 to 449 Ma along the belt of ultramafic rocks in Eastern Townships (St-Julien and Hubert, 1975, p. 355-356 and Fig. 2). Nevertheless, these old ages are real because a new determination of reserve muscovite which had yielded the 486 Ma age produced an age of 474 ± 15 Ma (to be published in the Geological Survey of Canada Paper, K-Ar isotopic ages, report 15, in preparation). This last age centres on early Middle Ordovician, and with the error, spans the entire Middle Ordovician.

The Rb-Sr isochron has relatively little scatter (MSWD of 1.11) and thus the isochron age of 466 ± 13 can reasonably be considered the age of the last chemical homogenization of the rocks. Whichever model is adopted, crystallization of a magma and near-synchronous metasomatism, or early crystallization of a magma and later homogenization or metasomatism, the isochron age is probably that of the secondary process.

The 466 ± 13 Ma age is about mid-Ordovician and is quite consistent with the K-Ar ages discussed above. Taken together, the Rb-Sr and K-Ar ages indicate that the ophiolite at least in the Thetford Mines-Black Lake area, was not heated above the muscovite argon blocking temperature, nor deformed at depth after Middle Ordovician (such as during the Acadian Orogeny). These ages compare well with the supposed age of the island arc volcanics of the Ascot and Weedon formations, and thus could be regarded as support for the model that the granitic bodies are related to that volcanism, as proposed by Laurent (1975).

If the high initial $^{87}Sr/^{86}Sr$ ratio of 0.7172 is interpreted as indicating a time interval between original magmatism and later homogenization, then it is faintly possible that the granitic bodies were originally intruded perhaps a few hundred million years before the mid-Ordovician. Thus, the isochron age could weakly support the model in which the granitic bodies are products of magmatic differentiation at or near a mid-oceanic ridge.

A third possible interpretation is that the granitic bodies intruded the peridotite and gabbro in an oceanic environment and then became metasomatically homogenized along with the introduction of radiogenic strontium during the mid-Ordovician polyphase deformation of the ophiolite.

And finally, a fourth interpretation is that the granitic bodies were generated by melting of granitic crust or overlying continental margin sediments as the ophiolite was being thrust over the continental edge, that the melts moved upward into the ophiolite sheet and became metasomatized during continued deformation associated with further movement and deformation of the sheet. In this interpretation, the granitic bodies are related neither to mid-ocean ridge magmatism nor to island arc volcanism, but to emplacement of the ophiolite allochthon.

References

Armstrong, R.L.
1978: Pre-Cenozoic Phanerozoic time scale – computer file of critical dates and consequences of new and in-progress decay-constant revisions; in Contributions to the Geologic Time Scale, ed. G.V. Cohee, M.F. Glaessner, and H.D. Hedberg; American Association of Petroleum Geologists, Studies in Geology No. 6, p. 73-91.

De, Aniruddha
1961: Petrology of dikes emplaced in the ultramafic rocks of southeastern Quebec; Princeton University, unpublished Ph.D. thesis, 201 p.

1972: Petrology of dikes emplaced in the ultramafic rocks of southeastern Quebec and origin of the rodingite; in Studies in Earth and Space Sciences, Harry H. Hess Volume, ed. R. Shagam, R.B. Hargraves and others; Geological Society of America, Memoir 132, p. 489-501.

Lamarche, R.Y.
1972: Ophiolites of southern Quebec; in The Ancient Oceanic Lithosphere; Canada Earth Physics Branch, v. 42, no. 3, p. 65-69.

Laurent, Roger
1975: Occurrences and origin of the ophiolites of southern Quebec, northern Appalachians; Canadian Journal of Earth Sciences, v. 12, no. 3, p. 443-455.

Laurent, Roger and Hébert, Yves
1977: Features of submarine volcanism in ophiolites from the Quebec Appalachians; in Volcanic Regimes in Canada, ed. W.R.A. Baragar, L.C. Coleman and J.M. Hall; Geological Association of Canada, Special Paper No. 16, p. 91-109.

Laurent, Roger and Vallerand, P.
1974: $^{40}Ar/^{40}K$ isochron age for the amphibolites of the ophiolitic complexes of the Appalachians of Quebec (abstract); in Program Abstracts, 3rd Circular; Geological Association of Canada-Mineralogical Association of Canada, p. 53.

Leech, G.B., Lowdon, J.A., Stockwell, C.H., and Wanless, R.K.
1963: Age determinations and geological studies, isotopic ages, report 4; Geological Survey of Canada, Paper 63-17, 140 p.

Riordon, P.H.
1954: Preliminary report on Thetford Mines-Black Lake area; Quebec Department of Mines, Preliminary Report No. 295, 23 p.

St-Julien, Pierre
1972: Geology of the Thetford Mines area; in Appalachian Structure and Stratigraphy in Quebec, ed. D.J. Glass; XXIV International Geological Congress, Montreal, Guidebook to Field Excursion A56-C56, p. 23-35.

St-Julien, Pierre and Hubert, Claude
1975: Evolution of the Taconian orogen in the Quebec Appalachians; in Tectonics and Mountain Ranges, John Rodgers Volume, ed. J.H. Ostrom and P.M. Orville; American Journal of Science, v. 275-A, p. 337-362.

Steiger, R.H. and Jäger, E., compilers
1977: Subcommission on Geochronology: convention on the use of decay constants in geo- and cosmochronology; Earth and Planetary Science Letters, v. 36, no. 3, p. 359-362.

5. Rb-Sr AGE STUDY OF THE MOULTON HILL GRANITE, SHERBROOKE AREA, QUEBEC

The isotopic compositions of eleven whole rock samples are listed in Table 1 and depicted in Figure 1. The analytical points do not form a single collinear trend but appear to fall on two roughly parallel lines. If a regression analysis is performed on all eleven samples an errorchron of age 505 ± 88 Ma, $^{87}Sr/^{86}Sr$ initial 0.7100 ± 0.0026 and very large MSWD of 12.2 is obtained. Conversely, the grouping of samples 2 plus 7 to 11 yields an isochron of age 397 ± 38 Ma, initial $^{87}Sr/^{86}Sr$ of 0.7152 ± 0.0015 and MSWD of 1.25 and of samples 1 plus 3 to 6 yields an errorchron of age 418 ± 162 Ma, $^{87}Sr/^{86}Sr$ initial 0.7100 ± 0.0027 and MSWD 3.24 which is much lower than that obtained for the eleven point errorchron.

From the isotopic evidence, the existence of the essentially parallel isochron and errorchron suggests the homogenization of two groups of rocks with differing Rb/Sr ratio at about 400 Ma ago. This is supported by the elemental concentrations measured for Rb and Sr and the geographical distribution of the samples. Samples falling on the isochron (high initial $^{87}Sr/^{86}Sr$ ratio, 0.7152) were collected from the southeast side of the body and have relatively high Rb contents ranging from 64 to 118 ppm, whereas samples falling on the 418 Ma errorchron (lower initial $^{87}Sr/^{86}Sr$ ratio, 0.7100) were collected from the northwest and have much lower Rb contents of 15 to 36 ppm. This division into two domains is supported by a comparable separation in the (less precise) X-ray fluorescence measurements of rubidium contents of nine other samples which were collected for the study but unused. The strontium contents are less definitive; somewhat higher in the southeastern high rubidium domain (72 to 178 ppm) and lower in the northwestern low rubidium domain (38 to 139 ppm).

If the assumption of the separate homogenization of the two domains at about 400 Ma has a factual basis, then it may be assumed that the current elemental compositions of the two domains are indicative of the compositions prior to the homogenization event. In this case the average $^{87}Rb/^{86}Sr$ and $^{87}Sr/^{86}Sr$ ratios of the two domains may be treated as a two point isochron to determine the age at which the two domains had the same initial $^{87}Sr/^{86}Sr$ ratio. Such computation results in an age of 620 Ma, and initial $^{87}Sr/^{86}Sr$ of 0.707.

Conversely, the disparate results may be interpreted in terms of the relative addition of rubidium and radiogenic strontium to the southeast side of the body in a homogenizing event at about 400 Ma. In either case the mechanism for the geographical separation of the two domains is obscure.

Geological Setting and Interpretation
by W.H. Poole

Geological Setting

The Moulton Hill granite is an elongate body of deformed metatrondhjemite and metagranodiorite, exposed northeast of Sherbrooke, Eastern Townships, Quebec (Fig. 2). The body, about 11 km long and as much as 1.5 km wide, has intruded felsic and mafic volcanics and associated, mainly pelitic, sedimentary rocks of the Ascot Formation (St-Julien, 1970; St-Julien and Lamarche, 1965; Lamarche, 1967). Clasts of the Ascot Formation and of the Moulton Hill granite occur in the unconformably overlying St. Francis Formation and nearby Lake Aylmer Formation both of Siluro-Devonian age (Lamarche, 1967). The Ascot Formation lacks fossils and is the oldest formation in the belt but is believed to be the same age as the lithologically correlative Tetagouche Group of northern New Brunswick, which is of Early and Middle Ordovician age (Arenigian to Caradocian), and of the Middle Ordovician Beauceville and St. Victor formations of the Magog Group lying along the northwest side of the Ascot Formation (St-Julien and Hubert, 1975).

The Ascot Formation contains a calc-alkaline volcanic assemblage and is believed to be, like the Tetagouche, a volcanic island arc assemblage generated above a subduction zone (St-Julien and Hubert, 1975). The Moulton Hill granite appears to be a deformed subvolcanic pluton (Table 2, Fig. 3) spatially and genetically related to Ascot volcanism. Both the Ascot Formation and the granite were deformed together; each contains the oldest penetrative schistosity surfaces (Lamarche, 1967). St-Julien and Lamarche (1965) mapped major overturned folds in the Ascot Formation and referred to a related schistosity being deformed by later, Acadian structures. Nevertheless, the same S_1 schistosity was mapped in the Siluro-Devonian strata, thus implying that all three units were penetratively deformed together during the Acadian orogeny.

According to regional and local geological arguments, the Moulton Hill granite should be of Early or Middle Ordovician age.

Interpretation

Fine muscovite in the schistose metatrondhjemite of sample 5 yielded a K-Ar age of 329 ± 14 Ma[1] (Wanless et al., 1968, p. 114-115), that is, about the Mississippian-Pennsylvanian boundary. The isotopic age probably relates to uplift and cooling through the argon blocking temperature during late Devonian and Carboniferous.

The regression line through all 11 plotted Rb/Sr analyses yielded an errorchron (MSWD of 12.2) of 505 ± 88 Ma with a relatively high initial $^{87}Sr/^{86}Sr$ ratio of 0.7100. The age centres on Early Ordovician and very weakly supports the correlation of the Ascot Formation with the Tetagouche Group if the granite is essentially the same age as the Ascot volcanics. The $^{87}Rb/^{86}Sr$ range within the 11 samples, from 0.3 to 3.7, is restricted. The relatively high initial $^{87}Sr/^{86}Sr$ ratio implies a time interval between crystallization and later chemical homogenization, or more likely, generation of magma from a relatively high $^{87}Sr/^{86}Sr$ source such as continentally-derived sediments or continental crust. Re-examination of the samples failed to identify many that could be argued to be unsatisfactory by petrographic character. Samples 3 and 5 are intensely sheared, contain brown-weathering carbonate aggregates, and muscovite has

[1] K-Ar age recalculated using the new constants recommended by Steiger and Jäger (1977). The time scale used in this report is that of Armstrong (1978), constructed using the new constants.

From: Rb-Sr and U-Pb Isotopic Age Studies in Current Research, Part C
Geol. Surv. Can., Paper 80-1C

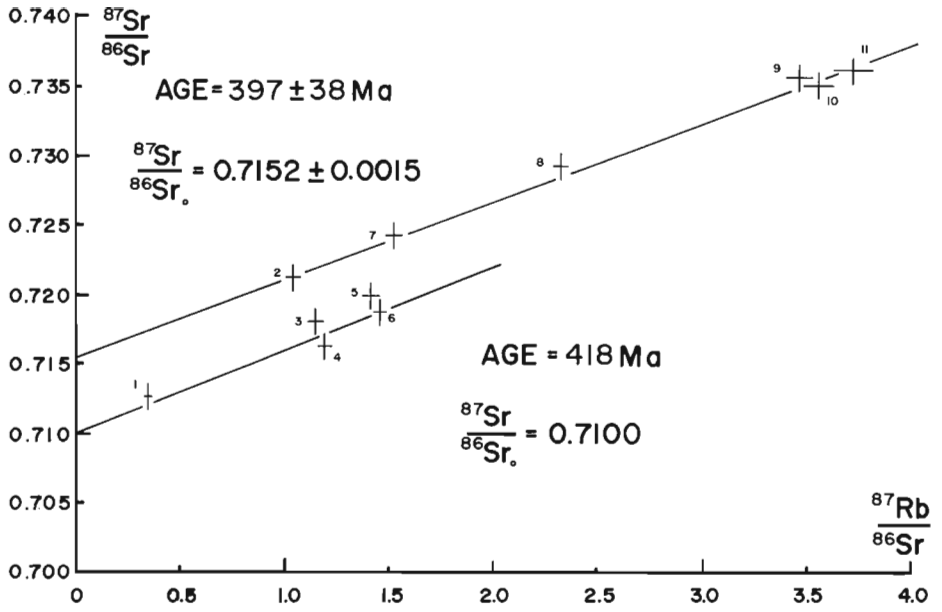

Figure 1. *Rb-Sr isochron diagram of the Moulton Hill granite, Sherbrooke area, Quebec.*

Table 1

Analytical data, whole rock samples, Moulton Hill granite, Sherbrooke area, Quebec

Sample No.	Rb ppm	Sr ppm	$^{87}Sr/^{86}Sr$ unspiked	$^{87}Sr/^{86}Sr$ spiked	$^{87}Sr/^{86}Sr$ average	$^{87}Rb/^{86}Sr$
1	15.29	* 128.6	0.7125	*0.7116	0.7121 ± 0.0011	0.344 ± 0.010
2	63.78	177.7	0.7210	0.7205	0.7207 ± 0.0011	1.039 ± 0.031
3	26.56	66.77	0.7177	0.7176	0.7177 ± 0.0011	1.152 ± 0.035
4	35.99	87.49	0.7164	0.7155	0.7159 ± 0.0011	1.191 ± 0.036
5	18.70	** 38.49	*** 0.7152	*0.7193	0.7193 ± 0.0011	1.406 ± 0.042
6	22.15	44.11	0.7184	0.7179	0.7181 ± 0.0011	1.454 ± 0.044
7	81.98	156.5	0.7231	0.7246	0.7239 ± 0.0011	1.517 ± 0.046
8	82.11	102.4	0.7287	0.7289	0.7288 ± 0.0011	2.322 ± 0.070
9	115.8	96.60	0.7354	0.7358	0.7356 ± 0.0011	3.471 ± 0.104
10	88.07	71.58	0.7346	0.7340	0.7343 ± 0.0011	3.562 ± 0.107
11	118.3	92.00	0.7364	0.7358	0.7361 ± 0.0011	3.723 ± 0.112

* Average of two determinations
** Average of three determinations
*** Not included in $^{87}Sr/^{86}Sr$ average

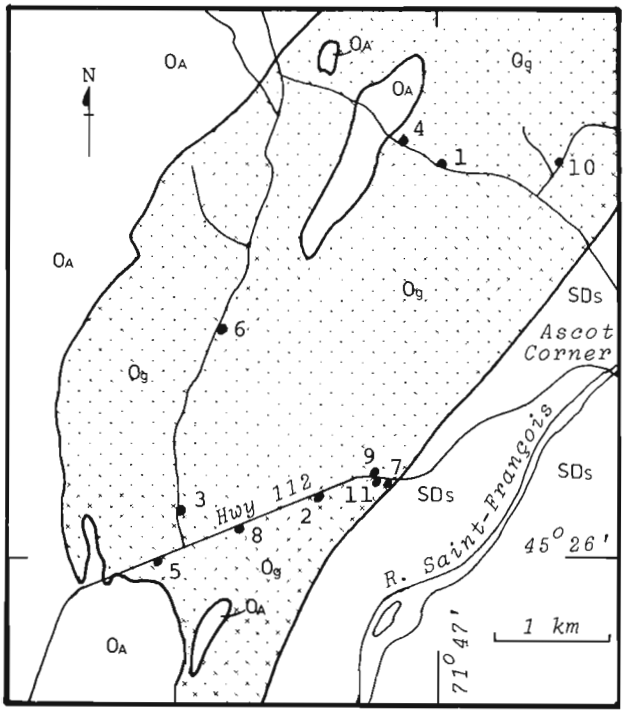

Siluro-Devonian
SDs St. Francis Gp.

Lower and Middle Ordovician
Og Moulton Hill granite
OA Ascot Fm.

Figure 2. *Location of samples within southern half of Moulton Hill granite, Sherbrooke area, Quebec. Geology generalized from St-Julien (1970).*

developed along the shear surfaces. The outcrops of green cataclastic granite of samples 1, 4 and 10 contain inclusions of mafic volcanics. Even with these analyses removed from the plot, the remaining analyses scatter excessively about any age line. The 505 ± 88 Ma errorchron does not provide a satisfactory age of the Moulton Hill granite.

The two parallel regression lines through the plotted points (Fig. 1) yield essentially early Devonian (Acadian) ages and may have some significance. Despite the differences in rubidium and strontium contents of samples of the two domains (see above), there are no apparent petrographically persistent lithological features of the samples which characterize the two domains. Samples 9, 10 and 11 of the southeastern domain do have 13 to 17 per cent potash feldspar (Table 2) but other samples in the domain as well as in the northwestern domain lack potash feldspar. The degree of retrogressive alteration and of foliation development is more or less uniform across both domains and is only locally more intense. The granite is charged with many mappable inclusions of Ascot volcanics, both felsic and mafic (Lamarche, 1967), but a domain boundary cannot be drawn to separate an area with abundant felsic volcanics from an area with abundant mafic volcanics. Despite the Acadian ages suggested by the lines, the granite must be older than the Devonian because the Siluro-Devonian strata rest unconformably upon it and contain clasts of it.

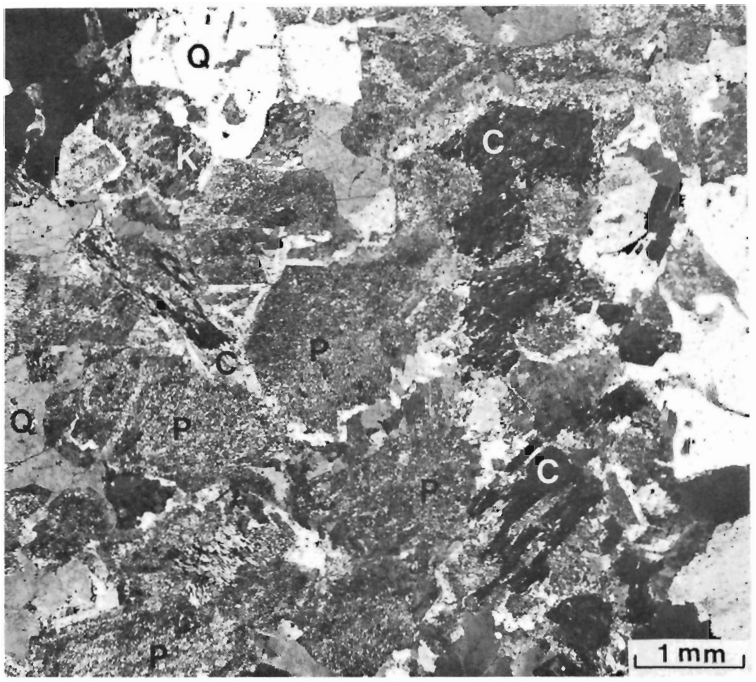

A. Less deformed variety characteristic of northern half of sample area. Sample 10, metagranodiorite. Intensely saussuritized plagioclase (P) is commonly rimmed with clear albite, quartz (Q) is strained, potash feldspar (K) is interstitial and mafic mineral (C) is completely altered to chlorite, muscovite and epidote. (GSC 203617 B)

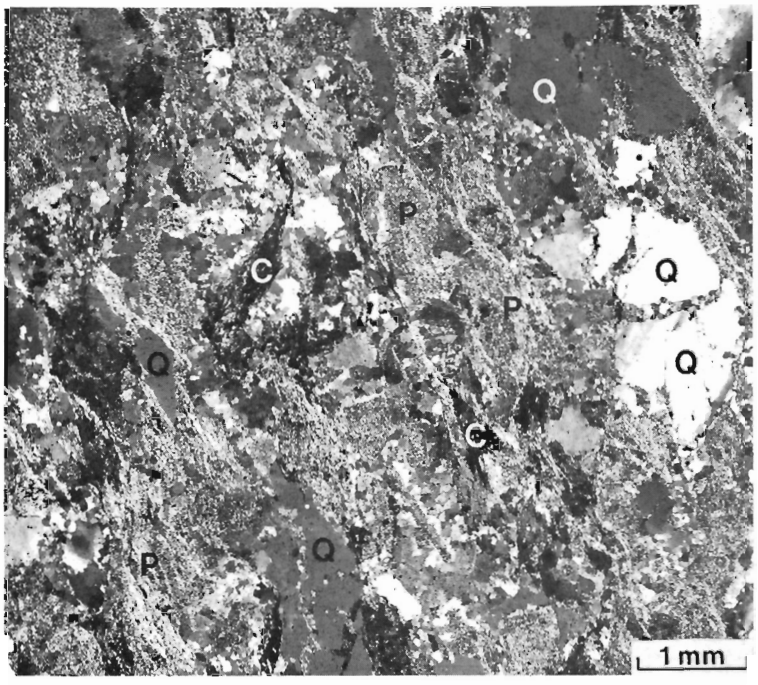

B. Schistose variety common in the southwestern part of the sample area. Sample 8, metatrondhjemite. Muscovitic schistose surfaces define a schistosity, saussuritized plagioclase (P) is deformed, quartz (Q) is more intensely deformed and some is polygonized, and mafic mineral (C) is completely altered to chlorite. (GSC 203617C)

Figure 3. *Photomicrographs of Moulton Hill granite.*

Table 2

Sample numbers and localities, Moulton Hill granite, Sherbrooke area, Quebec

Sample No. This work	Sample No. Field	Rock Type	Locality Latitude	Locality Longitude	N.T.S.
1	PB65-42	Metatrondhjemite, yellowish green-grey, medium grained	45°27'47"	71°47'00"	21 E/5
2	PB65-31	Metatrondhjemite, yellowish green-grey, medium grained, foliated	45°26'15"	71°47'52"	21 E/5
3	PB65-38	Metatrondhjemite, white with brown-weathering carbonate, sericite schist surfaces	45°26'10"	71°48'44"	21 E/5
4	PB65-40	Metatrondhjemite, yellow-green, coarse grained, foliated	45°27'53"	71°47'14"	21 E/5
5	PB65-35	Metatrondhjemite, white with brown-weathering carbonate, sericite schist surfaces	45°25'58"	71°48'52"	21 E/5
6	PB65-39	Metatrondhjemite, yellowish green-grey, coarse grained	45°27'02"	71°48'28"	21 E/5
7	PB65-24	Metatrondhjemite, yellow-green with 11% orange-pink albite, medium grained, foliated	45°26'19"	71°47'18"	21 E/5
8	PB65-32	Metatrondhjemite, grey, medium grained, foliated, schistose (Fig. 3B)	45°26'07"	71°48'21"	21 E/5
9	PB65-29	Metagranodiorite, yellow-green with 13% orange-pink microperthite, muscovitic, sericite schist surfaces	45°26'20"	71°47'27"	21 E/5
10	PB65-43	Metagranodiorite, greenish grey with 14% greyish pink potash feldspar (Fig. 3A)	45°27'48"	71°46'12"	21 E/5
11	PB65-27	Metagranodiorite, yellow-green with 17% orange-pink potash feldspar	45°26'19"	71°47'23"	21 E/5

If the granite was emplaced during the Ordovician and the crystallizing magma contained a uniform initial $^{87}Sr/^{86}Sr$ ratio but relatively rubidium-rich and rubidium-poor domains, then all points would plot on one regression line of Ordovician age if no younger episode of homogenization occurred. If on the other hand each domain was homogenized during the Devonian, with homogenization not crossing the domain boundary (which seems most improbable), two regression lines would result, each yielding a Devonian age. To produce a difference in the initial $^{87}Sr/^{86}Sr$ ratio of 0.005, the granite must have been emplaced about 220 Ma before the early Devonian, i.e. about 620 Ma or in the late Hadrynian, with a rather high initial $^{87}Sr/^{86}Sr$ ratio of 0.707. A Hadrynian age is geologically improbable but perhaps not entirely impossible since the Ascot Formation is the oldest unit in the belt.

I am therefore drawn to the conclusion that the different initial $^{87}Sr/^{86}Sr$ ratios and possibly, but not necessarily, the different rubidium and strontium contents are a product of a metasomatic process of Devonian age. Possibly the strontium isotopic ratios were altered by addition of radiogenic strontium to at least the southeastern domain, perhaps accompanied by addition of rubidium if the rubidium content was not uniform during original emplacement. Such a process would yield the two parallel regression lines of Devonian age. No confirming evidence of such a process can be offered, except to draw attention to the locally pervasive carbonatization of Ascot and St. Francis formations not far from the granite (St-Julien and Lamarche, 1965; Lamarche, 1967). A ferruginous carbonate of apparent hydrothermal origin has been locally introduced into all the stratified rocks, and some Devonian diorite and gabbro dykes and sills. Some carbonatized areas are irregularly shaped and more than 2 km long. The granite is not shown as partly carbonatized but nevertheless perhaps this process has given rise to the differing initial $^{87}Sr/^{86}Sr$ ratios of the two domains if not also the differing rubidium and strontium contents.

In conclusion, this Rb-Sr study has not satisfactorily provided an age of emplacement of the Moulton Hill granite. It has however suggested that the granite may have been altered and homogenized in some uncertain fashion during the Devonian. Clearly, an intriguing isotopic and geochemical problem has been touched upon and awaits further study.

References

Armstrong, R.L.
1978: Pre-Cenozoic Phanerozoic time scale – computer file of critical dates and consequences of new and in-progress decay-constant revisions; in Contributions to the Geologic Time Scale, ed. G.V. Cohee, M.F. Glaessner and H.D. Hedberg; American Association of Petroleum Geologists, Studies in Geology No. 6, p. 73-91.

Lamarche, R.-Y.
1967: Geology of Beavoir-Ascot Corner area, Sherbrooke, Richmond and Compton Counties; Quebec Department of Natural Resources, Preliminary Report No. 560, 16 p.

St-Julien, Pierre, compiler
1970: Orford-Sherbrooke area; Quebec Department of Natural Resources, Map 1619.

St-Julien, Pierre and Hubert, Claude
1975: Evolution of the Taconian orogen in the Quebec Appalachians; in Tectonics and Mountain Ranges, John Rodgers Volume, ed. J.H. Ostrom and P.M. Orville; American Journal of Science, v. 275-A, p. 337-362.

St-Julien, Pierre and Lamarche, R.-Y.
1965: Geology of Sherbrooke area, Sherbrooke County; Quebec Department of Natural Resources, Preliminary Report No. 530, 34 p.

Steiger, R.H. and Jäger, E., compilers
1977: Subcommission on Geochronology: convention on the use of decay constants in geo- and cosmochronology; Earth and Planetary Science Letters, v. 36, no. 3, p. 359-362.

Wanless, R.K., Stevens, R.D., Lachance, G.R., and Edmonds, C.M.
1968: Age determinations and geological studies, K-Ar isotopic ages, report 8; Geological Survey of Canada, Paper 67-2, Part A, 141 p.

6. A Rb-Sr STUDY OF DYKES ASSOCIATED WITH THE CHIBOUGAMAU PLUTON, QUEBEC

Errorchron Age = 2520 Ma
$^{87}Sr/^{86}Sr$ initial = 0.7021

The results of the isotopic analyses of eight samples are presented in Table 1 and depicted on a Rb-Sr isochron diagram, Figure 2. Figure 2 also shows the results of studies by Jones et al. (1974), and Brooks (1980), on rocks from the Chibougamau Pluton. Six of the eight analytical points determined in this study are reasonably collinear but yield an errorchron of age 2520 ± 141 Ma, $^{87}Sr/^{86}Sr$ initial 0.7021 ± 0.0009 and high MSWD 7.39. The other two points fall considerably off the six point errorchron, one to each side.

Geological Setting and Interpretation by Jayanta Guha and Ralph Thorpe

Geological Setting

The Chibougamau Pluton intrudes the volcanic and sedimentary assemblages of the east-west trending Matagami-Chibougamau greenstone belt as well as the Dore Lake Complex, a large stratiform mafic anorthositic complex. The exact time of emplacement of the Chibougamau Pluton is yet to be defined. It, along with its host rocks, was folded and metamorphosed during the Kenoran Orogeny. The possibility of an additional metamorphism at 2200 Ma has been indicated (Morris, 1977; Guha et al., 1979; Thorpe et al., in press).

This work was carried out on samples obtained in 1975 during the preliminary phase of a study of the dykes in the Chibougamau mining district (Maillet, 1978). The samples are from the northern flank of the pluton, mostly from the vicinity of Merrill Island (Table 2). At this locality a tongue of the central tonalite phase of the Chibougamau Pluton cuts across the diorite- meladiorite border zone and into the Dore Lake complex (Fig. 1). Northwestward from the tongue there is a gradual change in the lithologies of the dykes from equigranular tonalite to feldspar porphyry and finally to quartz feldspar porphyry. These dykes are believed to be cogenetic with the biotite tonalite phase of the Chibougamau Pluton (Maillet, 1978) and therefore samples from this series of dykes were thought to offer a chance to define an isochron.

Interpretation

The errorchron "age" based on a two error linear regression analysis of 6 out of 8 samples analyzed is 2520 ± 141 Ma ($\lambda^{87}Rb = 1.42 \times 10^{-11} a^{-1}$). The initial $^{87}Sr/^{86}Sr$ ratio is 0.7021 ± 0.0009.

Previous geochronological studies have shown the age of the Chibougamau Pluton to be about 2735 Ma based on a zircon U-Pb analysis (Krogh and Davis, 1971), and 2730 ± 100 Ma by the Rb-Sr isochron method (Verpaelst and Brooks, 1978; Brooks, 1980). These studies, however, have not dealt with the dykes related to the Chibougamau Pluton. A Rb-Sr isochron by Jones et al. (1974) for a suite of samples from the Chibougamau Pluton gave a date of 2509 ± 79 Ma ($\lambda^{87}Rb = 1.42 \times 10^{-11} a^{-1}$) with an initial $^{87}Sr/^{86}Sr$ ratio of 0.7005 ± 0.0002. This date was interpreted by them as that of Kenoran metamorphism. Recently Brooks (1980) has concluded that the best Rb-Sr isochron age for the Chibougamau pluton is 2730 ± 100 Ma. This is based on the data for 7 samples after 11 other samples were eliminated on the basis of their major element chemistry, volatile content and petrographic characteristics. Among the samples excluded were all seven comprising the Jones et al. (1974) isochron.

The data from the present study are shown in Figure 2. The results are similar to those of Jones et al. (1974), but data points for specimens 6 and 7 fall far from the general linear trend. When data for the latter specimens are eliminated, the scatter of the remaining points about the errorchron regression line is still sufficient to produce a high MSWD of 7.39. The selected data by Brooks lie on a steeper isochron with a lower initial ratio (0.7009 ± 0.0004) than that indicated by our data. Only our data points 2 and 4 agree well with the linear pattern defined by his selected data. Brooks pointed out that an errorchron can be calculated from the altered samples only, largely on the basis of data from Jones et al., at 2540 ± 150 Ma (initial ratio 0.7005 ± 0.0005). This errorchron, however, lies below most of the data points from the dykes. Despite the similarity of this age to the dyke age (2520 ± 141 Ma) the dyke samples may be distinguished from the altered samples by their consistently higher $^{87}Sr/^{86}Sr$ ratios and therefore can not be clearly associated with the 2540 Ma alteration event.

The present data for the felsic porphyry dykes spatially related to the Chibougamau Pluton do not clearly define a younger age than that defined for the pluton itself. However the higher initial ratio for the dykes suggests they could be younger. It is possible that the intrusion of the dykes was responsible for the alteration event at roughly 2540 Ma. In this case they could reflect late or post-kinematic events related to the Kenoran orogeny.

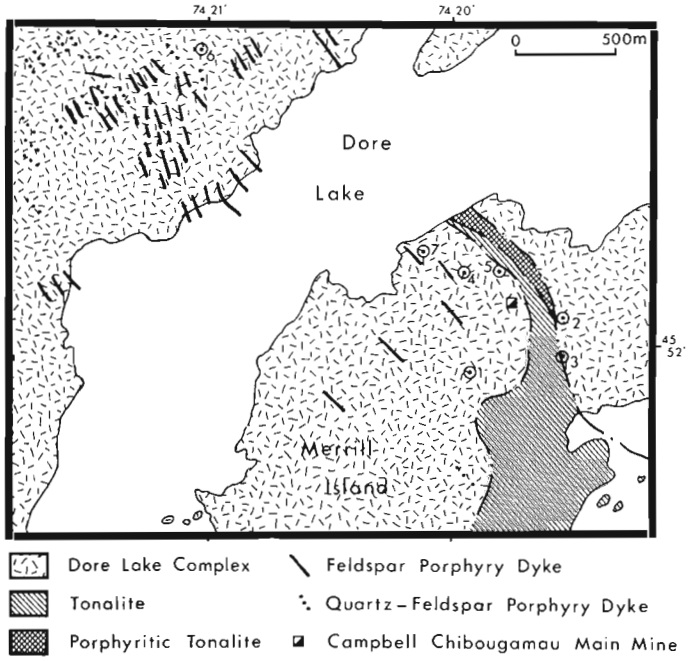

Figure 1. *Location map of the dyke specimens analyzed. Specimen 8 is from the Copper Rand mine, outside of the area shown.*

From: Rb-Sr and U-Pb Isotopic Age Studies in Current Research, Part C Geol. Surv. Can., Paper 80-1C

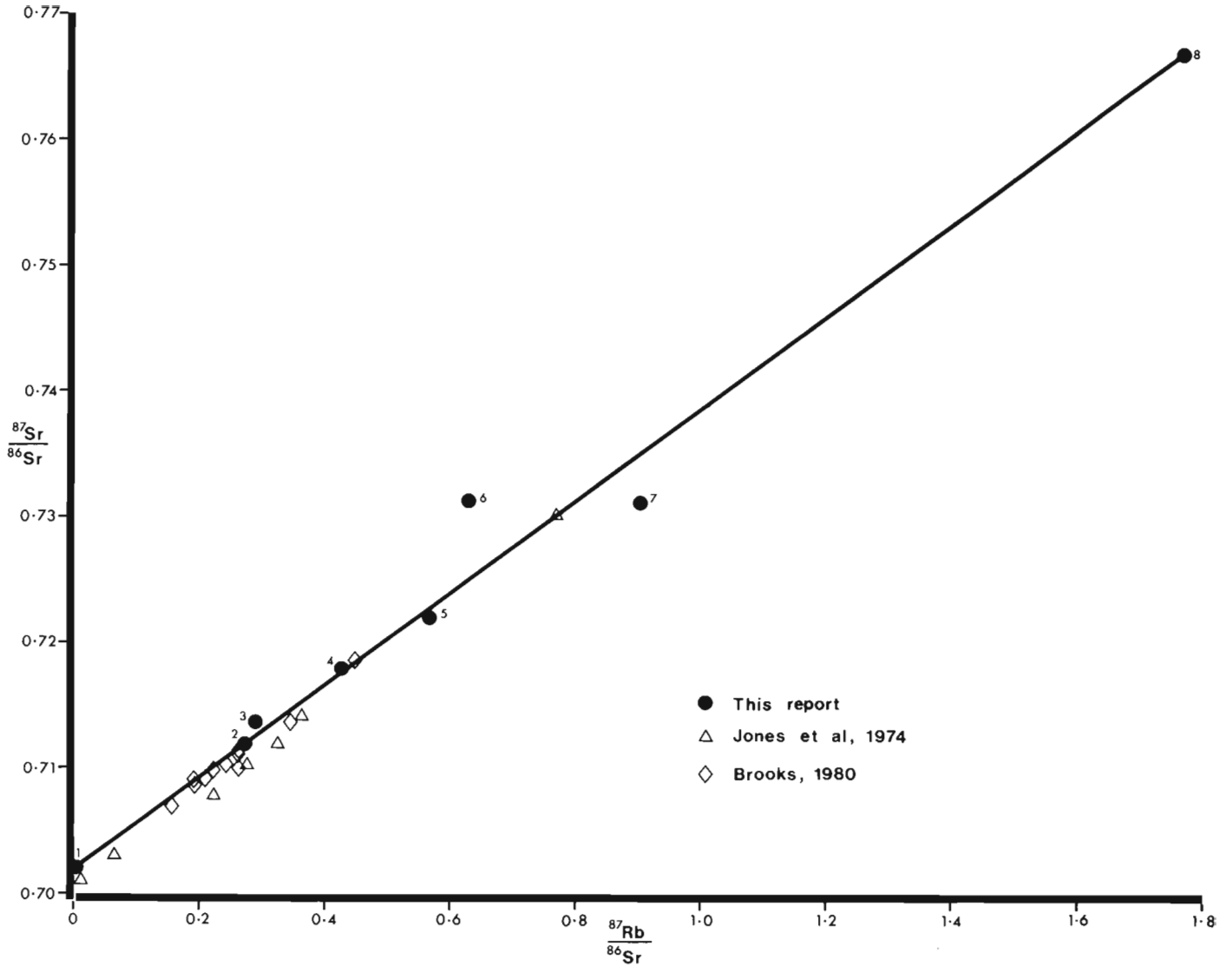

Figure 2. *Plot of the Rb-Sr data for felsic porphyry dykes cutting the Chibougamau Pluton. The data by Jones et al. (1974) and Brooks (1980) for the pluton are also shown. The black circles represent the data obtained in this study.*

Table 1

Analytical data, whole rock samples, for dykes associated with the Chibougamau Pluton, Quebec

Sample No.	Rb ppm	Sr ppm	$^{87}Sr/^{86}Sr$ spiked	$^{87}Rb/^{86}Sr$
1	0.320	297.4	0.7020 ± 0.0004	0.0031 ± 0.0001
2	21.88	230.8	0.7118 ± 0.0004	0.2741 ± 0.0055
3	19.10	192.0	0.7136 ± 0.0004	0.2876 ± 0.0058
4	46.35	315.6	0.7179 ± 0.0004	0.4246 ± 0.0085
5	43.11	319.7	0.7219 ± 0.0004	0.5673 ± 0.0113
6	21.65	98.99	0.7311 ± 0.0004	0.6323 ± 0.0126
7	66.27	211.9	0.7310 ± 0.0004	0.9042 ± 0.0181
8	41.59	67.87	0.7668 ± 0.0005	1.772 ± 0.035

Table 2

Sample Numbers and Localities from dykes associated with the Chibougamau Pluton, Quebec

Sample No. This work	Sample No. Field	Rock Type	Locality Latitude	Locality Longitude	N.T.S.
1	JM6a/v4	Feldspar porphyry	49°51'57"	74°19'56"	32 G/16
2	U1915(a)	Tonalite, chilled contact	49°52'04"	74°19'32"	32 G/16
3	JM6/1	Biotite tonalite	49°51'59"	74°19'32"	32 G/16
4	U1293(c)	Tonalite	49°52'10"	74°19'58"	32 G/16
5	JM6a/16	Tonalite	49°52'08"	74°19'48"	32 G/16
6	JM5b/18	Feldspar porphyry	49°52'12"	74°21'03"	32 G/16
7	U1657(b)	Biotite tonalite	49°52'39"	74°20'16"	32 G/16
8	JM-8/5	Feldspar porphyry	49°53'16"	74°15'50"	32 G/16

References

Brooks, C.
1980: The Rb/Sr geochronology of the Archean Chibougamau pluton, Quebec; Canadian Journal of Earth Sciences, v. 17, no. 6, p. 776-783.

Guha, J., Cimon, J., and Thorpe, R.I.
1979: Nouvelles données isotopiques et leurs implications sur les relations spatio-temporelles des minéralisations dans le secteur de Chibougamau, Québec; Compte rendu du Colloque Augustin Frigon sur l'industrie minière et l'exploration au Québec, Ecole Polytechnique, Université de Montréal, p. 117-118.

Jones, L.M., Walker, R.L., and Allard, G.O.
1974: The Rubidium-Strontium Whole-Rock Age of Major Units of the Chibougamau Greenstone Belt, Quebec; Canadian Journal of Earth Sciences, v. 11, p. 1550-1561.

Krogh, T.E. and Davis, G.L.
1971: Zircon U-Pb ages of Archean metavolcanic rocks in the Canadian Shield; Annual Report Geophysical Laboratory, Carnegie Institution Washington Yearbook 1970-1971, p. 241-242.

Maillet, J.
1978; Petrographie et géochimie des dyke du camp minier de Chibougamau, Québec; Unpublished M.Sc.A. thesis, Université du Québec à Chicoutimi, 150 p.

Morris, W.A.
1977: Paleomagnetism of the Gowganda and Chibougamau Formations: Evidence for 2200 m.y. – old folding and remagnetization event of the Southern Province; Geology, v. 5, no. 3, p. 137-140.

Thorpe, R.I., Guha, J., and Cimon, J.
Evidence from lead isotopes regarding the genesis of ore deposits in the Chibougamau region, Quebec; Canadian Journal of Earth Sciences. (in press)

Verpaelst, P. and Brooks, C.
1978: "Hot" and "Cold" Archean Tonalites (Abstract); in Abstracts with Programs, Geological Association of Canada/Mineralogical Association, v. 3, p. 509.

7. AGE DETERMINATIONS ACROSS THE CAYAMANT LINEAMENT, GRENVILLE PROVINCE, QUEBEC

1) Southeast of Lineament
   Isochron Age = 1229 ± 37 Ma
   $^{87}Sr/^{86}Sr$ initial = 0.7038 ± 0.0019

2) Southeast of Lineament
   Isochron Age = 1146 ± 65 Ma
   $^{87}Sr/^{86}Sr$ initial = 0.7039 ± 0.0011

3) Northwest of Lineament
   Isochron Age = 1193 ± 66 Ma
   $^{87}Sr/^{86}Sr$ initial = 0.7061 ± 0.0013

Group 1: Of seven samples analyzed isotopically five define an isochron of age 1229 ± 37 Ma, initial $^{87}Sr/^{86}Sr$ 0.7038 ± 0.0019 and MSWD 2.71. The results are presented in Table 1 and plotted in an isochron diagram Figure 1. Samples number 5 and 7 clearly fall below the line defined by the other five samples and have been excluded from the computation of isochron parameters.

Group 2: Four of the six samples analyzed are collinear defining an isochron of age 1146 ± 65 Ma, initial $^{87}Sr/^{86}Sr$ 0.7039 ± 0.0011 and MSWD 1.33 (Table 1 and Figure 2). Samples number 4 and 5 are essentially identical in $^{87}Rb/^{86}Sr$ and $^{87}Sr/^{86}Sr$ ratios and fall considerably above the isochron established by the other four points. The mutual agreement of the results of the two aberrant samples may document a geological event. Assuming an initial $^{87}Sr/^{86}Sr$ ratio of 0.7039, an age of about 1350 Ma can be calculated for these samples. Conversely, assuming the isochron age of 1146 Ma, an initial $^{87}Sr/^{86}Sr$ ratio of about 0.710 is indicated.

Group 3: Two sets of samples were collected from essentially the same area and analyzed isotopically as group 3. The first set, consisting of samples 2, 4, 5, 6 and 7 form an isochron of age 1193 ± 66 Ma, initial $^{87}Sr/^{86}Sr$ ratio of 0.7061 ± 0.0013 and small MSWD of 0.53. The second set, samples 1, 3 and 8 form a separate linear trend yielding a poorly defined isochron of age 1133 ± 109 Ma, initial $^{87}Sr/^{86}Sr$ 0.7035 ± 0.0020 and larger MSWD of 3.42. The results are presented in Table 1 and plotted in an isochron diagram Figure 3. Two separate linear trends are obviously involved in this instance; if all the samples from Group 3 are subjected to regression analysis the result is an errorchron of age 1208 Ma, initial $^{87}Sr/^{86}Sr$ of 0.7045 and MSWD of 10.69. On an isochron diagram, the line defined in this manner does not intersect any of the analytical points within their error margins.

The major thrust of this project was to establish whether the rocks northwest of the Cayamant Lineament are significantly older than those southeast of the lineament. This was not shown to be the case with respect to the area sampled and analyzed as Group 3; the age for the five point Group 3 isochron, 1193 ± 66 Ma, falls between the ages determined for the Group 1 and Group 2 rocks and the error limits associated with the Group 3 age overlap both the Group 1 and Group 2 ages. However the initial $^{87}Sr/^{86}Sr$ ratios associated with the Group 1 and 2 isochrons (0.7038 and 0.7039 respectively) are consistent with mantle derivation for these rocks whereas the initial ratio for the five point Group 3 isochron is somewhat higher at 0.7061. This may indicate a crustal prehistory for the Group 3 gneisses admitting the possibility of the suspected older age of emplacement.

Geological Setting and Interpretation

by James H. Bourne[1]

Introduction

Field mapping during the summers of 1969 and 1970 (Bourne, 1970a, b) revealed the presence of a major boundary called the Cayamant Lineament within the Grenville Province of southwestern Quebec (Fig. 4). The boundary separates a very complicated suite of grey biotite and hornblende gneisses to the northwest from marble and rusty-weathering sillimanite gneiss units, considered typical of the Grenville Supergroup, to the southeast. The lineament itself is poorly exposed and cannot be investigated directly.

One feature of note is the aeromagnetic pattern associated with each of the two areas of gneisses mentioned above. The biotite-hornblende gneisses to the northwest are associated with a pronounced northwest-southeast trending pattern of anomalies which continues out of the area investigated here for 140 km until it is affected by the Grenville Front Tectonic Zone. Throughout this area of northwest trending aeromagnetic anomalies the rocks appear to be very similar to the biotite-hornblende gneisses adjacent to the lineament. The marble and sillimanite gneisses to the southeast are associated with a strong aeromagnetic pattern oriented north-northeast. The boundary between these two different aeromagnetic domains is a zone of blob-shaped anomalies of no particular orientation.

The purpose of this investigation was to obtain age determinations from either side of the Cayamant Lineament, with a view to establishing whether or not the lineament forms a boundary between two different age groups of metamorphic rocks.

Results

The samples constituting Group 1 were collected along Hwy 105 from the garnet-sillimanite-K feldspar gneiss unit of the Grenville Supergroup. The samples were collected a considerable distance from the lineament in an attempt to eliminate any possible influence from this feature. An age of 1229 ± 37 Ma (Fig. 1) was obtained.

[1] Département des Sciences de la Terre, Université du Québec, Montréal, Québec.

From: Rb-Sr and U-Pb Isotopic Age Studies in Current Research, Part C Geol. Surv. Can., Paper 80-1C

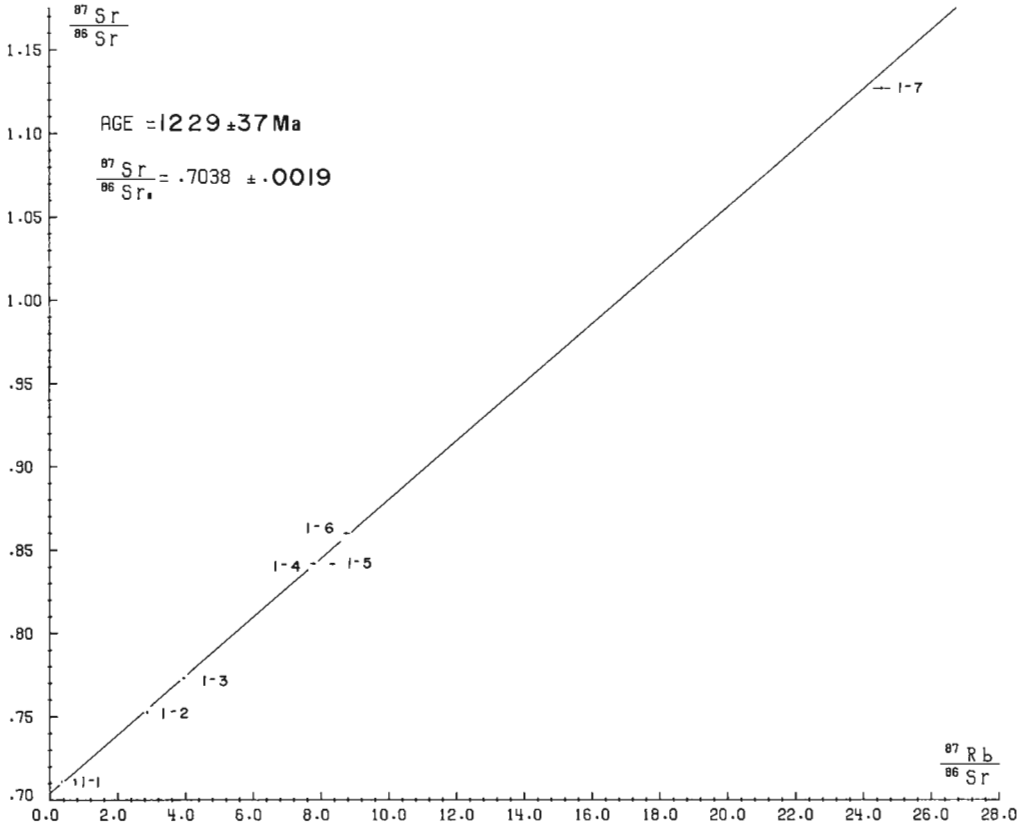

Figure 1. *Rb-Sr isochron, Group 1 samples, Cayamant Lineament, Grenville Province, Quebec.*

Table 1

Analytical data, whole rock samples, Cayamant Lineament region, Grenville Province, Quebec

Sample No.	Rb ppm	Sr ppm	$^{87}Sr/^{86}Sr$ unspiked	$^{87}Sr/^{86}Sr$ spiked	$^{87}Sr/^{86}Sr$ average	$^{87}Rb/^{86}Sr$
Group 1						
1-1	57.36	467.7	0.7110	0.7125	0.7108 ± 0.0011	0.355 ± 0.007
1-2	139.3	*140.5	0.7528	*0.7525	0.7526 ± 0.0011	2.871 ± 0.057
1-3	122.7	* 89.73	0.7728	*0.7731	0.7730 ± 0.0012	3.959 ± 0.079
1-4	114.7	42.63	0.8427	0.8409	0.8418 ± 0.0013	7.790 ± 0.156
1-5	97.14	33.70	0.8404	0.8430	0.8417 ± 0.0013	8.346 ± 0.167
1-6	151.7	* 50.15	*0.8601	0.8597	0.8600 ± 0.0014	8.758 ± 0.175
1-7	*155.0	18.28	1.1261	1.1277	1.1269 ± 0.0018	24.56 ± 0.49
Group 2						
2-1	18.33	690.8	0.7044	0.7058	0.7051 ± 0.0011	0.0768 ± 0.0015
2-2	83.14	509.3	0.7116	0.7114	0.7115 ± 0.0011	0.4726 ± 0.0095
2-3	109.1	230.7	0.7273	0.7272	0.7272 ± 0.0012	1.369 ± 0.027
2-4	90.64	131.4	0.7424	0.7425	0.7425 ± 0.0012	1.997 ± 0.040
2-5	95.07	137.3	0.7432	0.7420	0.7426 ± 0.0012	2.005 ± 0.040
2-6	157.2	220.4	0.7373	0.7370	0.7372 ± 0.0012	2.065 ± 0.041
Group 3						
3-1	41.23	696.6	0.7061	0.7056	0.7058 ± 0.0011	0.1714 ± 0.0034
3-2	89.02	313.9	0.7200	0.7202	0.7201 ± 0.0012	0.8211 ± 0.0164
3-3	96.47	302.7	0.7192	0.7196	0.7194 ± 0.0012	0.9227 ± 0.0185
3-4	85.93	*219.4	*0.7247	*0.7251	0.7249 ± 0.0012	1.134 ± 0.0227
3-5	120.4	283.7	0.7274	0.7277	0.7276 ± 0.0012	1.229 ± 0.025
3-6	137.0	237.6	0.7345	0.7349	0.7347 ± 0.0012	1.669 ± 0.033
3-7	141.6	193.0	0.7420	0.7424	0.7422 ± 0.0012	2.124 ± 0.042
3-8	154.6	191.1	0.7411	0.7411	0.7411 ± 0.0012	2.342 ± 0.047

*Average of two determinations

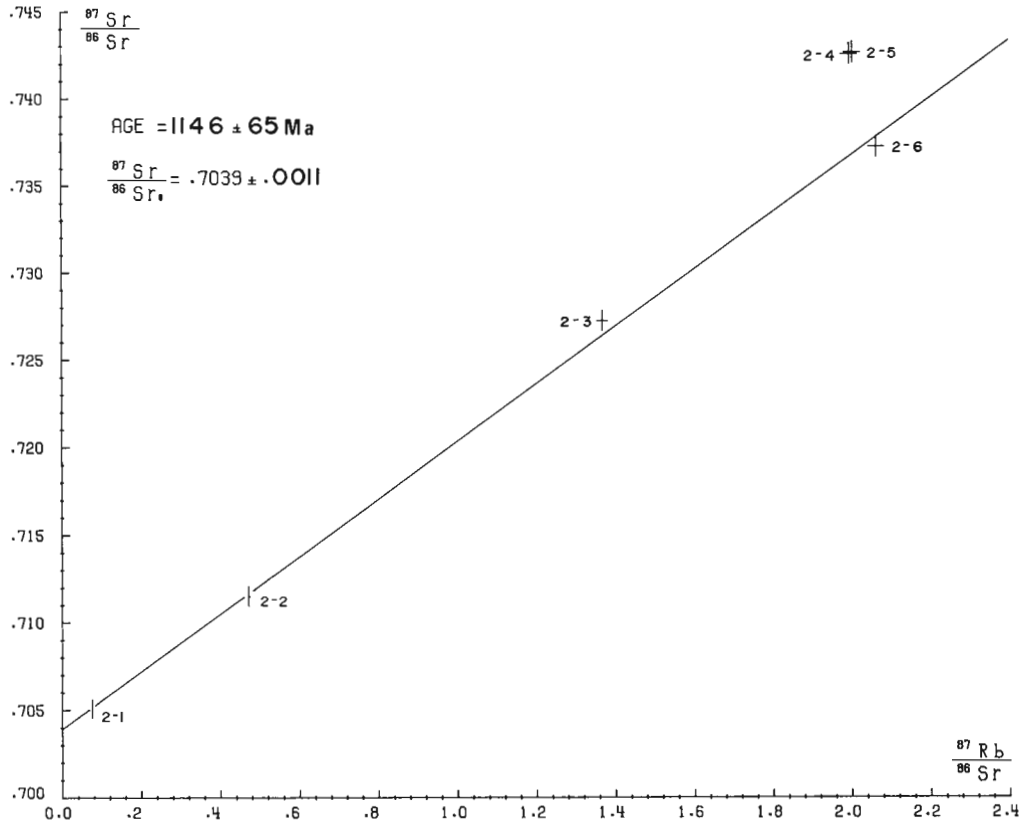

Figure 2. *Rb-Sr isochron, Group 2 samples, Cayamant Lineament, Grenville Province, Quebec.*

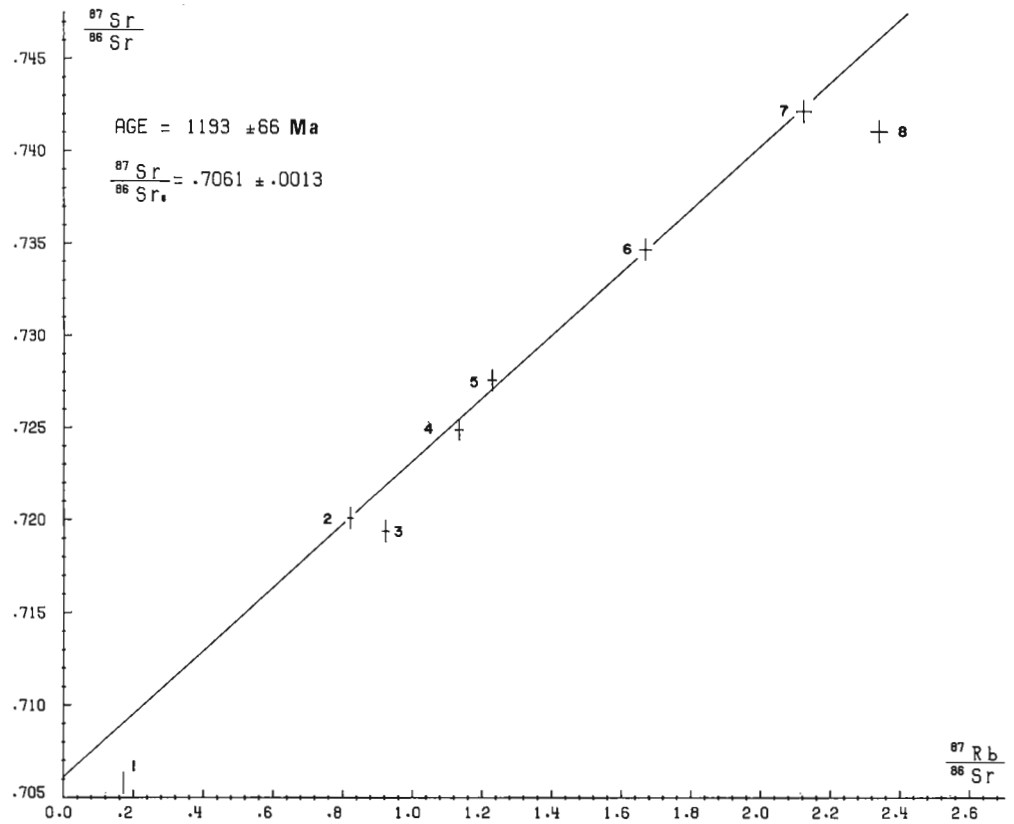

Figure 3. *Rb-Sr isochron, Group 3 samples, Cayamant Lineament, Grenville Province, Quebec. Only the isochron through the first set of samples (see text) is shown.*

Table 2

Sample localities and descriptions, Cayamant Lineament region, Grenville Province, Quebec

Sample Group	Rock Type	Latitude	Longitude	N.T.S.
1	Garnet sillimanite paragneiss Grenville Supergroup	46°01'	76°03'	31 K/1E
2	Garnet sillimanite paragneiss Grenville Supergroup	46°07'	76°12'	31 K/1E
3a and 3b	Medium grained, pink, biotite – granitic gneiss	46°28'	76°17'	31 K/8W

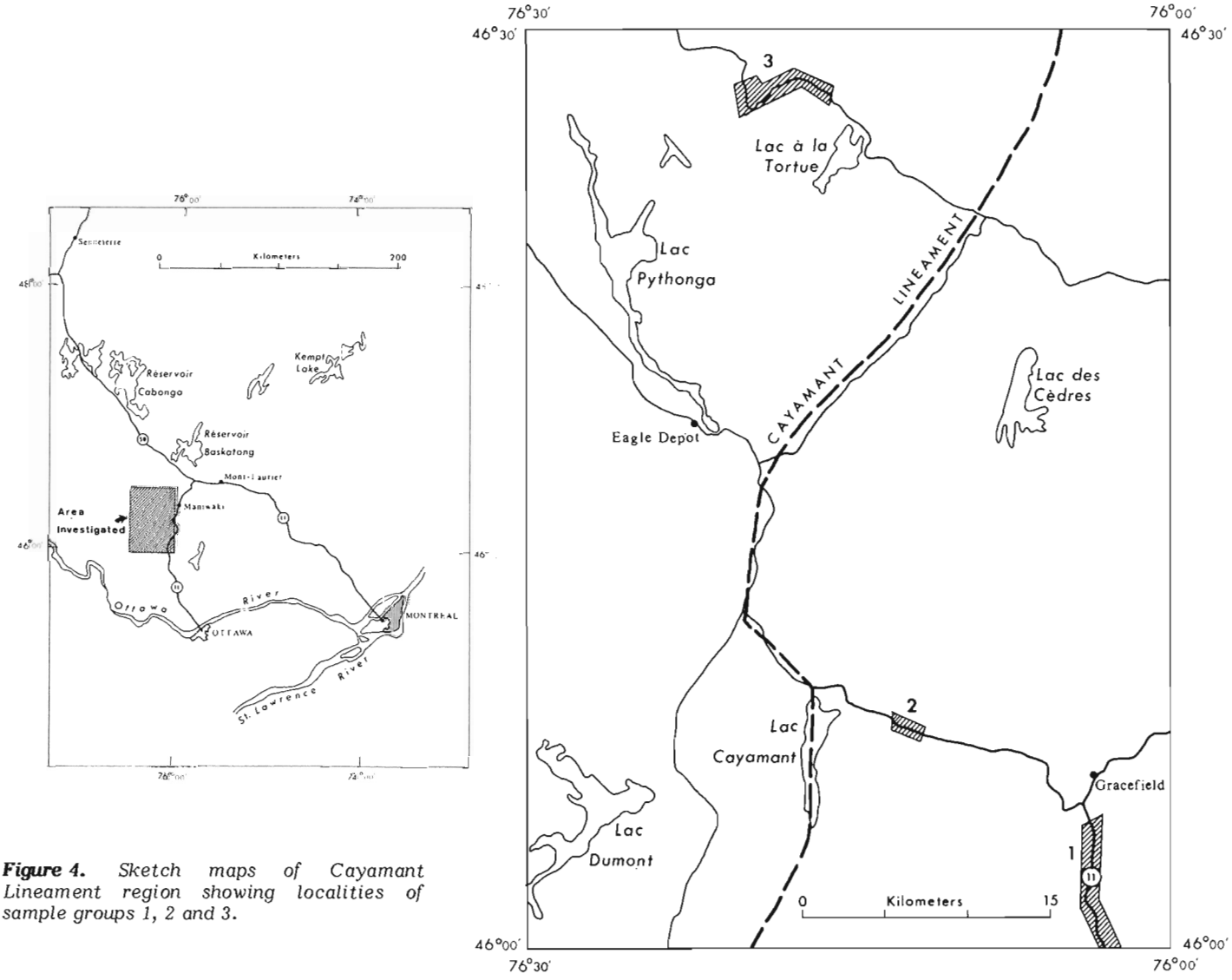

Figure 4. *Sketch maps of Cayamant Lineament region showing localities of sample groups 1, 2 and 3.*

Group 2 consists of numerous samples of garnet-sillimanite-K feldspar gneiss collected in the immediate vicinity of McGoey Lake near the town of Lac Cayamant. This is the closest outcrop of undoubted Grenville Supergroup paragneiss to the lineament, an age of 1146 ± 65 Ma (Fig. 2) was obtained for these rocks.

Three sample suites were collected on the northwest side of the lineament; two west of Lac Cayamant from the grey biotite-hornblende gneisses mentioned above and the third from a rather atypical, pink, rather homogeneous, granitic biotite gneiss (locality 3a). The purpose of this last sample was to ascertain if this particular rock type, unknown east of the lineament, was formed at a time related to the Grenvillian orogeny or at an earlier period.

The two suites of samples collected west of Lac Cayamant failed to yield enough variation in Rb/Sr ratio to enable reasonable isochrons to be determined. The pink granitic gneiss yielded an age of 1193 ± 66 Ma (Fig. 3). In an attempt to add more data points to isochron 3a, more samples of the unit were collected subsequently from the same general area (suite 3b). The isochron on the second suite of samples gave an age of 1133 ± 109 Ma and the combined data (suites 3a+3b) yield an errorchron age of 1208 Ma.

Discussion

The main thrust of the project was to determine whether the grey hornblende-biotite gneisses are significantly older than the metapelite rocks of the Grenville Supergroup in this portion of southwestern Quebec. This was not accomplished since no dates were obtained from the supposedly older rocks.

The results on the pink granitic gneiss are interesting since they are not significantly different from those obtained on the Grenville Supergroup rocks. In all cases, the surprisingly low initial ratios would suggest that no long period of pre-Grenvillian orogeny history is involved.

Four possible models to explain the above results can be proposed:

1. The Cayamant Lineament is simply a fault zone of minor importance, and the young ages from the granitic gneisses indicate that they and the hornblende-biotite gneisses were formed at the time of the Grenville Supergroup metamorphism. This possibility cannot be discounted but is unlikely in view of the fact that ages of approximately 1800 Ma have been obtained on hornblende-biotite gneisses similar to those described here, in the French River area of Ontario (Krogh and Davis, 1969). The model would necessitate the presence of a hitherto unrecognized boundary between the hornblende-biotite gneisses of the two regions.
2. The upper amphibolite (and locally granulite facies) metamorphism reset the older ages northwest of the lineament. Once again, this possibility cannot be disproved, however the low initial ratio obtained from the granitic gneiss militates against it. Furthermore the metamorphic grade of the hornblende-biotite gneiss does not appear to differ greatly from the gneiss dated by Krogh and Davis.
3. The age of the granitic gneiss is similar to that of the Grenville Supergroup, and both are collectively younger than the hornblende-biotite gneiss. This is a reasonable interpretation of the available data, and if correct is important in that it establishes that the western margin of the marble-metapelite units (i.e. the Cayamant Lineament) is not the limit of the Grenville Supergroup rocks in this area as previously thought. A possible interpretation might be that the lineament represents a zone of abrupt facies change, and that at least some of the rocks west of the lineament are time correlative with the Grenville Supergroup rocks.
4. The "young age" obtained from the granitic gneiss is due to a strong metasomatic episode which occurred at approximately the time indicated by the isochron. Wynne-Edwards et al. (1966) noted that the contact between the Grenville Supergroup rocks and those northwest of the lineament is a zone in which a pink migmatite has commonly developed. Doig (1977) obtained Rb-Sr whole rock ages ranging from 1370 to 1170 Ma on three samples of this unit, with initial ratios of 0.750, 0.728, and 0.707 respectively, and explained the enormous variation in the ratios by postulating the existence of a strong metasomatic event which was superimposed upon older gneisses, and which is but one of the many manifestations of the Grenvillian orogeny in this area. This isotopically disturbed zone is approximately 50 km wide according to Doig. Given the fact that the pink granitic gneiss is along strike from the area sampled by Doig, and in addition is only about 15 km or so from the lineament, it is not unreasonable to suggest a similar origin for the granitic rocks encountered here. This last mentioned hypothesis is the one personally favoured by the author at this time.

In conclusion, it can be stated that all ages reported herein are related directly to the Grenvillian orogeny, either through the metamorphism of pre-existing sedimentary rocks or (possibly) through the metasomatism of and resetting of the ages of older gneisses. It remains to be demonstrated that the grey hornblende-biotite gneisses, at a distance of more than 50 km from the Cayamant Lineament are significantly older than the ages presented here.

Acknowledgments

Many lively discussions with R. Doig have contributed greatly to the writers' knowledge of this portion of the Grenville Province.

References

Bourne, James H.
1970a: Geology of the Cayamant Lake area, Quebec; Ministère de Richesses Naturelles Québec, preliminary report 598, 20 p.

1970b: Geology of the Pythonga Lake area, Quebec; Ministère de Richesses Naturelles Québec, Open File Report GM-28638, 22 p.

Doig, R.
1977: Rb-Sr geochronology and evolution of the Grenville Province in northwestern Quebec, Canada; Geological Society of America Bulletin, v. 88, p. 1843-1856.

Fraser, J.A., Heywood, W.W., and Mazurski, M.A.
1978: Metamorphic Map of the Canadian Shield; Geological Survey of Canada, Map 1475A.

Krogh, T.E. and Davis, G.L.
1969: Geochronology of the Grenville Province; Carnegie Institution of Washington Yearbook, v. 67, p. 224-233.

Wynne-Edwards, H.R., Gregory, A.F., Hay, P.W., Giovanella, C.A., and Reinhardt, E.W.
1966: Mont Laurier and Kempt Lake map areas, Quebec; Geological Survey of Canada, Paper 66-32, 32 p.

8. FOLIATED AND RECRYSTALLIZED GRANITES FROM THE TIMBERLAKE PLUTON, ONTARIO

A) Foliated granites
Isochron Age = 1137 ± 173 Ma
$^{87}Sr/^{86}Sr$ initial = 0.7164 ± 0.0134

B) Recrystallized granites
Isochron Age = 994 ± 157 Ma
$^{87}Sr/^{86}Sr$ initial = 0.7276 ± 0.0124

C) Foliated and recrystallized granites combined
Isochron Age = 1070 ± 114 Ma
$^{87}Sr/^{86}Sr$ initial = 0.7216 ± 0.0089

Six foliated granite samples and six recrystallized granite samples were analyzed isotopically. Both groups formed isochrons with low MSWD values of 0.97 and 0.94 respectively. Both groups are extremely homogeneous with respect to Rb/Sr ratio. The measured Rb/Sr range in the foliated granites is 1.67 to 2.14 and in the recrystallized granites is almost identical at 1.77 to 2.28. The range in Rb/Sr ratios is only about 25 per cent of the average Rb/Sr ratio and it is this limited range that leads to the relatively high analytical uncertainties.

The analytical results are presented in Table 1 and depicted in isochron diagrams in Figures 1 and 2. If the results from the foliated and recrystallized samples are combined, a single isochron may be drawn through the analytical points yielding an age of 1070 ± 114 Ma, initial $^{87}Sr/^{86}Sr$ ratio of 0.7216 ± 0.0089 and MSWD of 0.91. This isochron is depicted in Figure 3.

Initial $^{87}Sr/^{86}Sr$ ratios are considerably higher than the range usually obtained for igneous rocks of this age and may indicate a significant history prior to isotopic homogenization at about 1100 Ma. The limited Rb-Sr range may be an indication of elemental homogenization at this time also.

Geological Setting and Interpretation
by A.J. Baer

Purpose of the Study

Timber Lake pluton is a well foliated, homogeneous granite cut locally by narrow shear-zones at a 30-45° angle to the foliation. the prime purpose of the study was to see if the material in the shear-zones would give an age younger than that of the pluton, and, in particular if the shearing was a Grenvillian event superimposed upon an older (Hudsonian ?) pluton. Samples from the foliated mass and from the apparently recrystallized shear-zones were dated separately.

Rock Description

The Timber Lake pluton is an elongated granite body about 35 km northeast of North Bay (Fig. 4). Foliation trends northwesterly, parallel with the long axis of the pluton, and dips about 50° to the southwest.

Outside of shear-zones, the granite is medium- to fine-grained, bright pink and leucocratic. Thin, platy aggregates of biotite and minor hornblende evenly distributed every few millimetres define an excellent foliation, reinforced by thin parallel lenses of quartz. The texture of the rock and the presence of occasional isoclinal fold hinges in mafic aggregates indicate that this foliation is a result of intense cataclastic deformation. As seen in thin section, the granite is now thoroughly recrystallized and the rock is therefore a blastomylonite. It comprises feldspar (60-70%) and quartz (20-40%) with less than 10 per cent biotite and minor hornblende and epidote. Plagioclase (An^{10}) and perthitic K-feldspar form anhedral grains commonly recrystallized as a mosaic, with triple junctions at 120°. This assemblage is compatible with the amphibolite facies of metamorphism.

Minor shear zones locally form abundant crenulations on a scale of a few centimetres to a few decimetres. Crenulations grade into narrow zones of remobilization where all traces of pre-existing foliation disappear (Fig. 5). These zones, commonly between 5 and 10 cm wide, trend east to east-southeast and appear to be vertical. Except for textural differences, the rock is similar to the rest of the pluton, and, in particular, the mineralogy appears to be the same.

Interpretation

Two interpretations of the isochrons are possible:

Case A. The ages obtained for the foliated and the recrystallized rocks in shear zones (respectively 1137 ± 173 Ma and 994 ± 157 Ma) indicate true ages of homogenization. In favour of this interpretation is the fact that relative ages of deformation match Rb-Sr ages. Shear-zones are undoubtedly younger than the foliation elsewhere in the pluton. Against this interpretation, one may say that the two ages are not significantly different, because of the very high analytical uncertainty (173 and 157 Ma). This uncertainty is due essentially to the great homogeneity of the rock, causing a clustering of points on the isochron. One may also argue that 994 Ma is similar to a K-Ar age of 940 Ma* (GSC 62-115, Leech et al, 1963) from the same area. This would indicate that during shearing the rock was close to 250-300°C, the blocking temperature for Ar. The lack of retrogression to greenschist facies and the style of deformation of shear-zones argue for higher temperatures of formation (Sibson, 1977). The case for two distinct events is not convincing, but a growing body of data from various parts of the Grenville Province suggests the possible existence of one peak of activity around 1150 ± 50 Ma and another around 950 ± 50 Ma (Baer, in preparation).

*951 Ma when adjusted for the 25th IGC decay constants adopted in 1977

From: Rb-Sr and U-Pb Isotopic Age Studies in Current Research, Part C Geol. Surv. Can., Paper 80-1C

Table 1

Analytical data, whole rock samples, Timber Lake granite, Ontario

Sample no.	Rb ppm	Sr ppm	$^{87}Sr/^{86}Sr$ unspiked	$^{87}Sr/^{86}Sr$ spiked	$^{87}Sr/^{86}Sr$ average	$^{87}Rb/^{86}Sr$
Foliated Granite						
1	111.8	66.93	0.7959	0.7950	0.7954 ± 0.0012	4.836 ± 0.145
2	118.6	68.25	0.7983	0.7965	0.7974 ± 0.0012	5.031 ± 0.151
3	124.1	65.28	0.8055	0.8057	0.8056 ± 0.0012	5.504 ± 0.165
4	118.9	62.08	0.8079	0.8086	0.8082 ± 0.0012	5.545 ± 0.166
5	124.8	59.90	0.8154	0.8162	0.8158 ± 0.0012	6.032 ± 0.181
6	136.8	63.86	0.8155	0.8148	0.8152 ± 0.0012	6.202 ± 0.186
Recrystallized Granite						
7	119.8	67.72	0.8016	0.8007	0.8012 ± 0.0012	5.122 ± 0.154
8	116.0	65.19	0.8025	0.8013	0.8019 ± 0.0012	5.152 ± 0.155
9	128.6	69.77	0.8031	0.8014	0.8022 ± 0.0012	5.339 ± 0.160
10	66.54	34.42	0.8054	0.8058	0.8056 ± 0.0012	5.597 ± 0.168
11	147.4	72.70	0.8126	0.8112	0.8119 ± 0.0012	5.870 ± 0.176
12	136.7	59.87	0.8204	0.8228	0.8216 ± 0.0012	6.611 ± 0.198

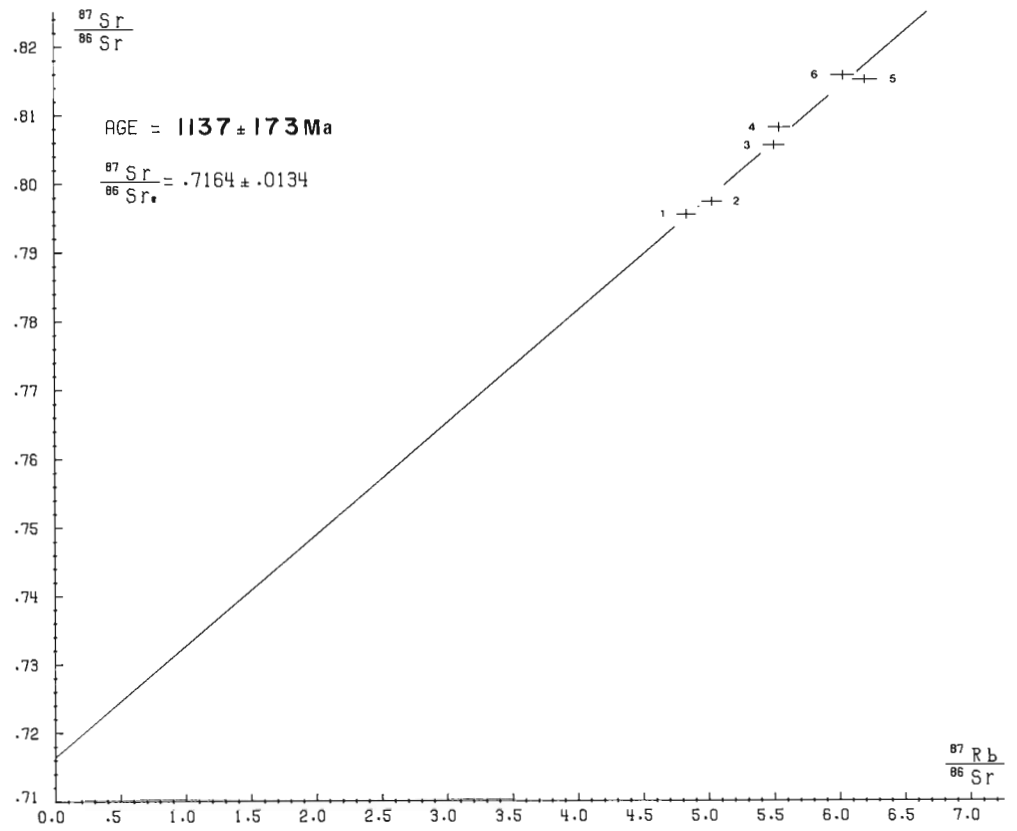

Figure 1. *Rb-Sr isochron, foliated granite, Timber Lake Pluton.*

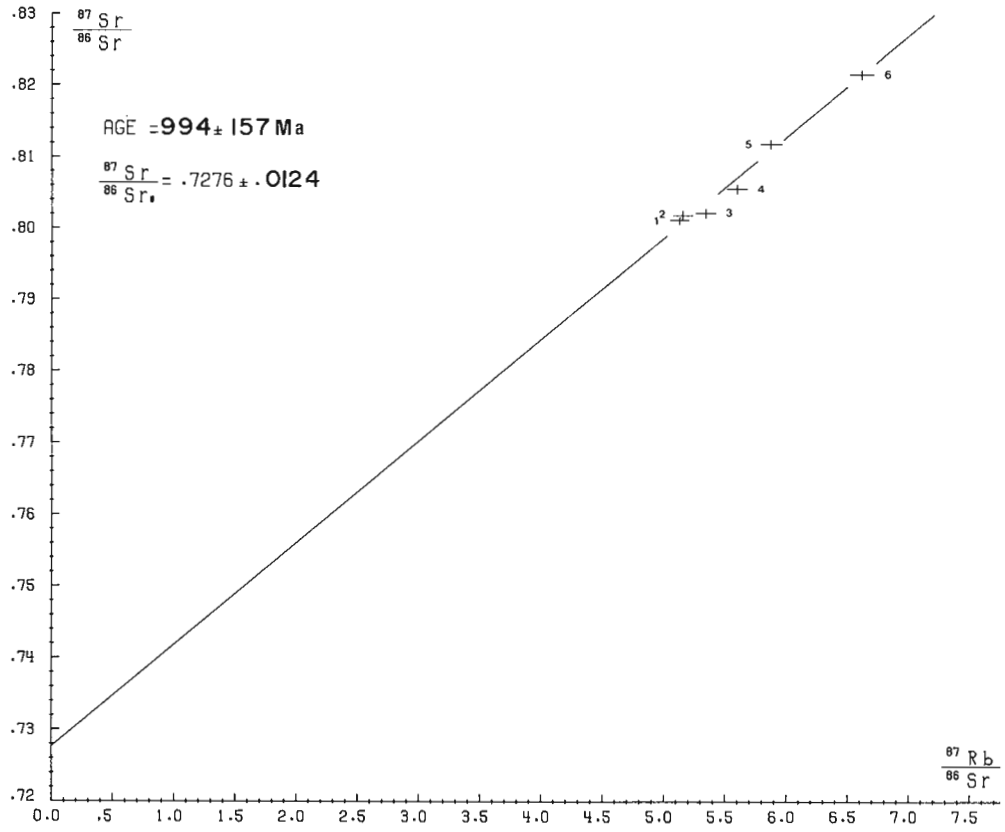

Figure 2. *Rb-Sr isochron, recrystallized granite, Timber Lake Pluton.*

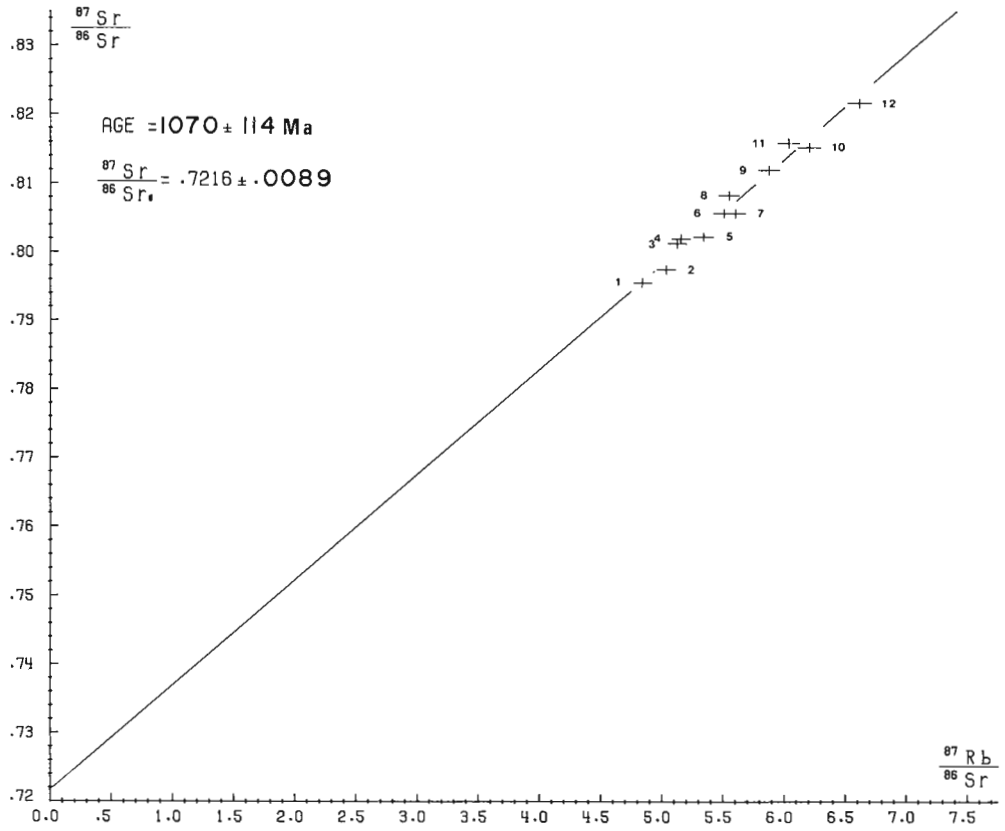

Figure 3. *Rb-Sr isochron, foliated and recrystallized granites combined, Timber Lake Pluton.*

Table 2

Sample numbers and localities, Timber Lake granite

Sample No.			Locality		
This work	Field	Rock type	Latitude	Longitude	NTS
1	BT-01-01B-71	medium grained, foliated granite	46°32'03"N	79°07'24"W	31 L/11 e
2	BT-01-03C-71	medium grained, foliated granite	46°31'15"N	79°05'14"W	31 L/11 e
3	BT-11-16-69-B6	medium grained, foliated granite	46°31'15"N	79°05'14"W	31 L/11 e
4	BT-11-16-69-B1	medium grained, foliated granite	46°31'15"N	79°05'14"W	31 L/11 e
5	BT-11-16-69-B8	medium grained, foliated granite	46°31'15"N	79°05'14"W	31 L/11 e
6	BT-11-16-69-B4	medium grained, foliated granite	46°31'15"N	79°05'14"W	31 L/11 e
7	BT-11-16-69-A5	medium grained, recrystallized granite	46°31'15"N	79°05'14"W	31 L/11 e
8	BT-11-16-69-A10	medium grained, recrystallized granite	46°31'15"N	79°05'14"W	31 L/11 e
9	BT-11-16-69-A2	medium grained, recrystallized granite	46°31'15"N	79°05'14"W	31 L/11 e
10	BT-11-16-69-A16	medium grained, recrystallized granite	46°31'15"N	79°05'14"W	31 L/11 e
11	BT-11-16-69-A13	medium grained, recrystallized granite	46°31'15"N	79°05'14"W	31 L/11 e
12	BT-11-16-69-A7	medium grained, recrystallized granite	46°31'15"N	79°05'14"W	31 L/11 e

Case B. As the ages obtained are not statistically different, only one isochron should be drawn, using all available points. This gives a date of 1070 ± 114 Ma. In this interpretation, the two geologically distinct events, blasto-mylonitization and shearing occurred within a short time interval, around 1070 Ma, and cannot be distinguished by Rb-Sr studies. This more conservative interpretation does not explain the fact that the date on shear-zone material is younger than the other. Initial $^{86}Sr/^{87}Sr$ ratios for both isochrons are extremely high by comparison with granitic rocks of this approximate age. An average ratio would probably be around 0.705-0.715. High initial ratios have commonly been interpreted as indicative of a long crustal history. A glance at the initial ratios obtained here (0.728 and 0.716) suggests therefore that the Timber Lake granite is very old and that the isochrons only date the latest thorough homogenization suffered by the rock. Closer examination indicates that this is probably not the case. The Sr content of analyzed samples is low, whereas the Rb content is about normal. As a result, Rb/Sr ratios are high (1.90 and 1.93 respectively for foliated and recrystallized samples). This means that in a plot of $^{87}Sr/^{86}Sr$ versus time (see Fig. 1 of Wanless and Loveridge, 1972) the slope of the line generated by such a high Rb/Sr ratio will be steep, and would intersect an approximate mantle evolutionary trend at about -150 Ma. It is doubtful, therefore, that the Timber Lake granite has a crustal history extending back much beyond 1300 Ma ago.

Origin of the Timber Lake Granite

The preceding interpretation is based on the assumption that the granite is a magmatic pluton. This appears reasonable, in view of the following facts:

From hand specimen, to outcrop, to mappable unit, the rock is extremely homogeneous. It does not display banding and its mineralogy seems to be everywhere the same. From analyses, Rb and Sr content are also extremely constant. Attempts at extending the range of $^{87}Rb/^{86}Sr$ ratios to obtain a better isochron have failed. Most samples were collected from an outcrop area about 30 x 60 m, but samples 1 and 2 of foliated rock come from a location 2 km away and their ratios hardly differ from those of other samples (Table 2). The textural, mineralogical and chemical homogeneity of the rock strongly favour an igneous, magmatic origin.

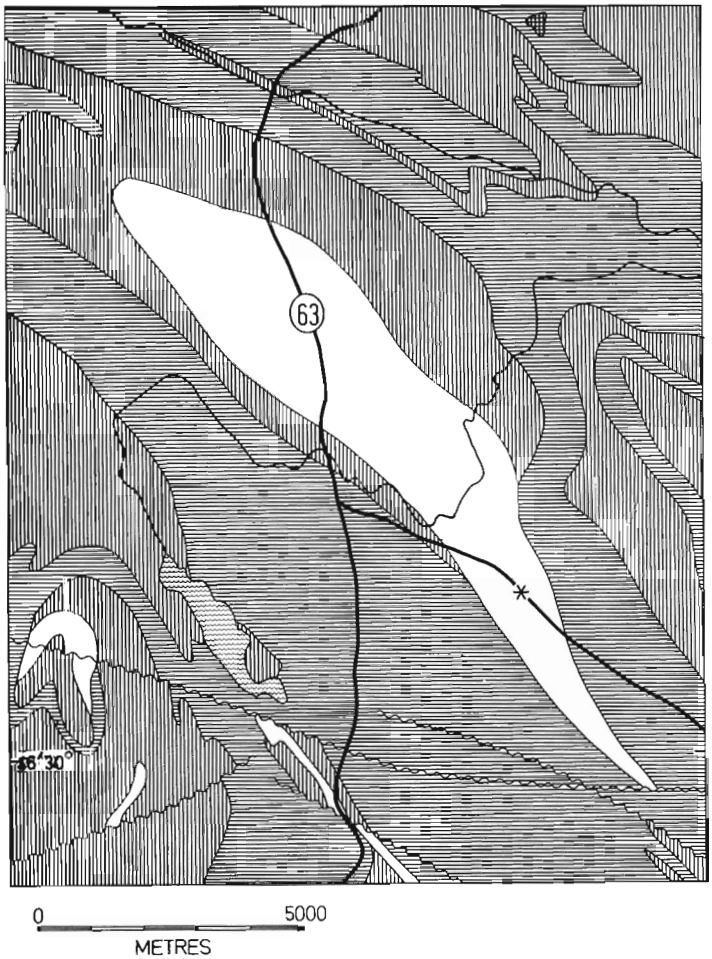

Figure 4. *Sketch map of Timber Lake pluton (after map 2361, Ontario Geological Survey, 1977). Sampling location shown by a star. Legend: vertical lines: biotite gneisses; horizontal lines: quartzofeldspathic gneisses, mainly quartz-rich and muscovite-bearing; cross-hatched: mafic rocks; white: granite and granodiorite; wave pattern: lake.*

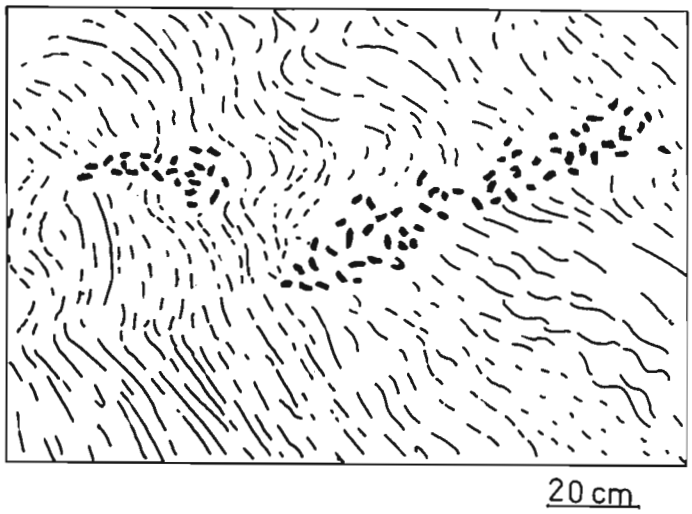

Figure 5. *Crenulated foliation in the granite with oblique, recrystallized shear-zones.*

Regional Correlation and Conclusions

Beside the K-Ar date of 940 Ma* already mentioned, two other Rb-Sr isochrons have been obtained in the area (Lumbers 1971). One, on the Mulock pluton, 25 km to the west-southwest gave a maximum age of 1175 Ma*, the other, on the Powassan-Bonfield pluton, 55 km to the south-southwest gave an age of 1302 ± 70 Ma*. The Mulock pluton is elongated northwest and lithologically similar to the Timber Lake granite. It is concordant with gneisses that surround it, but pegmatitic veins that cut the metasediments indicate an intrusive origin. Taking available data into account, the probable evolution of the area can be summarized as follows:

1. Granitic plutons were emplaced around 1300 Ma or shortly thereafter. They intruded a complex of gneisses that had been deformed previously. The northwesterly regional trend of the area was probably imposed upon it during intrusion.
2. A later deformation, or the end of the same one, affected the Timber Lake granite around 1140 Ma or 1070 Ma ago (depending upon which interpretation is chosen). This event was a mylonitization of the rock and probably represented a tightening of pre-existing folds in the gneisses surrounding the pluton. Temperatures were high, and the granite was in the amphibolite facies.
3. A final tectonic phase caused the formation of easterly trending shear-zones, possibly as early as 1070 Ma ago, but certainly no later than about 950 Ma ago. Although the time elapsed between the two deformations cannot be determined accurately, the divergence of structural trends implies that a major rearrangement of stress patterns occurred between the two events.
4. The region cooled to about 300°C around 940 Ma ago.

The timing of events in the area throws some doubt upon a generalized "Grenvillian orogeny" that would have occurred around 1050 Ma ago.

References

Leech, G.B., Lowdon, J.A., Stockwell, C.H., and Wanless, R.K.
1963: Age determinations and geological studies (Including isotopic ages – Report 4); Geological Survey of Canada, Paper 63-17, p. 76.

Lumbers, S.B.
1971: Geology of the North Bay area, districts of Nipissing and Parry Sound; Ontario Department of Mines, Geological Report 94.

Sibson, R.H.
1977; Fault rocks and fault mechanisms; Journal of Geological Society of London 133/3, 191-213.

Wanless, R.K. and Loveridge, W.D.
1972: Rubidium-Strontium isochron age studies, report 1; Geological Survey of Canada, Paper 72-23, p. 3.

*Adjusted using $\lambda^{87}Rb = 1.42 \times 10^{-11}\ a^{-1}$

9. Rb-Sr STUDIES OF THE HORSESHOE LAKE AND APISKO LAKE GRANITES, BERENS RIVER – DEER LAKE MAP AREA, MANITOBA AND ONTARIO

A) Horseshoe Lake granite
Isochron Age = 2557 ± 45 Ma
$^{87}Sr/^{86}Sr$ initial = 0.7024 ± 0.0010

B) Apisko Lake granite
Isochron Age = 2677 ± 165 Ma
$^{87}Sr/^{86}Sr$ initial = 0.7010 ± 0.0021

The results of isotopic analyses on ten whole rock samples from the Horseshoe Lake granite listed in Table 1 may be divided into two groups, sample numbers 1 to 8 with $^{87}Rb/^{86}Sr$ ratios less than 3.0 and samples 9 and 10 with $^{87}Rb/^{86}Sr$ ratios of 30.5 and 42.5 respectively. The results for samples 1 to 8 define a good isochron, Figure 1, of age 2557 ± 45 Ma, $^{87}Sr/^{86}Sr$ initial 0.7024 ± 0.0010 and MSWD 0.66. The high isotopic ratios of samples 9 and 10 permit calculation of individual Rb-Sr ages which are only minimally dependent on the assumed $^{87}Sr/^{86}Sr$ ratio. These are 2670 ± 53 and 2655 ± 53 Ma for samples 9 and 10 respectively, assuming an initial $^{87}Sr/^{86}Sr$ of 0.702.

Samples 9 and 10 were not included in the calculation of isochron parameters for two reasons: (1) because of their high isotopic ratios these two samples would strongly affect the calculated isochron age and (2) because the individual ages of these samples, 2670 ± 53 and 2655 ± 53 Ma, are significantly higher than the isochron age of 2557 ± 45 Ma obtained from samples 1 to 8.

The reason for the higher apparent ages associated with samples 9 and 10 is not clearly understood, but is probably associated with the coarse muscovite content of these samples (Table 3). The low strontium contents of 12.6 and 10.1 ppm obtained for these two samples (Table 1) is probably the result of a high proportion of muscovite in the fractions analyzed. Thus the 2670 and 2655 Ma ages are probably controlled by the muscovite; the rubidium and strontium contribution of the other minerals present having only a minor effect. Conversely the isochron age of 2557 Ma is controlled by the minerals which do not play a major part in the ages of samples 9 and 10 and of those, particularly the ones with the higher Rb/Sr ratios. If, of the samples comprising the isochron, those with the highest Rb/Sr ratios, samples 6, 7 and 8 are omitted from the isochron calculation the remaining samples (1 to 5) also yield an isochron but with a higher age 2599 ± 109 Ma, a lower intercept 0.7018 ± 0.0018 and a lower MSWD 0.19. This may indicate the existence of a relatively high Rb/Sr, lower age component (possibly microcline) in all Horseshoe Lake samples which dilutes the primary age. A comparable effect may be seen in the Rb-Sr isochron age of the Rice River Gneiss (I.F. Ermanovics, ibid.). The initial $^{87}Sr/^{86}Sr$ ratio of the Horseshoe Lake granite is marginally higher than commonly found for mantle derived rocks of this age supporting the hypotheses of a secondary component.

The isotopic results obtained on six whole rock samples from the Apisko Lake granite are presented in Table 2 and shown on an isochron diagram in Figure 2. All six samples are collinear yielding an isochron of age 2677 ± 165 Ma, initial $^{87}Sr/^{86}Sr$ 0.7010 ± 0.0021 and MSWD 1.14. The initial $^{87}Sr/^{86}Sr$ ratio is indistinguishable from those measured in mantle derived rocks of this age.

Geological Setting and Interpretation
by I.F. Ermanovics and W.D. Loveridge

Horseshoe Lake and Apisko Lake granites (nomenclature after Streckeisen, 1975) are potassic end-members of the late synkinematic, calc-alkaline plutonic intrusive suite in Berens subprovince (Ermanovics et al., 1979; Ermanovics, 1970). They form generally homogeneous, massive plutons whose rocks locally are weakly foliated and have recrystallized quartz mosaics. Modal analysis indicates equal parts of oligoclase-andesine, perthitic microcline and quartz. In 80 per cent of the modes Σ (quartz + feldspar) > 90%, and in 40 per cent of the modes Σ (quartz + feldspar) > 95%.

Horseshoe Lake granite

This 9x6 km, pear-shaped body intrudes Horseshoe Lake metadacites of amphibolite facies. The granite postdates metamorphism and is only locally foliated. It is coarse grained, pink, leucocratic and grades to granodiorite (sample number 3) containing 10 per cent brown biotite. Specimens 9 and 10 (Table 3) are fresh albite-microcline-muscovite granites of equant, medium grain, and like the granodiorite, represent border phases of the stock.

Samples 1 to 8 yield an isochron age of 2557 ± 45 Ma which is comparable to a K-Ar hornblende age (2570 ± 62 Ma, GSC 72-72) and a biotite age (2504 ± 68 Ma, GSC 72-73, Wanless et al., 1973) obtained from quartz diorite associated with the Horseshoe Lake metavolcanics. However, the two muscovite-bearing granites (samples 9 and 10) were treated separately and assuming an initial $^{87}Sr/^{86}Sr$ ratio of 0.702, yielded ages of 2670 Ma and 2655 Ma. These older ages are comparable with those obtained for the Apisko Lake granite.

A preliminary minimum U-Pb age measurement on zircon from the granite yielded ca. 2700 Ma (T. Krogh, Royal Ontario Museum, personal communication, 1979).

Apisko Lake granite

This body is oval-shaped with diameters of 40 and 13 km, and is part of a larger granodioritic batholith that intrudes amphibolite facies plutonic gneisses. Samples analyzed tend to fall closer to the granodioritic field and are texturally and compositionally (Table 5 and 6) more homogeneous than samples from Horseshoe Lake.

From: Rb-Sr and U-Pb Isotopic Age Studies in Current Research, Part C Geol. Surv. Can., Paper 80-1C

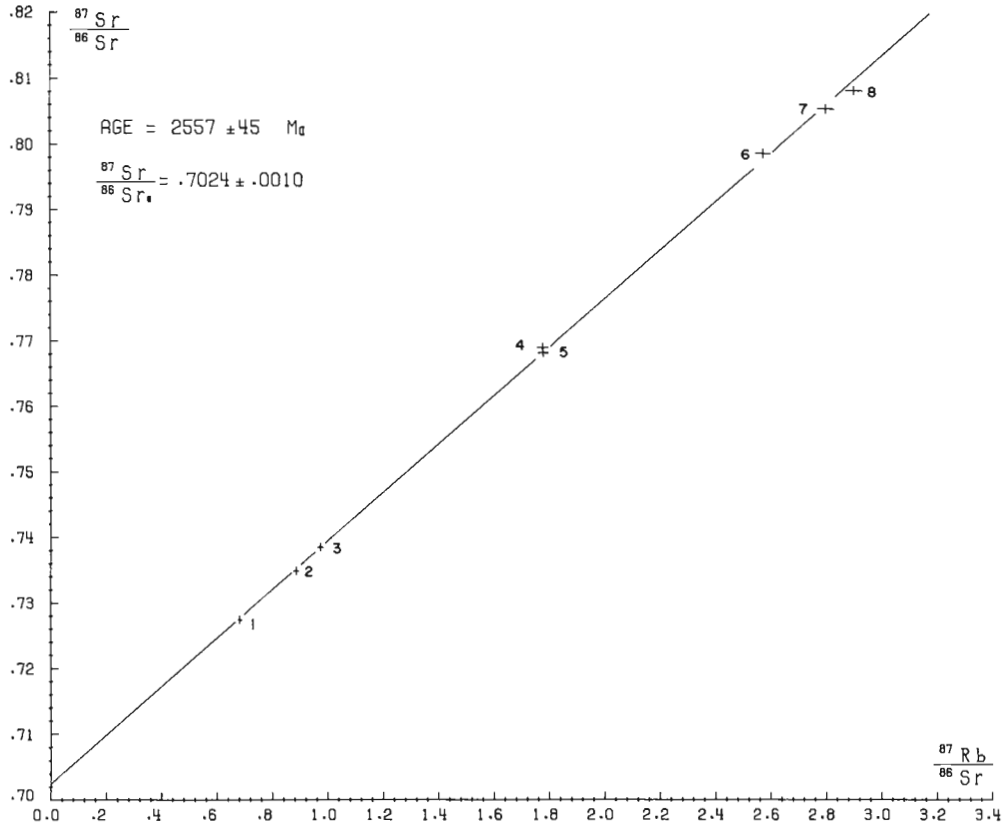

Figure 1. *Rb-Sr isochron Horseshoe Lake granite, Manitoba and Ontario.*

Table 1

Analytical data, whole rock samples, Horseshoe Lake granite, Manitoba and Ontario

Sample No.	Rb ppm	Sr ppm	$^{87}Sr/^{86}Sr$ unspiked	$^{87}Sr/^{86}Sr$ spiked	$^{87}Sr/^{86}Sr$ average	$^{87}Rb/^{86}Sr$
1	70.25	298.5	0.7278	0.7271	0.7274 ± 0.0011	0.6814 ± 0.0136
2	79.18	258.8	0.7354	0.7344	0.7349 ± 0.0011	0.8858 ± 0.0177
3	126.4	376.1	0.7384	0.7386	0.7385 ± 0.0011	0.9730 ± 0.0195
4	105.8	172.2	0.7679	0.7686	0.7682 ± 0.0011	1.779 ± 0.036
5	106.0	172.7	0.7691	0.7688	0.7690 ± 0.0012	1.777 ± 0.036
6	123.8	139.2	0.7983	0.7992	0.7987 ± 0.0012	2.575 ± 0.052
7	71.71	74.07	0.8064	0.8046	0.8055 ± 0.0012	2.803 ± 0.056
8	71.29	71.03	0.8086	0.8081	0.8083 ± 0.0012	2.906 ± 0.058
* 9	** 133.1	12.64		1.8803	1.8803 ± 0.0028	30.49 ± 0.61
*10	148.7	10.12	2.3340	2.3393	2.3366 ± 0.0035	42.54 ± 0.85

* Muscovite-bearing border phase
** Average of two determinations

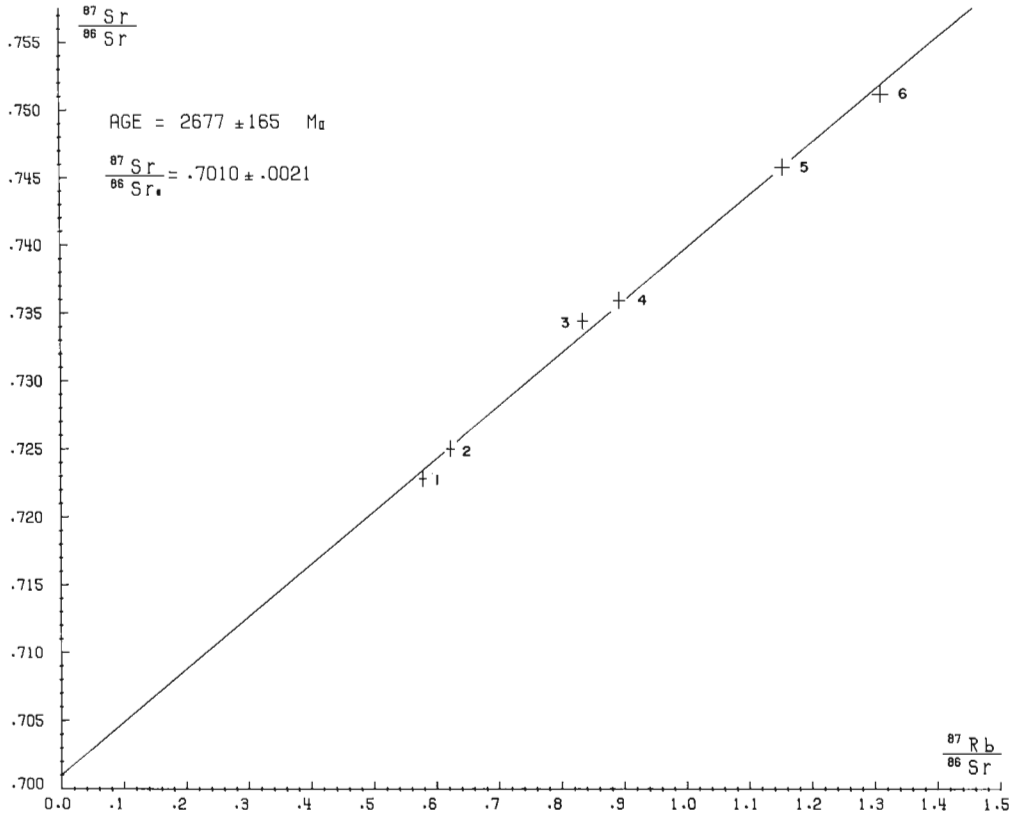

Figure 2. *Rb-Sr isochron Apisko Lake granite, Manitoba and Ontario.*

Table 2

Analytical data, whole rock samples, Apisko Lake granite, Manitoba and Ontario

Sample No.	Rb ppm	Sr ppm	$^{87}Sr/^{86}Sr$ unspiked	$^{87}Sr/^{86}Sr$ spiked	$^{87}Sr/^{86}Sr$ average	$^{87}Rb/^{86}Sr$
1	77.14	386.3	0.7231	0.7225	0.7228 ± 0.0011	0.5782 ± 0.0116
2	78.73	366.0	0.7253	0.7247	0.7250 ± 0.0011	0.6228 ± 0.0125
3	83.81	290.9	0.7341	0.7347	0.7344 ± 0.0011	0.8341 ± 0.0167
4	113.7	368.8	0.7357	0.7360	0.7359 ± 0.0011	0.8926 ± 0.0178
5	107.0	268.5	0.7452	0.7462	0.7457 ± 0.0011	1.154 ± 0.023
6	108.8	240.3	0.7510	0.7513	0.7512 ± 0.0011	1.311 ± 0.026

The Rb-Sr isochron age for the Apisko Lake granite is 2677 ± 165 Ma and a K-Ar biotite age on the same suite of samples is 2493 ± 72 Ma (GSC 72-75, Wanless et al., 1973). The isochron age is higher than that of the Horseshoe Lake granite but is very similar to the ages obtained on the muscovite bearing border phase of the Horseshoe Lake granite. The Apisko Lake isochron age is also in reasonable agreement with the 2700 Ma U-Pb age on zircons from the Horseshoe Lake granite.

Discussion

It is desirable to establish ages of crystallization for the Berens batholiths in the light of the preliminary U-Pb zircon age of 2700 Ma at Horseshoe Lake. A number of U-Pb zircon ages of late granodioritic plutonic rocks in Sachigo subprovince and Uchi subprovince (R.K. Wanless, personal communication, 1979; Krogh et al., 1974) are in the range 2705-2765 Ma. It is likely therefore that late plutonic rocks of the Berens subprovince also may have ages of crystallization in that range.

Table 3

Sample numbers and localities, Horseshoe Lake granite

Sample No. This work	Field	Rock Type	Locality Latitude	Longitude	N.T.S.
1	EE69-1203	Granite: zoned andesine-oligoclase with myrrmekite; 2% brown biotite	52°08'30"	95°47'30"	53 D
2	EE69-1201-2	Granite: as 1203	52°10'	95°49'	53 D
3	EE69-1202-1	Granodiorite: strained optics; 10% biotite	52°09'	95°48'30"	53 D
4	EE69-1190-1	Granite: quartz recrystallized; 3% chloritic biotite	52°11'20"	95°48'	53 D
5	EE69-1190-3	Granite: same rock and outcrop as 1190-1			
6	EE69-1205-1	Granite: pink, coarse grained; chloritic biotite 2%	52°09'20"	95°43'	53 D
7	EE69-1121-1	Granite: leucocratic, mafic = 0.5% (biotite); coarse grained; strained albite twin lamellae	52°08'	95°48'	53 D
8	EE69-1211-2	Granite: same rock and outcrop as 1211-1			
9	EE69-1165	Granite: medium grained, equant albite intergrown with microcline; 3% muscovite forms well developed grains 3 x 6 mm size	52°12'30"	93°48'30"	53 D
10	EE69-1166	Granite: as 1165	52°13'	95°48'	53 D

Table 4

Chemical analyses (wt. %), Horseshoe Lake granite

	Sample No. (this work)					
	1	2	3	6	7	9
SiO_2	73.2	72.7	69.0	75.6	79.6	77.7
Al_2O_3	13.8	14.3	14.4	12.7	11.5	12.3
TiO_2	0.37	0.33	0.57	0.19	0.14	0.08
Fe_2O_3	0.48	0.55	1.46	nf	0.24	0.13
FeO	1.5	1.2	2.1	1.2	0.40	0.30
MnO	0.06	0.06	0.11	0.06	0.02	0.08
MgO	0.75	0.52	1.6	0.39	0.17	0.14
CaO	1.5	1.4	3.1	0.90	0.45	0.29
Na_2O	4.1	4.4	4.9	3.8	3.2	4.7
K_2O	3.4	3.6	1.6	4.4	4.0	3.9
P_2O_5	0.15	0.15	0.30	0.09	0.03	0.05
CO_2	nf	nf	nf	nf	nf	nf
H_2O_T	0.40	0.50	1.1	0.50	0.60	0.30

nf = analyzed but not found
H_2O_T = total water

Table 5

Sample numbers and localities, Apisko Lake granite

Sample No. This work	Sample No. Field	Rock Type	Locality Latitude	Locality Longitude	N.T.S.
1	EE69-1093-1	Granite: as sample 1107-2 but strained; % microcline = plagioclase	52°35'30"	95°21'	53 D
2	EE69-1107-2	Granite: pink, coarse grained perthitic and poikilitic microcline and zoned oligoclase-andesine; 4% mafics (green-pale brown biotite)	52°30'30"	95°22'	53 D
3	EE69-1093-3	Granite: same rock and outcrop as 1093-1			
4	EE69-1088-1	Granite: as 1107-2	52°30'30"	95°29'	53 D
5	EE69-1097-2	Granite: as 1107-2; % microcline > plagioclase	52°32'	95°27'	53 D
6	EE69-1097-1	Granite: same rock and outcrop as 1097-2			

Table 6

Chemical analyses (wt. %), Apisko Lake granite

	Sample No. (this work)			
	2	3	4	6
SiO_2	71.3	72.9	72.1	75.6
Al_2O_3	14.0	13.9	13.9	13.4
TiO_2	0.55	0.38	0.35	0.11
Fe_2O_3	1.2	0.77	0.76	0.28
FeO	1.6	1.2	1.7	0.70
MnO	0.05	0.05	0.06	0.02
MgO	0.84	0.67	0.91	0.27
CaO	1.9	1.3	1.9	1.2
Na_2O	3.9	3.8	3.7	3.4
K_2O	4.2	4.4	3.7	5.0
P_2O_5	0.22	0.13	0.16	0.06
CO_2	nf	nf	nf	nf
H_2O_T	0.50	0.50	0.50	0.40

nf = analyzed but not found
H_2O_T = total water

If this is the case, the Apisko Lake isochron age and the age of the muscovite rich border phase of the Horseshoe Lake granite are reasonably close to the assumed age of crystallization whereas the Horseshoe Lake isochron is about 150 Ma younger. It may be possible to suggest an explanation for the difference in isochron ages of the Horseshoe Lake and Apisko Lake granites if a systematic compositional difference between these can be demonstrated.

K_2O contents (Table 4 and 6) for the two bodies are similar: Horseshoe Lake granite 3.4 to 4.4% with a lower value of 1.6% for the one granodiorite sample analyzed; Apisko Lake granite 3.7 to 5.0%, only slightly higher than the Horseshoe Lake values. Rubidium contents (Table 1 and 2) are also similar: Horseshoe Lake granite 70 to 126 ppm; Apisko Lake granite 77 to 114 ppm. However there is a substantial difference in Sr content: Horseshoe Lake granite 71 to 376 ppm (excluding the low strontium border phase samples 9 and 10); Apisko Lake granite 240 to 386 ppm. The higher Rb/Sr samples of the Horseshoe Lake granite which were shown previously to have the effect of lowering the isochron age, are also the samples with the lower strontium levels.

For purposes of comparison one may plot the analytical results for the Horseshoe Lake granite on the previously established Apisko Lake isochron. Three of the Horseshoe Lake granite samples (numbers 1, 2 and 3) have strontium contents within the range of those found for the Apisko Lake granite samples and these three samples also plot with an excellent fit on the Apisko Lake granite isochron. However the remaining five Horseshoe Lake granite samples, fall below the Apisko Lake granite isochron.

One may interpret these systematics as suggesting that the Horseshoe Lake granite is of the same Rb-Sr age and initial $^{87}Sr/^{86}Sr$ as the Apisko Lake granite but that more

recently the Horseshoe Lake granite samples with the lower strontium contents were significantly modified. This modification might have taken the form of secondary growth of microcline at a time close to the ca. 2500 Ma K-Ar biotite ages found in both granites. If this was the case, more than half of the strontium seen in Horseshoe Lake granite samples 7 and 8 would be of such a secondary origin. If a comparable amount of strontium had also been added to the other Horseshoe Lake granite samples, this could constitute 10 to 15% of the strontium in samples 1, 2 and 3 and 20 to 30% in samples 4 to 6. One might also extend this hypothesis to the Apisko Lake granite samples where the suggested secondary strontium would comprise some 10 to 15% of the total strontium in each sample. The above proportions (with respect to strontium), for the admixture of a secondary mineral at about 2500 Ma to a rock of primary age 2700 Ma, are sufficient to synthesize the measured Rb-Sr systematics for the two suites of samples.

Conclusions

It is demonstrated that Rb-Sr whole rock isochron ages obtained from homogeneous, massive, meso- to catazonal plutonic rocks may yield ages that are considerably younger than those obtained from U-Pb analyses on coexisting zircon (Horseshoe Lake granite, samples 1 to 8). It is suggested here that the primary age of the Horseshoe Lake and Apisko Lake granites are in the range 2700 to 2765 Ma and that the lower Rb-Sr isochron ages are due to the addition of a secondary component of lower age which particularly affects the systematics of the lower strontium samples. It is further suggested that microcline is the mineral responsible for this effect, which we hope to be able to demonstrate by further analytical work on mineral separates.

References

Ermanovics, I.F.
1970: Geology of Bernes River-Deer Lake map-area, Manitoba and Ontario – and a preliminary analysis of tectonic variation in the area; Geological Survey of Canada, Paper 70-29.

Ermanovics, I.F., McRitchie, W.C., and Houston, W.N.
1979: Petrochemistry and tectonic setting of plutonic rocks of the Superior Province in Manitoba; in Trondhjemites, Dacites and Related Rocks (Ed. F. Barker), Elsevier, Chapter X, p. 323-362.

Krogh, T.E., Ermanovics, I.F., and Davies, G.L.
1974: Two episodes of metamorphism and deformation in the Archean rocks of the Canadian Shield; in Carnegie Institute of Washington Yearbook 73, p. 573-575.

Streckeisen, A.
1975: To each plutonic rock its proper name; Earth-Science Reviews, v. 12, p. 1-33.

Turek, Andrew and Peterman, Zell E.
1971: Advances in the geochronology of the Rice Lake-Beresford Lake area, Southeastern Manitoba; Canadian Journal of Earth Sciences, v. 8, p. 572.

Wanless, R.K., Stevens, R.D., Lachance, G.R., and Delabio, R.N.
1973: Age determinations and geological studies, K-Ar isotopic ages, Report 11; Geological Survey of Canada, Paper 73-2.

10. Rb-Sr AGE OF THE RICE RIVER GNEISS, HECLA-CARROLL MAP AREA, MANITOBA AND ONTARIO

Isochron Age = 2674 ± 140 Ma
$^{87}Sr/^{86}Sr$ initial = 0.7010 ± 0.0006

The results of isotopic analyses on seven whole rock samples from the Rice River gneiss are presented in Table 1 and depicted on an isochron diagram in Figure 1. Six of seven sample points are collinear yielding an apparent isochron of age 2674 ± 140 Ma, $^{87}Sr/^{86}Sr$ initial 0.7010 ± 0.0006 and MSWD 0.84. Sample number 7 which falls considerably below the isochron formed by the other six points is thought by Ermanovics possibly to have been derived from greenstones rather than from the tonalitic orthogneiss that comprises the other six samples.

The age calculated for the six point isochron is strongly controlled by inclusion of sample number six which has an individual age of 2652 Ma when calculated assuming the isochron initial $^{87}Sr/^{86}Sr$ ratio of 0.7010. The high K_2O content of this sample (3.6%, Table 2) is at least a factor of two higher than that of the other six samples analyzed. If this atypical sample is excluded from the calculation of isochron parameters, a new isochron may be determined for samples 1 to 5 of age 2776 ± 287 Ma, initial $^{87}Sr/^{86}Sr$ 0.7009 ± 0.0008 and MSWD 0.89. The correspondence between the high K_2O content and low Rb-Sr age may indicate that the measured Rb-Sr age is a hybrid between the primary age and a younger age associated with the high potassium minerals.

The $^{87}Sr/^{86}Sr$ initial is compatible with direct derivation of these rocks from the mantle but, in light of their low Rb/Sr ratios, does not preclude a period of crustal residence in the order of a few hundred million years.

Geological Setting and Interpretation
by I.F. Ermanovics

Fifteen samples of Rice River gneiss (NTS 62 P, latitude 51°20'30", longitude 96°24'20") were collected over a distance of 400 m (across strike of unit) from islands in Rice River estuary to the first rapids in the river.

The gneiss is part of an assemblage of cataclastic rocks exposed along the shore of Lake Winnipeg, extending for 48 km from Wanipigow River estuary to Loon Straits (map units 7 and 11, Ermanovics, 1970). The rock is a medium grained, granoblastic, cataclastic lineated gneiss of problematical origin and is intercalated with coarse grained, porphyroclastic metatonalite and greenstone. Plagioclases are porphyroclastic and highly poikiloblastic with matrix materials. They lie in a fine grained recrystallized lensoid matrix of quartz, feldspar, minor biotite and chlorite, and 5 to 20 per cent subidioblastic green to pale brown amphibole. Lenticular mosaics of quartz and cigar-shaped pods of amphibole aggregates give the rock a lineated and banded look. The rocks are variably comminuted and recrystallized to give protomylonitic and blastomylonitic fabrics.

Rice River gneiss is a mixture of paragneiss (probably lower Black Island succession) and orthogneiss components. The member under discussion is probably orthogneiss (A. Brown, in preparation; personal communication, 1979) and may be a highly deformed variant of the coarse grained, porphyroclastic tonalite that at Hole River yielded a U-Pb zircon age of 3000 ± 10 Ma (Krogh et al., 1974). This hypothesis is corroborated by the relatively great abundance and similarity of zircons, and bulk chemistry (Ermanovics et al., 1979, Fig. 4) of both porphyroclastic tonalite and Rice River gneiss. Zircons from Rice River gneiss are clouded euhedra with darker metamict(?) cores yielding a U-Pb age of 2900 Ma (Krogh et al., 1974). This is interpreted to represent an updated age from 3000 Ma.

Rice River gneiss is cut by late granodioritic dykes (metamorphosed) whose U-Pb zircon age is 2715 ± 10 Ma (Krogh et al., 1974). The dykes are related to late plutonism in Berens subprovince where a U-Pb zircon age there also indicated ca. 2700 Ma (see preceding paper).

The present Rb-Sr whole rock analysis of Rice River gneiss indicates an isochron age of 2674 ± 140 Ma (regression of analyses 1 to 6). Interpretation of this age is problematical but may reflect a time of lower amphibolite facies metamorphism. Biotite from porphyroclastic metatonalite intercalated with Rice River gneiss gives a K-Ar age of 2430 ± 52 Ma (GSC 78-186, Wanless et al., 1979).

Analysis 7 falls well off the isochron. Inspection of Table 2 shows this sample to be Mg-rich, which is reflected by its 20 per cent mafic content (mainly amphibole). This sample may have been derived from greenstones related to those in the adjacent terrain, rather than from tonalitic orthogneiss.

Analysis 6 contains 3.6 per cent K_2O which is aberrantly large for these gneisses. This particular sample of fine- to medium-grained gneiss contained medium- to coarse-grained white feldspar (perthitic microcline) lenses that were thought to be autochthonous fractions of the gneiss at the time of isotope analysis. It now seems likely, however, that the microcline-rich fractions are allochthonous and related to the 2715 Ma old granodiorite dykes that intrude the gneiss. The high $^{87}Sr/^{86}Sr$ and $^{87}Rb/^{86}Sr$ ratios of sample 6 cause it to act as a 'lever' and unduly influence the slope of the isochron toward a younger age.

In light of the U-Pb zircon data this Rb-Sr whole rock age is likely a mixed age. It is possible that more judicious sampling may produce an age closer to that obtained by U-Pb methods. However, that the age may reflect a time of metamorphism is not precluded since similar whole rock ages are obtained for rocks of the Rice Lake belt 40 km southeast of the present sample site (Turek and Peterman, 1971).

Acknowledgments

I am indebted to A. Davidson and T. Krogh for their help in rationalizing the isotopic results presented here.

From: Rb-Sr and U-Pb Isotopic Age Studies in Current Research, Part C Geol. Surv. Can., Paper 80-1C

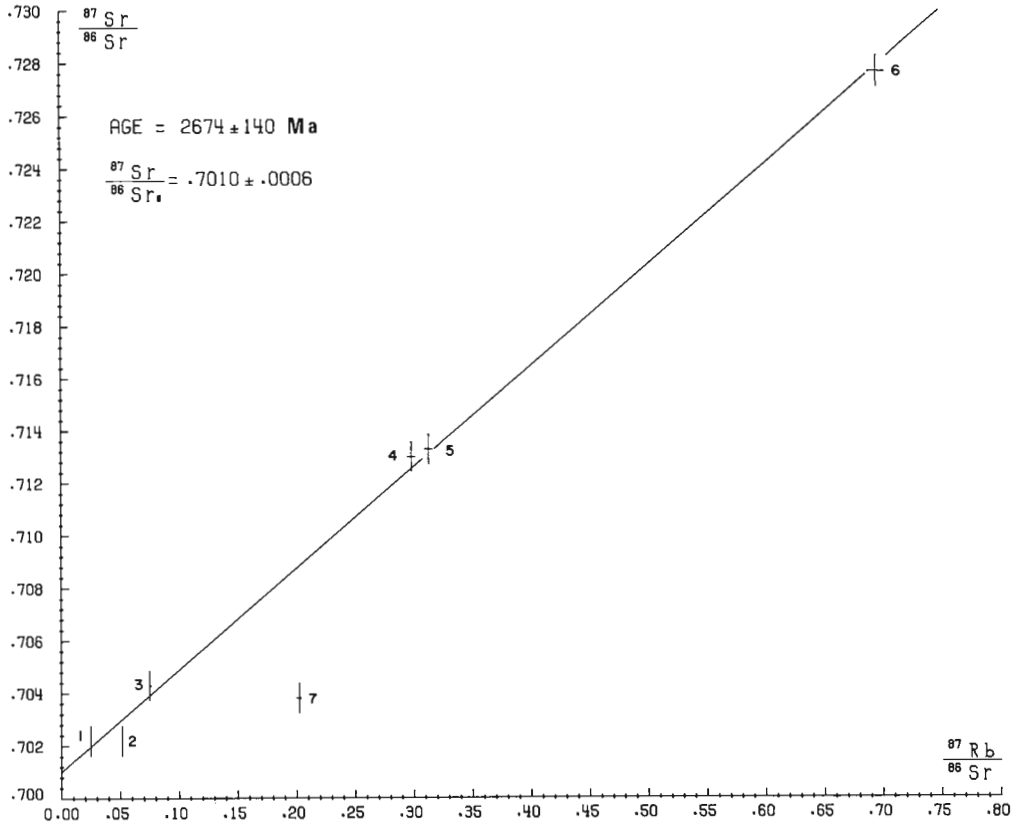

Figure 1. *Rb-Sr isochron Rice River gneiss, Hecla-Carroll map area, Manitoba and Ontario.*

Table 1

Analytical data, whole rock samples, Rice River gneiss, Manitoba and Ontario

Sample No.	Rb ppm	Sr ppm	$^{87}Sr/^{86}Sr$ unspiked	$^{87}Sr/^{86}Sr$ spiked	$^{87}Sr/^{86}Sr$ average	$^{87}Rb/^{86}Sr$
1	2.566	294.8	0.7019	0.7024	0.7022 ± 0.0011	0.0252 ± 0.0005
2	4.233	237.8	0.7021	0.7023	0.7022 ± 0.0011	0.0515 ± 0.0010
3	10.49	404.2	0.7043	0.7042	0.7043 ± 0.0011	0.0751 ± 0.0015
4	41.25	400.5	0.7126	0.7135	0.7130 ± 0.0011	0.2982 ± 0.0060
5	6.654	61.56	0.7138	0.7129	0.7133 ± 0.0011	0.3129 ± 0.0063
6	51.00	212.2	0.7276	0.7279	0.7277 ± 0.0011	0.6958 ± 0.0139
7	10.86	155.4	0.7036	0.7040	0.7038 ± 0.0011	0.2023 ± 0.0040

Table 2

Chemical analyses (wt. %), Rice River gneiss

	Sample No. (this work)						
	1	2	3	4	5	6	7
SiO_2	56.8	66.0	66.9	69.9	67.8	68.7	62.0
Al_2O_3	16.5	15.1	15.0	14.8	14.8	15.8	14.0
TiO_2	0.87	0.46	0.43	0.32	0.50	0.26	0.47
Fe_2O_3	0.61	0.06	0.39	0.19	1.0	nf	0.93
FeO	7.2	5.1	4.5	3.5	2.6	3.4	5.6
MnO	0.12	0.10	0.07	0.06	0.09	0.04	0.10
MgO	4.0	2.5	1.4	1.1	2.0	0.90	6.0
CaO	8.2	5.0	4.4	3.1	4.0	2.1	3.1
Na_2O	3.9	4.3	4.5	5.0	4.3	4.9	2.4
K_2O	0.31	0.34	0.44	1.5	1.7	3.6	1.4
P_2O_5	0.26	0.17	0.16	0.12	0.23	0.07	0.11
CO_2	0.07	nf	0.04	nf	0.27	0.11	nf
H_2O_T	1.3	1.2	1.0	0.80	0.8	0.70	3.1

Table 3

Sample numbers and localities, Rice River gneiss, Manitoba and Ontario

Sample No.		Locality		
This work	Field	Latitude	Longitude	N.T.S.
1	EEB-72-359	51°20'30"	96°24'20"	62 P/8
2	EEB-72-357	51°20'30"	96°24'20"	62 P/8
3	EE-72-148B	51°20'30"	96°24'20"	62 P/8
4	EEB-72-363	51°20'30"	96°24'20"	62 P/8
5	EEB-72-361	51°20'30"	96°24'20"	62 P/8
6	EE-72-144	51°20'30"	96°24'20"	62 P/8
7	EE-72-132	51°20'30"	96°24'20"	62 P/8

References

Ermanovics, I.F.
1970: Precambrian geology of Hecla-Carroll Lake map-area, Manitoba-Ontario; Geological Survey of Canada, Paper 69-42.

Ermanovics, I.F., McRitchie, W.C., and Houston, W.N.
1979: Petrochemistry and tectonic setting of plutonic rocks of the Superior Province in Manitoba; in Trondhjemites, Dacites and Related Rocks (Ed. F. Barker), Elsevier, Chapter X, p. 232-362.

Krogh, T.E., Ermanovics, I.F., and Davies, G.L.
1974: Two episodes of metamorphism and deformation in the Archean rocks of the Canadian Shield; in Carnegie Institute of Washington Yearbook 73, p. 573-575.

Turek, Andrew and Peterman, Zell E.
1971: Advances in the geochronology of the Rice Lake-Beresford Lake area, Southeastern Manitoba; Canadian Journal of Earth Sciences, v. 8, p. 572.

Wanless, R.K., Stevens, R.D., Lachance, G.R., and Delabio, R.N.
1979: Age determinations and geological studies, K-Ar isotopic ages, Report 14; Geological Survey of Canada, Paper 79-12.

11. TONALITE GNEISSES, WESTERN MELVILLE PENINSULA, DISTRICT OF FRANKLIN

Isochron Age = 2678 ± 112 Ma
$^{87}Sr/^{86}Sr$ initial = 0.7022 ± 0.0012

The isotopic results of six of the ten samples analyzed define an isochron giving an age of 2678 ± 112 Ma, initial $^{87}Sr/^{86}Sr$ ratio 0.7022 ± 0.0012, and MSWD 2.02. The remaining four analytical points fall considerably below this isochron and show no colinearities amongst themselves. The analytical results are displayed in an isochron diagram, Figure 1, and listed in Table 1. Figure 2 is an enlarged isochron diagram showing the points which define the isochron in greater detail.

The $^{87}Sr/^{86}Sr$ initial ratio of 0.7022 ± 0.0012 is in satisfactory agreement with ratios ascribed to the mantle at that age, indicating a deep crustal or mantle source.

Geological Setting and Interpretation
by T. Frisch

The samples analyzed come from a major map unit of relatively restricted occurrence north of Folster Lake in the Prince Albert Hills, an area within the Committee Fold Belt (Jackson and Taylor, 1972; Frisch, in press) of the Churchill Structural Province. The unit comprises grey tonalite gneisses with included amphibolite bodies, most of which are metadykes. Typically, the gneisses are composed of plagioclase (An_{25-29}), quartz, brown biotite and muscovite. Green hornblende, potassium feldspar, chlorite and epidote are minor constituents. Foliation is commonly poorly developed but is enhanced in zones of strong deformation. In such zones, where the rocks are cataclastic, epidote and chlorite are locally abundant, probably as a result of retrograde metamorphism. Under the microscope, many of the gneisses show a pronounced primary texture that is thought to be igenous: well-formed plagioclase laths, which may be zoned, are set in a finer grained matrix. Where deformation has been especially intense this texture is less obvious or even absent.

The amphibolite bodies show clear relict intrusive features, such as discordant contacts with gneiss and margins much finer grained than centres.

Chemically, the gneisses resemble the low-Al_2O_3 trondhjemites of Barker and Arth (1976) in that they have Al_2O_3 generally less than 15 per cent, low Rb (with one exception, less than 100 ppm) and low Sr (less than 300 ppm) and are associated with mafic magma (the metadykes), though this association may, of course, be fortuitous. Trends suggestive of magmatic differentiation of the tonalite are shown by plots of Sr-Ba, Ti-Zr and Rb-Sr and in the normative Q-Ab-Or diagram.

Further evidence that the gneisses are of igneous origin is provided by intrusive contacts with the Prince Albert Group of metasedimentary and metavolcanic rocks (Fig. 3). Xenoliths of mafic metavolcanic rocks are common in the tonalites near the contact with the Prince Albert Group and at one locality, tonalite has intruded acid metavolcanics and produced a hybrid rock with partially digested fragments of metavolcanic rock.

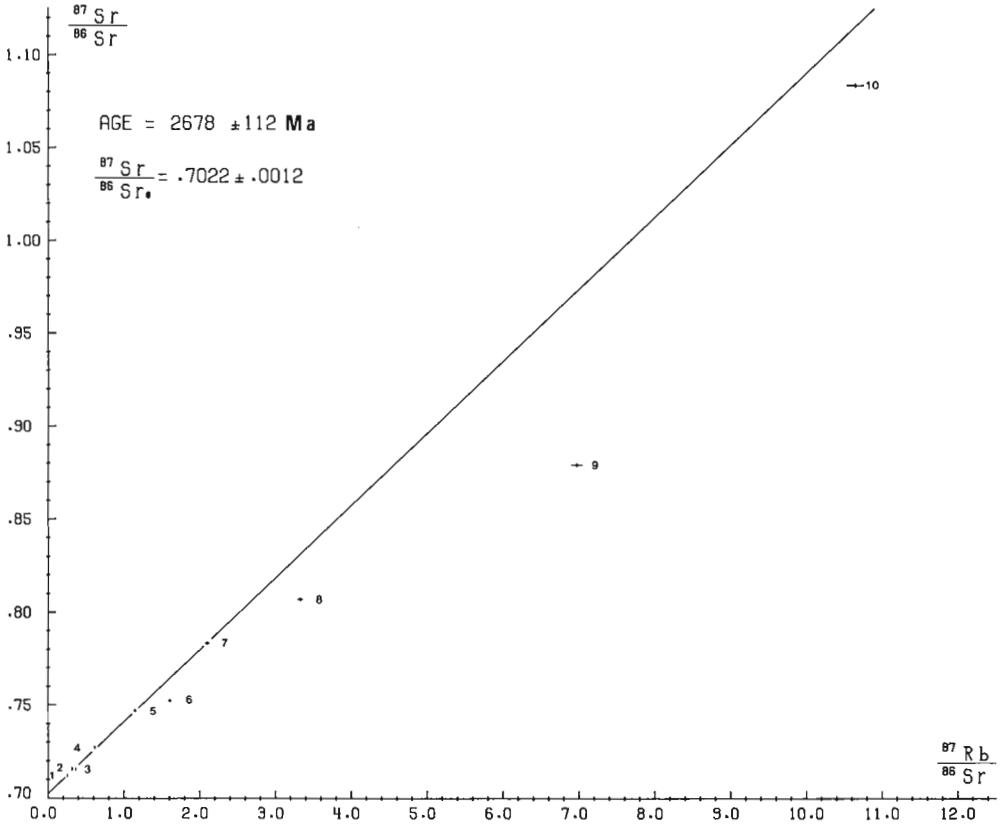

Figure 1. *Rb-Sr isochron, tonalite gneisses, Western Melville Peninsula.*

From: Rb-Sr and U-Pb Isotopic Age Studies in Current Research, Part C Geol. Surv. Can., Paper 80-1C

Table 1

Analytical data, whole rock samples, tonalite gneisses, Western Melville Peninsula

Sample No.	Rb ppm	Sr ppm	$^{87}Sr/^{86}Sr$ unspiked	$^{87}Sr/^{86}Sr$ spiked	$^{87}Sr/^{86}Sr$ average	$^{87}Rb/^{86}Sr$
1	22.99	258.6	0.7119	0.7117	0.7118 ± 0.0011	0.2572 ± 0.0051
2	18.15	164.8	0.7156	0.7154	0.7155 ± 0.0011	0.3186 ± 0.0064
3	29.74	234.6	0.7150	0.7157	0.7153 ± 0.0011	0.3667 ± 0.0073
4	35.75	166.9	0.7277	0.7268	0.7273 ± 0.0012	0.6196 ± 0.0124
5	57.88	145.8	0.7470	0.7465	0.7468 ± 0.0012	1.148 ± 0.023
6	74.74	134.6	0.7521	0.7526	0.7523 ± 0.0012	1.606 ± 0.032
7	45.33	62.37	0.7823	0.7842	0.7833 ± 0.0013	2.102 ± 0.042
8	108.5	94.37	0.8065	* 0.8071	0.8069 ± 0.0013	3.326 ± 0.067
9	59.33	* 24.62		* 0.8790	0.8790 ± 0.0014	6.971 ± 0.139
10	78.46	* 21.32		* 1.0832	1.0832 ± 0.0022	10.65 ± 0.21

*Average of two determinations

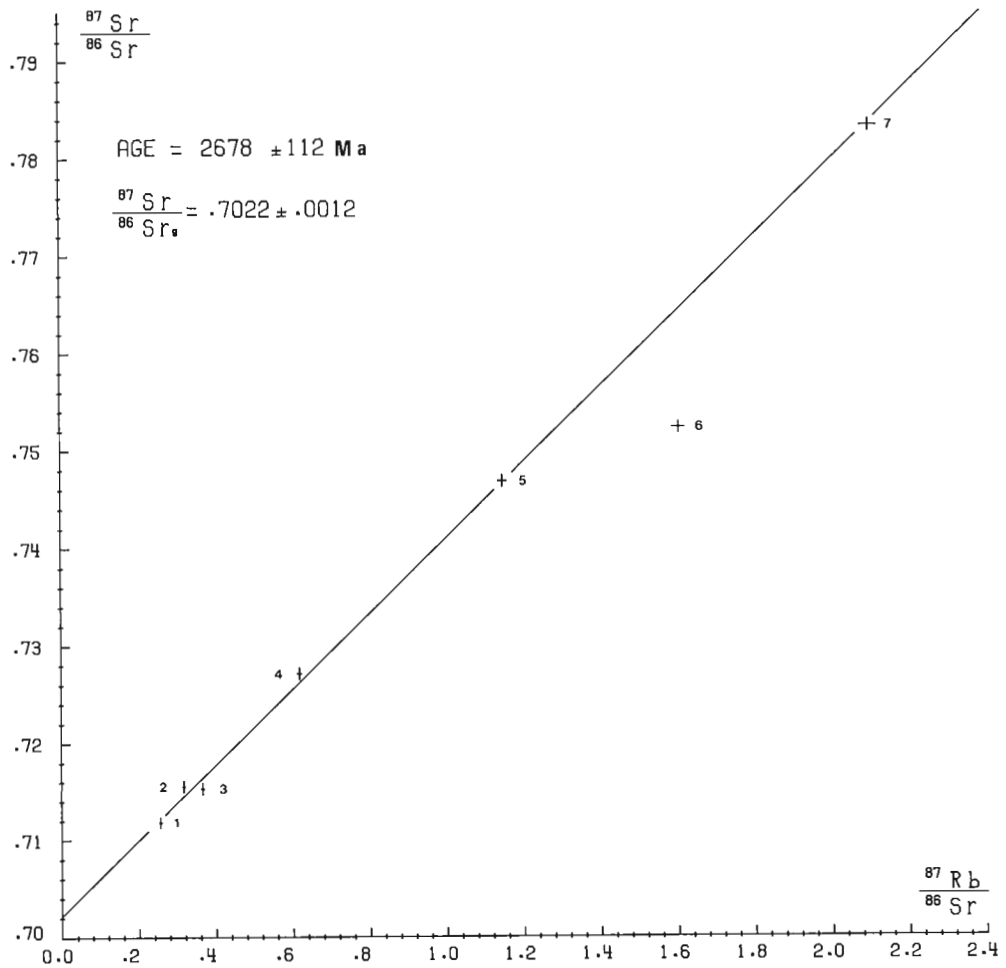

Figure 2. *Enlarged Rb-Sr isochron drawing, tonalite gneisses, Western Melville Peninsula.*

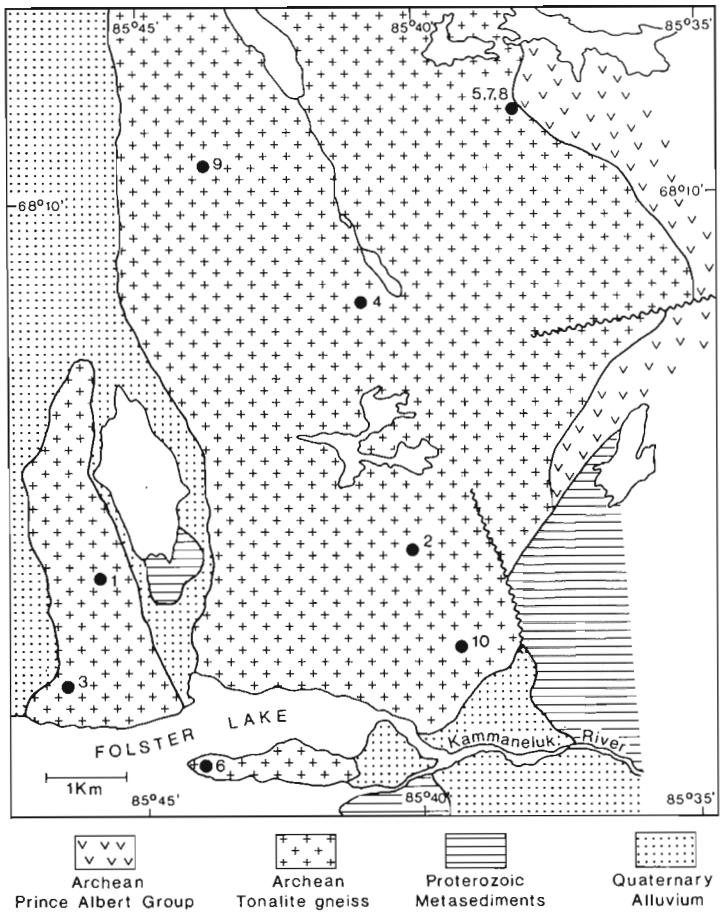

Figure 3. Geological setting and sample locations, tonalite gneisses, Western Melville Peninsula.

Table 2

Sample numbers and localities, tonalite gneisses, Western Melville Peninsula

Sample No. This work	Sample No. Field	Locality Latitude	Longitude	N.T.S.
1	FS-73-23	68°07'27"	85°45'48"	47 B/2
2	FS-73-126	68°07'37"	85°40'08"	47 B/2
3	FS-73-21	68°06'44"	85°46'26"	47 B/2
4	FS-73-127	68°09'18"	85°41'00"	47 B/2
5	FS-73-120	68°10'35"	85°38'12"	47 B/2
6	FS-73-125	68°06'11"	85°43'58"	47 B/2
7	FS-73-121	68°10'35"	85°38'12"	47 B/2
8	FS-73-122	68°10'35"	85°38'12"	47 B/2
9	FS-73-128	68°10'14"	85°43'50"	47 B/2
10	FS-73-19	68°06'57"	85°39'16"	47 B/2

The tonalite and mafic dykes and the Prince Albert Group were all metamorphosed in the amphibolite facies in Aphebian time or earlier. Granitic "back-veining" of the dykes indicates that the tonalites were remobilized possibly during the metamorphism or subsequently.

Ten samples of tonalitic gneiss were anlayzed in this study. All are superficially similar in lithology and chemistry but the samples vary in degree of cataclastic deformation and in Rb and Sr content. Samples 1 to 5 and 7 define an isochron giving an age of 2678 ± 112 Ma and an initial ratio of 0.7022 ± 0.0012. The low initial ratio is consistent with an igneous origin of the tonalite gneisses from a deep crustal source or the mantle. Samples 6, 8, 9, and 10 deviate markedly from the isochron but for no reason that is obvious. Three of these samples have heavily sericitized plagioclase and the fourth is cataclastic but these features are also well shown by samples 3 and 7, which are on, or close to, the isochron. Resetting of Rb-Sr systems seems to be a common feature of the more Rb-rich metamorphic rocks.

There are two possible interpretations of the isochron age: the age is that of (1) emplacement of the igneous protolith of the gneisses or (2) the metamorphism that produced the gneisses.

Massive K-feldspar-rich granitic rocks south and north of Folster Lake have a U/Pb concordia intercept age (measured on zircon) of 2706 Ma (Frisch, in press). This, combined with the Rb-Sr age reported here, suggests that a major igneous event occurred about 2700 Ma ago. The Prince Albert Group, which both the tonalite gneiss and the K-feldspathic granitic rock intruded, is known to be at least 2879 Ma old (Frisch op. cit.). All U/Pb and Rb/Sr age determinations in western Melville Peninsula have yielded Archean or earliest Aphebian minimum ages, so it seems likely that the major metamorphic and igneous events in this region took place in the Archean. Which type of event is dated in this particular study is not clear. However, the low initial $^{87}Sr/^{86}Sr$ ratio suggests a minimal time period between emplacement and metamorphism if it is the latter that is being dated.

References

Barker, F. and Arth, J.G.
1976: Generation of trondhjemitic-tonalitic liquids and Archean bimodal trondhjemite-basalt suites; Geology, v. 5, p. 596-600.

Frisch, T.
Precambrian geology of the Prince Albert Hills, western Melville Peninsula, Northwest Territories; Geological Survey of Canada, Bulletin. (in press)

Jackson, G.D. and Taylor, F.C.
1972: Correlation of major Aphebian rock units in the northeastern Canadian Shield; Canadian Journal of Earth Sciences, v. 9, p. 1650-1669.

12. ISOCHRON AGE OF A RE-METAMORPHOSED META-ULTRABASIC INCLUSION OF PRINCE ALBERT GROUP IN WALKER LAKE GNEISS COMPLEX, CENTRAL KEEWATIN

Isochron Age = 1679 ± 26 Ma
$^{87}Sr/^{86}Sr$ initial = 0.8260 ± 0.0697

The isotopic results obtained for four samples are given in Table 1 and plotted in Figure 1 and define an isochron of age 1679 ± 26 Ma, initial $^{87}Sr/^{86}Sr$ ratio of 0.8260 ± 0.0697 and low MSWD of 1.02. Strontium concentrations in the four samples are all very low; less than 1 ppm. The concomitant high $^{87}Rb/^{86}Sr$ ratios are associated with relatively high $^{87}Sr/^{86}Sr$ ratios resulting in the observed large uncertainty in the initial $^{87}Sr/^{86}Sr$ ratio.

Despite this analytical uncertainty, the $^{87}Sr/^{86}Sr$ ratio is sufficiently high to indicate a secondary origin for the rock suite.

Geological Setting and Interpretation
by Mikkel Schau

Samples were selected about one metre apart from each other from a single outcrop in a soapstone locality. At this locality a complex sequence of events has been deduced (Schau, in press). The Prince Albert Group including komatiite has in part been gneissified to form part of the Walker Lake Gneiss Complex. This has been intruded by a diabase dyke yielding K-Ar ages of 1891 ± 120 Ma on hornblende and 1613 ± 48 Ma on whole rock (personal communication, R.K. Wanless, June 1975) which has been subsequently deformed and partly altered by late granites. The samples were taken from a small pod of relict and partly made-over metakomatiite. It is very complex mineralogically and contains large variations in modes of minerals such as phlogopite over very short distances. The isochron is taken to date the metamorphic resetting of the phlogopite. This event is correlated with the emplacement of the latest granite and the deformation and partial recrystallization of the aforementioned metagabbroic dyke.

The isochron age is interpreted as the age of the intrusion of the late red granite and the high initial ratio as an indication that the strontium was homogenized at the time of intrusion following a considerable period in the crust.

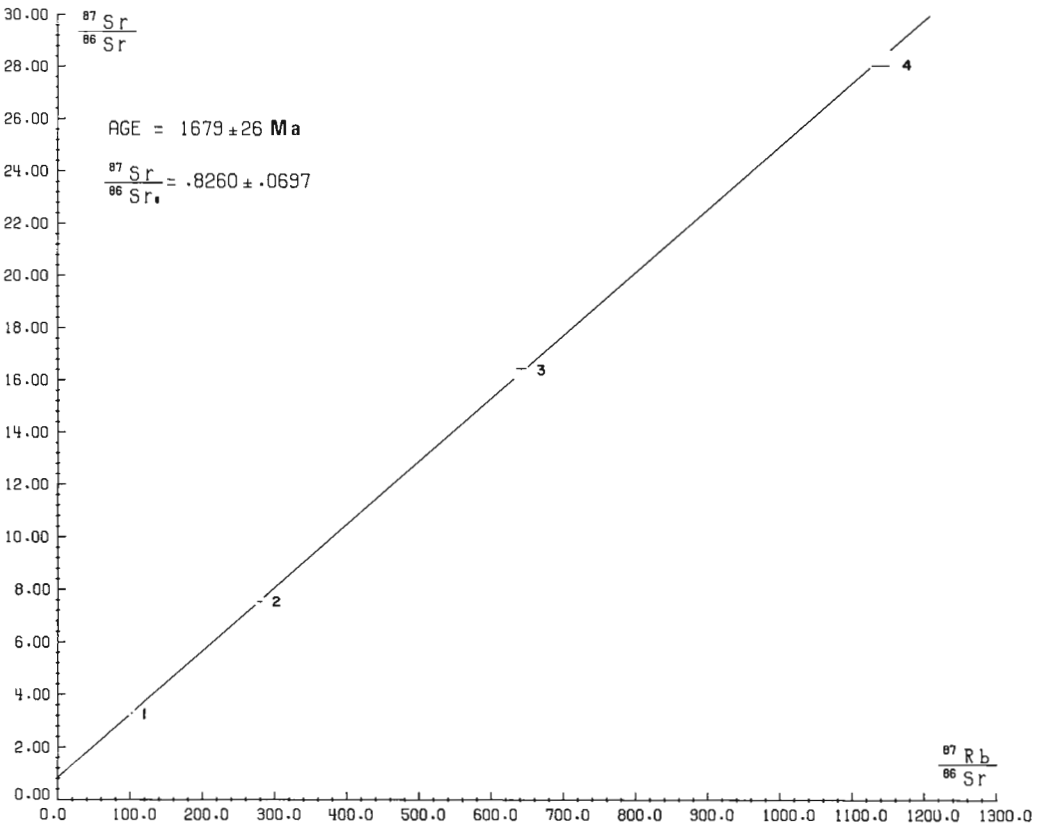

Figure 1. *Rb-Sr isochron, inclusion of Prince Albert Group in Walker Lake Gneiss Complex.*

From: Rb-Sr and U-Pb Isotopic Age Studies in Current Research, Part C Geol. Surv. Can., Paper 80-1C

Table 1

Analytical data, whole rock samples, inclusion of Prince Albert Group in Walker Lake Gneiss Complex

Sample No.	Rb ppm	Sr ppm	$^{87}Sr/^{86}Sr$ spiked	$^{87}Rb/^{86}Sr$
1	20.59	0.5812	3.2968 ± 0.0049	102.4 ± 2.1
2	51.81	0.5372	7.539 ± 0.011	278.8 ± 5.6
3	100.2	0.4520	16.463 ± 0.025	640.9 ± 12.8
4	193.4	0.4904	28.099 ± 0.042	1140.2 ± 22.8

Table 2

Sample numbers and localities, inclusion of Prince Albert Group in Walker Lake Gneiss Complex

Sample No.			Locality		
This work	Field	Rock Type	Latitude	Longitude	N.T.S.
1	*197 SMA 0010	Phlogopite meta-komatiite	66°46'12"N	91°52'55"W	56 J/13
2	198 SMA 0010	(talc-olivine-serpentine	66°46'12"N	91°52'55"W	56 J/13
3	199 SMA 0010	chlorite-phlogopite rock)	66°46'12"N	91°52'55"W	56 J/13
4	200 SMA 0010		66°46'12"N	91°52'55"W	56 J/13

*See Schau (1975, Table 5) (197=28, 198=27, 199=26, 200=25) for chemical analyses of specimens.

References

Schau, Mikkel

1975: Komatiitic and other ultramafic rocks of the Prince Albert Group, Hayes River Region, N.W.T.; in Report of Activities, Part A, Geological Survey of Canada, Paper 75-1A, p. 359-361.

Schau, Mikkel (cont.)

Geology of the Prince Albert Group in parts of Walker Lake and Laughland Lake map areas; Geological Survey of Canada, Bulletin No. 337. (in press)

13. Rb-Sr AGE OF THE LINEAMENT LAKE GRANODIORITE, DISTRICT OF MACKENZIE

Isochron Age = 2472 ± 31 Ma
$^{87}Sr/^{86}Sr$ initial = 0.7036 ± 0.0014

The results of isotopic analyses on 12 whole rock samples ranging in composition from diorite to granodiorite are given in Table 1 and depicted in an isochron diagram in Figure 1. Eleven sample points are collinear defining an isochron of age 2472 ± 31 Ma. initial $^{87}Sr/^{86}Sr$ 0.7036 ± 0.0014 and MSWD 1.37. Samples from four localities in three rock units all fall on the isochron within experimental error except for sample number 8. one of three samples analyzed from the foliated granodiorite/tonalite/diorite unit (Fig. 2).

The analytical project was undertaken in the following manner: five samples from sample location I were analyzed and an isochron of age 2479 ± 52 Ma. initial $^{87}Sr/^{86}Sr$ 0.7033 ± 0.0019 and MSWD 1.75 was established (note that these isochron parameters are very similar to those of the eleven point isochron). Pairs of samples from the three other sample locations were then analyzed and it was established that each of the resultant sample points fell on the original five point isochron except for sample number 8 from location II which fell below the line. However a satisfactory fit to the isochron was obtained from the results of analysis of a third sample from location II (in addition to one of the original pair).

We conclude from these results that we are unable to discriminate between the times of emplacement of these three bodies using the Rb-Sr whole rock approach and that the best age for the bodies sampled is the combined eleven point isochron age previously detailed. The results on sample number 8 document at least one location where the isotopic system has been disturbed.

The initial $^{87}Sr/^{86}Sr$ ratio is a little higher than commonly found for rocks of this age derived from the mantle and may indicate a short period of crustal residence.

Geological, Geochemical Setting and Interpretation
by E.M. Cameron

In 1972 a reconnaissance lake sediment geochemical survey was carried out over 93 000 km^2 of the Bear and Slave Structural Provinces. Uranium was found to be much more abundant in the Proterozoic terrane of the Bear Province compared to the Archean of the Slave (Cameron and Allan, 1973). However, within the Slave Province two strong and extensive uranium anomalies were found (Allan and Cameron, 1973). The most prominent of these is located in granitic terrane near the eastern margin of the Slave Province. It has been referred to as the Lineament Lake anomaly (Cameron and Durham, 1974). The other anomaly is also within a granitic area, near Yamba Lake in the central part of the Province (Folinsbee, 1949; Bostock, 1966).

Follow-up surveys were carried out on the Lineament Lake anomaly in 1973 and 1974 (Cameron and Durham, 1974; Dyck and Cameron, 1975). The anomalous nature of the area, originally defined by lake sediment reconnaissance, was confirmed by more detailed surveys, including uranium in water, radon in water, airborne gamma ray spectrometry and ground radiometry. No mineralization of possible economic interest was identified. The anomaly was ascribed to granitic rocks that contain a greater than average quantity of labile uranium.

It has been frequently observed that within Archean terrane there is an evolutionary cycle from sodic to potassic granites (Viljoen and Viljoen, 1969; Green and Baadsgaard, 1971). The potassic, more radioactive granites therefore tend to be the youngest in terranes of this age. The granites

Table 1

Analytical data, whole rock samples, Lineament Lake granodiorite

Sample No.	Rb ppm	Sr ppm	$^{87}Sr/^{86}Sr$ unspiked	$^{87}Sr/^{86}Sr$ spiked	$^{87}Sr/^{86}Sr$ average	$^{87}Rb/^{86}Sr$
1	127.7	*485.1	0.7295	0.7299	0.7297 ± 0.0012	0.7616 ± 0.0152
2	134.3	261.9	0.7583	0.7574	0.7578 ± 0.0012	1.483 ± 0.030
3	154.5	281.4		0.7611	0.7611 ± 0.0012	1.588 ± 0.032
4	157.9	*111.5	0.8510	* 0.8513	0.8512 ± 0.0014	4.083 ± 0.082
5	150.7	103.0		0.8523	0.8523 ± 0.0014	4.232 ± 0.085
6	244.0	136.3		0.8864	0.8864 ± 0.0014	5.178 ± 0.104
7	197.0	107.6	0.8953	0.8958	0.8956 ± 0.0014	5.296 ± 0.106
8	183.7	* 83.97	0.9173	* 0.9171	0.9172 ± 0.0015	6.328 ± 0.127
9	275.6	* 89.11		* 1.0267	1.0267 ± 0.0016	8.946 ± 0.179
10	294.5	82.57		1.0728	1.0728 ± 0.0017	10.317 ± 0.206
11	376.6	55.26		1.4034	1.4034 ± 0.0022	19.71 ± 0.39
12	415.4	53.26		1.5002	1.5002 ± 0.0024	22.56 ± 0.45

*Average of two determinations

From: *Rb-Sr and U-Pb Isotopic Age Studies in Current Research, Part C*
Geol. Surv. Can., Paper 80-1C

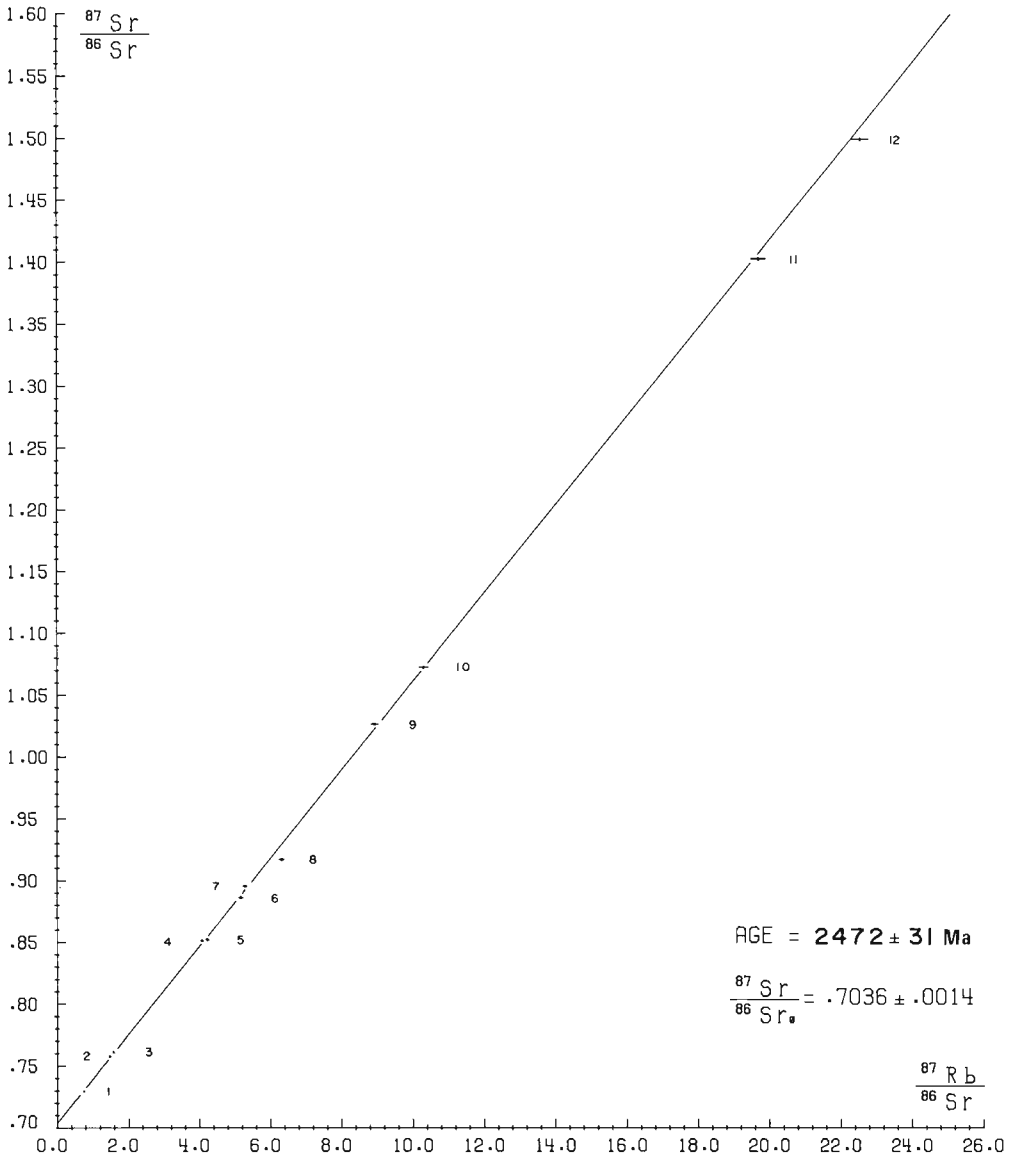

Figure 1. *Rb-Sr isochron Lineament Lake granodiorite, District of Mackenzie.*

of the Lineament Lake area, sampled in 1973, were submitted for geochronological studies because they possibly represent one of the youngest intrusive events within the Slave Province.

Until recently the only available geological map for this area was the 1:1 million map of Wright (1967). This showed the Lineament Lake area as part of a large region underlain by undivided granitic rocks. A preliminary map, based on 1:250 000 mapping, has recently been published by Henderson and Thompson (1980). They have mapped a number of intrusive bodies within the area. It is pertinent to quote part of their description of these rocks:

> "The quartz tonalite is a massive to locally weakly foliated, grey, coarse grained, biotite-rich pluton which is quite homogeneous throughout most of its outcrop area. It is characterized by abundant coarse masses of typically irridescent quartz up to one centimetre or more in size. . . it is intruded by the large granodiorite on its southeastern side, as shown by abundant dykes in the contact area.

"The diorite that occurs east of the quartz-tonalite is a rather heterogeneous massive but more commonly foliated, dark grey, equigranular, medium grained body whose contact with the quartz-tonalite was not observed but which may be gradational. It also is intruded by the granodiorite to the south and is in fault contact with the rocks to the east.

"The granodiorite to the south, which occurs as part of two large circular plutons, is a fairly homogeneous, massive to weakly foliated, commonly buff coloured, equigranular, medium grained, with moderate to low biotite content. It commonly contains muscovite of varied grain size. It contains few inclusions and intrudes all surrounding units.

"To the east is a large unit of undivided granodiorite, tonalite and locally, diorite. These rocks are almost everywhere strongly foliated and locally contain abundant small inclusions of mappable units of Yellowknife rocks. East of (Lineament Lake) the unit consists of a heterogeneous

Table 2

Sample numbers and localities, Lineament Lake area, District of Mackenzie

Sample No.		Locality			
This work	Field	Sample Locality	Latitude	Longitude	N.T.S.
1	CI-73-527	I	64°50'42"N	106°59'42"W	76 B/15
2	CI-73-526	I	64°50'42"N	106°59'42"W	76 B/15
3	CI-73-1109	III	64°49'03"N	106°42'54"W	76 B/15
4	CI-73-1098	II	64°55'21"N	106°42'54"W	76 B/15
5	CI-73-1102	III	64°49'03"N	106°42'54"W	76 B/15
6	CI-73-1523	IV	64°47'01"N	107°08'42"W	76 B/14
7	CI-73-1097	II	64°55'21"N	106°42'54"W	76 B/15
8	CI-73-1100	II	64°55'21"N	106°42'54"W	76 B/15
9	CI-73-531	I	64°50'42"N	106°59'42"W	76 B/15
10	CI-73-530	I	64°50'42"N	106°59'42"W	76 B/15
11	CI-73-1592	IV	64°47'01"N	107°08'42"W	76 B/14
12	CI-73-529	I	64°50'42"N	106°59'42"W	76 B/15

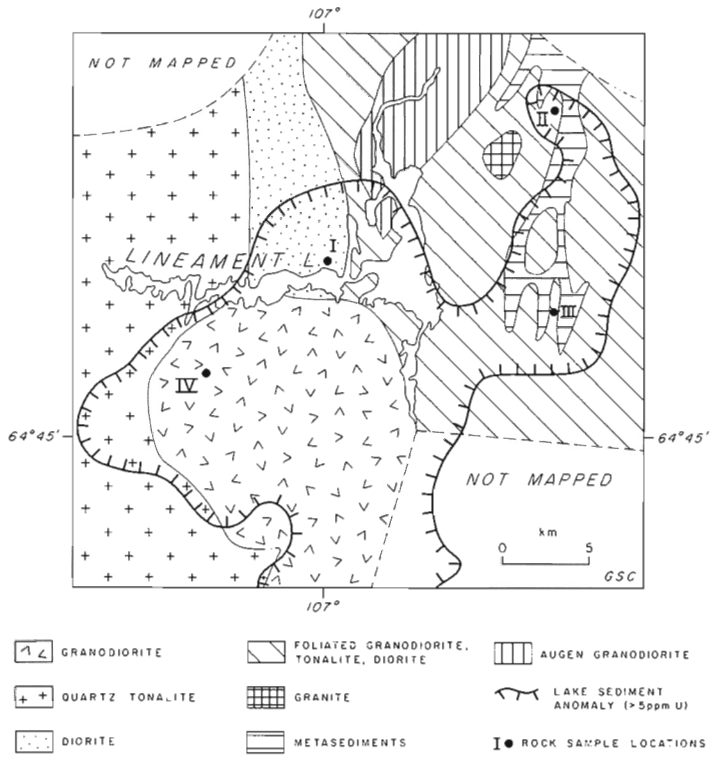

Figure 2. *Sample locations, Lineament Lake. District of Mackenzie. Geology after Henderson and Thompson, 1980.*

assemblage of small deformed inclusion-free plutons with intervening, more foliated, granodioritic rocks with abundant metasedimentary inclusions. The plutons are for the most part white, medium grained, equigranular, mafic moderate to poor granodiorites and tonalites. North of the lake a well foliated, biotite-rich, augen granodiorite body lies within the granodiorite. A single pluton of massive light pink, medium fine grained, mafic-poor granite intrudes the granodiorite."

It is clear from the disposition of the units relative to the uranium anomaly (Fig. 2), that the anomaly is related to the massive granodiorite, which intrudes all surrounding units. The most strongly radioactive portion of the anomaly lies on the northern part of this body. Note that the anomaly is larger in extent than the body as mapped.

It is possible that smaller masses of the uraniferous granodiorite intrude the surrounding units and thus broaden the surficial anomaly. Such masses may be represented in the sample collection from localities I, II, and III that lie outside the mapped limits of the massive granodiorite unit. Dr. P.H. Thomspon has identified granodiorite samples in the collection from locality I in the diorite unit. The undivided granodiorite/tonalite/diorite unit may, in part, be comprised of the uraniferous granodiorite.

Samples 1 to 3 are classified as diorite and the remainder, samples 4 to 12, as granodiorite or a leucocratic phase of the granodiorite pluton. While the massive granodiorite is intrusive into the diorite and other surrounding units, no age difference can be distinguished in the isochron, comprising samples from the four localities. The one exception is sample 8 from locality II which does not fall on the isochron and has been excluded from the computation of the 11 sample, 2472 Ma isochron. The five samples collected at locality I (Table 2) define an isochron of 2479 ± 52 Ma, initial $^{87}Sr/^{86}Sr$ = 0.7033 and MSWD = 1.75.

Acknowledgments

The samples were collected in the company of Chris Durham and George Thomas. Peter Thompson kindly examined thin sections of the samples and related these to the mapped rock units. I am also grateful to John McGlynn for reviewing this interpretation.

References

Allan, R.J. and Cameron, E.M.
1973: Uranium content of lake sediments, Bear-Slave Operation, District of Mackenzie; Geological Survey of Canada, Map 9-1973 (3 sheets).

Bostock, H.H.
1966: Geology of Itchen Lake, District of Mackenzie; Geological Survey of Canada, Map 8-1966.

Cameron, E.M. and Allan, R.J.
1973: Distribution of Uranium in the crust of the Northwestern Canadian Shield as shown by lake-sediment analysis. Journal of Geochemical Exploration, v. 2, p. 237-250.

Cameron, E.M. and Durham, C.C.
1974: Geochemical studies in the eastern part of the Slave Structural Province, 1973. With a contribuiton on the petrology of the volcanic rocks by Mariette Turay; Geological Survey of Canada, Paper 74-27, 22 p., 5 maps.

Dyck, W. and Cameron, E.M.
1975: Surface lake water uranium-radon survey of the Lineament Lake area, District of Mackenzie; in Report of Activities, Part A, Geological Survey of Canada, Paper 75-1A, p. 209-211.

Folinsbee, R.E.
1949; Lac de Gras, District of Mackenzie, Northwest Territories; Geological Survey of Canada, Map 977A.

Green, D.C. and Baadsgaard, H.
1971: Temporal evolution and petrogenesis of an Archean crustal segment at Yellowknife, N.W.T., Canada; Journal of Petrology, v. 12, p. 177-217.

Henderson, J.B. and Thompson, P.H.
1980: The Healey Lake map area (northern part) and the enigmatic Thelon Front, District of Mackenzie; in Current Research, Part A, Geological Survey of Canada, Paper 80-1A, p. 165-169.

Viljoen, M.J. and Viljoen, R.P.
1969: The geochemical evolution of granitic rocks of the Barberton region; in Upper Mantle Project, Geological Society of South Africa, Special Publication 2, p. 189-219.

Wright, G.M.
1967: Geology of the southeastern Barren Grounds; Geological Survey of Canada, Map 1216 A.

14. PENINSULAR SILL, TAKIJUQ LAKE, DISTRICT OF MACKENZIE

Isochron Age = 1816 ± 144 Ma
$^{87}Sr/^{86}Sr$ initial = 0.7079 ± 0.0022

Potassium-argon age determination work on whole rock samples from the Peninsular sill gave inconclusive results which led to this attempt to date the sill by the rubidium-strontium method. Five isotopically analyzed samples define an isochron indicating an age of 1816 ± 144 Ma with an initial $^{87}Sr/^{86}Sr$ ratio of 0.7079 ± 0.0022 and a small MSWD of 0.25. The analytical results are listed in Table 1 and are plotted as an isochron diagram in Figure 1.

The relatively high $^{87}Sr/^{86}Sr$ initial ratio is incompatible with the assumed mantle derivation of these rocks. Attainment of this ratio by minor assimilation of ^{87}Sr-rich country rock material is rendered unlikely by the substantial strontium content, in the order of 200 ppm, of the gabbro; a considerable crustal component would be required to produce the observed initial $^{87}Sr/^{86}Sr$ ratio. As there is no supporting evidence for a major assimilation of crustal material it appears necessary to invoke a more exotic contamination mechanism such as an isotope exchange with the country rock as envisioned by Pankhurst (1969) for the Insch mass of northeast Scotland.

Geological Setting and Interpretation
by J.C. McGlynn

The Peninsular sill intrudes the Recluse Formation of the Epworth Group. Similar sills intrude other units of the Epworth in what Hoffman (in press) defines as Zone 1 – the autochthonous zone – of the northern part of the Wopmay Orogen. The Peninsular sill is over 40 m thick and at observed contacts with Epworth strata dips about 10° to the west. The rock is fine- to medium-grained gabbro comprising pyroxene and basic plagioclase laths, minor quartz, less than 1 per cent biotite, and about 1 per cent iron oxides. Plagioclase is slightly altered to white mica and zoisite, and pyroxene grains are altered slightly to brown hornblende or light-green actinolite and chlorite. Coarser grained phases at the top of the sill contain more biotite, minor quartz, myrmekitic intergrowths and very minor amounts of potash feldspar, suggesting that the sill may be somewhat differentiated. Small angular inclusions of Epworth strata are scattered in a narrow zone along the top of the sill. The sedimentary rocks are recrystallized and contacts with the gabbro are sharp. There is no evidence of large scale assimilation of Epworth material into the gabbroic magma.

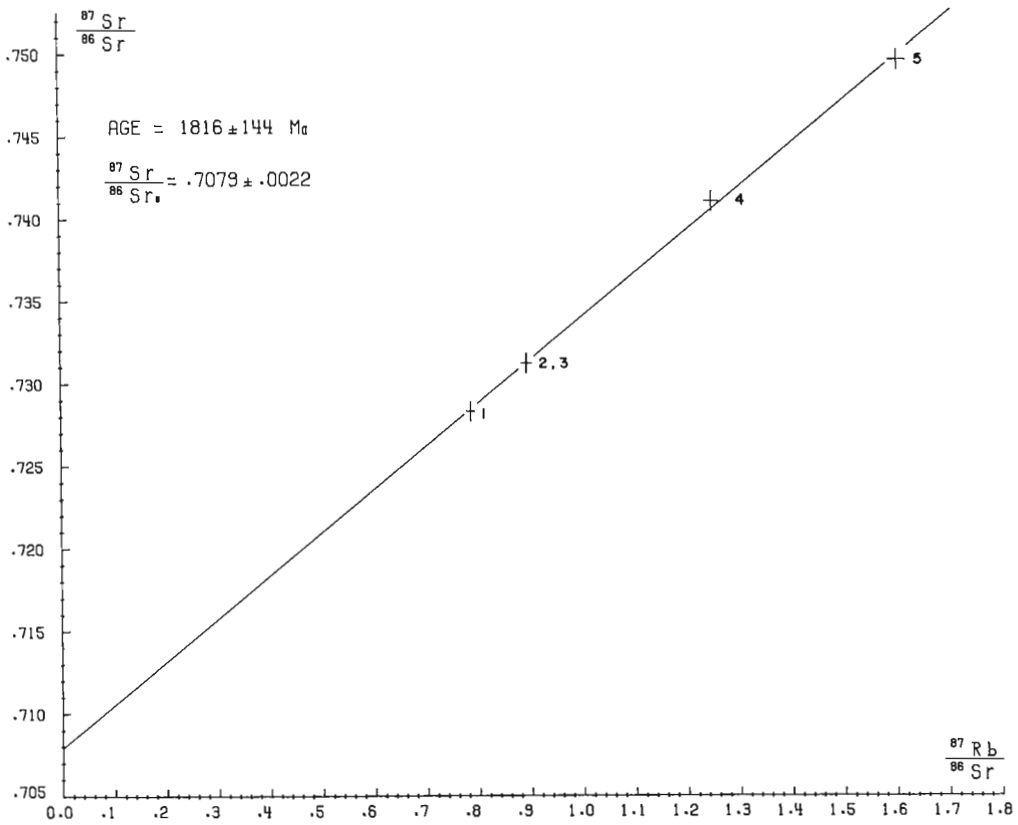

Figure 1. *Rb-Sr isochron, Peninsular sill, Takijuq Lake, District of Mackenzie.*

From: Rb-Sr and U-Pb Isotopic Age Studies in Current Research, Part C Geol. Surv. Can., Paper 80-1C

Table 1

Analytical data, whole rock samples, Peninsular sill, District of Mackenzie

Sample No.	Rb ppm	Sr ppm	$^{87}Sr/^{86}Sr$ unspiked	$^{87}Sr/^{86}Sr$ spiked	$^{87}Sr/^{86}Sr$ average	$^{87}Rb/^{86}Sr$
1	54.85	202.0	*0.7281	0.7286	0.7283 ± 0.0012	0.7855 ± 0.0157
2	63.81	*207.1		*0.7312	0.7312 ± 0.0012	0.8913 ± 0.0178
3	46.83	*151.6		*0.7312	0.7312 ± 0.0012	0.8936 ± 0.0178
4	76.65	*177.7		*0.7410	0.7410 ± 0.0012	1.248 ± 0.025
5	120.8	*217.9	0.7490	*0.7498	0.7495 ± 0.0012	1.604 ± 0.032

*Average of two determinations

Table 2

Sample numbers and localities, Peninsular sill

Sample No. This work	Field	Rock Type	Locality Latitude	Longitude	N.T.S.
1	JC-109	Gabbro	66°13'05"	112°57'55"	86 I/2
2	JC-40	Gabbro	66°05'54"	112°55'30"	86 I/2
3	JC-110	Gabbro	66°15'11"	112°57'48"	86 I/7
4	JC-49	Gabbro	66°21'36"	112°59'24"	86 I/7
5	JC-48	Gabbro	66°20'48"	112°58'00"	86 I/7

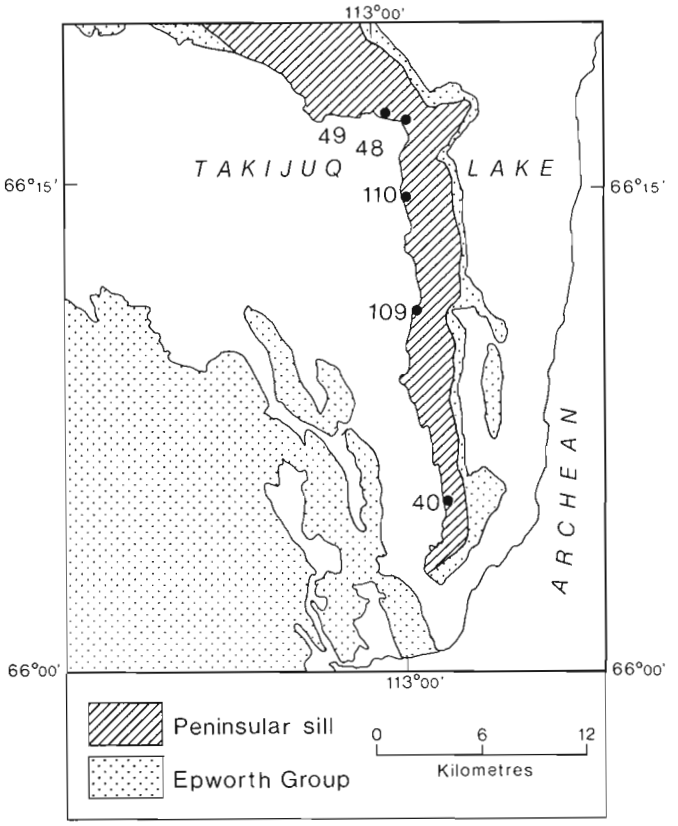

Figure 2. *Sketch map of Peninsular sill, Takijuq Lake and sample locations.*

The five samples analyzed isotopically for the isochron are from the upper part of the sill (Fig. 2). The isochron age is 1816 ± 144 Ma ($\lambda^{87}Rb = 1.42 \times 10^{-11} y^{-1}$). This is a reasonable minimum age of the intrusion. The initial $^{87}Sr/^{86}Sr$ ratio of 0.708 ± 0.002 is high for a gabbro of this age. The expected initial ratio for rocks derived directly from the mantle would be something less than 0.703. The high ratio is suggestive of some process of crustal contamination of the magma.

References

Hoffman, P.F.
Wopmay Orogen: A Wilson Cycle of early Proterozoic age in the northwest of the Canadian Shield: in The continental crust and its mineral deposits, D.W. Strangway (ed.), Geological Association of Canada, Special Paper. (in press)

Pankhurst, R.J.
1969: Strontium isotope studies related to petrogenesis in the Caledonian basic igneous province of NE Scotland; Journal of Petrology, v. 10, pt. 1, p. 115-143.

15. Rb-Sr STUDIES OF THE WILSON ISLAND GROUP, GREAT SLAVE LAKE, DISTRICT OF MACKENZIE

Isochron Age = 1846 ± 24 Ma
$^{87}Sr/^{86}Sr$ initial = 0.7048 ± 0.0008

The results of isotopic analyses on twelve whole rock samples and two mineral separates from the Wilson Island Group volcanics are given in Table 2. Six of these samples, numbers 1, 5, 8, 10 and 11 whole rocks and number 8 biotite were collected by E.W. Reinhardt in 1968; the remainder were collected by R.A. Frith in 1976 from the same volcanic sequence. Localities are listed in Table 3. Data points for the twelve whole rock samples are collinear yielding a Rb-Sr isochron (Fig. 1) of age 1846 ± 24 Ma, $^{87}Sr/^{86}Sr$ initial 0.7048 ± 0.0008 and MSWD 0.99. The biotite concentrate from sample number 8 yields a biotite-whole rock age of 1808 ± 72 Ma (initial $^{87}Sr/^{86}Sr$ 0.7117 ± 0.0070) and the muscovite concentrate from sample number 12 yields a muscovite-whole rock age of 1763 ± 38 Ma (initial $^{87}Sr/^{86}Sr$ = 0.7162 ± 0.0067) in reasonable agreement with its K-Ar age of 1742 ± 44 Ma (GSC 78-138, Wanless et al., 1979).

The initial $^{87}Sr/^{86}Sr$ ratio for the isochron of 0.7048 ± 0.0008 is somewhat higher than would be expected for rocks derived directly from the mantle at that time, indicating a secondary isotopic equilibration.

The isotopic results for six samples of Wilson Island Group sandstone, presented in Table 1, do not form an isochron and are plotted in Figure 3 for comparison with the isochron obtained on the volcanics.

Geological Setting and Interpretation
by R.A. Frith

Wilson Island Group - Volcanics

Eleven samples of volcanic rocks from the Wilson Island Group of rhyolitic to basaltic volcanics were sampled by E.W. Reinhardt in 1968 (R locations, Fig. 2) and by R.A. Frith in 1976 (F locations, Fig. 2). The analyzed samples yield collinear points forming an isochron of age 1846 ± 24 Ma, $^{87}Sr/^{86}Sr$ intercept of 0.7048 and MSWD[1] of 0.99 (Fig. 1). Despite the low initial ratio, widespread low grade regional metamorphism is recognized in the area sampled, manifested by mica grown both in the volcanics and the associated sediments of the group. If the isochron represents an age of metamorphic equilibration, the somewhat lower biotite-whole rock age of 1808 ± 72 Ma for sample number 8 indicates that the metamorphic episode was still in effect at that time. This is supported by a still younger muscovite-whole rock age of 1763 ± 38 Ma from sample number 12.

Wilson Island Group - Sandstones

Six samples of Wilson Island Group sandstone, mostly micaceous quartzites, were collected from the location shown in Figure 2. The results of analyses of these samples are shown in Figure 3 where they fall between the isochron derived from the Wilson Island Group volcanic rocks (above) and a parallel reference line with $^{87}Sr/^{86}Sr$ intercept 0.725. The sandstone results may also be interpreted as a metamorphic equilibration age. If this interpretation is correct, the initial ratios of the samples analyzed would range from 0.705 to 0.725 which is thought to be due to variable, but higher, rubidium content in the sandstones prior to the period of metamorphic equilibration.

Stratigraphic Relationship

The Wilson Island Group of volcanic and sedimentary rocks, as described by Stockwell (1933), Reinhardt (1969) and Hoffman et al. (1977) is the oldest sequence of supracrustal rocks of Proterozoic age in the East Arm of Great Slave

Table 1

Analytical data, whole rock samples, Wilson Island Group sandstone

Sample No.	Rb ppm	Sr ppm	$^{87}Sr/^{86}Sr$ spiked	$^{87}Rb/^{86}Sr$
13	57.57	31.94	0.8621 ± 0.0013	5.211 ± 0.104
14	100.4	45.08	0.8923 ± 0.0013	6.439 ± 0.129
15	195.8	68.40	0.9267 ± 0.0014	8.276 ± 0.165
16	161.9	54.09	0.9461 ± 0.0014	8.653 ± 0.173
17	130.5	32.40	1.0224 ± 0.0015	11.64 ± 0.23
18	258.8	16.61	1.888 ± 0.0028	45.05 ± 0.90

[1] The isotopic data were obtained in two runs with different orders of precision. The MSWD was calculated using the slightly higher error levels associated with the analyses of the Reinhardt samples (Table 1).

From: Rb-Sr and U-Pb Isotopic Age Studies in Current Research, Part C
Geol. Surv. Can., Paper 80-1C

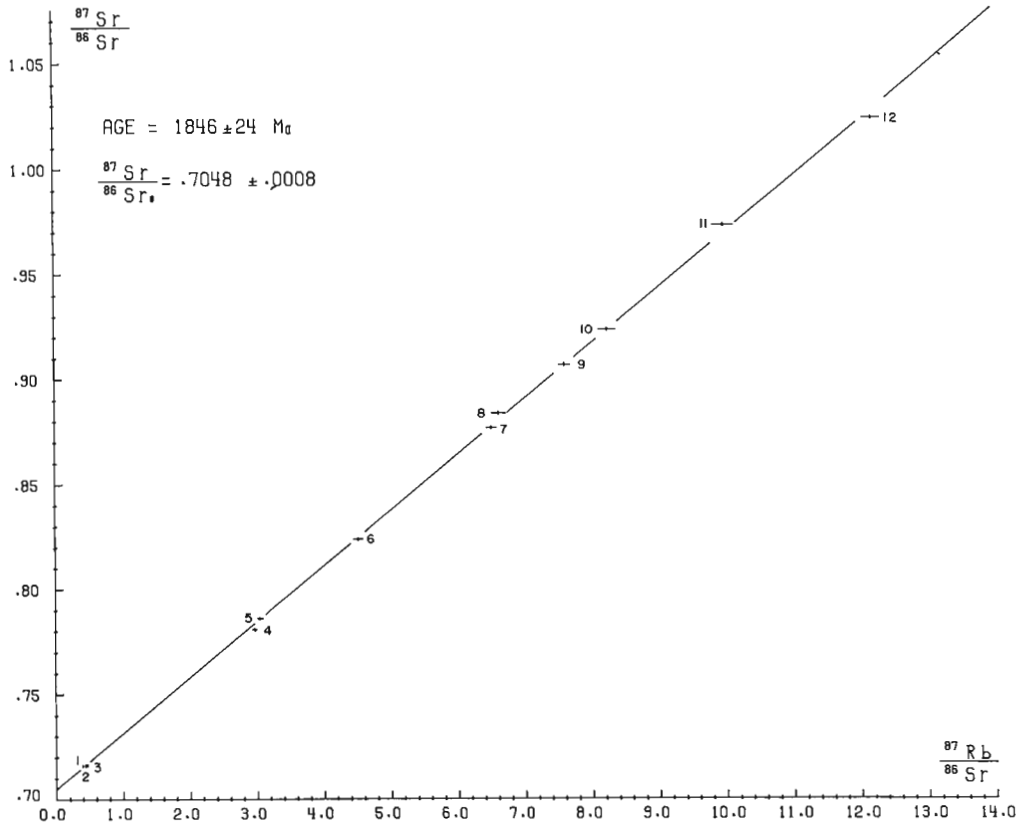

Figure 1. *Rb-Sr isochron Wilson Island Group volcanics, District of Mackenzie.*

Table 2

Analytical data, whole rock samples, Wilson Island Group volcanics

Sample No.		Rb ppm	Sr ppm	$^{87}Sr/^{86}Sr$ unspiked	$^{87}Sr/^{86}Sr$ spiked	$^{87}Sr/^{86}Sr$ average	$^{87}Rb/^{86}Sr$
1		32.38	238.7	0.7160	0.7163	0.7162 ± 0.0011	0.393 ± 0.012
2		65.19	437.7		0.7162	0.7162 ± 0.0004	0.4306 ± 0.0086
3		13.09	81.79		0.7163	0.7163 ± 0.0004	0.4627 ± 0.0093
4		113.3	110.6		0.7808	0.7808 ± 0.0005	2.962 ± 0.059
5		131.2	124.8	0.7867	0.7853	0.7860 ± 0.0013	3.044 ± 0.091
6		234.7	150.6		0.8239	0.8239 ± 0.0005	4.506 ± 0.090
7		228.3	101.6		0.8767	0.8767 ± 0.0005	6.496 ± 0.130
8		142.1	62.24	0.8845	0.8828	0.8836 ± 0.0014	6.610 ± 0.198
9		208.1	79.31		0.9067	0.9067 ± 0.0005	7.586 ± 0.152
10		107.8	37.98	0.9237	0.9233	0.9235 ± 0.0015	8.218 ± 0.247
11		91.50	26.62	0.9720	0.9740	0.9730 ± 0.0016	9.952 ± 0.299
12		157.3	37.42		1.0242	1.0242 ± 0.0006	12.15 ± 0.24
8	biotite	417.5	41.20		1.4738	1.4738 ± 0.0024	29.30 ± 0.88
12	muscovite	486.1	7.487		5.475	5.475 ± 0.008	187.7 ± 3.8

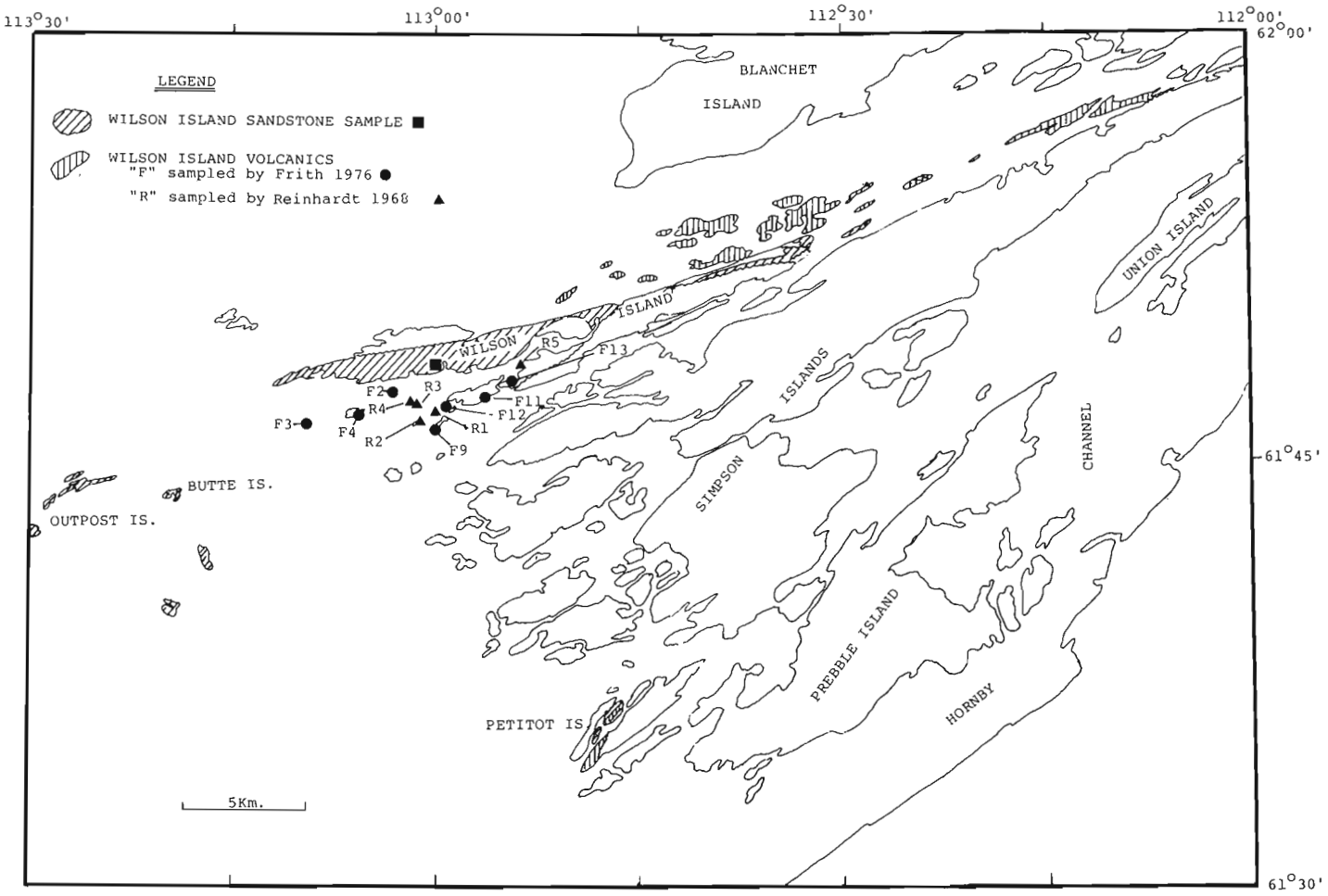

Figure 2. *Location map for samples of Wilson Island Group sandstone and volcanics.*

Table 3

Sample Number and localities, Wilson Island Group volcanics and sandstone, Great Slave Lake, District of Mackenzie

Sample Number			Locality		
This work	Map location	Field	Latitude	Longitude	N.T.S.
Wilson Island Volcanics					
1	R1	RM-470-1825-68	61°46'50"	113°00'00"	86 H/14
2	F13	FY-WIV-13-76	61°47'40"	112°54'20"	86 H/15
3	F11	FY-WIV-11-76	61°46'20"	112°56'20"	86 H/15
4	F9	FY-WIV-9-76	61°46'30"	112°59'40"	86 H/15
5	R2	RM-466-1814-68	61°46'40"	112°58'00"	86 H/15
6	F12	FY-WIV-12-76	61°46'55"	112°59'20"	86 H/15
7	F4	FY-WIV-4-76	61°46'30"	113°06'10"	86 H/14
8	R3	RMG-253-1025-68	61°47'17"	112°59'40"	86 H/15
9	F2	FY-WIV-2-76	61°46'15"	113°03'00"	86 H/14
10	R4	RMG-252B-1023-68	61°47'50"	112°58'50"	86 H/15
11	R5	RM-486-1914-68	61°48'30"	112°53'30"	86 H/15
12	F3	FY-WIV-3-76	61°46'55"	113°09'20"	86 H/14
Wilson Island Sandstones					
13		FY-WIS-10-76	61°48'15"	113°02'15"	86 H/14
14		FY-WIS-3-76	61°48'15"	113°02'15"	86 H/14
15		FY-WIS-7-76	61°48'15"	113°02'15"	86 H/14
16		FY-WIS-4-76	61°48'15"	113°02'15"	86 H/14
17		FY-WIS-1-76	61°48'15"	113°02'15"	86 H/14
18		FY-WIS-11-76	61°48'15"	113°02'15"	86 H/14

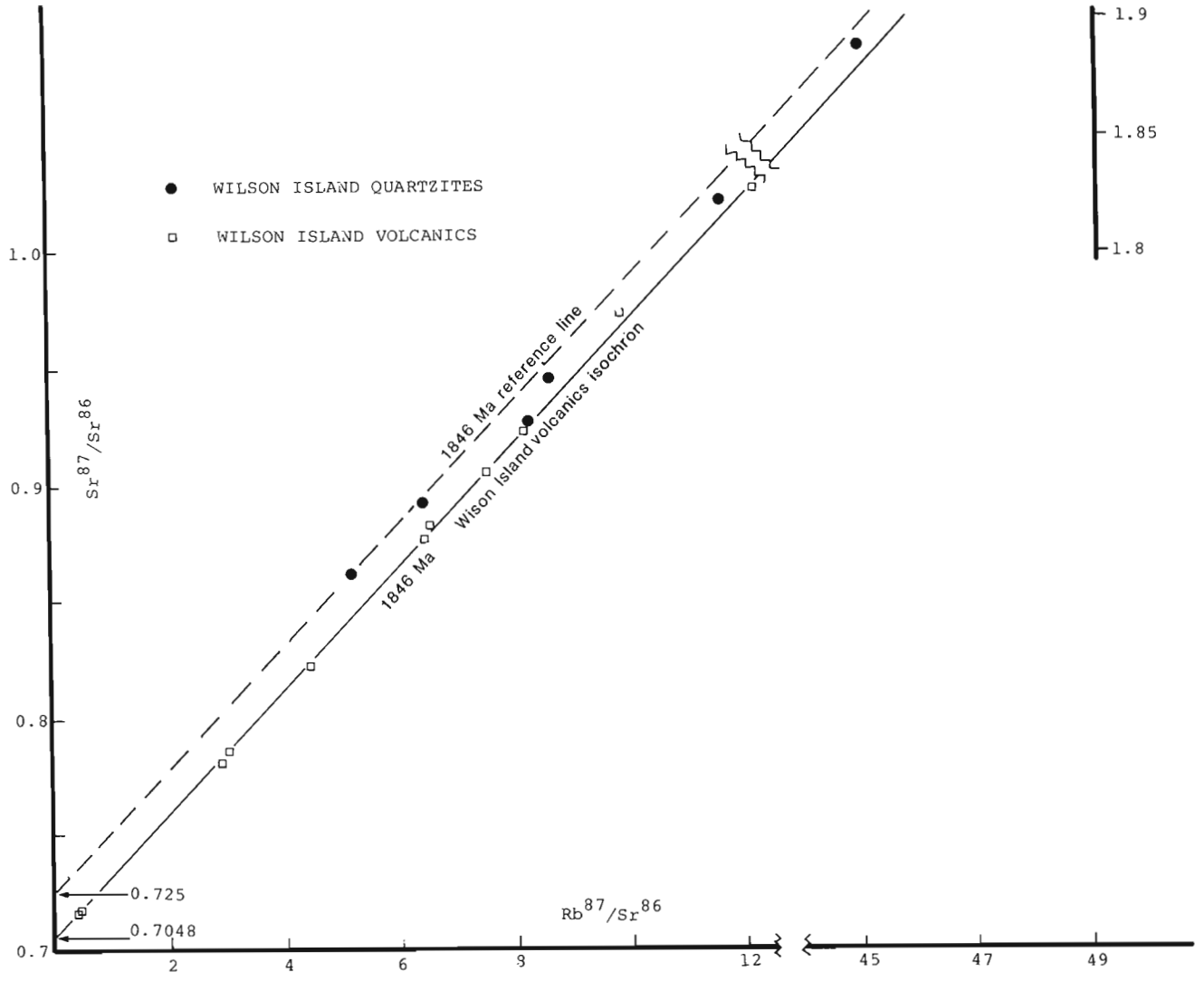

Figure 3. *Rb-Sr isotopic distribution from the Wilson Island quartzites compared with a metamorphic equilibration isochron derived from the Wilson Island volcanics.*

Table 4

Summary of Rb-Sr and K-Ar mineral ages from the Wilson Island Group

Sample No.	Lithology	Method	Age (Ma)	Comment
8 biotite	Wilson Island volcanics	Rb-Sr	1808 ± 72	Age of crystallization
12 muscovite	Muscovite pegmatite in Wilson Island volcanics	Rb-Sr	1763 ± 38	Blocking temperature
*12 muscovite		K-Ar	1742 ± 44	Blocking temperature
*18 muscovite	Wilson Island Sandstone	K-Ar	1775 ± 42	Blocking temperature

*12 Musc. GSC 78-138, 18 Musc. GSC 78-137; Wanless et al., 1979.

Lake. Arkoses and small pebble conglomerates occur in the sedimentary succession, which is interlayered with the volcanics. These locally contain granitoid clasts which may be derived from Archean basement rocks. In one sample location (F2, Fig. 2) chloritic granite-gneiss pebbles form a conspicuous part of a conglomeratic layer within a volcanic pyroclastic succession. The Sosan Group of the Great Slave Supergroup may provide a minimum age as it contains mylonitized pebbles which may be derived from Wilson Island Group quartzite. This mylonitization predates the deposition of the Great Slave Supergroup and probably postdates an early metamorphism of the Wilson Island rocks (Hoffman et al., 1977).

Contact relationships between the Archean basement and the Wilson Island Group are not well understood. Hoffman et al. (1977) considered that the Wilson Island Group is allochthonous, derived by nappe thrusts from the south. This explains the absence of a basal unconformity in the study area.

Discussion

Metamorphic grade is mostly greenschist in the sample region. Muscovite is abundant in the quartzites and biotite is locally present in the volcanic rocks. Pegmatite, which appears to cut the penetrative deformation, contains muscovite of younger age.

Deformation increases southward from the sample area. In the Petitot Islands the Wilson Island Group has been mylonitized, producing rocks similar to mylonitized clasts found in the Sosan (Hoffman et al., 1977).

Near Butte Island, sedimentary rocks have been metamorphosed to upper amphibolite grade, but these rocks have been extensively retrograded (Hoffman, personal communication 1980). If the high grade metamorphism predates the mylonitization of the Wilson Island Group, as Hoffman suggests, then the 1846 Ma isochron may be the same as the age of retrograde metamorphism observed in the high grade metasediments of Butte Island.

The 1846 Ma age defined by the volcanics of the Wilson Island Group has several time-stratigraphic correlatives in the East Arm of Great Slave Lake which include the dioritic laccoliths that intrude both the Great Slave Supergroup and the Blachford Igneous Suite at about 1860 Ma (Davidson, personal communication 1980). Also, K-Ar ages of hornblende and muscovite, derived from the mylonitized rocks of the Simpson Island region (Geological Survey of Canada, unpublished data), indicate a resetting of muscovite about 1855 Ma ago.

However there are several younger mineral ages from the Wilson Island Group (Table 4) that indicate a "tailing off" of metamorphism to about 1750 Ma. The Seton Island Formation volcanic rocks have been dated by the Rb-Sr whole rock technique at 1805 ± 18 Ma (Geological Survey of Canada, unpublished data) and 1832 ± 10 Ma (Baadsgaard et al., 1973) suggesting that the same metamorphism affected some rocks of the Great Slave Supergroup.

References

Baadsgaard, H., Morton, R.D., and Olade, M.A.D.
1973: Rb-Sr Isotopic Age for the Precambrian Lavas of the Seton Formation, East Arm of Great Slave Lake, Northwest Territories; Canadian Journal of Earth Sciences, v. 10, p. 1579-1582.

Hoffman, P.F., Bell, I.R., Hildebrand, R.S., and Thorstad, L.
1977: Geology of the Athapuscow Aulacogen, East Arm of Great Slave Lake, District of Mackenzie; in Report of Activities, Part A, Geological Survey of Canada, Paper 77-1A, p. 117-129.

Reinhardt, E.W.
1969: Geology of the Precambrian rocks of Thubun Lakes map area in relationship to the McDonald Fault System, District of Mackenzie; Geological Survey of Canada, Paper 69-21, p. 29.

Stockwell, C.H.
1933: Great Slave Lake-Coppermine River area, District of Mackenzie; Geological Survey of Canada, Summary Report, 1932, p. 37-63.

Wanless, R.K., Stevens, R.D., Lachance, G.R., and Delabio, R.N.
1979: Age determinations and geological studies, K-Ar isotopic ages, Report 14; Geological Survey of Canada, Paper 79-2.

16. Rb-Sr AGE OF THE COTTERILL LAKE GRANITES, INDIN LAKE AREA, DISTRICT OF MACKENZIE

Isochron Age = 2532 ± 126 Ma
$^{87}Sr/^{86}Sr$ initial = 0.7027 ± 0.0019

Table 1 presents the results of isotopic analyses on ten whole rock samples from the Cotterill Lake granites, which were collected in 1973 from locations shown in Figure 1. Nine of the resultant sample points are collinear and yield a Rb-Sr isochron of age 2532 ± 126 Ma, initial $^{87}Sr/^{86}Sr$ 0.7027 ± 0.0019 and MSWD 1.16, which is shown on an isochron diagram in Figure 2. Sample point number 10 falls somewhat below the line defined by the other nine samples.

Geological Setting and Interpretation
by R.A. Frith

The regional geology of the Indin Lake map area has been described by Fortier (1949), Frith (1973, 1978) and by Frith et al. (1974 and 1977). The Cotterill granites are irregular, megacrystic bodies of granite and granodiorite that intrude 3.25 Ga tonalitic basement (unpublished preliminary U-Pb zircon data, Geochronology Laboratories, Geological Survey of Canada) and migmatites derived from Yellowknife Supergroup rocks (≤ 2.67 Ga, Frith, in preparation).

Similar megacrystic rocks form part of the Basler – Eau Claire plutonic complex that has been dated at 2510 ± 110 ma (McGlynn, 1972). Other nearby anatectic granites of the Meyer Lake complex have been dated at 2473 ± 101 Ma with an initial ratio of 0.711 (Frith et al., 1977). Some undated megacrystic granites intrude the southeastern and northeastern parts of the map area. All of these megacrystic granites contrast with their gneissic to migmatitic host rocks in their massive homogeneous appearance. However, their elongate but irregular shapes and the presence of local augen textures, suggest that like the Basler plutonic and Meyer Lake migmatite complexes, they were intruded during or slightly after the major regional deformation (D_2 of Frith, 1978) and the thermal metamorphic episode that produced large porphyroblasts in the Yellowknife sedimentary rocks (M_2 of Frith, 1978).

The low $^{87}Sr/^{86}Sr$ initial ratio (.7027) of the Cotterill Lake granites, if interpreted according to Faure and Powell (1972) and Moorbath (1975), would indicate a mantle origin or a short crustal residence for these rocks. However, granulite facies metamorphism at Ghost Lake (Robertson, 1974) and the presence of anatectic granites with high $^{87}Sr/^{86}Sr$ ratios, as shown for granites of the Meyer Lake migmatite complex, indicate that anatectic processes were active in the region. Contact relationships of the Cotterill Lake bodies are generally gradational. Megacrysts observed in the bodies, which range from 5-60 per cent of the rock, may also be present in the migmatitic host rocks, as much as 2 km from the granites, suggesting that formation of porphyroblasts of microcline was locally an important rock-forming process.

The preferred origin for the Cotterill Lake granites is similar to that proposed for Archean granitoids by Bridgwater and Fyfe (1974), who recognized three principal types, including: synvolcanic plutons of tonalitic or dioritic composition; metasomatized gneisses and migmatite; and quartz- and potash-rich granite plutons. The Cotterill Lake granites fall in the last category. Bridgwater and Fyfe would have these rocks developed by progressive melting of initial sial from the base of the crust upward. The late potash granitoids would form from the higher levels with less internal heat and intrude only where rheological, partly melted host-rock conditions exist. This mode of formation and intrusion would involve varying degrees of mixing with country rock to form hybrid granites and granodiorites rich in quartz, micas, alkali-feldspar and trace elements such as U, Pb and Rb. On the other hand, Sr would tend to remain behind with Ca locked into plagioclase structures, as suggested by Frith and Currie (1976) and would not overly influence the $^{87}Sr/^{86}Sr$ ratio upward.

Table 1

Analytical data, whole rock samples, Cotterill Lake granites District of Mackenzie

Sample No.	Rb ppm	Sr ppm	$^{87}Sr/^{86}Sr$ unspiked	$^{87}Sr/^{86}Sr$ spiked	$^{87}Sr/^{86}Sr$ average	$^{87}Rb/^{86}Sr$
1	76.26	402.0	0.7233	0.7230	0.7232 ± 0.0012	0.5484 ± 0.0110
2	140.9	476.2	0.7337	0.7327	0.7332 ± 0.0012	0.8554 ± 0.0171
3	135.2	454.8		0.7344	0.7344 ± 0.0012	0.8594 ± 0.0172
4	135.2	394.4		0.7377	0.7377 ± 0.0012	0.9911 ± 0.0198
5	143.6	384.8		0.7429	0.7429 ± 0.0012	1.079 ± 0.022
6	138.9	340.1		0.7459	0.7459 ± 0.0012	1.181 ± 0.024
7	130.2	316.9	0.7472	0.7470	0.7471 ± 0.0012	1.188 ± 0.024
8	166.6	*331.3	0.7562	*0.7553	0.7556 ± 0.0012	1.453 ± 0.029
9	146.5	281.9		0.7577	0.7577 ± 0.0012	1.502 ± 0.030
10	*134.8	*247.5		*0.7561	0.7561 ± 0.0012	1.575 ± 0.032

*Average of two determinations

From: Rb-Sr and U-Pb Isotopic Age Studies in Current Research, Part C Geol. Surv. Can., Paper 80-1C

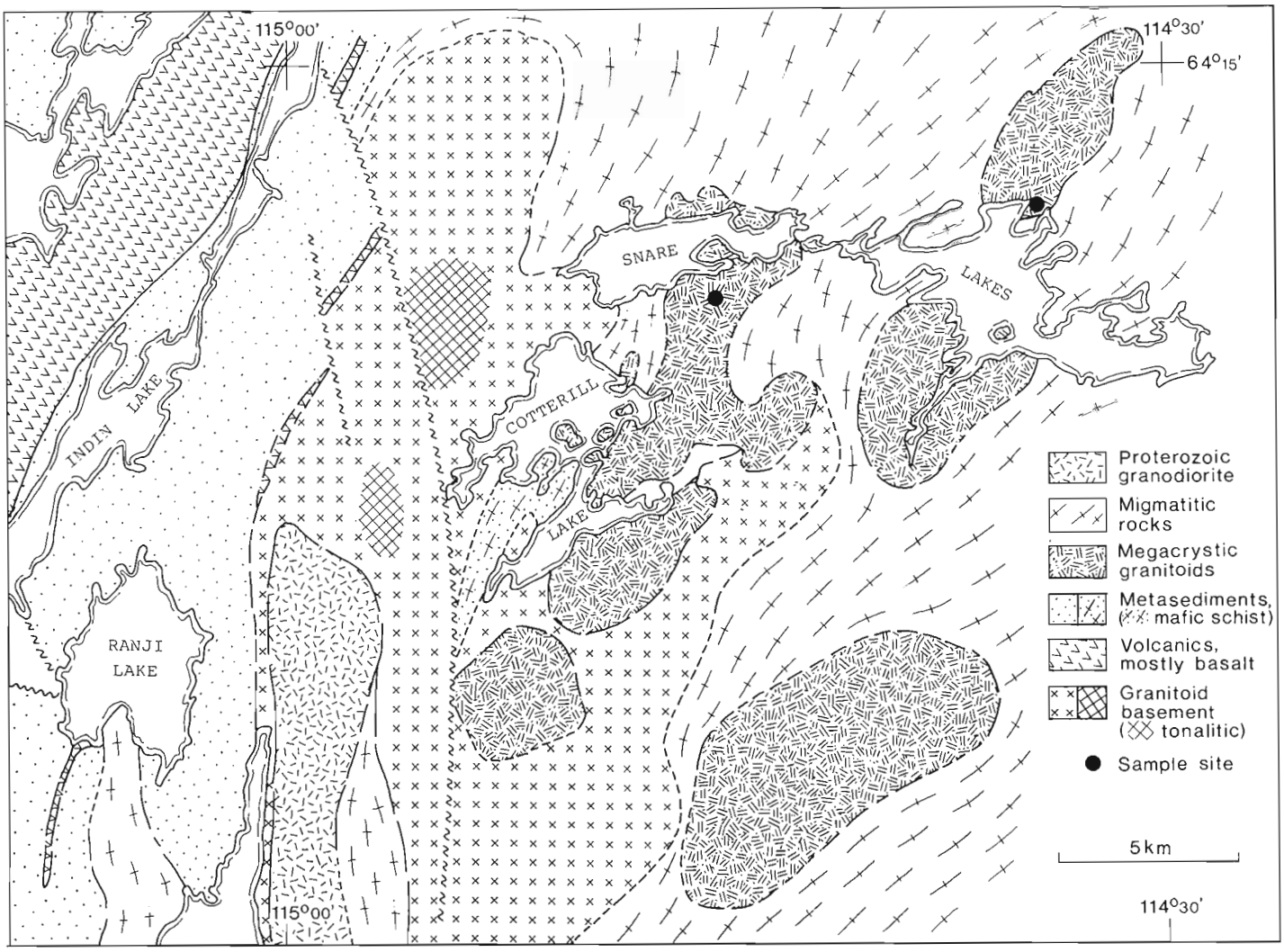

Figure 1. *Sample sites for the Cotterill Lake granite bodies.*

Table 2

Sample numbers and localities, Cotterill Lake granites, District of Mackenzie

Sample Number	Locality			
This work	Field	Latitude	Longitude	N.T.S.
1	FYT-666-5	114°35'	64°12'30"	86 B/2
2	FYT-1320-7	114°46'	64°11'	86 B/2
3	FYT-666-9	114°35'	64°12'30"	86 B/2
4	FYT-1320-8	114°46'	64°11'	86 B/2
5	FYT-1320-3	114°46'	64°11'	86 B/2
6	FYT-666-8	114°35'	64°12'30"	86 B/2
7	FYT-666-2	114°35'	64°12'30"	86 B/2
8	FYT-1320-9	114°46'	64°11'	86 B/2
9	FYT-666-7	114°35'	64°12'30"	86 B/2
10	FYT-1320-11	114°46'	64°11'	86 B/2

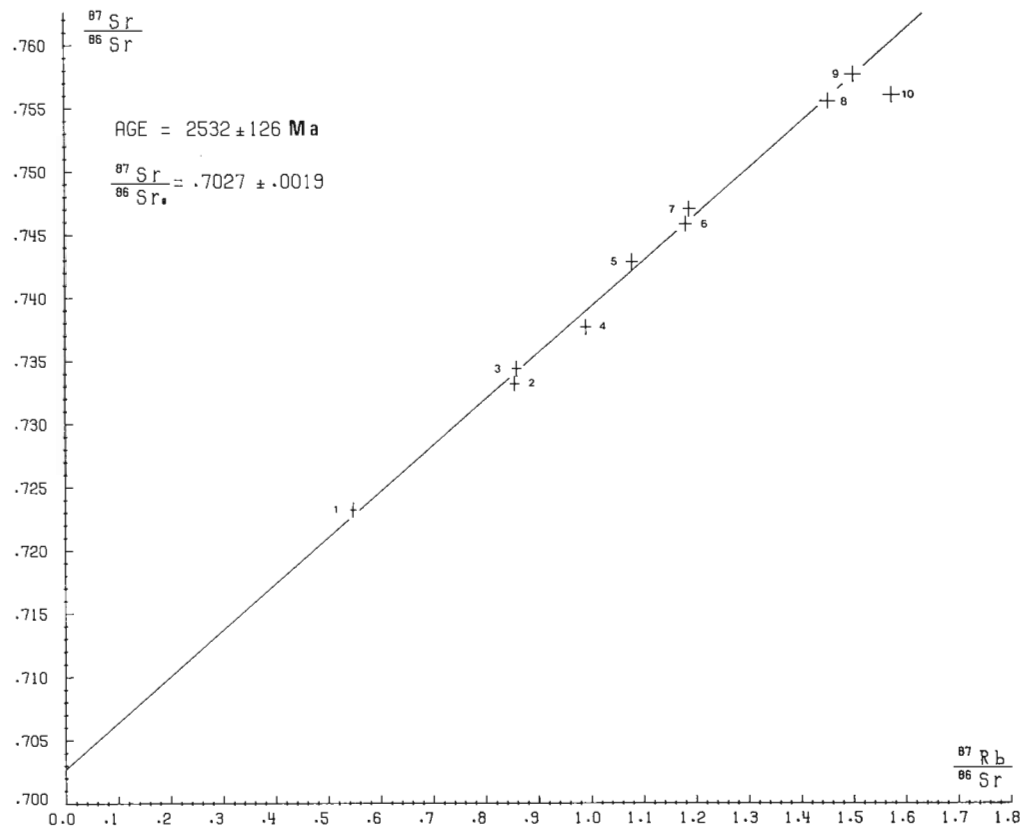

Figure 2. *Rb-Sr isochron Cotterill Lake granites, District of Mackenzie.*

References

Bridgwater, D. and Fyfe, W.S.
1974: The Pre-3 b.y. Crust: Fact-Fiction-Fantasy; Geoscience Canada, v. 1, no. 3, p. 7-11.

Faure, G. and Powell, J.C.
1972: Strontium isotope geology; Springer-Verlag Heidelberg, 188 p.

Fortier, Y.O.
1949: Indin Lake, E/2, District of Mackenzie; Geological Survey of Canada, Map No. 49-10a and Paper 49-10.

Frith, R.A.
1973: The geology of the Bear-Slave boundary in the Indin Lake area, in Report of Activities, Part A, District of Mackenzie; Geological Survey of Canada, Paper 73-1A, p. 146-148.

1978: Tectonics and metamorphism along the southern boundary between the Bear and Slave Structural Provinces; in Metamorphism in the Canadian Shield; Geological Survey of Canada, Paper 78-10, p. 103-114.

Geology of the Indin Lake map area, District of Mackenzie; Geological Survey of Canada, Paper, in preparation.

Frith, R.A. and Currie, K.L.
1976: A model for the origin of the Lac St. Jean anorthosite massif; Canadian Journal of Earth Sciences, v. 13, p. 389-399.

Frith, R.A., Frith, R., Helmstaedt, H., Hill, J., and Leatherbarrow, R.
1974: Geology of the Indin Lake area, District of Mackenzie; in Report of Activities, Part A, Geological Survey of Canada, Paper 74-1A, p. 165-171.

Frith, Rosaline, Frith, R.A., and Doig, R.
1977: The geochronology of the granitic rocks along the Bear-Slave Structural Province boundary, northwest Canadian Shield; Canadian Journal of Earth Sciences, v. 14, p. 1356-1373.

McGlynn, J.C.
1972: Basler Lake granite, District of Mackenzie; in Wanless, R.K. and Loveridge, W.D., 1972, Rubidium-Strontium Isochron Age Studies. Report 1; Geological Survey of Canada, Paper 72-23, p. 15-20.

Moorbath, S.
1975: Evolution of Precambrian crust from strontium isotopic evidence; Nature, v. 254, p. 395-398.

Robertson, D.K.
1974: Lead isotope ratios and crustal evolution of the Slave Craton at Ghost Lake, Northwest Territories. Canadian Journal of Earth Sciences, v. 11, p. 819-827.

17. ZIRCON AGES FROM A GRANULITE-ANORTHOSITE COMPLEX AND A LAYERED GNEISS COMPLEX NORTHEAST OF BAKER LAKE, DISTRICT OF KEEWATIN

Uranium-lead, upper concordia intercept ages were obtained on pairs of zircons from:

1. *the granulite-anorthosite complex exposed along the Chesterfield fault zone, sample number WN-505-78, age* 2573^{+28}_{-5} *Ma, and*
2. *a gneiss complex north of the Chesterfield fault zone, sample number WN-506-78, age* 2675^{+33}_{-11} *Ma.*

The analytical results are listed in Table 1. Corrections for contamination lead introduced during the analytical processing, and common lead in the zircon crystals, amount to less than one per cent of the radiogenic lead present in the samples processed. Thus, errors associated with these parameters are negligible. A concordia plot of the data is shown in Figure 1. For both samples the pairs of data points are close enough to the concordia curve to define the intercept ages with satisfactory precision. Assuming reasonable co-linearity, a third data point on each line would not substantially affect the intercept age, so further analyses were not undertaken.

A description of the zircons analyzed is presented in Table 2.

Geological Settings and Interpretations
by Mikkel Schau

1. A minimum "late Archean" age for charnockitic gneiss from granulite-anorthosite complex along Chesterfield fault zone near Baker Lake

WN-505-78 Age 2573^{+28}_{-5} Ma

Location: 64°05'N, 93°56'W

A granulite-anorthosite complex is exposed along the Chesterfield fault zone (Schau and Ashton, 1978) where it is cut by a granitoid plutonic complex which has yielded a rubidium-strontium whole rock errorchron of 2.5-2.4 Ga (more work is underway by W.D. Loveridge to better define this age).

The granulite-anorthosite complex consists of granulites with considerable compositional variety but mainly of intermediate composition (plagioclase + orthopyroxene ± clinopyroxene ± garnet ± quartz) into which a most spectacular layered complex consisting of an upper(?) gabbroic noritic anorthosite (Wright, 1967) and associated (and lower?) layered anorthositic to melanocratic iron gabbros and norites has been introduced.

The sample was taken on the north side of an anticlinal core of charnockitic gneiss very near the unexposed contact with layered anorthositic gabbro. The sample was interpreted in the field as a charnockitic gneiss, which was considered part of the granulitic sequence intruded by the anorthosite complex, but petrographic work has identified the presence of charnockitic-mangeritic rocks within the anorthosite suite. Whether the rocks at the sampled locality belong to the igneous suite or the intruded suite is now not clear.

Nevertheless, the zircon date is a minimum age of an event which affected the anorthosite-granulite complex and combined with the errorchron mentioned above suggests a minimum age of latest Archean for the whole complex.

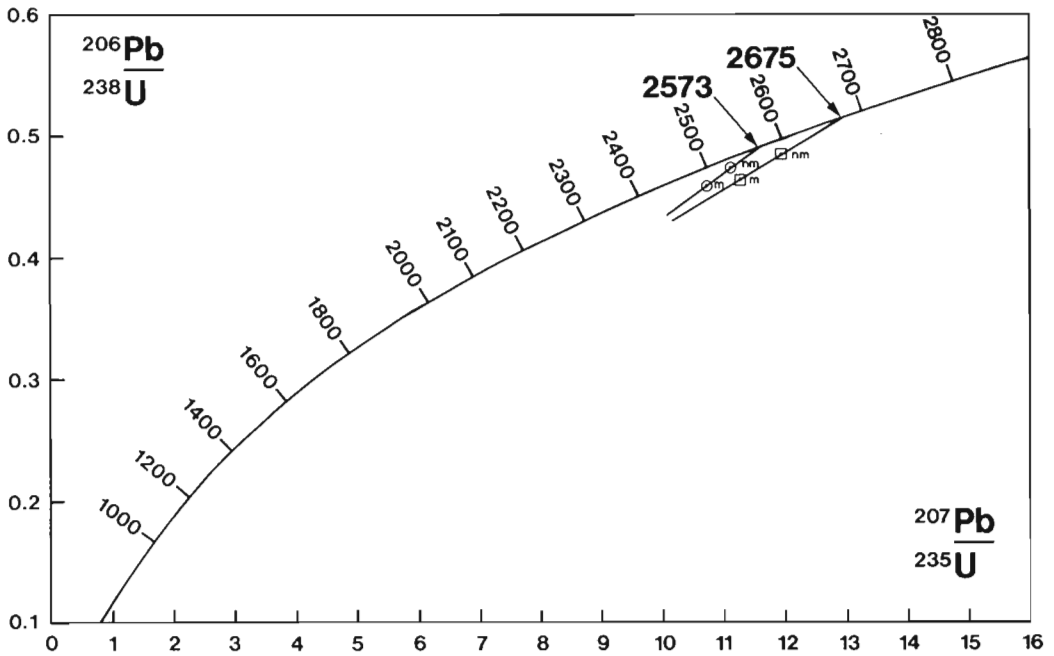

Figure 1. *Concordia diagram showing analyses of zircon fractions from a Granulite-Anorthosite Complex and a Layered Gneiss Complex northeast of Baker Lake.*

From: *Rb-Sr and U-Pb Isotopic Age Studies in Current Research, Part C Geol. Surv. Can., Paper 80-1C*

Table 1

Analytical data for zircon samples from two complexes northeast of Baker Lake

Sample No.	Size (μm)	*Pb (ppm)	U (ppm)	Age (Ma) $^{206}Pb/^{204}Pb$	$^{206}Pb/^{238}U$	$^{207}Pb/^{235}U$	$^{207}Pb/^{206}Pb$	Concordia (Ma)	K/Ar (Ma)
Wn-505-78	+149 n.m.	230.1	414.5	6870	2497	2532	2561	2573^{+28}_{-5}	
	+149 m	318.8	628.0	4130	2439	2501	2552		
Wn-506-78	+149 n.m.	150.9	263.7	6799	2550	2602	2642	2675^{+33}_{-11}	b 1895 ± 44
	+149 m	196.4	362.9	4210	2460	2547	2616		

*Radiogenic Pb, m = magnetic, n.m. = nonmagnetic, b = biotite, λ_{238} U = $1.55125 \times 10^{-10}a^{-1}$, λ_{235} U = $9.8485 \times 10^{-10}a^{-1}$, $^{238}U/^{235}U = 137.88$

Table 2

Description of zircon concentrates as analyzed, samples number WN-505-78 and WN-506-78

WN-505-78

Fraction 1, +100 mesh (149 μ), nonmagnetic, hand picked

The analyzed material consisted of essentially clear, very rounded elongated zircons. The more spherical grains were removed by hand-picking. The grains are amber coloured, internally complex with fractures, striae and inclusions but no evident zoning. Length to breath ratios range up to 3:1.

Fraction 2, +100 mesh (149 μ), magnetic, hand picked

Same as fraction 1, no visible distinction.

WN-506-78

Fraction 1, +100 mesh (149 μ), nonmagnetic hand picked

The analyzed zircon consisted essentially of subhedral to rounded crystals and fragments. 85 per cent were clear honey-coloured and 15% were red-orange. In the latter variety the centres tended to be less intensely coloured than the margins. Also the more strongly coloured grains showed indications of a fine "fishbone" internal structure possibly indicating zoning of the crystals. In finer fractions zoning is quite evident. Internal lines and fractures and bubble inclusions, are common. Elongation ranges up to 4:1.

Fraction 2, +100 mesh (149 μ), magnetic, hand picked

Essentially similar to fraction 1, but the crystals and fragments contain more black specks and bubble inclusions. These zircons also appear to be more strongly coloured than the nonmagnetic variety and consist of 75 per cent clear, honey to tan coloured and 25 per cent distinctly orange-red in colour.

2. Leucocratic layer in amphibole-rich gneiss: age of late Archean for a gneissic complex in the Armit block, District of Keewatin

WN-506-78 Age 2675^{+33}_{-11} Ma

Location: 64°11'N, 93°59½'W

A gneiss complex north of the Chesterfield fault zone near Baker Lake (Heywood and Schau, 1978) is in fault contact with a granulite-anorthosite complex (see WN-505-78) and both these complexes are intruded by a granitoid plutonic complex on which an Rb-Sr errorchron (unpublished) indicates 2.5-2.4 Ga. (Work is continuing on the Rb-Sr systematics on these rocks.)

The gneiss complex consists of well layered biotite, biotite-hornblende, or hornblende gneisses with local layers rich in epidote and occasional inclusions of chlorite and/or talc schists. The sample was taken from a leucocratic layer in a biotite-bearing hornblende quartz plagioclase gneiss (Schau and Ashton, 1979).

The zircon date provides a minimum date for the age of this gneiss complex in the Armit block.

References

Heywood, W.W. and Schau, Mikkel
1978: A subdivision of the Northern Churchill Structural Province; in Current Research, Part A, Geological Survey of Canada, Paper 78-1A, p. 139-143.

Schau, Mikkel and Ashton, K.E.
1979: Granulites and plutonic complexes northeast of Baker Lake, District of Keewatin; in Current Research, Part A, Geological Survey of Canada, Paper 79-1A, p. 311-316.

Wright, G.M.
1967: Geology of the Southeastern Barren Grounds, parts of the Districts of Mackenzie and Keewatin; Geological Survey of Canada, Memoir 350.

18. A URANIUM-LEAD AGE OF ZIRCONS FROM VOLCANICS AND SEDIMENTS OF THE BACK RIVER VOLCANIC COMPLEX, EASTERN SLAVE PROVINCE, DISTRICT OF MACKENZIE

Uranium-lead analyses were performed on zircon concentrates from a rhyolite sample 77-E-695-LQ-2 collected by M.B. Lambert in 1977 and a greywacke HBA-J-82-1-74 collected by J.B. Henderson in 1974. The results are listed in Table 1 and shown on a concordia diagram, Figure 1. Table 3 is a description of the zircon concentrates as analyzed.

The two sets of age results for the zircons from the rhyolite sample are almost identical (Table 1) and yield an average $^{207}Pb/^{206}Pb$ age of 2667 ± 7 Ma. As there is no separation between the analytical points, the $^{207}Pb/^{206}Pb$ results provide a minimum age for the rhyolite sample.

A parallel case exists for the greywacke sample. The age results are very similar for these two analyses as well, more discordant than for the rhyolite, but yielding a similar average $^{207}Pb/^{206}Pb$ age of 2672 ± 7 Ma which may be taken as a minimum age for the greywacke.

However, since the $^{207}Pb/^{206}Pb$ ages for the greywacke and the rhyolite agree within the analytical uncertainty, despite the differing degrees of discordance, it is probable that they represent the primary age of these rocks units. This is the interpretation that is depicted in the concordia diagram, Figure 1. The upper intersection with the concordia curve of the chord defined by the four analytical point yields an age of 2667 Ma but the lower intersection yields a slightly negative age. A better estimate is probably the average of the four $^{207}Pb/^{206}Pb$ ages, 2670 ± 4 Ma.

Geological Setting and Interpretation
by M.B. Lambert and J.B. Henderson

1. Rhyolite dome 2667 ± 7 Ma ($^{207}Pb/^{206}Pb$ zircon)
2. Greywacke 2672 ± 7 Ma ($^{207}Pb/^{206}Pb$ zircon)

The Back River volcanic complex (Fig. 2) covers an area about 40 km long and 20 km wide in the eastern Slave Province, centred about 480 km northeast of Yellowknife, N.W.T. The complex is an essentially flat lying succession of volcanics surrounded by more highly deformed metagreywacke-mudstone turbidites. Both the volcanics and sediments are part of the Yellowknife Supergroup of Archean age. Zircons were analyzed from samples collected from both volcanics and sediments in an attempt to confirm an Archean age for the complex and perhaps to determine the time span of volcanism.

Geological Setting

The Back River Complex records a history of volcanism that began with the effusion of basaltic and andesitic magma on the seafloor, producing submarine domal ridges of breccia and pillow lavas. The volcanic pile gradually emerged and explosive eruptions of voluminous felsic pyroclastics produced a subaerial ash-flow field. Water-laid tuffs, ash flows, landslide debris and volcaniclastic sands accumulated in shallow margins along the flanks of the volcano. Eruptions culminated in cauldron subsidence and development of two ring-fracture systems in the southern half of the complex. Rhyolite dykes and domes rose along ring fractures and in shallow seas marginal to the emergent volcanic pile in the northern half (Fig. 2).

The bulk of the volcanics are andesitic to dacitic rocks comprising pillow lavas, breccias, massive flows and domes, water-laid and air-fall tuffs, ash flows and pyroclastic breccias. Basalt pillow lavas, breccias and volcaniclastic sediments form a minor part of the complex along the northern margin.

Sediments completely surround the complex. At the present level of erosion they conformably underlie the volcanics in the northern part of the complex but interfinger with volcanics locally along the eastern and western margins. The sediments are dominantly greywacke-mudstone turbidites but iron formation, containing carbonate, sulphide and silicate facies occurs near the contact with volcanics. Thin members of felsic volcanic breccia and water-laid tuffs occur in the sediments up to 10 km from the main volcanic complex. The greywackes are composed dominantly of felsic volcanic rock fragments and quartz derived mainly from the adjacent volcanic complex or other volcanic complexes similar to it but not preserved.

The flat lying volcanic complex has behaved as a stable buttress against which the much less competent sediments have been complexly deformed. The metamorphic grade of the volcanic complex and the immediately adjacent sediments is greenschist although amphibolite grade is reached in small areas along the northern and southern margins of the complex near tonalitic to granodioritic plutons.

Various aspects of the geology of the volcanics and sediments are discussed in greater detail in Baragar, 1975; Henderson, 1975; Lambert, 1976, 1977, 1978.

Sample Descriptions

Two samples, one from the volcanic complex and one from the sediments, were collected for radiometric dating of zircons (Fig. 2, Table 2).

The first is from a rhyolite body along the southern end of the complex which is interpreted to represent a late stage in the evolution of the complex. The body, about 1700 m long and 200 to 300 m wide is one of a series of small domes or intrusions that lie within the outer ring complex. The rhyolite is a white to pink weathering, massive to brecciated rock. Fresh rock is pale greenish- to bluish-grey, sparsely porphyritic rhyolite containing phenocrysts of quartz and plagioclase 2 to 5 mm across in an aphanitic matrix.

The second sample is an unusually coarse greywacke or fine sedimentary breccia collected 1 km from the east side of the complex. It is composed of subangular quartz, felsic volcanic rock fragments, chert, intraformational mudstone clasts and minor plagioclase. Maximum grain size is 7 mm although most are less than 3 mm and grade to a quartzo-feldspathic-argillaceous matrix. The metamorphic mineral assemblage is chlorite-muscovite. Zircons occur as detrital grains in the matrix and probably in the felsic rock fragments as well.

From: Rb-Sr and U-Pb Isotopic Age Studies in Current Research, Part C
Geol. Surv. Can., Paper 80-1C

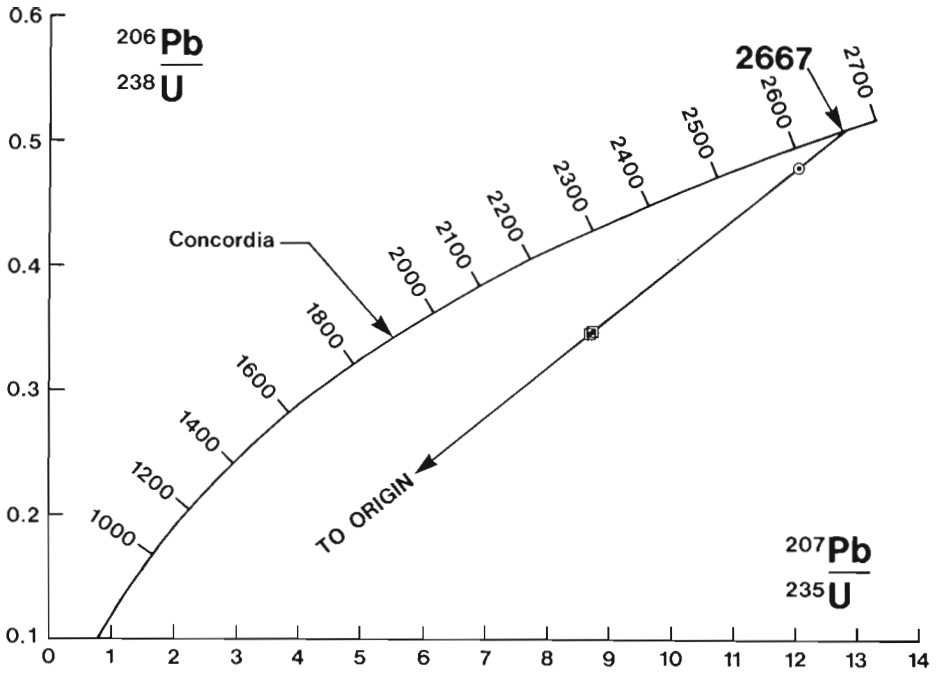

Figure 1. *Concordia diagram showing the results of analysis of zircon concentrates from rhyolite (circle) and greywacke (squares), Back River volcanic complex, District of Mackenzie.*

Table 1

Analytical data, zircon fractions rhyolite and greywacke,
Back River volcanic complex, District of Mackenzie

*Fraction number		R1	R2	G1	G2
Fraction size (μm)		-105 + 88	-74 + 64	-93 + 74	-74 + 64
Magnetic or nonmagnetic		nm	nm	-	-
Weight (mg)		11.48	8.82	15.93	16.63
Total Rb, ng		653.2	619.8	426.5	449.2
Pb blank %		0.3	0.3	0.4	0.9
Observed $^{206}Pb/^{204}Pb$		3903	12850	711	777
Abundances	^{204}Pb	0.0204	0.0032	0.1333	0.1126
(^{206}Pb = 100)	^{207}Pb	18.414	18.180	19.837	19.603
	^{208}Pb	13.852	13.646	24.818	23.538
Radiogenic Pb ppm		155.8	177.0	91.78	94.05
%		99.02	99.85	94.25	95.09
Uranium ppm		286.3	324.6	218.33	226.1
Atomic ratios	$^{206}Pb/^{238}U$	0.48133	0.48120	0.35133	0.34921
	$^{207}Pb/^{235}U$	12.056	12.037	8.8179	8.7742
	$^{207}Pb/^{206}Pb$	0.18165	0.18141	0.18202	0.18222
Ages (Ma)	$^{206}Pb/^{238}U$	2533	2533	1941	1931
	$^{207}Pb/^{235}U$	2609	2607	2319	2315
	$^{207}Pb/^{206}Pb$	2668	2666	2671	2673

* R1 and R2 = 77-E-695-LQ-2 rhyolite
G1 and G2 = HBA-J-82-1-74 greywacke

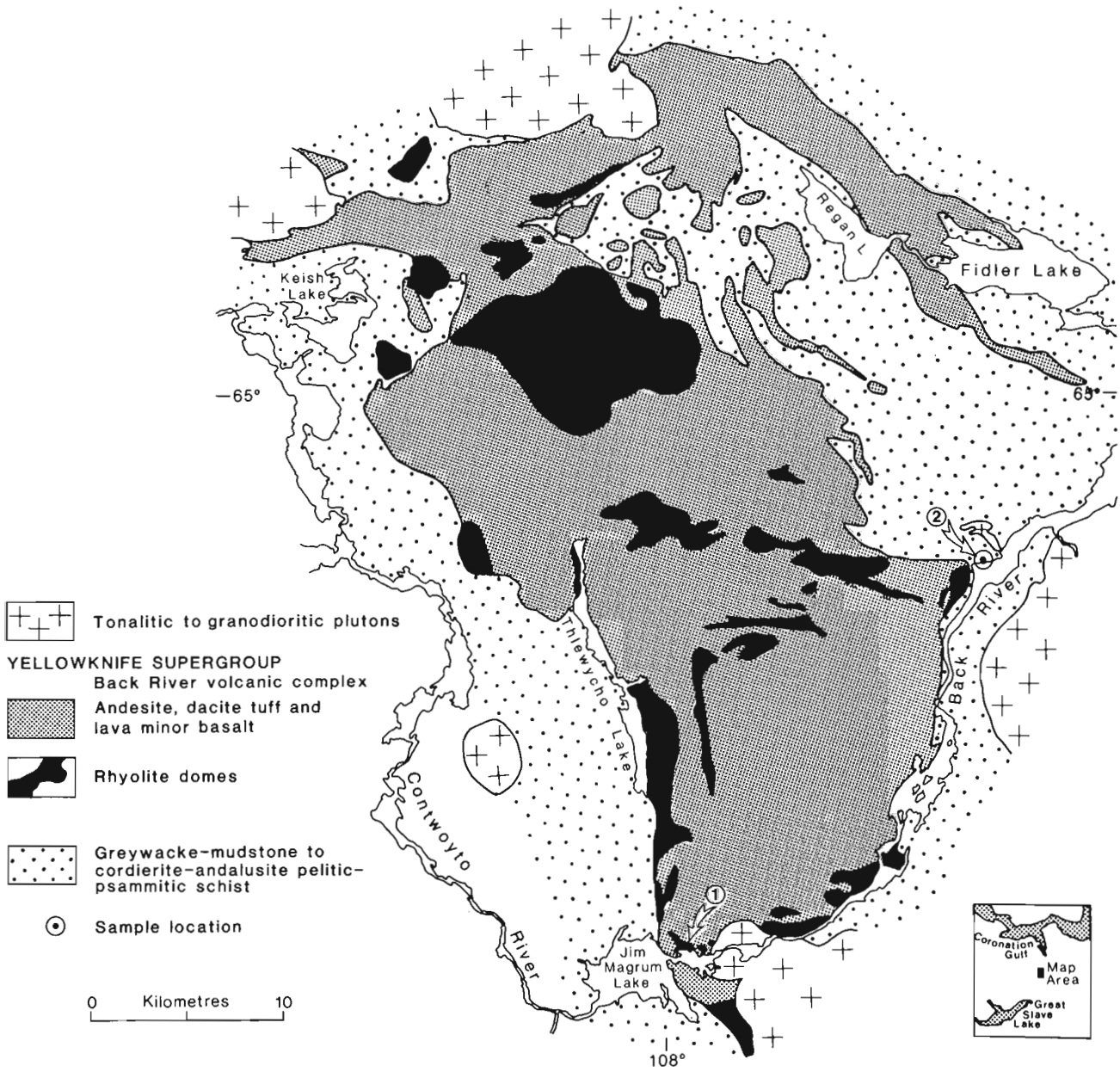

Figure 2. *Geological map of Back River area. Localities 1 and 2 show the rhyolite and greywacke sample sites, respectively.*

Table 2

Sample numbers and localities

Sample No.			Locality		
This work	Field	Rock Type	Latitude	Longitude	N.T.S.
R1 and R2	77E-695LQ2	Rhyolite	64°44'30"N	107°58'15"W	76 B/12
G1 and G2	HBA-J-82-1-74	Greywacke	64°55'30"N	107°43'45"W	76 B/13

Table 3

Description of zircon concentrates as analyzed,
Back River volcanic complex, District of Mackenzie

Fraction R1, -140 + 170 mesh, (-105 + 88 μ) nonmagnetic

These zircons were light- to medium-amber coloured, subhedral to partially rounded. Most are fragments of crystals but the few complete crystals have an elongation ratio up to 2.8:1. Inclusions and internal fractures and imperfections are common. Occasional crystals are almost translucent and have very imperfect, nonuniform birefringence. These may be cyrtolite, which has been identified by X-ray diffraction in other fractions. Non-zircon impurities consisted of about 5% unidentified opaque grains.

Fraction R2, -200 + 250 mesh, (-74 + 64 μ) nonmagnetic

Essentially similar to R1 but of generally darker amber colour with some approaching orange-brown. There is evidence of a quantity of very fine material adhering to zircon grain surfaces. There is a higher proportion of translucent grains in this fraction and inclusions and internal imperfections are more abundant. Cores are evident in some. Birefringence is also more disturbed, increasingly so with colour intensity. The concentrate contains approximately 5% unidentified opaque impurities.

Fraction G1, -160 + 200 mesh (-93 + 74 μ)

The analyzed zircon consisted of pale- to medium-brown, euhedral to rounded crystals and crystal fragments. Granular, rod and bubble inclusions were observed in about 50% of the crystals, zoning is clearly evident in at least 75% and one crystal was observed to have a distinct core. The zoned crystals have more internal fractures and imperfections than do the unzoned, clearer ones. Elongation range up to 2.5:1.

Fraction G-2, -200 + 250 mesh (-74 + 64 μ)

Essentially identical to fraction G1.

Discussion

The discordant zircon data at 2670 ± 4 Ma clearly confirm the Archean age of the supracrustal rocks and give a minimum age of volcanism. These preliminary data correspond reasonably well with zircon data from Yellowknife supracrustal rocks elsewhere in the Slave Province. For example, at Yellowknife, Green and Baadsgaard (1971) reported a zircon $^{207}Pb/^{206}Pb$ age of 2650 Ma from a dacite in the Kam volcanics while a single population of zircons from the Burwash greywackes at Yellowknife have a $^{207}Pb/^{206}Pb$ age of 2680 Ma (R.K. Wanless, personal communication). A single population of zircons from a felsic volcanic breccia near Snofield Lake in the northernmost Slave Province have a somewhat younger $^{207}Pb/^{206}Pb$ age of 2510 Ma (R.K. Wanless personal communication).

References

Baragar, W.R.A.
1975: Miscellaneous data from volcanic belts at Yellowknife, Wolverine Lake and James River, N.W.T.; in Report of Activities, Part A, Geological Survey of Canada, Paper 75-1A, p. 281-286

Green, D.C. and Baadsgaard, H.
1971: Temporal evolution and petrogenesis of an Archean crustal segment at Yellowknife, N.W.T, Canada; Journal of Petrology, v. 12, p. 177-217.

Henderson, J.B.
1975: Sedimentological Studies in the Yellowknife Supergroup in the Slave Structural Province; in Report of Activities, Part A, Geological Survey of Canada, Paper 75-1, p. 325-330.

Lambert, M.B.
1976: The Back River Volcanic Complex, District of Mackenzie; in Report of Activities, Part A, Geological Survey of Canada, Paper 76-1A, p. 363-367.

1977: The southwestern margin of the Back River Volcanic Complex, District of Mackenzie; in Report of Activities, Part A, Geological Survey of Canada, Paper 77-1A, p. 179-180.

1978; The Back River Complex – a cauldron subsidence structure of Archean age; in Current Research, Part A, Geological Survey of Canada, Paper 78-1A, p. 153-158.

19. A CONCORDANT URANIUM-LEAD AGE FOR ZIRCONS IN THE ADAMANT PLUTON, BRITISH COLUMBIA

Essentially concordant uranium-lead ages averaging 169 ± 4 Ma were obtained on three fractions of one zircon sample from the hornblende diorite-quartz monzonite zone at the southwest corner of the Adamant Pluton. The ages and associated analytical results are listed in Table 2. Corrections for the 1.8 nanograms of contaminant lead introduced during the analytical processing of the sample are in the order of ten per cent of the sample lead present, reflecting the low lead content of these zircon fractions. Common lead contents are also high ranging from seven to fourteen per cent of total lead in the zircons. The relatively high corrections to the total lead compositions required by these nonradiogenic components probably introduce a somewhat higher than normal uncertainty (Sullivan and Loveridge, this report) to the calculated radiogenic lead parameters.

The age of 169 ± 4 Ma presented above is the average of nine isotopic age results determined on three fractions. As the error associated with the measurement of $^{207}Pb/^{206}Pb$ ages in this age range is much higher than that associated with the measurement of $^{206}Pb/^{238}U$ and $^{207}Pb/^{235}U$ ages, it might be possible to derive a more precise age by averaging only the latter two ratios for the three zircon fractions. However, this result, 168 ± 3 Ma is essentially indistinguishable from the former figure.

A description of the zircons analyzed is presented in Table 1. Figure 2 shows the results of analyses of the three zircon fractions on a concordia diagram.

Geological Setting and Interpretation
by D. Shaw

Introduction

The Adamant Pluton is a zoned, igneous body with an elongated, ellipsoidal map outline (Fig. 1). The long axis, in plan view, is aligned east-west and is 25.6 km long. The maximum width of the pluton is 6.4 km. The core of hypersthene-augite monzonite is successively enclosed by a mixed zone of hornblende-quartz monzonite and granodiorite, a zone of biotite-hornblende granodiorite and a zone of quartz diorite (Fox, 1969).

The northwest-southeast regional, structural trend is modified in the vicinity of the Adamant Pluton to a pronounced and easily apparent structural aureole associated with the igneous mass.

Regional Deformation

Three major phases of deformation are recognized in the Northern Selkirk Mountains. The earliest phase is attributed to Caribooan orogenic activity (Read and Wheeler, 1975; Read, 1975, 1976) and generated at least one large scale nappe in the region adjacent to the Adamant Pluton (Van der Leeden, 1976; Brown et al., 1977). A planar fabric (S_1) produced during this phase is generally parallel to primary bedding (S_0) throughout the northern Selkirk Mountains (Brown et al., 1977).

During the Middle Jurassic extensive deformation and metamorphism occurred throughout the northern Selkirk Mountains. Two phases of folding, separated by the peak of regional[1] metamorphism, are recognized. Both phases generated folds with a regional northwest-southeast strike; axial planes of the earlier phase generally dip towards the east whilst those of the latter dip towards the west. A pronounced planar fabric (S_2) is associated with folds of the former phase. Interference of phase two and phase three folds has given rise to the Selkirk structural fan (Brown and Tippett, 1978). The east-west elongate Adamant Pluton sits astride the northwesterly trending fan axis.

Emplacement of Adamant Pluton with respect to structural history

The outer zone of the body contains a metamorphic, planar fabric composed of thin, one centimetre or less, alternating mafic (biotite and hornblende) and silicic (quartz and feldspar) layers. This fabric is parallel/subparallel to the contact except where it is taken around the hinges of folds. These folds contain a planar fabric, composed of biotite plates, that is parallel to the axial surface of the folds themselves. Only one phase of folding is recognized in the outer zone of the pluton. The strength of the folded fabric and the intensity of the folding decrease as the core of the pluton is approached.

Phase two folds and fabric in the adjacent country rock can be traced into the perimeter zones of the pluton where they are correlated with folds and fabric located therein.

The deformed, metamorphic fabric in the outer zones is believed to be a mimetic feature after the igneous fabric generated during the emplacement of the body.

Table 1

Description of zircon concentrates as analyzed, Adamant Pluton, British Columbia

Fraction 1, +80 mesh (+177 μ), nonmagnetic, hand picked
The analyzed material consisted of very pure, clear, colourless, euhedral prismatic zircon crystals and crystal fragments. Bubble and rod-shaped inclusions and dark streaks were observed in some grains. Most whole crystals are considerably elongated (up to 8:1) while elongated fragments indicate even higher length to breadth ratios. There is no optical indication of zoning, but rare twinned crystals were observed.
Fraction 2, +80 mesh (+177 μ), magnetic
Very similar to the nonmagnetic fraction, except that 15-20% of these contain obvious black and red-brown granular inclusions in addition to rods and bubbles. Hand picking was not required for the magnetic fraction.
Fraction 3, -200 +230 mesh (-74 to +62 μ), nonmagnetic
This fine, nonmagnetic fraction consisted of about 70% clear, colourless, less euhedral crystals with somewhat rounded terminations, and about 30% zircon fragments. The longer crystals again had elongation ratios up to 8:1. Bubble and rod inclusions were noted in some grains.

From: Rb-Sr and U-Pb Isotopic Age Studies in Current Research, Part C Geol. Surv. Can., Paper 80-1C

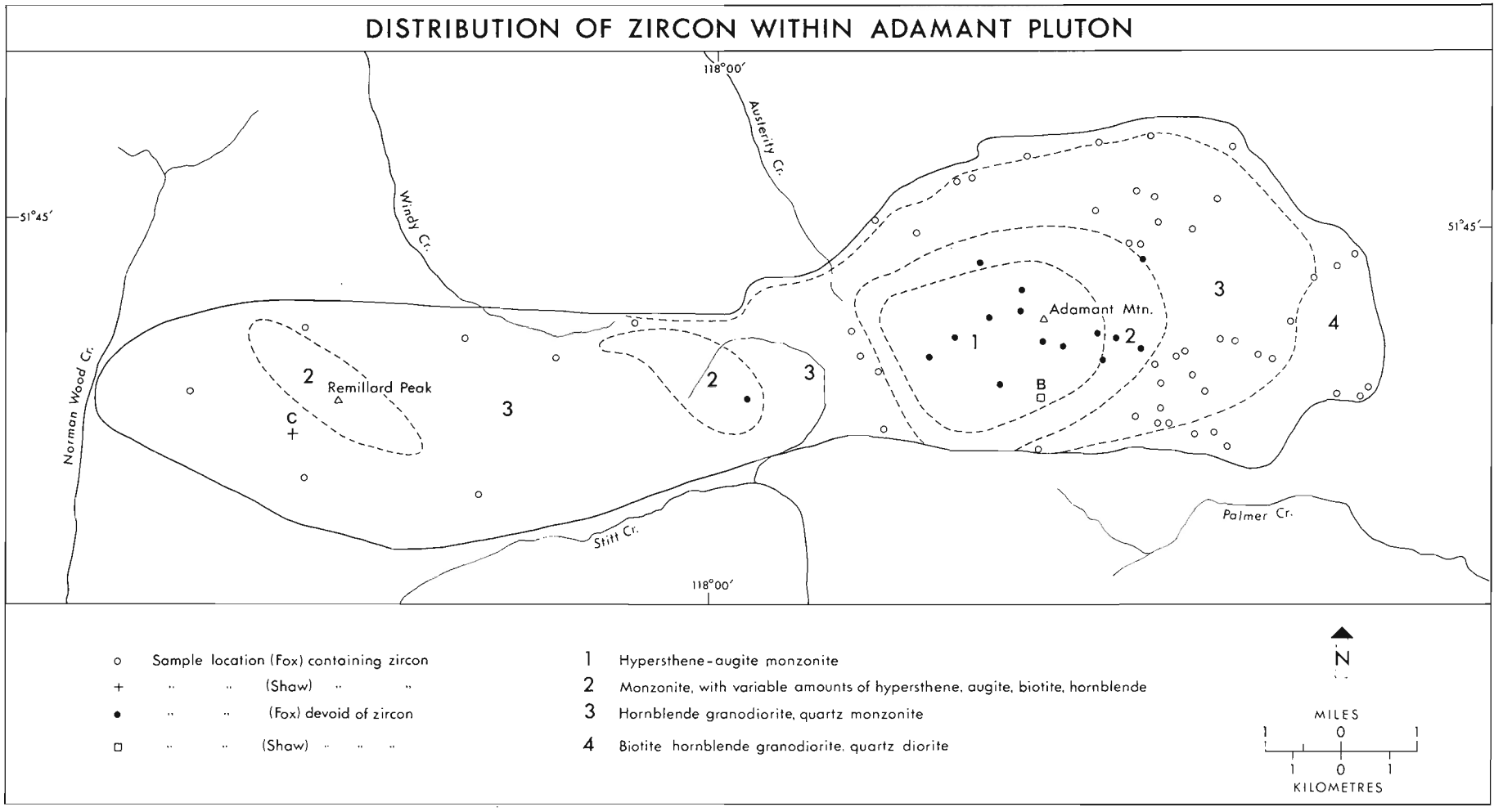

Figure 1. *Sample location and distribution of zircon within the Adamant Pluton, British Columbia.*

Table 2

Analytical data, zircon fractions, Adamant Pluton, British Columbia

Fraction number		1	2	3
Fraction size (μm)		+177	+177	-74+62
Magnetic or nonmagnetic		nm	m	nm
Weight (mg)		8.16	5.91	5.22
Total Pb, ng		23.0	19.2	18.5
Pb blank, %		8.0	9.5	9.9
Observed $^{206}Pb/^{204}Pb$		343	231	312
Abundances (^{206}Pb = 100)	^{204}Pb	0.1466	0.2555	0.1335
	^{207}Pb	7.106	8.7009	6.911
	^{208}Pb	21.298	24.739	25.085
Radiogenic Pb ppm		7.57	7.45	8.91
%		91.60	85.92	92.56
Uranium ppm		272.5	273.6	313.0
Atomic ratios	$^{206}Pb/^{238}U$	0.026675	0.026229	0.026360
	$^{207}Pb/^{235}U$	0.18209	0.17883	0.17984
	$^{207}Pb/^{206}Pb$	0.049506	0.049444	0.049479
Ages (Ma)	$^{206}Pb/^{238}U$	169.7	166.9	167.7
	$^{207}Pb/^{235}U$	169.9	167.1	167.9
	$^{207}Pb/^{206}Pb$	171.9	169.0	170.6

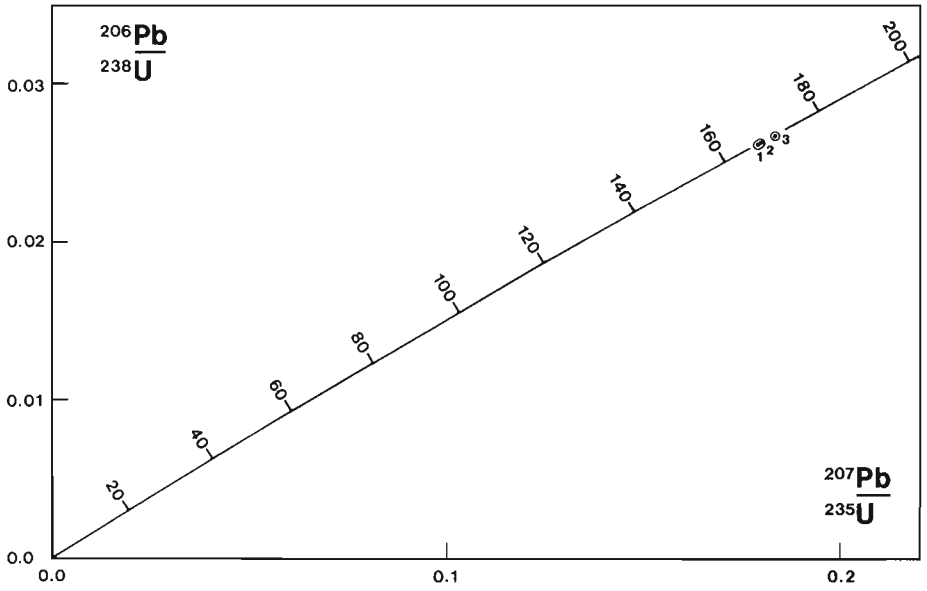

Figure 2. *Concordia diagram showing the results of analyses of three zircon fractions from the Adamant Pluton, British Columbia.*

From the above fabric relationship it appears that the pluton could have been emplaced before or during formation of the second phase folds. However the highly discordant trend of the elongate pluton argues against synkinematic emplacement.

Adjacent to the western end of the body the axial surface trace of a major phase one fold and associated minor structures (Brown et al., 1977) exhibits a similar type of re-orientation to that shown by the axial surfaces of phase two and phase three structures. Finite element analysis performed by Shaw, has shown that the manner of the re-orientation of the phase two and phase three axial surface traces is consistent with the body being pretectonic with respect to those phases. The similarity of the re-orientation of the phase one axial surface trace with those of the later phases indicates that the pluton also predates the earliest phase.

Field data has shown that the Adamant Pluton can be no younger than the second phase of deformation, and is probably older.

Experimental data indicates that the pluton may predate the earliest phase of deformation.

Sampling

Three groups of samples were collected and analyzed for zircon content.

Sample group A was assembled from the Adamant Pluton collection of Fox (1969). All of the samples in this group were collected from the biotite-hornblende granodiorite and quartz diorite zones.

Sample group B was collected by Shaw and consists entirely of samples from the hypersthene-augite monzonite core zone, collected at locations in the extreme south of that zone (Fig. 1).

Sample group C was collected by Shaw and consists entirely of samples from a single location within the hornblende granodiorite and quartz monzonite zone at the southwest corner of the pluton (Fig. 1).

Zircons were found to be abundant in sample groups A, and C, group B was devoid of zircons. The zircon fractions analyzed in this study are from sample group C; a medium grained, foliated, biotite hornblende granodiorite collected at an elevation of 6750' from a cirque on the southwest slope of Mt. Remillard (lat. 51°42'30", long. 118°07'50").

Discussion

The distribution of zircon is confined to the hydrated, outer zones of the pluton, the anhydrous inner two zones being devoid of zircon (Fig. 2). Chemically the body is essentially homogeneous, the only differences between core and perimeter zones being a small variation in SiO_2 and MgO content (Fox, 1969). Petrological differences between core and perimeter reflect on addition of water to the outer zones, the degree of hydration decreasing away from the perimeter of the body. This progressive hydration and associated recrystallization is thought by Fox (1969) to have occurred during regional metamorphism. It has already been shown that recrystallization of the outer zones of the body commenced before the second phase of deformation, unless the mimetic growth of the metamorphic fabric occurred after the original igneous fabric had been folded during the second phase of deformation which is unlikely.

During the second phase of deformation further mineral growth occurred in the outer zones as a biotite fabric was generated parallel to the axial surfaces of phase two folds.

It is suggested that the zircons present in the outer zones of the pluton were nucleated and grew during this ongoing phase of thermal metamorphic activity. This activity peaked between the second and third phases of deformation after which time new mineral growth was greatly reduced. With decreasing temperature the solidus point for the metamorphic minerals would be arrived at. With respect to the Adamant Pluton zircons the solidus point-blocking temperature was reached approximately 170 Ma ago. Consequently the apparent age derived from the zircons of sample group C is related to regional metamorphic activity in the northern Selkirk Mountains, and does not reflect the timing of emplacement of the igneous body.

References

Brown, R.L., Perkins, M.J., and Tippett, C.R.
1977: Structure and stratigraphy of the Big Bend area, British Columbia; in Report of Activities, Part A, Geological Survey of Canada, Paper 77-1A, p. 273-275.

Brown, R.L. and Tippett, C.R.
1978: The Selkirk Fan structure of the southeastern Canadian Cordillera; Geological Society of America Bulletin, v. 89, p. 548-558.

Fox, P.E.
1969: Petrology of the Adamant Pluton, British Columbia; Geological Survey of Canada, Paper 67-61, 101 p.

Read, P.B.
1975: Lardeau Group, Lardeau map-area, west half, British Columbia; in Report of Activities, Part A, Geological Survey of Canada, Paper 75-1A, p. 28.

1976: Lardeau map-area (82 K west-half), British Columbia; in Report of Activities, Part A, Geological Survey of Canada, Paper 77-1A, p. 95-96.

Read, P.B. and Wheeler, J.O.
1975: Lardeau west-half geology; Geological Survey of Canada Open File 288.

Van der Leeden, J.
1976: Stratigraphy, structure and metamorphism in the Northern Selkirk Mountains, southwest of Argonaut Mountain, southeastern British Columbia; unpublished M.Sc. thesis, Carleton University, Ottawa, Ontario, 166 p.

NOTE TO CONTRIBUTORS

Submissions to the *Discussion* section of *Current Research* are welcome from both the staff of the Geological Survey and from the public. Discussions are limited to 6 double-spaced typewritten pages (about 1500 words) and are subject to review by the Chief Scientific Editor. Discussions are restricted to the scientific content of Geological Survey reports. General discussions concerning branch or government policy will not be accepted. Illustrations will be accepted only if, in the opinion of the editor, they are considered essential. In any case no redrafting will be undertaken and reproducible copy must accompany the original submissions. Discussion is limited to recent reports (not more than 2 years old) and may be in either English or French. Every effort is made to include both *Discussion* and *Reply* in the same issue. *Current Research* is published in January, June and November. Submissions for these issues should be received not later than November 1, April 1, and September 1 respectively. Submissions should be sent to the Chief Scientific Editor, Geological Survey of Canada, 601 Booth Street, Ottawa, Canada, K1A 0E8.

AVIS AUX AUTEURS D'ARTICLES

Nous encourageons tant le personnel de la Commission géologique que le grand public à nous faire parvenir des articles destinés à la section discussion *de la publication* Recherches en cours. *Le texte doit comprendre au plus six pages dactylographiées à double interligne (environ 1500 mots), texte qui peut faire l'objet d'un réexamen par le rédacteur en chef scientifique. Les discussions doivent se limiter au contenu scientifique des rapports de la Commission géologique. Les discussions générales sur la Direction ou les politiques gouvernementales ne seront pas acceptées. Les illustrations ne seront acceptées que dans la mesure où, selon l'opinion du rédacteur, elles seront considérées comme essentielles. Aucune retouche ne sera faite aux textes et dans tous les cas, une copie qui puisse être reproduite doit accompagner les textes originaux. Les discussions en français ou en anglais doivent se limiter aux rapports récents (au plus de 2 ans). On s'efforcera de faire coincider les articles destinés aux rubriques* discussions *et* réponses *dans le même numéro. La publication* Recherches en cours *paraît en janvier, en juin et en novembre. Les articles pour ces numéros doivent être reçus au plus tard le 1er novembre, le 1er avril et le 1er septembre respectivement. Les articles doivent être renvoyés au rédacteur en chef scientifique: Commission géologique du Canada, 601, rue Booth, Ottawa, Canada, K1A 0E8.*

AUTHOR INDEX